

NUREG/CP-0041, V. 1  
c. 1

NUREG/CP-0041  
Vol. 1



\*NW28526\*

Proceedings of the U.S. Nuclear Regulatory Commission

---

---

NUCLEAR WASTE  
MANAGEMENT  
LIBRARY

# Tenth Water Reactor Safety Research Information Meeting

SANDIA NATIONAL LABORATORIES  
823 LIBRARY, MS-0731  
P. O. BOX 5800  
ALBUQUERQUE, NM 87185-5800

## Volume 1

- Plenary Session
- Integral Systems Experiments
- Separate Effects Experimental Programs
- Model Development Experimental Programs
- 2D/3D Research Program
- Foreign Programs in Thermal Hydraulics

Held at  
National Bureau of Standards,  
Gaithersburg, Maryland  
October 12-15, 1982

---

---

**U.S. Nuclear Regulatory  
Commission**

Office of Nuclear Regulatory Research



The views expressed in these proceedings are not necessarily those of the U. S. Nuclear Regulatory Commission.

The submitted manuscript has been authored by a contractor of the U.S. Government under contract. Accordingly the U.S. Government retains a nonexclusive, royalty-free license to publish or reproduce the published form of this contribution, or allow others to do so, for U.S. Government purposes.

Available from

GPO Sales Program  
Division of Technical Information and Document Control  
U.S. Nuclear Regulatory Commission  
Washington, DC 20555

Printed copy price: \$11.00

and

National Technical Information Service  
Springfield, VA 22161

Proceedings of the U.S. Nuclear Regulatory Commission

---

---

# Tenth Water Reactor Safety Research Information Meeting

## Volume 1

- Plenary Session
- Integral Systems Experiments
- Separate Effects Experimental Programs
- Model Development Experimental Programs
- 2D/3D Research Program
- Foreign Programs in Thermal Hydraulics

Held at  
National Bureau of Standards  
Gaithersburg, Maryland  
October 12-15, 1982

---

---

Date Published: January 1983

Compiled by: Stanley A. Szawlewicz, Consultant

**Office of Nuclear Regulatory Research  
U.S. Nuclear Regulatory Commission  
Washington, D.C. 20555**

## ABSTRACT

This report is a compilation of papers which were presented at the Tenth Water Reactor Safety Research Information Meeting held at the National Bureau of Standards, Gaithersburg, Maryland, October 12-15, 1982. It consists of six volumes. The papers describe recent results and planning of safety research work sponsored by the Office of Nuclear Regulatory Research, NRC. It also includes a number of invited papers on water reactor safety research prepared by the Electric Power Research Institute and various government and industry organizations from Europe and Japan.

PROCEEDINGS OF THE  
TENTH WATER REACTOR SAFETY RESEARCH  
INFORMATION MEETING

October 12-15, 1982

PUBLISHED IN SIX VOLUMES

GENERAL INDEX

VOLUME 1

- PLENARY SESSION
- INTEGRAL SYSTEMS EXPERIMENTS
- SEPARATE EFFECTS EXPERIMENTAL PROGRAMS
- MODEL DEVELOPMENT EXPERIMENTAL PROGRAMS
- 2D/3D RESEARCH PROGRAM
- FOREIGN PROGRAMS IN THERMAL HYDRAULICS

VOLUME 2

- ANALYSIS OF TRANSIENTS IN LIGHT WATER REACTORS
- FUEL BEHAVIOR AND FISSION PRODUCT RELEASE
- SEVERE ACCIDENT ASSESSMENT
- SEVERE ACCIDENT SEQUENCE ANALYSIS

VOLUME 3

- HUMAN FACTORS RESEARCH
- INSTRUMENTATION AND CONTROL RESEARCH
- OCCUPATIONAL RADIATION PROTECTION
- SAFETY/SAFEGUARDS INTERACTION

VOLUME 4

- MATERIALS ENGINEERING RESEARCH

VOLUME 5

- MECHANICAL/STRUCTURAL ENGINEERING
- LOAD COMBINATIONS
- SEISMIC SAFETY MARGINS
- STRUCTURAL ENGINEERING
- ELECTRICAL EQUIPMENT QUALIFICATION
- PROCESS CONTROL AND ACCIDENT MITIGATION

VOLUME 6

- RISK ANALYSIS
- EPRI SAFETY RESEARCH PROGRAM

PROCEEDINGS OF THE  
TENTH WATER REACTOR SAFETY RESEARCH  
INFORMATION MEETING

held at the

NATIONAL BUREAU OF STANDARDS  
GAITHERSBURG, MARYLAND

October 12-15, 1982

TABLE OF CONTENTS - VOLUME 1

PREFACE . . . . . xi

PLENARY SESSION

Chairman: L. H. Sullivan, NRC

Introductory Remarks  
R. B. Minogue, NRC . . . . . 1

Scaling Rationale in Reactor Safety Research  
L. S. Tong, NRC . . . . . 20

INTEGRAL SYSTEMS EXPERIMENTS

Chairman: Garnet Donald McPherson, NRC

Introduction to Integral Systems Experiments Session  
Garnet Donald McPherson, NRC . . . . . 38

Results of Recent LOFT Experiments  
L. P. Leach, D. J. Hanson, and D. L. Batt, EG&G Idaho . . . . . 40

Semiscale Program FY 82-83 Highlights  
D. J. Shimeck, EG&G Idaho . . . . . 53

Experiment Design and Scaling Analysis for the BWR FIST  
J. E. Thompson, J. A. Findlay, and W. A. Sutherland, GE . . . . . 60

LOBI Experimental Programme Results and Plans: Status  
September 1982  
W. L. Riebold, L. Piplies, and H. Stadtke, JRC Ispra . . . . . 71

ROSA-III Program for BWR LOCA/ECCS Integral Test  
K. Tasaka, M. Suzuki, Y. Anoda, H. Kumamaru, H. Nakamura,  
T. Yonomoto, and M. Shiba, JAERI . . . . . 91

Summary of Two-Bundle Loop Experimental Results  
M. Naitoh, M. Murase, Hitachi Co. Ltd., and R. Tsutsumi,  
Toshiba Corp. . . . . 95

The French Integral Loop, a Joint CEA-EDF-FRAMATOME Project  
R. Deruaz, CEA-CENG, and J. C. Megnin, Framatome . . . . . 108

INTEGRAL SYSTEMS EXPERIMENTS (Cont'd)

18 Degree Sector Test Apparatus (ESTA) Test Results  
H. Nagasaka, M. Katoh, I. Onodera, and H. Aoki, Toshiba Corp. 118

PKL System Effects Test - Status of PKL II Tests  
B. Brand, H. Liebert, R. Mandl, and J. Sarkar, KWU, FRG . . . 121

RELAP-5 Application to Integral Experiments  
V. H. Ransom, EG&G Idaho . . . . . 141

SEPARATE EFFECTS EXPERIMENTAL PROGRAMS

Chairman: W. D. Beckner, NRC

NRC/EPRI/W Flecht-Seaset Program, Natural Circulation Results,  
163-Blocked Bundle Results  
L. E. Hochreiter, Westinghouse . . . . . 152

Heat Transfer from a Vertical Tube Bundle Under Natural  
Circulation Conditions  
M. J. Gruszczynski and R. Viskanta, Purdue Univ. . . . . 180

Thermal-Hydraulic Experiment Facility (THEF)  
J. S. Martinell, EG&G Idaho . . . . . 188

NRC/DAE Reactor Safety Research Data Bank  
E. T. Laats, EG&G Idaho . . . . . 195

Payoffs from the BWR Refill/Reflood Program  
J. A. Findlay and W. A. Sutherland, General Electric . . . 202

MODEL DEVELOPMENT EXPERIMENTAL PROGRAMS

Chairman: M. W. Young, NRC

TRAC-BWR Heat Transfer  
R. W. Shumway and R. E. Phillips, EG&G Idaho . . . . . 218

Experimental Data for Nonequilibrium Post-CHF Heat Transfer  
in a Vertical Tube  
D. Evans, S. Webb, J. C. Chen, and S. Neti, Lehigh Univ. . . 227

Phenomenological Modeling of Two-phase Flow in Water Reactor  
at ANL  
M. Ishii and G. De Jarlais, ANL . . . . . 232

An LDA In Situ Study of Droplet Hydrodynamics Across Grid  
Spacers in PWR-LOCA Reflood  
S. L. Lee, S. K. Cho, K. Rob, H. J. Sheen, and M. Aghili,  
State University of New York at Stony Brook . . . . . 253

2D/3D RESEARCH PROGRAM  
Chairman: L. H. Sullivan, NRC

|   |     |
|---|-----|
| Findings in CCTF Core I Test<br>Y. Murao, T. Sudoh, T. Iguchi, J. Sugimoto, H. Akimoto,<br>T. Okubo, and K. Hirano, JAERI . . . . .               | 275 |
| SCTF Core-I Reflood Test Results<br>H. Adachi, Y. Sudo, M. Sobajima, T. Iwamura, M. Osakabe,<br>A. Ohnuki, Y. Abe, and K. Hirano, JAERI . . . . . | 287 |
| TRAC Analysis Support for the 2D/3D Program<br>K. A. Williams, LANL . . . . .   | 307 |

FOREIGN PROGRAMS IN THERMAL HYDRAULICS  
Chairman: L. Harold Sullivan, NRC

|  |     |
|--|-----|
| TRAC-BD1 Calculation for Two-Bundle Loop Integral Response<br>M. Naitoh, T. Matsumoto, M. Murase, Hitachi Co. Ltd.,<br>and R. Tsutsumi, Tokyo Electric Power Co. . . . . | 347 |
| ROSA-IV Program for the Experimental Study on Small-Break LOCAs<br>and the Related Transients in a PWR<br>K. Tasaka, JAERI . . . . .                                     | 353 |
| TRAC-BD1 Calculation of ESTA Test<br>N. Abe, M. Katoh, JAERI, and H. Nagasaka, H. Aoki,<br>Toshiba Corp. . . . .   | 356 |
| The CATHARE Code and its Qualification on Analytical Experiments<br>G. Houdayer, EDF, J. C. Rousseau and B. Brun, CEA France . . . . .                                   | 359 |
| NEPTUN Bundle Boil-off and Reflooding Experimental Program Results<br>S. N. Aksan, EIR Switzerland . . . . .   | 363 |
| HDR Core Barrel Dynamics for Large and Small Breaks Including<br>Nonlinear Structural Impact Phenomena<br>L. Wolf, KFK GmbH, FRG . . . . .                               | 375 |



## PREFACE

This report, published in six volumes, includes 160 papers which were presented at the Tenth Water Reactor Safety Research Information Meeting. The papers are printed in the order of their presentation in each session. The titles of the papers and the names of the authors have been updated and may differ from those which appeared in the Final Agenda for this meeting.

Five papers, which were submitted for presentation at the meeting but could not be scheduled, are also included in this report. They are the following:

Calculations of Pressurized Thermal Shock Problems with the SOLA-PTS Method, B. J. Daly, B. A. Kashiwa, and M. D. Torrey, LANL, (Pages 113-130, Volume 2)

Hydrogen Migration Modeling for the EPRI/HEDL Standard Problems, J. R. Travis, LANL, (Pages 131-144, Volume 2)

Independent Code Assessment at BNL in FY 1982, P. Saha, U. S. Rohatgi, J. H. Jo, L. Neymotin, G. Slivik, and C. Yuelys-Miksis, BNL, (Pages 145-168, Volume 2)

Experimental Evidence for the Dependence of Fuel Relocation upon the Maximum Local Power Attained, D. D. Lanning, PNL, (Pages 285-296, Volume 2)

PRA Has Many Faces - Can the Safety Goal Be Well-Posed? H. Bargmann, Swiss Federal Institute for Reactor Research, (Pages 105-114, Volume 6).

INTRODUCTORY REMARKS  
TENTH WATER REACTOR SAFETY RESEARCH INFORMATION MEETING  
BY  
ROBERT B. MINOGUE, DIRECTOR  
OFFICE OF NUCLEAR REGULATORY RESEARCH  
OCTOBER 12, 1982

On behalf of the Nuclear Regulatory Commission I would like to welcome all of you to the Tenth Water Reactor Safety Research Information Meeting. The large attendance at this meeting reflects the strong international interest in resolving the remaining nuclear safety issues that require research.

We sponsor this conference each year because we believe the nuclear industry, the Department of Energy (DOE), and other countries have a major interest in understanding our research and how it may relate to safety questions of mutual interest. We are all involved in performing research to ensure that nuclear power plants and other nuclear facilities are designed and operated safely and reliably. Since our programs deal with closely related issues, our goal in sponsoring this annual meeting is to provide an opportunity for dialogue that will lead to an increased level of understanding of each others' programs and will serve as a catalyst for increasing the level of cooperation and coordination among U.S. government agencies, the American nuclear industry, and research activities from other countries. Through consolidated research program planning we can improve the efficiency of all our efforts by making more effective use of resources and eliminating unnecessary duplication of effort.

The objective of the NRC nuclear safety research program is to support our regulatory program, that is, to conduct the research needed to develop a technical basis for sound decisions on regulatory issues and improve nuclear safety. This is being accomplished through the (a) identification and definition of means to improve the consistency and coherency in the level of protection afforded by NRC regulations, (b) improvement of the understanding of phenomena necessary for analyzing safety issues, and (c) development of risk assessment methods for evaluating regulatory issues and the application of these methods to regulatory decisions and to setting priorities for research.

In my talk, I will identify some of the NRC's more prominent research programs on water reactor safety and then discuss Plant Aging and Severe Accident Research, in more detail.

Our research to increase our understanding of operating reactors includes a significant program in the area of human engineering, particularly with respect to improvements in the operator/machine interface. We are also evaluating the potential for malfunctions of plant control, protection, instrumentation, and electric systems to determine the impact on safety.

In view of the large number of operating reactors, we have a major effort of research centered on maintaining the integrity of the primary coolant pressure boundary, which is aimed at understanding life-cycle related problems, detecting them, and interpreting the results of inservice inspection. The research also includes the evaluation of mechanical and electrical equipment survivability and operability in accident situations, and studies of seismic safety margins and risks.

We are continuing to stress improvements in methodology of probabilistic risk assessment techniques and the data base to support those methods. We are placing increased emphasis on applications of probabilistic risk assessment. We foresee an increasing use of these methods in the licensing review process and in setting research priorities. Our probabilistic risk assessment efforts will be augmented by increased use of systems reliability analysis and evaluation, including human error rate data analysis.

Much of our large-break loss-of-coolant-accident (LOCA) research has been or is being completed. Program completions are reflected by the reduced LOCA tests in Semiscale and the planned termination or conversion of the NRC LOFT program to an international consortium in which we would be participants. We foresee a substantial increase in the use of these and other experimental facilities to study complex reactor system transients over a wide range of conditions.

As regards computer codes, we foresee more emphasis on the application of codes for a better understanding of the progression and consequences of complex transients and accidents in both reactor and containment systems, and much more emphasis on best estimate, or realistic modelling, rather than limiting case models for licensing review. An important aspect of our code development work will be codes used for application in risk assessments.

## Plant Aging

The first program area of research for operating reactors I would like to discuss in some detail is plant aging. This includes research on reactor vessels, steam generators, other parts of the primary coolant pressure boundary, electrical and mechanical components, piping, and nondestructive examination techniques.

As plants become older, our research in support of the safety of these plants is being directed at an increased understanding of time-related effects such as degradation of components caused by prolonged exposure to operating environments. We are also looking at the methods of examination and testing to determine the conditions of components, with emphasis on understanding the limitations of these methods, and interpreting the safety significance of their results.

Our research includes a comprehensive aging program directed at identifying which components are of most concern from a safety viewpoint as they age, and what conditions are of most concern in terms of deterioration of these safety-related components. We believe the major portion of the research associated with aging will be carried out through research on factors that affect individual components, since it is the combination of the component and its environment that we must understand.

Let me first address reactor pressure vessel research factors.

At this time, the dominant safety concern with reactor pressure vessels is long-term embrittlement of certain older vessels and pressurized thermal shock. Progressive embrittlement of pressure vessel steel by fast neutron irradiation has been recognized as a potential safety problem from the very beginning of the nuclear power program and was taken into account for pressure vessels designed, fabricated, inspected, and operated in accordance with the Boiler and Pressure Vessel Code of the American Society of Mechanical Engineers. However, as a precaution, a program of surveillance of irradiated coupons has been required by our regulations; and surveillance data and research results have shown that some of the older vessels, in particular the ones with copper-contaminated welds, are especially susceptible to neutron-irradiation embrittlement. For these vessels, the nil-ductility transition temperature has risen more rapidly than expected and is continuing to rise. Thus, these particular vessels are becoming more susceptible to overcooling transients.

A number of approaches can be used in research to help resolve this issue. First is a careful examination of potential over-cooling transients to identify steps that can be taken to reduce the likelihood of such transients (operator training, improved operating procedures, or system modifications). On a longer term basis, extension of current and past studies on mechanisms of pressure vessel failure, for example, studies of crack propagation and behavior of nonuniformly embrittled vessels, would permit a more realistic appraisal of the consequences of an over-cooling transient. Closely related to this are studies of the actual coolant temperatures affecting the vessel and of mixing phenomena, such as those being carried out by EPRI. My personal view is that the

prospects are excellent for long-term resolution of this issue by attention to reduction of the likelihood of over-cooling transients, that is, I am confident that the longer term program will show the adequacy of the short-term steps taken by our licensing people. As a cautious backup, we are looking also at ways that neutron exposure levels could be reduced and assessing the feasibility and practicability of in-place annealing.

Now let me discuss the aging problems in steam generators and our current research in this area.

There are many different forms of degradation in steam generators that have been identified to date. These include stress corrosion cracking, wastage, intergranular attack, denting, erosion-corrosion, fatigue cracking, pitting, fretting, and support plate degradation. One or more of these forms of degradation has affected at least 40 operating PWRs and has resulted in extensive steam generator inspections, tube plugging, repair, and even replacement. Recently, steam generators from a U.S. manufacturer in other countries have experienced tube wear associated with flow-induced vibration because of a new integral pre-heater design.

The primary focus of the current NRC approach to steam generator research is directed at assessing primary system integrity. This is accomplished primarily through the requirements for inservice inspection, leak rate monitoring, and tube plugging. This approach is directed at the symptoms

and not the cause of steam generator degradation, which lies primarily in secondary system design and operations. The current NRC position considers the industry as being responsible for eliminating the problem at its source; and U.S. industry, in fact, has a major research effort to determine and eliminate the causes of these problems.

NRC's steam generator research program mainly addresses improved eddy-current inspection techniques for steam generator tubing, stress corrosion cracking of steam generator tubing, and evaluation of tube integrity.

The objective of the eddy-current program is to upgrade and improve eddy-current inspection probes, techniques, and associated instrumentation for inservice inspection of steam generator tubing to improve the ability to identify and characterize tube defects.

The stress corrosion cracking program is developing data and models that will be used to predict the stress corrosion cracking initiation and service life of Inconel 600 steam generator tubing. The testing program includes variables that influence stress corrosion cracking such as temperature, stress, strain and strain rate, metallurgical structures and processing, and ingredients in the primary and secondary coolant.

Initially, under our sponsorship, and with participation by EPRI and other industry groups, a program was developed around a steam generator with service-induced degradation that was removed from the Surry Nuclear Generating Station. More recently, this has developed into an international program that will allow a broader technical base for definition of this research program and should allow for more generic applicability of the results.



The current program at the facility includes the validation of the accuracy and confidence limits of nondestructive inspection instrumentation and techniques and for burst and collapse tests on field degraded tubes to validate tube integrity models. It is also being used to develop data for validating stress corrosion cracking predictive models, for chemical cleaning and decontamination, for dose-rate reduction, and for secondary side characterization. In addition, statistically based sampling models for inservice inspection programs will be confirmed or improved by using this first confirmed data base. We also expect to make this test facility available to individual organizations on a cost-recovery basis to allow the fullest use of its unique capabilities.

Let me now discuss our research on plant aging as it is directed at electrical and mechanical components.

This program is evaluating mechanical and electrical equipment qualification with respect to its survivability and operability in accident situations and includes studies of seismic safety margins and risks. We currently have underway research on accelerated aging methodologies for different types of electrical equipment subjected to qualification tests in simulated normal service conditions and accident environments. The continuing refinement of these methodologies is expected to lead to more valid qualification test results for "aged" components. This should ensure, to an even greater degree, that no unforeseen anomalies caused by aging will occur under actual event conditions.

Our mechanical equipment qualification effort consists of several projects focused on validating or developing adequate procedures for the dynamic (including seismic) and environmental qualification of mechanical equipment and the dynamic (including seismic) qualification of electrical equipment.

A generic problem in light water reactor piping is stress-corrosion cracking. In boiling water reactors, this continues to be a troublesome problem ranging from cracks in small-diameter piping to cracks in the emergency core cooling system and the largest primary-system recirculation lines such as the recent problems at Nine Mile Point Nuclear Station. The cracks, normally located in stainless steel that was sensitized by thermal-mechanical effects in the manufacturing process, are difficult to detect until substantial leakage occurs. Our research related to piping and associated welds is aimed at developing an independent capability for prediction, detection, and control of stress-corrosion cracking.

To complement the aging program, we are conducting research to develop reliable, reproducible nondestructive examination techniques. This includes the interpretation and analysis of results of techniques that could be used for examining steam generator tubes, piping, and vessels. In addition, we are continuing our efforts to evaluate on-line detection methods such as acoustic emission. If this method can be demonstrated as practical and applicable to a full-scale plant, it would give us early detection of potential safety problems. Since it is practical to apply several of these techniques only at specific periods such as shutdown, we recognize the importance of understanding the mechanism of deterioration and particularly the rate so that proper actions can be taken to ensure that

deterioration does not progress to an unacceptable level between inspections. Conversely, if the period between inspections is not fixed, this program will aid in identifying the desired frequency of inspections.

Some of the corrective actions that are coming out of the aging and nondestructive examination research could result in maintenance requirements. Therefore, our long-term plans anticipate a greater need to look at repair welding, sleeving of steam generator tubes, plugging of tubes, testing of pumps and valves in service, and replacement of components.

#### Severe Accident Research

The second major program area of reactor safety research I would like to discuss with you today is severe accident analysis.

The conclusions drawn from safety reviews of reactors are highly dependent on accident source-term assumptions. Knowing the source term under various accident scenarios is basic to the formulation of well-founded engineering practices and sound operations and to our ability to regulate based on realistic assessments.

A major effort is being put forth in the U.S. and around the world to develop needed data and to establish the best estimate for source terms to project reactor accident scenarios.

We have a significant effort underway for improving our understanding of complex system transients and the phenomenology of accidents involving fuel damage. This information should improve our understanding of

needed plant and staff operational capabilities in the event of such transients or accidents. We expect this work to provide a more realistic quantification of fission product behavior ("source term") and the post-accident radiation levels to which in-containment equipment will be exposed, as well as a better definition of the possible accident loads on containment. This effort will also provide information for design of improved safety systems and mitigation features. The information developed in this program will improve NRC's ability to implement the proposed safety goal by providing better information for best-estimate analyses and for use in risk assessments.

If meaningful regulations addressing severe accidents are to be developed, a rational structure for decision-making is needed. The safety goals and numerical guidelines proposed in a recent NRC discussion paper (NUREG-0880, "Safety Goals for Nuclear Power Plants") offer some possible criteria against which to judge whether existing requirements need to be modified. Probabilistic risk assessment establishes the formal logical methodology to be used in evaluating severe accident safety issues in terms of the proposed safety goal. The limitations and usefulness of probabilistic risk analysis in the context of severe accident analysis must be carefully established if this methodology is to be used correctly in evaluating safety needs.

However, there are major uncertainties in severe accident analysis because the calculations are based on information that is either incomplete or largely judgmental at this time. Therefore, the identification, quantification, and reduction of important uncertainties is of substantial significance in our severe accident research program.

The largest uncertainties in severe accident analysis are thought to be associated with phenomenology. Although some of these uncertainties can be reduced by the development of better analytical methods, expansion of the data base by experiment, and a better understanding of physical phenomena and human interactions, in fact, the nature of the severe accident analysis involves a degree of uncertainty that will never be entirely eliminated.

Our research program in this area is intended to:

1. Develop methods and data to evaluate accident sequence likelihood and associated uncertainty,
2. Develop both detailed and more simplistic (fast-running) methods and data to define accident physical processes, consequences, and associated uncertainty, and
3. Develop a method and data to evaluate benefits (risk reduction) and costs associated with plant design and operational modifications.

The development of methods and data involves not only the refinement of current severe accident probabilistic risk analysis methods but also the development of more rigorous severe accident risk analysis methods and supporting experimental data to validate the simplified probabilistic methods for use. As part of our severe accident program, insights into issues will be gained by applying best-estimate codes such as RELAP, TRAC, MARCH-CORRAL, and CRAC. In addition to the MARCH code, we are developing a new risk code (MELCOR). These latter codes address the physical behavior of the degraded core.

We recently completed an assessment of MARCH that highlighted the significant difficulties in validating such models because of an inadequate phenomenological data base. Unfortunately, the new code, MELCOR, will also suffer from the same lack of sufficient verification information and will depend on information that will be generated by new research into severe fuel damage phenomena.

The NRC research program, together with efforts of EPRI, IDCOR, and international research programs, is attempting to answer the questions: (1) When does containment fail?; (2) How does it fail?; (3) What and how much gets out?; and (4) Where are the radionuclides that didn't get out? Our source-term work is focusing on the mechanisms of transport or depletion of fission products as they pass, or fail to pass, from the fuel to the atmosphere under the possible conditions present in the primary coolant system and in the containment building.

The NRC research program on the behavior and containment of fission products is concentrated at ORNL, Battelle Columbus, Sandia, and INEL. First, continuation of fission-product release experiments at ORNL will measure fission product release rates from short segments of discharged commercial PWR/BWR fuel elements. The experiments are being conducted out-of-pile in an induction furnace within a hot cell at isothermal temperatures between 1300<sup>o</sup> C and 2600<sup>o</sup> C. A second program at ORNL is examining samples of trace irradiated fission product simulators. The objectives are to determine fission product release rates, rate of fuel and structural aerosol release, physical and chemical characteristics of released species, behavior of the mixed aerosols in containment and

perhaps the primary system, and effects of hydrogen ignition on fission product and aerosol transport and physical and chemical characteristics. A third program at ORNL is reviewing the chemical behavior of major iodine species in aqueous solutions. The goals are to determine the reaction kinetics up to 150<sup>0</sup> C, measure partition coefficients and establish the existence of hypoiodous acid. The tests do not involve radioactive materials.

The last major effort at ORNL is the aerosol transport test program in steam in the Nuclear Safety Pilot Plant (NSPP). The objective of the program is to provide experimental data on the behavior of aerosols released into containment under assumed LWR accident conditions. Components of the LWR core melt aerosol to be considered are those species derived from fuel, cladding, structural materials, concrete and coolant. Effects of moisture, in-vessel sprays and fogs, auxiliary cleanup systems, and containment equipment on aerosol behavior and removal will be studied.

At Sandia National Laboratories, fission product vapor phase chemistry is being studied to identify the chemistry and interactions that may affect the transport of fission products from the fuel into the reactor containment. The chemistry and transport of fission products in typical steam and hydrogen environments will be compared with thermodynamic calculations.

A major part of our study of the related phenomenology is the Severe Fuel Damage (SFD) series in the Power Burst Facility. Phase I of the program, which is now underway, will provide integral scoping data. The tests will provide data on (a) hydrogen generation and fission product release from the reactor core at various heating rates, (b) assessing the effects of burnup and absorber materials, and (c) the characteristics of the severely damaged fuel. Higher temperatures, potentially up to the fuel melting point, will be achieved in a possible Phase II program. The major emphasis in the Phase II tests would be to measure fission product transport under prototypic conditions for severe accident sequences. The system will include measurements of the relative timing of volatile fission product and aerosol release, time-dependent measurement of aerosol release in the primary system, specific measurement of selected fission product chemical forms, discrete characterization of aerosol release and integral fission product and aerosol retention.

A program of separate-effects phenomenological experiments has also been started in the annular core research reactor (ACRR) on the mechanisms involved in the formation and relocation of fuel debris and on the characterization of the debris. These experiments will provide continuous visual diagnostic data for unprotected accident sequences. They will also provide debris characterization for reflood quenching at various times in the accident sequences. Data from these separate-effects experiments will be used to expand the Power Burst Facility data base and to develop phenomenological models of the major processes. These separate-effects experiments effectively supplement the larger-scale integral Phase I SFD tests in the Power Burst Facility and they will substantially broaden the data base for model development.



We intend to participate in the Marviken V program. In fact, our recent experience in participating with EPRI in the planning of the proposed multinational Marviken V aerosol transport test program is a good example of the value of experts from many countries cooperating as a working group to resolve tough technical issues related to test definition, data needs, and test component selection. We believe that these efforts will lead to the formulation of the best technical program possible to meet the needs of all the participants. An equally important aspect of the proposed Marviken V program is that the shared financial support of the participants allows an important program such as Marviken to go forward that otherwise would have been a prohibitive undertaking for any one country alone.

A major emphasis of this multinational program will be fission product attenuation within the primary system. Aerosols will be generated by vaporizing nonradioactive fission product simulants to represent the aerosol source expected during core-melt accidents. The primary objective is to create a large-scale data base on the behavior of vapors and aerosols within typical LWR primary systems for the verification of the transport models for risk-dominant accident scenarios. The secondary objective is to provide a large-scale demonstration of the behavior of aerosols in primary systems. These test results can then be more reliably extrapolated to full-scale application if source behavior is quantified by the PBF Phase II severe fuel damage studies of molten fuel.

We have for many years enjoyed broad-scope safety research information exchange agreements with many other countries. Several special programs of coordinated work have occurred within the scope of

these agreements, and latest among these is the recent decision for direct participation in our severe fuel damage program by the United Kingdom and Japan. Of course, we all know of the work with the 2L'3D program, and many of you may be aware of the coordination of work on probabilistic risk assessment between ourselves and the U.K. We expect that these examples of international cooperation will be multiplied in the years ahead.

We also view as particularly important the program planned by the French on the Phebus reactor, in which NRC plans to participate. The European community also plans a longer term project on Severe Fuel Damage at the Joint Research Center at Ispra in which the NRC is also a participant.

Upon completion of this work, in fact from results already achieved, we will have a much better understanding of what might happen in the course of a real accident and the identity, quantities, and behavior of radionuclides that may be released. We will also have a series of simulation models that have been calibrated with experimental results and are capable of extrapolation to accident sequences that have not been analyzed in detail.

How will these tools allow us to do a better job of regulating the nuclear industry? A number of areas stand out as immediate beneficiaries of the source term research -- such areas as equipment qualification, probabilistic risk assessment, and definition of siting and emergency planning requirements. As soon as the results of the near-term source term work are available, the technical analyses used to support the NRC

emergency planning regulations and their implementation will be reexamined to determine whether any changes should be made. The development of siting criteria will be continued with a reexamination of the sensitivity studies to gain insight into siting parameters important to safety.

Equipment qualification requirements will be reviewed with an eye towards the environment within which safety systems may have to operate in the event of an accident. The range of physical conditions in the primary coolant system and in the containment building will be much better known in terms of the parameters that a system will have to deal with to accomplish its function. The equipment qualification program will therefore have a much firmer basis for establishing performance requirements.

A particularly important area of application will be to risk models and best-estimate codes for risk assessments. The usefulness of risk assessment should be improved through a better understanding of the phenomenology of accidents involving fuel damage that will permit a more realistic treatment.

The revised source-term data base will be particularly useful to us in our current evaluations of the effectiveness and need for additional plant features to reduce the risk of severe accidents.

During the course of this conference, I am sure these and many other important reactor safety issues will be intensively discussed. I look forward to these discussions because I believe they will serve to increase our level of understanding of each others' research programs -- and therefore enhance the cooperative and coordinated efforts among our various research activities.

## SCALING RATIONALE IN REACTOR SAFETY RESEARCH

L. S. Tong

### I. Introduction

The requirement of a sound and valid scaling rationale is necessary for application of the scaled experimental results to a real industrial plant. It is particularly important in reactor safety research, because the results of simulated severe accident tests are not expected to be checked in an actual reactor and thus the wrongly scaled experimental data could mislead the reactor designer or operator to an unsafe condition. We are now applying research results to safety analysis. To avoid misleading applications, we bring up scaling rationale again. The word "scaling" here is in a very broad sense. This paper is to review the existing scaling rationale (or simulation criteria) of research in the field of thermal-hydraulics, structure, and metallurgy; and to call researchers' attention to the scaling rationale in future reactor safety research efforts.

### II. General Requirements of Integral and Separate-Effect Experiments

For a complex physical process, a single set of scaling criteria may only be valid in a restricted regime in space (or phase in time) of an integral test, but not necessarily applicable for entire process at all times. Scaling criteria can be studied separately for each region (or phase) of the physical process by simulating the principal controlling phenomena of the region (or phase) in a separate-effect test. Therefore, the controlling phenomena must be identified in the study of a specific region (or phase), and the characteristic groups of this controlling phenomena should be preserved in simulation. For example, a two-phase flow regime changes from a bubbly flow to a slug flow and

then to an annular-dispersed flow as the void fraction increases. The characteristic groups are different from each other in these flow regimes <sup>1\*</sup>. Another example is a LOCA which consists of blowdown and reflood phases. The characteristic groups in the blowdown phase are again different from that of the reflood phase.

In separate-effect experiments of a reactor accident, the input conditions should simulate the actual reactor conditions. The transient environmental (or boundary) conditions should be consistent with the accident scenarios of the reactor or the integral test. The assumption of "limiting case" of accident may lead to unwarranted conservatism, and may result in design requirements that inhibit the ability to cope with actual accidents. Any deviations of the test conditions from the best estimated reactor conditions must be noted along the data to indicate the probability of actually being at each deviated condition and the estimated possible biases in the end results for each deviation. Any sensitivity or statistical studies should be conducted around the best estimated condition in application.

Computer codes based on first principles could simplify the simulation efforts of experiments, because the scale effects and regime transitions are built-in as equations and boundary conditions in the codes as long as the computation cell size is small enough to describe the controlling phenomena. Thus the analytical models in codes for a component can be validated by separate-effect tests in the region of the interest. The uncertainty of a model can also be determined over the application range of data base.

While the size scaling effects on the component models have been validated through small- and large-size separate-effect tests, the result of interactions

---

\*The superscript is the number of the reference.

between the components of a large system may be obtained from the result of interactions in a scaled down system test. The size scaling effect of the components in an integral system test can be assumed the same as that of a separate-effect test. This extrapolation is valid only when the size scaling range of the component models covers the size scaling range of the integral system study. This is the basis of most reactor safety research experiments conducted for predicting the behavior of large size commercial reactors.

### III. Scaling Criteria for Large Break and Small Break LOCAs

A comparison of the scaling criteria for large break and small break LOCAs is shown in Table 1. In essence, for a large break LOCA the ratio of power/volume should be preserved<sup>2</sup> to maintain a correct time history of a fast transition of flow regimes and heat transfer mechanisms (e.g. CHF, rewet, etc); while the core and system height should be preserved for a small break LOCA to maintain a correct water level by the gravitational effect in a slow transient. Another important feature should be closely simulated is the by-pass flow area between the upper plenum and the downcomer (at the connection of exit nozzle of core barrier and vessel). If this bypass flow area is too large, (e.g. 6% for LOFT compared with 1-2% for commercial PWRs), the amount of steam binding in both small and large break LOCAs will be greatly reduced. Particularly in a small break LOCA, a test facility with a large bypass flow area will not be able to detect the early core uncovering which was detected in Semiscale small break test S-UT-8. In this case the core uncovering is the controlling phenomenon and the time to uncovering determines the degree of core damage.

The scaling effect of a two-phase flow in a horizontal pipe during a small break LOCA test in Semiscale and LOFT was analyzed by N. Zuber<sup>1</sup>. He found that:

- (1) the boundary of a stratified flow and an intermittent slug flow or annular-dispersed flow depends on the non-dimensional liquid depth (H/D) and the vapor Froude number ( $F_r$ ). Thus

$$F_r = j_g \sqrt{\rho_g} / \sqrt{g \Delta \rho D} = f_1 (H/D)$$

which is shown in Figure 1 where the scaling distortions of Semiscale and LOFT are evaluated on the basis of their power to volume ratio (R) and size scale (S).

$$R = \frac{j_{gm}}{j_{gp}} = \frac{1}{S} \left( \frac{D_p}{D_m} \right)^2$$

Therefore,

$$\left( j_g \sqrt{\rho_g} / \sqrt{g \Delta \rho D} \right)_m = \frac{1}{S} \left( \frac{D_p}{D_m} \right)^{5/2} \left( j_g \sqrt{\rho_g} / \sqrt{g \Delta \rho D} \right)_p$$

where  $\Delta = \frac{1}{S} (D_p/D_m)^{5/2}$  is a scale distortion, and  $\Delta = 1$  for PWR. S is a scale-down factor from the commercial PWR, and it is 1500 and 64 for Semiscale and LOFT respectively,  $\Delta$  is 1.46 for Semiscale and 0.176 for LOFT. These are the values used in Figure 1. It should be noted that the times for flow regime boundary changes are not isochronous and flashing reduces the requirement of vapor flux to change the flow regime.

- (2) The propensity of liquid entrainment or vapor pull-through at the break in a stratified horizontal flow were analyzed. The result shows that the liquid entrainment in a PWR is bracketted by the scale of Semiscale and LOFT; and a PWR has a higher propensity for vapor pull through due to the vortex flow than either LOFT or Semiscale. A vortex was observed during a small break LOCA test in Semiscale with a hole at the side of a horizontal pipe as shown in Figure 2.



The scaling effect of counter-current flow limit (CCFL) in a vertical channel was studied at Creare and BCL. In a saturated liquid and vapor flow (no condensation), the scaling correlations suggested by Kutateladze and Wallis for CCFL are:

$$\text{Kutateladze: } K_g = j_g / [g \sigma (\rho_l - \rho_g / \rho_g^2)]^{1/4} = \text{constant, const.} = 3.2 \text{ for water.}$$

$$\text{Wallis: } J_g = j_g / [g D (\rho_l - \rho_g) / \rho_g]^{1/2} = \text{constant, const.} = 0.17 \text{ for water.}$$

The data from Creare and BCL were plotted on  $K_g$  and  $J_g$  in saturated steam/water flows at various sizes of annulus in Figure 3, which indicates that  $K_g$  should be used for scaling of saturated steam/water (or air/water) flows. The condensation effect in a subcooled water would enhance the liquid going down and possibly create flow oscillations.

#### IV. Scaling Criteria of Material Properties of Heat Transfer Media

The scaling and modelling criteria in two-phase flow and boiling heat transfer in Freon for scaling steam-water mixtures were tested by F. Mayinger.<sup>3</sup> The results are formulated in the following:

$$(\rho_l / \rho_g)_{H_2O} = (\rho_l / \rho_g)_{R12} = f(p/p_c), \quad \text{Scaling for density ratio.}$$

$$(X_i)_l, H_2O = (C_i)_l (X_i)_l, R12, \quad \text{Scaling for property } i \text{ of liquid,}$$

$$(X_i)_g, H_2O = (C_i)_g (X_i)_g, R12, \quad \text{Scaling for property } i \text{ of vapor,}$$

$$(\partial X_i / \partial p)_{H_2O} = C_{ip} (\partial X_i / \partial p)_{R12}, \quad \text{for property change rate with pressure.}$$

$C_i$ 's are constants determined empirically.

Thus non-dimensional groups like Nu, Re, Pr, Fr, etc. can be calculated from the property-scaling relationships of these two fluids. Compounded phenomena like critical heat flux in a Freon flow were tested in a full scale rod bundle as reported by Stevens<sup>4</sup> and Tong et al<sup>5</sup>. The critical heat flux or onset of deficient cooling in PWR core is usually tested by a 5x5, 6x6, or 7x7 square full scale rod bundle with true lattice and real grid to simulate an open-lattice core. In a test section, the water gap between the rod bundle and the wall should be carefully designed to minimize the boundary flow bypass effect. The critical power of a closed-channel BWR core can be tested by a full size replica of a BWR fuel channel (either 7x7 or 8x8 square bundle), so that the void centering effect of a high void two-phase flow is simulated in a BWR rod bundle. Since no analytical model or scaling criteria exists for the critical heat flux or boiling transition, it must be tested in a true geometry.

#### V. Scaling Criteria of Structure Analysis

To model the containment structure in events of pressurization loading and seismic excitation, the Pi groups are developed respectively by using the Buckingham Pi Theorem<sup>6</sup>. These Pi groups are listed in Tables 2 and 3. The parameters used in the groups are listed in Table 4. It should be noted that some of the Pi groups in Table 2 are different from that in Table 3 because of the difference in controlling phenomena. The insignificant Pi groups in each phenomenon may be eliminated for convenience of designing simulation tests.

#### VI. Scaling Criteria for Temperature Effect

In most chemical reactions; the reaction rate varies with absolute temperatures according to the Arrhenius model as:

$$R = Ae^{-E/kT}$$

where

R is the reaction rate.

A is a constant for the material.

E is the activation energy (ev).

k is Boltzmann's constant.

T is the absolute temperature ( $^{\circ}$ K).

The Arrhenius model is used for scaling the temperature effect in an accelerated tests of qualifying equipment and predicting the strain to initiate stress corrosion cracking.

1. Qualification Tests -- A reactor component is required to be tested under LOCA or MSLB conditions at the end of its qualified life (40 years). Thus to scale (or simulating) the aging of the component to the end of 40 years, it is necessary to accelerate the process of aging by exposing the prototype to an elevated temperatures.

In addition to accelerating the thermal aging of materials to simulate environmental or chemical degradation, it is also necessary to accelerate the degradation process due to radiation. This is usually done by giving a lifetime integrated radiation dose (typically 50 megarad for equipment in the containment) over a short period of time ( $<1$  megarad/hour). However, recently Sandia National Laboratory has shown that some materials exhibit higher rates of degradation at low dose rates. A correction factor has to be applied.

The LOCA/MSLB simulation normally exposes the equipment to a steam temperature and pressure profile simulating as close as possible that expected in containment as a result of the design basis accident. The equipment will typically be subjected over a 60 day period to the full anticipated accident environment.

2. Stress corrosion cracking test -- A steam generator tube SCC takes a long time to be initiated at an operating temperature of 290°C. However, this process can be accelerated at high temperatures to save the time of testing. High temperature corrosion tests were conducted at BNL to determine the relationship of % strain to initiate SCC versus temperatures. The relationship for scaling of SCC of an Inconel 600 tubing with 0.01% Carbon was determined as:

$$\frac{1}{\% \text{ Strain}} = Ke^{-Q/RT}$$

and the value of K and Q are  $1.5 \times 10^4$  and 13.5kcal respectively. T is the absolute temperature (°K). Thus the strain required to initiate SCC is about 12.5% in the current steam generators at an operating temperature of 290°C as shown by extrapolation in Figure 4. The validity of this scaling criterion extrapolation lies on the fact that no discontinuity should exist along the line of extrapolation.

## VII. Conclusions

1. Scaling criteria (or non-dimensional characteristic groups of parameters) of a phenomenon can be developed from analytical models or empirical correlations with thorough physical understanding of the phenomenon.
2. In testing scaled models, the characteristic groups according to the scaling criteria of the principal controlling phenomena must be preserved.
3. The principal controlling phenomena may change outside the region (or phase) specified for the scaling criteria. Whenever the values of the physical parameters are out of the valid region (or phase), the test must be stopped to avoid misleading results.

4. A probabilistic approach should be used to evaluate the realism of the assumed test conditions of a simulated test.
5. A sound scaling rationale of a test assures the applicability of the test results. Thus the scaling criteria of a proposed test must be examined before the acceptance of the test.
6. The validity of the scaling rationale of an experiment represents the usefulness and applicability of the experiment. Therefore, the achievement of the experiment can be evaluated accordingly.

## REFERENCE

1. N. Zuber, "Problems in Modeling of Small Break LOCA," NUREG-0724, 1980.
2. L. J. Ybarrondo, P. Griffith, S. Fabric, and G. D. McPherson, "Examination of LOFT Scaling," ASME paper 74-WA/HT-53, 1974.
3. F. Mayinger, "Scaling and Modelling Laws in Two-phase Flow and Boiling Heat Transfer," International Heat Transfer Conference 1981.
4. G. F. Stevens and R. V. MacBeth, "The Use of Freon 12 to Model Forced Convection Burnout in Water: The Restriction on the Size of the Model," ASME 70-TH-20.
5. L. S. Tong, F. E. Motley, and J. O. Cermak, "Scaling Law of Flow Boiling Crises," 4th International Heat Transfer Conference, Versailles, 1970.
6. W.E. Baker, P.S. Westine and F.T. Dodge, Similarity Methods in Engineering Dynamics, Rochelle Park, New Jersey, Hayden Book Company, Inc. 1973.

Table 1. LOCA SCALING

| PHASES   | BREAK SIZES | CONTROLLING PHENOMENA   | MAJOR PARAMETER PRESERVED  |
|----------|-------------|---|--|
| BLOWDOWN | LARGE BREAK | <ol style="list-style-type: none"> <li>1. TIME TO CHF AND REWET</li> <li>2. STORED HEAT DISTRIBUTION</li> </ol>                     | POWER/VOLUME<br>BREAK AREA/VOLUME  |
|          | SMALL BREAK | <ol style="list-style-type: none"> <li>1. WATER INVENTORY AND DISTRIBUTION</li> <li>2. DECAY HEAT REMOVAL</li> </ol>                | HEIGHT OF LOOP AND<br>STEAM GENERATORS<br><br>PRIMARY COOLANT<br>LOSING RATE |
| REFLOOD  | LARGE BREAK | <ol style="list-style-type: none"> <li>1. CCFL IN DOWNCOMER AND FLOW BYPASS</li> <li>2. STEAM BINDING</li> </ol>                    | CORE HEIGHT<br>FLOW BYPASS AREA  |
|          | SMALL BREAK | <ol style="list-style-type: none"> <li>1. CORE UNCOVERY LEVEL AND STEAM BINDING</li> <li>2. CORE RECOVERY LEVEL AND TIME</li> </ol> | CORE HEIGHT<br><br>FLOW BYPASS AREA  |

Table 2 . Major Pi Terms For Pressurization Loading

$$\pi_1 = \ell_i$$

$$\pi_2 = \theta_i$$

$$\pi_3 = \rho_i$$

$$\pi_4 = N_i$$

$$\pi_5 = \sigma_i$$

$$\pi_6 = E_i$$

$$\pi_7 = \nu$$

$$\pi_8 = \frac{P_o}{\sigma}$$

$$\pi_9 = \frac{\rho_o}{\rho}$$

$$\pi_{11} = \frac{F}{\sigma L^2}$$

$$\pi_{12} = F_i$$

$$\pi_{15} = \epsilon$$

$$\pi_{16} = \frac{x}{L}$$

$$\pi_{17} = \frac{v \rho^{1/2}}{\sigma^{1/2}}$$

$$\pi_{18} = \frac{a \rho L}{\sigma}$$

$$\pi_{19} = \frac{\dot{m}}{\rho^{1/2} \sigma^{1/2} L^2}$$

$$\pi_{20} = \frac{t \sigma^{1/2}}{L \rho^{1/2}}$$

$$\pi_{21} = \frac{P}{\sigma}$$

$$\pi_{22} = \frac{P(t)}{\sigma}$$

$$\pi_{23} = \frac{T \sigma^{1/2}}{L \rho^{1/2}}$$



Table 3. Major Pi Terms For Seismic Excitation

|  |  |
|--|--|
| $\pi_1 = \ell_i$   | $\pi_{15} = \epsilon$                                    |
| $\pi_2 = \theta_i$                                       | $\pi_{16} = \frac{x}{L}$                                 |
| $\pi_3 = \rho_i$   | $\pi_{17} = \frac{v \rho^{1/2}}{\sigma^{1/2}}$           |
| $\pi_4 = N_i$  | $\pi_{18} = \frac{a \circ L}{\sigma}$                    |
| $\pi_5 = \sigma_i$                                       | $\pi_{19} = \frac{\dot{m}}{\rho^{1/2} \sigma^{1/2} L^2}$ |
| $\pi_6 = E_i$  | $\pi_{20} = \frac{t \sigma^{1/2}}{L \rho^{1/2}}$         |
| $\pi_7 = \nu$  | $\pi_{24} = \frac{A \rho L}{\sigma}$                     |
| $\pi_8 = \frac{p_o}{\sigma}$                             | $\pi_{25} = \frac{v \rho^{1/2}}{\sigma^{1/2}}$           |
| $\pi_9 = \frac{\rho_o}{\rho}$                            | $\pi_{26} = \frac{X}{L}$                                 |
| $\pi_{10} = \frac{\beta_i}{L^2 \rho^{1/2} \sigma^{1/2}}$ | $\pi_{27} = \frac{\omega L \rho^{1/2}}{\sigma^{1/2}}$    |
| $\pi_{11} = \frac{F}{\sigma L^2}$                        | $\pi_{28} = \frac{T_e \sigma^{1/2}}{L \rho^{1/2}}$       |
| $\pi_{12} = F_i$   |  |

Table 4. List of Parameters

| <u>Symbol</u> | <u>Parameter</u>   | <u>Fundamental Units of Measure</u> | <u>Reason for Using in Analysis</u> |
|---------------|--|-------------------------------------|-------------------------------------|
| L             | Characteristic Length  | L                                   | Geometry                            |
| $l_1$         | Other Lengths Relative to L                                      | -                                   |                                     |
| $\theta_1$    | Angles   | -                                   |                                     |
| $\rho$        | Mass Density of Concrete or Other Reference Material             | $FT^2/L^4$                          | Inertial Effects                    |
| $\rho_1$      | Density of Steel or Other Materials Relative to Reference $\rho$ | -                                   |                                     |
| $\sigma$      | Characteristic Strength of Structure                             | $F/L^2$                             | Strength of Structural Materials    |
| $E_1$         | Moduli Relative $\sigma$   | -                                   |                                     |
| $\sigma_1$    | Strengths Relative $\sigma$                                      | -                                   |                                     |
| $\nu$         | Poisson's Ratio  | -                                   |                                     |
| $N_1$         | Number Reinforcing Bars  | -                                   | Prestress in Concrete               |
| F             | Prestress Force in Bar   | F                                   |                                     |
| $F_1$         | Prestress Force Other Bars Relative F                            | -                                   |                                     |
| g             | Acceleration Gravity   | $L/T^2$                             | Dead Weight Effects                 |
| $K_1$         | Strain Rate Coefficient  | $FT/L^2$                            | Strain Rate                         |
| $\rho_0$      | Density of Air   | $FT^2/L^4$                          | Atmospheric Conditions              |
| $P_0$         | Atmospheric Pressure   | $F/L^2$                             |                                     |
| $S_1$         | Coefficient of Equivalent Viscous Damping                        | $FT/L$                              | Equivalent Viscous Damping          |
| c             | Strain Anywhere on Structure                                     | -                                   | Response Being Observed             |
| x             | Displacement of Any Point on Structure                           | L                                   |                                     |
| v             | Velocity of Point on Structure                                   | $L/T$                               |                                     |
| a             | Acceleration of Point on Structure                               | $L/T^2$                             |                                     |
| t             | Time   | T                                   |                                     |
| $\dot{n}$     | Leakage Rate   | $FT/L$                              |                                     |
| P             | Applied Maximum Pressure   | $F/L^2$                             |                                     |
| T             | Duration of Pressure Loading                                     | T                                   |                                     |
| p(t)          | Applied Pressure History   | $F/L^2$                             |                                     |
| A             | Acceleration Amplitudes  | $L/T^2$                             | Applied Earthquake Loading          |
| V             | Velocity Amplitudes  | $L/T$                               |                                     |
| X             | Displacement Amplitudes  | L                                   |                                     |
| $\omega$      | Frequency  | $1/T$                               |                                     |
| $T_e$         | Earthquake Time Duration   | T                                   |                                     |

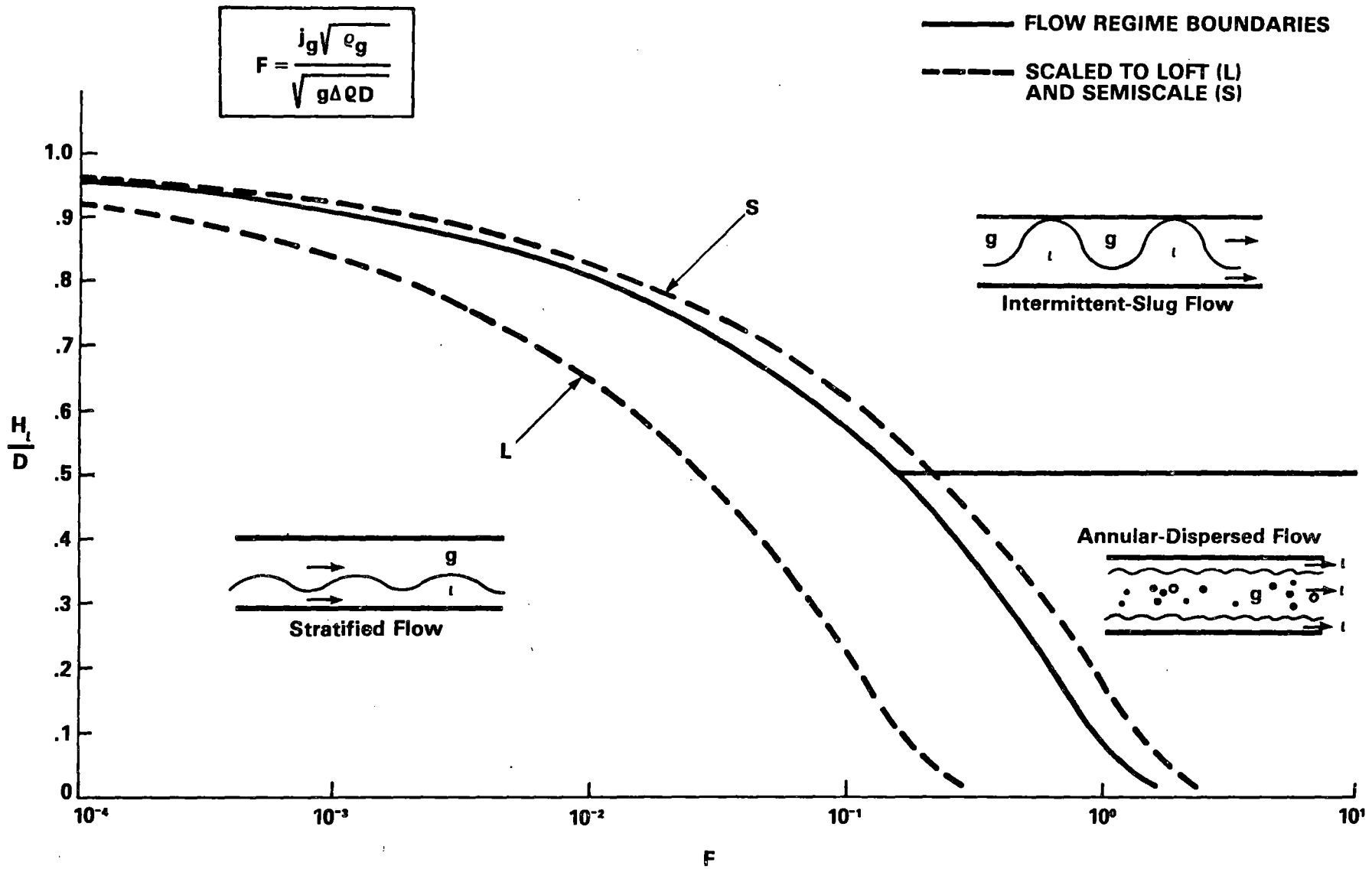


FIG. 1 DUKLER-TAITEL FLOW REGIME MAP

Fig. 2

Steam



Liquid



mixture  
Vortex



31  
2:13:43

11111111  
00000000  
10000000  
: : : : :  
MNONON  
MNONON

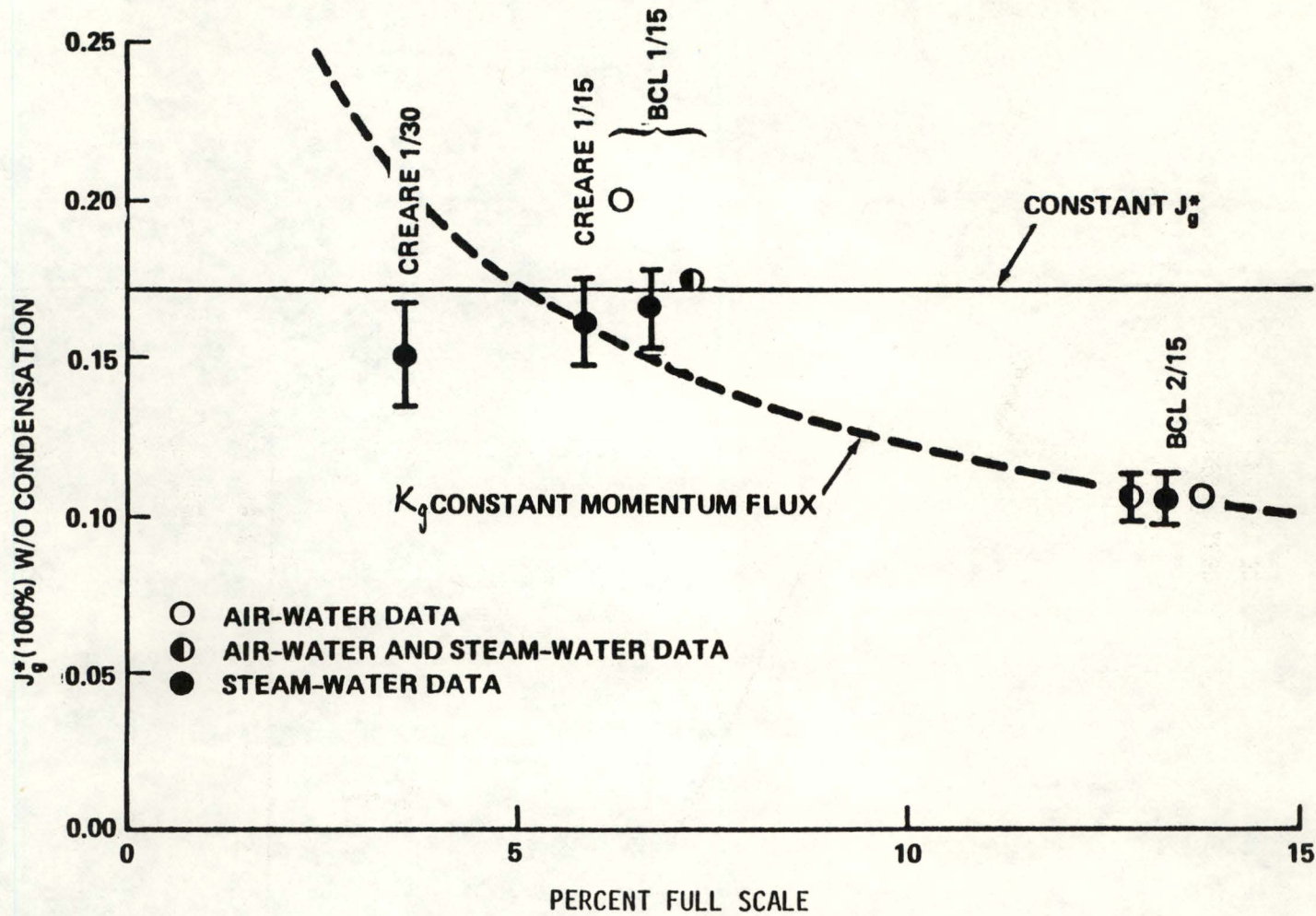


FIGURE 3 - EMPIRICALLY DETERMINED GAS FLOW FOR 100% BYPASS W/O CONDENSATION AS A FUNCTION OF SCALE SIZE.

SCC INITIATION  
CERT .01% C

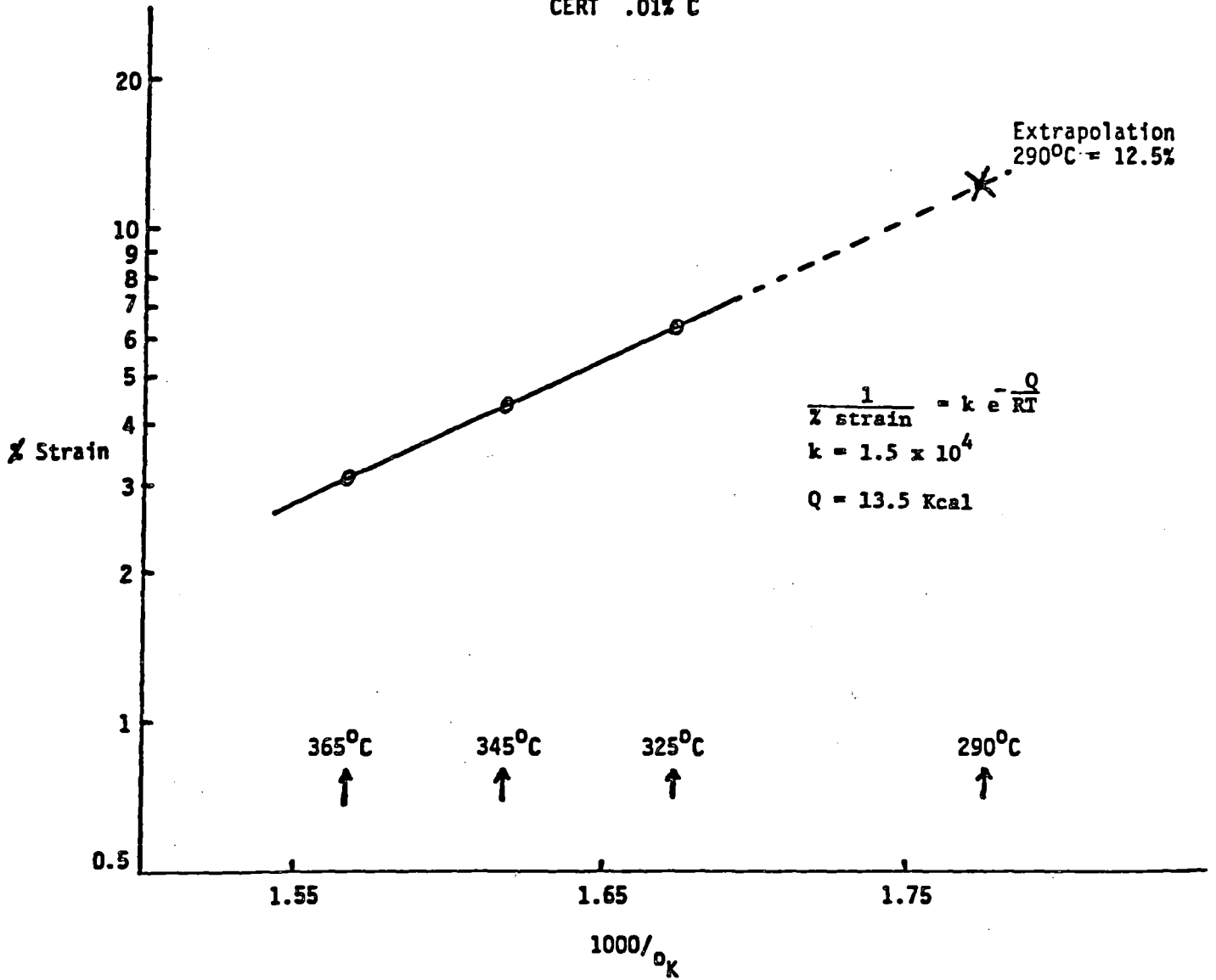


Figure 4

WATER REACTOR SAFETY RESEARCH INFORMATION MEETING    OCTOBER 12-15, 1982

Introduction to Integral Systems Experiments Session    October 12, 1982  
by Dr. G. Donald McPherson

At last year's meeting, for the first time, we grouped the reports of several integral systems experiments - both domestic and foreign - into an Integral Systems session. In view of the success of that arrangement, the organizers of the year's meeting made a special effort to group reports of as many as possible of the world's integral systems into this first technical session.

The agenda shows that by reducing the amount of time devoted to NRC's integral system facilities and by expanding the session to the end of the day, we have managed to include reports on all the major integral systems representing both PWR's and BWR's. In the former area, we have the familiar LOFT, Semiscale, LOBI and PKL, and in addition, we have a newcomer called BETHSY from France. In the BWR area, we have the Full Integral Simulation Test which was announced last year as the extension of the Two Loop Test Assembly work, ROSA III, Hitachi's Two-Bundle Loop, plus a newcomer from Japan called the 18 Degree Sector Test. Then, to end the day we will hear a report on Applications of a Computer Code to Integral Experiments. That code is RELAP-5 which was developed in close association with the LOFT and Semiscale experimental programs. I trust that you will find this an interesting, informative session.

- - - - -

By way of introduction to the first presentation, let me recall that at this time last year, the LOFT program was at a cross-roads leading to three alternative futures:

1. Early termination of its test program in 1982
2. Termination of its test program in 1983, following a series of tests requested by the NRC commissioners.
3. Continuation on from NRC's program under the leadership of the Department of Energy and in the form of an International Consortium.

In the end, course 2 was followed, while the DOE continued to pursue the International Consortium concept.

Today, LOFT is again at the cross-roads of two alternatives: With one final test remaining in the NRC program, either we will do that test in February and then shut down the facility, or we will proceed directly into the International Consortium test program, delaying NRC's final test until the end. Details of the Consortium arrangement are being worked out under the leadership of the DOE and under the aegis of the OECD's Nuclear Energy Agency. A decision on the course to be followed should be made within the month.

OVER.....

When we last met here, LOFT had just completed an intermediate break followed by a significant core uncover. During the year, INEL has performed 5 additional tests:

- two ATWS tests - one initiated by a loss-of-feed-water
  - one initiated by a loss-of-offsite-power
- one boron-dilution operational transient
- a "worst-case Appendix K" large break involving a loss-of-offsite-power
- and an operational transient mini-series involving control-rod withdrawal

I will now introduce the first speaker to discuss the results of these tests.



## RESULTS OF RECENT LOFT EXPERIMENTS<sup>a</sup>

L. P. Leach  
D. J. Hanson  
D. L. Batt.  
EG&G Idaho, Inc.

Five experiments were performed in the Loss-of-Fluid Test (LOFT) facility during the past year. In accordance with the overall objectives of the LOFT Program, all of these experiments were performed for the purposes of (a) improving reactor safety through improved understanding of accident phenomena and (b) aiding the development and verification of computer codes used for reactor safety assessment. The experiments conducted spanned a wide range of potential accident scenarios, including large and small break loss-of-coolant accidents (LOCAs), control rod withdrawal accidents, uncontrolled boron dilution, and anticipated transients without scram (ATWS). This summary describes these experiments and presents results available at the time of this writing from the experiments and experiment prediction calculations. In addition, a brief overview is given for the remaining experiment planned in the LOFT Program.

The LOFT facility<sup>1</sup> is a 50-MW(t) pressurized water reactor (PWR) designed to perform integral system experiments. The system includes all of the primary, auxiliary, and emergency systems of commercial PWRs except that an air-cooled condenser is used in place of a turbine generator. The system is extensively instrumented with both the normal process instruments used in commercial PWRs and special instrumentation to monitor parameters of interest during the experiments. The LOFT core contains 1300 5.5-ft-long fuel rods.

---

a. Work supported by the U.S. Nuclear Regulatory Commission, Office of Nuclear Regulatory Research under DOE Contract No. DE-AC07-76ID01570.

### ATWS Experiment L9-3

Experiment L9-3<sup>2</sup> represented an ATWS leading to the maximum primary coolant system pressure in a PWR. A special relief valve system was added to the LOFT primary coolant system. The special system was scaled to yield pressures in the range of Service Level C pressure limitations for PWRs of the same "vintage" as LOFT, that is, late 1960s to early 1970s. The normal reactor scram circuitry was inhibited, and the simulated accident was initiated by a complete loss of feedwater to the steam generator. Accident recovery procedures patterned after those designed for commercial PWRs were used to return the LOFT plant to normal operating conditions. An experiment prediction was performed with the RELAP5 computer code.

Results of the experiment conformed to expectations in many respects; however, the peak pressure reached was significantly less than predicted. This was because the scaled safety valve flow was higher than expected. It should be noted that the peak pressure reached in this LOFT experiment is not indicative of the peak pressure that would be reached in a worst case ATWS in a commercial PWR, as the LOFT core neutronics are indicative of conditions 2/3 through core life in a commercial PWR core. Core neutronics early in core life would lead to higher pressures, as the moderator temperature coefficient would be more positive.

The experiment predictions did not show a good quantitative match with the experiment data due to overstatement of the safety valve flow and the calculation of pressurizer response. A postexperiment calculation performed with only these factors corrected showed good agreement with the experiment data.

### Boron Dilution Experiment L6-6

Experiment L6-6<sup>3</sup> was conducted to evaluate the methods for calculating uncontrolled boron dilution accidents in a PWR from a cold refueling condition. Unborated water was injected into the LOFT system starting at a cold condition and continuing until the reactor reached

criticality, with two different recirculation rates in the system simulating shutdown cooling. A simple mixing model was used to calculate the time to criticality.

Results of this experiment confirmed the use of complete mixing models for volumes included in the main recirculation path, regardless of the recirculation flow rate. Significant mixing was also observed in volumes outside the main recirculation path. Based on using these models, it appears as though sufficient time is available between count rate alarms and criticality to take corrective action.

#### Large Break LOCA Experiment L2-5

Experiment L2-5<sup>4</sup> represented a double-ended offset shear of the reactor inlet pipe. The reactor coolant pumps were shut off very early in this experiment in an attempt to prevent the early core rewet observed in prior large break Experiment L2-3, and thereby confirm that the early rewet was due to the action of the primary coolant pumps. Experiment prediction calculations for Experiment L2-5 were performed with the RELAP5 computer code.

Experiment L2-5 results compared very well with expectations and the predictions with the RELAP5 computer code. This experiment thereby confirms the overall ability to accurately predict the behavior of large break LOCAs.

#### Transient Experiment L6-8

Experiment L6-8 consisted of six separate transients: two uncontrolled rod withdrawals, three small break LOCA simulations, and a natural circulation cooldown event. Experiment prediction calculations for all of these transients were performed with the RELAP5 computer code.

Data from Experiment L6-8 were not evaluated at the time of this writing, but results and conclusions will be presented in the meeting.

### ATWS Experiment L9-4

Experiment L9-4 will simulate a loss of all feedwater ATWS coincident with loss of offsite power. Although this ATWS is not expected to result in peak pressures as high as those observed in ATWS Experiment L9-3, it will be somewhat more challenging to the computer code because of the need to predict natural circulation phenomenon. The recovery procedure for Experiment L9-4 is intended to investigate recovery in PWRs with low-head high-pressure injection pumps and no, or a failed, power-operated relief valves. The RELAP5 computer code was also used for these experiment prediction calculations.

Experiment L9-4 was not completed at the time of this writing, but results will be available and presented in the meeting.

### Fuel Ballooning Experiment L2-6

Experiment L2-6, the last experiment planned for the LOFT Program, is intended to address Code of Federal Regulations (10 CFR 50) Appendix K licensing concerns relative to the ballooning of pressurized fuel rods in a PWR during a large break LOCA. This experiment will be similar to the previously conducted large break LOCA experiments, except that emergency core coolant will be inhibited until ballooning and rupture of the pressurized fuel rods in the center fuel bundle occur. These fuel rods will be prepressurized to have a pressure indicative of that which would occur in end-of-life fuel. This will be the largest ballooning and blockage test performed in a reactor, and will aid in the development and verification of fuel behavior models. In addition, data will be obtained on fission product release and transport.

Experiment L2-6 is planned to be conducted near the end of February 1983.

## References

1. D. L. Reeder, LOFT System and Test Description (5.5-Ft Nuclear Core 1 LOCEs), NUREG/CR-0247, TREE-1208, July 1978.
2. P. D. Bayless and J. M. Divine, Experiment Data Report for LOFT Anticipated Transient Without Scram Experiment L9-3, NUREG/CR-2717, EGG-2195, May 1982.
3. B. D. Stitt and J. M. Divine, Experiment Data Report for LOFT Boron Dilution Experiment L6-6, NUREG/CR-2733, EGG-2197, June 1982.
4. P. D. Bayless and J. M. Divine, Experiment Data Report for LOFT Large Break Loss-of-Coolant Experiment L2-5, NUREG/CR-2826, EGG-2210, August 1982.

# Results of Recent LOFT Experiments

L.P. Leach  
D.J. Hanson  
D.L. Batt



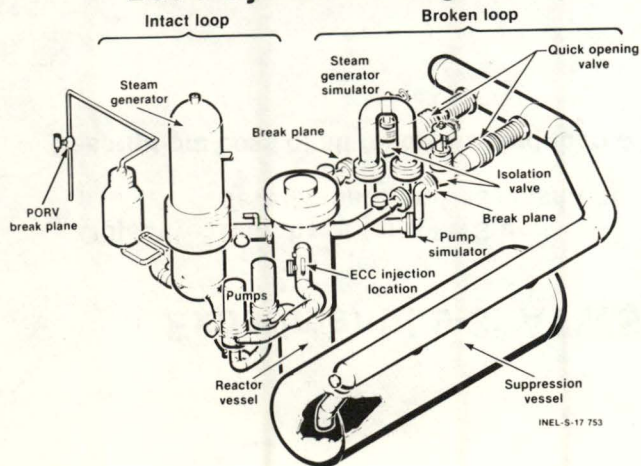
# Introduction

- LOFT Overview
- Results of recent experiments
- Plans for final experiment

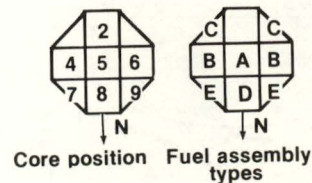
S2 10 261

4.5

## LOFT System Configuration

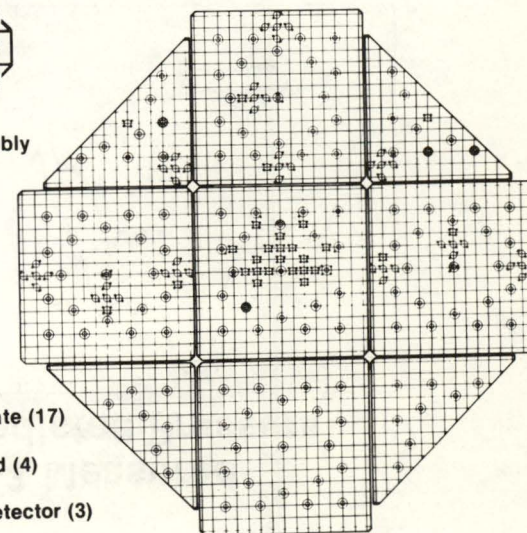


## LOFT First Core Instrumentation Location



### Legend

- Guide tube
- Fuel rod
- Neutron source
- Thermocouple (196)
- Thermocouple lower tie plate (17)
- ⊕ Dummy thermocouple
- × Neutron flux detector, fixed (4)
- Neutron flux scan (4)
- Conductivity liquid level detector (3)



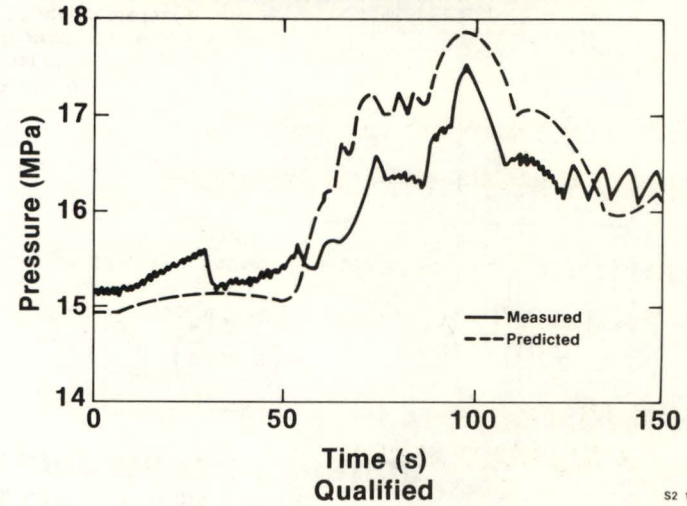
## Experiment L9-3: ATWS

Objective: Data base for ATWS code development and assessment

Description: Loss of all feedwater induced ATWS

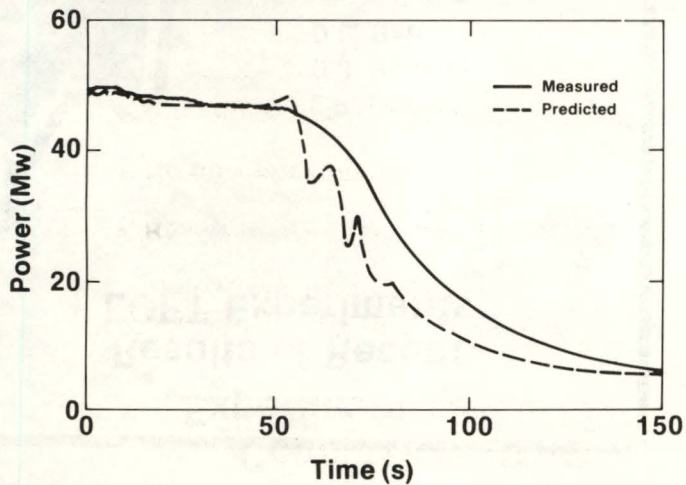
S2 10 260

### L9-3 Measured and Predicted Pressure



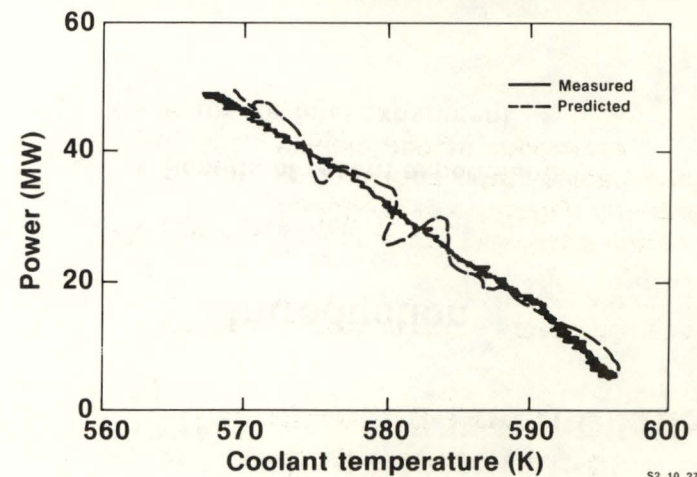
S2 10 265

### L9-3 Measured and Predicted Power



S2 10 266

### L9-3 Measured and Predicted Power Versus Fluid Temperature



S2 10 273

## Conclusions from Experiment L9-3 ATWS

- Pressurizer response and relief valve flow models need improvement
- Reactivity feedback well predicted
- No new phenomena
- Smooth recovery without control rod insertion

S2 10 259

## Experiment L6-6: Uncontrolled Boron Dilution

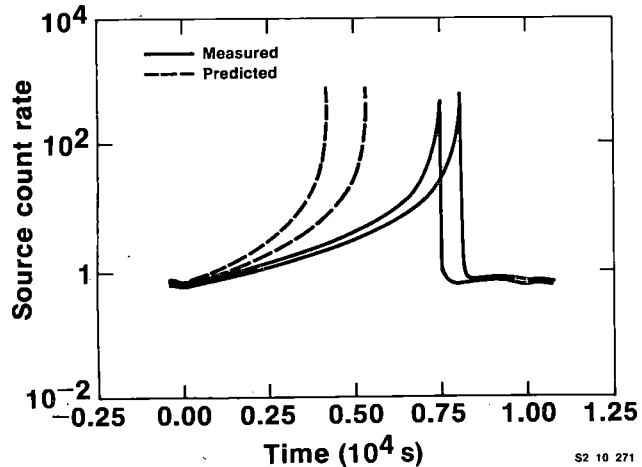
**Objective:** Assess mixing model calculations of time to alarm and criticality

**Description:** Two cold demineralized water injections to criticality; different recirculation rates; primary coolant system pumps unpowered

S2 10 255

47

## L6-6 Predicted and Measured Source Count Rate



S2 10 271

## Conclusions from Experiment L6-6 Boron Dilution

- Simple mixing model is conservative
- Some mixing of volumes occurs outside flow path
- Effect of recirculation rate is small
- Adequate time exists from alarm to criticality

S2 10 256



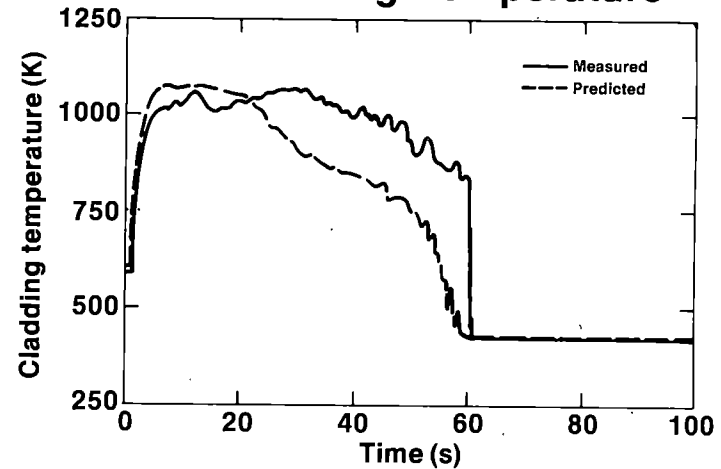
## Experiment L2-5: Large Break LOCA

**Objective:** Large break LOCA with thermal-hydraulic conditions calculated to inhibit rewet and confirm theory of causes of rewet in earlier experiments

**Description:** Double-ended cold leg break LOCA from 12 kW/ft initial Maximum Linear Heat Generation Rate (MLHGR); rapid primary coolant pump coastdown

S2 10 257

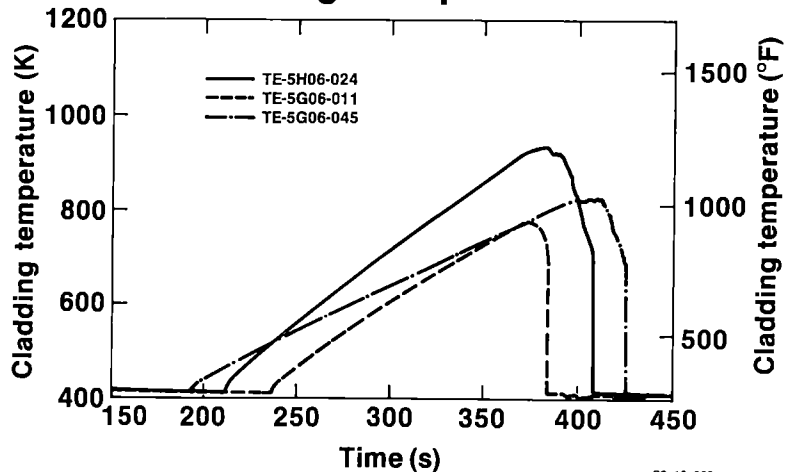
## L2-5 Predicted and Measured Peak Cladding Temperature



S2 10 262

48

## L2-5 Measured Fuel Rod Cladding Temperatures



S2 10 268

## Conclusions from LOCA Experiment L2-5

- No bottom up early rewet - confirms theory
- Good comparison of predictions with results
- ECC performance good at higher fuel temperatures
- No failure of pressurized fuel

S2 10 258

# Experiment L6-8: Transient Experiments

## Objective:

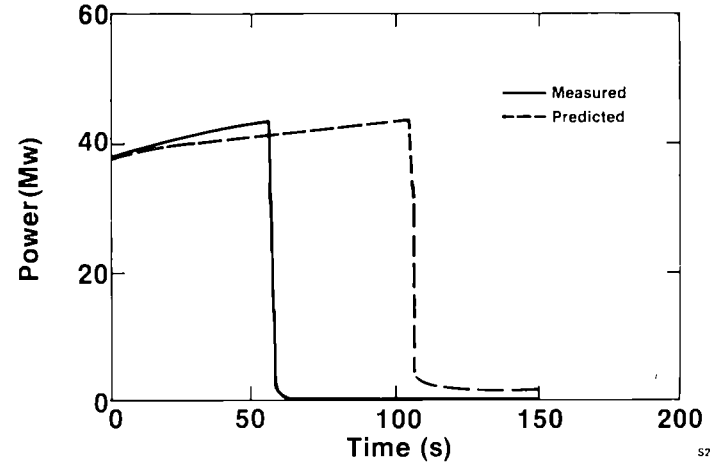
- Provide data base for uncontrolled rod withdrawal calculations
- Provide recovery procedures for small break LOCAs of size of steam generator tube

## Description:

- Two uncontrolled rod withdrawals
- Three small break LOCAs with different recovery strategies
- Natural circulation cooldown

S2 10 253

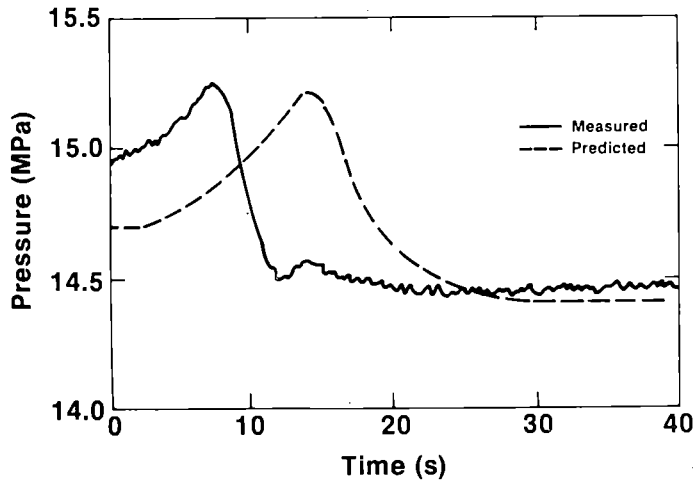
## L6-8B1 Predicted and Measured Power



S2 10 263

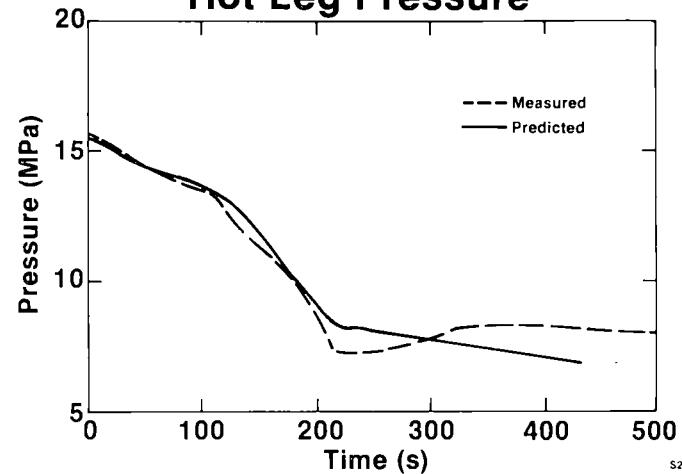
49

## L6-8B2 Predicted and Measured Pressure



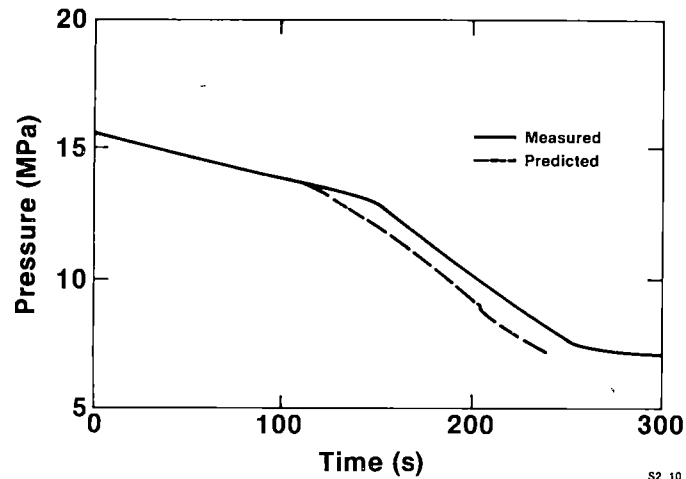
S2 10 267

## L6-8C1 Predicted and Measured Hot Leg Pressure



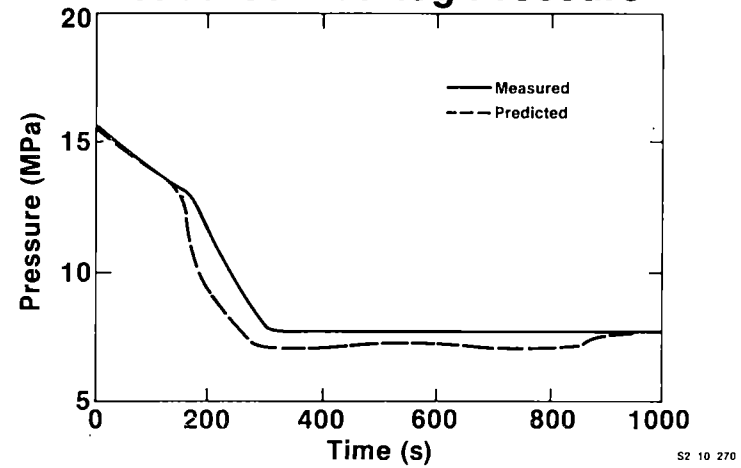
S2 10 264

**L6-8C2 Predicted and Measured Hot Leg Pressure**



S2 10 269

**L6-8C3 Predicted and Measured Hot Leg Pressure**



S2 10 270

50

**Small Break Transient Pump Power  
and Pressure Temperature Plot  
(will be presented)**

**Conclusions from Experiment L6-8  
(will be presented)**

## **Experiment L9-4: ATWS**

**Objective:** Extend data base for ATWS code development and verification with experiment more challenging to code (but less severe to system)

**Description:** Loss of offsite power ATWS with no PORV and low pressure HPIS

S2 10 251

**L9-4 ATWS Measured and Predicted Pressure  
(will be presented)**

## **Experiment L2-6: Large Break LOCA with Moderate Fuel Damage**

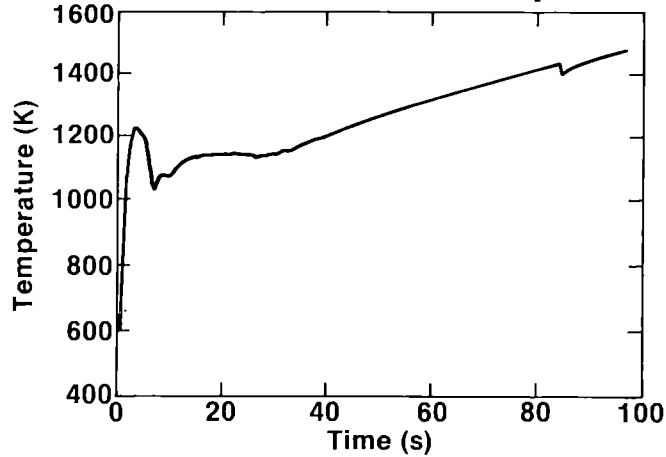
**Objective:** Large break fuel ballooning and rupture experiment for model development and verification

**Description:** Large break LOCA from end-of-life fuel conditions (high internal pressure/low MLHGR) with ECC inhibited until fuel rod rupture

S2 10 252

**Experiment L9-4 ATWS Preliminary Results  
(will be presented)**

## L2-6 Predicted Peak Cladding Temperature (16 kW/ft, no ECC, PCPs operating)



S2 3543

## Predicted Decay of Isotope Groups Released for L2-6 (12 kW/ft) (Curies)

| Isotope group   | Time after cladding rupture |                    |            |
|-----------------|-----------------------------|--------------------|------------|
|                 | 2.5 min                     | 30 days            | 120 days   |
| Noble gases     | $7.28 \times 10^5$          | $2.03 \times 10^3$ | 6          |
| Halogens        | $7.85 \times 10^5$          | $2.47 \times 10^3$ | Negligible |
| Volatile solids | $6.70 \times 10^4$          | 93                 | 17         |
| Other solids    | $3.43 \times 10^5$          | $4.18 \times 10^3$ | 958        |
| <b>Total</b>    | $1.92 \times 10^6$          | $8.77 \times 10^3$ | 981        |

S2 10 254

## Conclusions

- Substantial extension of data base for reactor safety evaluations
- Application of analytical models requires careful consideration of key variables for each transient type
- LOFT experiments confirm efficacy of plant protection systems and recovery methods

S2 10 274

## SEMISCALE PROGRAM FY 82-83 HIGHLIGHTS<sup>a</sup>

D. J. Shimeck  
EG&G Idaho, Inc.

Experiments and analyses conducted by the Semiscale Program in the past year have encompassed a number of water reactor safety issues. Efforts continued on completing the analysis of extensive natural circulation cooling experiments performed in FY-81. Effort was also extended toward analyzing data from numerous small-break loss-of-coolant experiments performed since the TMI-2 accident. Recent results from this effort have highlighted the value of experimental results in validating computer code capabilities. In terms of new experimental work, three test series were performed: an intermediate break series, secondary side feedwater and steam line breaks, and primary coolant system feed and bleed experiments. Each is briefly reviewed below.

The Semiscale Program and test facility are located at the Idaho National Engineering Laboratory and operated by EG&G Idaho for the U.S. Department of Energy. The system is a small-scale model of the primary coolant system of a pressurized water reactor (PWR) nuclear generating plant. It incorporates the major components of a PWR and is capable of attaining typical operating pressures and temperatures. As configured for testing performed in FY-82, the system was designated Mod-2A.

Experiments in the Intermediate Break series consisted of cold leg primary coolant pipe breaks of 22, 50, and 100% of the scaled pipe flow area. The primary objective of the series was to provide data between the extensive large-break (200% pipe area) and small-break (<10% pipe area) data bases that have been compiled in Semiscale. Analysis of the results identified no unanticipated thermal-hydraulic phenomena, and indicated a

---

a. Work supported by the U.S. Nuclear Regulatory Commission, Office of Nuclear Regulatory Research under DOE Contract No. DE-AC07-76ID01570.

gradual shift with decreasing break size from the large-break-type, early departure-from-nucleate-boiling-dominated transient to the loop-seal-governed core level depression and boiloff characteristic of small breaks.

Secondary side feedwater line break experiments involved three different break sizes in the small-break end of the spectrum (5 to 27% maximum break area). System behavior was characterized by rapid primary pressurization following loss of heat sink in the affected generator. The conservatisms incorporated in the experimental procedures were typical of those used in licensing calculations. The primary objective was to characterize primary-to-secondary heat transfer behavior during a secondary side blowdown as a function of inventory. Results showed the heat transfer rate degraded rapidly over a very narrow range of secondary inventory ( $\sim 10\%$ ). Furthermore, the inventory at which degradation occurred was found to be break-size dependent, increasing with break size, and occurred with substantial quantities of water remaining in the secondary. These results are presently being incorporated into code verification studies, and ultimately may influence licensing assumptions used in secondary side break analyses.

During the analysis of small-break loss-of-coolant experiments, an interest was taken in explaining large differences in the core uncover behavior of two 5% cold leg break experiments performed in the Mod-2A system, which were essentially identical except for vessel upper head hydraulic resistance. Resistance of the flow path through the upper head was increased such that the core bypass at operating conditions dropped from about 4% down to 2%. Classically, the core level depression caused by the formation of liquid "seals" in the pump suction U-traps is thought to be limited to the elevation of the bottom of the suction, about midcore. However, with the lower bypass, a total depression of the level below the core occurred and, consequently, the remainder of the transient was more severe. Data analysis identified the key phenomena contributing to the behavior as steam generator tube flooding that, coupled with the pump suction head, was capable of depressing the vessel level to the bottom of the core. Code predictions for various facilities that indicated similar

behavior were previously met with skepticism. Subsequent refinement of the calculations, however, duplicated the observed Semiscale behavior. This information has been disseminated, and illustrates the value of interaction between experimental and code program efforts.

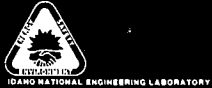
The Semiscale Program coordinated an extensive analysis of primary coolant system feed and bleed cooling that included experimentation and code calculations. Information from the study has delineated the parameters that establish the ultimate capabilities of feed and bleed. Data analysis has further identified transient thermal-hydraulic phenomena that impact feed and bleed behavior. The RELAP5 code was verified against Semiscale data and used to extrapolate to large plant behavior, and different scenarios. The final results have predicted viable feed and bleed capability over a wide range of conditions, but have also shed light on the potential limits to feed and bleed as a cooling mechanism.

Modifications are being made to the Semiscale facility prior to the start of FY-83 testing. A new, more accurately scaled, pressurizer is being installed. Additional capabilities for simulating plant controls and more accurately measuring relief flows are being incorporated. The system will be redesignated Mod-2B. Two major experiment series will be conducted in FY-83. The first will include investigation of multiple system failure accidents, which have as a common event the loss of offsite power, and subsequent evaluation of recovery procedures. The second will be a steam generator tube rupture series.



## Semiscale Program FY 82-83 Highlights

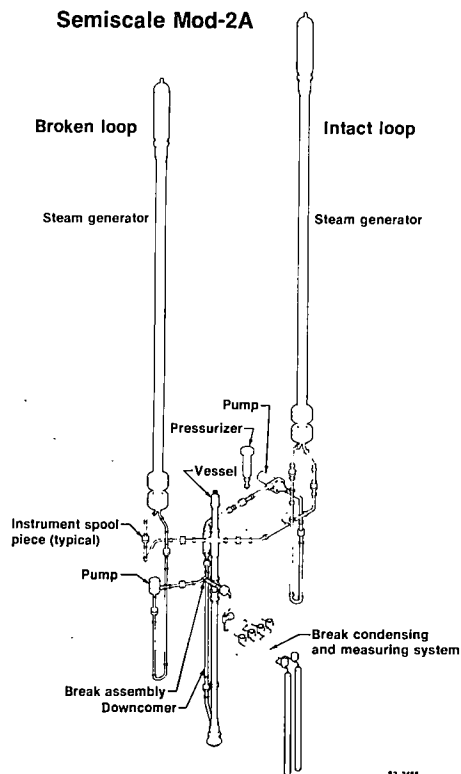
D.J. Shimeck



## Semiscale Mod-2A FY-82 Program

- Natural Circulation Analysis
- Intermediate break series
- Feedwater and steam line breaks
- Primary feed and bleed experiments
- Continued small-break analysis

S2 10 168



S2 1466

## Semiscale Feedline Break Experiments

### Objective:

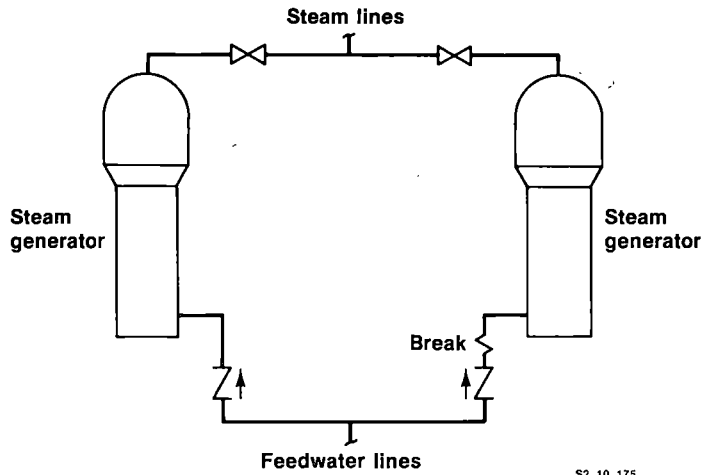
- Evaluate primary-to-secondary heat transfer behavior during feedwater line break

### Scenario:

- Feedline break initiated from full power
- Scram on high primary pressure
- Communication between generators

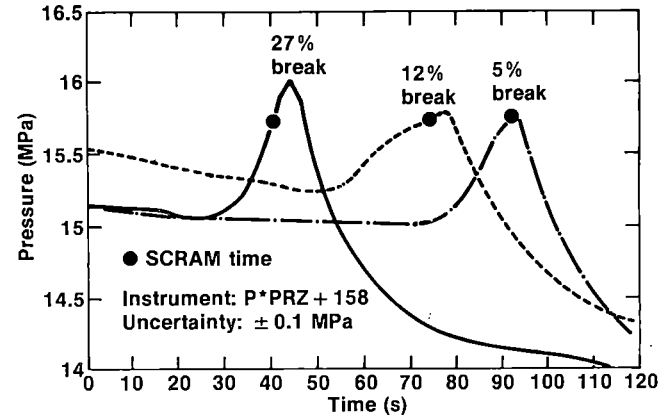
S2 10 172

### Feedline Break Scenario



S2 10 175

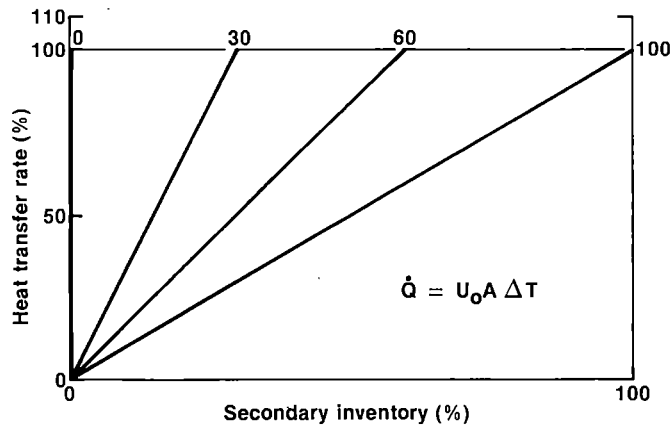
### Primary Pressure Response for Feedline Breaks



S2 10 174

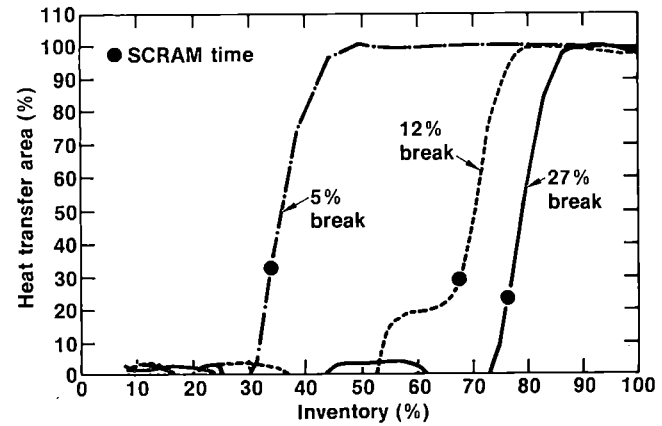
57

### Feedline Break Heat Transfer Assumptions



S2 10 178

### Heat Transfer Versus Secondary Inventory



S2 10 173

## Feedline Break Experimental Results

- Sharp degradation in primary-to-secondary heat transfer noted over narrow secondary inventory range
- Degradation influenced primarily by change in secondary hydraulics
- Secondary inventory at onset of degradation is break-size dependent
- Rapid primary pressurization followed loss of secondary sink

S2 10 171

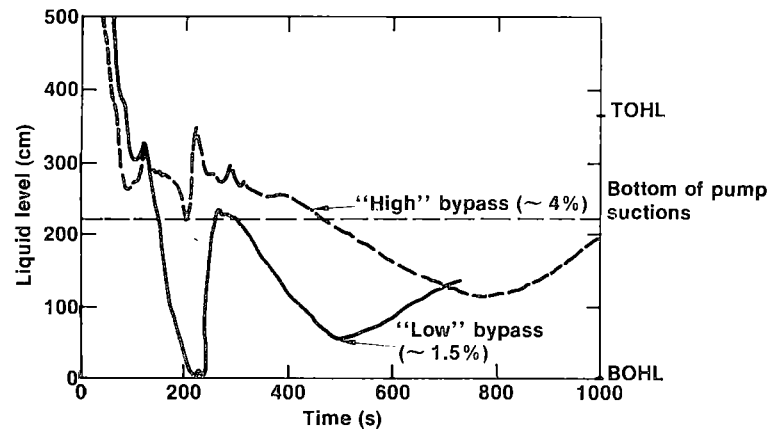
## Unanticipated Core Uncovery Evaluation

- 5% cold leg break experiment (repeat)
- Reduced vessel upper head bypass
- Significant change in transient behavior and core voiding
- Reassessment of code predictive capabilities

S2 10 170

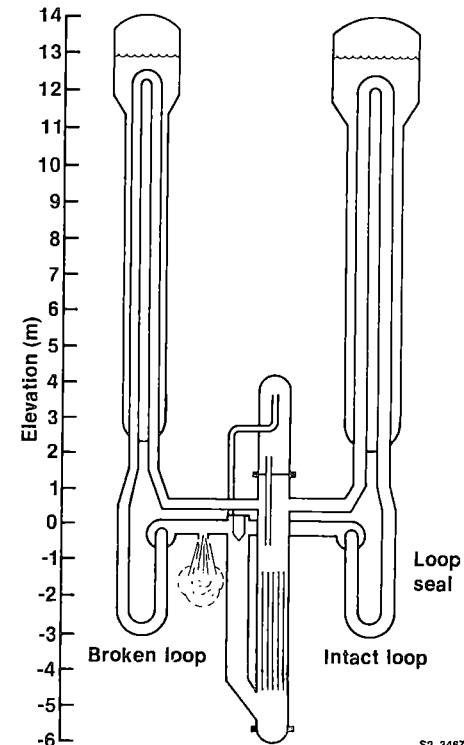
53

### Influence of Bypass on Core Level 5% Cold Leg Break



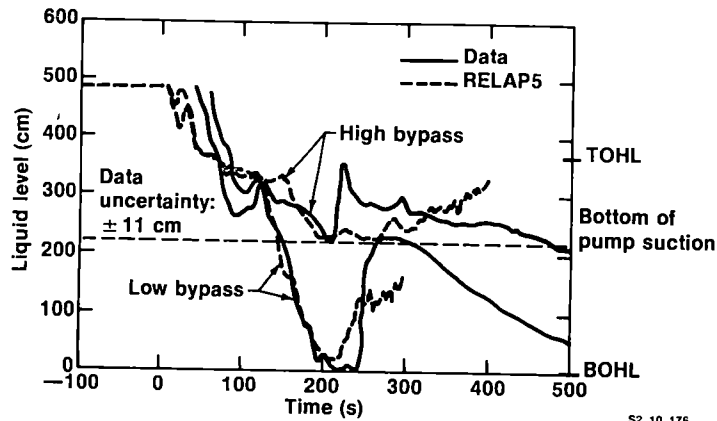
S2 10 177

### Mass Distribution Prior to Loop Blowout Seal



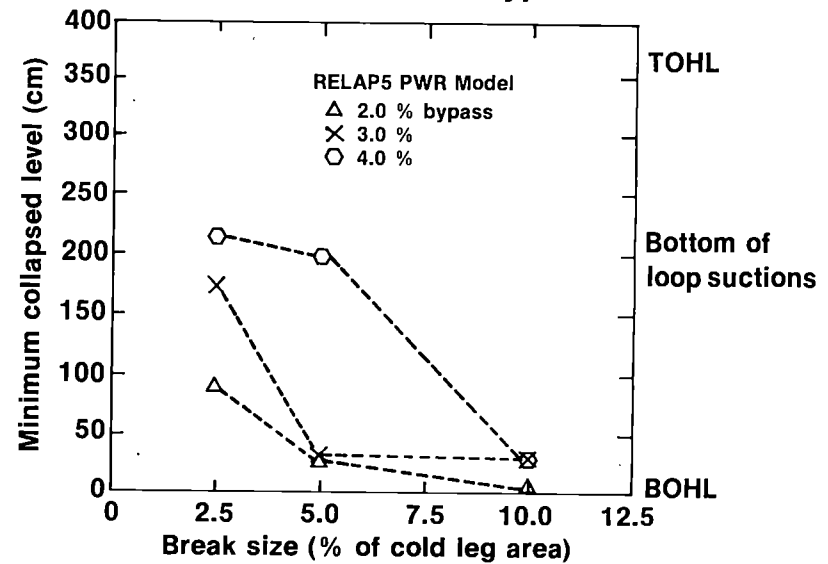
S2 3467

## RELAP5 Prediction of Bypass Influence



S2 10 176

## Core Level Depression Sensitivity to Break Size and Bypass



S2 3591

59

## Core Level Depression Phenomena

- Steam generator tube flooding is driving phenomenon
- PWR sensitivity to upper head bypass predicted with RELAP5
- Accurate condensation/holdup calculations important to SBLOCA predictions

S2 3592

## Semiscale Mod-2B FY-83 Program

| Experiment Series            | Analyses  |
|------------------------------|---|
| Loss-of-offsite power        | <ul style="list-style-type: none"> <li>• Aggravating ESF failures</li> <li>• Recovery procedures</li> <li>• Benchmark against full-scale data</li> </ul>  |
| Steam generator tube rupture | <ul style="list-style-type: none"> <li>• Accident signatures for single and multiple generator ruptures</li> <li>• Tube ruptures as compounding failure</li> <li>• Alternative recovery procedures</li> <li>• Assess computer models</li> </ul> |

S2 10 167

**EXPERIMENT DESIGN AND SCALING ANALYSIS  
FOR THE BWR FIST**

**J. E. Thompson  
J. A. Findlay  
W. A. Sutherland**

**General Electric Company  
Nuclear Fuels Engineering Department  
San Jose, California**

**BWR FIST SPONSORS:**

**U.S. NUCLEAR REGULATORY COMMISSION  
ELECTRIC POWER RESEARCH INSTITUTE  
GENERAL ELECTRIC COMPANY**

## BWR FIST PROGRAM

The Full Integral Simulation Test (FIST) program is an extension of BWR safety technology into the areas of small break LOCAs and operational transients. To tie back with the existing data base, DBA LOCAs will also be performed. The FIST facility is an integral system capable of full power steady state operation and real time simulation of transients, including power excursions and/or degraded systems. It is a full height simulation of the reactor vessel and internals with scaled regional volumes, and includes all major interfacing systems and automatic trip signals. Combined with a full size electrically heated bundle, this provides full scale values for fluid conditions, velocities, and static heads. The program provides data for evaluation of the governing phenomena, for development and qualification of thermal hydraulic methods, and for evaluation of reactor system operating information.

## FIST SCALING APPROACH

Factors considered in the design of the FIST facility include BWR design features important to scaling, the system parameters and phenomena which must be accurately simulated, and experience gained from design of previous scaled facilities.

As illustrated in Figure 1, the BWR system consists of a pressure vessel with internal recirculation flow. Two external loops draw flow from the downcomer region and drive the internal jet pumps.

The compactness of this system, being within a single vessel and with a minimum of external piping, simplifies the scaling. The large volume to surface area ratio characteristic of a compact system also reduces the impact of increases in heat loss that may be encountered with scaled systems. Since each fuel bundle in a BWR is individually channeled, the resultant lack of cross flow in the core region means that thermal hydraulic conditions within the core can be accurately simulated by a single bundle with typical boundary conditions imposed at the inlet and outlet plenums.

Key phenomena considered in the design of the FIST facility are shown in Figure 2, along with the parameters which will be independently controlled in the tests. The relation between these two groups of parameters governs the scaling basis chosen for the facility. For example, the need to simultaneously produce accurate pressure, level, and inventory responses in FIST, coupled with the choice of power as a controlled parameter, results in the choice of a full height volume scaled vessel capable of operating at full pressure.

#### FIST SIMULATION OF THE BWR

The FIST simulation of the BWR vessel and internals is shown in Figure 3. The full height vessel contains typical internals and a single full length full power electrically heated bundle. Combined with volume scaling of all internal regions, this provides full scale values for fluid conditions, velocities, and

static heads. The fact that the bundle is full size insures that bundle flow, void distribution, and heat transfer is correctly simulated. Two independent external loops and internal jet pumps are included to provide recirculation flow typical of the BWR.

Figure 4 summarizes the FIST simulation of BWR trip signals. Major system functions that are actuated automatically, such as emergency core cooling system (ECCS) activation and main steam isolation valve (MSIV) closure, are also handled in FIST by automatic action. By triggering these events based on actual system response, instead of on timers set to reflect anticipated response, a more representative system simulation is achieved. Typical reactor level instrumentation is used in the FIST facility, which serves both as input to the trip system and to obtain data for evaluation of the system information that is supplied to the operator.

The major interfacing systems on the BWR are simulated in the FIST facility, as shown in Figure 5, so as to provide correct boundary conditions to the system. The main steam line is simulated up to the MSIV, including five safety/relief valves for the five SRV groups in the BWR and the automatic depressurization system (ADS) function of one of the groups. The heated feedwater system assures a correct inlet temperature for steady state operation. All ECC Systems, and the reactor core isolation cooling (RCIC) system, are also simulated.



## FIST DESIGN EVALUATION

Evaluation of the FIST facility design is ongoing. Separate effects studies have been performed as a part of the facility design activity to evaluate the characteristics of specific components, such as jet pump performance. To evaluate the system performance of the FIST facility, a comparative analysis of the BWR and FIST designs have been performed using the best estimate thermal-hydraulic code TRAC. The calculations are complete, and the analysis and evaluation of the results is in progress. Data collected during shakedown testing, which is now starting, will also be used to evaluate facility performance. Tests to characterize specific performance areas, such as system heat loss, are also being performed during this phase.

## PROGRAM SUMMARY

The FIST program provides a comprehensive integral system simulation capability for investigation of both LOCAs and operational transients. The program will yield data for evaluation of governing phenomena, for development and qualification of thermal hydraulic methods, and for evaluation of reactor system operating information.

PREVIOUS REPORTS IN BWR FIST SERIES

BWR Full Integral Simulation Test (FIST) Program Test Plan,  
J. E. Thompson, General Electric Company, NUREG/CR-2575,  
April 1982.

## BWR FEATURES IMPORTANT IN SCALING

- SINGLE VESSEL
- CHANNELED BUNDLES
- INTERNAL FLOWS
- DISTINCT REGIONS
- TWO DRIVE PUMP LOOPS

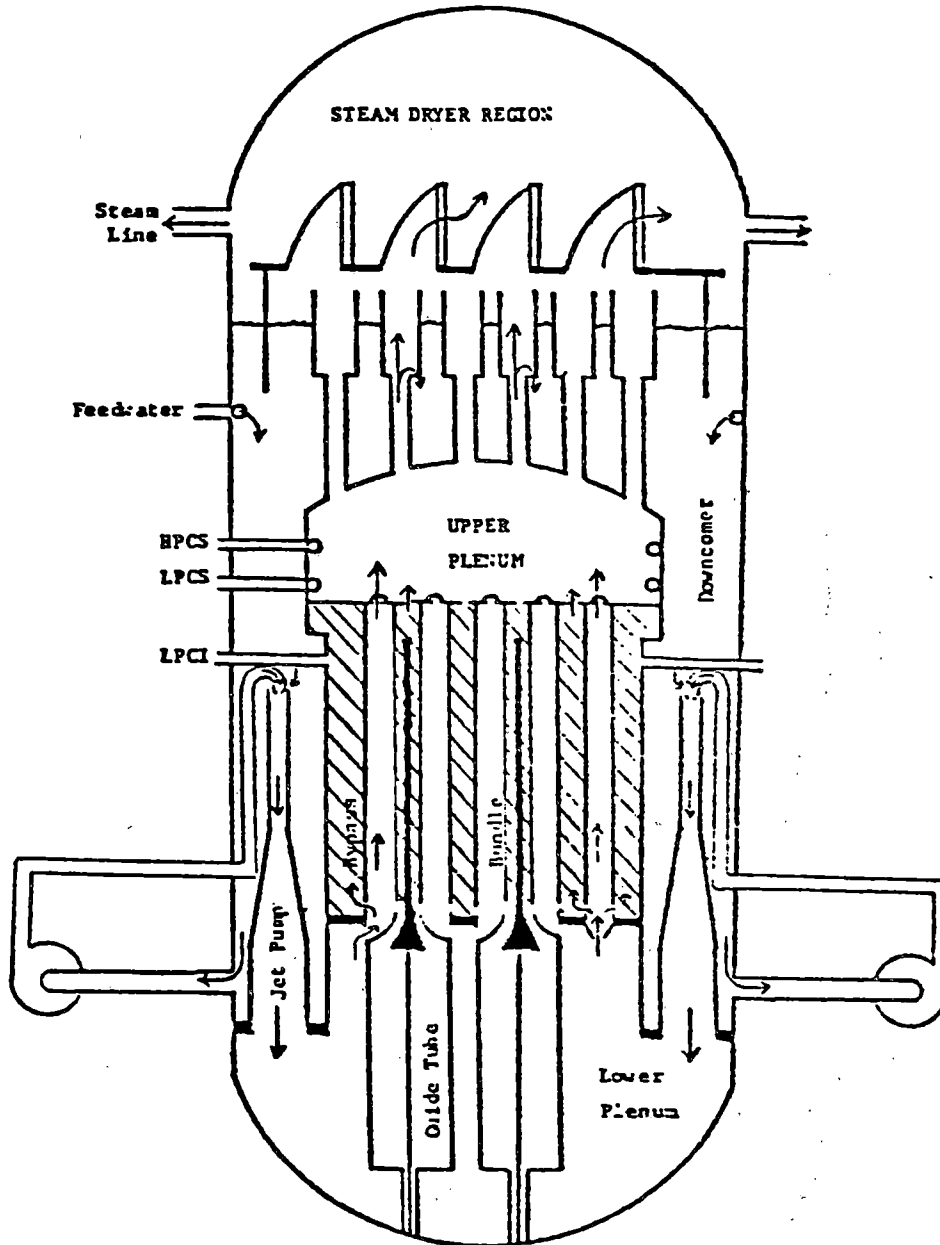


FIGURE 1

## PHENOMENA IMPORTANT IN SCALING

- CONTROLLED PARAMETERS

- POWER
- BREAK AREA/LOCATION
- BOUNDARY FLOWS
- INITIAL CONDITIONS
- TRIP LOGIC

- KEY PHENOMENA

- PRESSURE
- BREAK FLOW
- INVENTORY
- LEVEL
- INTERNAL FLOWS
- LOOP FLOWS
- BUNDLE FLOW/HT

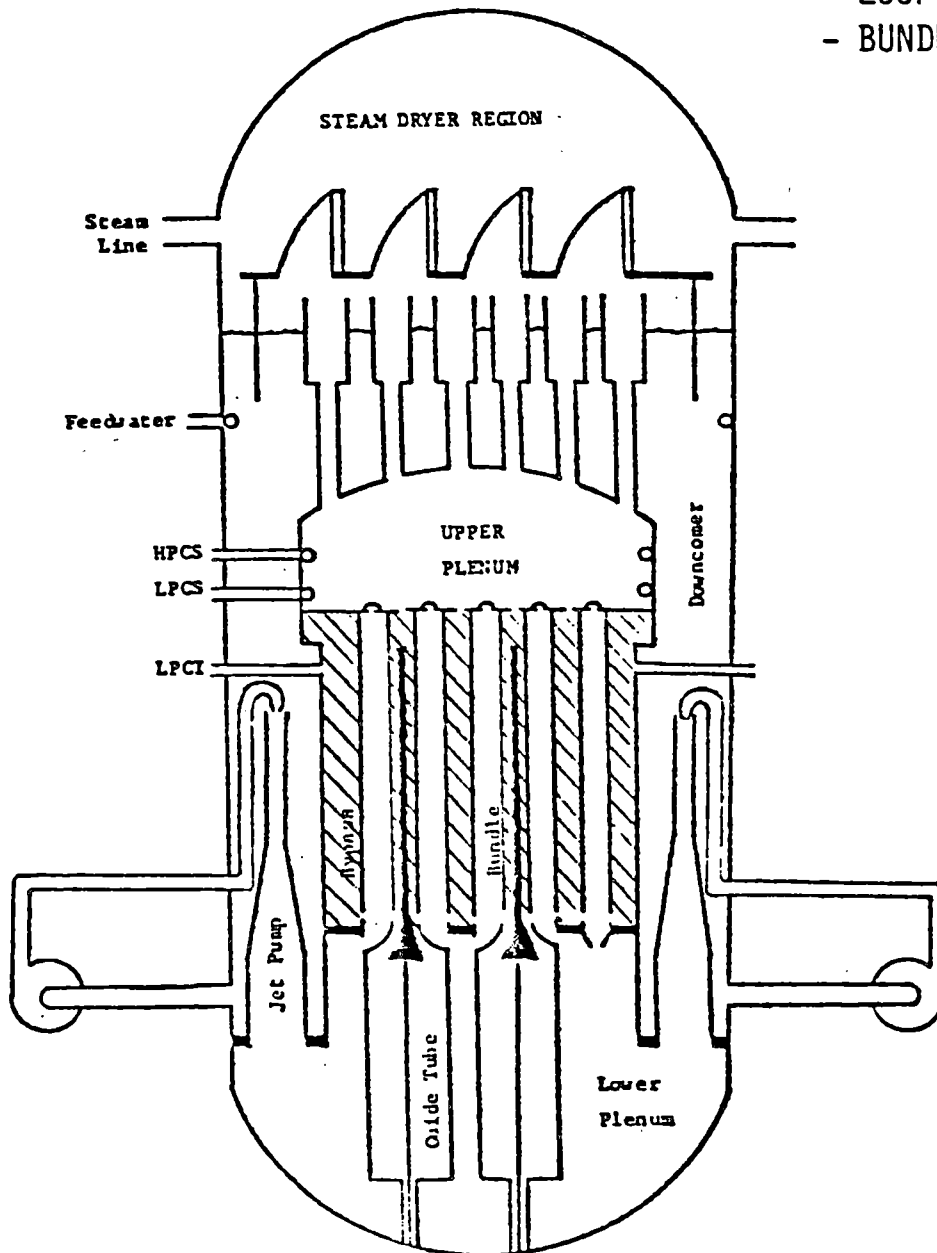


FIGURE 2

# FIST SIMULATION OF BWR VESSEL AND INTERNALS

- FULL PRESSURE
- FULL LENGTH, FULL POWER BUNDLE
- SCALED VOLUMES/BREAK AREA
- FULL HEIGHT VESSEL
- TYPICAL INTERNAL HARDWARE
- TWO DRIVE PUMP LOOPS

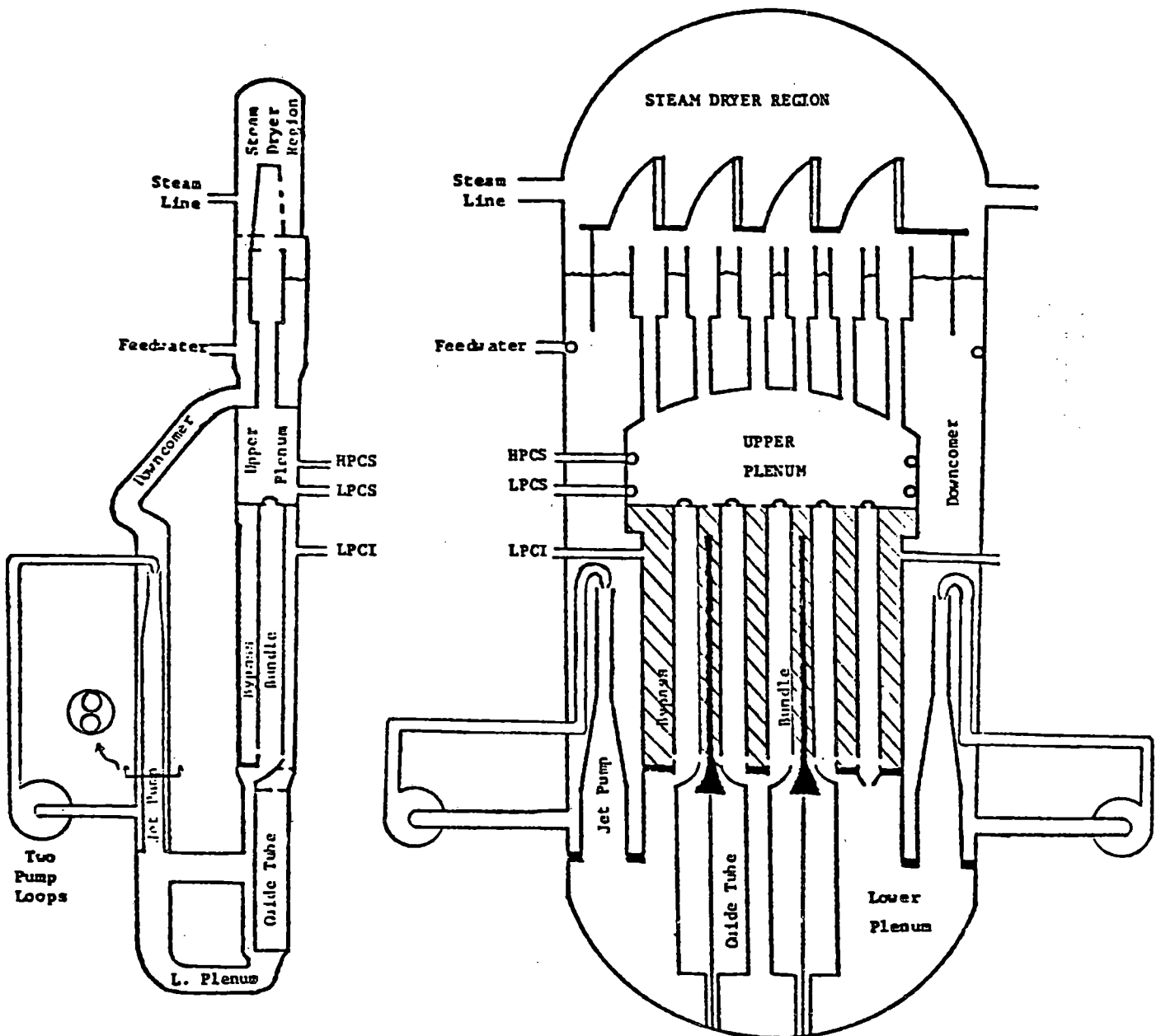


FIGURE 3  
68

FIST SIMULATION OF BWR  
TRIP SIGNALS

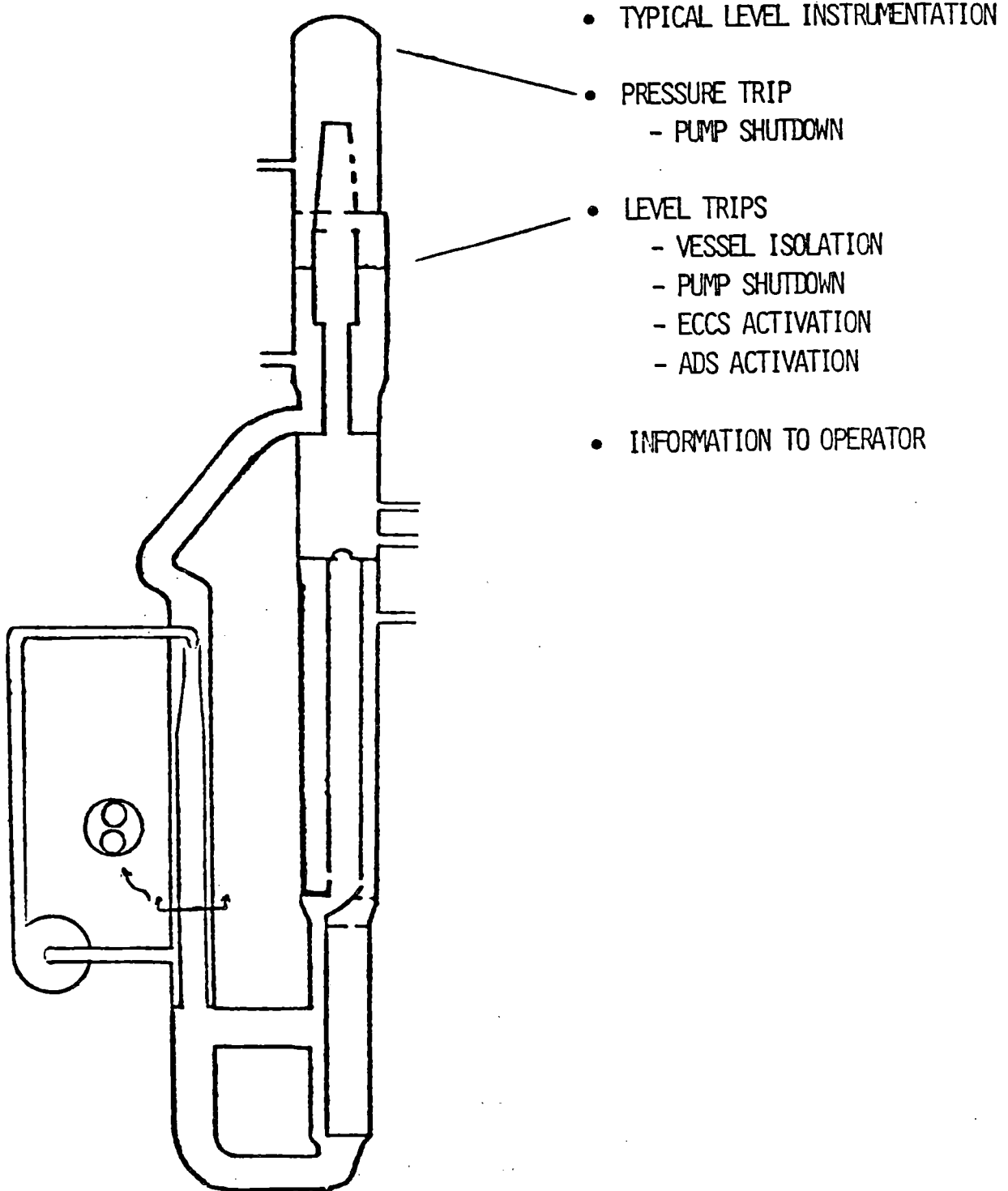


FIGURE 4

FIST SIMULATION OF BWR  
SYSTEMS

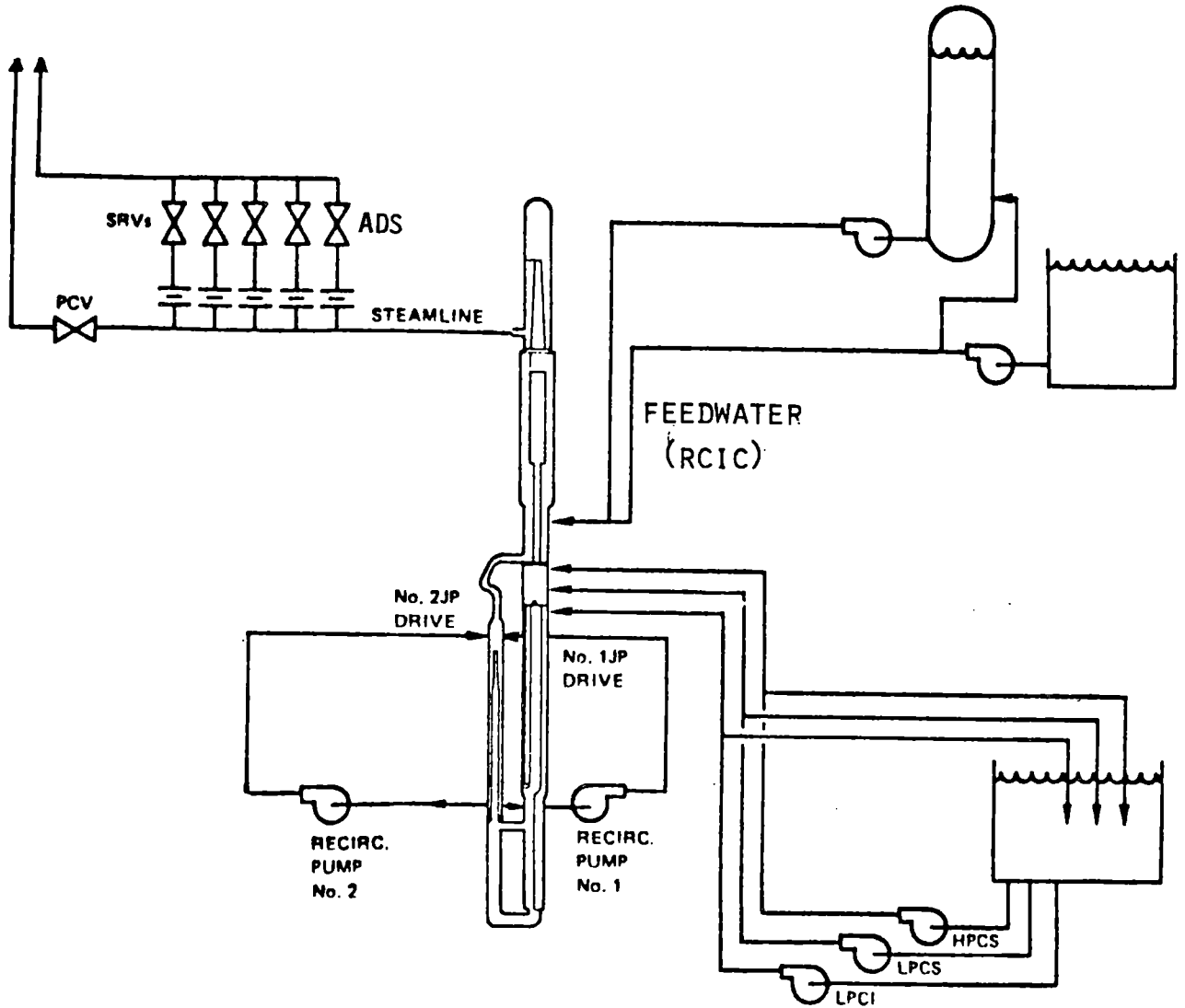


FIGURE 5

LOBI Experimental Programme Results and Plans:

Status September 1982

W. L. Riebold, L. Piplies, H. Städtke

Commission of the European Communities  
EURATOM, Joint Research Centre - Ispra Establishment  
LOBI Project, Heat Transfer Division  
I-21020 ISPRA/Varese (I)

1. Introduction

The LOBI Project is being executed in the framework of an R&D contract between the Bundesminister für Forschung und Technologie (BMFT), Bonn/FRG, and the Commission of the European Communities.

The LOBI test facility / 1 / was built and is operated by the EURATOM Joint Research Centre (J.R.C.) in Ispra, Italy; it is at present the only high-pressure integral system test facility in Europe for the investigation of pressurized water reactor (PWR) loss-of-coolant accidents (LOCA).

The overall objective of the LOBI experimental programme is to provide and/or extend the data base required for assessing the computer code capabilities to predict integral system blowdown-refill experiments and accidents for a range of system components operation conditions and for pipe ruptures of different sizes and at various locations within the primary cooling system.

In the first part of the LOBI test programme, a total of 25 large break blowdown tests with different break sizes and different break locations were successfully performed during the period December 1979 to June 1982, see Table 1.

The present paper aims at highlighting the analysis results obtained till now from the LOBI Programme by (1) considering the influence of three important test parameters on blowdown, (2) showing the test prediction capability of the RELAP4/MOD6 code and (3) illustrating the importance of pump behaviour simulation. The three test parameters investigated are (1) the ECC water injection mode which was varied between cold leg injection, combined cold and hot leg injection and no injection at all, (2) the break size which ranged from 2 x 1A down to 1 x 0.25A, and (3) the downcomer gap width of 50 and 12 mm. For this purpose, a comparative results analysis of those seven tests out of a total of 25 was performed which are evidenced by a frame in Table 1.

A short outline of the presented status of the LOBI Project, and of the plans for the forthcoming experimental programme concludes the paper.

2. Test Facility and Design Rationals / 1 /

The LOBI facility is similar to the Semiscale and LOFT facilities of the USNRC; it has a two-active-loop configuration and was designed as a 1 : 712 mo-



del of a four-loop 1300 MWe PWR primary cooling system to simulate the transient thermal-hydraulic behaviour of the latter during the blowdown and the initial re-fill period of a LOCA. See Fig. 1. The "intact loop" represents three unbroken loops of the reference plant; within the "single" or "broken loop" pipe ruptures of different sizes can be simulated at three different break positions (hot leg, cold leg, pump suction leg). The test facility operates at normal (KWU) PWR conditions of 290°/320°C and 155 bar on the primary side, and 210°C feedwater temperature and 54 bar on the secondary side. The closed loop secondary cooling system contains a condenser simulating the turbines, which is followed by a cooler to reduce the condensate temperature to 210°C at the inlet to the feedwater pump and to the steam generators.

For the primary circuit, very detailed attention was paid to scaling: all coolant volumes of the individual components and of the pipework between them, the mass flows in the two loops (7 and 21 kg/s) and the heating power (5,3 MW for the LOBI 8 x 8 rod bundle) have been scaled by a factor of 712 with respect to the reference plant. Heat transfer surfaces, i.e. heater rods (3.9 m) and SG U-tubes are full length. All component heights and elevations have been preserved 1 : 1 to retain the correct gravitational heads.

An exception to this scaling concept is the annular shaped downcomer: since no general scaling concept for the downcomer gap size is available at present, LOBI tests have been performed with two different gap widths of 50 and 12 mm.

The LOBI heater rods are directly electrically heated hollow tubes. A stepped cosine profile for the axial heat flux distribution is achieved by five sections with different tube wall thicknesses. The fission power and the release of the decay-heat and of the stored energy of the nuclear fuel rods are simulated by an appropriate electrical power-time curve which has to be determined prior to each test based on pre-test predictions / 2 /.

In the present test facility configuration only the accumulator ECC injection system is represented. ECC water can be supplied from two accumulators, one for each loop; cold or hot leg as well as combined injection can be simulated.

### 3. The Influence of ECC Water Injection Mode / 3 /

#### 3.1 Introduction

For the pressurized water reactors at present in operation the emergency core cooling (ECC) water injection is performed according to the vendor type at different locations: either only into the cold leg, or (KWU reactor) into both the cold and hot leg (combined injection) of the primary cooling system.

The effect of these different injection modes on the course of a LOCA, in particular on the bundle temperature behaviour was investigated with the LOBI facility using a downcomer gap width of 12 mm which represented a nearly correct simulation of the reactor downcomer.

- For this purpose the results of the following three tests were analysed:
- Test A1-66 with ECC injection into the cold leg only (between main coolant pump and vessel)
  - Test A1-07 without ECC injection
  - Test A1-06 with combined ECC injection into the cold leg and hot leg (between vessel and steam generator).

In all three tests, a double-ended 2 x 1A break in the cold leg was simulated starting from nominal operation conditions. The pressurizer was connected to

the intact loop hot leg. The pump speeds were controlled such as to simulate the pump behaviour of the reference plant. The decay heat and the stored energy in the nuclear fuel rod were simulated by a stepwise reduced electrical heating power which was shut off at 30 s (!) into the transient and corresponds to about 6 full power seconds.

The good agreement in the initial and boundary conditions (heating power, pump speeds) provides a good basis for a comparison of these three tests.

### 3.2 Results

The emergency core cooling water causes a decrease in the depressurization rate; this decrease is the strongest in the case of combined injection as a consequence of the amount of coolant inventory increase.

For the three tests under consideration, the thermal response of the LOBI heater rod bundle is different: Fig. 2 shows that the combined injection (A1-06) is much more efficient than the cold leg injection (A1-66). With combined injection already at 5 s after injection started, rewetting of the bundle occurs contemporaneously at the bottom and at the top, and the whole bundle is rewetted at about 45 s after begin of injection, having a temperature of 140°C. At the same time into the transient, with cold leg injection only, and also with no injection at all (A1-07) the heater rod temperatures, after having passed the maximum value of about 600°C, decrease only gradually and are still at about 500°C. In the case of combined injection a small negative two-phase core mass flow is established during the refill period resulting in an upward flow of saturated fluid within the downcomer and thus preventing ECC water penetration from the cold leg injection into the downcomer. This result is supported by the fluid temperatures measured in the downcomer, see Fig. 3: with combined injection, except for a few subcooled water and superheated steam temperature spikes, the fluid temperature also in the upper downcomer region is at saturation temperature. For cold leg injection only, much more subcooled water temperature spikes occur indicating a higher degree of ECC water penetration into the downcomer; the small 12 mm downcomer gap width causes a too strong limitation of this penetration process, such that only a small amount of ECC water reaches the lower plenum. These results are supported by the fluid density measurements in the lower plenum.

The total time history of the LOBI bundle behaviour is recorded in a film where selected heater rod temperatures for the three tests are shown simultaneously. Two frames of this film are represented in Fig. 4 showing the heater rod temperatures at 13 s (5 s before ECC injection started) and at 85 s into the transient.

### 3.3 Conclusion

LOCA experiments in the LOBI facility with different modes of ECC injection show a much more effective bundle cooling with combined cold and hot leg injection than with cold leg injection only. It must however be pointed out, that the small 12 mm downcomer gap width caused a too negative result for the core cooling efficiency of only cold leg ECC injection due to an atypically *high* vapour velocity in the downcomer, inhibiting ECC water penetration.

## 4. Influence of Break Size for Large Breaks / 4 /

### 4.1 Introduction

The influence of the break size on blowdown in the LOBI facility with 50 mm downcomer gap width has been investigated through a comparative analysis of essential results of four tests which covered a break size spectrum ranging from 1 x 0.25A to 2 x 1A: B-R1M (1 x 0.25A), A2-55 (1 x 0.5A), A2-59 (1 x 1A) and A1-04R (2 x 1A).

All four tests were cold leg break tests with ECC water injection from the accumulator into the intact loop cold leg only. The pressurizer was connected to the intact loop hot leg. The different break sizes were simulated by convergent-divergent nozzles of different throat diameter.

It must be noted that the downcomer gap width of 50 mm is out-of-scale with respect to both power to volume and pressure drop scaling criteria<sup>1</sup>. Thus break sizes of 2 x 1A, 1 x 1A, 1 x 0.5A and 1 x 0.25A represent break sizes of 2 x 0.75A, 1 x 0.75A, 1 x 0.38A and 1 x 0.19A respectively, when reference is made to the ratio of break size to actual primary system volume of the LOBI facility with the 50 mm downcomer gap width installed.

The power supplied to the rod bundle was programmed to follow the calculated energy release from an appropriate nuclear fuel model during the simulated transient / 2 /. The feedwater mass flow to the steam generator secondary side was reduced to zero after blowdown was started.

### 4.2 Results

The effect of break size on depressurization rate of the primary cooling system during blowdown is shown in Fig. 5 which compares the pressure responses in the intact loop cold leg (see the "short time" plot in the insert) which are almost identical to the lower plenum pressure responses. The depressurization rate clearly decreases with the break size which limits the rate of discharge and hence the depletion of primary system fluid inventory during both the subcooled and the subsequent saturated phase of the blowdown transient. In the early transient the depressurization rate changes with the occurrence of flashing at various locations in the primary cooling system.

Immediately following the start of blowdown the system pressure drops quickly to the saturation pressure corresponding to hot legs and upper plenum fluid temperatures. For the four blowdown tests with 2 x 1A, 1 x 1A, 1 x 0.5A and 1 x 0.25A break the saturation pressure in the upper vessel region is reached within 100 ms, 200 ms, 400 ms and 1 s respectively. Thereafter a flashing front propagates through the whole primary cooling system. The transition from subcooled to saturated conditions in the cold legs occurs at 3.4 s, 5.4 s, 7.5 s and 8.5 s for the break sizes decreasing from 2 x 1A down to 1 x 0.25A.

As the primary system fluid inventory depleted due to fluid discharge through the break, heater rod bundle heat transfer degraded considerably causing departure from nucleate boiling (DNB) over the whole heated length for the 2 x 1A and 1 x 1A break tests. For the 1 x 0.5A test, DNB occurred only

---

<sup>1</sup> A volume scaled downcomer would yield a 7 mm gap width whereas a 25 mm gap width would preserve the same pressure drop due to wall friction as in the reference plant.

in the upper bundle region whilst no boiling crisis was observed in the 1 x 0.25A test. The onset of DNB for the spectrum of break sizes considered is shown in Fig. 6 where the average times with one standard deviation are presented (TC's time response is not accounted for).

After the occurrence of DNB a first rewet of the bundle was observed for each test where boiling crisis was experienced, see Fig. 7 which illustrates the envelopes of heater rod temperatures (central and intermediate zones of the 8 x 8 square lattice) in the middle part of the bundle (level 6), see also Fig. 6. This very first rewet is mainly caused by a reestablished core flow in the 2 x 1A and 1 x 1A tests. For the 1 x 0.5A test where relatively low quality fluid persisted in the bundle during the early transient, rewet was caused by the initial decay of the heating power. In the larger 2 x 1A and 1 x 1A break tests the initial rewet was followed by the onset of dryout at about 14 s and 24 s, respectively. No dryout occurred in the 1 x 0.5 A and 1 x 0.25A tests. The temperature rise after dryout in the 2 x 1A test was generally higher and more rapid than in the 1 x 1A test.

Figure 8 depicts fluid densities at core entrance for each of the four break sizes. This density in the 2 x 1A test drops quickly soon after initiation of blowdown due to large core flow reversal and then recovers as positive core flow is momentarily reestablished. Thereafter the density decreases continuously with the core mass flow and starts to recover again only when ECC injection starts. The same trend characterizes the 1 x 1A blowdown transient. Here, however, the initial drop of density is very mild. The 1 x 0.5A and 1 x 0.25A blowdown transients are characterized by relatively high core entrance fluid density.

#### 4.3 Conclusion

The thermohydraulic conditions (fluid flow, heat transfer) in the rod bundle (core) are directly related to the break size dependent break mass flow and hence, coolant depletion. As a consequence, early DNB over the whole heated length of the bundle was observed to occur certainly for break sizes of 1 x 1A and larger; no DNB at all is certainly to be expected for break sizes of 1 x 0.25A and less. The transition between no DNB and overall DNB occurs within the intermediate region, e.g. DNB only in the upper part of the bundle for 1 x 0.5 break size. After an initial rewet caused by a re-established positive core flow, dryout was measured only for the larger 2 x 1A and 1 x 1A break tests.

### 5. Influence of Downcomer Volume and Gap Width / 5 /

#### 5.1 Introduction

An exception to the general scaling concept of the LOBI facility is the annular shaped downcomer.

Although the downcomer problematic is well known from the Semiscale test programme / 6 /, no general scaling concept for the downcomer gap size is available at present. The rational scaling criteria may also be different for the different LOCA periods (blowdown, refill period), depending on the governing physical phenomena.

For this reason it has been decided to perform the LOBI blowdown tests with two different downcomer gap widths. The gap width of 50 mm results in 6.3 times too large a downcomer volume and therefore in a strong distortion

of the mass distribution within the scaled system. The 12 mm gap width was chosen as a compromise between the volume scaled downcomer (7 mm gap width) and a downcomer which would yield the same pressure drop due to wall friction as in the reference reactor (25 mm gap width for the scaled facility). For the downcomer filler a honeycomb structure was used in order to reduce the amount of stored heat in the downcomer walls<sup>1</sup>. Although the 12 mm gap width still gives too large a downcomer volume (1.7 times larger than the volume scaled downcomer), the volume and mass distribution is a more representative one of the reactor cooling system.

The influence of downcomer volume and gap width during the blowdown and early refill period was investigated by a comparative results analysis of two tests:

- A1-04R with 50 mm downcomer gap width
- A1-66 with 12 mm downcomer gap width.

Both tests were double-ended offset shear (2 x 1A) cold leg break tests with ECC injection from the accumulator into the intact loop cold leg only. All other initial and boundary conditions were equal for the two tests except

- the heating power which was different due to different thermohydraulic core conditions / 2 /
- the flow resistance of the accumulator injection line, which for the A1-66 test was increased in order to obtain a smaller and more reactor-typical ECC injection rate.

## 5.2 Results

There is no significant effect of the downcomer volume and gap size on the thermohydraulic behaviour during the first 2 s into the transient when subcooled fluid conditions persisted in the downcomer region, see Fig. 9 to 12.

However, during the subsequent saturated blowdown period the downcomer volume strongly affects the course of the transient: after fluid evaporation has started also in the cold regions of the system, the reduction of the depressurization rate (Fig. 9), the re-establishment of a positive core mass flow (Fig. 12) and the resulting improvement of the core cooling (Fig. 11) are much more pronounced in test A1-04R where the initial liquid amount in the downcomer is 3.64 times higher than in test A1-66. As a consequence, completely different conditions existed in the primary system at the time when the ECC injection from the accumulator started: Large amount of residual water in the lower plenum, positive core mass flow and low heater rod temperatures for test A1-04R with the large downcomer volume, and reduced residual mass in the lower plenum, nearly stagnation conditions in the core and relatively high heater rod temperatures for test A1-66 with the small downcomer volume. The heater rod temperature behaviour in test A1-04R with the large downcomer is qualitatively quite similar to the cladding temperature behaviour observed in the large break LOFT test L2-3 / 7 /.

Fig. 13 shows calculated results for the upper downcomer region. The amount of ECC water penetrating the downcomer results to be significantly affected by the downcomer gap width:

---

<sup>1</sup> The downcomer walls are not thermally insulated.

- For the large (50 mm) gap width, the penetration - indicated by a sudden increase of downcomer inlet mass flow - starts at about 2.5 s after ECC injection had initiated, and soon amounts to about 60 % of the totally injected mass flow; of the ECC water reaching the lower plenum, a small part results in a water inventory increase (Fig. 10), and the major part contributes to the persistence of a positive core mass flow (Fig. 12) and, hence an improved core cooling (Fig. 11). Apparently, the amount of vapour produced within the upper downcomer region and the resulting superficial vapour velocity were not large enough to cause counter-current flow limitation to such an extent as to prevent the refill of the pressure vessel.
- For the small (12 mm) gap width the penetration starts at about 5 s after ECC injection initiated, and amounts to only about 30 % of the totally injected mass flow; apparently, due to the larger (factor 4) surface-to-flow area ratio a larger amount of vapour was produced within the upper downcomer region, and the resulting higher superficial vapour velocity caused a significantly stronger prevention from ECC water penetration. The ECC water reaching the lower plenum contributes prevalently to the water inventory increase (Fig.10), since no significant effect on the core mass flow is obtained (Fig.12).

A further significant difference to the large gap width case consists in the occurrence of a periodical voiding of the lower plenum through the downcomer into the cold leg pipes starting at about 30 s into the transient. This effect might be attributed to a larger amount of heat released from the hot wall within the lower part of the pressure vessel and possibly from the core inlet region, both being at a high temperature level.

The refill behaviour in both cases described above is probably further adversely affected by the fact that the containment back pressure was not simulated in these LOBI tests; as a consequence, a too large break mass flow persisted for an untypically extended time period, and an increased amount of ECC water by-passed the pressure vessel.

### 5.3 Summary

The influence of the annular downcomer volume and gap width on the course of a LOCA transient was demonstrated by two LOBI tests A1-04R and A1-66. These showed that the course of a LOCA transient is significantly affected

- during the blowdown period by the downcomer volume, and
- during the refill period by the downcomer gap width.

As a consequence of the effect of the downcomer volume, the thermo-hydraulic conditions within the primary cooling system at the time into the transient when ECC injection starts, may differ substantially and, hence, further affect the course of the refill process and the ECC effectiveness.

## 6. Comparison of Prediction and Experimental Results / 8 /

### 6.1 Introduction

The LOBI experimental programme is accompanied by prediction calculations using large blowdown computer codes. The prediction effort performed in the LOBI "Programme and Analysis" Group includes

- (1) Sensitivity studies to identify the governing parameters and to support the test programme planning

- (2) Simulation calculations to determine transient control curves for those components of the test facility which are not reactor typical, e.g. the electrically heated bundle and the LOBI coolant circulation pumps
- (3) Pre-test predictions using specified initial and boundary conditions
- (4) Post-test predictions with measured initial and boundary conditions for test analysis and code assessment purposes.

For the large break test programme all prediction calculations performed in the LOBI Analysis Group were done with the REALP4/MOD6 code developed at EG&G in Idaho Falls / 9 /. For an improved user convenience an SI input/output conversion package has been added to the original code version which is described in / 10 /. As far as the experimental results are also available to the Community Member States, the following institutions have participated in the test prediction programme using the same version of the RELAP4 code: the Commissariat a l'Energie Atomique (CEA) in France and the University of Pisa in Italy. In addition, most of the tests were also predicted by the Gesellschaft für Reaktorsicherheit (GRS) in Germany with the German blowdown code DRUFAN01/02. Advanced safety codes like RELAP5 and TRAC-PF1 will be used in the near future for the LOBI test prediction after the conversion of these codes to IBM/AMDAHL versions has been completed.

## 6.2 Results

Measured and calculated values for three key parameters, the pressure and density in the lower plenum and the heater rod temperature in the high powered middle section of heater rod bundle, are given in Fig. 9 to 11 for test A1-04R and A1-66. Both tests simulate a large break in the cold leg pipe between pump and pressure vessel of a PWR / 11, 12 /. The main difference between the two tests is the scaling criteria for the downcomer region which resulted in different values for the downcomer volume and gap width. The test results are described more in detail in the preceding chapter 5, where the influence of the downcomer size on the blowdown transient is discussed.

The measured and predicted quantities show a good qualitative, and in most cases, also a good quantitative agreement during the blowdown and most of the refill transients. This includes the depressurization rate, the mass inventory in the lower plenum, the time for the Departure from Nucleate Boiling (DNB) for the heater rod bundle and the maximum heater rod temperature.

Discrepancies between measured and predicted values which have been found for the later blowdown and refill period are related to the deficiency of the RELAP4 code in describing: (1) Phase separation processes in vertically and horizontally oriented components of the test facility, (2) three-dimensional flow patterns in components with multiple flow path connections (upper and lower plenum, downcomer upper annulus), (3) thermal non-equilibrium processes which occur when subcooled liquid is injected into components which contain saturated vapour, (4) heat transfer in the post-DNB (film boiling) region and rewetting processes.

It is expected that some of these problems are solved in the RELAP5 code which handles inhomogeneous two-phase flow and thermal non-equilibrium conditions by a two-fluid model. For this reason predictions for selected LOBI tests will be repeated using RELAP5 when the IBM/AMDAHL version of this code is implemented.

## 7. Simulationg of Pump Behaviour / 13 /

### 7.1 Introduction

During a LOCA transient the primary pump may undergo conditions where head, flow and speed can be negative. Additionally, the occurrence of two-phase flow leads to a strong change in the pump characteristics. Therefore the behaviour of the LOBI pump under two-phase flow conditions was investigated experimentally<sup>1</sup>. This experimental programme comprises some specific experiments on the influence of pressure and void fraction and a thorough investigation of five pump characteristics charts at different pressures and void fractions. It is believed that this programme covers the full range of conditions of pressure and void fraction to be expected during a loss-of-coolant accident. Results were presented in / 14 /.

The three objectives of the LOBI pump two-phase flow tests were:

- (1) to provide a basis for describing the pump behaviour in the pre- and post-test calculations for the LOBI tests. Since in many computer codes the homologous curves are used, this concept was also chosen for the evaluation of the LOBI pump two-phase tests.
- (2) to determine the pump speed-time control curves for LOBI tests.
- (3) to develop a more general pump model using the two-phase LOBI pump data as a basis.

### 7.2 Results

The LOBI pump and the main coolant pump of the reference plant are different in their characteristics data and consequently in their hydraulic behaviour, see Fig. 14. Therefore the speed of the LOBI pumps are controlled during a test as function of time to ensure that the influence of the LOBI pumps on the thermohydraulic behaviour of the LOBI facility is similar to that of the pumps in the reference plant. This means that the LOBI pump is used as a "variable flow resistance simulator".

Necessary for the determination of a LOBI pump speed control curve is a set of quantities (as  $\Delta p$ ,  $\dot{M}$  ...) which describes the thermohydraulic state at the pump. These data may come from a calculation for the reference plant or from a calculation for the LOBI facility with an "ideal reactor model pump". Using this set of data and the LOBI pump two-phase flow characteristics the speed control curves can be determined.

After having available the complete LOBI pump head two-phase data this procedure was applied to a certain number of A1-tests.

An example is given in Figures 15 and 16. These curves are valid for a 2A break between vessel and steam generator. As shown here, the result may be, that for the same case the pump speeds in the LOBI facility and in the reference plant differ considerably (Fig. 15), but that the pressure differences across the pumps - which determine the mass flow - are nonetheless very similar (Fig. 16).

---

<sup>1</sup> The tests were carried out at WCL, Hamilton (Canada); evaluation was performed at JRC, Euratom, Italy.



### 7.3 Summary

To ensure that the pump influence on the LOCA transient is similar in both the reference and the experimental plant, it is necessary that the differential pressure across the pump shows the same time behaviour. It is, hence, not sufficient to simulate the pump speed behaviour unless both pumps have the same specific speed.

## 8. LOBI Programme Plans / 15, 16 /

### 8.1 Introduction

The future LOBI programme plans will comprise both further loss-of-coolant experiments (LOCE) and Special Transients experiments (STE).

The test facility modifications required in view of the forthcoming small break loss-of-coolant experiments programme (LOCEP) and special transients experiments programme (STEP) tests are at present under way; they are scheduled to be terminated in April 1983.

### 8.2 LOBI Test Facility Modifications: LOBI-MOD2

The original objectives of the LOBI experimental programme were prevalently oriented towards large break loss-of-coolant tests and are clearly reflected in the design of both the mechanical parts of the test facility and the measurement instrumentation and data acquisition system. As a consequence, the test facility configuration which was operated until June 1982 exhibits a series of deficiencies which in view of the forthcoming small break LOCEP and STEP tests have to be removed.

These test facility modifications aim to achieve an optimal adaptation of the performance characteristics to specific needs of small break and special transients tests. They include

- new inverted U-tube steam generators with (1) rigorously (to within 6 %) scaled volumes of the primary and secondary side, (2) 1 : 1 scaled heights on both sides, (3) an intensive instrumentation with 47 and 44 measurement channels on the primary and secondary side respectively, and (4) a secondary side operation pressure of up to 100 bars / 16 /
- modifications of the secondary cooling circuit by (1) installing isolation valves in both the feedwater and the steam lines, and pressure relief valves in the steam lines to allow steam generator blowdown, (2) adding the auxiliary feedwater system (AFS), and (3) installing mass flow measurement devices within the steam lines / 15 /
- a new reactor pressure vessel model exhibiting a total of 17 nozzles for measurement devices penetration allowing very closely axially spaced differential pressure measurements in both the bundle and the downcomer region with the aim to determine collapsed and mixture levels and void distribution / 15 /
- installation of the high pressure injection system (HPIS) within the primary cooling system / 15 /
- modifications of the instrumentation system with the aim to reduce the measuring range, to improve the accuracy and to slow down the time response
- installation of a new data acquisition system consisting of a computer controlled disc system with a software controlled signal scanning rate variation between 20 and 1000 samples per second / 15 /

- an improved thermal insulation of the primary loop system / 15 /.

After completion of these modifications the test facility will be referred to as LOBI-MOD2.

### 8.3 LOBI Loss-of-Coolant Experiments Programme (LOCEP) Plans

The LOBI loss-of-coolant experiments programme (LOCEP) according to present commitments and plans will run at least until the end of 1987. It will be subdivided into two phases, see Fig. 17:

- (1) Upon conclusion of the presently running test facility modification phase in April 1983, the A1-programme phase will continue until the end of 1984. During this period a total of 16 small and intermediate break tests will be executed; they are composed of 12 A1-, 3 A2- and 1 B-test. These tests are covering a break size spectrum ranging from 0.4 % to 10 % and include two quasi steady-state natural circulation tests, see Table 2.

The objectives of these 16 tests are essentially the following / 15 /:

- the experimental investigation of the natural circulation characteristics of the primary loop system, particularly with respect to heat transport performances between reactor and steam generators, under single- and two-phase flow conditions
- the establishment of mixture levels due to phase separation, and their behaviour as function of break location and size and of pump operation mode
- the heat removal characteristics of both the steam generator secondary side and the secondary loop system which may be operated in different modes according to reactor plant type, and safety and emergency system operation mode applied by the utility.

- (2) The A1-programme phase is planned to be followed by the A2-programme phase during which several B-tests will be executed alternating with the A2-tests in the framework of an interweaving test programme. The A2- and the B-tests to be performed during this programme phase have as yet been defined only preliminarily. Although the break size to be simulated with these tests will cover again the whole range of interest, emphasis is placed on small and intermediate size break tests.

According to the original LOBI programme plans, the LOBI LOCE programme should continue after 1987 performing and concluding the B-test programme. However, for the time being it is hard to anticipate to which extent after 1987 needs will persist for further investigations in the LOCA problems area.

### 8.4 LOBI Special Transients Experiments Programme (STEP) Plans

A Special Transients experiments programme (STEP) is intended to be performed with the LOBI-MOD2 facility. This programme is at present being set up; it foresees two programme phases which shall be executed from 1983 onwards in parallel to the LOBI LOCEP tests:

- during 1983 and 1984, a feasibility study shall be performed including experiment design calculations and the execution of two or three scoping tests; this study aims at setting up a final test matrix for the STEP
- from 1985 onwards, it is proposed to perform - on average - two or three Special Transients tests per year, at the expense of a corresponding number of LOCA tests, and according to the relative shift of importance between LOCA and Special Transients tests at that time.

So far, two preliminary proposals were made for a LOBI STEP which were subject of several discussions. As a result, two lists have been produced, one reporting a total of 11 different transients to be considered which are further subdivided in short term and long term transients; another list reports a total of 8 different phenomena which are anticipated to play a governing role during the various transients or during different time periods of one transient. The combination of both lists should yield the basis for defining a preliminary test matrix.

#### References

- / 1 / W.L.Riebold, H.Städtke: "LOBI - Influence of PWR Loops on Blowdown. First Results." Trans. Am. Nucl. Soc. 38,734(1981).  
Paper presented at the 9th Water Reactor Safety Research Information Meeting of the USNRC, October 26-30, 1981, Gaithersburg/MD,USA.
- / 2 / H.Städtke, L.Piplies: "Performance of Directly Heated Rods as Nuclear Fuel Rod Simulators in the LOBI Facility". Proceedings of the International Symposium on Fuel Rod Simulators, Gatlinburg, Tennessee, October, 1980.
- / 3 / W.L.Riebold, F.Chenneaux, R.Kirmse: "Einfluß des Notkühlwasser-Einspeisemodus auf den Blowdown in LOBI-Experimenten." ISSN 0720-9207,S.187, Jahrestagung Kerntechnik '82, 4.-5. May 1982, Mannheim.
- / 4 / L.Piplies, C.Addabbo, W.L.Riebold: "Influence of Break Size on Blowdown for Large Breaks." Paper presented at the "International Meeting on Thermal Nuclear Reactor Safety", August 29 - September 2, 1982, Chicago/Illinois, USA.
- / 5 / H.Städtke, D.Carey, W.L.Riebold: "Influence of Downcomer Volume and Gap Width on Blowdown." Paper presented at the "International Meeting on Thermal Nuclear Reactor Safety"; August 29 - September 2, 1982, Chicago/Illinois, USA.
- / 6 / T.K.Larson, E.A.Harvego: "Semiscale Program Summary: A Review of Mod 3 Results", Nuclear Safety, Vol.22, No.2, May-June, 1981.
- / 7 / P.G.Prassinis et al.: "Experiment Data Report for LOFT Power Ascension Experiment L2-3", NUREG/CR-0792, TREE, July, 1979.
- / 8 / H.Städtke, W.Kolar, W.Brewka: "Vorausrechnung der LOBI-Versuche mit RELAP4/MOD6 - Vergleich Experiment und Rechnung." ISSN 0720-9207,S.191, Jahrestagung Kerntechnik '82, 4.-5. May 1982, Mannheim.
- / 9 / "RELAP4/Mod 6 - A Computer Code for Transient Thermal Hydraulic Analysis of Nuclear Reactors and Related Systems", CDAP-TRO03, January, 1978. EG&G Idaho Inc.
- / 10 / W.Kolar, W.Brewka: "RELAP4/Mod 6 Input Card Description for International Units", Technical Note No. I.06.01.81.40, April, 1981, JRC, Ispra.
- / 11 / H.Städtke: Test Prediction for LOBI Test A1-04R". Communication No. 3808, April, 1981, JRC, Ispra.

- / 12 / H.Städtke: "Prediction - Experiment Comparison Report on LOBI Test A1-66", Communication No. 3937, March, 1982, JRC, Ispra.
- / 13 / L.Piplies, W.Kolar: "Pumpenverhalten unter Störfallbedingungen: Zweiphasen-Kennfelder der LOBI-Pumpe." ISSN 0720-9207, S.195, Jahrestagung Kerntechnik '82, 4.-6. May 1982, Mannheim.
- / 14 / L.Piplies, W.Kolar: "Two-Phase Performance Characteristics of the LOBI Pump." Paper presented at the 9th Water Reactor Safety Research Information Meeting, October 26-30, 1981, Gaithersburg/MD, USA.
- / 15 / W.L.Riebold, L.Piplies: "The LOBI-Project Small Break Experimental Programme". Paper presented at the ANS-EPRI Specialists Conference on Small Breaks in LWRs, August 25-27, 1981, Monterey/California, USA.
- / 16 / W.L.Riebold, T.Fortescue, K.H.Günther: "Design and Instrumentation of LOBI U-tube Steam Generators for Small Break and Special Transients Tests." Paper presented at the "International Meeting on Thermal Nuclear Reactor Safety", August 29 - September 2, 1982, Chicago/Illinois, USA.

Table 1: **LOBI LARGE BREAK TESTS** (1980-1982)

|                          |              | BREAK SIZE                       |                         |          |       |                 |       |          |       |           |                  | MODE             |
|--------------------------|--------------|----------------------------------|-------------------------|----------|-------|-----------------|-------|----------|-------|-----------|------------------|------------------|
|                          |              | 2 × 1A                           |                         | 2 × 0.5A |       | 1 × 1A          |       | 1 × 0.5A |       | 1 × 0.25A |                  |                  |
| BREAK LOCATION           | COLD         | A1-04<br>A1-04R                  | A1-66                   | B-101    | B-222 | A2-59<br>A2-59R |       | A2-55    |       | B-RTM     |                  | COLD LEG INJ.    |
|                          | LEG          | A1-01<br>A1-02<br>A1-03<br>A1-05 | A1-06<br>A1-72<br>A1-74 |          |       |                 | A1-69 |          | A1-68 |           | A1-67            | COMBINED INJECT. |
|                          |              |                                  | A1-07                   |          |       |                 |       |          |       |           |                  | NO INJECT.       |
|                          | PUMP SUCTION |                                  |                         |          |       |                 |       |          |       |           |                  | COLD LEG INJ.    |
|                          | LEG          |                                  | A1-70                   |          |       |                 |       |          |       |           |                  | COMBINED INJECT. |
| HOT                      |              |                                  |                         | B-302    |       |                 |       |          |       |           | COLD LEG INJ.    |                  |
| LEG                      |              | A1-10A<br>A1-10B                 |                         |          |       |                 |       |          |       | A1-73     | COMBINED INJECT. |                  |
|                          |              | 50                               | 12                      | 50       | 12    | 50              | 12    | 50       | 12    | 50        | 12               |                  |
| DOWNCOMER GAP WIDTH (MM) |              |                                  |                         |          |       |                 |       |          |       |           |                  |                  |

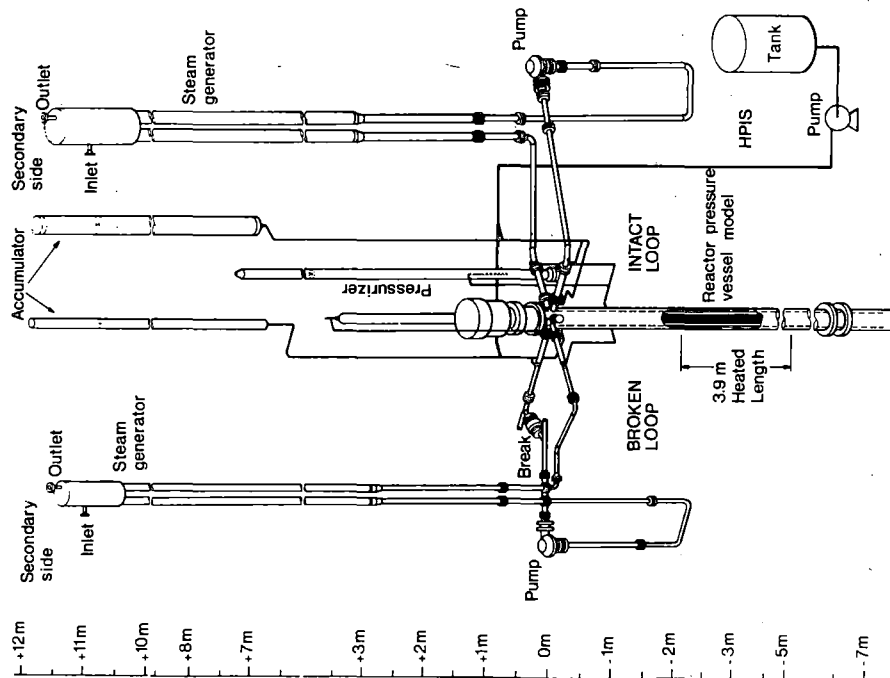


FIG. 1 LOBI Test Facility

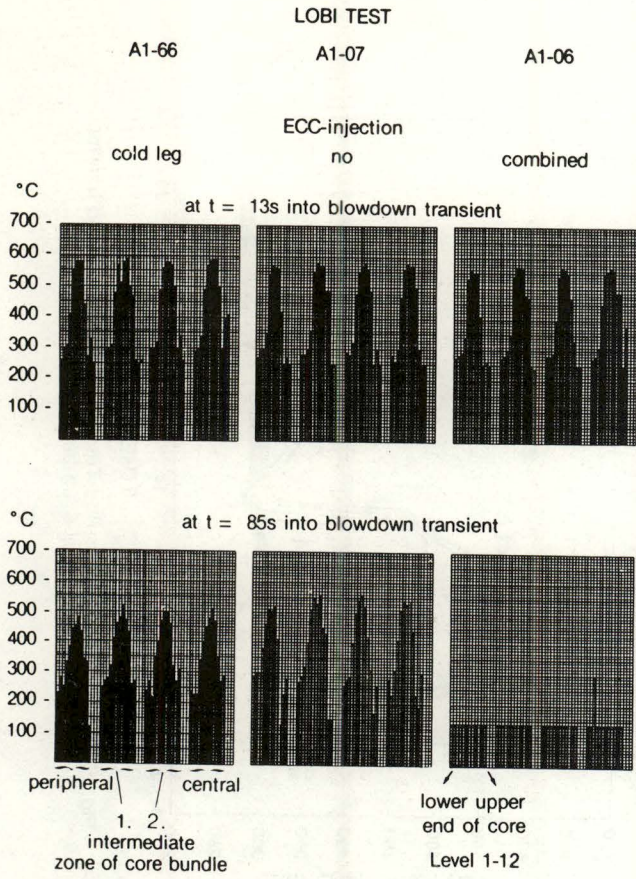


Fig. 4: Heater Rod Surface Temperatures at t = 13 s and t = 85 s into the blowdown transient: Influence of ECC Injection Mode

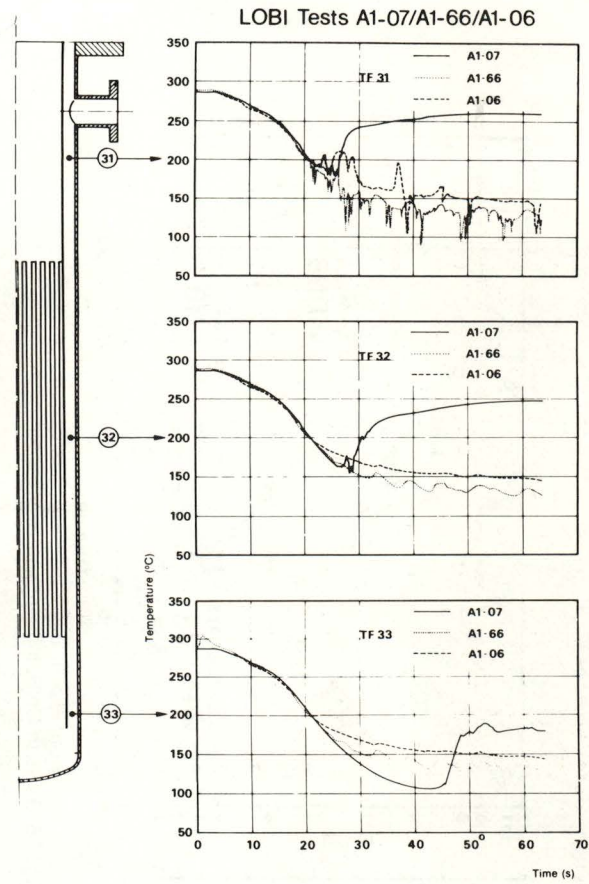


Fig. 3: Downcomer Fluid Temperatures: Influence of ECC Injection Mode

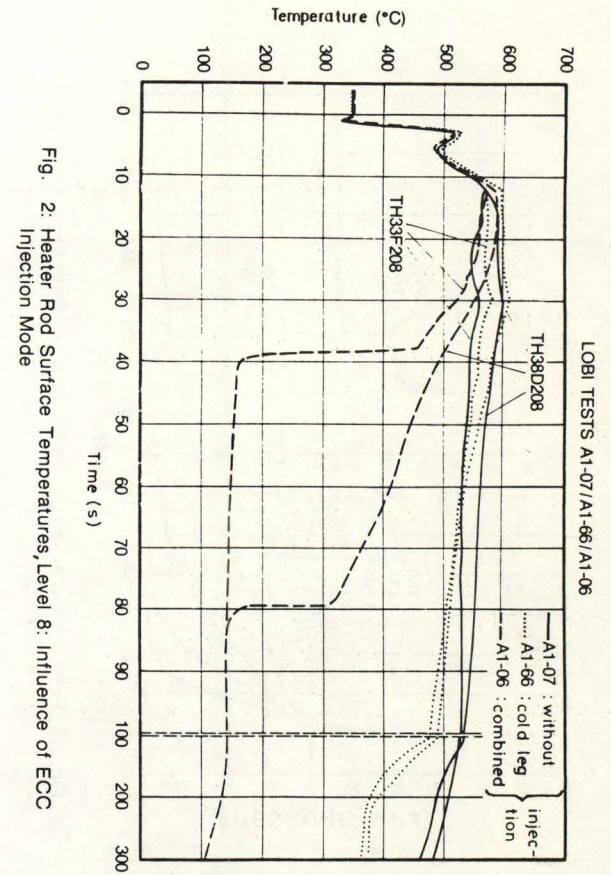


Fig. 2: Heater Rod Surface Temperatures, Level 8: Influence of ECC Injection Mode

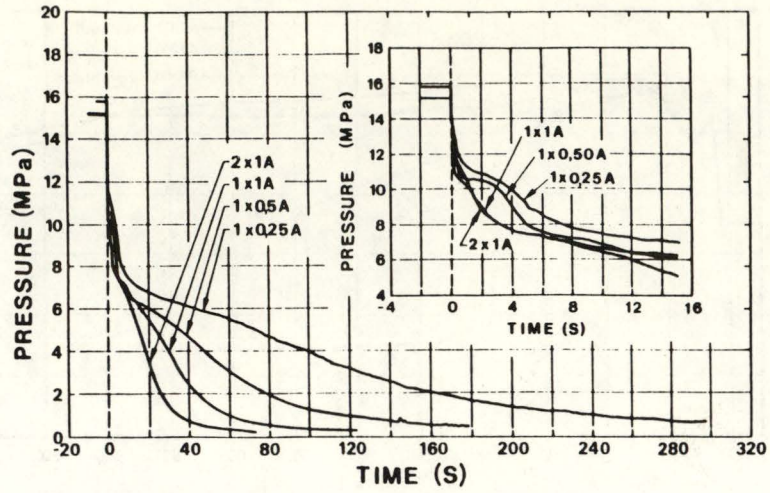


Fig. 5: Pressure Behaviour in the Intact Loop Cold Leg: Influence of Break Size

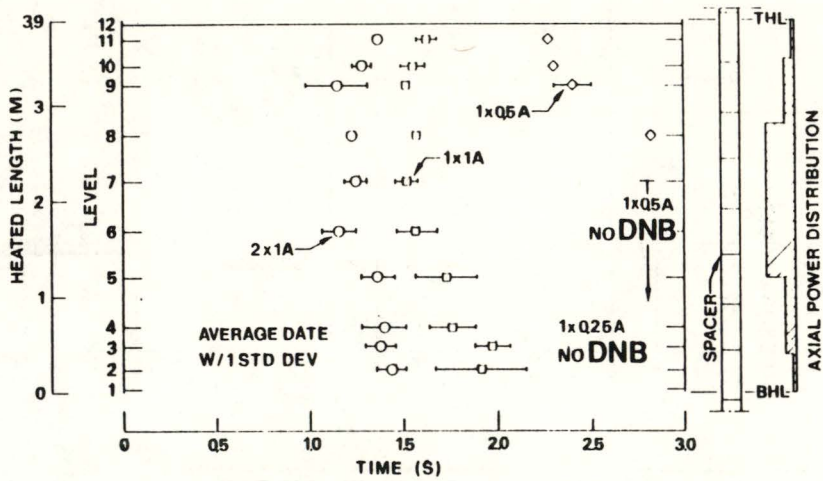


Fig. 6: Time to DNB: Influence of Break Size

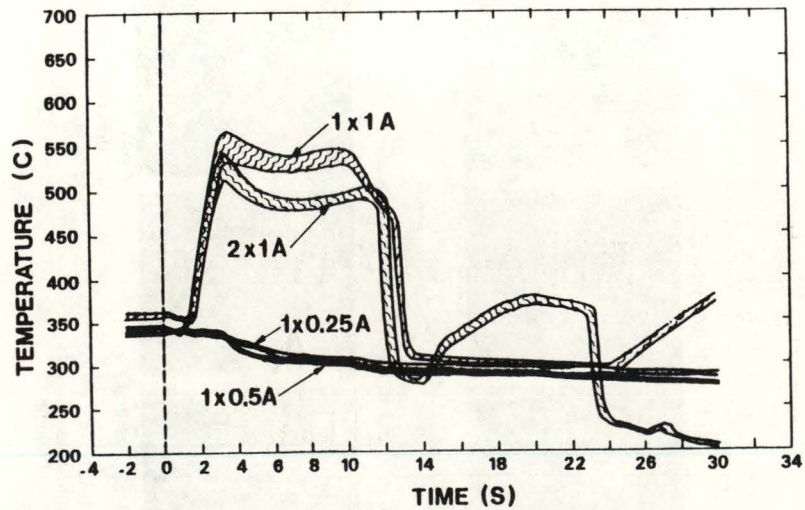


Fig. 7: Envelopes of Heater Rod Temperatures (Central and Intermediate Zones) at Level 6: Influence of Break Size

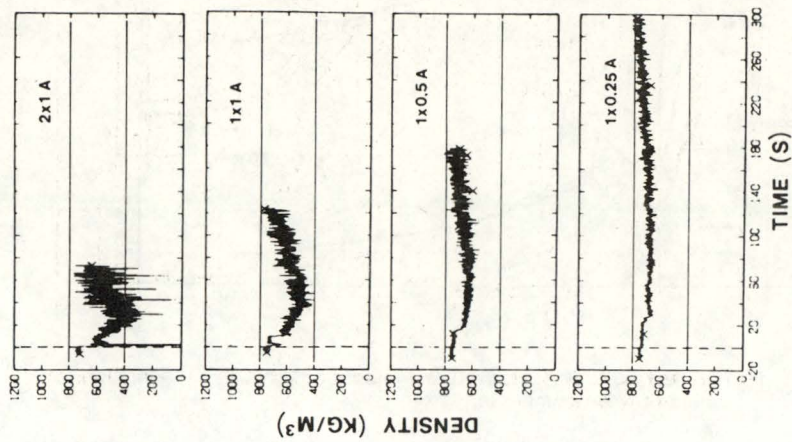


Fig. 8: Fluid Density at Core Entrance: Influence of Break Size

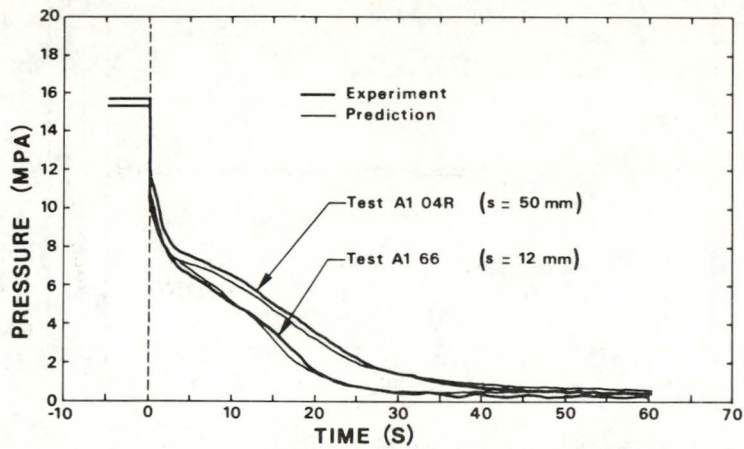


Fig. 9: Pressure in Lower Plenum: Influence of Downcomer Gap Width (s)

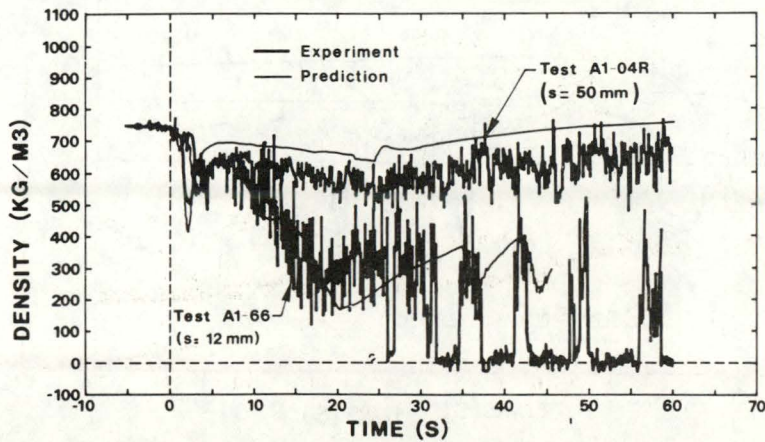


Fig. 10: Fluid Density in Lower Plenum: Influence of Downcomer Gap Width (s)



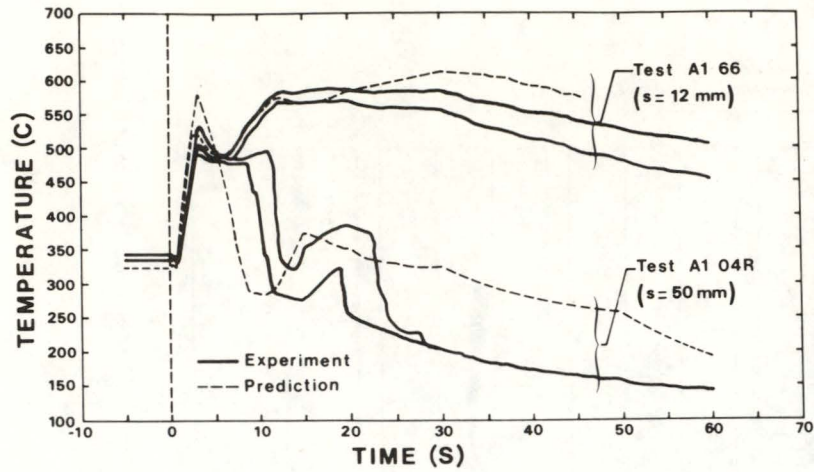


Fig. 11: Heater Rod Surface Temperatures, Middle Section of Bundle: Influence of Downcomer Gap Width (s)

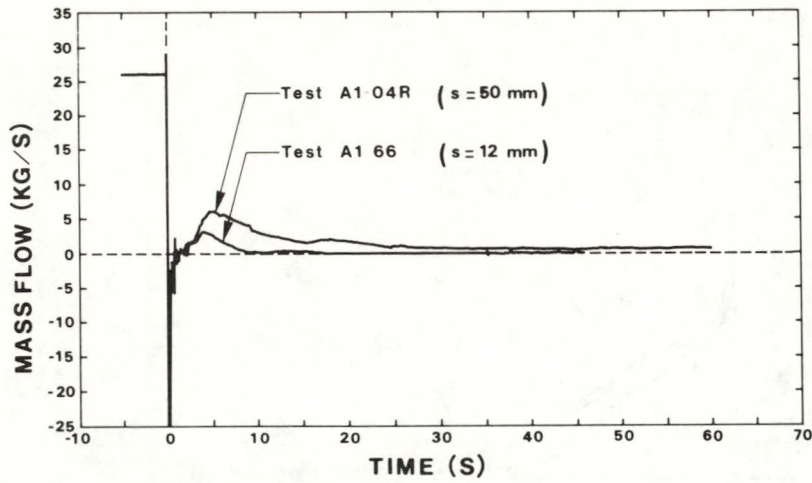


Fig. 12: Calculated Mass Flow in Core Middle Section: Influence of Downcomer Gap Width (s)

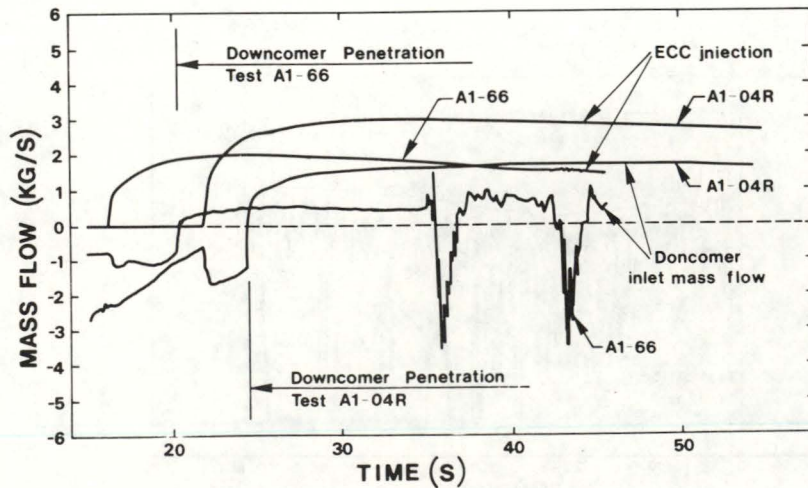


Fig. 13: ECC Injection Mass Flow and Liquid Mass Flow at Downcomer Inlet, Results of Test Predictions

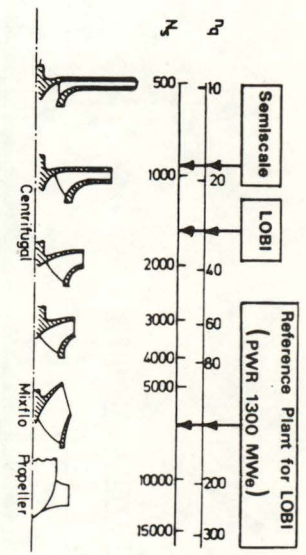


Fig. 14: Specific Pump Speeds

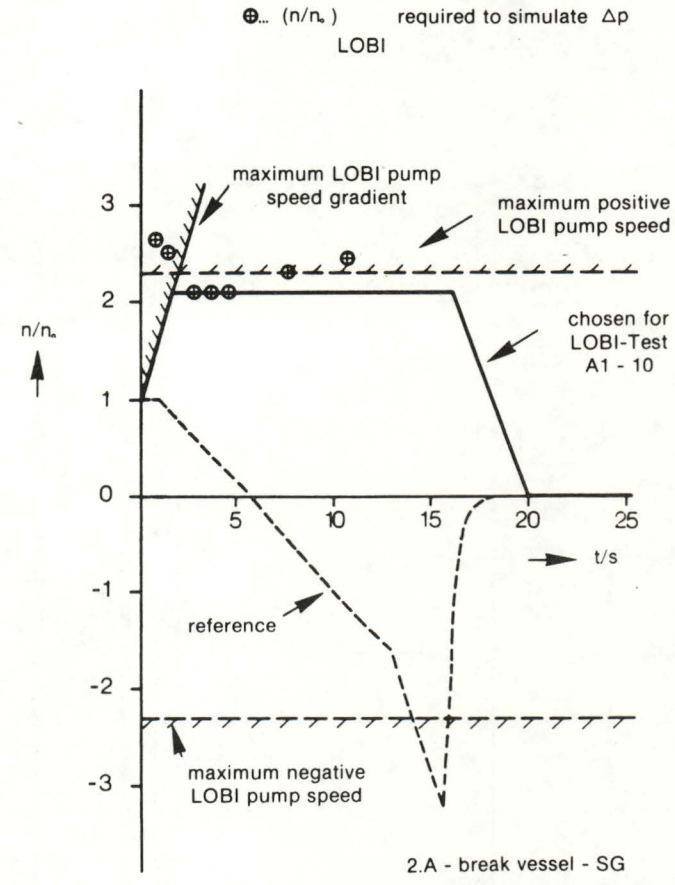


Fig. 15: Pump Speed Behaviour (Broken Loop Pump)

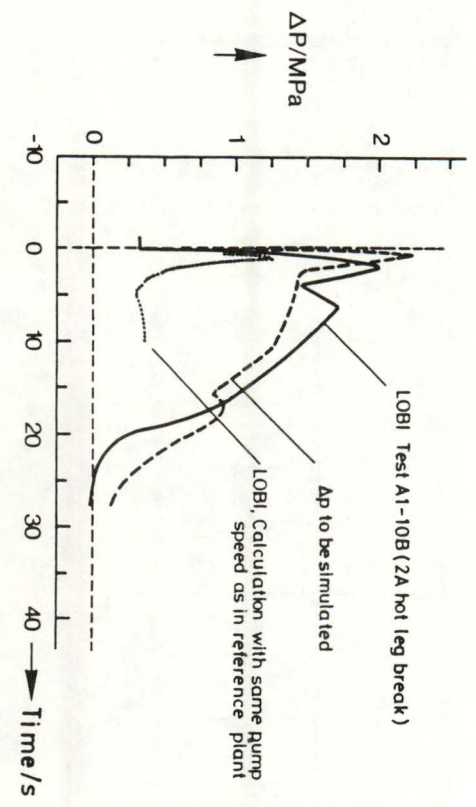


Fig. 16: Differential Pressure across Pump of Broken Loop (Comparison)

FIG. 17 **LOBI - LOCEP & - STEP PLANNING** (SEPT. 1982)

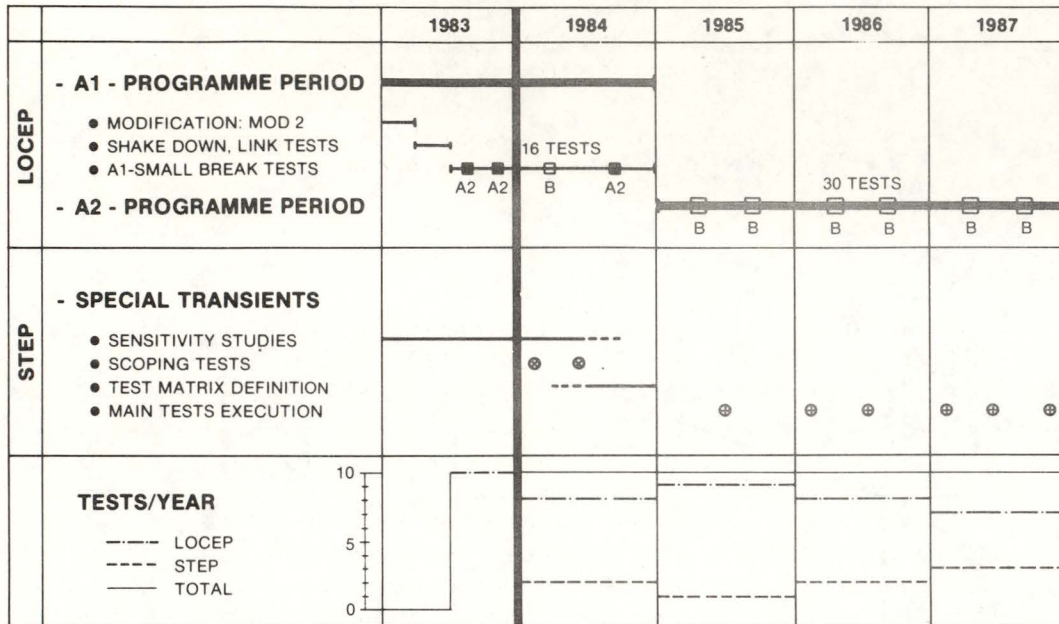


Table 2: **LOBI SMALL BREAK A1-TESTS PRELIMINARY** (1983-1984)

|                         |                  | BREAK SIZE |      |           |        |           |        |            |        |        |                     | ACCU<br>INJECTION<br>MODE |
|-------------------------|------------------|------------|------|-----------|--------|-----------|--------|------------|--------|--------|---------------------|---------------------------|
|                         |                  | 1 × 0.1A   |      | 1 × 0.02A |        | 1 × 0.01A |        | 1 × 0.004A |        |        |                     |                           |
| BREAK<br>LOCATION       | COLD             |            |      |           |        |           | X(2/4) | X(2/4)     | X(2/4) | X(4/4) | NO<br>INJECT.       |                           |
|                         | LEG              | X(2/4)     |      |           | X(2/4) | X(2/4)    |        |            |        |        | COMBINED<br>INJECT. |                           |
|                         | PRESSUR-<br>IZER |            |      |           |        |           |        |            | X(2/4) |        | NO<br>INJECT.       |                           |
|                         | Relief<br>Valve  |            |      |           |        |           |        |            |        |        | COMBINED<br>INJECT. |                           |
|                         | HOT              |            |      |           |        |           |        |            |        |        | NO<br>INJECT.       |                           |
|                         | LEG              | X(1/4)     |      |           | X(2/4) |           |        |            |        |        | COMBINED<br>INJECT. |                           |
|                         |                  | H.L.       | C.L. | H.L.      | C.L.   | H.L.      | C.L.   | H.L.       | C.L.   | H.L.   | C.L.                |                           |
| HPIS INJECTION LOCATION |                  |            |      |           |        |           |        |            |        |        |                     |                           |

A paper presented at the Tenth Water Reactor Safety Research Information Meeting, October 12-15, 1982, Gaithersburg, Maryland, USA

### ROSA-III Program for BWR LOCA/ECCS Integral Test

K. TASAKA, M. SUZUKI, Y. ANODA, H. KUMAMARU,  
H. NAKAMURA, T. YONOMOTO, M. SHIBA

Japan Atomic Energy Research Institute  
Tokai-mura, Ibaraki-ken, 319-11, Japan

#### Introduction

The Japan Atomic Energy Research Institute (JAERI) initiated the Rig of Safety Assessment Number 3 (ROSA-III) program in 1978 to conduct an integral system effect test on a Loss-of-Coolant Accident (LOCA) in a Boiling Water Reactor (BWR) to study the fundamental thermal-hydraulic phenomena during a LOCA and the effectiveness of the Emergency Core Cooling System (ECCS).

The objectives of the ROSA-III program are;

1. To study the BWR LOCA scenario comprehensively varying the test conditions on the break, ECCS and other parameters,
2. To identify any problem area or unexpected phenomena in a BWR LOCA, and
3. To provide experimental data for the computer code assessment.

#### Test Facility

The ROSA-III test facility is designed to simulate the major components and responses of the 1100-MW (electric) BWR/6 (251-848) system during a LOCA. The maximum operating pressure and the fluid temperature cover the BWR fluid conditions both in the steady state and in the transient, i.e., 9.0 MPa and 576 K (303°C).

The facility is a volumetrically scaled system of the BWR/6 and the volume of each component of the primary cooling system is scaled down to 1/424 of the corresponding volume of the BWR/6 system. The relative elevation of each component is also simulated.

The core is installed in the pressure vessel and consists of four half-length 8×8 fuel bundles heated electrically. Each fuel bundle contains 62 fuel rods and two water rods arranged in an 8×8 square array with a 16.16-mm pitch. The heated length of the core is 1880 mm and the outside diameter of the fuel rod is 12.27 mm. Each fuel rod is a sheathed electric heater with nicrome as the heater and Inconel 600 as the sheath. The maximum heat generating rate in the core is 4.2 MW.

The ROSA-III test facility has two recirculation loops. One is a broken loop and the other is an intact loop. Each loop is furnished with one recirculation pump and two jet pumps. Jet pumps are installed outside the vessel for satisfactory simulation of the volume and the height.

The facility has three different types of ECCSs, namely, the high pressure core spray (HPCS), the low pressure core spray (LPCS), and the low pressure coolant injection (LPCI) systems. The flow rate of each system is scaled to 1/424 of the BWR condition. The break device consists of two blowdown valves, one quick shutoff valve, and two orifices or nozzles. The break area can be varied by changing the size of the orifice or nozzle.

#### Schedule and Test Matrix

The BWR LOCA/ECCS integral tests were initiated in 1978 in JAERI using the ROSA-III test facility. More than sixty integral tests in nine test series have been conducted up to now. They are

- (1) Base test series (6 tests),
- (2) Single failure test series (4 tests),
- (3) Small break test series (17 tests),
- (4) Break area parameter test series (10 tests),
- (5) Double-ended test series (9 tests),
- (6) Natural circulation test series (30 tests),
- (7) Discharge line break test series (3 tests),
- (8) Steam line break test series (3 tests), and
- (9) Small break sensitivity test series (9 tests).

The three test series (5), (8) and (9) are still going on and the test program will be completed in March 1983.

#### Conclusions obtained from Test Results

The following conclusions have been obtained from the experimental analysis of the test results:

- (1) The scenario of LOCA without HPCS actuation is similar for various size breaks in the recirculation line except for the differences in the mechanism for rapid depressurization and the time span of the transients. System pressure decreases rapidly due to fall of the downcomer liquid level and uncovering of the recirculation line for break areas greater than 5% and after ADS actuation at (L1 + 120 s) for break areas less than 5%.
  - a) Lower plenum flashing (LPF) initiated at a system pressure of 6.4 MPa results in temporal recovery of core liquid level and improved core cooling.
  - b) The fuel surface dries out from top of core following the mixture level fall in the core after LPF.
  - c) The feedwater line flashes at a system pressure of 2.2 MPa slowing down the depressurization, and resulting in the temporal acceleration of core uncovering for the break areas less than 1%.
  - d) The LPCS initiated at a system pressure of 2.2 MPa rewets the low power region at the top and the bottom of the core due to falling back water from the upper plenum. The LPCS is sufficient to quench the whole core for break areas smaller than 1%.
  - e) The LPCI initiated at a system pressure of 1.6 MPa results in reflooding and quenching of the whole core.
- (2) The cladding surface temperature transient can be strongly correlated to the mixture level transient in the core.
- (3) The severest single failure assumption for core cooling is the HPCS failure irrespective of the break area for recirculation line break.

- (4) The thermo-hydraulic phenomena during a LOCA are similar for break areas greater than 85% for recirculation pump discharge line breaks and 121% for suction line breaks.
- (5) For breaks with break areas less than 85%, the thermo-hydraulic phenomena during a LOCA are similar irrespective of the break location in the recirculation line.
- (6) In a steam line break upstream of MSIV, the actuation of ECCS is delayed considerably because the upper downcomer liquid level is kept above the tripping level for ECCS for a long time due to high void fraction in the downcomer, therefore, a large part of the core is uncovered to steam environment.
- (7) For a steam line break, the cladding surface temperature transient cannot be correlated to the liquid level transient outside the core-shroud, which is monitored in a BWR.
- (8) The multi-channel effects are small on the thermal-hydraulic phenomena during a LOCA.
- (9) The peak cladding temperatures (PCTs) observed in recirculation line breaks and steam line breaks are lower than 1000 K, being well below the present safety criteria of 1473 K. The highest PCT in recirculation line breaks is 940 K observed in a 50% break. The PCT in a recirculation pump discharge line break is higher than the PCT in a suction line break with the same break area. The highest PCT in steam line breaks is 1000 K observed in a 100% break upstream of the main steam isolation valve (MSIV).
- (10) The decay heat power can be removed by natural circulation if the liquid level in downcomer is maintained above the jet pump suction level.

#### References

1. K. TASAKA, M. SOBAJIMA, M. SUZUKI and M. SHIBA: Study on the similarity between ROSA-III experiment and BWR LOCA (preanalysis of ROSA-III), JAERI-M 6703 (1976).
2. Y. ANODA, K. TASAKA, M. SUZUKI, Y. KOIZUMI and M. SHIBA: ROSA-III system description, JAERI-M 9243 (1980).
3. Y. ANODA, K. TASAKA, H. KUMAMARU and M. SHIBA: ROSA-III system description for fuel assembly No. 4, JAERI-M 9363 (1981).
4. K. TASAKA and M. SHIBA: ROSA-III program at JAERI for BWR LOCA/ECCS integral tests, proceedings of the ANS/ENS topical meeting on thermal reactor safety, April 6 ~ 9, 1980, Knoxville, Tennessee, USA, 427-435.
5. K. SODA, K. TASAKA and M. SHIBA: Boiling water reactor LOCA/ECCS integral tests at ROSA-III facility of JAERI, a paper presented at international seminar on nuclear reactor safety heat transfer, September 1 ~ 5, 1980, Dubrovnik, Yugoslavia.
6. M. SHIBA, K. TASAKA, Y. KOIZUMI and Y. ANODA: Small break LOCA experiment in ROSA-III, proceedings of the IAEA meeting on current nuclear power plant safety issues, October 20 ~ 24, 1980, Stockholm, Sweden, IAEA-CN-39/69.
7. M. SHIBA: Break area parameter test series of ROSA-III for BWR LOCA/ECCS integral tests, a paper presented at the ninth water reactor safety research information meeting, October 26 ~ 30, 1981, Gaithersburg, Maryland, USA.

8. Y. KOIZUMI, K. TASAKA, et al.: Analysis of 5% small break LOCA experiment at ROSA-III, proceedings of the ANS specialist conference on small breaks in LWRs, August 25 ~ 27, 1981, Monterey, California, USA.
9. K. TASAKA, M. SHIBA, Y. KOIZUMI, et al.: ROSA-III base test series for a large break loss of coolant accident in a boiling water reactor, Nucl. Technol. 57, 179-191 (1982).
10. K. TASAKA, M. SUZUKI, Y. KOIZUMI, Y. ANODA, H. KUMAMARU and M. SHIBA: The LOCA/ECC system effects tests at ROSA-III changing the break area as test parameter, proceedings of the international meeting on thermal nuclear reactor safety, August 29 ~ September 2, 1982, Chicago, Illinois, USA.
11. M. KATO, N. ABE, K. ITOYA, F. MASUDA and K. TASAKA: ROSA-III small break test analysis by RELAP5/MOD1, *ibid.*
12. Y. ANODA, K. TASAKA, Y. KOIZUMI, et al.: Experiment data of ROSA-III integral test RUN 912 (5% split break test without HPCS actuation), JAERI-M 82-010 (1982).
13. K. TASAKA, Y. ANODA, H. KUMAMARU, et al.: Comparison report for CSNI international standard problem 12 (ROSA-III RUN 912) JAERI-M 82-120 (1982).

---

See the additional pages for this paper, 94a, 94b, 94c, and 94d, which were submitted for publication after this report was paginated.

ROSA-III PROGRAM FOR BWR LOCA/ECCS INTEGRAL TEST

PRESENTED BY  
KANJI TASAKA

JAPAN ATOMIC ENERGY RESEARCH INSTITUTE

CONTENTS

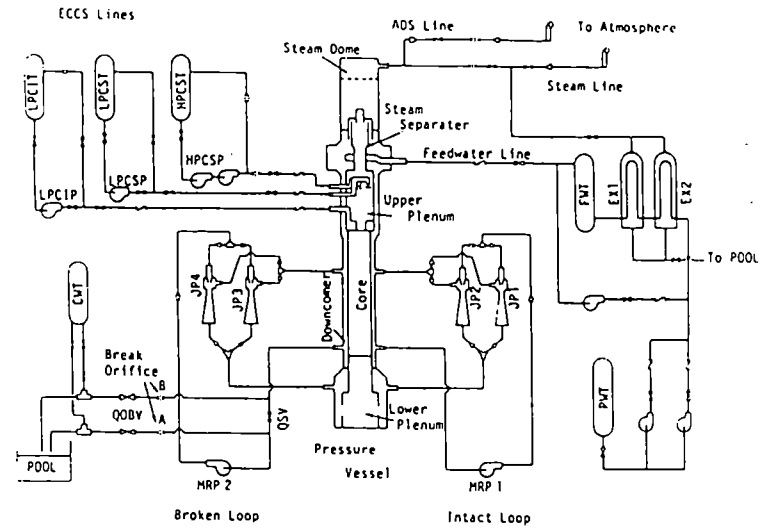
1. OBJECTIVES
2. TEST FACILITY
3. SCHEDULE AND TEST MATRIX
4. CONCLUSIONS OBTAINED FROM TEST RESULTS

OBJECTIVES

1. TO STUDY THE BWR LOCA SCENARIO COMPREHENSIVELY VARYING THE BREAK CONDITIONS, ECCS CONDITIONS AND OTHER PARAMETERS.
2. TO IDENTIFY ANY PROBLEM AREA OR UNEXPECTED PHENOMENA IN A BWR LOCA.
3. TO PROVIDE EXPERIMENTAL DATA FOR THE COMPUTER CODE ASSESSMENT.

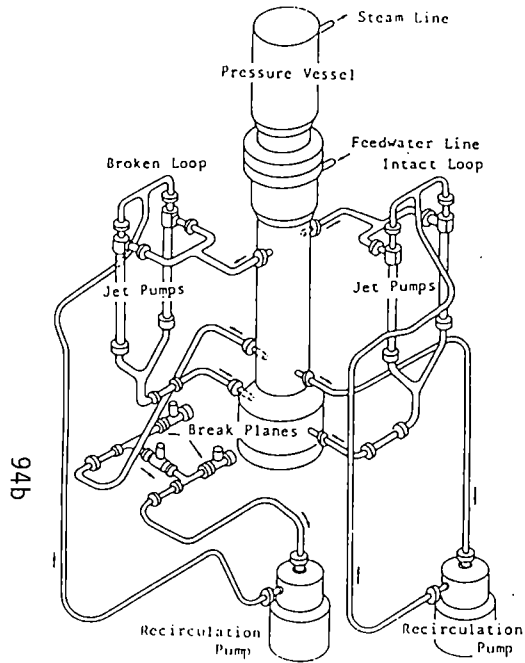
|                                | BWR/6-251 | ROSA-III | BWR<br>ROSA |
|--------------------------------|-----------|----------|-------------|
| No. of Recirc. Loops           | 2         | 2        | 1           |
| No. of Jet Pumps               | 24        | 4        | 6           |
| No. of Separators              | 251       | 1        | 251         |
| No. of Fuel Assemblies         | 848       | 4        | 212         |
| Active Fuel Length (m)         | 3.76      | 1.88     | 2           |
| Total Volume (m <sup>3</sup> ) | 621       | 1.42     | 437         |
| Power (MW)                     | 3800      | 4.24     | 896         |
| Pressure (MPa)                 | 7.23      | 7.23     | 1           |
| Core Flow (kg/s)               | 15400     | 36.4     | 424         |
| Recirculation Flow (ℓ/s)       | 2970      | 7.01     | 424         |
| Feedwater Flow (kg/s)          | 2060      | 4.86     | 424         |
| Feedwater Temp. (K)            | 489       | 489      | 1           |

ROSA-III FLOW SHEET



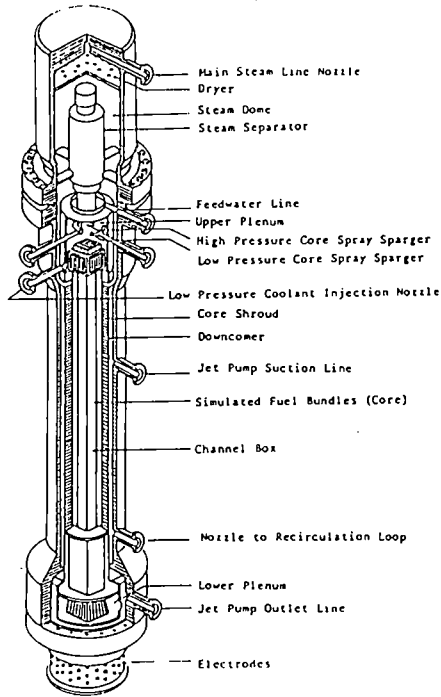


# ROSA-III Test Facility

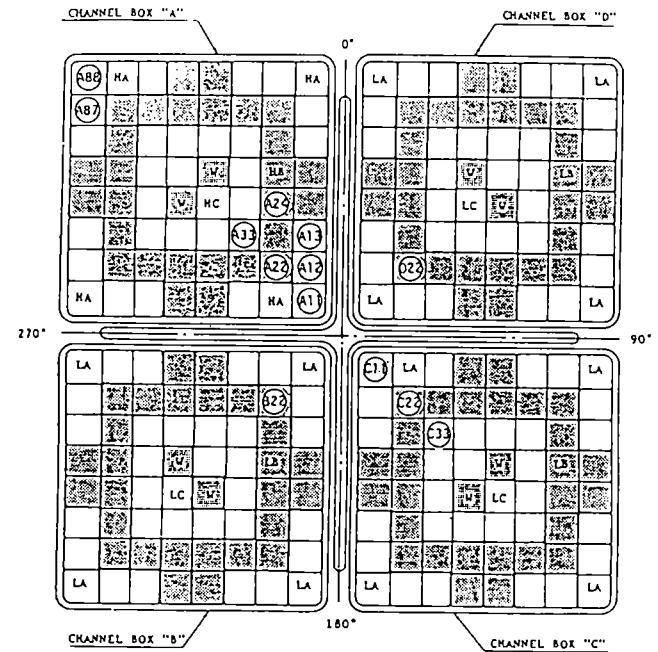


94b

# Pressure Vessel



# Core Cross Section



| Region                  | HA   | HB    | HC    | LA    | LB    | LC    | U   |
|-------------------------|------|-------|-------|-------|-------|-------|-----|
| Linear Heat Rate (kW/m) | 18.5 | 16.81 | 14.41 | 13.21 | 12.01 | 10.29 | 0.0 |
| Local peaking factor    | 1.1  | 1.0   | 0.875 | 1.1   | 1.0   | 0.875 | 0.0 |
| No. of Rods             | 20   | 28    | 14    | 60    | 84    | 42    | 8   |

\* note Radial peaking factor is 1.4

| YEAR | TEST SERIES   |
|------|---|
| 1978 | BASE TEST SERIES  |
| 1979 | SINGLE FAILURE TEST SERIES  |
| 1980 | SMALL BREAK TEST SERIES   |
| 1981 | BREAK AREA PARAMETER TEST SERIES<br>DOUBLE-ENDED BREAK TEST SERIES<br>NATURAL CIRCULATION TEST SERIES   |
| 1982 | DISCHARGE LINE BREAK TEST SERIES<br>STEAM LINE BREAK TEST SERIES<br>SMALL BREAK SENSITIVITY TEST SERIES |

## CONCLUSION 1

THE LOCA SCENARIO IS SIMILAR FOR VARIOUS SIZE BREAKS IN THE RECIRCULATION LINE EXCEPT FOR THE DIFFERENCES IN THE MECHANISM FOR RAPID DEPRESSURIZATION AND THE TIME SPAN OF THE TRANSIENTS.

|         |   |                      |
|---------|---|----------------------|
| RAPID   | DEPRESSURIZATION AFTER  | RLU IN A LARGE BREAK |
| +       |   | ADS IN A SMALL BREAK |
| 6.4 MPa | LPF - TEMPORARY IMPROVEMENT IN CORE COOLING - CORE UNCOVERING |                      |
| +       |   |                      |
| 2.2 MPa | FWF - SLOWS DOWN THE DEPRESSURIZATION                         |                      |
| 1       | LPCS - REWETS THE FUEL SURFACE AT TOP OF CORE                 |                      |
| +       |   |                      |
| 1.6 MPa | LPCI - REFLOODING - TURNAROUND - QUENCHING                    |                      |

## CONCLUSION 2

THE CLADDING SURFACE TEMPERATURE TRANSIENT CAN BE STRONGLY CORRELATED TO THE MIXTURE LEVEL TRANSIENT IN THE CORE.

Test Conditions

## Break Conditions

Position : Recirculation Pump Inlet

Area : 0,1,2,5,15,25,50,75,100,200%

ECCS Conditions : HPCS Failure

## Steady State Conditions

Steam Dome Pressure : 7.3 MPa

Lower Plenum Subcooling : 11 K

Core Exit Quality : 14 %

CONCLUSIONS :

1. THE LOCA SCENARIO IS SIMILAR FOR VARIOUS SIZE BREAKS IN THE RECIRCULATION LINE.
2. THE CLADDING SURFACE TEMPERATURE TRANSIENT CAN BE STRONGLY CORRELATED TO THE MIXTURE LEVEL TRANSIENT IN THE CORE.
3. THE SEVEREST SINGLE FAILURE ASSUMPTION FOR CORE COOLING IS THE HPCS FAILURE IRRESPECTIVE OF THE BREAK AREA FOR RECIRCULATION LINE BREAK.
4. FOR RECIRCULATION PUMP DISCHARGE LINE BREAKS WITH BREAK AREAS GREATER THAN 85%, THE THERMO-HYDRAULIC PHENOMENA DURING A LOCA ARE SIMILAR.
5. FOR BREAKS WITH BREAK AREAS LESS THAN 85%, THE THERMO-HYDRAULIC PHENOMENA DURING A LOCA ARE SIMILAR IRRESPECTIVE OF THE BREAK LOCATION IN THE RECIRCULATION LINE.
6. IN A STEAM LINE BREAK LOCA, A LARGE PART OF THE CORE IS UNCOVERED TO STEAM ENVIRONMENT DUE TO DELAY IN ECCS ACTUATION IF BREAK IS ASSUMED UPSTREAM OF MSIV.
7. IN A STEAM LINE BREAK, THE CLADDING SURFACE TEMPERATURE TRANSIENT CANNOT BE CORRELATED TO THE LIQUID LEVEL TRANSIENT OUTSIDE THE CORE-SHROUD.
8. MULTI-CHANNEL EFFECTS ARE SMALL.
9. PCT OBSERVED IN RECIRCULATION LINE BREAKS AND STEAM LINE BREAKS ARE LOWER THAN 1000 K, BEING WELL BELOW THE PRESENT SAFETY CRITERIA OF 1473 K.
10. THE DECAY HEAT POWER CAN BE REMOVED BY NATURAL CIRCULATION IF THE LIQUID LEVEL IN DOWNCOMER IS MAINTAINED ABOVE THE JET PUMP SUCTION LEVEL.

SUMMARY OF TWO-BUNDLE LOOP EXPERIMENTAL RESULTS

Masanori NAITOH, Michio MURASE

Energy Research Laboratory,  
Hitachi Ltd.  
Moriyama-cho, Hitachi, Ibaraki 316  
JAPAN

and  
Ryoosuke TSUTSUMI

Uchisaiwai-cho, Chiyodaku, Tokyo 100  
JAPAN

JOINT STUDY OF JAPAN BWR UTILITIES,  
HITACHI CO. LTD. AND TOSHIBA CORPORATION

## SUMMARY OF TWO-BUNDLE LOOP EXPERIMENTAL RESULTS

Masanori NAITOH, Michio MURASE, and Ryoosuke TSUTSUMI

BWR Loss of coolant integral tests are being conducted as a joint study program of Japan BWR utilities, Hitachi Ltd., and Toshiba Corporation. The first series of the tests, which were focused on the simulation of a recirculation line break, has been finished. And the facility is now being modified for the second series of the tests to simulate other breaks of a feed water line, a core spray line, and a drain line than a recirculation line. The second tests will start at January 1983.

This paper presents the results of the first test series. The facility (TBL-1) simulates a reference BWR/5-251 plant with 764 fuel bundles by 2 heater bundles<sup>1)2)</sup>. The TBL-1 test parameters were a break diameter, a bundle power combination, and an ECCS operation mode. A bundle power combination was mainly 4MW+6MW for the two bundles, and several tests with 4+4 MW and 5+5 MW combinations were performed. A break diameter was from 4mm(2%) to 28mm(100%) which simulated the design basis accident.

The large break test results indicated that the flow paths for falling water from the upper plenum and updraft steam from the lower plenum were separated in the two bundles after the termination of the lower plenum flashing, and that the flow separation affected rod surface temperatures<sup>3)</sup>. A simple conceptional mechanism for the flow path separation was derived from a relation of an upper tie plate and an inlet orifice CCFL characteristics. The small difference in water mass between the two bundles is thought to induce large variations in the updraft steam and falling water flow rates. From this flow path separation, heatup initiation of

rods was early and local in the bundle with much falling water and was delayed in the bundle with much updraft steam. The peak cladding temperature (PCT) was higher in the early heatup bundle even with lower power than in the delayed heatup bundle when CCFL at the bundle inlet was continued until the reflooding period. In smaller breaks, the parallel channel effect was not significant because of the low depressurization and low steam generation rates, and consequently, the thermal-hydraulic responses were similar in the two bundles. Peak cladding temperatures (PCTs) in each bundle were very much difference due to the flow path separation, when CCFL at the bundle inlets was continued until the reflooding period was reached. However, when the feed water flashing made the depressurization rate low and CCFL at the bundle inlet was broken due to a lower steam generation rate in the lower plenum, the difference of PCTs became smaller due to a weak parallel channel effect.

The peak cladding temperature in the two bundles slightly changed by the break size and it was always lower than the calculation results for the reference BWR/5-251 plant by the safety evaluation model, or the licensing code.

The fuel rod temperature was estimated from the test results with the heater rods. The bundle power was decided to simulate decay heat of a fuel bundle, which was ANS+20%, considering the difference of heat capacity. However, the actual bundle power was higher than the prearranged value due to time delay of power control system and the limit of a computer memory. And moreover, the heat transfer coefficient was very higher than the value used for the determination of the bundle power. This means that the heat flux from a heater rod was higher than the estimated value for the fuel rod. Considering these differences, the fuel rod temperature was estimated to be lower than that of the heater rod.

Reference

- 1) M.Naitoh, M.Murase, and R.Tsutsumi, "Large Break Integral Test with TBL-1 (Hitachi BWR Integral Facility)", Paper presented at the 9th Water Reactor Safety Research Information Meeting, Gaithersburg, Maryland (October 1981).
- 2) M.Murase, et. al., "Two-Bundle Loop for LWR Large-Break Integral test", Trans. Am. Nucl. Soc., Vol.41, P.390 (1982).
- 3) M.Murase, M.Naitoh, and T.Gomyoo, "BWR Loss of Coolant Integral Test : Parallel Channel Effect", Paper presented at the International Meeting on Thermal Nuclear Reactor Safety, Chicago, Illinois (1982).

Table 1 Scale of the Facility

| ITEM                            | BWR/5<br>251 | TBL    | Scale   |
|---------------------------------|--------------|--------|---------|
| Fuel Bundle                     | 764          | 2      | 2/764   |
| Power (MW)                      | 3293         | 10     | 2.3/764 |
| Fuel Rod                        | 63           | 63     | 1       |
| Water Rod                       | 1            | 1      | 1       |
| Power Distribution              | —            | Cosine | —       |
| Active Fuel Length (m)          | 3.708        | 3.708  | 1       |
| Rod Diameter (mm)               | 12.52        | 12.52  | 1       |
| Vessel Volume (m <sup>3</sup> ) | 596          | 1.55   | 2/764   |
| Operational Pressure (MPa)      | 7.0          | 7.0    | 1       |
| Operational Temperature (°C)    | 285          | 285    | 1       |

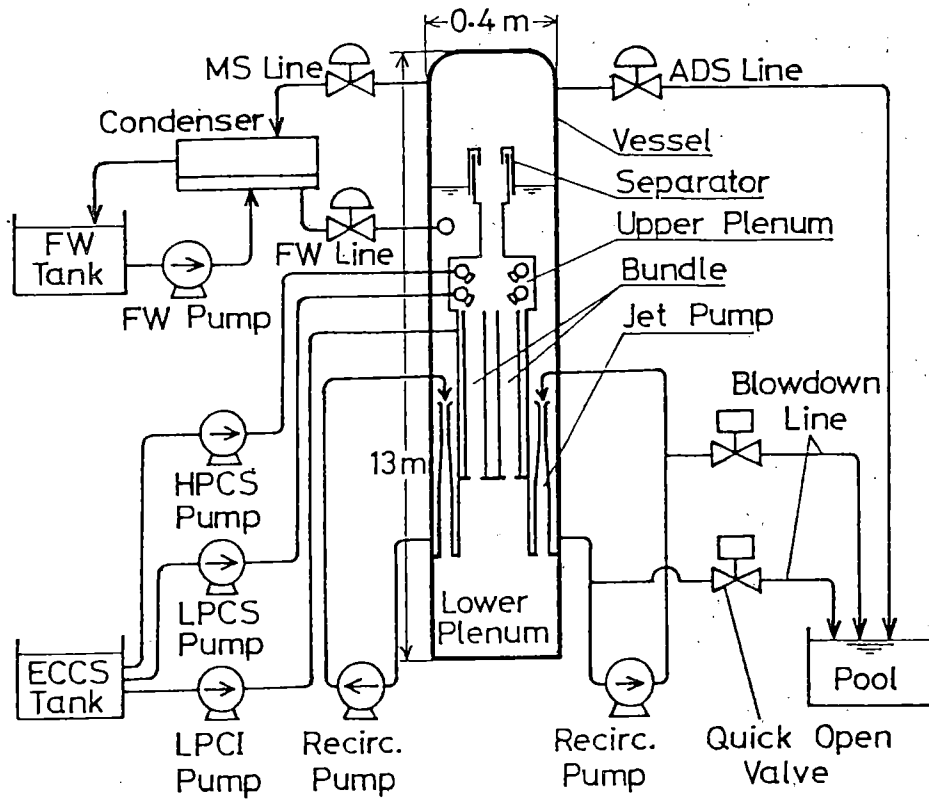


Fig.1 Facility Outline

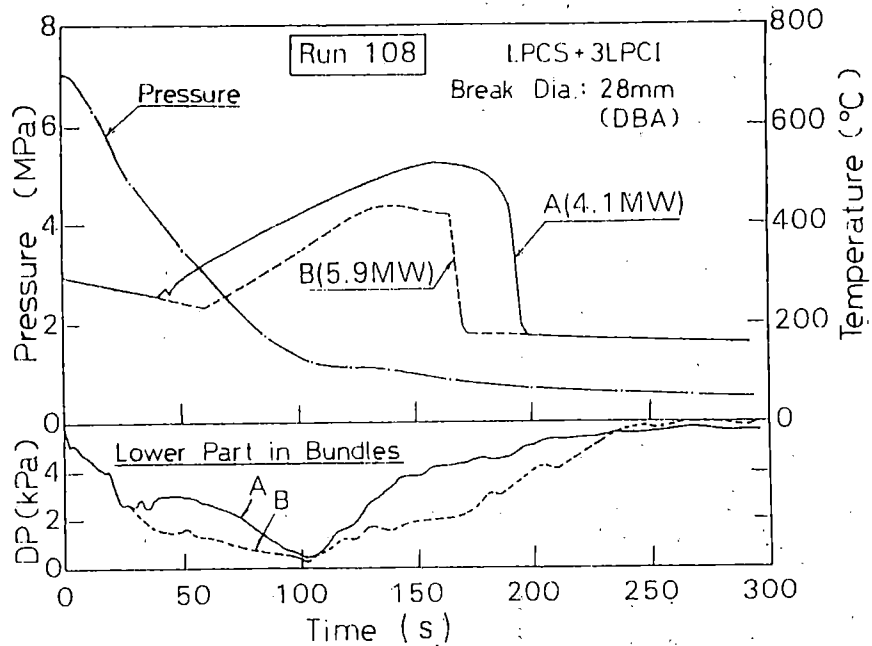
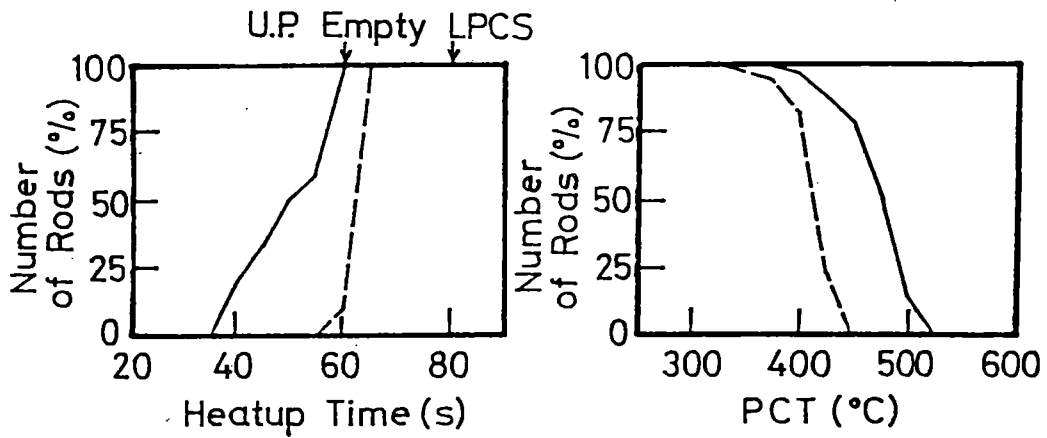


Fig.2 Difference of Rod Surface Temperatures



— Bundle-A (4.0-4.1MW), --- Bundle-B (5.9MW)

1. Run 108 (LPCS+3LPCI)



2. Run 107 (HPCS+LPCS+LPCI)

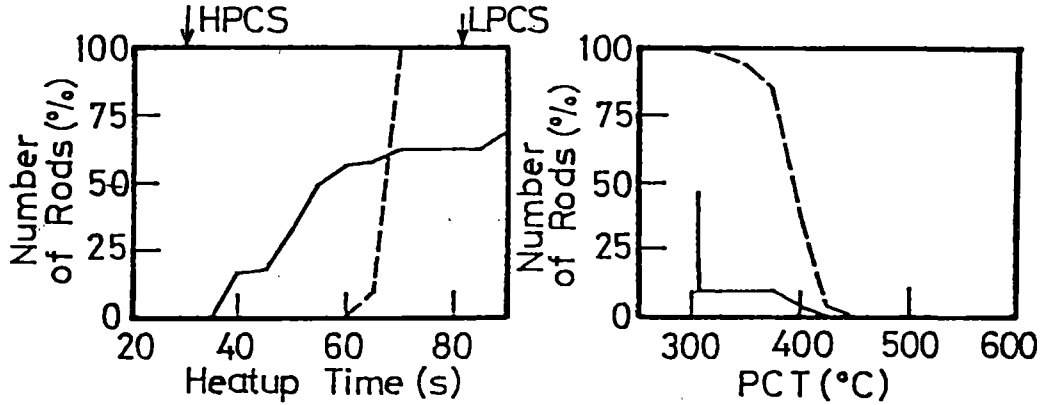


Fig.3 Heatup Time and PCT of Each Rod

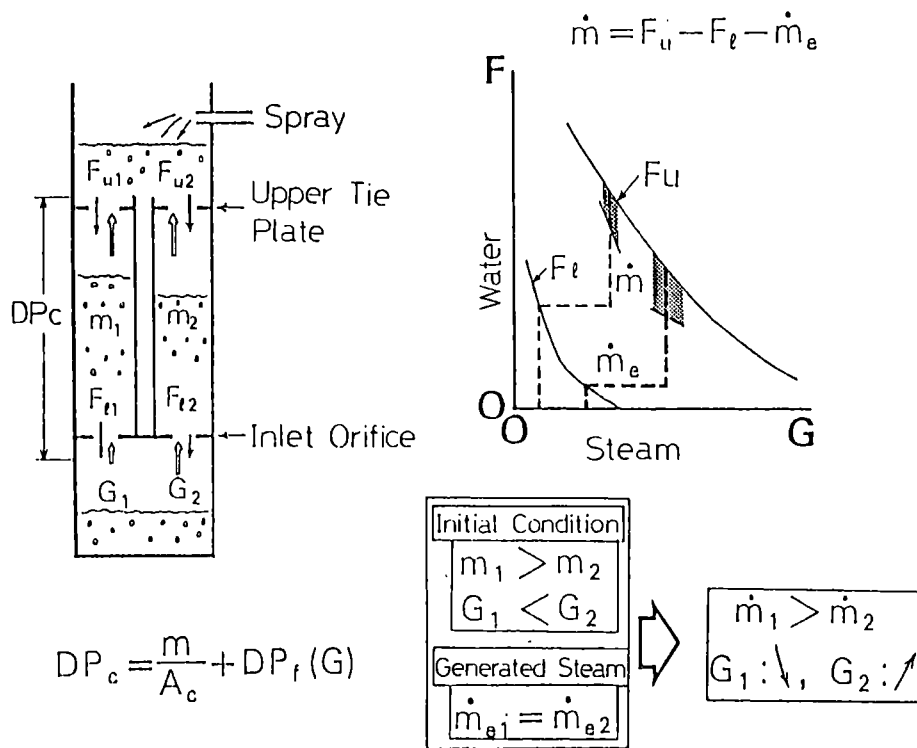


Fig. 4 Mechanism of Flow Path Separation

Table 2 Condition for Flow Path Separation

|                 |                                 | Initial Condition          |   |                            |   |
|-----------------|---------------------------------|----------------------------|---|----------------------------|---|
|                 |                                 | $m_1 < m_2$<br>$G_1 > G_2$ |   | $m_1 = m_2$<br>$G_1 = G_2$ |   |
| Generated Steam | $\dot{m}_{e1} = \dot{m}_{e2}$   | X                          | O | X                          | X |
|                 | $\dot{m}_{e1} \gg \dot{m}_{e2}$ | O                          | O | O                          | O |
|                 | $\dot{m}_{e1} > \dot{m}_{e2}$   | X                          | O | X                          | O |

O : Separation  
 X : No Separation

$\left| \frac{dF_u}{dG} \right| < \left| \frac{dF_l}{dG} \right|$

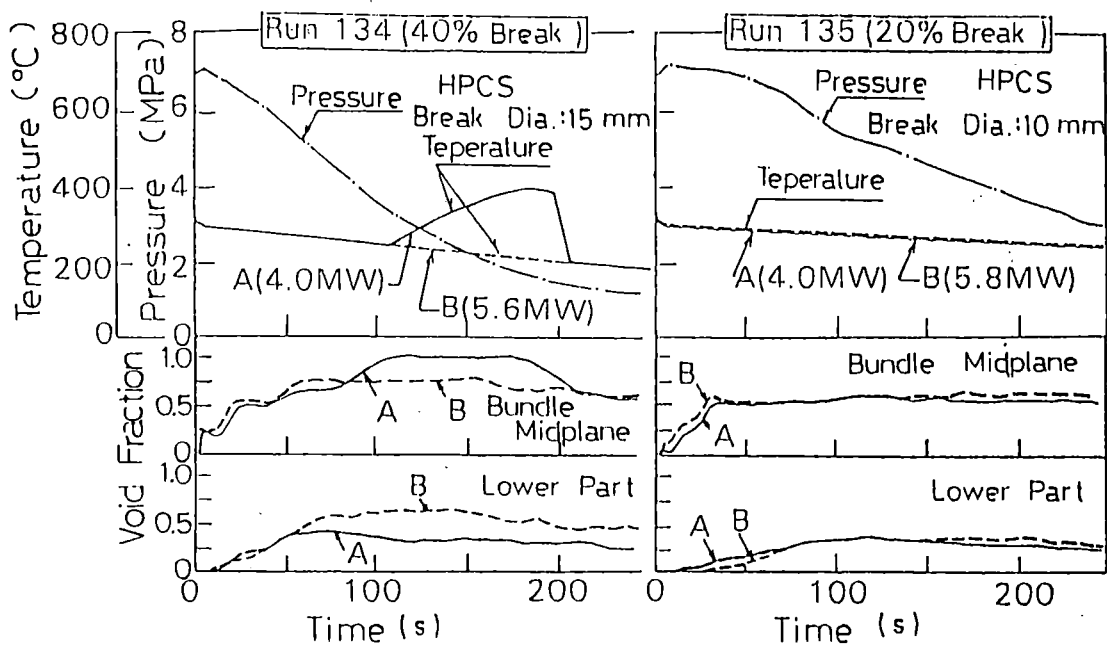


Fig. 5 Effect of Break Area

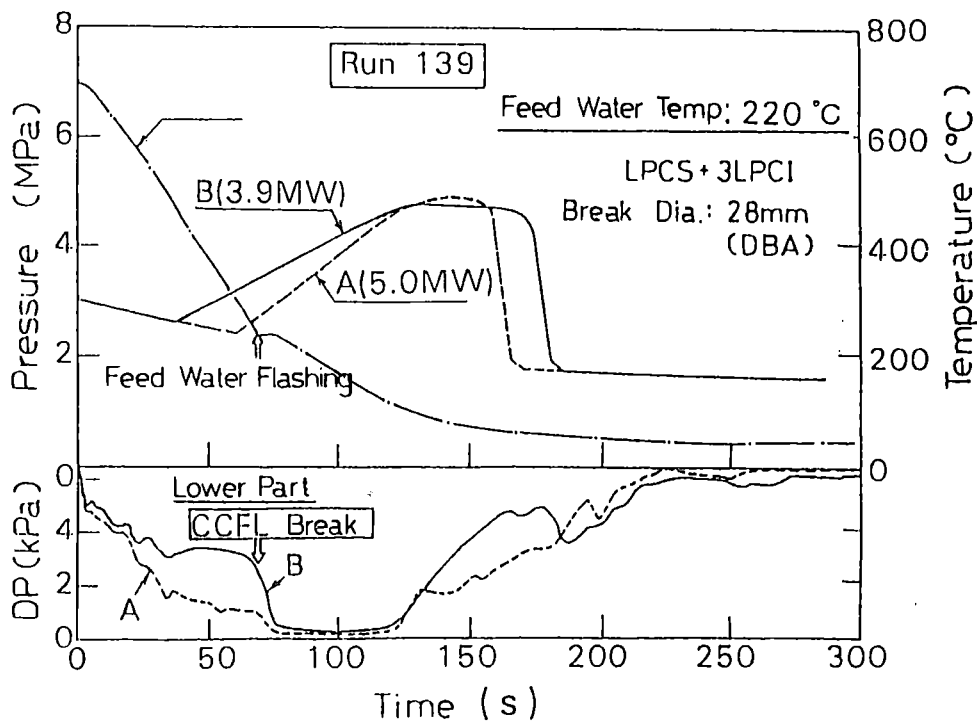


Fig. 6 Effect of Feed Water Flashing on Temperature

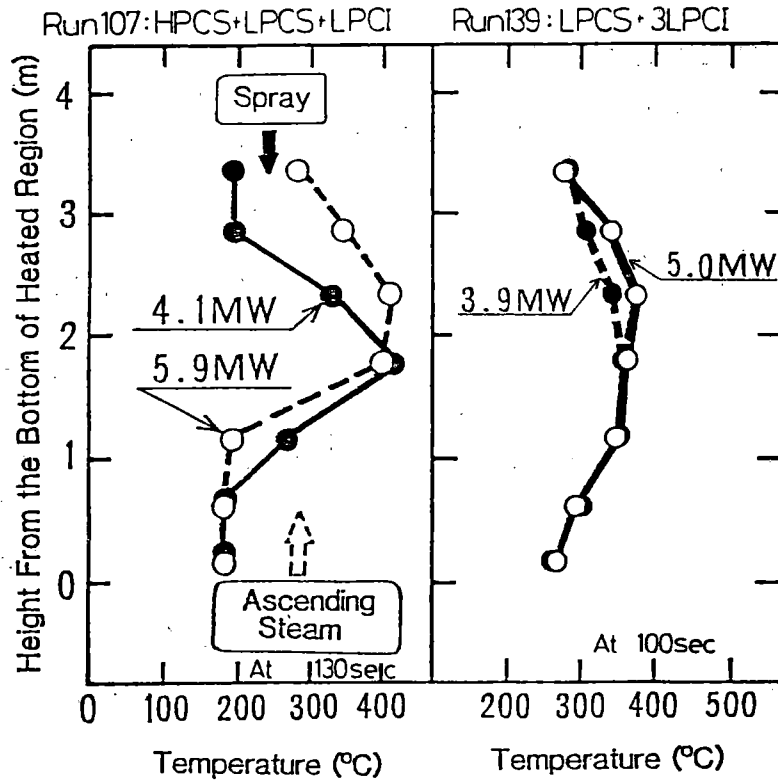


Fig. 7 Axial Temperature Distribution  
(Runs 107 and 139 : Bundle A—, Bundle B----)

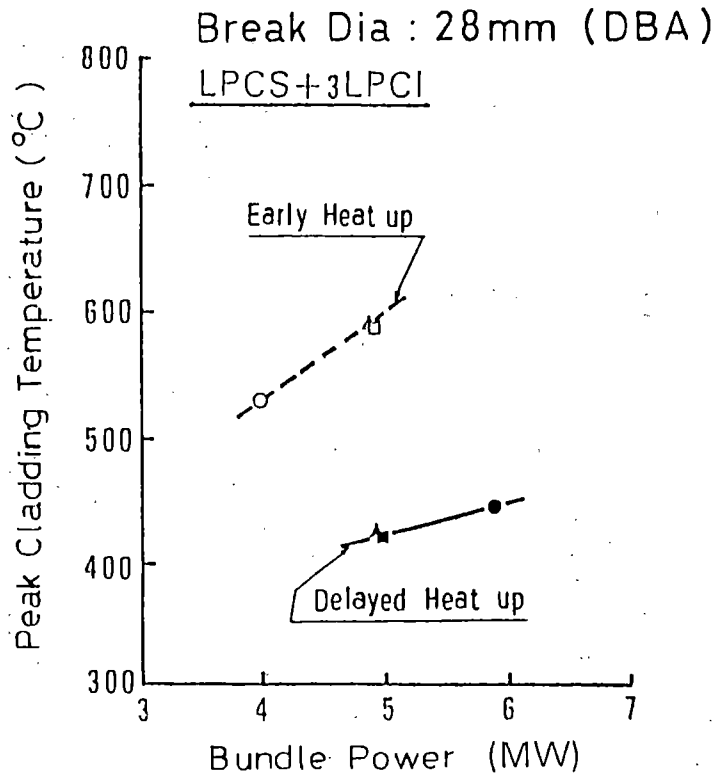


Fig. 8 Peak Cladding Temperature with Parallel Channel Effect

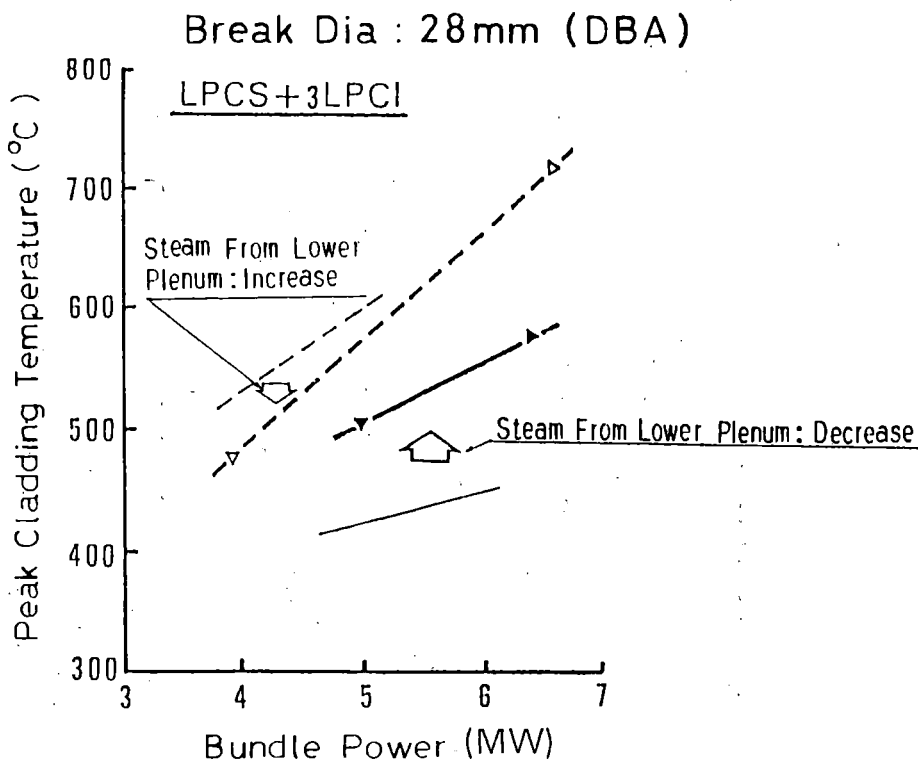


Fig. 9 Peak Cladding Temperature After Inlet Orifice CCFL Break Down

TEST RESULT

| Symbol | Power (MW) | ECCS           |
|--------|------------|----------------|
| ●—     | 4 + 6      | LPCS+3LPCI+ADS |
| —x—    | 5 + 5      |                |
| —△—    | 4 + 6      | HPCS           |

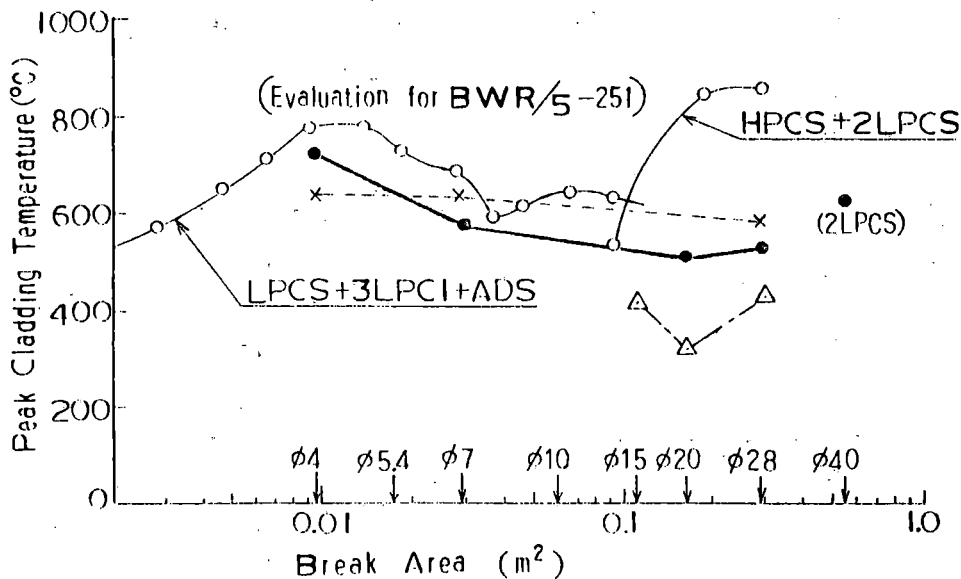


Fig.10 Effect of Break Area on P.C.T.

$$Q_{acc} = Q_g - Q_f$$

$$Q_{acc} = \rho \cdot C_p \cdot \frac{dT}{dt}$$

$$Q_f = A \cdot h(T_w - T_f)$$

Table 3 Comparison of Heat Capacity

|        |                 | Heat Capacity ( $\rho \cdot C_p$ ) |           |
|--------|-----------------|------------------------------------|-----------|
|        |                 | [J/cm $\cdot$ °C]                  | Ratio (%) |
| Fuel   | Zr-2            | 0.63                               | 23        |
|        | UO <sub>2</sub> | 2.12                               | 77        |
|        | He Gas          | 10 <sup>-5</sup>                   | 0         |
|        | Total           | 2.75                               | 100       |
| Heater | Inconel 600     | 1.79                               | 59        |
|        | Ni-Cr 5         | 0.40                               | 13        |
|        | BN              | 0.84                               | 28        |
|        | Total           | 3.03                               | 100       |

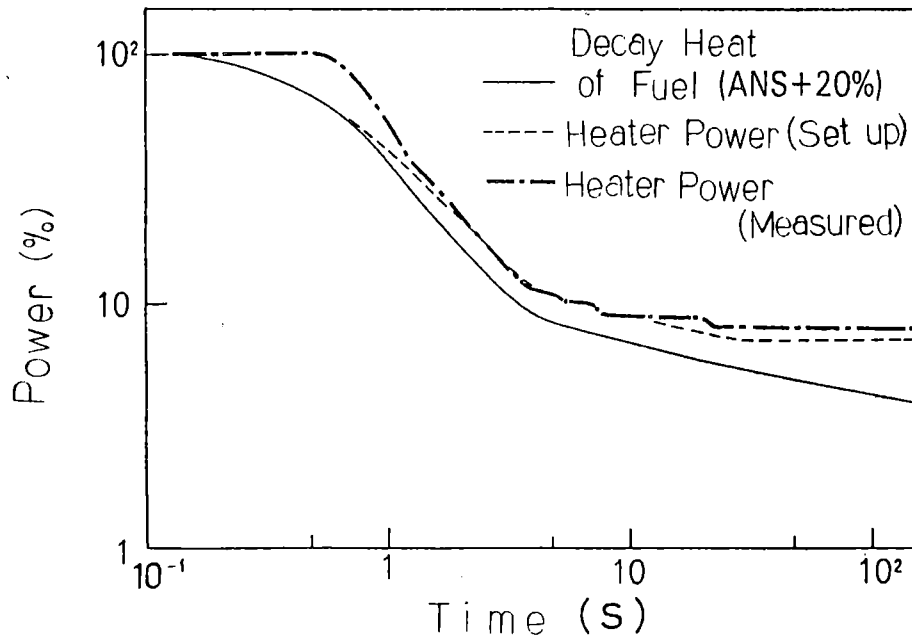


Fig II Decay Heat Simulation

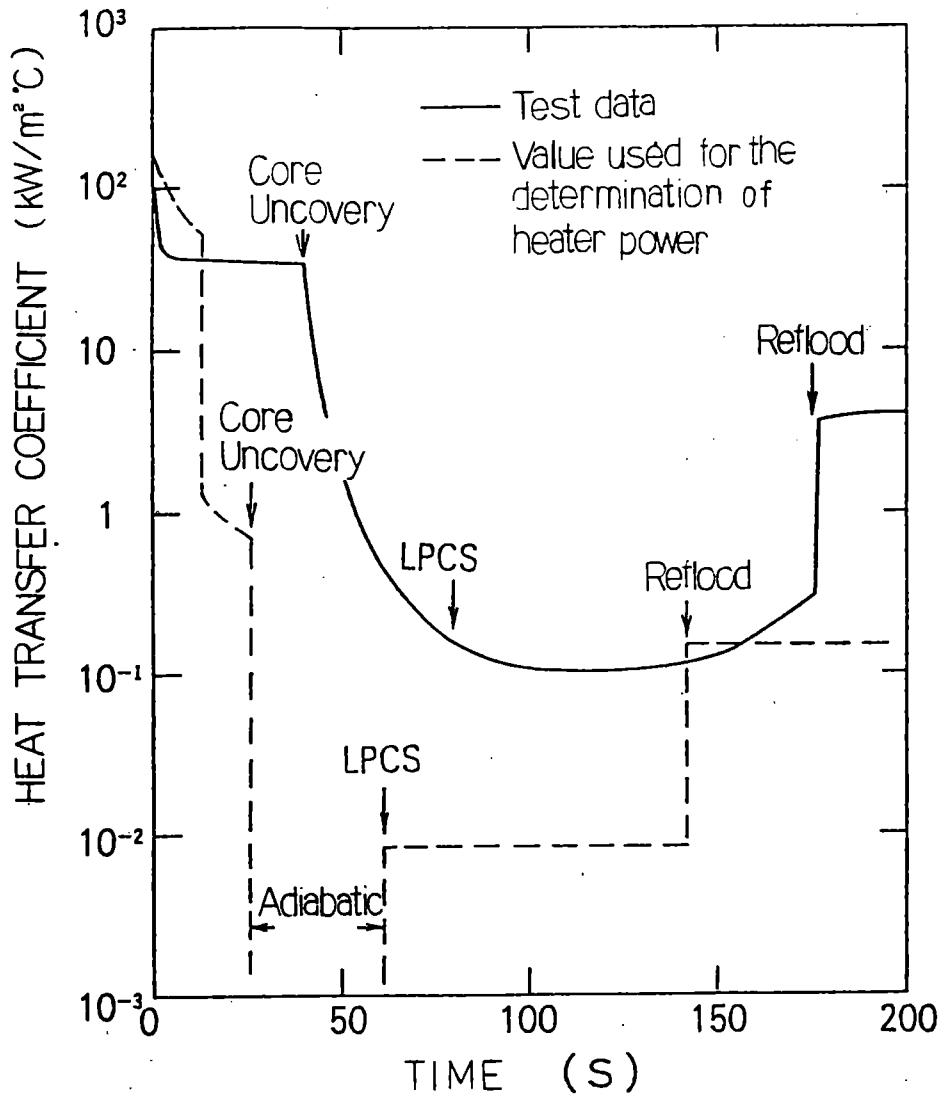


Fig.12 HEAT TRANSFER COEFFICIENT

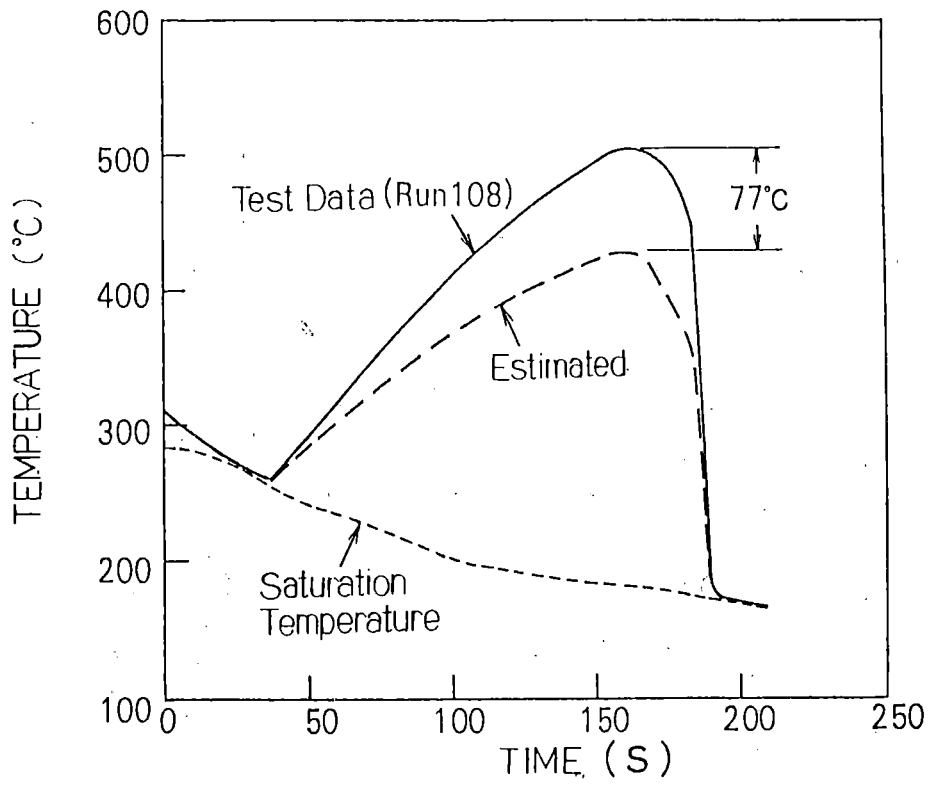


Fig.13 Estimation of Fuel Rod Temperature

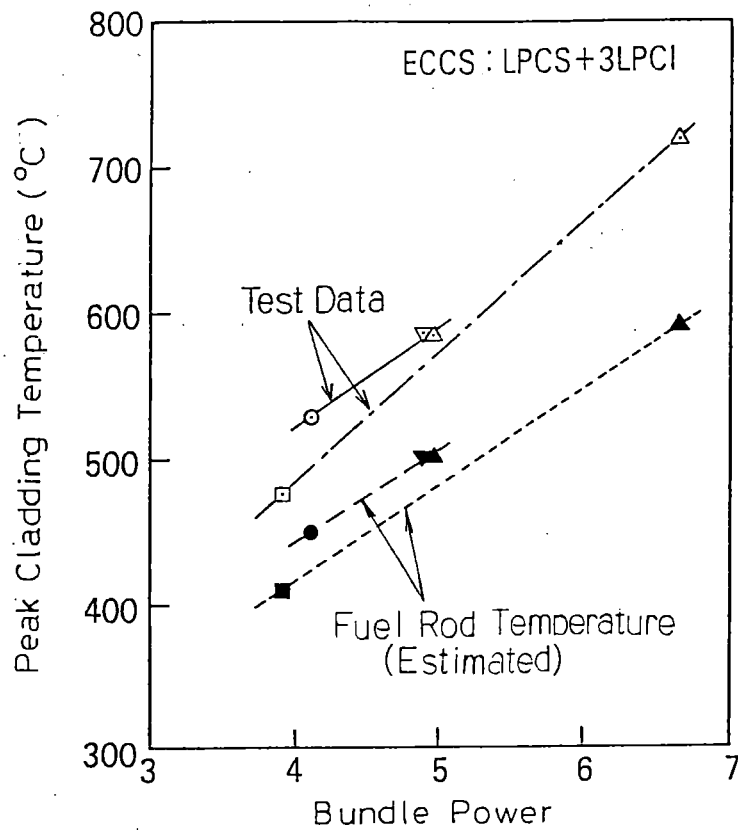


Fig.14 Estimation of Fuel Rod P.C.T.



The French integral loop,  
a joint CEA-EDF-FRAMATOME project

by

R. DERUAZ\* and J.C. MEGNIN\*\*

\* CEA-CENG

\*\* FRAMATOME

## 1. INTRODUCTION

A rather large number of nuclear plant units, PWR type, are in operation, under construction or planned in France and, consequently, the partners of the french nuclear programme CEA-EDF and FRAMATOME are closely concerned with nuclear safety problems.

With regard to the thermalhydraulic behaviour of reactors in accidental or incidental situations, several tools are currently elaborated among which mainly :

- the safety code CATHARE which is developed within the above-mentioned three-party framework and supported by a programme of analytical experiments which has been undertaken several years ago
- accidental sequence simulators which are derived from Cathare or other two phase models and aim at training operators and qualifying operation procedures

In this context and as a complement to current work in thermalhydraulics related to nuclear safety, CEA-EDF and FRAMATOME are planning to build an integral loop, which is considered to be of special interest to investigate post-accidental situations where the primary coolant is in two-phase state and during which the action of operators is likely to help the plant coming back to a safe condition.

## 2. OBJECTIVES

This integral facility is expected to play a prominent part in the improvement of PWR safety. It will in particular enable :

- to better identify and understand the successive physical phenomena occuring along the transients as well as their interaction which cannot be studied on separate effect tests.
- to assess safety codes which are needed to transpose the experimental results to reactors.

- to validate the physical bases of operation procedures
- to analyse the modifications of safeguard systems which are expected to improve the coolability of reactors
- to initiate, within a rather short time, studies related to accidents possibly occurring in the future on a power unit.

### 3. MAIN CHARACTERISTICS

#### 3.1. Reference reactor

The selected reference reactor is the CP1 FRAMATOME

PWR : 3 loops, 2775 thermal megawatts, 17 x 17 fuel bundle design.

#### 3.2. General design

The scale factor of the facility, which is issued from a compromise between economical aspects and the need for a reasonable representativity (size of the core, steam generators, piping diameter) with respect to the different situations to be investigated, will be  $f = 10^{-2}$ .

Volumes of the components and core power will be scaled by  $f$  while the scale will be 1/1 for elevations. The maximum pressure will be 170 bar at a temperature of structures close to 400°C. This couple (P,T) corresponds roughly to (120 bar, 600°C) which enables the investigation of most cases where the core is expected to get uncovered.

The number of loops will be the same as for the reference reactor (fig. 1).

The facility will be equipped with the devices through which operators can act upon the events which are taking place, which implies in particular :

- active primary pumps
- active steam generators with a good representation of secondary sides
- safety injection systems
- relief valves on the pressurizer and the secondary circuit

### 3.3. Test vessel (fig. 2)

3.3.1. The core will be cylindrical and will include 419 full length, indirectly heated, 17 x 17 geometry heater rods, together with guide thimbles. The clad, which will be made of stainless steel and insulated from the resistance elements with boron nitride, will be capable of undergoing temperatures of 1000°C. Heater rods will be designed to provide a cosine axial power profile ( $f_z = 1.5$ ).

The total power will reach a maximum value of 3MW which represents 10% of the nominal power scaled by  $f$ , and the radial distribution will be uniform ( $f_{xy} = 1$ ).

The core by-pass, which is up flow in normal operation, will be represented.

3.3.2. Nozzles will be such that the elevation of the low inner generating line of the cold leg is identical with those of the reference reactor, while the centerline will be preserved for the hot leg.

#### 3.3.3. Lower plenum :

- the volume is scaled by  $f$  but the elevation is not 1/1
- at the extent possible, the resistance coefficient will be preserved.

3.3.4. The upper plenum will not contain scaled internal structures, but provisions will be made to be able, if necessary, to modify the extent of steam-water separation in this volume.

3.3.5. Upper head : flow communications with both the downcomer and the upper plenum will be represented by calibrated orifices.

3.3.6. The downcomer will be external (tubular geometry) in order to avoid problems which are related to the use of an annular geometry for example : large thermal inertia, heat transfer from the uncovered core to the downcomer not representative, small hydraulic diameter, impossibility to preserve both volume and CCFL conditions, increase of difficulties for instrumentation.

Perforated cross-pieces will be introduced to act upon mixing between loops.

#### 3.4. Primary coolant piping

The Froude number which is generally recognized as a good criterion with respect to flow regime transitions, countercurrent flow limitation, stratified flow in horizontal pipes, will be preserved for the hot leg. This gives a diameter equal to 120 mm which is also applied to the cold and the crossover legs. The resulting distortion on pressure drop and Kutateladze number - more adequate for example for the expulsion of the water plug in the ascending part of the crossover leg - is not very large. This criterion is combined with volume scaling which determines the length of pipes.

#### 3.5. Primary coolant pumps

Pumps will be designed both to get the initial conditions of transients ( $\Delta T$  across the core in normal operation) with a reduced power, and as a tool for operators to influence cooling of the core. This leads to two operating ranges, respectively 5 to 15% and 100% of the nominal flow rate scaled by  $f$ . As far as possible diffusers will be represented as well as the whole resistance coefficient (pump off, unlocked rotor).

#### 3.6. Steam generators (fig. 3)

The main characteristics of steam generators will be :

- all elevations 1/1 with the exception of the steam dome
- volumes and heat transfer surface between primary and secondary side scaled by  $f$ . Each steam generator will contain 34 U tubes with the same inner diameter and same thickness as on the reference reactor (tests are underway to verify this last point).

Six tube heights will be provided, lying between 9 to 10.5 meters, and the arrangement of the U tubes will be such that the tube lane is well scaled.

- external multitubular downcomer to avoid a too small hydraulic diameter as it would be the case with an annular geometry.
- no moister separator-dryers : gravity separation occurs due to the low power level
- feedwater system : feedwater flow rate and temperature will be adjustable, and the circuit will include a header and quick closing valves, while provisions will be made to simulate a feed line rupture.
- steam system equipped with a header, quick closing valves, safety and relief valves with adjustable opening and closing set points.
- spray condenser capable of extracting the maximum core power

### 3.7. Pressurizer

The pressurizer will be equipped with :

- heaters and spray systems for control of pressure
- a relief circuit with safety and relief valves which set points will be adjustable
- a surge line connected to the hot leg of either the intact or the broken loop.

### 3.8. Safety injection systems

High pressure, low pressure and accumulator injection will be provided.

- HPIS :
  - . The maximum pressure will be 170 bar and water temperature will be adjustable
  - . the flow rate will be controlled by the pressure of the primary circuit in order to simulate typical conditions of the reference reactor, but the possibility will also exist to adjust its value at different levels.

- . the injection points will be located in the hot and cold legs, at the top of the downcomer, in the lower and upper plenum, at the pump seal.

- LPIS :

The same principles will be adopted for LPIS.

Actuation of LPIS will be possible at different pressures

( $P_{\max} = 20$  bar).

- Accumulators

3 accumulators will be used, volume scaled. The nitrogen pressure will be adjustable and water injected at room temperature. The injection lines will preserve the reference resistance coefficient and will include sectioning and check valves. The injection points will be located in the cold leg, the upper and lower plenum, and the downcomer.

### 3.9. Breaks (fig. 4)

The following locations are foreseen :

- small and/or intermediate breaks :

- . steam generators : main feedwater line, U tubes (external piping)
- . cold and hot legs
- . lower plenum and upper head
- . pressurizer (aspersion lines, relief valves)

- Large breaks : cold leg only

### 3.10. Incondensable gas

It will be possible to inject in the core a flow rate of incondensable gas simulating gas release in case of core uncovering.

### 3.11. Instrumentation

Two kinds of instrumentation will equip the integral facility :

- plant instrumentation with, as far as possible, the same detecting elements at the same location as in the reference reactor
- physical instrumentation allowing detailed information on thermalhydraulic phenomena occuring in the facility during the transients.

### 4. SCHEDULE

The facility is planned to be operational in 1986.



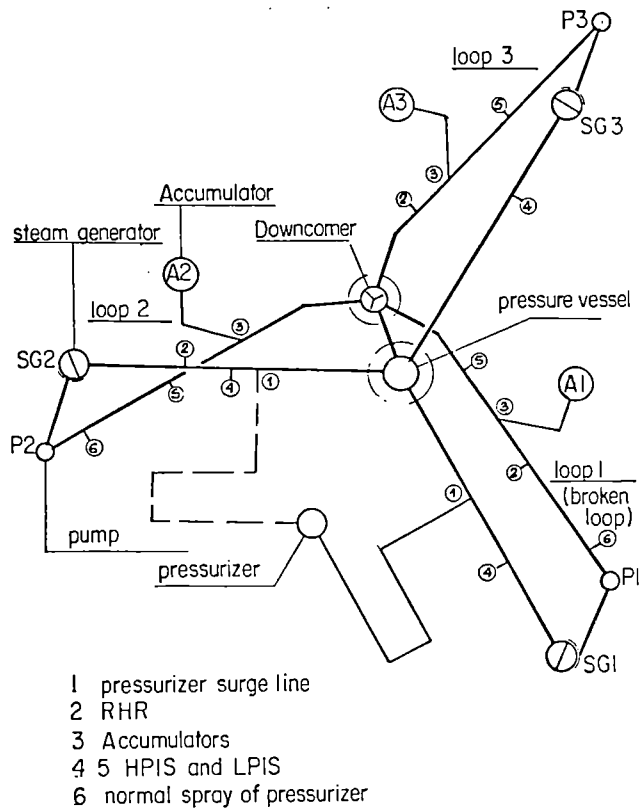


**Fig. 1 Primary coolant piping  
 Top view**

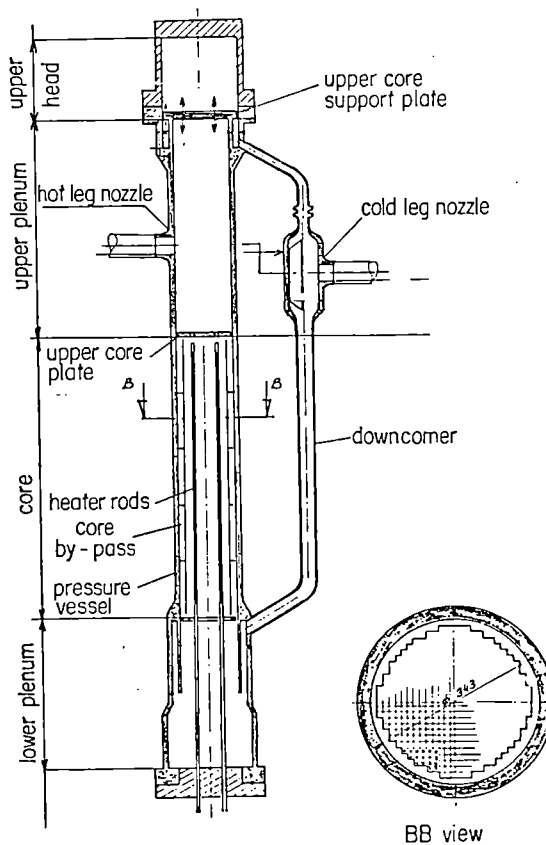


**Fig. 2 Test vessel**

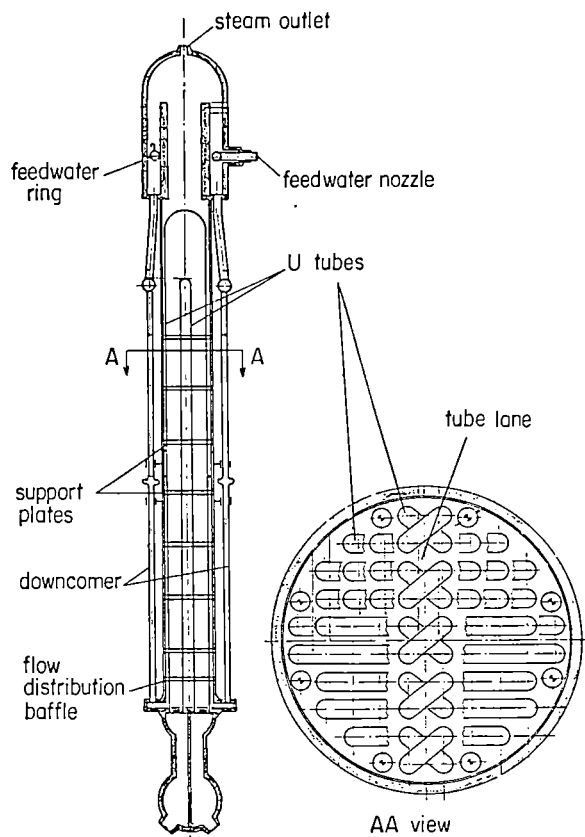


Fig. 3 Steam generator

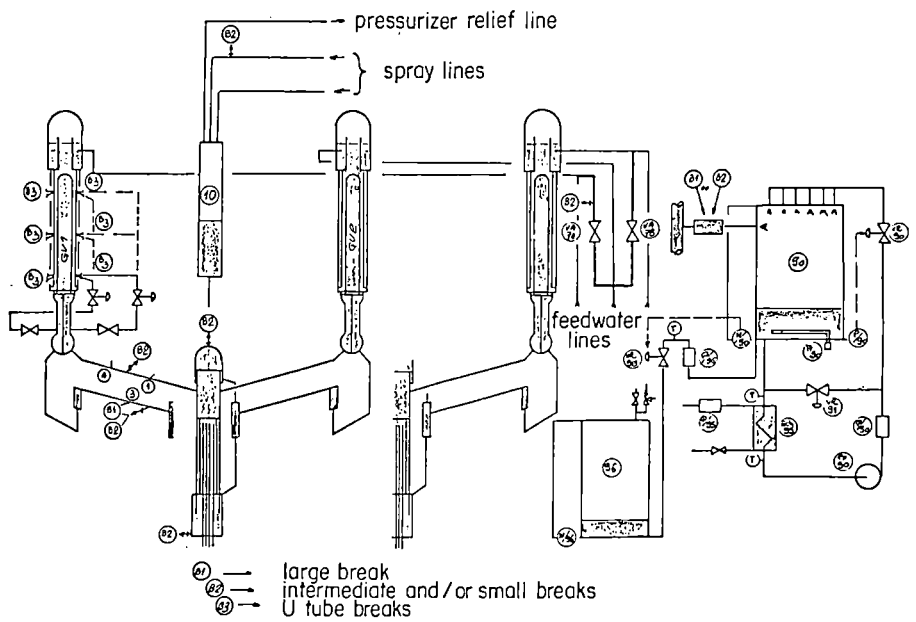


Fig. 4 Break location and flow measuring system

## SUMMARY

### 18 Degree Sector Test Apparatus (ESTA) Test Results

H. Nagasaka  
M. Katoh  
I. Onodera  
H. Aoki

TOSHIBA CORPORATION  
NUCLEAR ENGINEERING LABORATORY

#### 1. INTRODUCTION

Eighteen degree sector test apparatus (ESTA), which mocks up BWR plant, has been constructed and refill-reflood phenomena during LOCA conditions have been studied. Specifically, the main concern of this study is to clarify how CCFL and CCFL breakdown phenomena at various flow restricted components affect the refill-reflood phase. The objective of this study is to confirm the conservatism of current safety evaluation models and to present the data base for best estimate code qualification and verification.

This paper deals with separate effects tests of CCFL and CCFL breakdown phenomena at the upper tie-plate (UTP).

#### 2. TEST FACILITY

ESTA is full height from jet pump bottom to standpipe top and main components within shroud are cut into an 18° sector. Lower plenum, guide tube and jet pump regions have scaled volumes. ESTA is an atmospheric facility. Steam generation is simulated by steam injection from a boiler. Steam is injected into each bundle, bypass, lower plenum and steam dome. As to core and bypass, radial steam profiles are simulated. ESTA uses a saturated water line to establish initial upper plenum (UP) two-phase mixture conditions. All ECCS, that is, high pressure core spray (HPCS), low pressure core spray (HPCS) and low pressure coolant injection (LPCI) are included. ESTA has 0.8(m)X1.5(m) UP windows to observe

and to record UP two-phase thermohydraulic behavior.

Key measurements for the understanding of CCFL and CCFL breakdown phenomena at UTP are UP pressure, UP collapsed levels, UP temperature distribution, UTP temperature transients, bypass temperature distribution and bundle drainage rates.

### 3. TEST RESULTS AND DISCUSSION

#### 3.1 Multi-bundle UTP CCFL characteristics

ESTA multi-bundle UTP CCFL characteristics tests were conducted by injecting steam into the bundles and supplying saturated water into the UP, with bypass filled with saturated water. CCFL bundle drainages agreed with Wallis type correlation, derived from the single bundle tests.

#### 3.2 Spray Water Temperature Effect on CCFL Breakdown Phenomena

To examine spray water temperature effect on CCFL breakdown phenomena, tests were conducted by varying spray water temperature. Test procedure was first to inject steam into the core and to supply saturated water into the UP using the saturated water line, with bypass filled with saturated water. After steady two-phase mixture level was built up in the UP, saturated water supply was stopped and then spray was initiated.

For higher spray temperature test, UP  $\Delta P$  increased further after spray initiation. Therefore more liquid collected in the UP. For lower spray temperature test, UP  $\Delta P$  decreased and became oscillatory due to CCFL breakdown associated with the accumulation of subcooled water on peripheral bundle region. CCFL breakdown occurred at predominantly at peripheral bundles. The other central bundles still remained in CCFL condition.

#### 3.3 UP Collapsed Level Oscillatory Phenomena

To clarify UP collapsed level oscillatory phenomena, associated with CCFL breakdown, the most typical test showing this oscillation is to be explained. In this test, UP was initially empty and bypass filled with saturated water. Under this conditions, subcooled water was sprayed into the UP, while steam was injected into the core.

At spray initiation, spray was exposed to steam environment and its heat absorption efficiency was high so that nozzle neighboring temperature was relatively high and UTP temperature almost saturated. Hence, two-phase mixture level increased due to CCFL, and nozzle neighboring temperature decreased due to spray drops travelling a shorter distance in the steam environment. When the two-phase mixture level reached the sparger level, spray was basically injected into a liquid continuous two-phase mixture. That shielded the subcooled liquid from the steam and allowed the UTP to become subcooled. CCFL breakdown then occurred and the spray was again exposed to steam environment, thus  $UP \Delta P$  became oscillatory.

### 3.4 LPCI Effect on CCFL Breakdown Phenomena

To examine LPCI effects on CCFL breakdown phenomena, HPCS and HPCS+LPCI operation tests were conducted. For both tests, UP was initially filled with two-phase mixture. For HPCS+LPCI test, bypass water was drained from the bottom of the bypass at a rate equal to the LPCI flow, while for HPCS test the bypass bottom was closed. The leakage paths between bundles and bypass were blocked.

For HPCS+LPCI operation, CCFL breakdown occurred due to peripheral bundle steam condensation effect across the fuel bundle channel walls, whereas for HPCI operation breakdown did not occur appreciably. CCFL breakdown occurred at predominantly at peripheral bundles. The other central bundles still remained in CCFL condition.

## 4. CONCLUSION

- (1) Multi-bundle UTP CCFL characteristics agree with Wallis type CCFL correlation, consistent with single channel test results.
- (2) The minimum spray subcooling to produce CCFL breakdown ranges between 40(K) and 60(K) for the typical BWR conditions of these tests.
- (3) Interactions between spray condensation and CCFL breakdown retain a uniform liquid pool in the upper plenum that slowly oscillates near the spray injection elevation.
- (4) LPCI promotes CCFL breakdown due to peripheral bundle steam condensation effect across the fuel bundle channel walls.
- (5) CCFL breakdown occurs predominantly at peripheral bundles. The other central bundles still remain in CCFL condition.
- (6) Peripheral bundle drainage rates after CCFL breakdown are much higher than CCFL controlled drainage rates.



---

PKL SYSTEM EFFECTS TEST  
- STATUS OF PKL II TESTS -

---

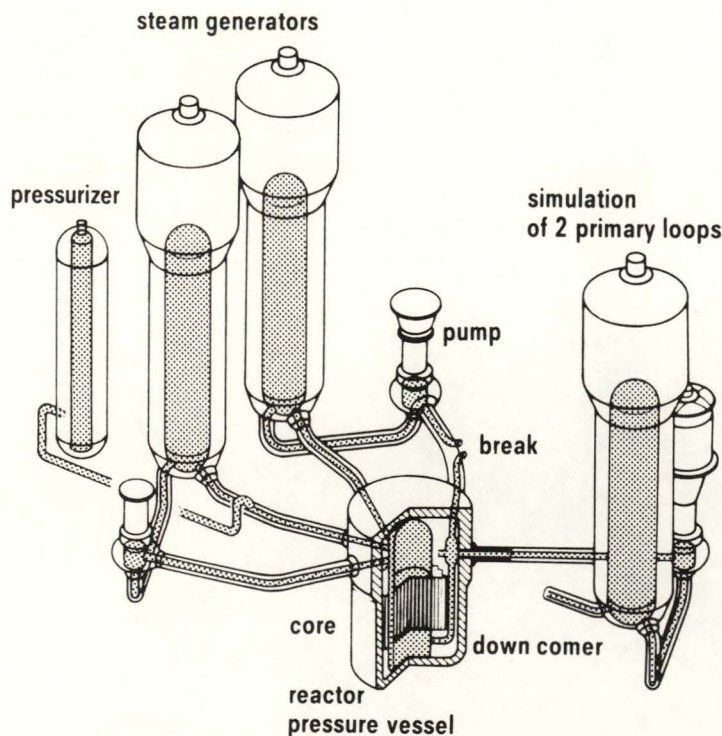
B. BRAND, H. LIEBERT, R. MANDL, J. SARKAR  
KRAFTWERK UNION AG, ERLANGEN

## 1. Introduction

The PKL test facility (fig. 1) is a scaled down model of a 1300 MWe KWU PWR primary system for the investigation of the low pressure phase of a LOCA. The PKL system represents all primary components including reactor pressure vessel, downcomer and 3 loops with steamgenerators and pump simulators. The design pressure of 40 bar allows to simulate large break LOCA conditions including the End-of-Blowdown Phase and the Refill/Reflood Phase so that the accumulator injection at 26 bar can be simulated. Due to the high pressure level, also an interesting phase during a small break LOCA, can be investigated. As already reported in previous presentations several test series had been performed by the simulation of

- Refill/Reflood behaviour of a PWR system under large break conditions (PKL IA/IB) /1/
- Steady state and transient conditions of a small break LOCA (PKL IC/ID) /2/ and
- End-of-Blowdown phase for a large break /3/.

A first scoping test was carried out to investigate the test procedure. This test demonstrated the cooling capability of the hot side injected water for a cold leg break transient (combined injection ECC system) and stimulated the plans to include the EoB-phase already in the PKL II test series.



### PKL - Systems Effects Tests:

- interplay between components
- code verification

|                 | PWR   | PKL          |
|-----------------|-------|--------------|
| number of rods  | 45548 | 314 (+ 26)   |
| volume scale    | 145   | 1            |
| elevation scale | 1     | 1            |
| primary loops   | 4     | 2 + 1 double |
| ECC - injection | 8     | 4 + 2 double |

PKL Simulation of 4 - Loop PWR

Fig. 1

After these tests the facility was modified for blowdown requirements, a new test bundle was installed and the instrumentation and data acquisition capacities were increased.

Within the international cooperation on reactor safety research between the US, Japan and Germany (known as 2D/3D agreement) additional instrumentation supplied by US-NRC was also installed to increase the experience with newly developed instruments (under low pressure refill/reflood conditions) for the 2D/3D program.

In a shakedown period for PKL II, terminated in August this year, several refill/reflood tests were performed to check the instrumentation behaviour. The test data have not yet been evaluated completely but some results related to instrumentation behaviour will be presented.

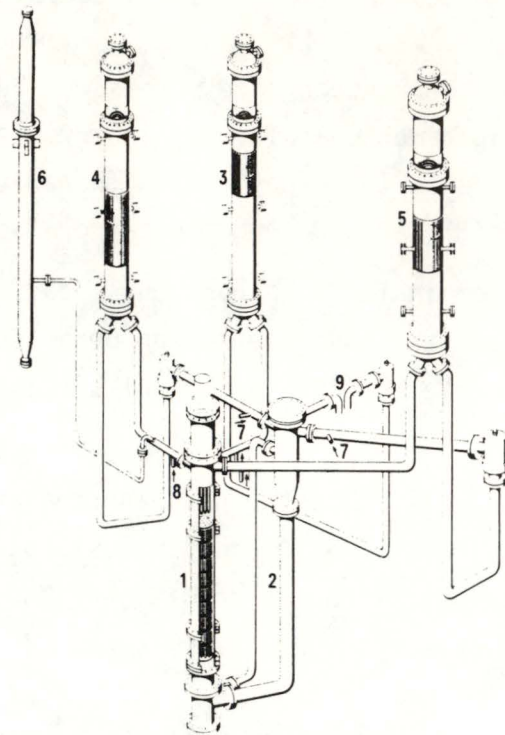
The major goal of the PKL II series will be tests including the end-of-blowdown (EoB) phase with test parameters which will be geared to Best Estimate conditions while PKL I tests were oriented towards licencing conditions. The test procedure will be discussed later on in this presentation.

## 2. PKL System Modifications

As in all LOCA test facilities specific scaling laws have to be observed such as:

- all elevations in scale 1:1 to account for effect gravity
- heat transfer in core and steam generator (SG) within original geometries and the same specific values (e.g. power density)
- reduction of the core dimensions (power scaling) requires equivalent volume scaling which in the case of PKL II is 1:145 (1:12 in diameter; figure 2)
- friction pressure losses should be kept similar
- relation between heat capacity of structures and primary fluid should be as close as possible.





- 1 Pressure Vessel
- 2 Downcomer
- 3 Steam Generator 1 (Broken Loop)
- 4 Steam Generator 2 (Intact Loop)
- 5 Steam Generator 3 (Double Loop)
- 6 Pressurizer
- 7 Cold Leg ECC Injection
- 8 Hot Leg ECC Injection
- 9 Cold Leg break

Reactor: 1300 MWe Standard

Elevation Scaling: 1 : 1

Volume and Power Scaling: 1 : 145

| Component             | Volume [m <sup>3</sup> ] | Scaling Ratio |
|-----------------------|--------------------------|---------------|
| Core                  | 0,196                    | 1 : 127       |
| Downcomer             | 0,257                    | 1 : 122       |
| Lower Plenum          | 0,152                    | 1 : 134       |
| Upper Plenum          | 0,428                    | 1 : 137       |
| Steam Generator       | 0,590                    | 1 : 159       |
| Pressurizer           | 0,512                    | 1 : 131       |
| Loops                 | 0,598                    | 1 : 192       |
| <b>Primary System</b> |                          |               |
| ● without Pressurizer | 2,364                    | 1 : 151       |
| ● with Pressurizer    | 2,876                    | 1 : 148       |

**PKL II Test Facility – Volume Scaling**

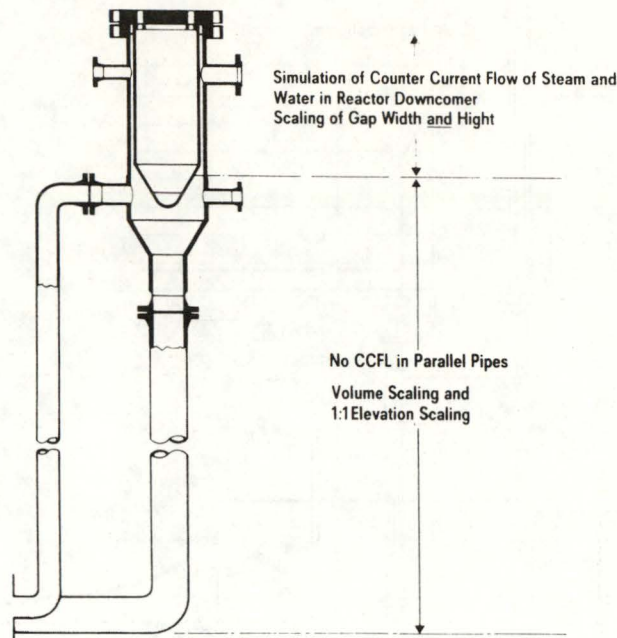
Fig. 2

In order to correctly simulate flow rates and stagnation points in the system including the blowdown phase, the volumes of all components had to be scaled more accurately.

This required some significant modifications:

- reduction of lower plenum volume
- increase of upper plenum volume (upper head)
- separation of the annular downcomer gap (available in PKL I as an option)

An important component for the system behaviour - namely the downcomer - had to be closely investigated. A purely geometrical reduction of the reactor downcomer would lead to an annular downcomer gap width of 22 mm. In this case pressure losses and structural heat release would deviate by a factor of 12 from the desired values. An external pipe downcomer is able to simulate this much better but would disproportionately promote the limitation of counter current flow (CCFL) of steam (up) and water (down). Therefore the PKL II downcomer configuration (fig. 3) is



Simulation of Downcomer in PKL II  
- CCFL and Volume Scaling -

Fig. 3

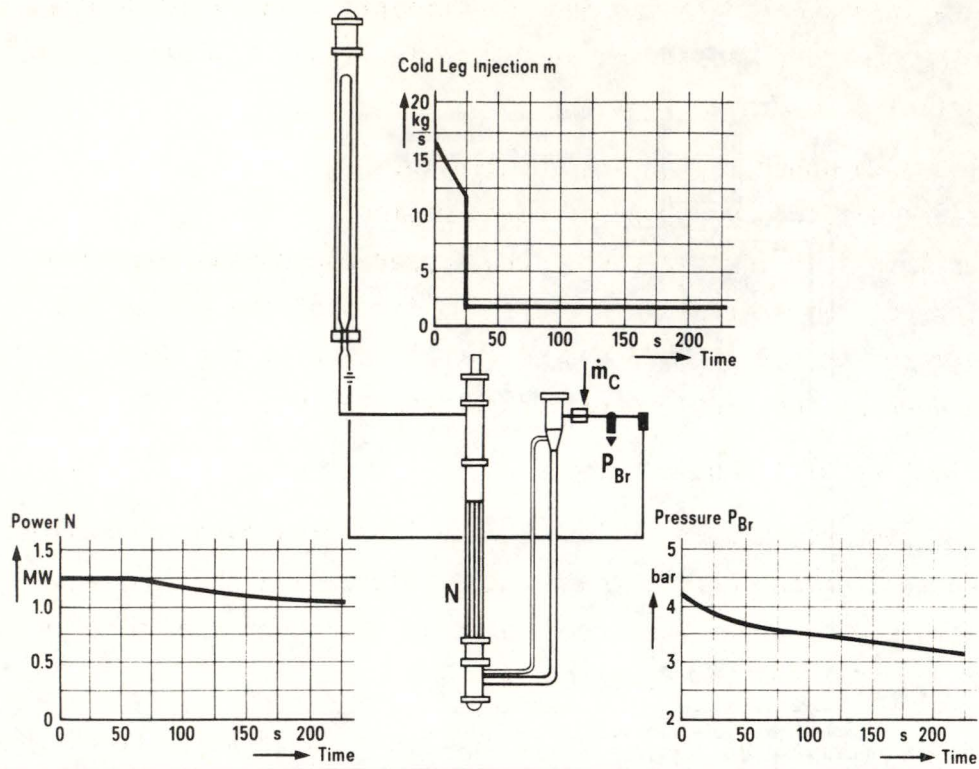
split in 2 zones. The lower part with two parallel pipes simulates correctly pressure losses, heat release, volume and vertical elevation but underestimates CCFL. The upper part consisting of a vessel and a filler piece with an annular gap of 22 mm simulates the CCFL behaviour of the whole downcomer. Following results of Battelle Columbus /4/ the gap length of the downcomer must be also reduced when it's width is reduced. So a gap width of 22 mm requires only a length of about 600 mm. This was the basis for the PKL II downcomer design.

### 3. Experience with Instrumentation in a PKL II Shake Down Test

As mentioned the shake down tests were carried out under low pressure conditions, simulating only the Refill/Reflood phase of a large break LOCA. Test II A-9 simulated test conditions of a 200 % cold leg break with cold side injection.

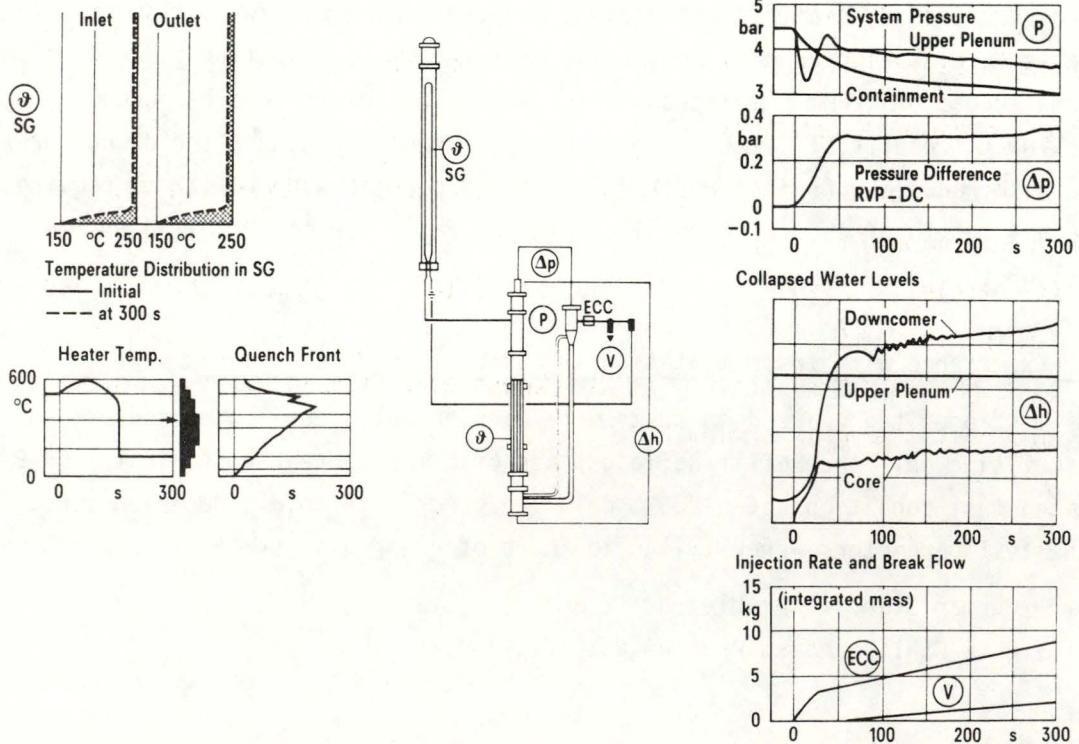
The test parameters were similar to those of run K 9 in series I B which was the

- German Standard Problem No. 2 and
- OECD/CSNI Standard Problem No. 10.



PKL II - Test Parameters for Shakedown Test II A - 9

Fig. 4



PKL II - Results of Shakedown Test II A - 9

Fig. 5

Compared to run K 9 the total power was reduced by the presence of unheated rods (8 %) in the new bundle. Further, the pump resistances, especially in the intact loops, were increased following new investigations on pump behaviour during reflood. The boundary conditions are given in figure 4. Figure 5 summarizes the most important data of the test:

- pressure in upper plenum and containment
- pressure difference upper plenum/downcomer
- water levels in lower plenum, core, upper plenum and downcomer
- heated rod temperatures and quenching times of the center rod
- integrated injection rate and entrained water at the break
- cool down of the steam generator secondary side.

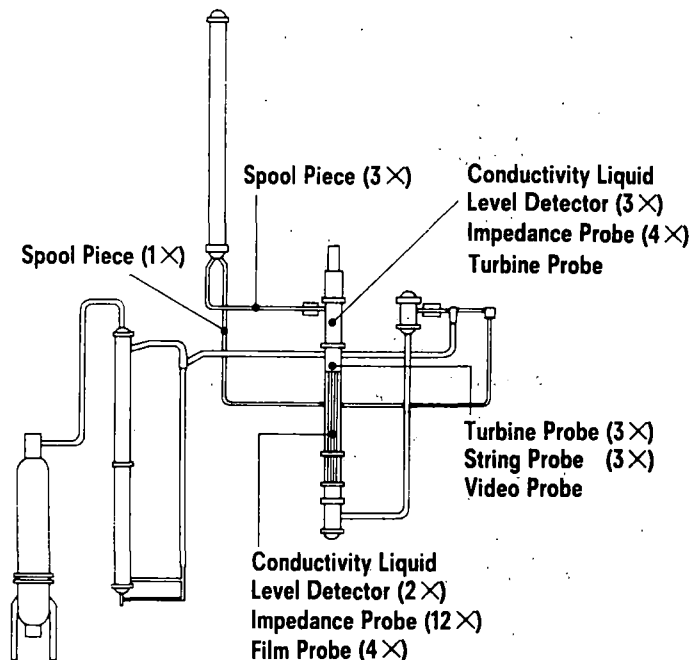
Two important results should <sup>be</sup> pointed out:

- o Higher pump resistance influenced the loop flow rates and the entrainment of water from the core into the upper plenum and the hot legs. In this test nearly no water was accumulated in the upper plenum nor entrained into the SG (very low cooldown rate).
- o A partial bypass of ECC water to the break could be observed long before the downcomer was filled to the elevation of the cold legs. This was the result of the scaled downcomer gap.

One aspect of investigation was to qualify the increase of information by the US-NRC supplied instrumentation /5/6/7/ in comparison to the "standard" flooding instrumentation (No. and position of instruments see Fig. 6).

The core region is equipped with

- impedance probes (IP) to measure local void fraction and fluid velocity in subchannels
- conductivity liquid level detectors (CLLD) to detect the mixture or swell level rise and
- film probes to measure film thickness and film velocity of de-entrained water at the flow channel.



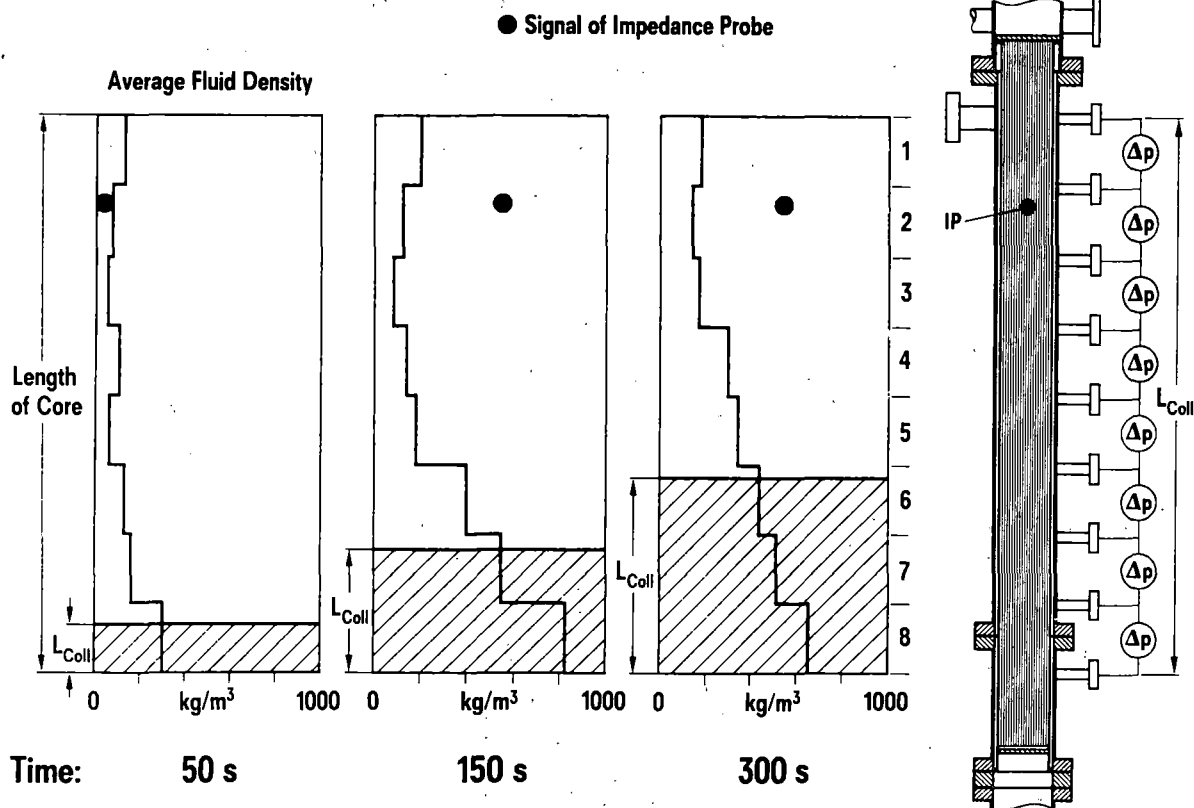
List of Measurands

| Measurand                 | Temperature | Level      | Flow      | Pressure  | Density   | Capacitance/<br>Conductivity Sensors | Drag Forces |
|---------------------------|-------------|------------|-----------|-----------|-----------|--------------------------------------|-------------|
| Pressure Vessel           | 418         | 97         | 46        | 5         | 46        | 13                                   | —           |
| Downcomer                 | 20          | 3          | 2         | 5         | 2         | 2                                    | —           |
| Steam Generator           | 128         | 16         | 14        | 6         | —         | —                                    | —           |
| Loops                     | 43          | 9          | —         | 15        | 12        | 4                                    | 12          |
| Separator/<br>Containment | 12<br>2     | 1<br>1     | —<br>2    | —<br>1    | —         | —                                    | —           |
| <b>Total: 937</b>         | <b>623</b>  | <b>127</b> | <b>64</b> | <b>32</b> | <b>60</b> | <b>19</b>                            | <b>12</b>   |

PKL II Instrumentation

List of all Instruments and Location of NRC Supplied Instrumentation

Fig. 6



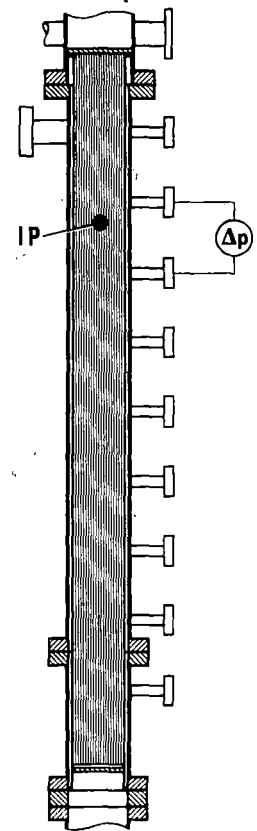
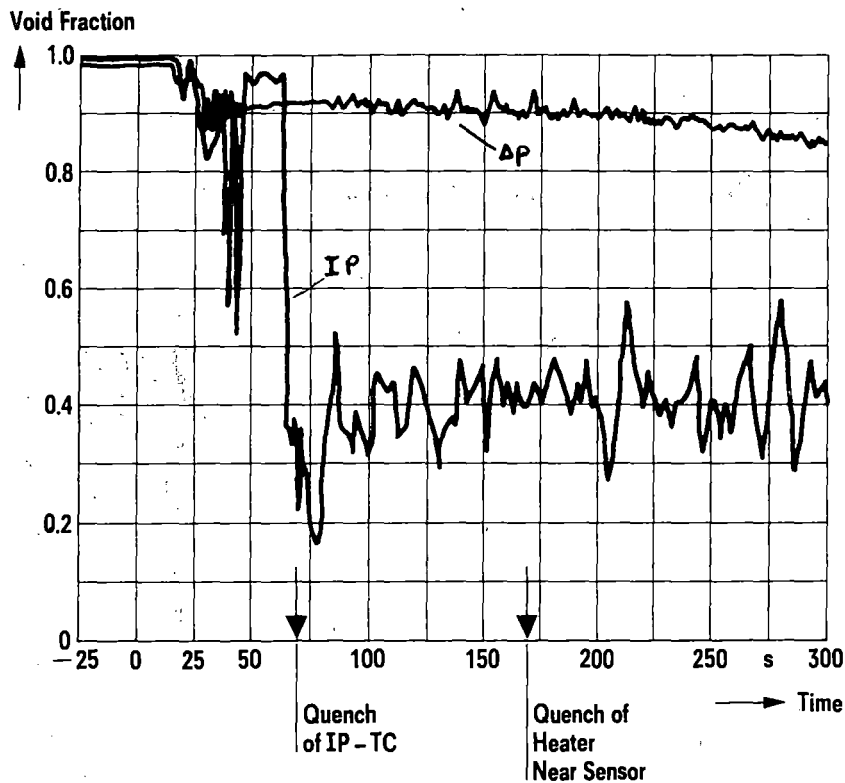
PKL II A Shakedown Test (cold leg injection)

Collapsed Level Measurement, Density Distribution and 1 Impedance Probe Signal

Fig. 7

The average density distribution is measured by 8 dp cells along the heated zone. Figure 7 indicates the axial density distribution for 3 time "windows" (50, 150, 300 sec) of the test. As expected for a cold leg injection test the higher water concentration exists always at the lower end. The signals indicate that water is very soon entrained to the top of the core even for very low water inventories (see collapsed level) and it generates (by separation) a somewhat higher density below the tie plate.

The results of the void measurement of one core impedance probe (IP) in the upper part of the bundle is added to these graphs. The first time window shows good comparison with the dp-data but a big difference exists in the later test period. The reason for this deviation can be seen in fig. 8, where the average void fraction (from dp) and the impedance probe void fraction are plotted versus time.



**PKL II A Shakedown Test (cold leg injection)  
Comparison of  $\Delta p$  and Impedance Probe**

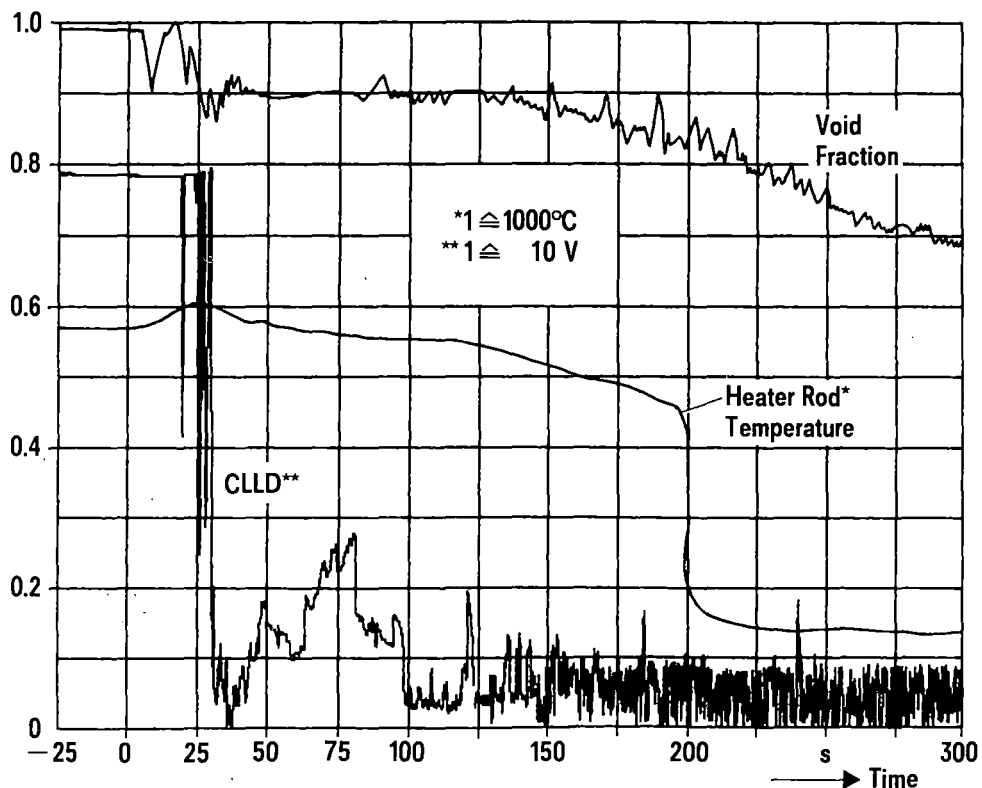
Fig. 8

After a relatively good agreement at the beginning the IP drops to significantly lower values (at around 70 sec). At the same time the temperature sensor next to the probe indicates rewetting of the unheated rod (low heat capacity) where the probe is located while the heated rods nearby quench much later. This effect

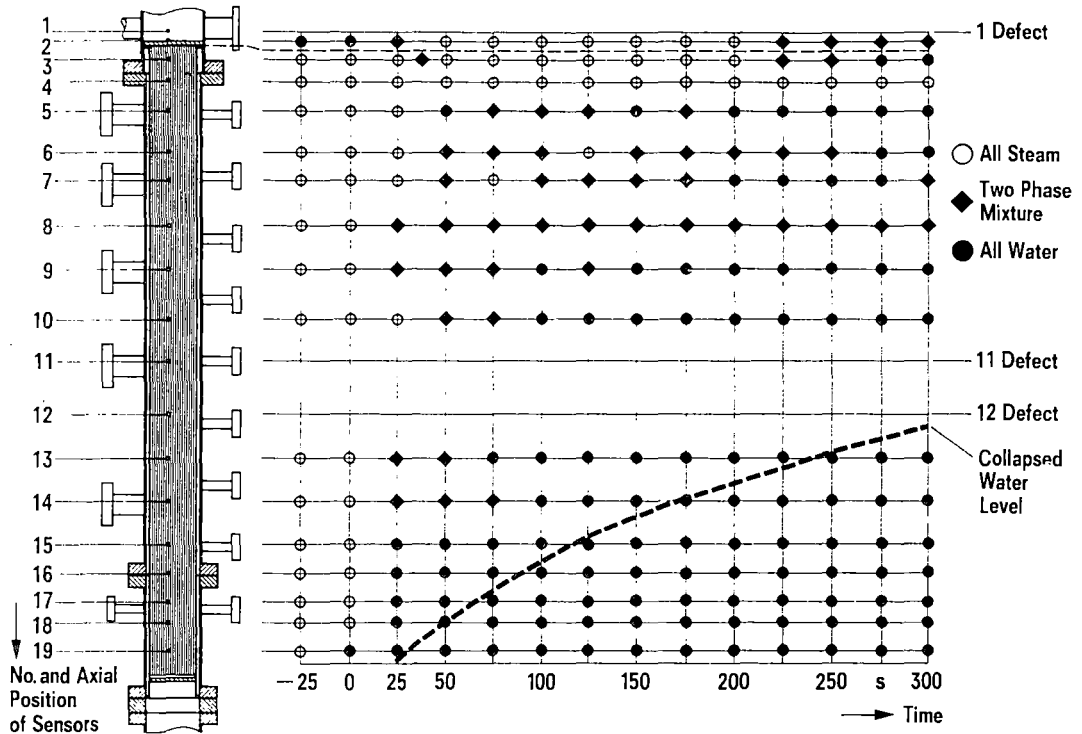
is already known from a 3 x 3 bundle instrumentation test (with visual observation) /8/ and it is caused by bridging of the two sensors with a water film on the rod surface. As soon as the bridging effect takes place the void signals appear to be systematically too low.

As long as the probe remains at high temperatures this measuring technique is successful. An improvement to avoid bridging effects would be desirable.

The conductivity liquid level detectors had been previously used in LOFT blowdown tests; however there are not many consistent results available from flooding tests. Figure 9 shows an analog recording of a probe signal measured near core mid-plane compared to the equivalent dp-void fraction measurement and to a heater rod temperature nearby in the core. As soon as the first water droplets are entrained along the subchannel the probe signal drops down to a low level (water film on the probe); after that the signal rises again due to the dryout effect caused by the steam but does not reach dry conditions again. The signal indicates that for flooding conditions (low amount of stored heat in the sensors) the data evaluation must be made very carefully. There are hints that not the signal amplitude but the signal frequency may allow a flow pattern detection but in any case a computerized interpretation seems to be very difficult. The classical interpretation of CLLD signal as "bubble plot" overpredicts the water inventory in the core region (see fig. 10).



PKL II Shakedown Test (cold leg injection) Fig. 9  
 CLLD, Heater Rod Temperature and Average Void Fraction above Core Mid - plane

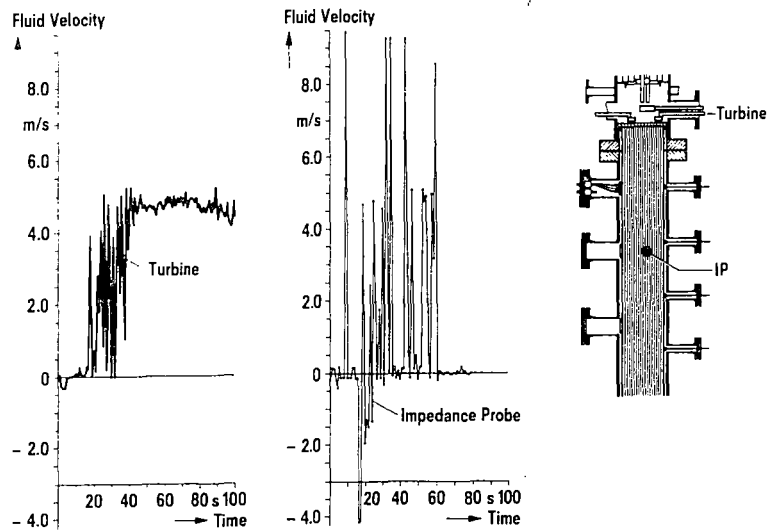


PKL II Shakedown Test  
CLLD Bubble Plot

Fig. 10

In the vicinity of the tie plate the NRC supplied instrumentation allows a better interpretation of the flow conditions than before (only dp-measurement). The results of the combination of

- impedance probe velocity calculation below the tie plate and of a
- turbine probe for fluid velocity are shown in figure 11.



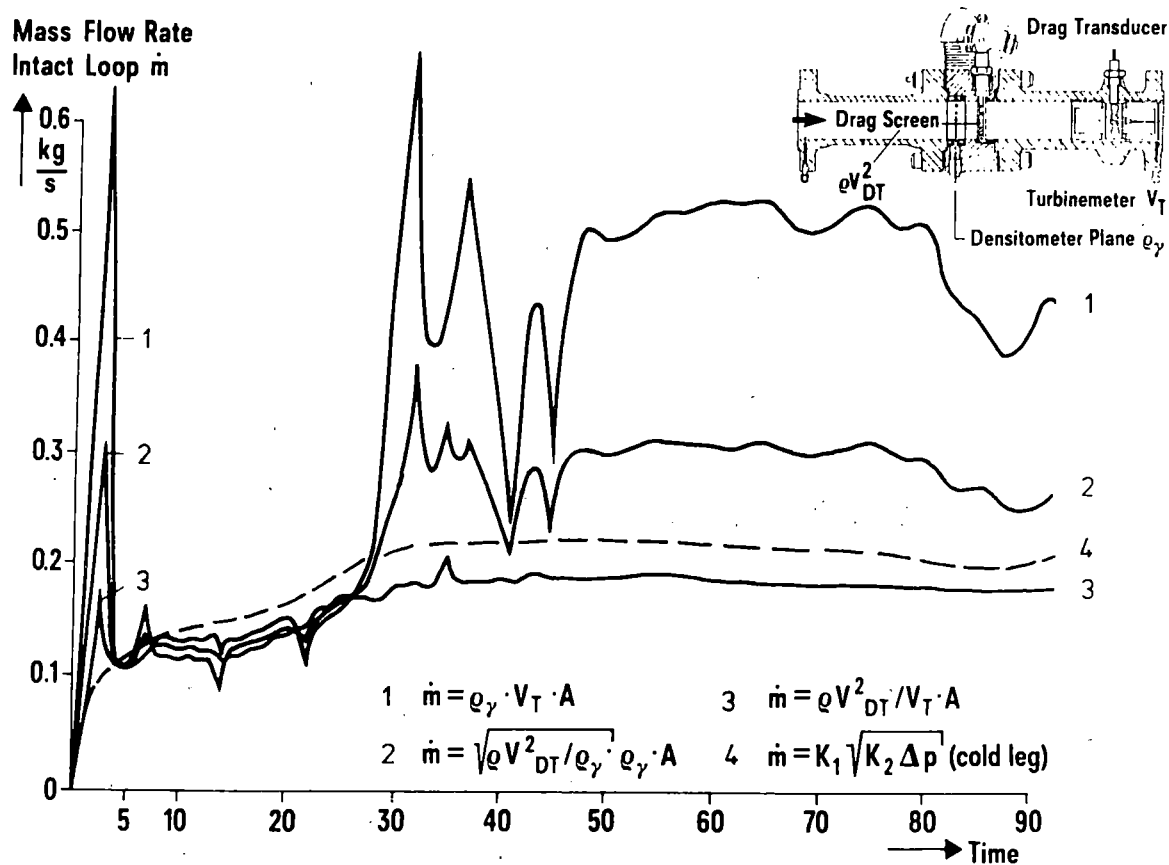
PKL II A Shakedown Test (cold leg injection)  
Upper Tieplate Turbine Probe and Core Impedance Probe Measurement

Fig. 11



The comparison shows for the first 60 seconds some similarity although the turbine signals are more continuous than the core impedance probe data. After rewetting of the sensor surface (see fig. 8) the velocity calculation does not show reasonable results any more. The signals of the string probes near to the turbine have not yet been analyzed.

US-NRC supplied also 4 Instrumented Spool Pieces to measure two phase flow in the hot legs (3) and in the broken cold leg (1). Due to the expected high void fractions the 3-beam densitometer was designed especially for PKL with low energy sources ( $Fe_{55}$ ,  $Am_{241}$ ,  $Cd_{109}$ ) and a detector with equivalent sensitivity. Calibration tests showed a good density measurement with the Iron source at high void levels.

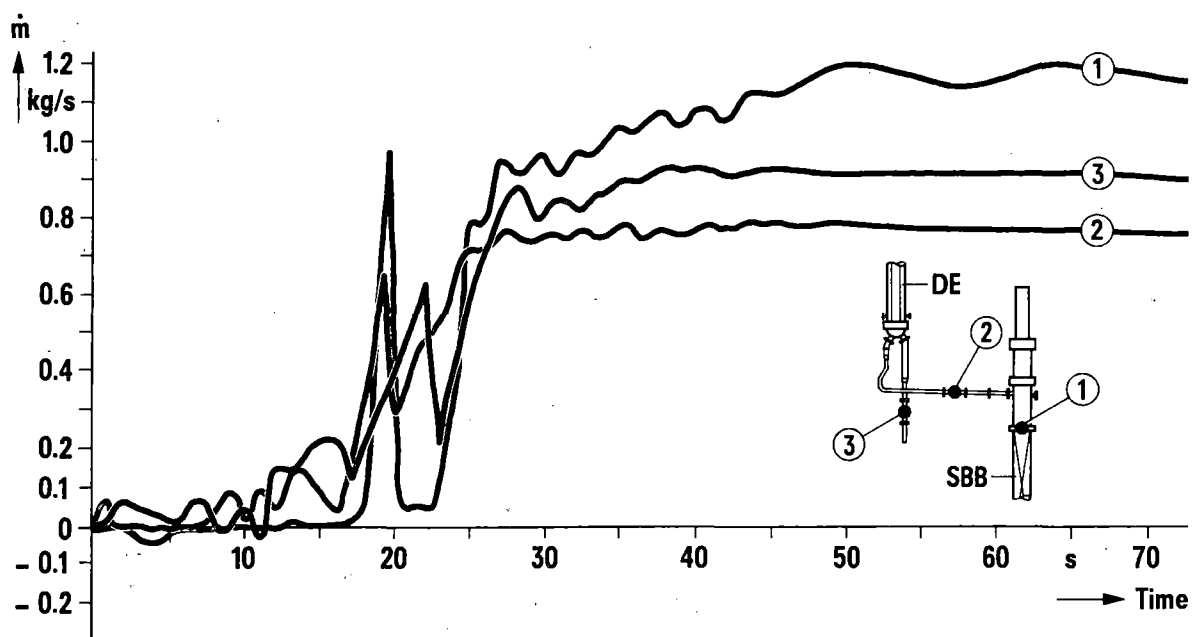


PKL II A Shakedown Test(cold leg injection) Fig. 12  
 Comparison of Various Spool Piece Signal Combinations and an Orifice Measurement

Figure 12 compared the calculated mass flow rates for one hot leg spool piece using the 3 possible combinations of signals ( $\gamma$  + drag;  $\gamma$  + turbine; drag + turbine). Good results in comparison to the measured cold leg flow rate (superheated steam) show the drag/turbine combination. The discrepancies in the later test period are caused by an averaging procedure of all 3  $\gamma$ -signals (when Am, Cd have low accuracy).

This possibly requires a software modification. The results indicate that for a "classical" combination with 3 systems ( $\chi$ , turbine, drag) the possibility of cross checking gives a higher degree of confidence than the combination of only 2 systems (e.g. dragbody and  $\chi$ -density).

A comparison of the total flow rates at the tie plate (turbine signal + steam density), in the hot legs (spool pieces) and in the cold legs (1 spool piece and 2 orifice plate measurements) is shown in figure 13.



**PKL II A Shakedown Test (cold leg injection)  
Mass Balance**

Fig. 13

The local turbine seems to overpredict the total flow rate using saturated steam density for mass flow calculation. These Spool Piece Systems turned out to be a successful measurement device in low pressure region with high void fractions.

The first appraisal of the - conventional - instrumentation and the US-NRC supplied instruments can be summarized as follows:

- the additional instruments contribute additional information in core, upper plenum and loops
- turbines and spool pieces perform well
- impedance probes have (besides failure due to leakages) their specific behaviour caused by water bridging. (Film probe sensors have not yet been analyzed).
- CLLD probes in upper plenum show almost - wet - signals during flooding. CLLD core probes seem to be also influenced by rewetting effects and have the tendency to overpredict water inventory.
- Pictures from video probe next to the tie plate show poor image resulting from the flow regime (froth). A different probe position would be desirable
- more analytical work in excess of the "standard" procedures is required in order to extract all potential information
- detailed discussions of the results, operability and of potential improvements in analysis with the instrument suppliers will follow.

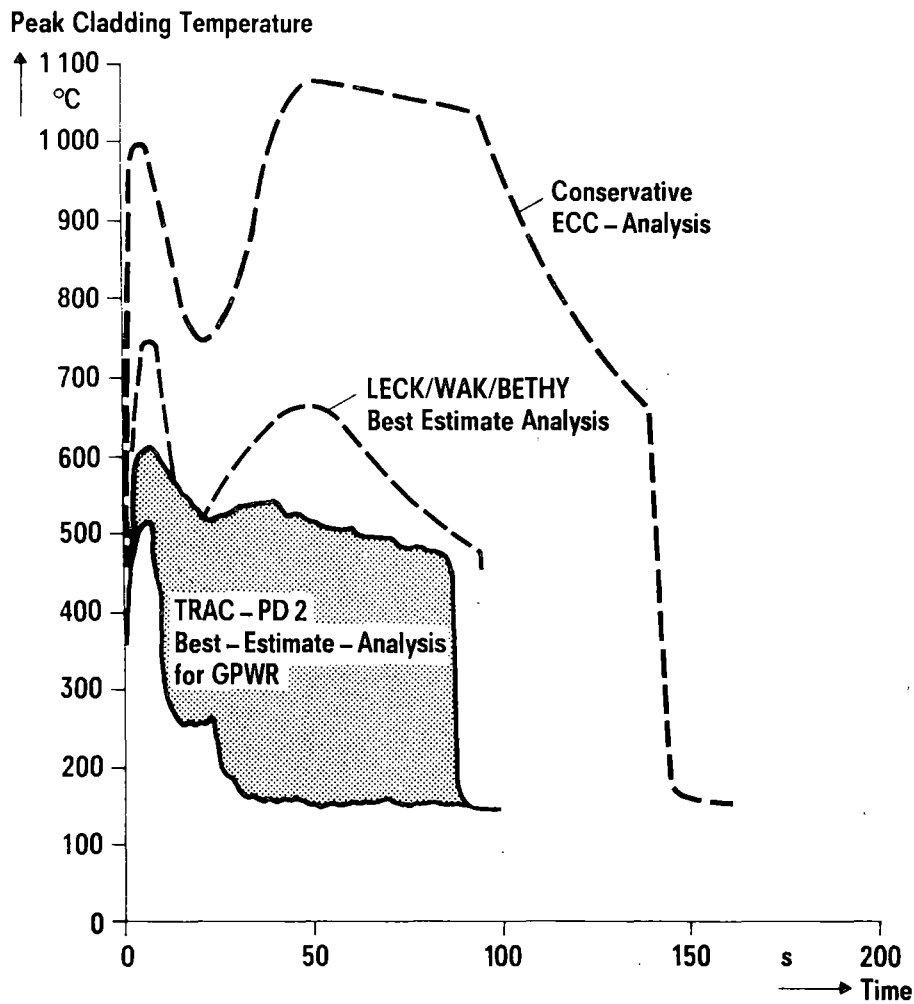
#### 4. Simulation of the End-of-Blowdown-Phase in PKL II

Up to now the flooding tests in PKL and in most of the other reflood facilities were performed with the assumption of a completely voided primary system prior to refill. The cooling capacity of the accumulator injection during the end of the blowdown phase (EoB) was also neglected. Test parameters were oriented on the so called - licencing - requirements such as:

- 20 % higher decay heat generation than that specified by ANS
- reduced ECC capacity
- no quenching during EoB
- conservative values for heater rod gap conductance etc.

The results of code calculations and equivalent tests indicate high cladding temperatures and long quench times (see fig. 14).

For - best estimate conditions - which are the more realistic ones the codes predict much lower temperature levels and a shorter time to rewet the core especially in the case of combined hot and cold leg ECC injection (e.g. TRAC results for GPWR /9/).



1300 MW - PWR, 200% Cold Leg Break

**Peak Cladding Temperatures with Conservative and Best - Estimate Analysis**

Fig. 14

The PKL II tests will be oriented to these more realistic conditions. PKL is designed for a max. pressure of 40 bar, so that the accumulator injection starting at 26 bar (KWU system) will be simulated. In the following the procedure to reach the correct blowdown conditions is described:

Before the test steady state conditions will be established:

- stagnant steam filled system at 40 bar
- pressurizer isolated and at 80 bar
- SG secondary side filled with saturated water at specified conditions e.g. 55 bar
- core heated up to precalculated temperatures e.g. 550 ° C at the hot spot.

Then the conditioning phase (40 to 26 bar) will be initiated with the aim of establishing the correct thermohydraulics by the time the pressure of 26 bar is reached.

This is done by:

- initiation of blowdown (break valve opened)
- opening of surgeline valve, critical flow into the system
- injection of - residual - water from reservoirs to supply water inventory to the loops
- termination of the above mentioned injection when reaching 26 bar.

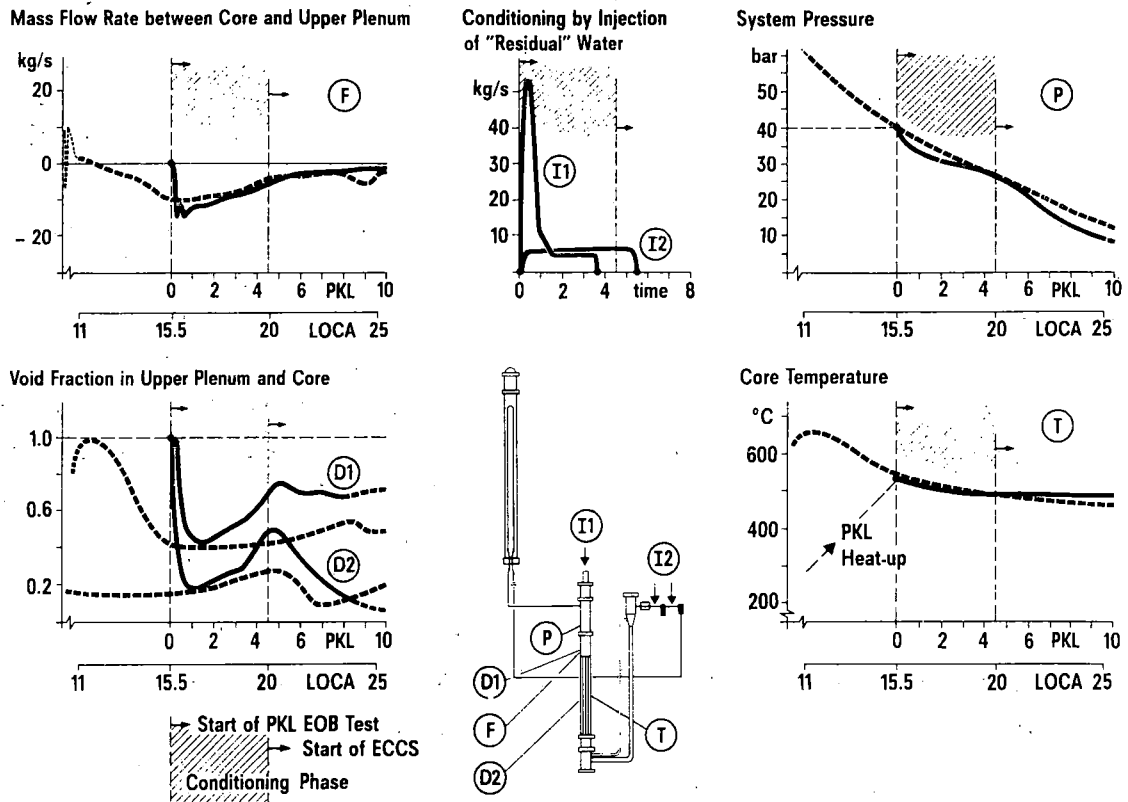
Then the test phase starts with ECC injection.

During the conditioning phase the most important thermohydraulic conditions for the core cooling must be established. These are

- pressure level and pressure gradient
- core mass flow rate and
- fluid density in the core region.

The amount of water injection will be precalculated by system codes like DRUFAN or TRAC. There are three calculation steps for a specified break size and location.

1. a PWR transient starting from normal operation
2. a PKL transient starting from "normal" operation assuming PKL would be designed for full pressure (160 bar)
3. a PKL transient starting at 40 bar.



**PKL II End of Blowdown - Conditioning of the Test**  
**Results of First Calculations by GRS with the DRUFAN Code**

Fig. 15

First results of such a comparison are very encouraging.

Fig. 15 summarizes the most important results of calculation steps 2. and 3. for a 200 % cold leg break. The comparison is plotted for the time 11 to 25 seconds which covers also the transient above 40 bar and below 26 bar.

The calculation (3) starting at 40 bar simulates the injection of - residual - water into the upper head of the pressure vessel and next to the break (see plot I1 and I2).

The other plots show the comparison of

- system pressure (P)
- core temperature (T)
- mass flow rate from core to upper plenum (F) and
- void fraction in core (D 1) and upper plenum (D 2)

All plots show reasonably good agreement at the end of the conditioning phase. In case of deviations (e.g. higher void) these will not cause improved cooling conditions in the core during the conditioning phase.

More precalculation will be performed for all test parameters so that the confidence in this test procedure will be improved.

For the EoB tests more instrumentation (dp-independent) will be installed and the US-NRC supplied instruments (especially spool pieces and CLLD) are expected to contribute useful data on liquid level and density in the transition phase between blowdown and refill/reflood.

It is planned to start with these EoB-tests in summer of next year.

## References

- /1/ D. HEIN et al.  
PKL Reflood Experiment - Influence of Injection Mode  
and Loop Resistance  
European Two Phase Flow Group Meeting 1978, Stockholm
- /2/ H. WEISSHÄUPL, B. BRAND  
PKL Small Break Tests and Energy Transport Mechanisms  
ANS Specialist Conference on Small Breaks, August 1981, Monterey Cal.
- /3/ B. BRAND, D. HEIN, P. WEISS  
PKL I Findings - PKL II Plans  
9th Water Reactor Safety Information Meeting, Oct. 1981 Gaithersburg
- /4/ A. SEGER, R.P. COLLIER  
Development of a Mechanistic Model for ECC Penetration in a  
PWR Downcomer  
NUREG/CR-1426, Battelle Columbus Laboratories (1980)
- /5.1/ B.G. EADS, J.O. HYLTON  
Development of impedance sensors at ORNL  
for measurement of two-phase flows  
7th Water Reactor Safety Research Information Meeting  
Gaithersburg, Maryland, Nov. 5 - 9, 1979
- /5.2/ R.A. HESS, C.J. REMENYIK  
Development of film thickness and velocity probes for use  
in simulated reactor LOCA experiments  
NRC Reactor Safety Instrumentation Review Group Meeting,  
Oak Ridge, Tennessee, July 30, 1980



- /6.1/ D.E. MENKHOUSE  
Operation and Maintenance Manual Turbine Flowmeter  
Measurement System  
EGG-3D-5661, December 1981
- /6.2/ R.F. SMELLIE, M.A. HATCH, E.F. WILSON  
Primärkreislauf (PKL) SPOOL PIECE  
Technical Manual  
EGG, San Ramon Operations, MES-011, January 1981
- /6.3/ H. MEYER-CHRISTIANS, R.O. ALBERTSON  
PKL Operation and Maintenance Manual Conductivity Liquid  
Level Measurement System  
EGG-3D-5176, April 1981
- /7/ PKL Video Probe System Technical Manual  
LA-DRAFT-TM  
Rev. 0 6/82, June 1982
- /8/ J.E. HARDY, W.H. LEAVELL, H. LIEBERT, J.A. MULLENS  
Transient Testing of an In-Core Impedance Flow Sensor  
in a 9-Rod Heated Bundle  
ORNL/NUREG/TM-389, February 1981
- /9/ F. MOTLEY, K.A. WILLIAMS  
TRAC PD2 Calculation of a Double Ended Cold Leg Break in a  
Reference German PWR  
paper presented at 2D/3D Coordination Meeting  
Nov. 3 - 7, 1980, Los Alamos

## RELAP5 APPLICATION TO INTEGRAL EXPERIMENTS<sup>a</sup>

By

V. H. Ransom

EG&G Idaho, Inc.

RELAP5 is a one-dimensional light water reactor (LWR) transient analysis code. The outstanding features of the code are its versatility, fast running, and ease of use. The released version of the code, RELAP5/MOD1, is available from the National Energy Software Center and is being maintained. Error corrections and minor improvements are added to the code periodically as updates (cycle 18 contains the latest updates to the code). The RELAP5/MOD1 code contains the necessary models for simulation of LWR depressurization and operational transients. This version of the code is particularly well suited to simulation of small break loss-of-coolant accidents (LOCAs) and has been used extensively at the Idaho National Engineering Laboratory (INEL) in support of the Semiscale and LOFT testing programs. The major limitation of RELAP5/MOD1 is the lack of reflood modeling capability, specifically the nonequilibrium heat transfer process in the subcooled boiling and post-CHF regimes.

During 1982 new modeling capabilities were completed in addition to the maintenance activities related to RELAP5/MOD1. An interim version of the code, RELAP5/MOD1.5, containing most of the new features was released to the NRC for use by NRC contractors in August of 1982. RELAP5/MOD1.5 contains reflood modeling capability and associated nonequilibrium heat transfer and vapor generation models, a steady state initialization branch, a jet mixer component, boron feedback in the reactor kinetics model, and added control system components. This version of the code is only available through the NRC. A MOD2 version of RELAP5 is scheduled for release to the NRC in

---

a. Work supported by the U.S. Nuclear Regulatory Commission, Office of Nuclear Regulatory Research under DOE Contract No. DE-AC07-76ID01570.

mid-1983. This will be a complete modeling capability for pressurized water reactors with limited modeling capability for boiling water reactor (BWR) systems.

A significant development during this past year has been the addition of interactive execution capability to RELAP5. This feature permits the code to be used in a nuclear plant analyzer mode. A demonstration of this capability was conducted several times, wherein a simple plant model was executed interactively and remotely by means of a standard telephone line to the INEL computer. The RELAP5 Nuclear Plant Analyzer capabilities are described in more detail in a specific presentation at this meeting.

RELAP5/MOD1 has been applied extensively in the Semiscale and LOFT programs for experiment planning, safety analysis, pretest prediction, posttest analysis, and typicality studies. A mutual benefit has derived from these applications. A better understanding of the experiments has resulted, the relation between the experiments and full scale plant behavior has been better understood, and the code development has benefited from the experimental feedback. The three examples of typicality studies reviewed herein relate the experimental results related to PWR behavior. These studies have yielded enhanced understanding of PWR behavior with respect to reactor operation and safety.

The first example consists of results from a recent series of Semiscale small break tests, S-UT-6 and S-UT-8. Both tests are 5% cold leg break LOCA simulations, but Test S-UT-6 had an upper head to cold leg bypass or leakage of 3.4%, while Test S-UT-8 had a bypass of 1.4% that corresponds to a low bypass PWR design. A RELAP5 model for a generic PWR was used to compare predicted core level behavior at full scale to the S-UT-6 result. The full scale calculated result showed complete core uncover for a brief period at approximately 200 s while the experiment showed only modest core level depression. Since the test results showed expected behavior and the calculation atypical behavior, the analytical result was viewed with scepticism even though the generic PWR model had a bypass ratio less than 0.5% (the calculation was made some time prior to the experiment). Following Test S-UT-6, changes were made in the upperhead geometry to make the Semiscale system correspond more closely with a low bypass ratio PWR (the bypass

was reduced from 3.4 to 1.4%). Test S-UT-8 was a repeat of Test S-UT-6 except for the modified bypass ratio. The results of Test S-UT-8 showed a core level depression almost identical to the RELAP5 generic PWR calculation result. The reason that the core uncover exists is that condensation in the upside of the steam generator tubes results in a relatively large hydrostatic head on the upside compared to the downside. This coupled with the pump loop seal produces an imbalance of pressure that depresses the core level. The effect of high bypass ratio is to mitigate this effect. The code calculations, because of the detail available, are of great help in understanding such phenomena. The example given here illustrates the progress in code physical accuracy that has been achieved, the potential utility of a system code in understanding safety experiments, and the possible benefit of using a best estimate calculation for licensing purposes (a pessimistic evaluation model analysis does not predict as severe a core level depression as obtained in the best estimate calculation).

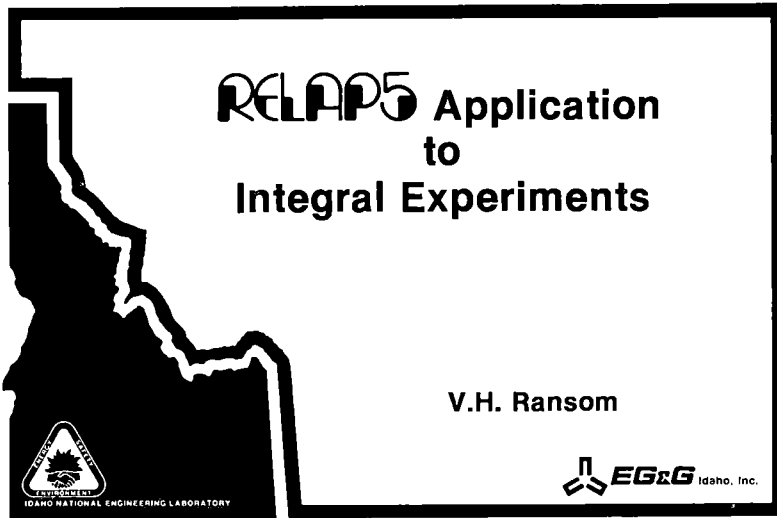
The second example of code application benefit is from the recent Semiscale feed and bleed Experiment S-SR-2. This test was conducted to evaluate the feasibility of decay heat removal by a primary system feed and bleed using high pressure injection system (HPIS) and the power operated relief valves (PORV). The test was conducted with the steam generator secondaries dry to simulate the condition resulting from station blackout with loss-of-feed to the steam generators. The Semiscale injection rate was scaled to correspond to HPIS without benefit of charging pumps. The test results indicated that a steady state feed and bleed operation was feasible, but was not conclusive because of system tolerance with respect to primary mass leakage, scaled HPIS and PORV flow. The RELAP5/MOD1 code was used to model the S-SR-2 test and very close agreement with data was achieved. RELAP5 was subsequently used to analyze a station blackout transient with feed and bleed for a full scale PWR (RESAR). The results showed that a steady state system subcooled state could be achieved using HPIS and charging pumps. Analysis also indicated the feasibility of achieving a subcooled steady state using only HPIS. In this example it was possible to relate the experimental result to generic PWR system behavior in spite of experimental tolerances that were atypical of a full scale system.

The third example is from the LOFT program and concerns the conclusions with respect to pump operation during a small break LOCA. Tests L3-5 and L3-6 were conducted to investigate whether the reactor coolant pumps should be tripped off or left running in the early phase of a SBLOCA. The experimental results showed that beyond 300 s of LOCA operation a greater system mass loss occurred if the pumps were left running. The RELAP5/MOD1 code was able to closely simulate both the experiments and in particular showed the same trends with respect to system mass loss. Subsequently a typicality study was made using a RELAP5 model for a full scale Zion plant. In particular the effect of geometric and elevation differences between the Zion plant and LOFT were simulated. The trend, with respect to system mass loss for the Zion simulation, was similar to the LOFT results, except that greater system mass was lost with the pumps running beyond 1300 s of LOCA operation as compared to the 300 s observed in LOFT. The calculations also showed an early (500 s) Zion level depression for early pump trip. Thus, the typicality study, in collaboration with LOFT results, indicated the desirability of some delay in pump trip (up to 20 min). This conclusion was not obvious from the experiment alone.

The three examples given here of code use in interpreting and applying results from integral experiments are only a sample, but clearly indicate the value of coupling best estimate system analysis with the experiment.

## REFERENCES

1. V. H. Ransom et al., "RELAP5/MOD1 Code Manuals--Volume 1: System Models and Numerical Methods," NUREG/CR-1826, EGG-2070, March 1982.
2. V. H. Ransom et al., "RELAP5/MOD1 Code Manuals--Volume 2: User Guide and Input Requirements," NUREG/CR-1826, EGG-2070, November 1980.
3. R. J. Wagner and V. H. Ransom, "RELAP5 Nuclear Plant Analyzer Capabilities," ANS Winter Meeting, Washington D.C., November 14-19, 1982.
4. D. G. Hall, "RELAP5 Development Project Code Development and Configuration/Quality Control Procedures," EGG-CDD-5776, February 1982.
5. H. Chow, R. A. Riemke, and V. H. Ransom, "The Application of RELAP5 to Three Separate Effects Test," ANS Winter Meeting, Washington D.C., November 14-19, 1982.
6. V. H. Ransom and D. L. Hicks, "Hyperbolic Two-Pressure Models for Two-Phase Flow," To be submitted to Journal of Applied Physics.
7. R. J. Wagner and F. Aguilar, "Study of RELAP5 Parallelism and Proposal for NRC In-House Nuclear Plant Analyzer," EGG-CDD-5819, April 1982.
8. D. J. Shimeck et al., "Analysis of Primary Feed and Bleed Cooling in PWR Systems," EGG-SEMI-6022, September 1982.
9. S. M. Modro et al., "RELAP5 Analysis of LOFT and ZION Nuclear Power Plant Small Break LOCAs," EGG-M-15282, ANS International Meeting on Thermal Nuclear Reactor Safety, August 29--September 2, 1982.



## Presentation Outline

- RELAP5
- Application Examples
  - Semiscale
  - LOFT
- Summary
  - Code improvement schedule

S2 3849

146

## RELAP5

- Generic LWR best-estimate LOCA and transient code
- Economic
  - User convenient
  - Fast running
- Versatile
  - Experiment support
  - Plant/component analysis
  - Plant analyzer

S2 3850

## RELAP5 Release Sequence

| Version | Date      | Capabilities                                  |
|---------|-----------|---|
| MOD1    | Dec. 1980 | PWR blowdown, SBLOCA, transients              |
| MOD1.5* | Aug 1982  | Added reflood and improvements                |
| MOD2    | July 1983 | All PWR transients and limited BWR transients |

\* Internal release to NRC contractors

S2 3851

## RELAP5 Application in Integral Experiments

- Planning/safety analysis
- Experiment pre-prediction
- Posttest analysis (assessment)
- Typicality studies

S2 3852

## RELAP5/MOD1 PWR Typicality Applications

- Semiscale
  - PWR core bypass effects
    - S-UT-6 and S-UT-8
  - PWR feed and bleed operation
    - S-SR-2
- LOFT
  - SBLOCA pump operation
    - L3-5 and L3-6

S2 3865

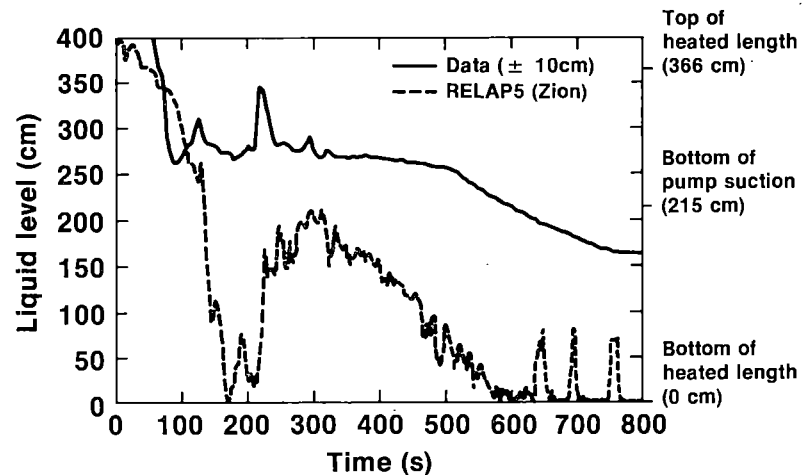
147

## Semiscale Tests S-UT-6 and S-UT-8

- Objective: Evaluate the effect of core bypass for SBLOCA
- Test conditions:
  - MOD 2A system
  - SBLOCA (5%)
  - Non UHI
  - 3.4% and 1.4% upper head bypass

S2 3853

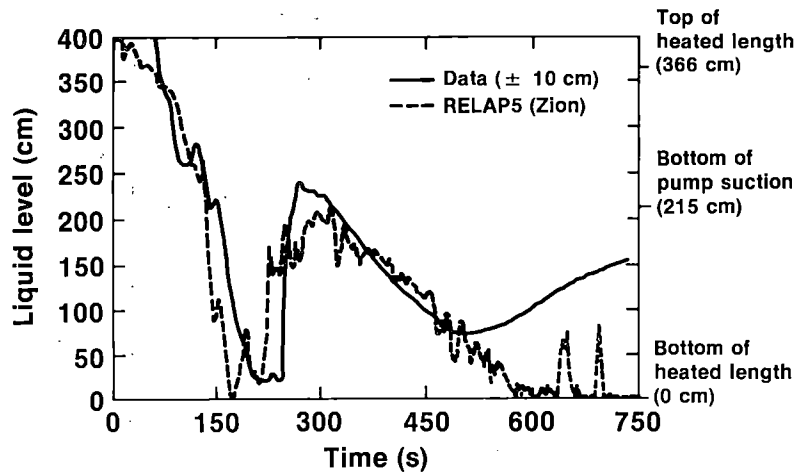
## Core Collapsed Liquid Levels S-UT-6: 5% Break, 3.4% Bypass



S2 3858



### Core Collapsed Liquid Levels S-UT-8: 5% Break, 1.4% Bypass



S2 3860

### Core Bypass Typicality Conclusions

- Bypass magnitude
  - Significant effect on transient levels
- Unanticipated phenomena
  - Loop seal coupling with steam generator

S2 3859

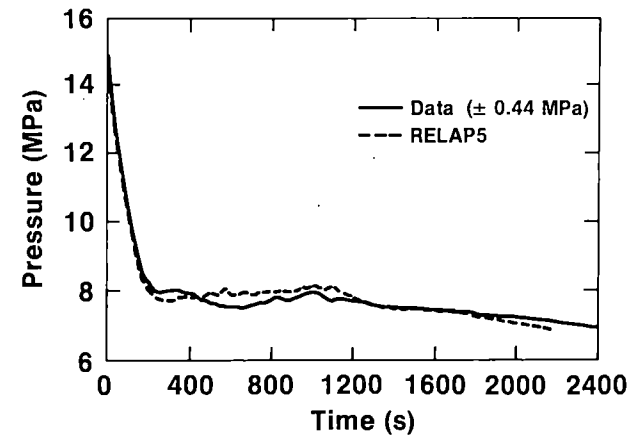
148

### Semiscale Test S-SR-2, Point 3

- Objective: Establish feasibility of steady-state primary feed and bleed cooling
- Test conditions:
  - Mod 2a system
  - Feed - Low head HPIS (Zion) no charging pumps
  - Bleed - PORV latched open
  - Net core power 40 kW (2%)
  - Pumps - natural circulation
  - Steam generators - dry secondary

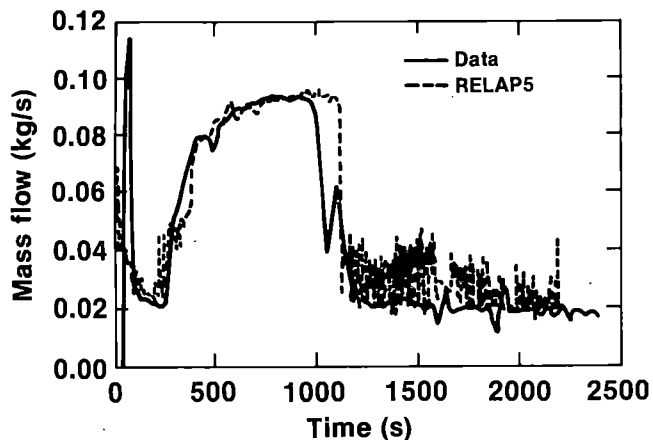
S2 3854

### S-SR-2 System Pressure Feed and Bleed Operation



S2 3857

### S-SR-2 PORV Flow



S2 3856

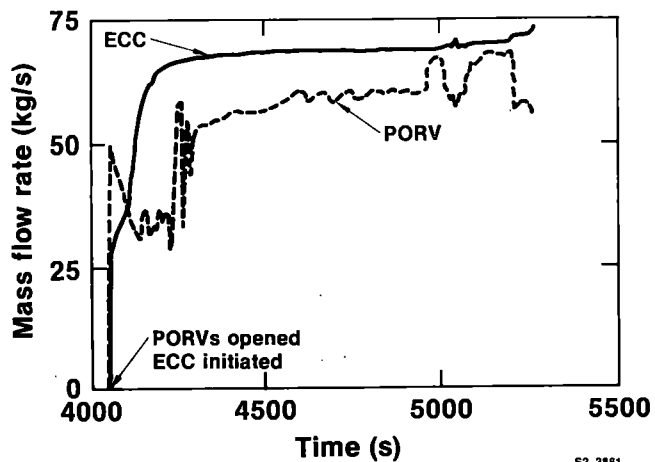
### RESAR Feed and Bleed Analysis

| Time (s) | Event                       |
|----------|-----------------------------|
| 0.0      | Loss of offsite power       |
| 0.5      | Scram                       |
| 3875     | Steam generators dry out    |
| 4052     | PORV latched open           |
| 4100     | HPIS and charging initiated |
| 4500     | Hot leg subcooled           |
| 5260     | Primary system 95% liquid   |

S2 3855

149

### RELAP5 Calculated PORV and ECC Flows RESAR Feed and Bleed Operation



S2 3861

### Feed and Bleed Typicality Conclusions

- Cooling feasible in full scale
  - HPIS and charging
  - HPIS only
- Marginal S-SR-2 result
  - System tolerances/scale

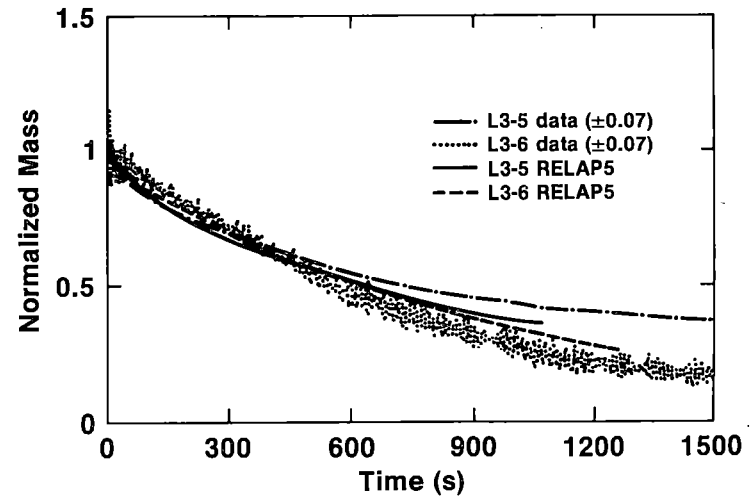
S2 3844

## LOFT L3-5, L3-6

- Objective: Evaluate effect of pump operation
- Test conditions:
  - Small break LOCA - 2.5%
  - L3-5 early pump trip
  - L3-6 delayed pump trip

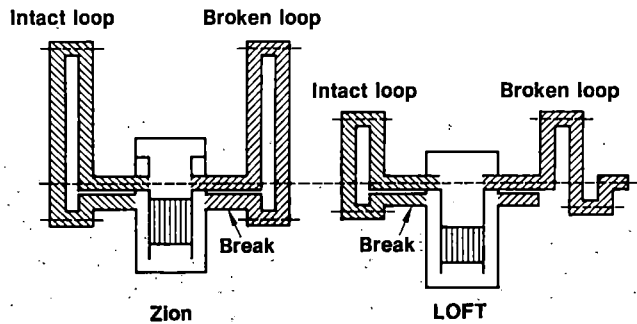
S2 3862

## L3-5 and L3-6 Normalized Coolant Mass



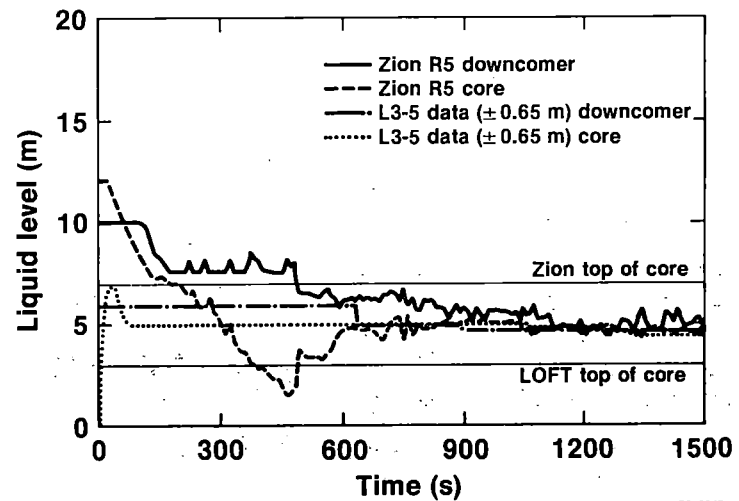
S2 3846

## Zion - LOFT Geometric Comparison



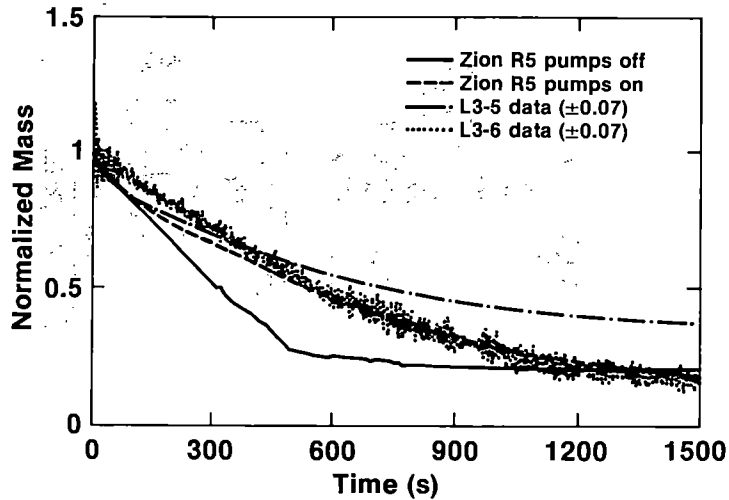
S2 3864

## Calculated Zion Levels Compared to L3-5 Data, Early Pump Trip



S2 3847

## Normalized Coolant Mass Zion Calculated and LOFT



S2 3848

## SBLOCA Pump Operation Typicality Conclusions

- Elevation/geometric effects
  - Break flow quality
  - Mass inventory loss
  - System liquid levels
- Typical PWR system
  - Core uncover for early pump trip
  - Delayed pump trip (up to 20 min) desirable

S2 3845

151

## RELAP5 Improvement Schedule

| Model                         | MOD1   | MOD1.5  | MOD2           |
|-------------------------------|--|---|----------------|
| Hydrodynamics<br>Constitutive | Fixed annular/mist trans<br>Equ. heat transfer<br>and vapor gen                                    | Fixed annular/mist trans<br>Equ. recompression                                  |                |
| Components                    | No noncondensable<br>HX effect<br>Ideal separator<br>No turbine or condenser<br>Parallel branching | No noncondensable<br>HX effect<br>No turbine or condenser<br>Parallel branching |                |
| Conduction/Fuel               | Fixed axial mesh<br>Fixed gap  | Fixed gap   |                |
| Kinetics                      | Old ANS decay heat<br>Linear feedback<br>No boron  | Old ANS decay heat  |                |
| Controls                      | No min/max, delay,<br>lead/lag, or inverse   | No lead/lag,<br>or inverse  |                |
| Numerics                      | Mat. Courant DT<br>User DTmax Control  | Mat. Courant DT<br>User DTmax control   | Some DT limits |

S2 3866

## Conclusions

- RELAP5 correctly simulates PWR system behavior
- Analysis can be used to examine typicality
  - Geometric differences
  - Leakage or flow path effects
  - Operation differences
- Code application coupled with refinement
  - Increased reliability
  - Expanded typicality role

S2 3863

NRC/EPRI/W FLECHT-SEASET PROGRAM

- NATURAL CIRCULATION RESULTS
- 163-BLOCKED BUNDLE RESULTS

Presented By

L. E. Hochreiter

Westinghouse Nuclear Tehcnology Division

## INTRODUCTION

The FLECHT-SEASET program is a cooperative research and development program between the US NRC, EPRI, and W. The goals of the program are to examine flow blockage heat transfer to address large break LOCA concerns, as well as to examine the different cooling modes in natural circulation.

## NATURAL CIRCULATION SYSTEMS EFFECTS TASK

The objectives of this task is to examine the systems response and steam generator heat transfer for different natural circulation cooling modes. The test series is specifically designed to address post TMI-Accident and accident recovery concerns. The experiments have investigated the different natural circulation cooling modes as well as the transition between modes. The test facility was originally designed for reflood heat transfer systems effects tests, however, nearly all the scaling requirements for natural circulation are the same as those for reflood with the exception of sytem pressure. The test facility is full height, has PWR resistances and preserves the proper power-to-volume ratio. An active secondary side has been added to the two full height steam generators such that a forced flow or boiling secondary side in the steam generators can be used. The one parameter which is not modeled is the sytem pressure.. The desired pressure for small break situations is 600 - 1200 psia, whereas the original design pressure for the FLECHT-SEASET systems effects facility was 60 psia. The concern about the lower pressure in the test was the flow regime transitions could occur at different mass fluxes in the test relative to the PWR because of the lower density resulting

in different natural circulation cooling modes. Two changes in the test facility design were incorporated to compensate for the lower pressure design. The test facility design was increased from 60 to 150 psia. This was the highest pressure we could go to without a major redesign effort. The hot legs which were normally 3-inch (unbroken loop) and 1 1/2-inch (broken loop) were enlarged to 6-inch and 3-inch respectively. Enlarging the cold legs permitted operation at prototypical decay powers and steam generation rates such that stratified flow would exist at the lower pressures in the hot legs rather than a dispersed flow. The concern was that two-phase and reflux condensation cooling modes could be very difficult to obtain with the smaller hot legs.

Tests have been run to observe the effects of:

- a.) non-condensable gas injection into the generators
- b.) cold leg and upper plenum injection
- c.) minimum and maximum heat sink effects
- d.) power effects in single phase natural circulation
- e.) complete loss of heat sink and recovery.

The test results indicate stable heat removable capability in each cooling mode. The non condensable gas effects in single and two-phase act to block off selected tubes and to slightly increase the primary system pressure. The two phase natural circulation case was forced back into single phase as selected tubes apparently filled with the gas. For refluxing, it is believed that the non-condensable acts to spread the steam generator heat flux out over a larger portion of the generator. The primary system also pressurizes to help create a larger primary to secondary temperature difference. Examples of the non-condensable effects are shown on the attached figures.

When draining mass from the system to go from single phase to two-phase, the two-phase flow reaches a peak at  $\sim 85\%$  of the original mass inventory. This is about the same inventory value that semiscale observed. However, more mass had to be drained from the FLECHT-SEASET system to reach stable reflux as compared to semiscale. Typically, stable reflux was reached at  $\sim 40\%$  of the original mass inventory, where as semiscale reached reflux at 50 - 60% of the original mass inventory. The lower mass in FLECHT-SEASET is due to the lower pressure in the facility which results in a higher hot leg superficial velocity.

We feel that the natural circulation data developed from the FLECHT-SEASET program will compliment the Semiscale and PKL data as well as provide additional information for model development and system code verification.

#### 163-ROD BUNDLE FLOW BLOCKAGE PROGRAM

The objectives of the 163-rod bundle flow blockage program are to develop a data base and analysis method to examine PWR flow blockage heat transfer. A loop schematic for the 163-rod bundle test facility is given as well as a cross section of the test section.

Example of the 163-rod bundle hardware are also shown. A non-coplanar blockage distribution is used for two-21-rod bundle islands in the center of 163-rod bundle. The blockage sleeves which simulate the ballooned rods are also shown in photographs of the bundle.

A series of constant flooding rate, variable flooding rate, and gravity feed flooding rate tests have been conducted at test conditions which match the previously conducted 161 unblocked bundle tests. Examples of the rod temperatures, vapor temperatures and heat transfer are shown for the unblocked 161-rod bundle and blocked 163-bundle. Preliminary analysis

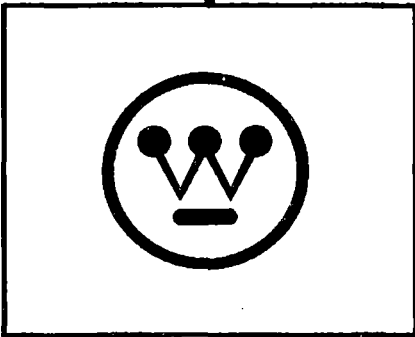


of the data indicates that the blockage in the 163-rod bundle promotes improved heat transfer in and downstream (three to four feet) of the blockage zone in nearly all cases. At the 10 foot location, some of the blocked rods did show poorer heat transfer than the unblocked rods, however, the absolute value of the temperature is low ( $\sim 1500^{\circ}\text{F}$ ) and the blocked to unblocked rod temperature difference is only  $50^{\circ}\text{F}$ .

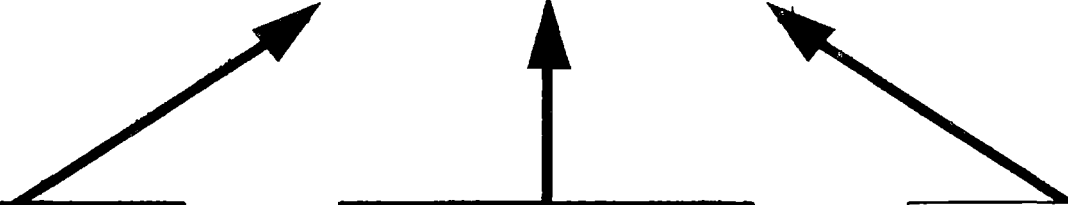
The current plan for analyzing the FLECHT-SEASET data is for W to develop component flow blockage heat transfer models which can be inserted into the Battelle Northwest COBRA-TF code. W will supply the models (consistent with COBRA-TF) and Battelle will insert the models and make the code operational. W will then verify the models using the FLECHT-SEASET 21-rod bundle data, FEBA data, and 163-rod bundle data. The goal is to provide a mechanistic assessment of flow blockage heat transfer which can then be used to address Appendix K changes.

FLECHT-SEASET PROGRAM

USNRC  
L.H. Sullivan  
R. Lee



EPRI  
K.H. (Bill) Sun  
A. Singh



# NATURAL CIRCULATION SYSTEMS EFFECT TASK OBJECTIVES

- Provide a single and two-phase natural circulation data base over a range of natural circulation cooling modes
- Examine system response in each cooling mode
- Examine steam generator heat transfer in each cooling mode

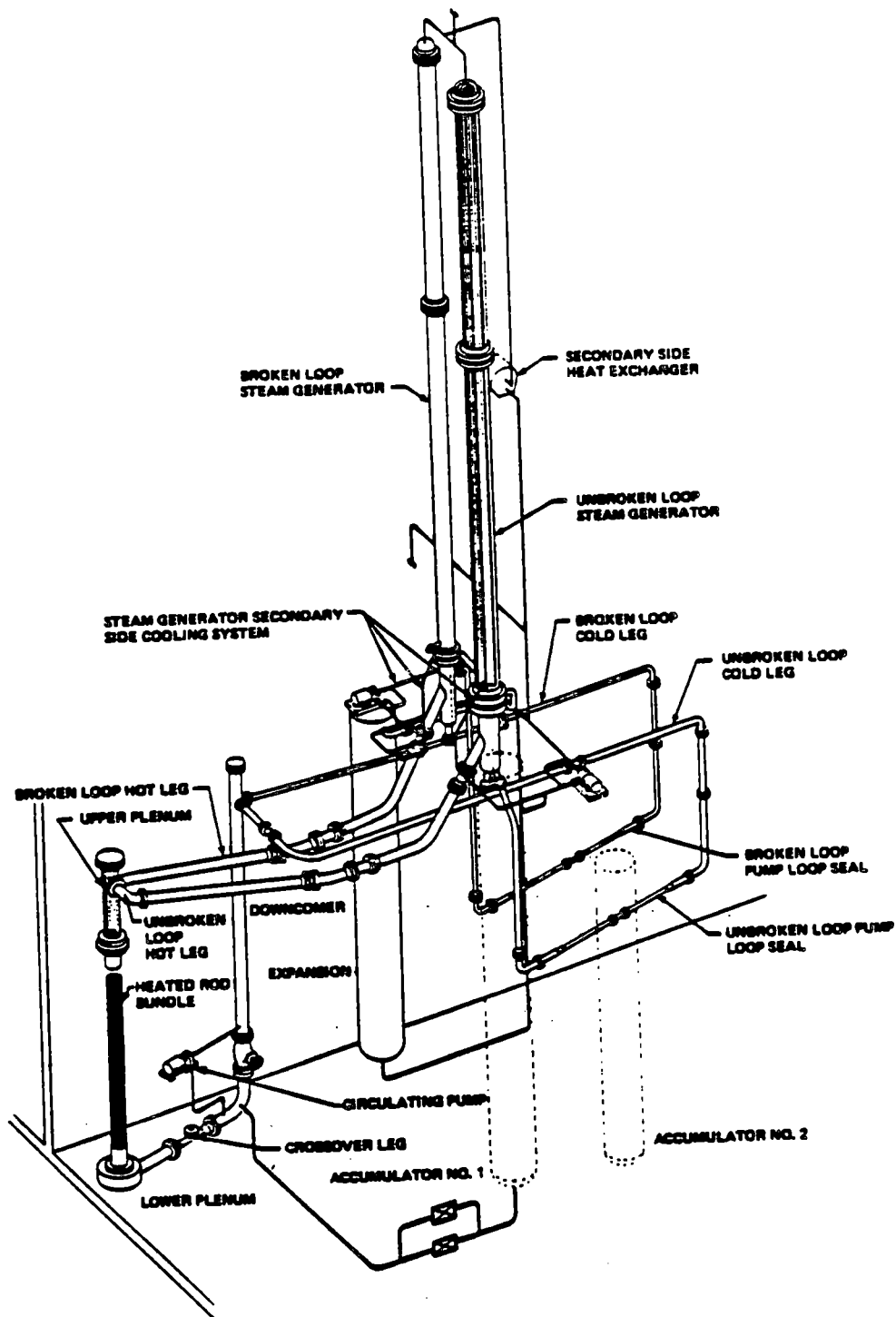


Figure 6-1. FLECHT SEASET Systems Effect Natural Circulation and Reflux Condensation Test Facility

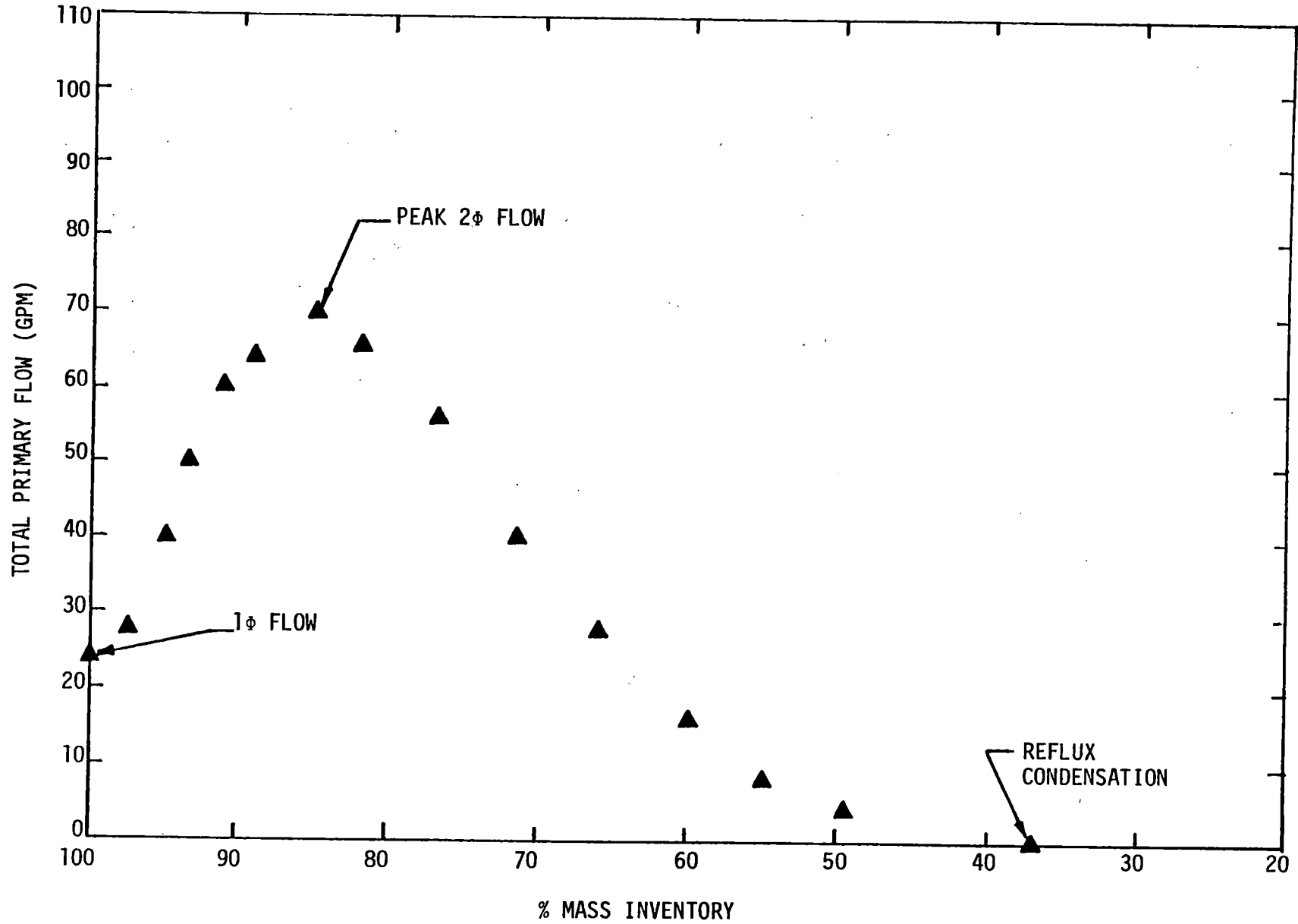
## TEST MATRIX EXAMINED

- Power effects for single phase natural circulation
- Cold leg and upper plenum injection effects during single, two-phase and reflux condensation
- Non-condensable gas injection
- Loss of heat sink
- Increase of heat sink
- Single phase and boiling effects on steam generator secondary side

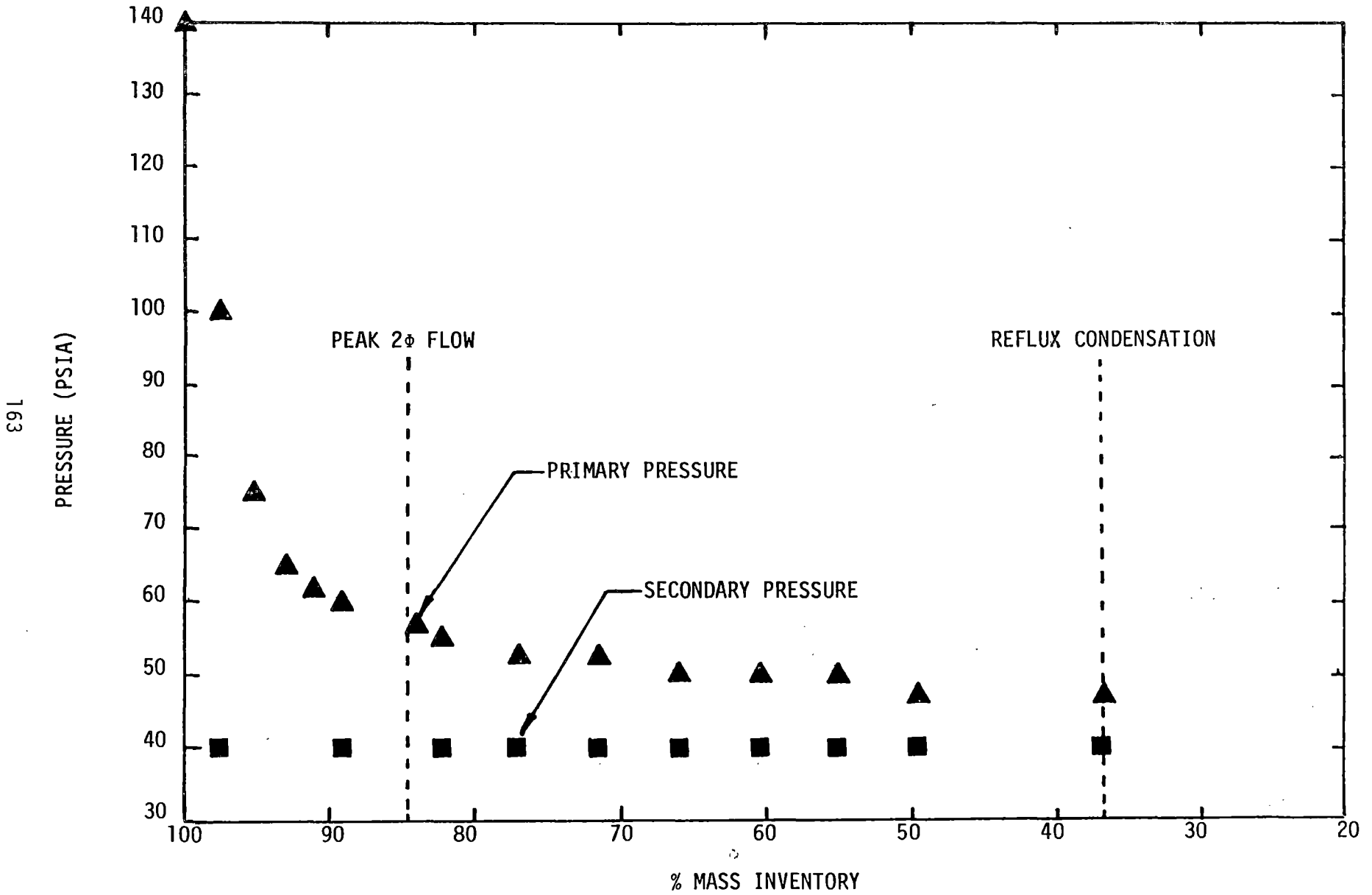
# CONCLUSIONS

- The FLECHT SEASET Facility can operate in a stable fashion in all three natural circulation cooling modes
- The effects of noncondensable gas were observed to
  - Not change single phase cooling
  - Could force a two-phase cooling situation back into single phase as tubes plugged
  - Would only increase primary side pressure to spread out the steam generator heat flux in reflux condensation
- If natural circulation would stall due to cold water injection the pressure would rise, then recover
- If the steam generators were boiled dry, the system would easily be recovered by introducing secondary side water

NATURAL CIRCULATION FLOW RATE AS A FUNCTION OF  
PRIMARY SYSTEM MASS INVENTORY



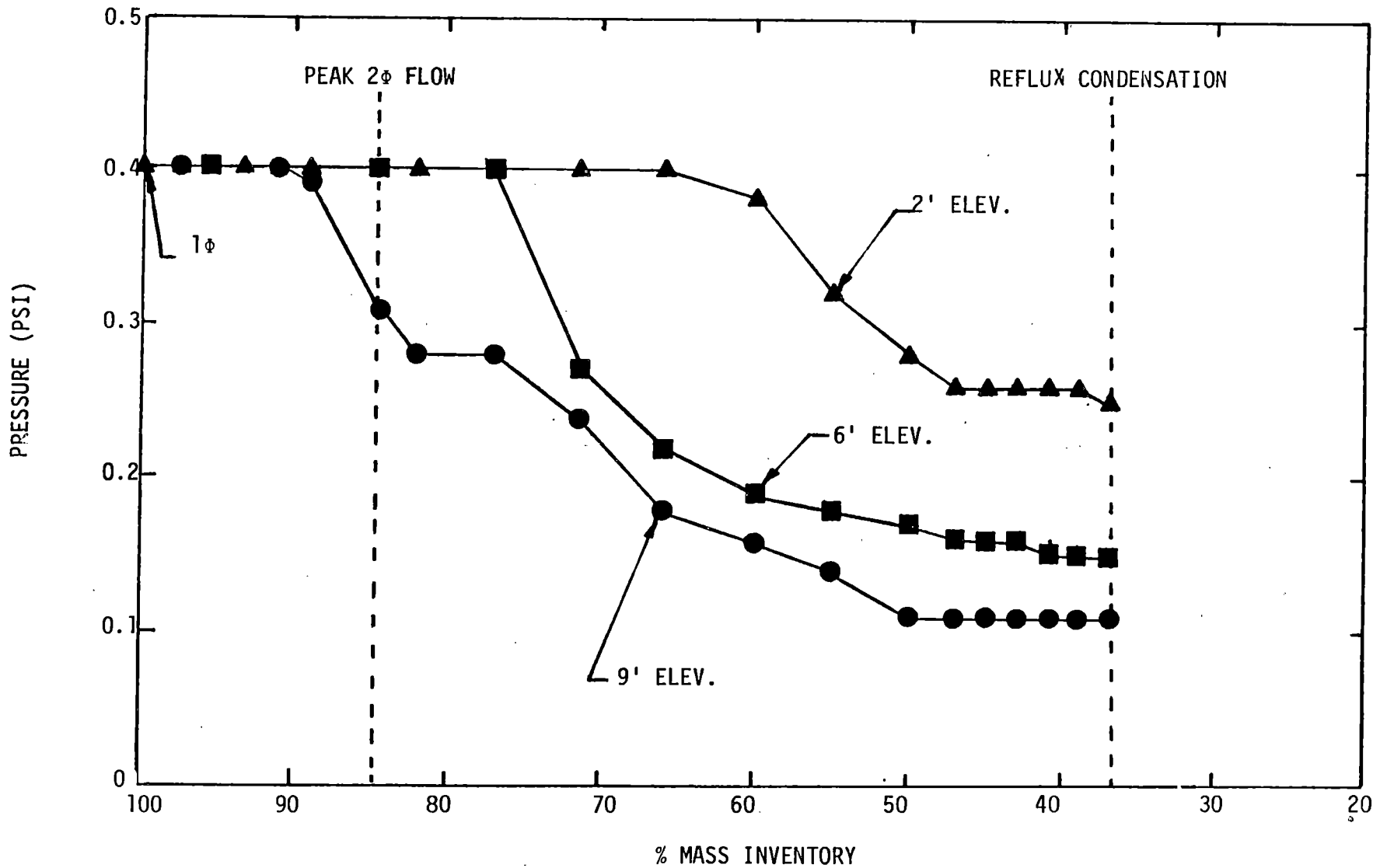
NATURAL CIRCULATION SYSTEM PRESSURES AS A FUNCTION OF  
PRIMARY SYSTEM MASS INVENTORY



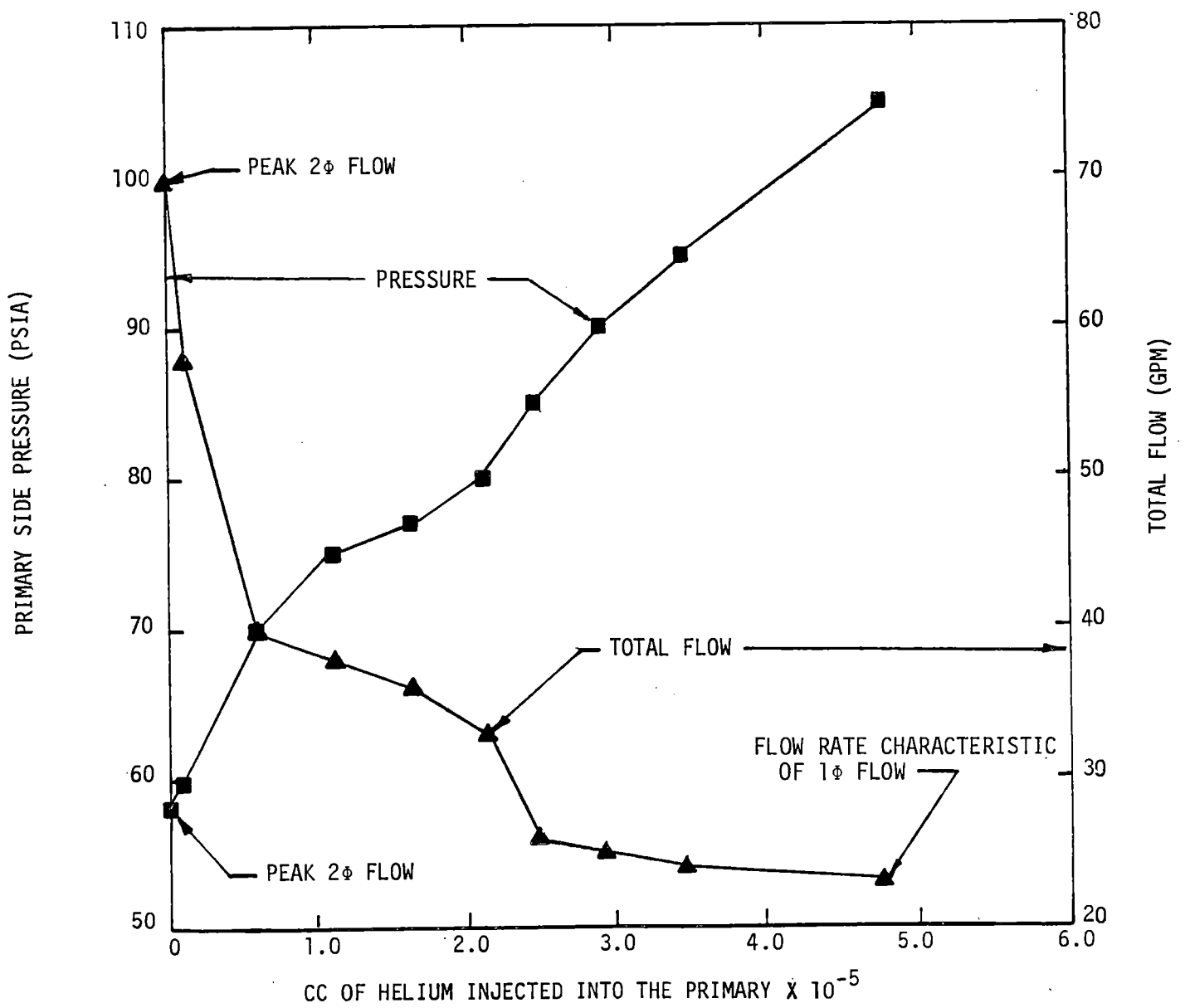


NATURAL CIRCULATION ROD BUNDLE DIFFERENTIAL PRESSURE READINGS AS A FUNCTION OF PRIMARY SYSTEM MASS INVENTORY

164

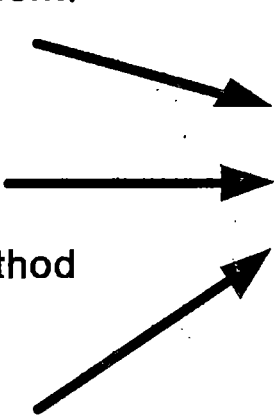


NATURAL CIRCULATION TOTAL FLOW AND PRIMARY PRESSURE  
 AS A FUNCTION OF HELIUM INJECTED INTO THE PRIMARY;  
 2 $\phi$  PEAK FLOW WAS THE INITIAL CONDITION



## FLOW BLOCKAGE HEAT TRANSFER

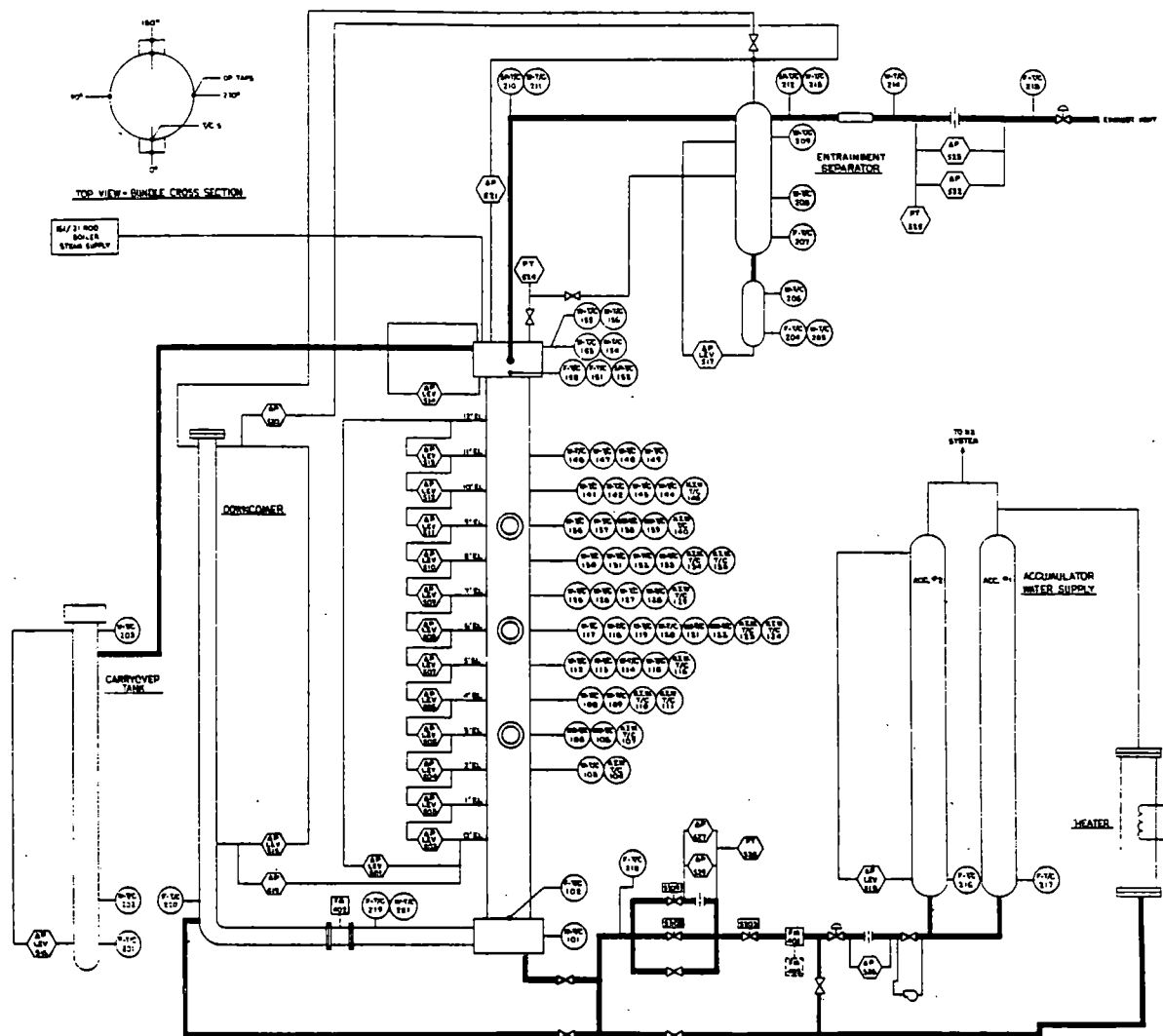
- 17x17 Unblocked FLECHT Tests
  - Geometry effects, data base for blockage
  - Provide data for reflood code development/ verification (TRAC, RELAP MOD-6)
- 21 - Rod Bundle Tests
  - Assesses blockage geometry and configuration effects
  - Provide data for Blockage Analysis Method
- 17x17 Blocked Bundle FLECHT Tests
  - Blockage and bypass effects
  - Address current licensing criteria
  - Assess Blockage Analysis Method



To assess the APP K  
steam cooling/flow  
blockage rule and to  
provide a data base  
for a rule change

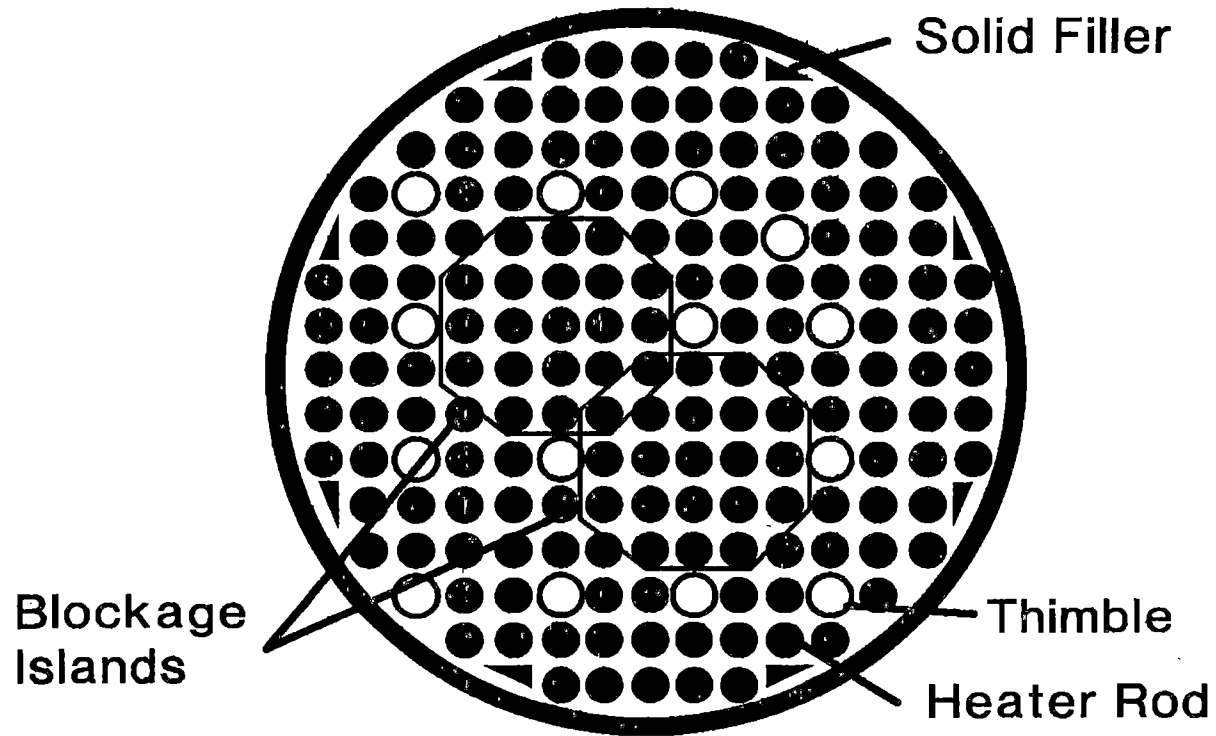
# OBJECTIVES OF THE 163 BLOCKED BUNDLE

- To obtain, evaluate, and analyze 163 blocked bundle thermal-hydraulic data to determine the effects of flow blockage and bypass on reflood heat transfer
- To develop models to describe the flow blockage heat transfer
- To work with Battelle Northwest Laboratory to develop and verify flow blockage models for COBRA-TF



**161-Rod Blocked Bundle Task Loop Instrumentation**

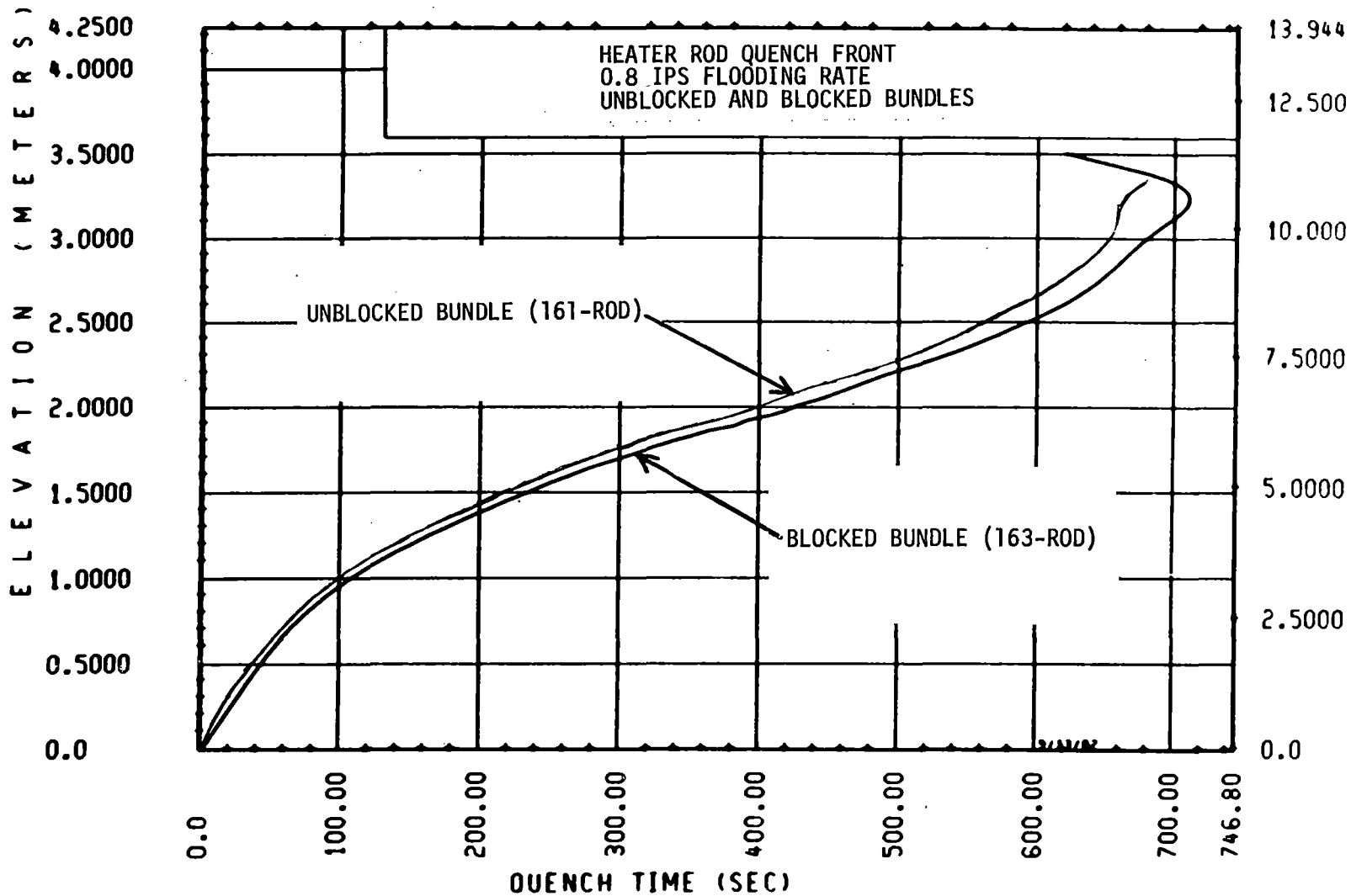
# 21-ROD BLOCKAGE ISLANDS IN 163 ROD BUNDLE



159

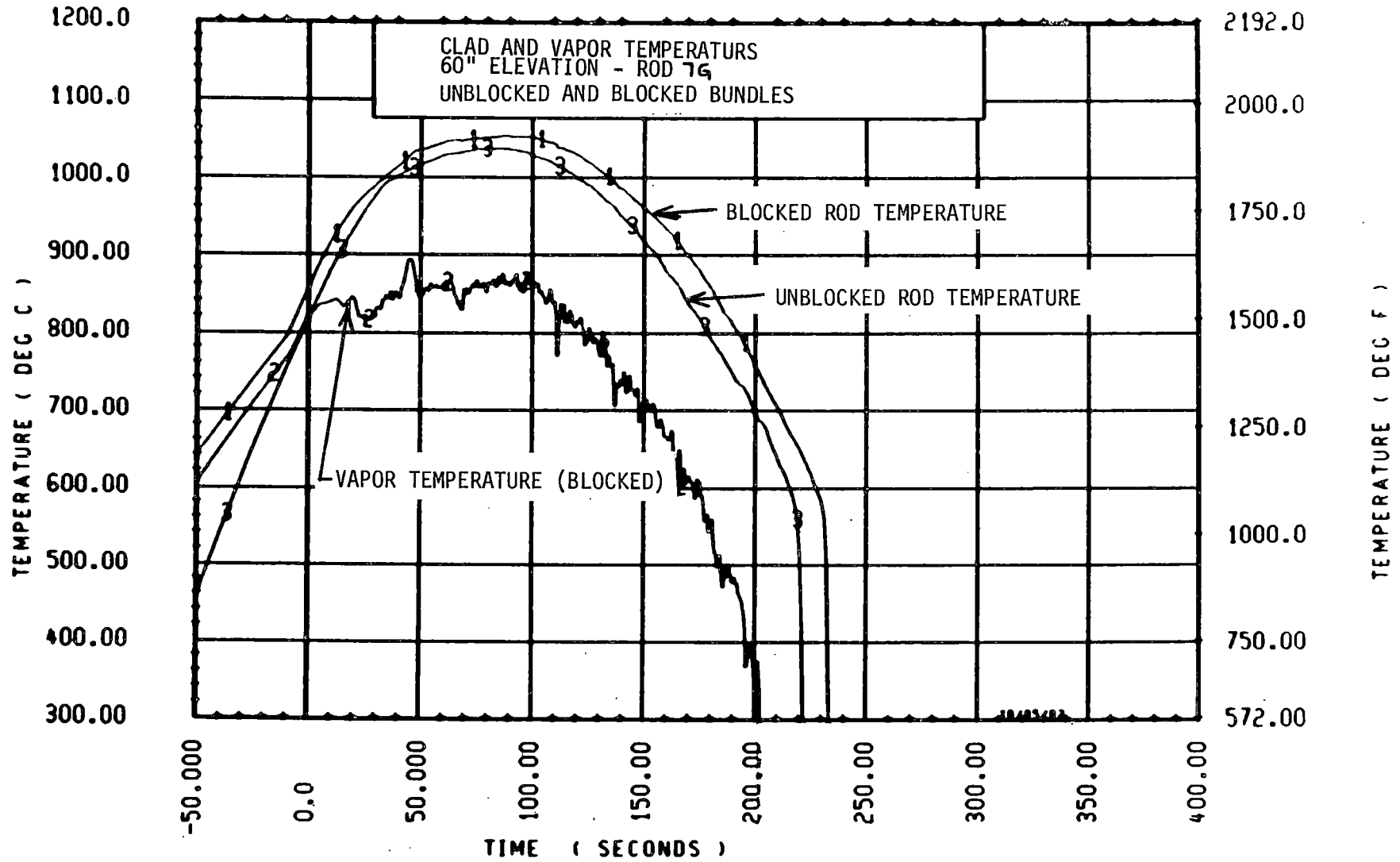
## Bundle Statistics

|                         |          |           |                           |                       |                         |
|-------------------------|----------|-----------|---------------------------|-----------------------|-------------------------|
| Housing Inside Diameter | 194.0 mm | 7.625 in. | Cross-Sectional Flow Area | 15476 mm <sup>2</sup> | 23.989 in. <sup>2</sup> |
| Housing Wall Thickness  | 5.08 mm  | 0.200 in. | Filler Dimensions         | 19.43 mm x 8.64 mm    | 0.765 in. x 0.340 in.   |
| Rod Diameter            | 9.50 mm  | 0.374 in. | 163 Heater Rods           | -                     | -                       |
| Thimble Diameter        | 12.3 mm  | 0.484 in. | 14 Thimbles               | -                     | -                       |
| Rod Pitch               | 12.6 mm  | 0.496 in. | 8 Fillers                 | -                     | -                       |

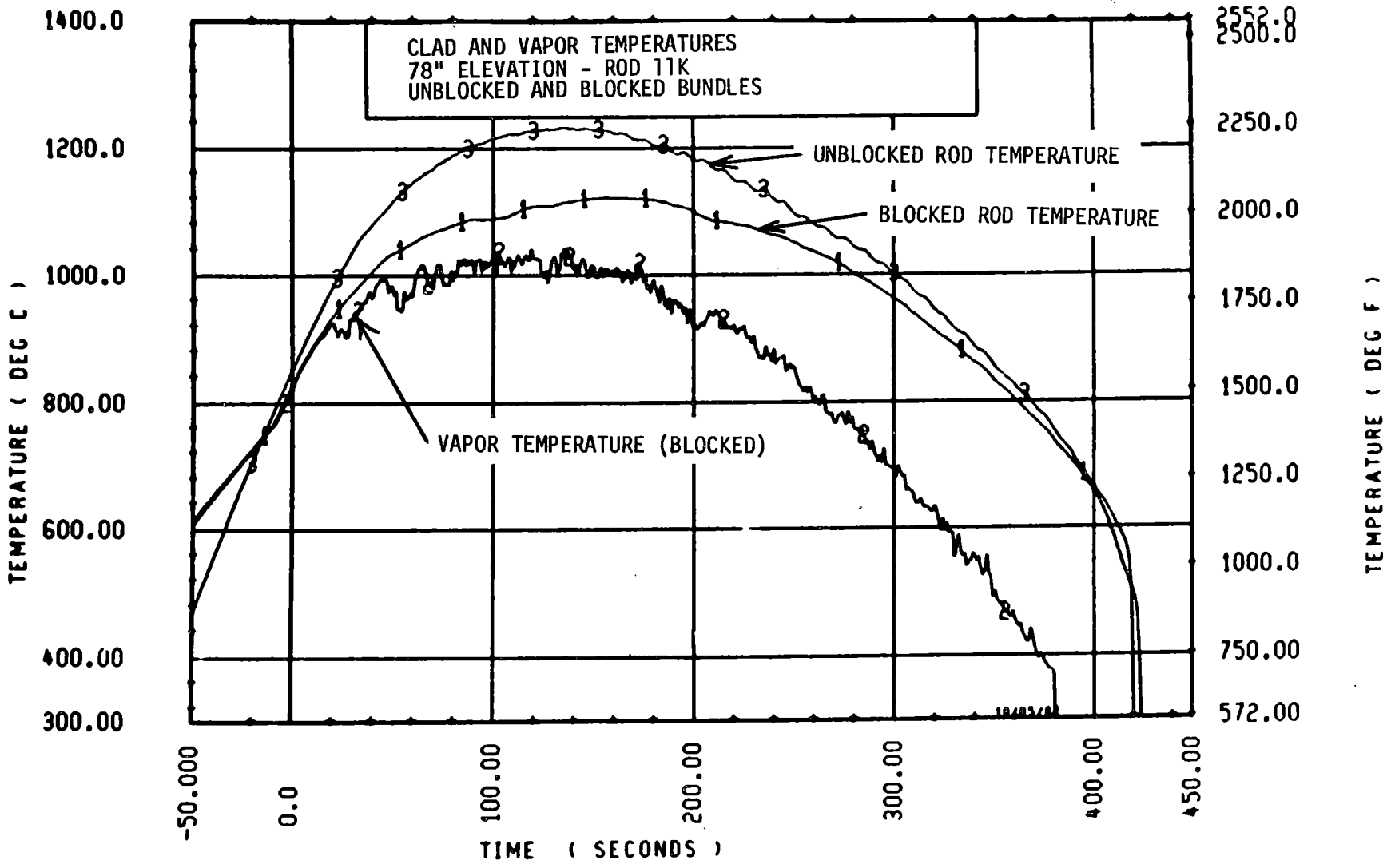


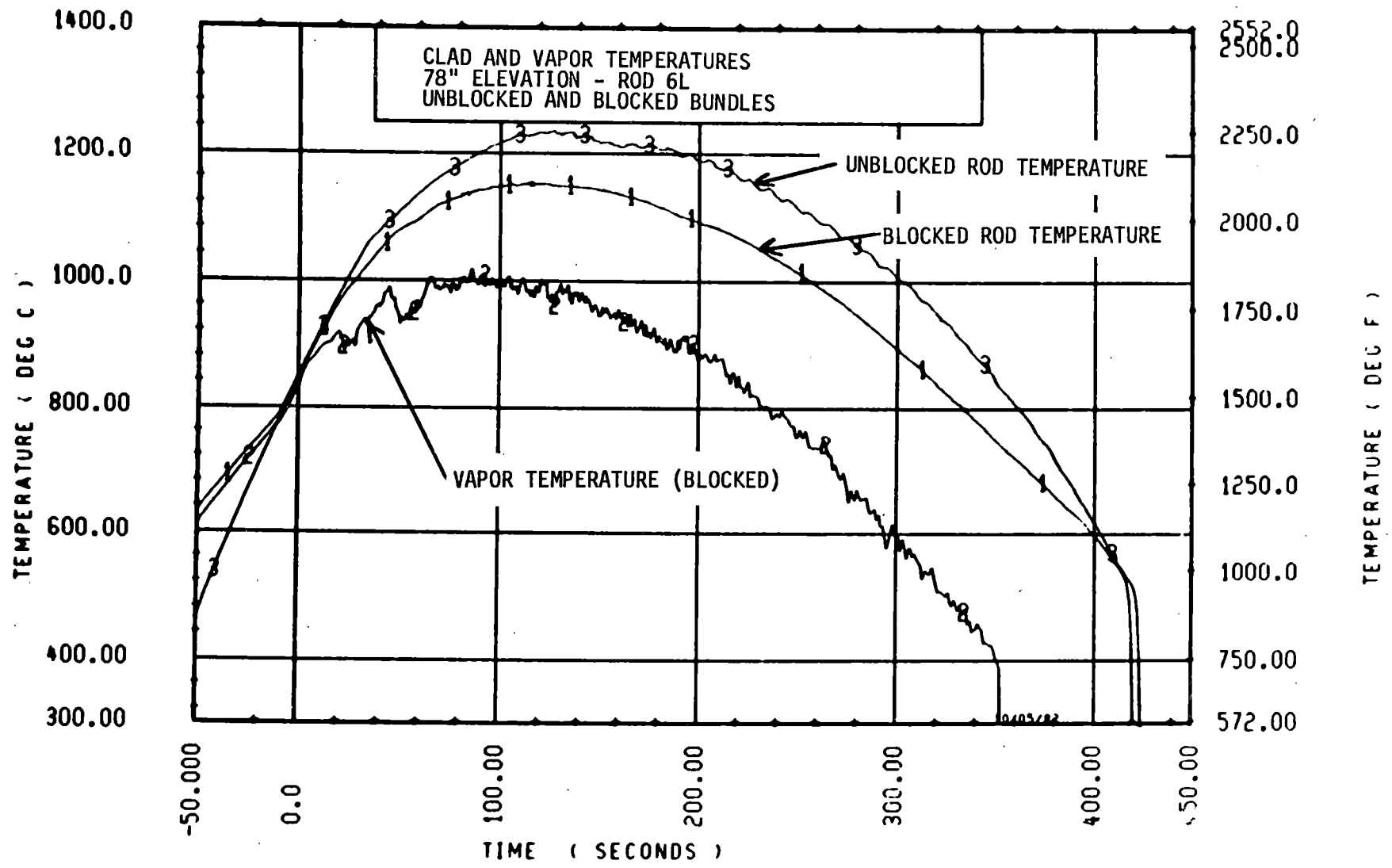
ELEVATION ( FEET )

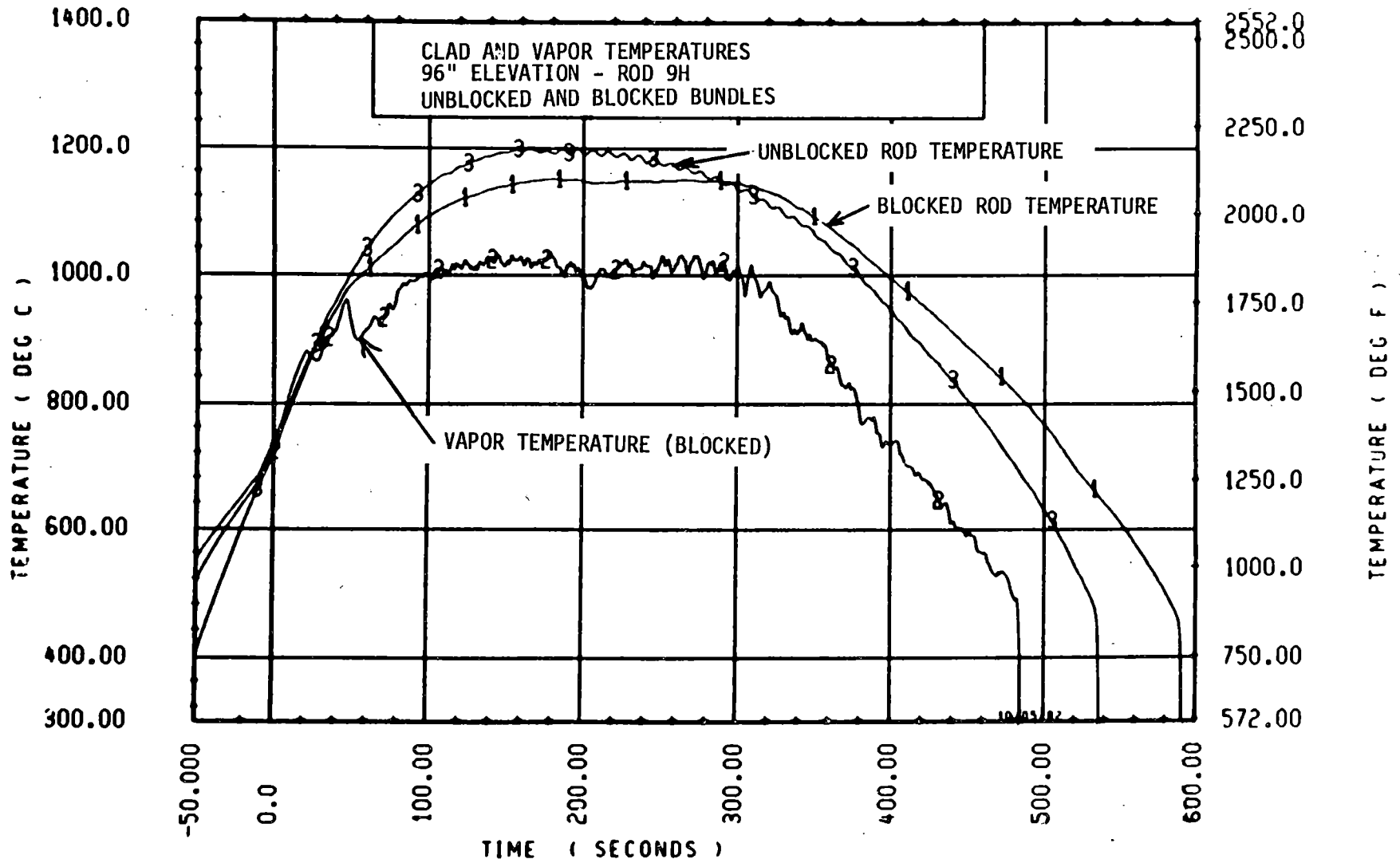
171

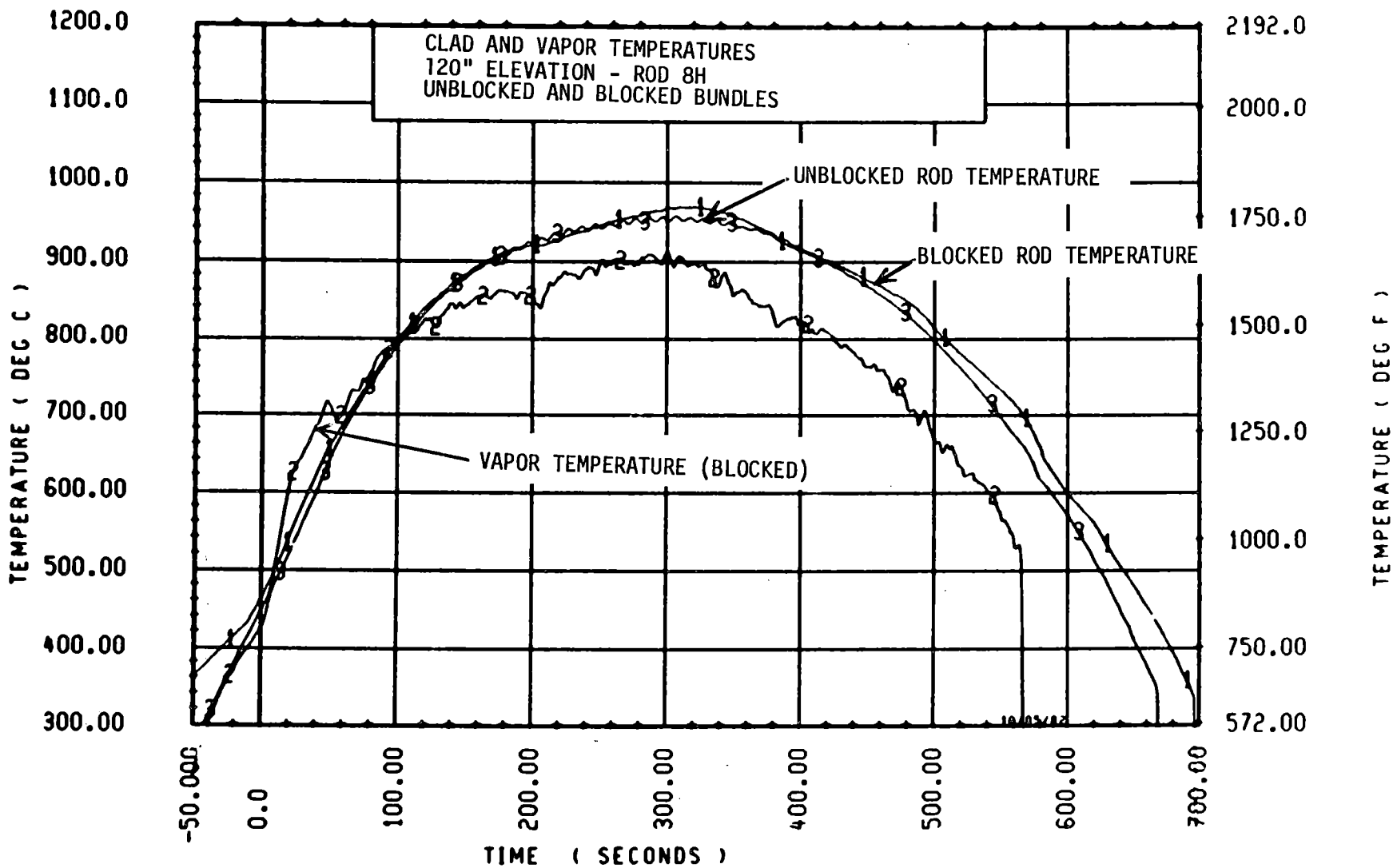


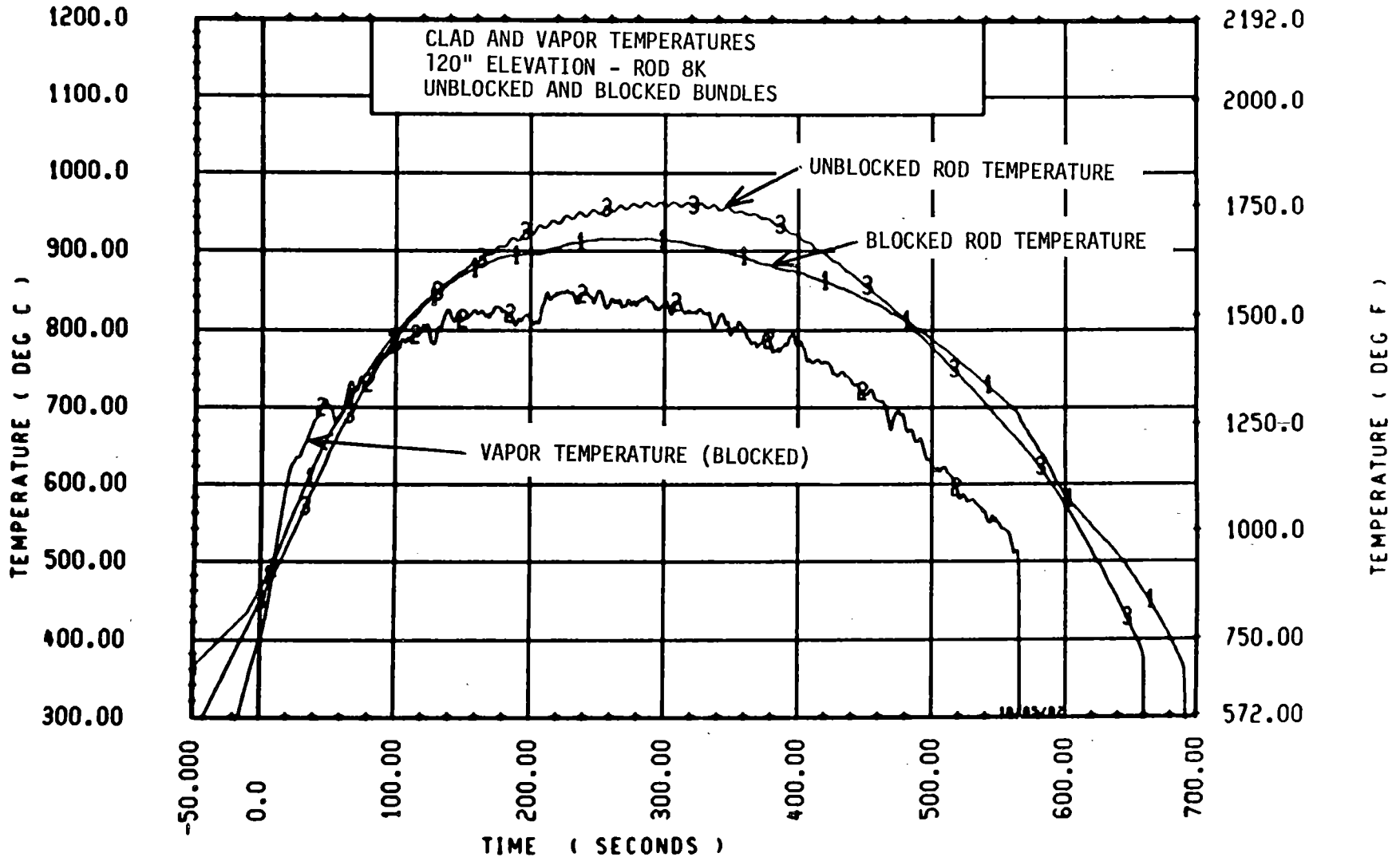




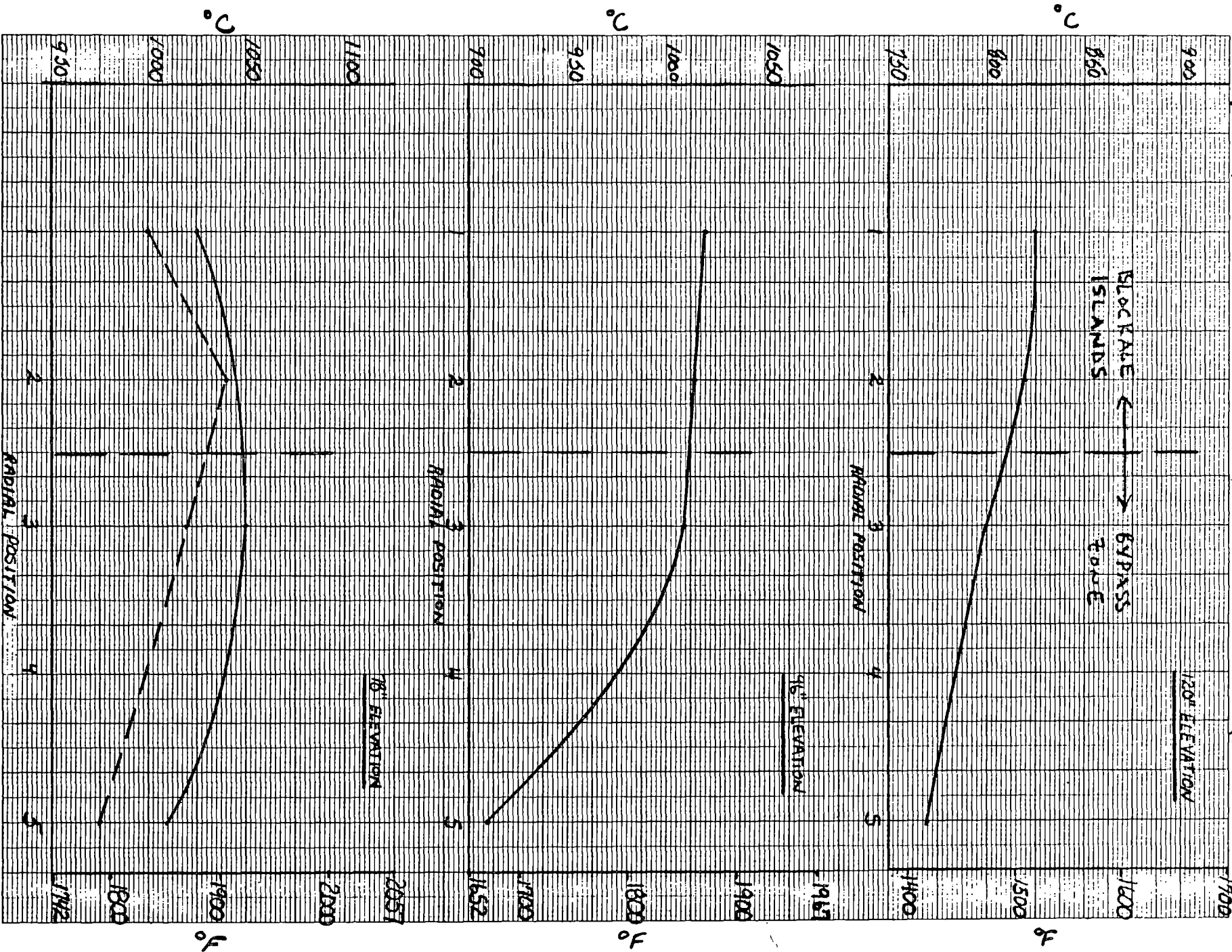








AVERAGE RADIAL VAPOR TEMPERATURES (100 - 150 SEC)



## DATA ANALYSIS AND FLOW BLOCKAGE MODEL DEVELOPMENT

- An agreement has been reached between BNWL, EPRI, NRC, and Westinghouse by which Westinghouse will develop flow blockage component for COBRA-TF
- BNWL will input the flow blockage models into COBRA-TF and make them operational
- Westinghouse will assess the models against FLECHT-SEASET 21 rod bundle data, KfK FEBA data, and the 163 blocked bundle data

# CONCLUSION

- Preliminary analysis of the 163 blocked bundle data indicates
  - Blocked bundle heat transfer improvement in and immediatency downstream of the blockage zone (6-9 feet)
  - Some small heat transfer penalty at the 10 foot elevations for a few rods, pattern is not consistant
- An analysis plan has been developed to model the observed heat transfer effects



HEAT TRANSFER FROM A VERTICAL TUBE  
BUNDLE UNDER NATURAL CIRCULATION CONDITIONS

by

M.J. Gruszczynski and R. Viskanta  
Heat Transfer Laboratory  
School of Mechanical Engineering  
Purdue University  
West Lafayette, IN 47907

PROJECT SUMMARY

Experiments

This paper highlights results of work covering steady-state and transient heat transfer for longitudinal flow of water outside a vertical tube bundle (rods) under natural convection circulation conditions. This type of fundamental information is needed for realistic modeling of the thermal-hydraulic behavior of light water nuclear reactors under transient or accident (e.g., TMI-2) conditions. It is also necessary for the development of computer models to simulate a wide range of postulated nuclear reactor accidents in order to gain insight into measures that can be taken to improve reactor safety.

A rectangular natural circulation loop (thermosyphon) was used to measure the average heat transfer coefficients to water at atmospheric pressure. A seven-tube test bundle having a pitch-to-diameter tube ratio of 1.25 was used as a test heat exchanger. The bundle was 1.219 m long, and the outside tube diameter of the copper tubes was 0.01905 m. A circulating flow was established in the loop because of buoyancy differences in its two vertical legs. The test bundle was heated by circulating water through the bundle. A similar type of tube bundle was used for the other (cold) leg of the loop. Steady state heat transfer measurements were over a range of thermal conditions, and the dynamic response of the loop was studied. About 80 steady-state test runs were performed with the test bundle in a counter-flow and parallel-flow arrangements. The experiments are described and the results are discussed in detail elsewhere [1].

Results and Discussion

The analysis of the effective flow resistance parameter  $R$  indicates that a plot of  $RA_f^2$  versus  $1/Re$  would be a straight line of the form [1],

$$R A_f^2 = C_R/Re + K_T A_f^2, \quad (1)$$

where  $A_f$  and  $Re$  are the cross sectional flow area and the Reynolds number, respectively, in the section containing the test tube bundle. The constant  $C_R$  is composed of the individual friction factors for each loop component, and  $K_T$  is the total form loss coefficient for flow in the loop. Analysis of experimental data [6] has shown that  $C_R = 18,340$  and  $K_T A_f^2 = -5$ . This indicates that the form losses in the loop have only a minor influence on the pressure drop around the loop, and the major factor controlling the frictional pressure drop is the first term on the right hand side of Eq. (1). The form loss coefficient  $K_T A_f^2$  was found to be small but negative by a least squares fit. This was due to experimental errors and the approximations used in calculating the

driving temperature difference for determining the resistance parameter  $R$ . When numerical values for the hydraulic diameters, flow areas, and the lengths of the components are substituted into the defining equation, the constant  $C_R$  can be expressed as

$$C_R = 4a_L + 114 a_1 + 161 a_2, \quad (2)$$

where  $a_1$ ,  $a_2$ , and  $a_L$  are the individual friction factor coefficients in the Fanning<sup>1</sup> friction factor relation,  $f = a_L/Re^b$ . Taking  $a_L = 16$  and  $b = 1$  [2] and assuming that  $a_1 = a_2$  since the porosities are approximately equal [3], this yields that  $a_1 = 66.5$ . Noting that 90% of the data lies in a range for  $C_R$  of  $13,000 < C_R < 20,000$ , this gives a range for  $a_1$  of  $47 < a_1 < 72$ .

The average Nusselt number is based on the average convective heat transfer coefficient for heat transfer to the circulating fluid in the loop from the outside walls of the test tube bundle is used. The hydraulic diameter ( $D_h = 0.0138m$ ) of the tube bundle. The thermophysical properties of water were evaluated at the average temperature of the fluid. Since it has not been conclusively established in the literature what should be the appropriate correlating heat transfer parameters in a natural circulation loop average Nusselt numbers are presented in terms of Reynolds, Rayleigh and Grashof-to-Reynolds number ratio.

The effect of thermophysical property variation with temperature on heat transfer was found to be best correlated by including the Prandtl number dependence on the average Nusselt number. A plot of  $Nu/Pr^{0.43}$  versus  $Re$  is shown in Figure 1. Counter-flow tests (A through D) are correlated by a least squares fit of the form

$$\overline{Nu} = 0.0667 Re^{0.80} Pr^{0.43}, \quad 80 < Re < 300 \quad (3)$$

and parallel-flow tests (E) are correlated by

$$\overline{Nu} = 0.0814 Re^{0.80} Pr^{0.43}, \quad 80 < Re < 300 \quad (4)$$

For  $Re > 300$ , the average Nusselt number is overpredicted by Eqs. (3) and (4). Since the data are quite scattered, no correlation is given for  $Re > 300$ . The average Nusselt numbers are higher for parallel-flow tests than for counter-flow. This is expected, since higher flow rates have been obtained for equivalent heating rates. The results also show that there is poor correlation between the data for  $Re > 300$  which indicates that the Reynolds number is not the only correlating parameter.

The dependence of the heat transfer parameter  $\overline{Nu}/Pr^{0.43}$  on the Rayleigh number is shown in Figure 2. The counter-flow tests are correlated by a least squares fit,

$$\overline{Nu} = 0.00116 Ra^{0.67} Pr^{0.43}, \quad 6 \times 10^4 < Ra < 5 \times 10^5 \quad (5)$$

and the parallel-flow tests by

$$\overline{Nu} = 0.00173 Ra^{0.67} Pr^{0.43}, \quad 6 \times 10^4 < Ra < 5 \times 10^5 \quad (6)$$

Again, for  $Ra > 5 \times 10^5$ , Eq. (5) does not correlate the experimental data. The exponent on the Rayleigh number is approximately 2.5 times higher than that usually expected for laminar free convection conditions [2].

In our attempt to determine if heat transfer from the tube bundle to the fluid in the natural circulation loop behaves like combined forced and natural convection, the Grashof-to-Reynolds number ratio  $Gr/Re$  was used as a correlating parameter. The counter-flow tests are correlated by a least squares fit,

$$\bar{Nu} = 0.0192 \left[ \frac{Gr}{Re} \right]^{1.2}, \quad 75 < Gr/Re < 250 \quad (7)$$

and data for parallel-flow tests by

$$\bar{Nu} = 0.0191 \left[ \frac{Gr}{Re} \right]^{1.3}, \quad 75 < Gr/Re < 250 \quad (8)$$

For  $Gr/Re$  ratios above 250, the data points are quite scattered, and no meaningful least squares fits could be found. The combined convection heat transfer analysis in infinite rod arrays [4] has used the  $Gr/Re$  number ratio, where the Grashof number is based on an average heat flux along the length of the rod, as a correlating parameter. This Grashof-Reynolds number ratio is equivalent to  $NuGr/Re$ . The analysis [4] only covers values of  $Gr/Re$  ratios up to 70 ( $GrNu/Re = 680$ ) assuming fully developed flow and heat transfer with a constant heat flux along the length of the rod. The numerical results are outside the range of present experimental data.

### Conclusions

Steady-state heat transfer results were correlated in terms of non-dimensional parameters that govern fluid flow and heat transfer in the system. The pressure drop around the loop was found to depend on the Reynolds number alone. Laminar forced flow friction factor correlations were found to correlate the total flow resistance in the loop. Heat transfer results were not predicted by laminar forced flow correlations but were found to depend on the Reynolds, Rayleigh, and Prandtl numbers.

The empirical equations (3) and (4) with the Reynolds number as the governing parameter correlate the experimental data the best. Since the heating rate of the fluid determines the magnitude of the mass circulation rate of the fluid, one would expect a relation of this form to yield the best correlation.

### Acknowledgements

This work was supported by the U.S. Nuclear Regulatory Commission through a subcontract from Argonne National Laboratory. The authors are indebted to Dr. Paul A. Lottes for his interest and many helpful discussions.

References

- [1] Gruszczynski, M.J., "Heat Transfer from a Vertical Tube Bundle under Natural Circulation Conditions", Thesis, Purdue University, August 1982.
- [2] Incropera, F.P., and DeWitt, D.P., Fundamentals of Heat Transfer, Wiley Book Co., New York, 1981.
- [3] Sparrow, E.M., and Loeffler, A.L., "Longitudinal Laminar Flow Between Cylinders Arranged in Regular ARrays", AIChE Journal, Vol.5, pp. 325-330, 1959.
- [4] Yang, J.M., Analysis of Combined Convection and Heat Transfer in Infinite Rod Arrays, in Heat Transfer 1978, Volume 1, National Research Council of Canada, Ottawa, 1978, pp. 49-54.

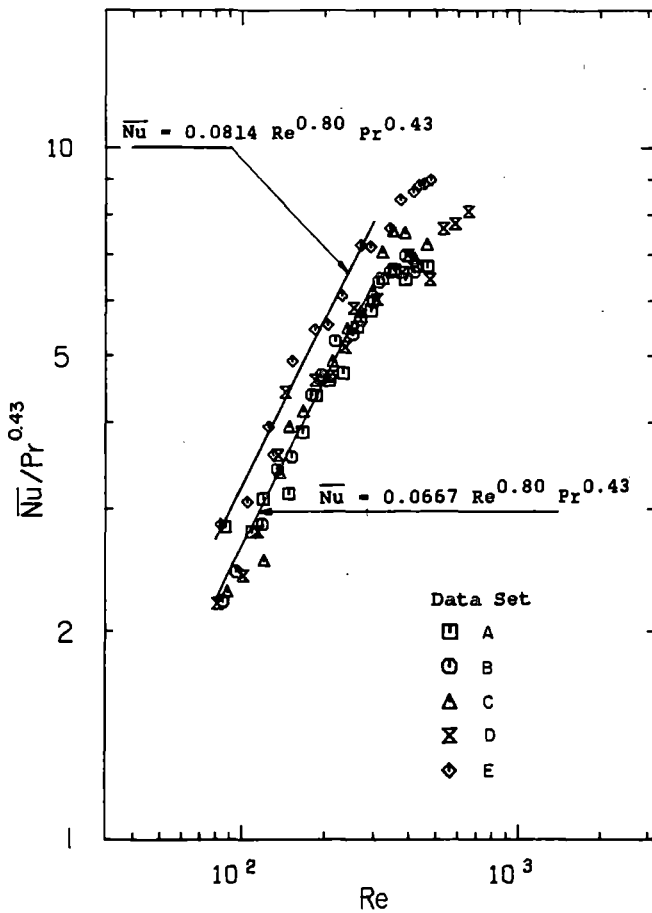


Figure 1. Heat transfer parameter dependence on Reynolds number

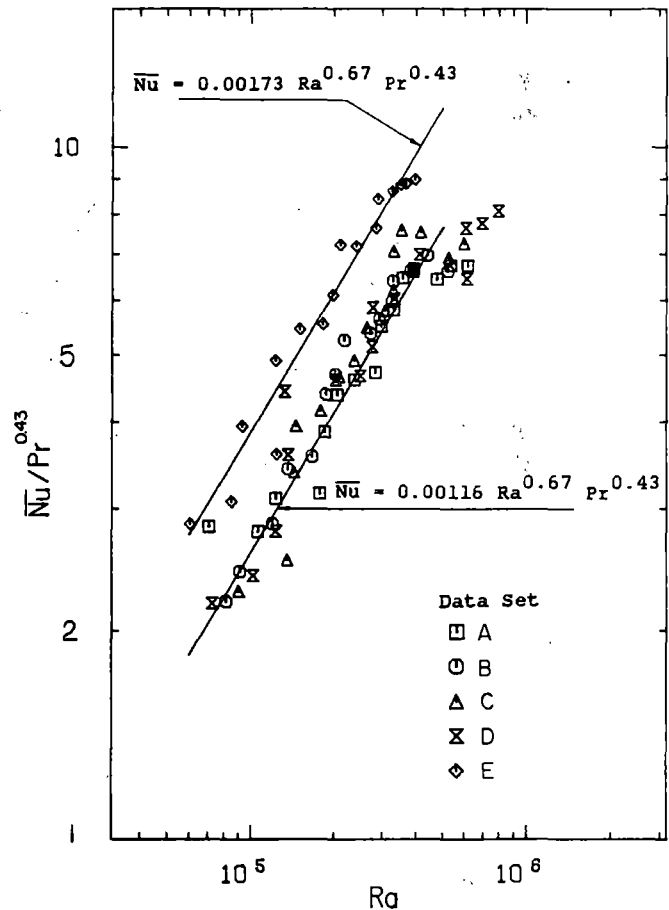


Figure 2. Heat transfer parameter dependence on Rayleigh number

HEAT TRANSFER TO WATER FROM A VERTICAL  
TUBE BUNDLE UNDER NATURAL  
CIRCULATION CONDITIONS

by

M.J. Gruszczynski and R. Viskanta  
School of Mechanical Engineering  
Purdue University  
West Lafayette, IN 47907

PROJECT OBJECTIVES

- Measure and Correlate Steady-State Pressure Drop in a Tube Bundle Under Natural Circulation Conditions
- Measure and Correlate Steady-State Heat Transfer From a Tube Bundle Under Natural Circulation Conditions
- Predict the Transient Behavior of the Natural Circulation Loop and Compare with Experimental Data

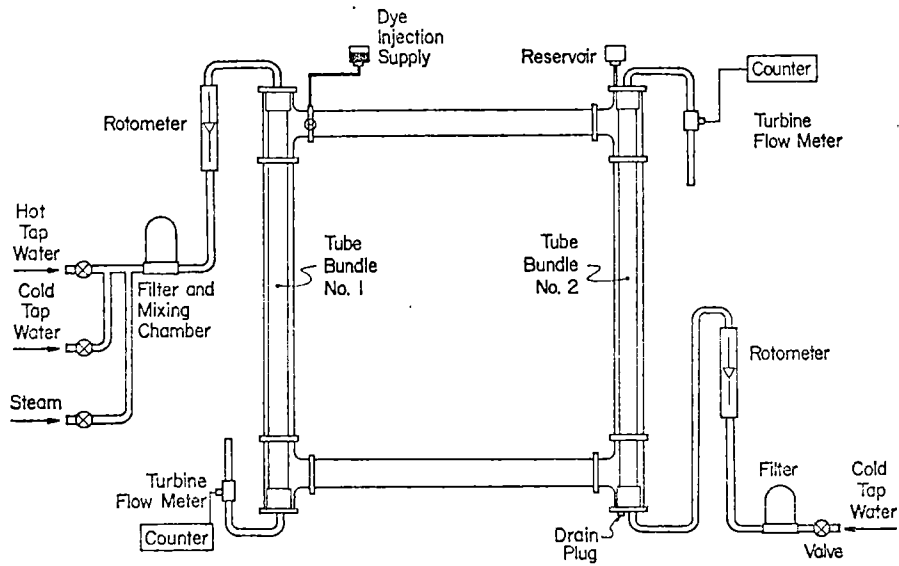


Figure 2. Schematic diagram of the experimental loop

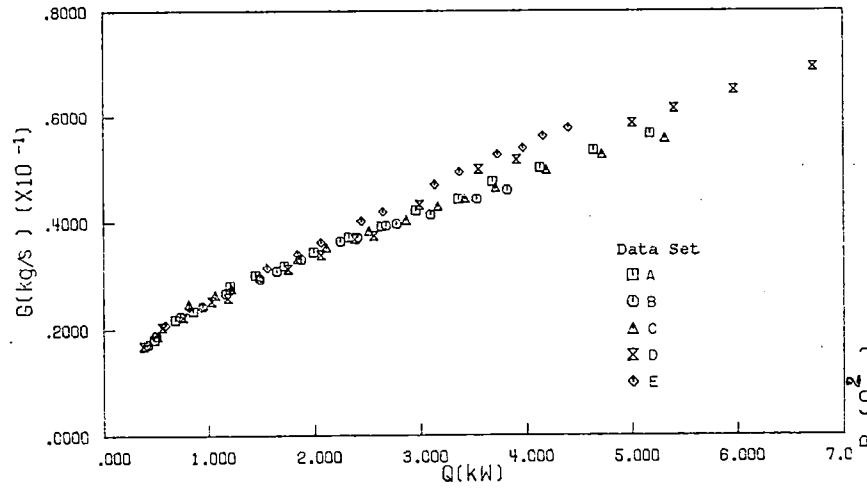


Figure 11. Variation of flow rate with heating rate

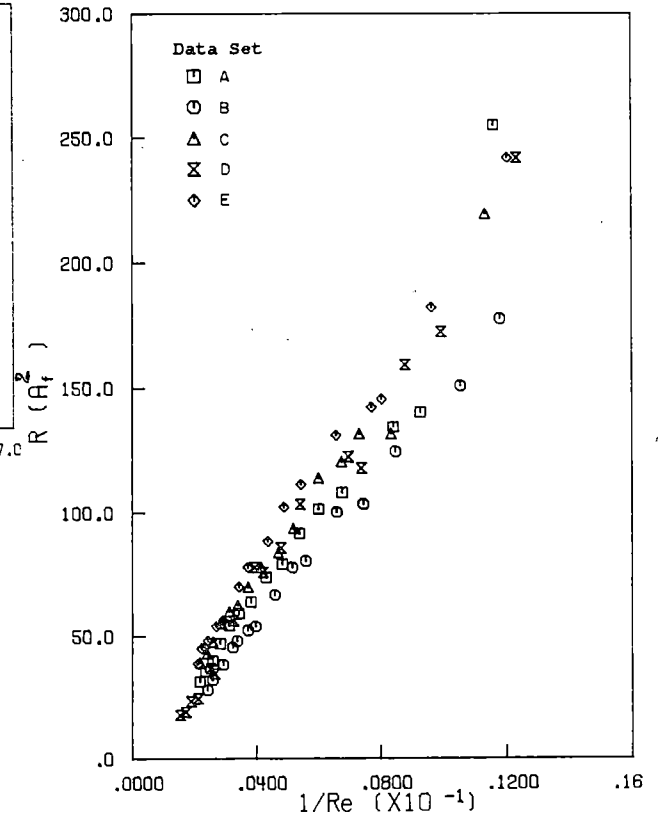


Figure 14. Dependence of effective flow resistance parameter on Reynolds number

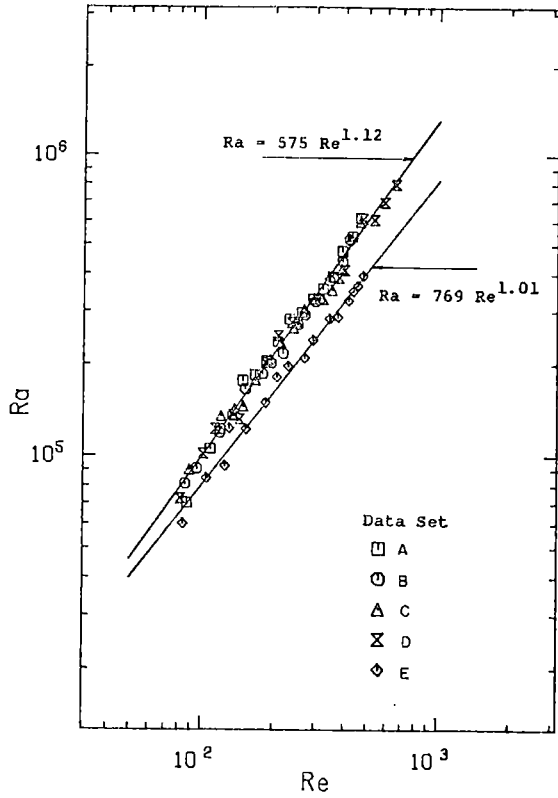


Figure 13. Rayleigh number dependence on Reynolds number

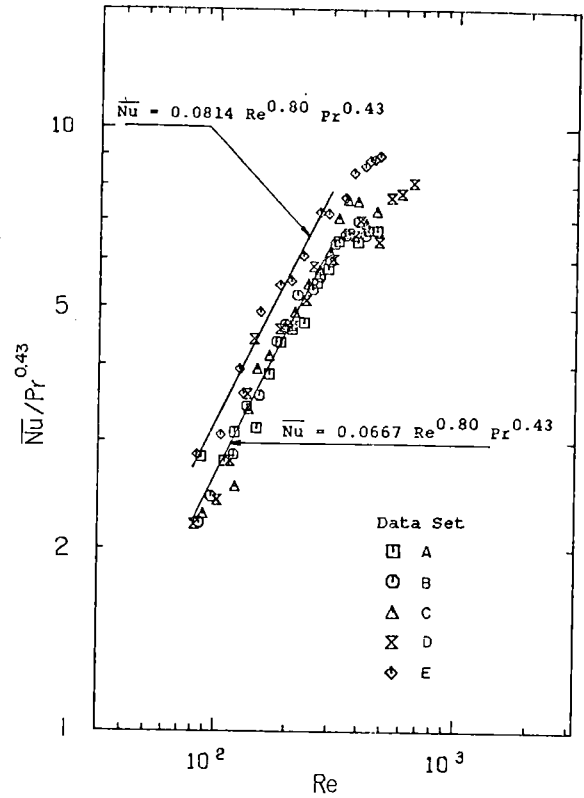


Figure 19. Heat transfer parameter dependence on Reynolds number

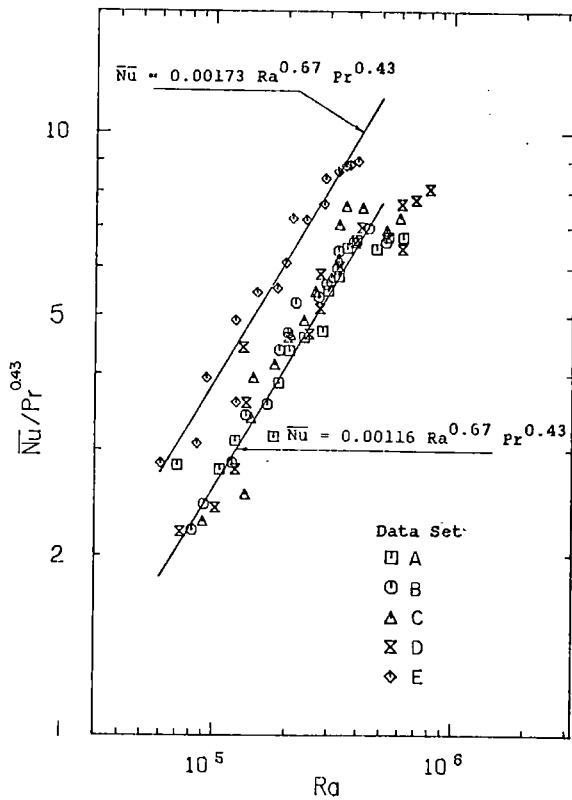


Figure 21. Heat transfer parameter dependence on Rayleigh number

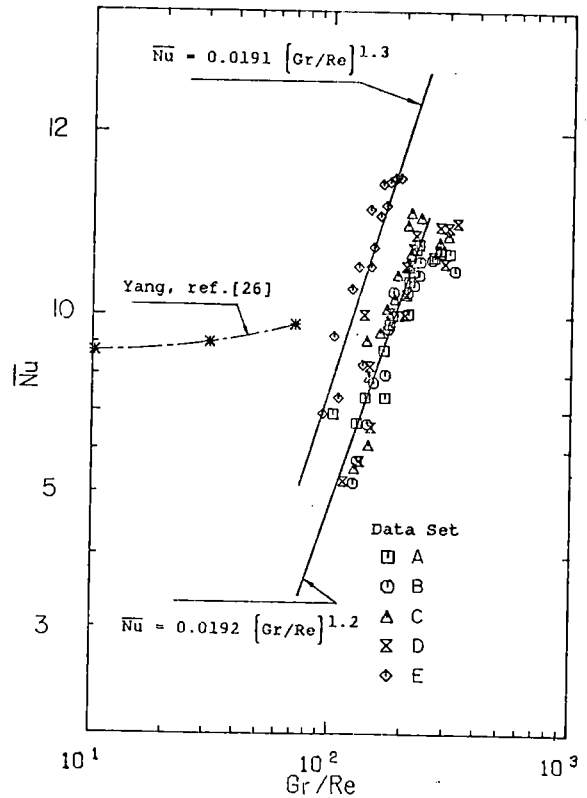


Figure 22. Average Nusselt number dependence on Grashof to Reynolds number ratio

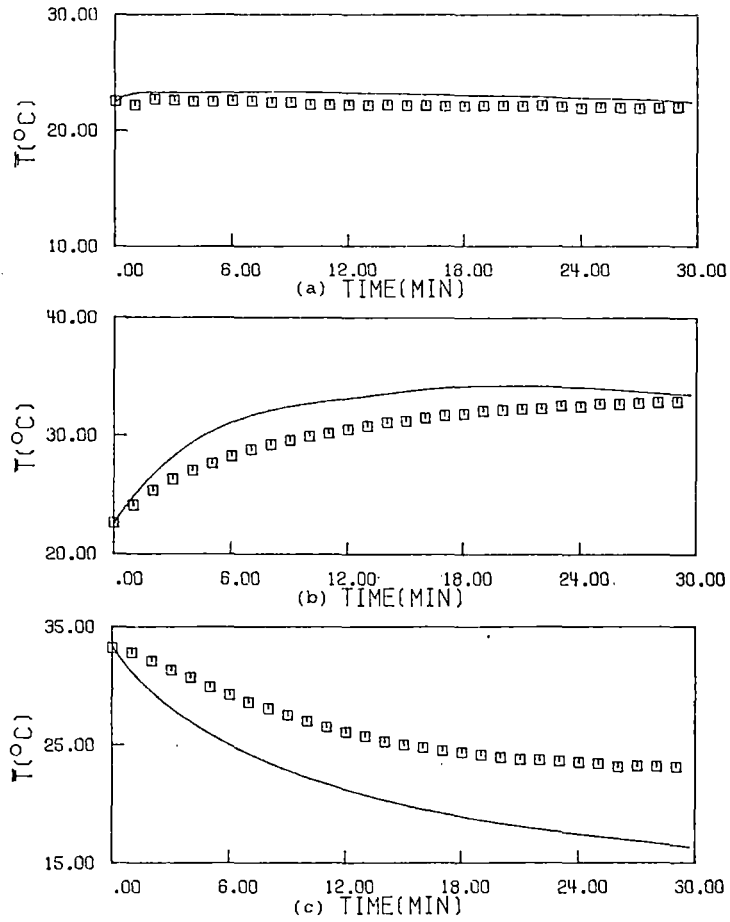


Figure 26. Average temperature variation with time of the loop for the transient tests:  
 (a) Tr-1, (b) Tr-2, (c) Tr-3

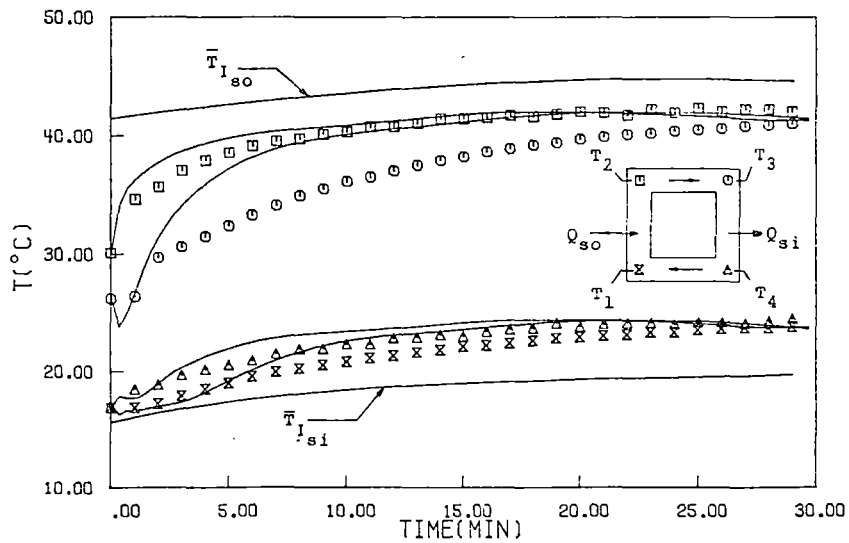


Figure 27. Local temperature variation with time in the loop for transient test Tr-2



## THERMAL-HYDRAULIC EXPERIMENT FACILITY (THEF)<sup>a</sup>

J. S. Martinell  
EG&G Idaho, Inc.

This paper provides an overview of the Thermal-Hydraulic Experiment Facility (THEF) at the Idaho National Engineering Laboratory (INEL). The overview follows two distinct paths. The first deals with a description of the major test systems, measurements, and data acquisition system. The second presents objectives, facility configuration, and results for major experimental projects recently conducted at the THEF. Plans for future projects are also discussed.

The THEF is located in the Water Reactor Research Test Facility (WRRTF) area at the INEL. The facility comprises two major test systems, auxiliary support equipment, measurement systems, and a central data acquisition system. The two major test systems include the Blowdown Facility (BF), and the Two-Phase Flow Loop (TPFL).

The BF is a stainless steel, high pressure (15.5 MPa), high temperature (620 K) facility capable of steady state or transient operation. The system has a volume of approximately  $0.3 \text{ m}^3$ , with test piping ranging in inside diameter from 1 to 10 cm. The system is versatile and provides access for rapid reconfiguration for support of a wide range of experiments.

The TPFL is a large, two-phase steam/water test system consisting of a once-through steam system and a closed-loop liquid recirculation system. Piping and components are carbon steel, with test section operating limits of 6.9 MPa and 560 K. The steam supply contains  $85 \text{ m}^3$  of saturated liquid storage, providing maximum steam flow of 25 kg/s for 4 minutes. The

---

a. Work supported by the U.S. Nuclear Regulatory Commission, Office of Nuclear Regulatory Research, under DOE Contract No. DE-AC07-76ID01570.

maximum liquid flow rate is 420 kg/s. Current configuration provides a horizontal test section with an inside diameter of 28 cm.

Auxiliary support equipment such as power controllers, compressors, makeup, and drain are shared by both systems. Instrumentation is available for making detailed measurements on either system. Transducer output are amplified, acquired, and processed on a central computerized data acquisition system.

The THEF was constructed to provide experimental capability in the areas of separate effects thermal-hydraulic phenomena investigation, instrument development and calibration, and component performance assessment. The facility has been used to support INEL programs involved in water reactor safety research for the NRC. Examples of recently conducted projects include two-phase instrumented spool calibration, subcooled critical flow nozzle characterization, and postcritical heat flux (CHF) heat transfer investigation.

The TPFL was configured in the fall of 1980 to support calibration and performance assessment of two-phase flow instrumentation developed by the 2D/3D program for use in the Japan Atomic Energy Research Institute Slab Core Test Facility (SCTF). Test system piping was modified to provide simulation of the SCTF upper plenum, hot leg, and steam generator inlet. Instrumentation tested included densitometers, drag devices, turbines, and optical probes. Results indicated excellent agreement between measured two-phase flows and reference values.

The BF has been configured for several subcooled critical flow nozzle characterization studies to support LOFT experimental needs and code assessment and development projects. Results of these experiments have provided data from which size and subcooling effects on subcooled critical mass flow through nozzles have been assessed.

The existing data base from which correlations on post-CHF heat transfer have been developed is lacking in data at conditions experienced during large-break blowdown experiments. The BF was configured in the spring of

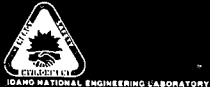

1982 to provide nonequilibrium, dispersed-flow, post-CHF data over a range of conditions designed to help fill this void. Results of the experiments have produced data which will enable model and code assessment and development in an effort to improve heat transfer analysis capabilities.

Several potential projects for use of the THEF have been proposed and planning has been initiated. One such project would provide experimental data on bubble dynamics in an inverted U-tube geometry representative of the involute at the inlet of a once-through steam generator. Experiment planning and facility preparation to provide data on two-phase flow regime effects on critical mass discharge from a branch line have been initiated. A project to address experimental determination of two-phase regime transition boundaries in large pipes with varying configurations has also been proposed.

In summary, the THEF is a versatile, thermal-hydraulic test facility capable of providing experimental data to address a broad range of water reactor safety needs.

# Thermal-Hydraulic Experiment Facility (THEF)

J.S. Martinell

S2 10 190

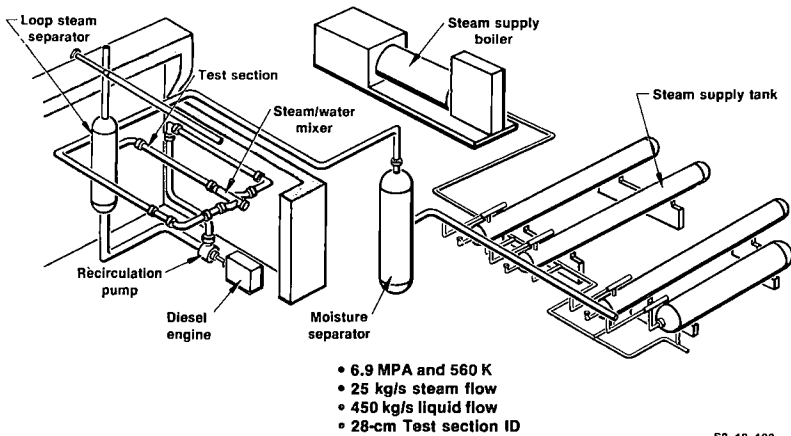
## Objectives

- Present THEF summary description
- Review experimental projects conducted at THEF
- Discuss future THEF projects

S2 10 191

151

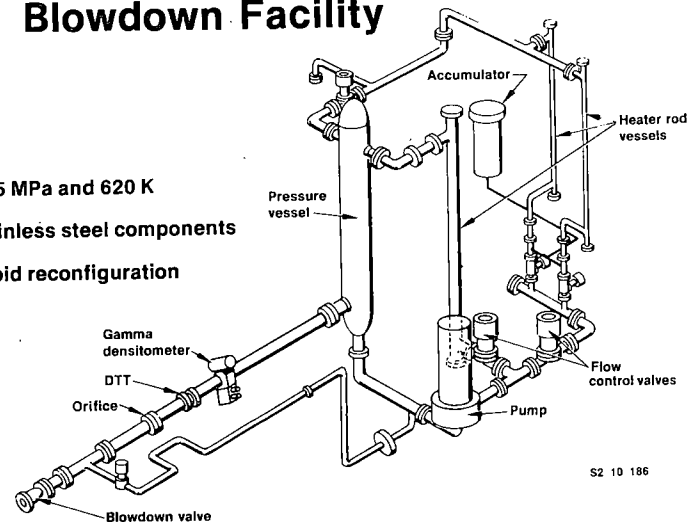
## Two-Phase Flow Loop



S2 10 192

## Blowdown Facility

- 15.5 MPa and 620 K
- Stainless steel components
- Rapid reconfiguration



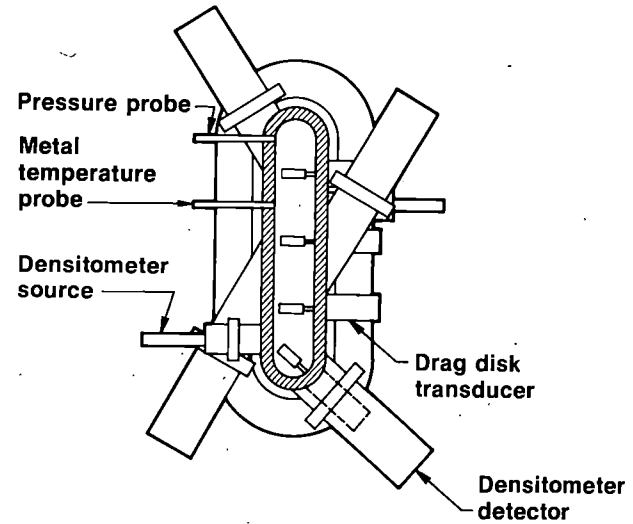
S2 10 186

## THEF Experiment Application

- Separate effects thermal-hydraulic phenomena
- Instrument calibration/development
- Component performance assessment

S2 10 188

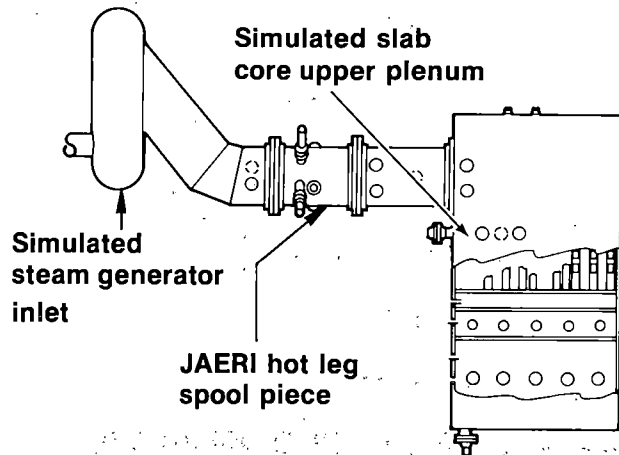
## 2D/3D Instrument Test Spool Piece



S2 10 183

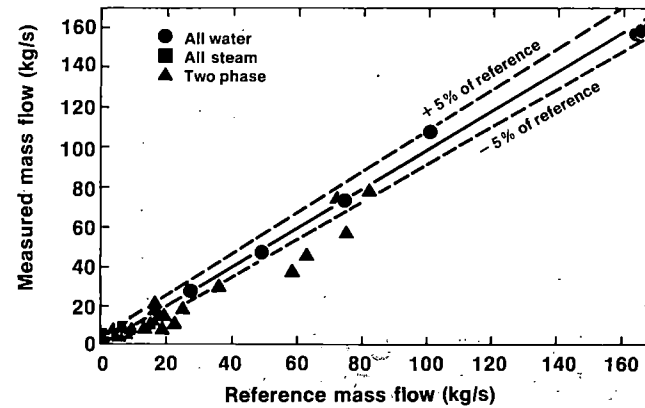
192

## 2D/3D Instrument Testing



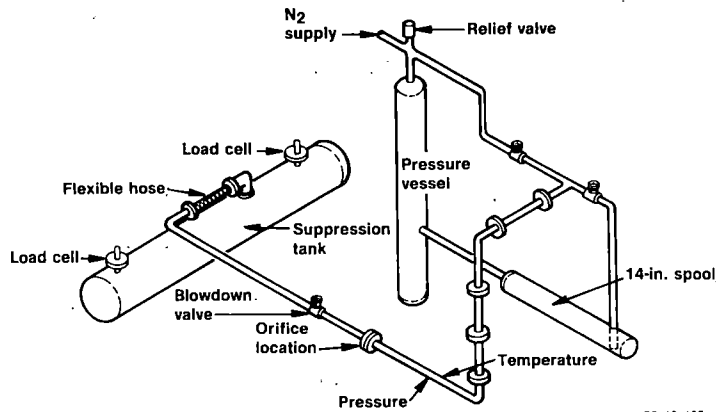
S2 10 184

## 2D/3D Instrument Test Results



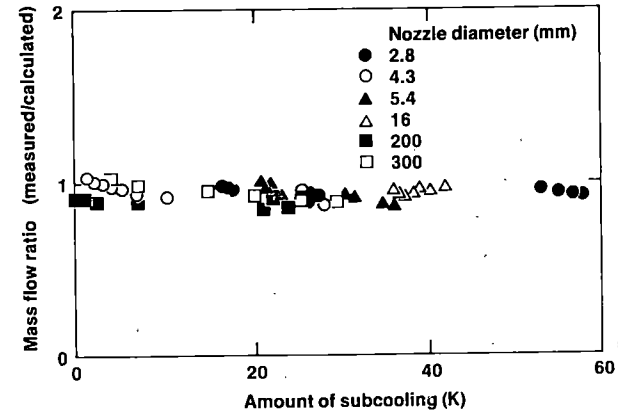
S2 10 181

## Subcooled Critical Flow Testing



S2 10 185

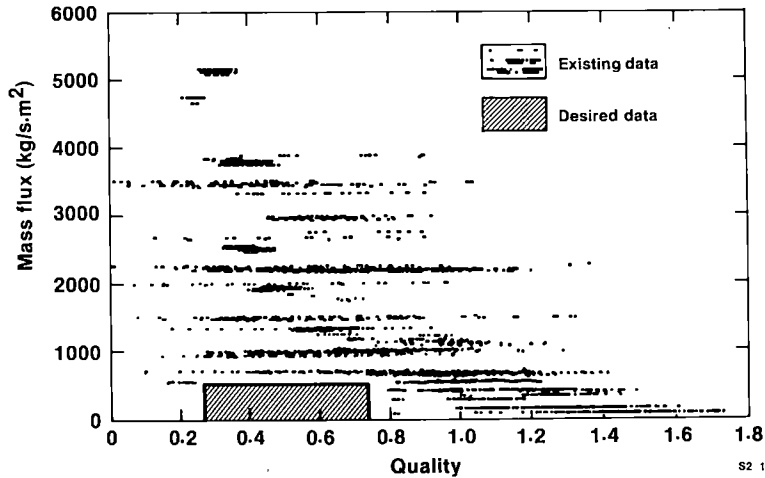
## Scale and Subcooling Effect on Critical Flow



S2 10 180

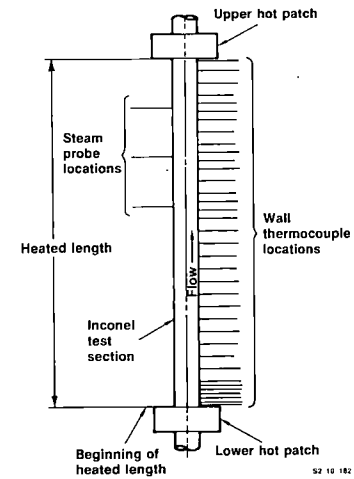
103

## Post-CHF Tests



S2 10 187

## Post-CHF Test Section



S2 10 182

## Post-CHF Test Data Obtained

### Steady state, fixed quench front

- 0.21, 0.40, and 0.69 MPa
- 15 to 25 kg/s.m<sup>2</sup>
- 0.20 to 0.47 inlet quality
- 700 to 1050 K

### Transient, moving quench front

- 0.70, 3.5, and 7.0 MPa
- 15 to 65 kg/s.m<sup>2</sup>
- 5 K subcooled to 0.47 quality at inlet
- 700 to 1100 K

S2 10 179

## Planned/Potential THEF Projects

- Bubble dynamics behavior in inverted U-bend
- Critical flow in branch lines
- Two-phase flow regime development and transition

S2 10 189

## NRC/DAE REACTOR SAFETY RESEARCH DATA BANK<sup>a</sup>

E. T. Laats

EG&G Idaho, Inc.

In 1976, the United States Nuclear Regulatory Commission (NRC) established the NRC/Division of Accident Evaluation (DAE) Data Bank to collect, store, and make available data from the many domestic and foreign water reactor safety research programs. This program has since grown from the conceptual stage to a useful, usable service for computer code development, code assessment, and experimentation groups in meeting the needs of the nuclear industry. Data from 20 facilities are now processed and permanently stored in the Data Bank, which utilizes the Control Data Corporation (CDC) CYBER 176 computer system located at the Idaho National Engineering Laboratory (INEL). New data and data sources are continually being added to the Data Bank. In addition to providing data storage and access software, the Data Bank program supplies data entry, documentation, and training and advisory services to users and the NRC. Management of the NRC/DAE Data Bank is provided by EG&G Idaho, Inc.

The major nuclear reactor test facilities contributing their data to the Data Bank are identified on Table 1. The Data Bank contains data from approximately 350 tests from these facilities. Each facility has a specific purpose in the water reactor safety effort. All of these facilities, however, provide data that will contribute to the overall water reactor safety research objective of safe, acceptable nuclear power production.

The user has immediate access to the Data Bank by typing commands from his own computer terminal. These on-line data storage, retrieval, and graphics capabilities enable him to manipulate test data, produce data plots on the terminal screen, and make data comparisons. The user may also be

---

a. Work supported by the U.S. Nuclear Regulatory Commission, Office of Nuclear Regulatory Research, under DOE Contract No. DE-AC07-76ID01570.



TABLE 1. FACILITIES THAT ARE DATA SOURCES FOR NRC/DAE DATA BANK

---

Browns Ferry  
FEBA  
FLECHT-COSINE  
FLECHT-SEASET  
FLECHT-SKEWED  
Goeta  
Halden  
Loss-of-Fluid Test (LOFT)  
Marviken  
NEPTUN  
National Reactor Universal (NRU)  
Power Burst Facility (PBF)  
Peach Bottom  
ROSA-III  
Semiscale  
Single Heated Bundle Facility (SHBF)  
Slab Core Test Facility  
Steam Sector Test Facility (SSTF)  
Thermal-Hydraulic Test Facility (THTF)  
Two Loop Test Apparatus (TLTA)  
2D/3D  
Cylinder Core Test Facility (CCTP)

---

sent test data on magnetic tape, to be processed on another computer of the user's choice.

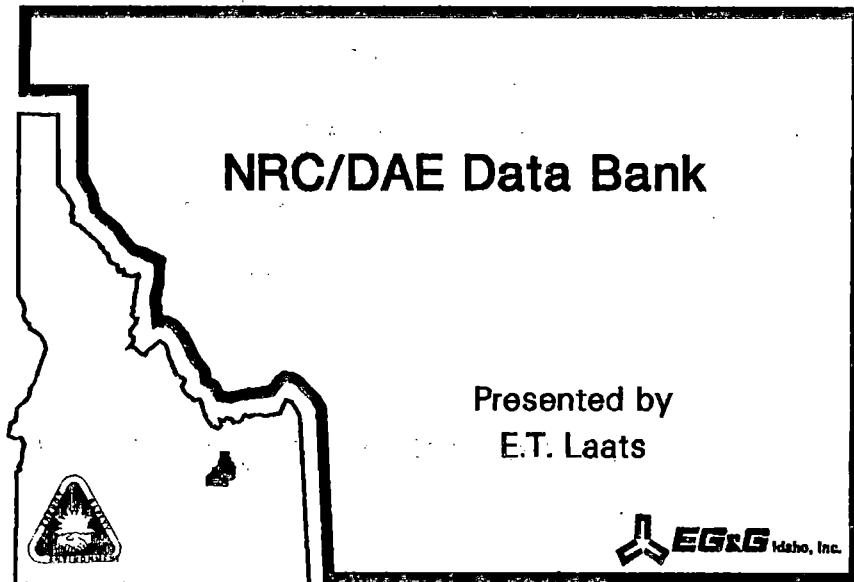
In addition to the data manipulation and plotting capabilities available through on-line computer terminal use, two other important features are accessible. First, a directory of Data Bank contents is stored and retrievable through a series of simple user-input commands.<sup>1</sup>

The directory lists the test facilities, gives the test names, identifies the Experiment Data Report (EDR) for each test and gives an abstract from each identified EDR, provides a listing of the measurement types for each test, as well as identifying which instruments have their data stored in the Data Bank. The second feature is the ability to also store in the INEL computer the results from computer code calculations. The Data Bank software may then be used to simultaneously plot selected calculated results and the corresponding experiment data. Computer codes such as RELAP4, RELAP5, and TRAC are currently used in this mode.

Any United States citizen may utilize the services of Data Bank, pending approval of the NRC and the Department of Energy. The procedure to receive approval may be obtained from the NRC/DAE Data Bank Administrator at EG&G Idaho, Inc.

#### REFERENCE

1. N. R. Scofield et al., "Introductory User's Manual for the U.S. Nuclear Regulatory Commission Reactor Safety Research Data Bank," NUREG/CR-2531, February 1982.



## General Information

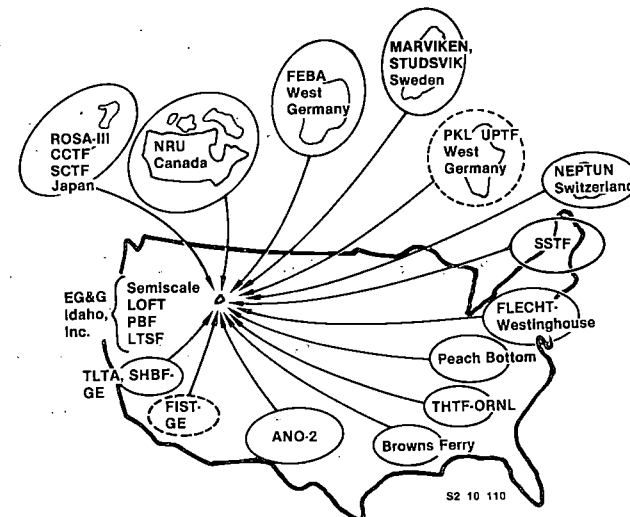
- Repository of qualified experiment data from worldwide test facilities
- Started in 1976
- Administered by EG&G Idaho for NRC/DAE
- Located at INEL

ETL982-2

## Overview

- General information
- Repository
- Hardware and software
- On-line data retrieval/graphics
- Data distribution
- Other services
- Costs
- New user procedure

ETL982-1



## Data Bank Hardware and Software

- 2 CDC Cyber 176 computers
- INEL Scientific Data Management System (ISDMS)
- Tektronix Plot 10

ETL982-4

## Basic Six Command Sequence

LOGIN,UID,PW

BEGIN,MASTER

MAGNUM

ATTACH,CWAF,UIC,DBSCOM

FINDC,1,CHANNO

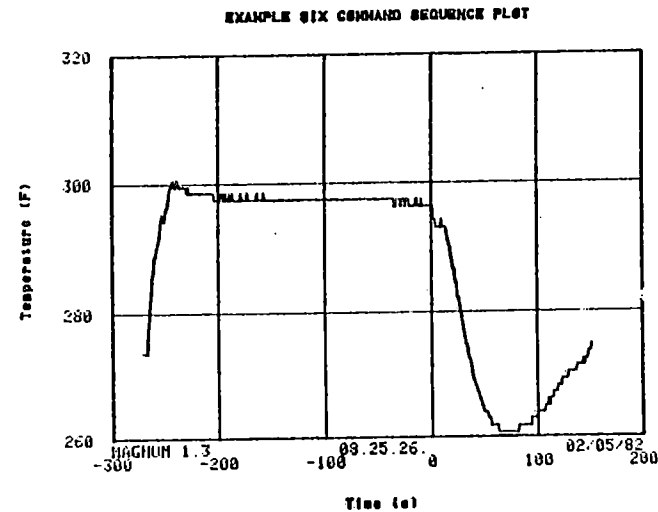
PLOT,1

ETL982-8

## On-line Data Retrieval and Graphics

- Basic 6 command sequence to retrieve and plot
- Many variations to customize plot
- 3 on-line information sources to aid user

ETL982-5

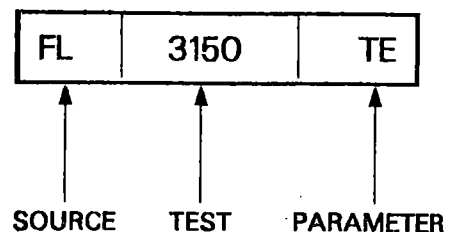


## On-line Information Sources

- User's Manual
- List of tests (brief)
- List of tests (detailed)
- Example plotting session

ETL982-8

## UIC Unique Identifier Code



ETL982-9

## Outline of User's Manual

- Introduction
- Overview of Data Bank and ISDMS
- Use of major processors
- Examples
- Printed off-line, mailed to user

ETL982-10

## Detailed List of Tests

- Facility name
- Test name
- Instrument type
- Reference, abstract
- Interactive prompting

ETL982-11

## Off-line Data Distribution

- Magnetic tape
- Simple format, instructions

ETL982-12

## Other Services

- User assistance
- Documentation upgrade
- Training sessions

ETL982-13

## Costs

- Terminal connect time (~ \$5.00 per hour)
- On-line data processing time (~ 4 cents per cp second)
- Data file storage time (\$1 to \$200 per test)
- Data tape creation services (\$50 to \$300 per test)
- Other costs, non-data bank  
Hardware (terminal mode)  
Telephone connect time

ETL982-14

## Procedure to Become Data Bank User

- Send letter of request to NRC, DOE, EG&G Idaho (Data Bank Administrator)
- Accompany letter to EG&G Idaho with purchase order

ETL982-15

PAYOFFS FROM THE  
BWR REFILL/REFLOOD PROGRAM

J. A. Findlay  
W. A. Sutherland

General Electric Company  
Nuclear Fuels Engineering Department  
San Jose, California

BWR REFILL-REFLOOD PROGRAM SPONSORS:

U.S. NUCLEAR REGULATORY COMMISSION  
ELECTRIC POWER RESEARCH INSTITUTE  
GENERAL ELECTRIC COMPANY

## BWR REFILL/REFLOOD PROGRAM

Results from the Refill/Reflood Program provide an extensive full scale, multi-channel, multi-dimensional data base of system performance under LOCA conditions. The data show the two-phase hydrodynamic parallel channel behavior that occurs in an array of multiple channels when there is a two-phase level in the lower plenum. And the data show the regional mixing and steam condensation of subcooled ECCS water injected into the system. The effectiveness of the ECC Systems and the beneficial effects of the multi-dimensional phenomena are demonstrated. The understanding of controlling phenomena that has been gained from this program has contributed substantially to the development of the BWR multi-dimensional best estimate analysis model, and the data base that has been obtained provides an important source for qualification of this model. A principal payoff from the program is its contribution to the closure of BWR LOCA issues by demonstrating effective core reflooding and providing the technology for greater confidence in calculation of LOCA consequences.

## FULL SCALE, MULTI-DIMENSIONAL LOCA DATA

The full scale 30 degree Sector Steam Test Facility, shown schematically in Figure 1, provided Refill/Reflood system performance data which has been used to identify and evaluate the controlling phenomena and to develop and assess best estimate analysis methods. The facility mocks up 58 individual fuel



bundles, the surrounding peripheral and interstitial bypass region, upper and lower plenums, guide tubes, jet - pump flow paths, downcomer, and ECCS injection systems. Being the only large test facility of this type, the information obtained from it is unique. Both separate effects tests, used to evaluate specific phenomena, and system response tests, used to evaluate system refill-reflood performance during blowdown transients, have been carried out.

#### DEMONSTRATION OF BWR ECCS EFFECTIVENESS

The system response tests demonstrate rapid reflooding of the fuel channels by the ECC Systems during blowdown transients over the range of interest (e.g., different break sizes, ECC temperatures, etc.). As shown in Figure 2, due to CCFL at the inlet orifices that holds up water entering the channels from the bypass, all channels start reflooding upon initiation of ECCS injection, even before the lower plenum is refilled. The subcooled water from the bypass, Figure 3, flows through holes in the bundle lower tie plate. This subcooled bypass liquid also cools the channel walls, providing an additional source of core cooling.

#### MULTI-DIMENSIONAL BENEFITS DEMONSTRATED

These tests also demonstrate beneficial effects of multi-channel interaction, Figure 4, that is not seen in single channel refill-reflood tests. The free communication in the bypass region

leads to upper plenum liquid draining into the bypass without counter current flow limiting. Localized subcooling in the upper plenum near the spray spargers, as shown in Figure 5, leads to early breakdown of CCFL at the upper tieplates in the peripheral channels. The localized subcooling in the upper plenum also leads to a balance in the drainage rate such that a two-phase mixture level forms in the upper plenum. This pool, which forms after the bypass fills, distributes spray water to all channels.

The subcooled LPCI water, injected into the peripheral bypass, condenses steam and cools the channel walls as it flows toward the center of the core. The bypass fills rapidly, with subcooling being greatest at the periphery and spreading across the core. Bypass filling is augmented by the upper plenum draining through the top-of-bypass openings.

Liquid hold up in the majority of the channels is due to CCFL at the inlet orifices. This is shown schematically in Figure 4. These channels each contain the same mass of liquid, the equal pressure differentials being dominated by static head. A small number of channels undergo a transition to co-current upflow through the SEO's, which vents additional steam from the lower plenum. The two-phase level is prevented from reaching the jet pump exit where venting steam would also carry liquid out the jet pumps much like an air lift pump. As a result more liquid is retained inside the shroud, contributing to the refill-reflood. The upflow bundles receive liquid from the bypass at rates equal to or greater than the counter flow bundles, with the result that

a considerable quantity of water is carried up these channels with the steam.

#### SYSTEM RESPONSE AND CONTROLLING PHENOMENA

Evaluation of the SSTF refill-reflood test results provides new insights and understanding of multi-dimensional phenomena, Figure 6. This understanding of the affect these phenomena have on controlling the system response provides increased confidence in, and materially improved the ability to, model the multi-dimensional BWR system. In addition, interpretation of results from other multiple channel facilities is substantially improved.

#### QUALIFICATION OF BEST ESTIMATE MODELS

The Refill/Reflood Program produced a complete range of multi-dimensional phenomena and system interactions data for final qualification of multi-dimensional best estimate models. The TRAC code has been set up to model the SSTF facility, Figure 7, and is currently being evaluated against this test data. Upon completion of the qualification, the TRAC code will be a tool that can calculate with confidence the consequences of a LOCA and quantify the evaluation model margin.

## CLOSE BWR LOCA ISSUES

The Refill-Reflood Program results have made a significant contribution to the closing of LOCA issues, Figure 8. The system response tests clearly demonstrate the effectiveness of the ECC Systems in mitigating the effects of a break in the primary system. Core reflooding of all channels begins without delay upon initiation of the ECC Systems, and there is a residual pool of water in the upper plenum during this period which also distributes coolant over the top of all channels, as well.

A clear understanding of system response has developed, and the analytical methods for confidently calculating the consequences of the LOCA are being developed and qualified.

PREVIOUS REPORTS IN BWR REFILL-REFLOOD SERIES

BWR Refill-Reflood Program Task 4.1 - Program Plan,  
G. W. Burnette, General Electric Company,  
NUREG/CR-1972, January, 1981.

BWR Refill-Reflood Program Task 4.2 - Core Spray  
Distribution Experimental Task Plan, T. Eckert,  
General Electric Company, NUREG/CR-1558, November, 1980.

BWR Refill-Reflood Program Task 4.2 - Core Spray  
Distribution Final Report, T. Eckert, General Electric  
Company, NUREG/CR-1707, March, 1981.

BWR Refill-Reflood Program Task 4.3 - Single Heated  
Bundle Experimental Task Plan, D. D. Jones,  
L. L. Myers, J. A. Findlay, General Electric Company,  
NUREG/CR-1708, March, 1981.

BWR Refill-Reflood Program Task 4.3 - Single Heated  
Bundle Experimental Task Plan, Addendum I, Stage 3 -  
Separate Effects Bundle, D. D. Jones, General Electric  
Company, NUREG/CR-1708 - Add. I, March, 1981.

BWR Refill-Reflood Program Task 4.3 - Single Heated  
Bundle Final Report, W. A. Sutherland, J. E. Barton,  
J. A. Findlay, General Electric Company, NUREG/CR-2001,  
June 1982.

BWR Refill-Reflood Program Task 4.4 - CCFL/Refill System  
Effects Tests (30 Sector) Experimental Task Plan,  
D. G. Schumacher, General Electric Company, NUREG/CR-1846,  
July, 1981.

BWR Refill-Reflood Program Task 4.4 - CCFL/Refill System  
Effects Tests (30 Sector) Experimental Task Plan,  
Addendum A, SSTF CCFL/Refill Shakedown Plan,  
D. G. Schumacher, T. Eckert, General Electric Company,  
NUREG/CR-1846, Add. A, September 1981.

BWR Refill-Reflood Program Task 4.4 - CCFL/Refill System  
Effects Tests (30 Sector) Experimental Task Plan,  
Addendum B, 30 SSTF CCFL/Refill Separate Effect Test  
Plan, D. G. Schumacher, General Electric Company,  
NUREG/CR-1846, Add. B, September 1981.

BWR Refill-Reflood Program Task 4.4 - CCFL/Refill System  
Effects Tests (30 Sector) Experimental Task Plan,  
Addendum C, 30 SSTF CCFL/Refill BWR/6 System Response  
Test Plan, D. G. Schumacher, General Electric Company,  
NUREG/CR-1846, Add. C, January 1982.

BWR Refill-Reflood Program Task 4.4 - CCFL/Refill System Effects Tests (30 Sector) Experimental Task Plan, Addendum D, SSTF CCFL/Refill with ECCS Variation Test Plan (BWR/4 ECCS Geometry), D. G. Schumacher, General Electric Company, NUREG/CR-1846, Add. D, January 1982.

BWR Refill-Reflood Program Task 4.4 - 30 SSTF Description Document, J. E. Barton, D. G. Schumacher, J. A. Findlay, S. C. Caruso, General Electric Company, NUREG/CR-2133, May 1982.

BWR Refill-Reflood Program Task 4.4 - CCFL Refill System Effects Tests (30 Sector) - SSTF System Response Test Results, D. G. Schumacher, T. Eckert, J. A. Findlay, General Electric Company, NUREG/CR-2568, March 1982.

BWR Refill-Reflood Program Task 4.4 - CCFL Refill System Effects Tests (30 Sector) - Evaluation of Parallel Channel Phenomena, J. A. Findlay, General Electric Company, NUREG/CR-2566, March 1982.

BWR Refill-Reflood Task 4.7 - Model Development Task Plan, J. G. M. Andersen, General Electric Company, NUREG/CR-2057, March 1981.

BWR Refill-Reflood Program Task 4.7 - TRAC/BWR Component Development, M. M. Aburomia, General Electric Company, NUREG/CR-2135, May 1981.

BWR Refill-Reflood Program Task 4.8 - Model Qualification Task Plan, J. A. Findlay, General Electric Company, NUREG/CR-1899, January 1981.

FIGURE 1 - FULL SCALE MULTIDIMENSIONAL DATA

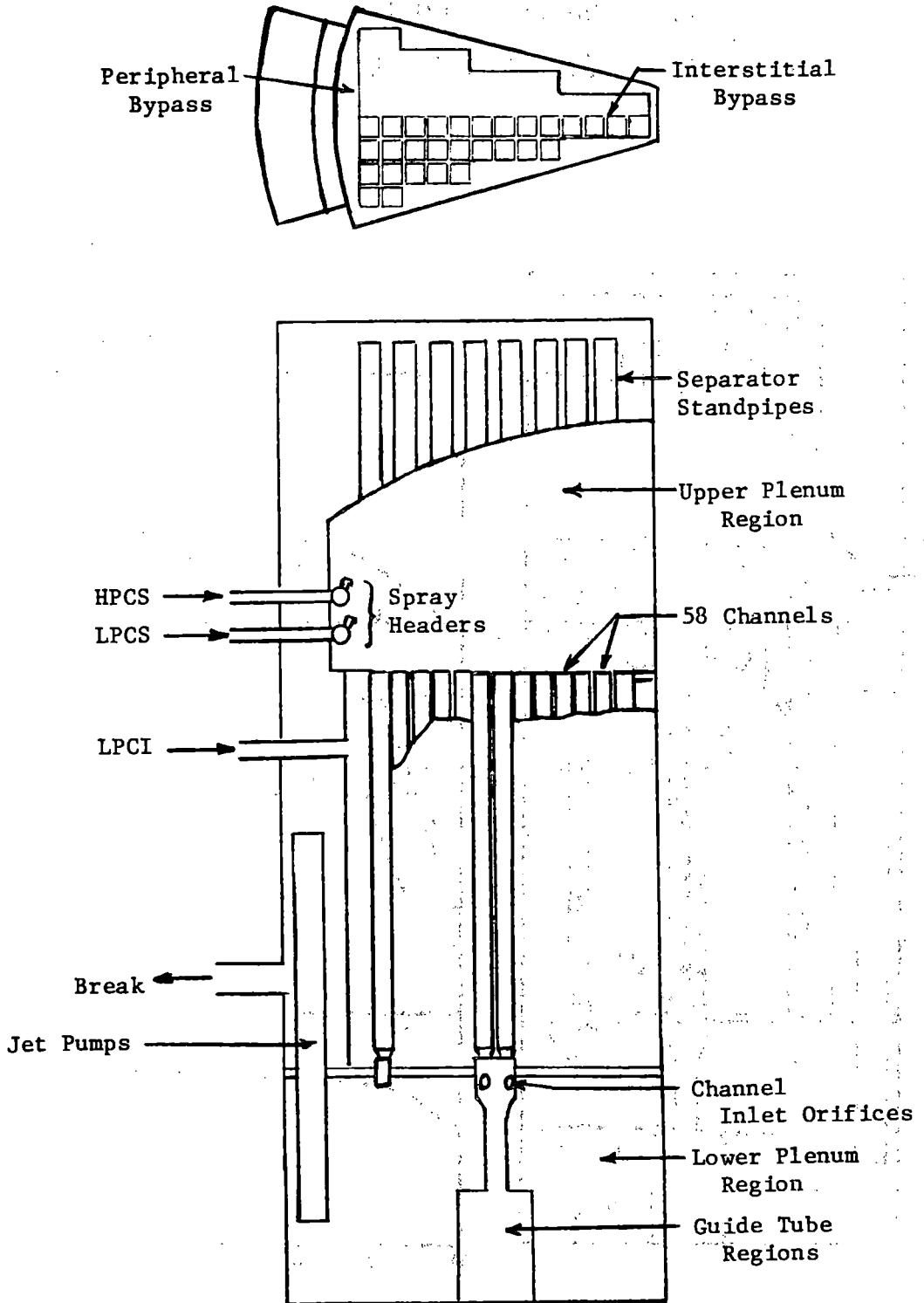


FIGURE 2 - ECCS EFFECTIVENESS DEMONSTRATED

- ① Bypass Supplies Water to All Channels
- ② Inlet Orifice Holds Up Water in All Channels
- ③ All Channels Promptly Reflood
- ④ Liquid Continuous Region in Upper Plenum

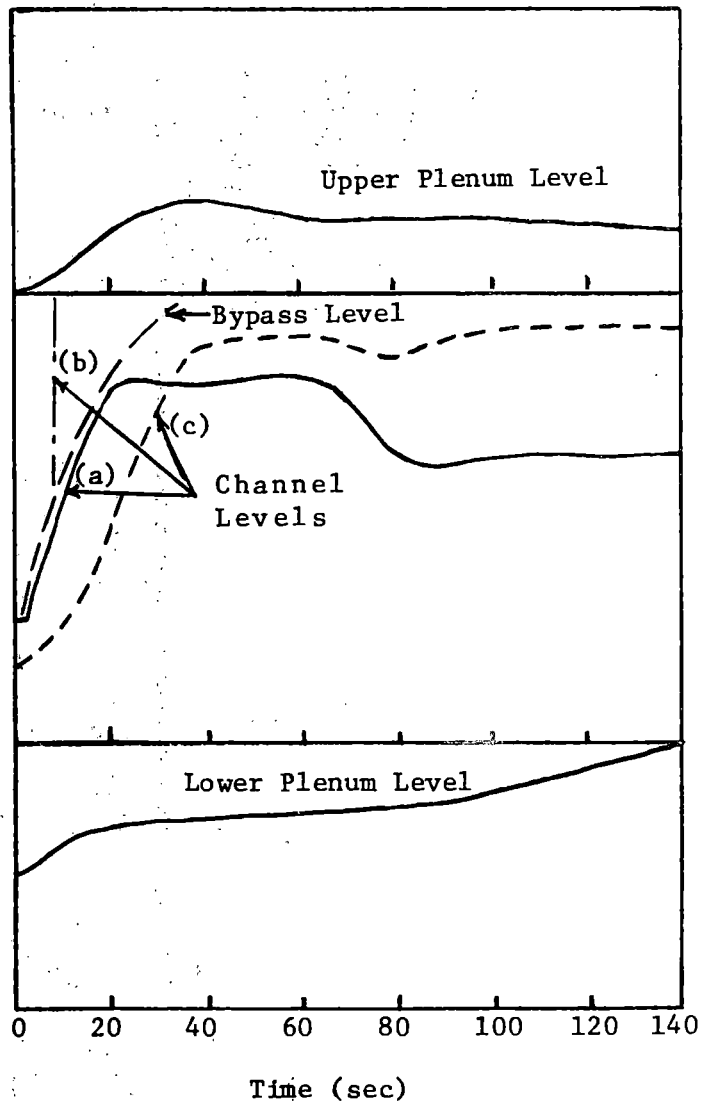
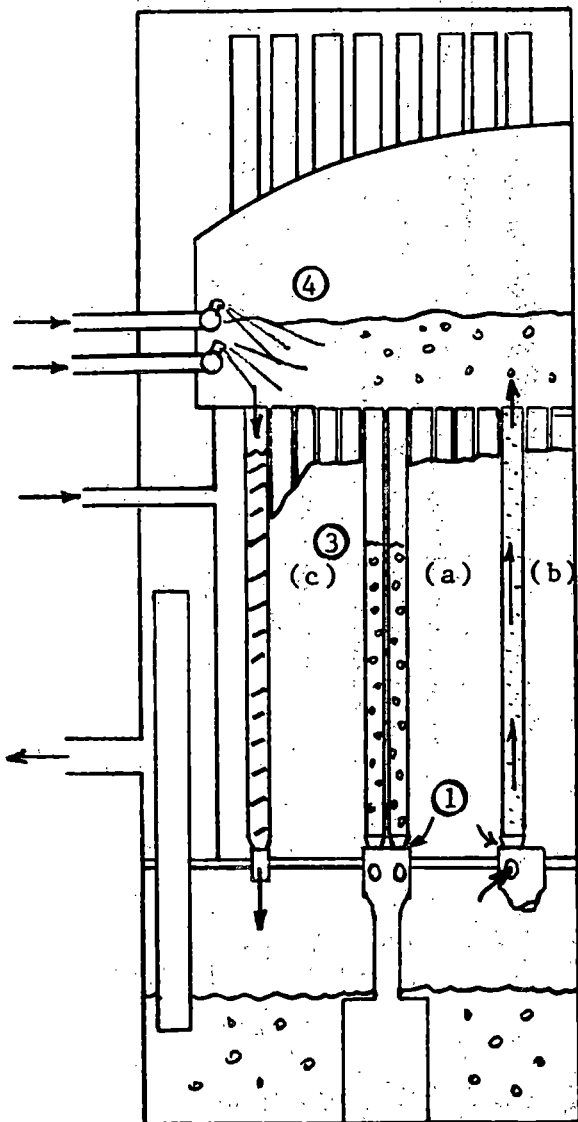




FIGURE 3 - BYPASS SUPPLIES SUBCOOLED WATER TO ALL CHANNELS

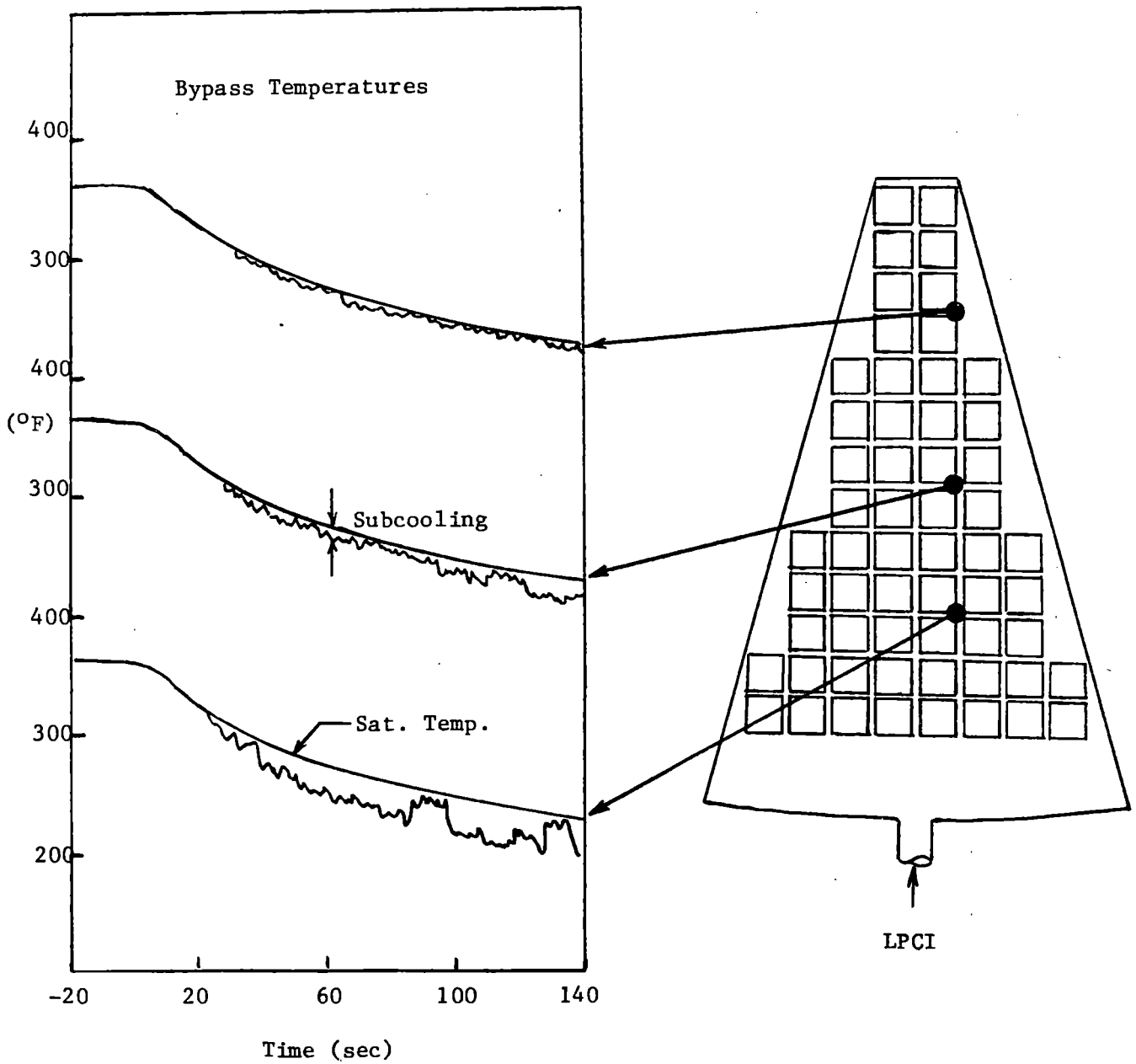


FIGURE 4 - MULTIDIMENSIONAL EFFECTS DEMONSTRATED

- ① NO CCFL AT TOP-OF-BYPASS
  - BYPASS REGION FILLS RAPIDLY
- ② PERIPHERAL UPPER PLENUM SUBCOOLING
  - UPPER TIE PLATE CCFL BREAKDOWN
- ③ PARALLEL CHANNEL FLOW
  - UPPER PLENUM DRAINS TO LOWER PLENUM
  - LOWER PLENUM STEAM VENTED

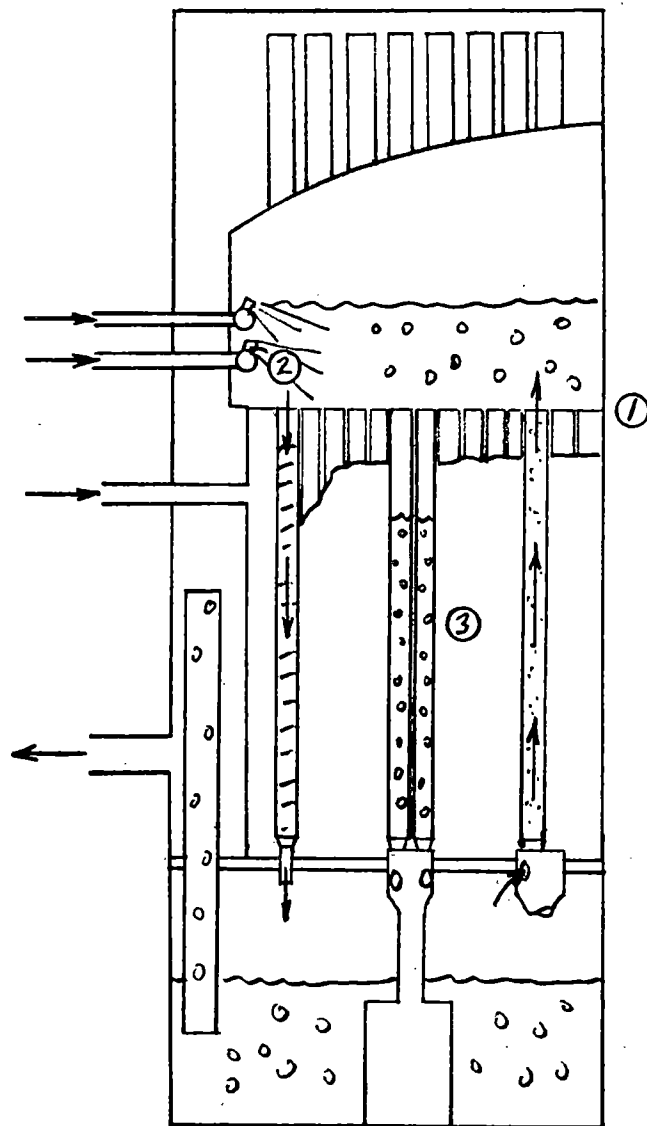


FIGURE 5 - UPPER PLENUM LIQUID CONTINUOUS REGION DEMONSTRATED

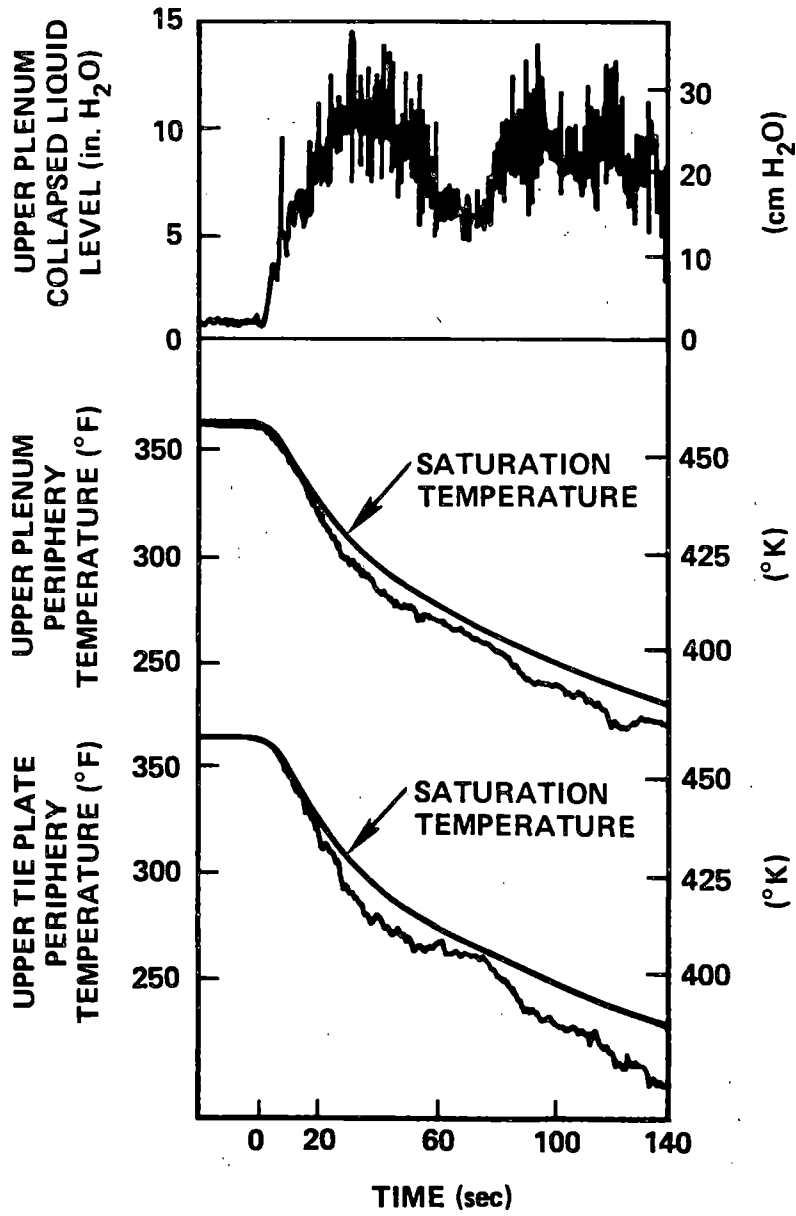


FIGURE 6 - PARALLEL CHANNEL PHENOMENA DEMONSTRATED

- ① FLASHING FORMS LEVEL IN LOWER PLENUM
- ② ORIFICE CCFL HOLDS UP WATER IN CHANNELS
- ③ CHANNEL HYDRAULIC STABILITY
  - PARALLEL CHANNEL REGIMES
  - STEAM FLOW SPLIT
- ④ UTP CCFL
  - LIQUID CONTINUOUS REGION IN UPPER PLENUM
- ⑤ NO CCFL AT TOP-OF-BYPASS
  - REGION FILLS RAPIDLY

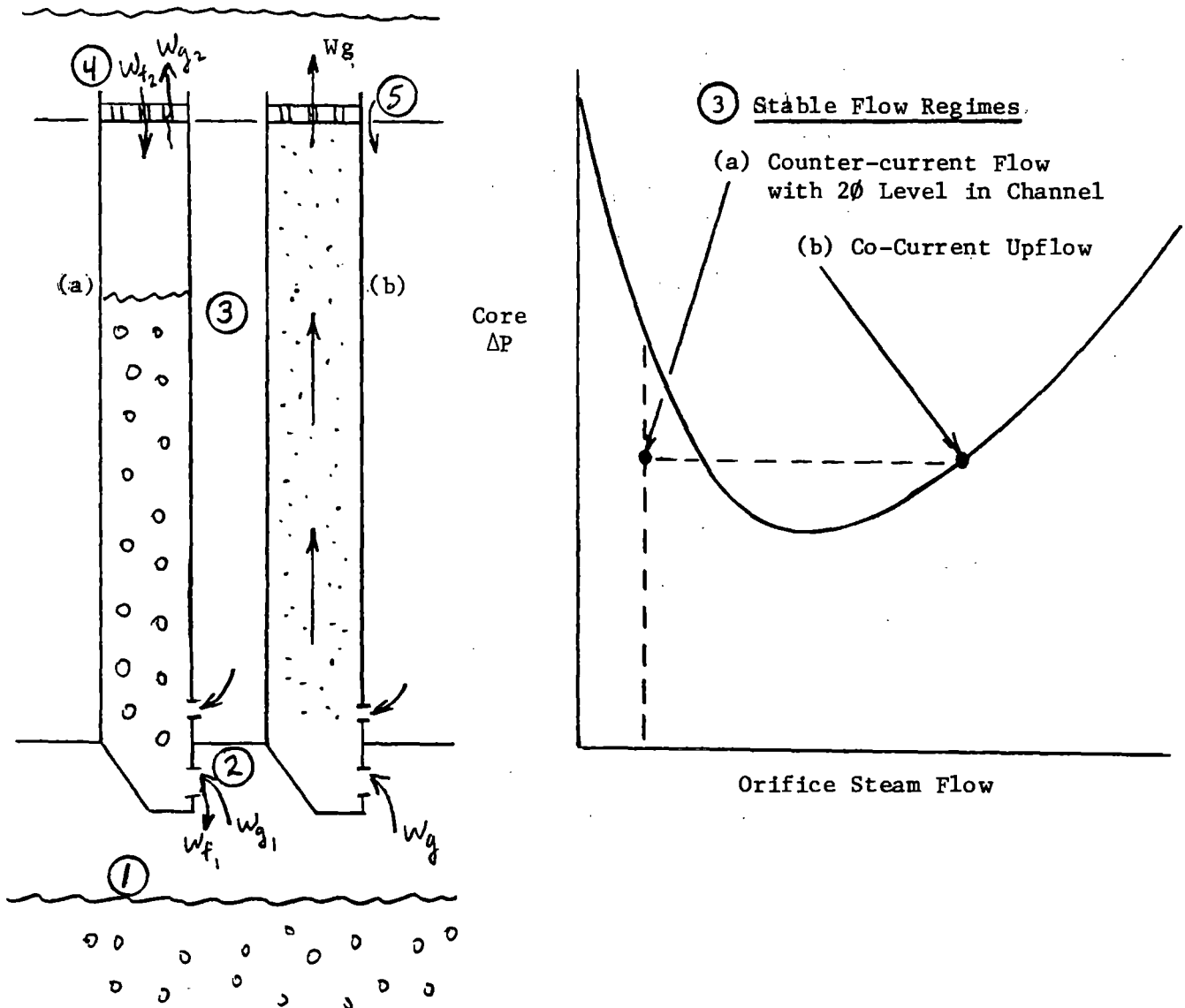


FIGURE 7 - QUALIFICATION OF MULTIDIMENSIONAL MODEL

(BWR TRAC CODE)

- DIVERSE DATA CHALLENGES CODE
  - PARALLEL CHANNEL FLOW
  - ECCS MIXING
  - CCFL AND CCFL BREAKDOWN
- SEPARATE EFFECTS TESTS EVALUATE PHENOMENA
- REFILL/REFLOOD SYSTEM RESPONSE TRANSIENTS

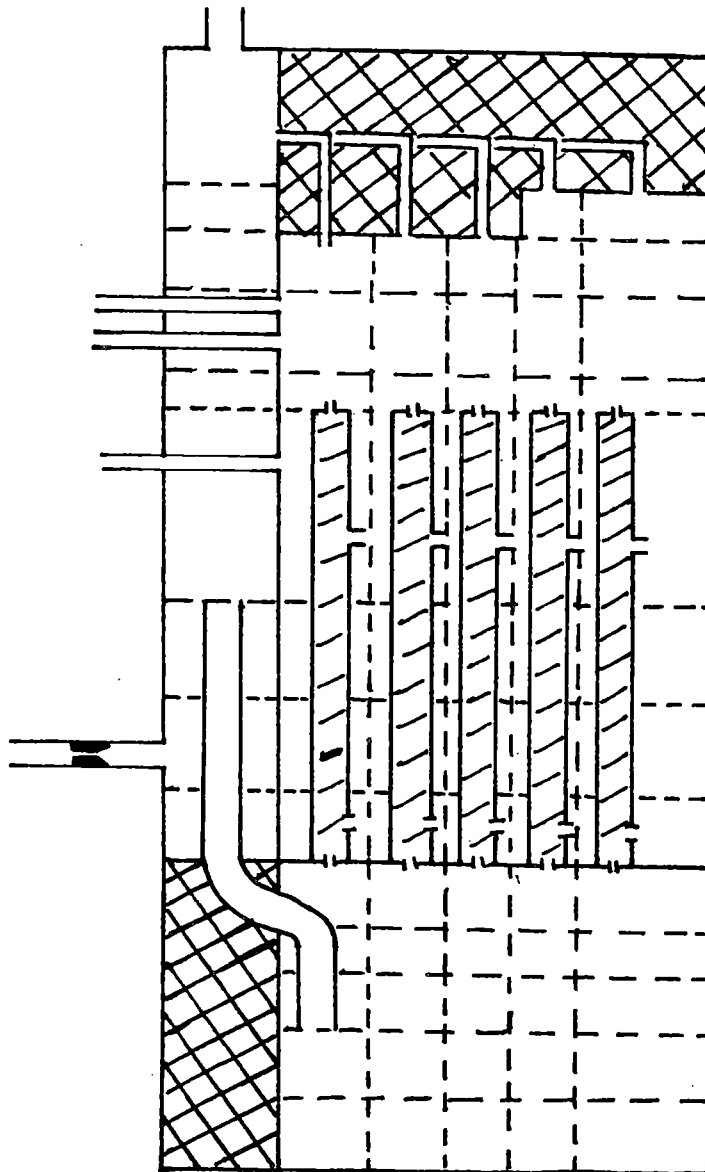


FIGURE 8 - CONTRIBUTION TO CLOSING LOCA ISSUES

- ECCS EFFECTIVENESS DEMONSTRATED
  - RAPID CORE REFLOOD
  - UPPER PLENUM LEVEL DISTRIBUTES SPRAY
  
- SYSTEM RESPONSE RESULTS APPLIED
  - MULTIDIMENSIONAL CONTROLLING PHENOMENA EVALUATED
  - LOCA MODELS IMPROVED
  
- BEST-ESTIMATE MODEL QUALIFIED
  - DIVERSE FULL SCALE DATA CHALLENGES CODE
  
- CONFIDENCE IN LOCA CALCULATIONS
  - QUANTIFY LARGE MARGINS

## TRAC-BWR HEAT TRANSFER<sup>a</sup>

R. W. Shumway and R. E. Phillips  
EG&G Idaho, Inc.

This paper discusses the TRAC-BWR heat transfer project. The TRAC-BD1/MOD1 code is under development at the Idaho National Engineering Laboratory<sup>1,2</sup> to provide the US Nuclear Regulatory Commission with a detailed, best estimate code for the analysis of the loss-of-coolant accidents and abnormal operating events, including anticipated transients without scram in boiling water reactor (BWR) systems. The TRAC-BWR heat transfer project results will be used in MOD1, but another goal is to determine those areas which are important for BWR transient analysis where more experimental data or improved heat transfer correlations are needed. TRAC-BD1/MOD1 will be used to review license applications, perform audit calculations, and evaluate operating guidelines. The code has been used to evaluate BWR Refill/Reflood Experiments and is now being used to design and plan tests for the BWR FIST Program. Several authors<sup>3,4,5</sup> have reviewed heat transfer packages used for the analysis of transients in pressurized water reactors. The TRAC-BWR heat transfer project will develop a best estimate heat transfer package for use in the TRAC-BD1 code and assess the package for the prediction of BWR transients. The heat transfer package will be developed within the framework of TRAC-BD1 and the specific product will be coding and subroutines containing best estimate correlations for the TRAC-BWR code.

### Model Development and Implementation

The TRAC-PD2<sup>6</sup> heat transfer correlation package was used as the starting point for developing the TRAC-BWR heat transfer package. Modifications to the TRAC-PD2 heat transfer package to make it applicable for BWR analysis were the addition of a radiation heat transfer model,<sup>7</sup> inclusion of a critical quality-boiling length correlation for the departure from nucleate

---

a. Work supported by the U.S. Nuclear Regulatory Commission, Office of Nuclear Regulatory Research under DOE Contract No. DE-AC07-76ID01570.

boiling,<sup>8</sup> addition of a subcooled boiling model, and the reintroduction of the modified Zuber critical heat flux correlation for low flow conditions.<sup>9</sup> Recent improvements are: streamlining of the heat transfer coefficient selection logic to decrease computer time, the introduction of vapor film properties into convective and film boiling regimes, changing the liquid deficient cutoff from 96% void fraction to 96% equilibrium quality, and implementation of Webb-Chen-Sundaram<sup>10</sup> interfacial heat transfer into dispersed droplet flow. As the assessment of the package proceeds, additional changes will be made as necessary.

### Developmental Assessment

The heat transfer package is being assessed by comparing calculations with steady state experimental data<sup>11</sup> and transient data. The percent change in heat transfer correlations needed to make TRAC accurately predict the data will be applied to BWR reactor base case calculations to find the effect of heat transfer uncertainties on reactor transients. If the effect is acceptably small, the heat transfer package will need no further changes. The acceptance criteria and method of implementing it are given in Reference 12.

The prediction of high pressure-high mass flux dryout data and film boiling data is generally acceptable, but low pressure data is more difficult because the two-phase flow is less homogeneous. Under low pressure-low velocity situations, flow oscillations that were numerically stable were encountered suggesting deficiencies in the interfacial shear formulation. (The Andersen-Ishii interfacial shear formulation, which is based on Ishii's data, is implemented into the code.) Recent discussions with Dr. M. Ishii have resulted in changes to the interfacial drag, which have greatly reduced the oscillations while maintaining reasonable slip ratios. However, film boiling data indicates that much larger convective heat transfer coefficients are needed.



## Summary

The TRAC-BWR heat transfer task is aimed at providing a best estimate heat transfer capability for BWR transient analysis. Many significant improvements have been made and an assessment and acceptance plan have been formulated. The need for void fraction data at low mass flux values has become evident.

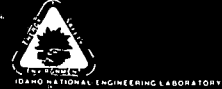
## References

1. J. W. Spore et al., TRAC-BD1 User's Manual, NUREG/CR-2178, 1981.
2. W. L. Weaver et al., "TRAC-BWR Transient Reactor Analysis Codes for Boiling Water Reactors," Ninth Water Reactor Safety Research Information Meeting, Gaithersburg, Maryland, October 26-30, 1981.
3. L. S. Tong, "Heat Transfer in Reactor Safety," Sixth International Heat Transfer Conference, Vol. 6, Toronto, Canada, 1978, pp. 285-309.
4. Y. Y. Hsu and L. H. Sullivan, "1981 Updating of Best Estimate Heat Transfer Package for Transient CHF and Post-CHF Regimes During Blowdown and Reflood Phases," Third CSNI Specialists Meeting on Transient Two-Phase Flow, Pasadena, California, March 23-25, 1981.
5. T. A. Bjornard and P. Griffith, "PWR Blowdown Heat Transfer," Thermal and Hydraulic Aspects of Nuclear Reactor Safety, Vol. 1, New York: American Society of Mechanical Engineering, 1977, pp. 17-41.
6. Safety Code Development Group, TRAC-PD2, An Advanced Best-Estimate Computer Program for Pressurized Water Reactor Loss-of-Coolant Accident Analysis, LA-8709-MS, NUREG/CR-2054, April 1981.
7. J. W. Spore, M. M. Giles, R. W. Shumway, "A Best Estimate Radiation Heat Transfer Model Developed for TRAC-BD1," 20th ASME/AIChE National Heat Transfer Conference, Milwaukee, Wisconsin, August 2-5, 1981.
8. R. E. Phillips, R. W. Shumway, K. H. Chu, "Improvements to the Prediction of Boiling Transition in BWR Transient Calculations," 20th ASME/AIChE National Heat Transfer Conference, Milwaukee, Wisconsin, August 2-5, 1981.
9. R. W. Shumway and R. E. Phillips, "TRAC-BWR Heat Transfer," NRC Heat Transfer Workshop, February 1981.
10. S. W. Webb, J. C. Chen, R. K. Sundaram, "Vapor Generation Rate in Nonequilibrium Convective Film Boiling," 7th International Heat Transfer Conference, Munich, West Germany, September 6-10, 1982.

11. R. E. Phillips and R. W. Shumway, TRAC-BWR Heat Transfer: Model Description and Steady State Experimental Assessment, WR-CD-82-064, May 1982.
12. R. E. Phillips and R. W. Shumway, Sample BWR Heat Transfer Sensitivity Study, EGG-CDD-5731, January 1982.

## TRAC-BWR Heat Transfer

Presented by  
R.W. Shumway



## Purpose

- **Best estimate heat transfer model development and assessment for use in TRAC-BD1/MOD1 relative to BWR transient analysis requirements**
- **Aid experimental programs by showing where data and/or correlation improvements are needed.**

S2 3511

222

## Assessment Methodology

- **Quantitative assessment**
  - **Steady state test data**
  - **Transient test data**
- **Qualitative assessment**
  - **BWR/6 transients**
- **Acceptance criteria**

S2 3513

## Steady State Test Cases

1. **Christensen** Subcooled and saturated nucleate boiling in channels
2. **Marchature** Subcooled and saturated nucleate boiling, forced and natural convection in tubes
3. **Frigg** Subcooled and saturated nucleate boiling, plus CHF in rod bundles
4. **Bennett** Post-CHF heat transfer in tubes
5. **Heinman** Forced convection to steam in tubes
6. **Lehigh** Forced convection film boiling in tubes, low pressure
7. **INEL** Forced convection film boiling in tubes, low and high pressure

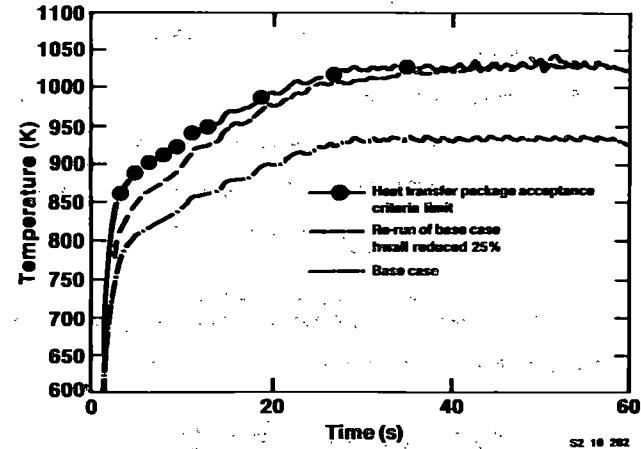
S2 3541

## Transient Test Cases

1. DSF-P1 (GOTA) Test 78    Top bundle spray
2. Semiscale S075            Bottom reflood with void measurements
3. FLECHT 9077              Bottom reflood with steam temperature measurements
4. F-SEASET 35557          Boiloff and steam cooling
5. THTF 3.06.B&C            Upflow film boiling
6. GE Atlas loop 16-rod test   Transient CHF

S2 3540

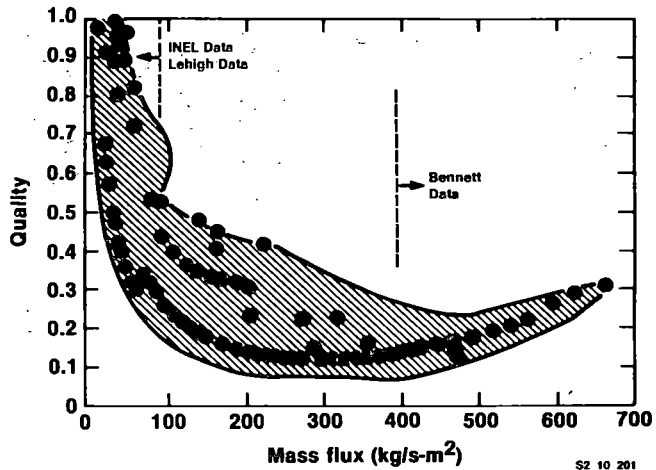
## BWR6 Turbine Trip Transient



S2 10 282

223

## Mid-Core Quality vs Mass Flux BWR6 10% Break



S2 10 201

## Interfacial Heat Transfer

### SSD

Saha-Shiralkar-Dix correlation

$$\Gamma_v = 6300 \left(1 - \frac{P}{P_c}\right)^2 \left(\frac{\rho_v J_v}{\alpha}\right) \frac{K_v (T_v - T_g) (1 - \alpha)}{(\rho_v \sigma D h_f^3)^{1/2} h_{fg}}$$

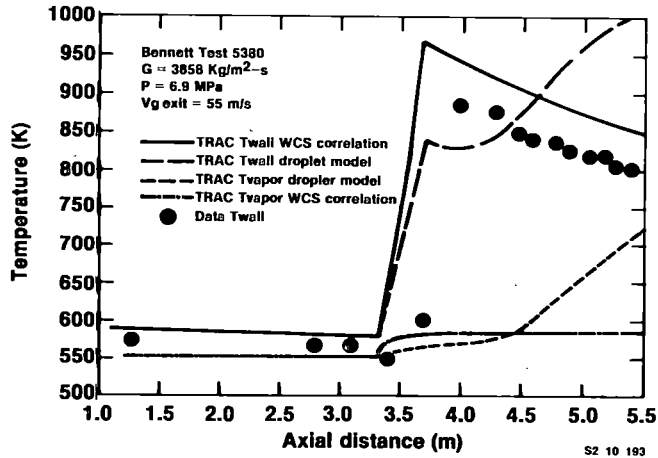
### WCS

Webb-Chen-Sundaram correlation

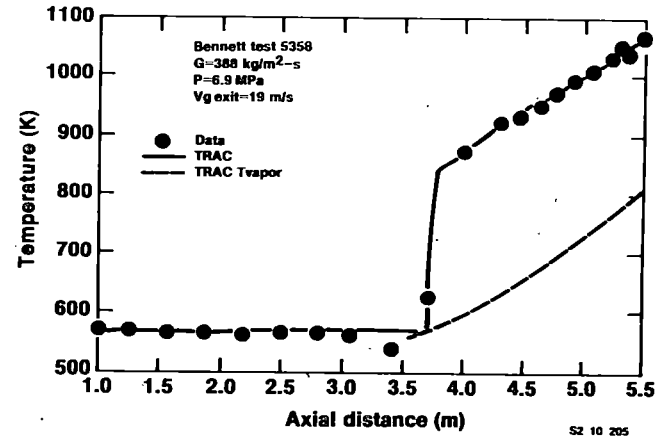
$$\Gamma_v = 1.32 \left(\frac{P}{P_c}\right)^{-1.1} \left(\frac{\rho_v J_v}{\sigma H_{om}}\right)^2 \frac{K_v (T_v - T_g) (1 - \alpha H_{om})^{2/3}}{\rho_v \sigma D h_{fg}}$$

S2 10 187

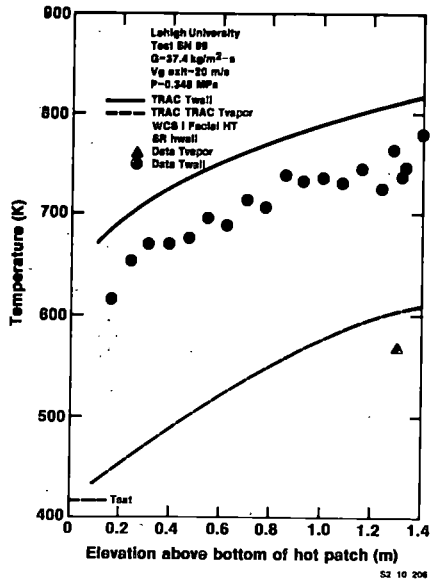
## High Mass Flux - High Pressure



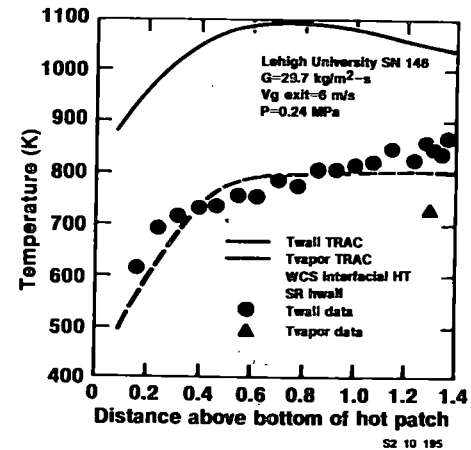
## Medium Mass Flux - High Pressure



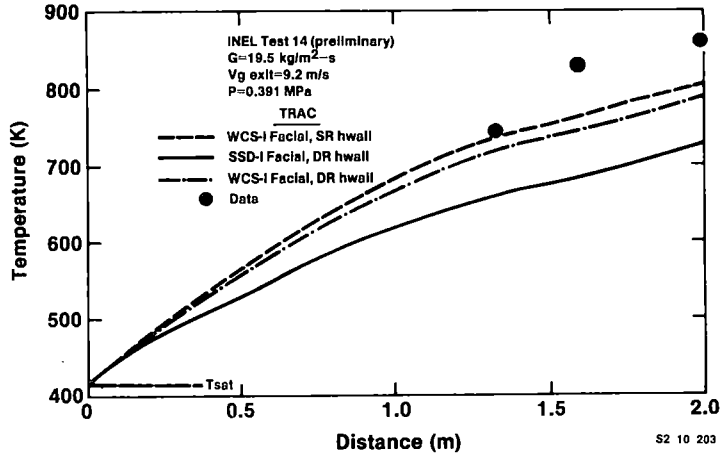
## Low Mass Flux - Low Pressure



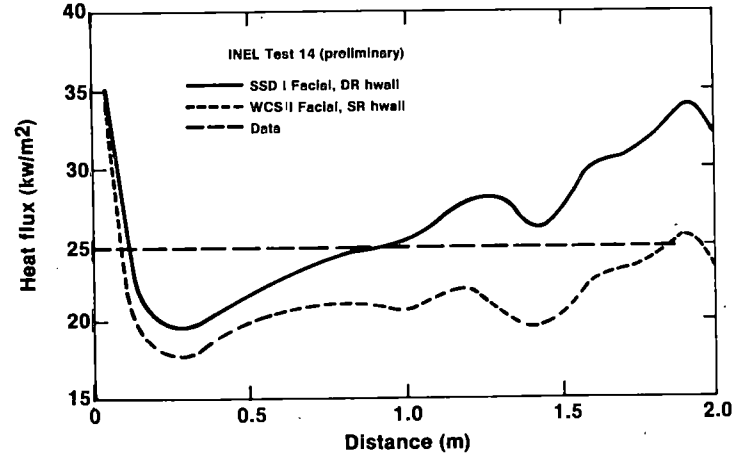
## Low Mass Flux - Low Inlet Quality Low Pressure



### Vapor Temperature Profile

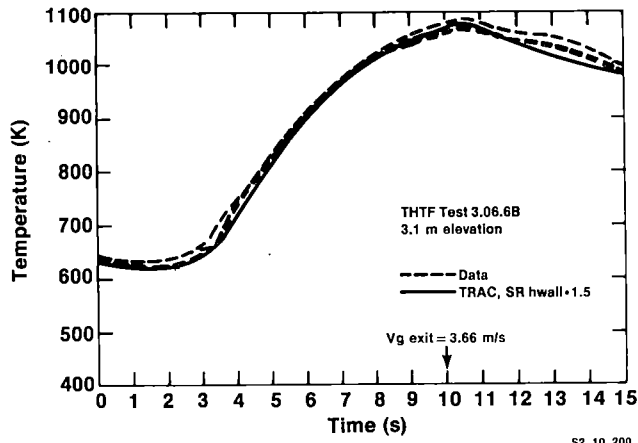


### Wall Heat Flux

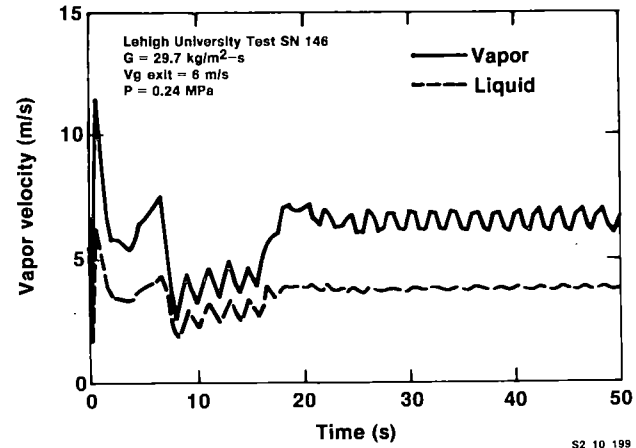


225

### High Pressure Transient Test



### TRAC Phase Velocity-Improved Drag



## Conclusion

- **Medium to high mass flux**
  - TRAC boiling curve looks good
- **Low mass flux (important BWR area)**
  - TRAC film boiling needs improvement
  - TRAC vapor generation reduced
  - Higher vapor temperature necessitates high wall heat transfer coefficients
  - Unsure of  $V^2$  term in WCS correlation
- **Film boiling void fraction and steam temperature data is needed**

S2 3512

EXPERIMENTAL DATA FOR NONEQUILIBRIUM  
POST-CHF HEAT TRANSFER IN A VERTICAL TUBE

by

D. Evans, S. Webb, J. C. Chen, and S. Neti

Institute of Thermo-Fluid Engineering and Science  
Lehigh University  
Bethlehem, PA 18015

In post-CHF convective boiling, under both blowdown and reflood conditions of nuclear safety concern, one often finds that wall heat flux, wall temperature, fluid equilibrium quality, and the local heat transfer coefficient all vary with axial position. A number of experimental investigations have reported data for the axial variations of these parameters. However, to improve our capability for modeling post-CHF heat transfer, one needs to also know the axial variation of fluid actual quality and vapor superheat. Experimental measurements of these two nonequilibrium parameters are scarce and data on axial variations of  $T_v$  and  $X_a$  are essentially not available at this date.

In this past year, a program at Lehigh University under the sponsorship of the U.S. NRC has attempted to obtain experimental measurements of the nonequilibrium vapor superheat and fluid actual qualities for post-CHF boiling heat transfer in a vertical tube. The experimental technique has been described in the previous Water Reactor Safety Research Information Meeting and is documented in References 1 and 2. Figure 1 shows a sketch of the test section, consisting of an Inconel tube having inside diameter of 15.4 mm. The test section was heated by D.C. current flow through the tube wall. At three locations along the length of the 1.35 m long tube,



ports were provided for insertion of vapor probes for measurement of vapor superheats. During the tests, the test section was first preheated to post-CHF wall temperatures prior to the start of vertically upward two-phase flow. By careful control of operating conditions, it was possible to obtain a flow upward progression of a quench front through the length of the test section. During this slow "reflood" process, it was possible to obtain measurements of wall heat flux, wall temperature, and nonequilibrium vapor temperature as functions of distance above the quench front. Due to the low quench front propagation velocity (of the order of 8 mm/sec) the movement of the quench front location was a small fraction of the fluid residence time (time required for the fluid to traverse the length of the test section). According to transient convective heat transfer theory, the thermal hydraulic data thus obtained are quasi-steady state.

Figure 2 shows a sample plot of the measured axial wall temperature profiles at various times during a quench run. The upward progression of the quench front, starting at the bottom of the test section, is clearly obvious. Figure 3 shows the data cross plotted as  $T_{wall}$  vs. time, for several axial locations. It is seen that the temperature history at any given axial location shows the familiar period of precursor cooling, followed by a rapid quench. From such measurements, it was possible to determine the location of the quench front as a function of time, as indicated in Figure 4 for a sample case.

Differentially aspirated vapor probes [1] in the test section were used to measure vapor superheats at one or more of the probe locations. Figure 5 shows a plot of the vapor superheat measured at one probe station as a function of the quench history. Combining such information with knowledge of the quench front location, it was then possible to determine

the variation of vapor superheat as a function of axial distance from the quench front. A sample of the final result is shown in Figure 6. The results of this high inlet quality run show an almost linear increase in the vapor superheat with distance from the quench front. Other runs have shown that with decrease in the inlet quality the vapor superheat was close to zero for up to 0.3 m from the quench front. Beyond that initial .3 m, the vapor superheat was found to rise rapidly, attaining a magnitude of several hundred degrees C at a distance of 1 m from the quench front location. Such experimental data on the axial variation of nonequilibrium superheats are being utilized to model the nonequilibrium source term (commonly denoted as  $\Gamma$ ), for post-CHF heat transfer [3].

#### References

1. S. Nijhawan, J. C. Chen, R. K. Sundaram, and E. J. London, "Measurement of Vapor Superheat in Post-CHF Boiling," Journal of Heat Transfer, vol. 102, no. 3, 465 (1980).
2. S. Nijhawan, J.C. Chen and R. K. Sundaram, "Parametric Effects on Vapor Nonequilibrium in Post-Dryout Heat Transfer," ASME Paper No. 80-WA/HT-50 (1981).
3. S. Webb, J. C. Chen, and R. K. Sundaram, "Vapor Generation Rate in Nonequilibrium Convective Film Boiling," 7th International Heat Transfer Conference, Munich (1982).

#### Nomenclature

|                   |                                    |                             |
|-------------------|------------------------------------|-----------------------------|
| G                 | mass flux                          | Kg/m <sup>2</sup> -s        |
| P                 | test section pressure              | kPa                         |
| Q                 | heat flux                          | Kw/m <sup>2</sup>           |
| t                 | time, seconds                      | = 5.2 times snapshot number |
| T <sub>v</sub>    | vapor temperature, vapor superheat | °C                          |
| T <sub>wall</sub> | wall temperature, wall superheat   | °C                          |
| X <sub>a</sub>    | actual quality                     |                             |
| X <sub>in</sub>   | inlet quality                      |                             |
| $\Gamma$          | nonequilibrium source term         |                             |

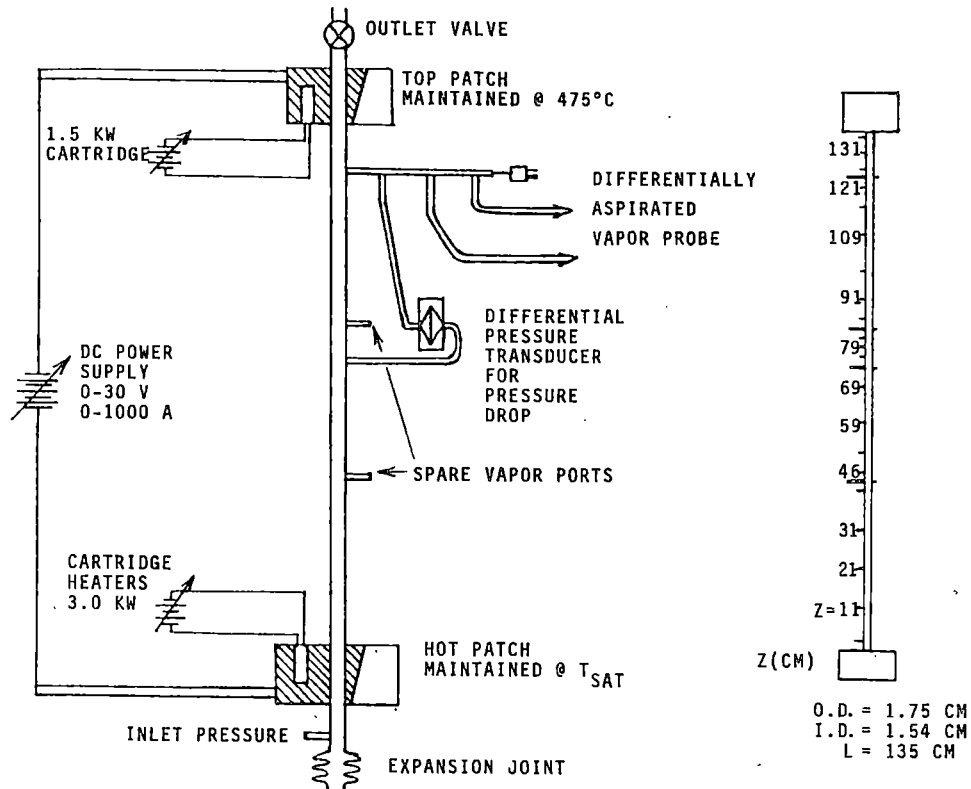


Figure 1 Schematic of test section and wall thermocouple locations

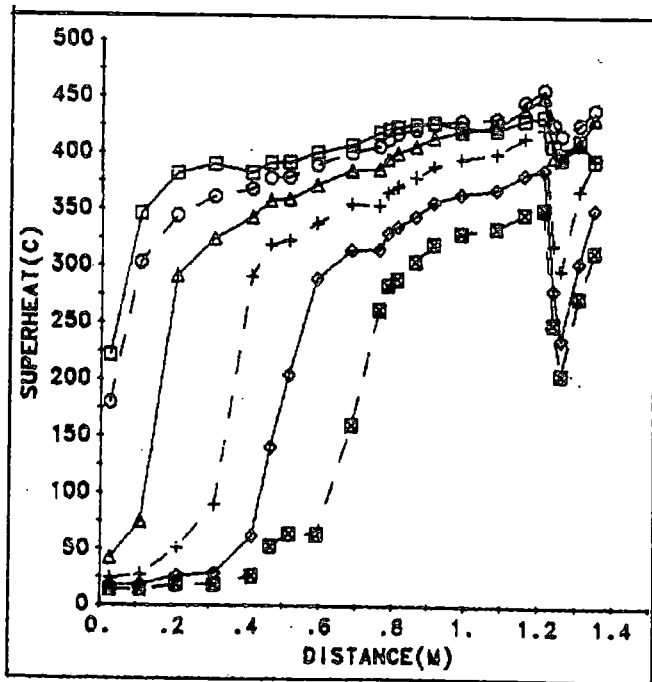


Figure 2 Wall superheat vs. distance along test section at 30 sec time intervals.  $P = 461 \text{ kPa}$ ,  $G = 29 \text{ Kg/m}^2\text{-s}$ ,  $Q = 35.9 \text{ Kw/m}^2$ ,  $X_{in} = 0.72$

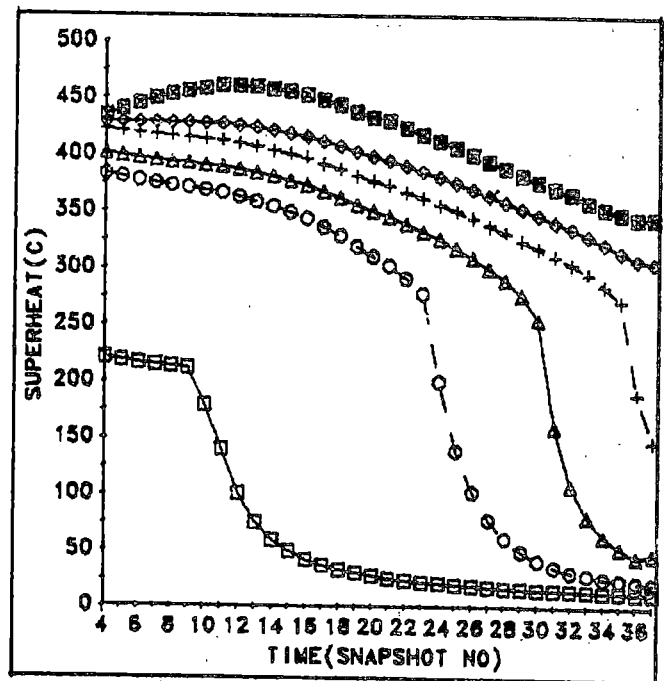


Figure 3 Wall superheat vs. time at several axial locations. Time in sec =  $5.2 \times$  snapshot no.  
 $\square$  0.025 m,  $\circ$  0.41 m,  $\triangle$  0.59 m,  $+$  0.79,  $\diamond$  0.914 m,  $\blacksquare$  1.21 m  
 (vapor probe at 1.24 m)

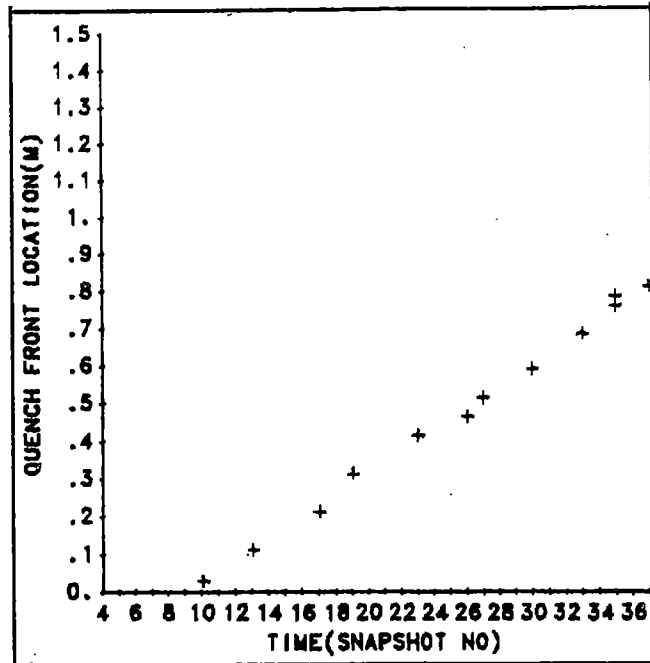


Figure 4 Quench front location vs. time.  
Time in sec = 5.2 x snapshot no.

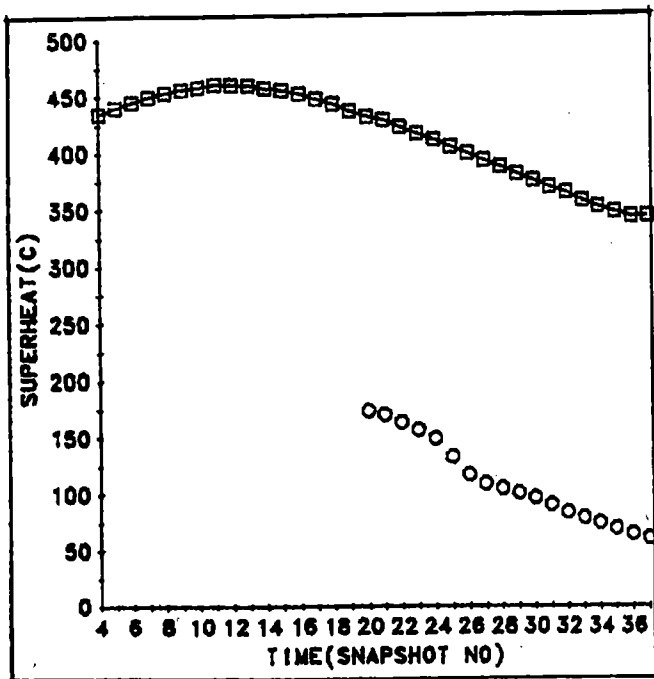


Figure 5 Vapor and wall superheat at 1.21 m from inlet.  
 $P = 461 \text{ kPa}$ ,  $G = 29 \text{ Kg/m}^2\text{-s}$ ,  
 $Q = 35.9 \text{ Kw/m}^2$ ,  $X_{in} = 0.72$

- wall superheat
- vapor superheat

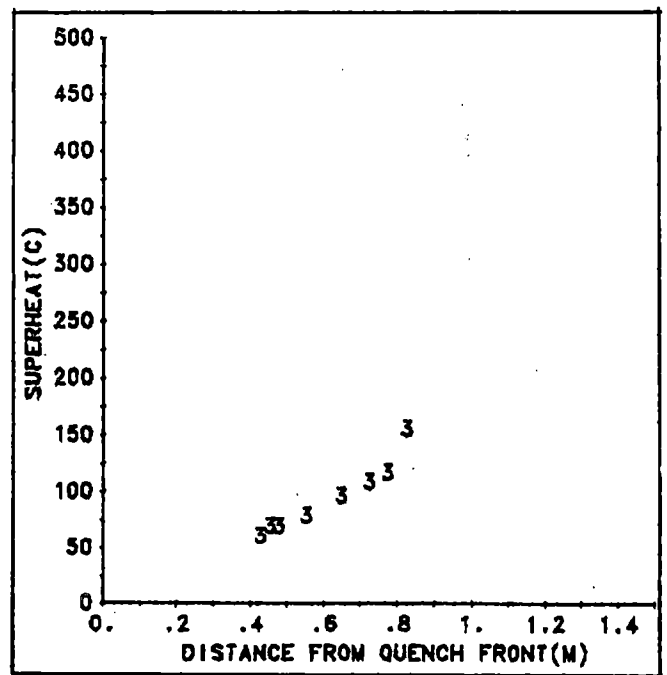


Figure 6 Variation of vapor superheat with distance from quench front

Phenomenological Modeling of Two-phase Flow  
in Water Reactor at ANL  
(Inverted Annular Flow Modeling)

by

M. Ishii and G. De Jarlais

Reactor Analysis and Safety Division  
Argonne National Laboratory

## Abstract

In predicting two-phase flow phenomena in nuclear reactors under various accident conditions, the interfacial transfer terms are among the most essential factors in the modeling. The interfacial geometry and thermo-hydraulics at the interface often dominate these two-phase flow phenomena. Among the various two-phase flow regimes, the inverted annular flow is relatively less well understood due to its special heat transfer conditions. However, this regime is quite important in terms of LWR accident analyses, since the peak cladding temperature often strongly depends on the thermo-hydraulics in this inverted annular flow and subsequent droplet dispersed flow. In view of this, the inverted annular flow transfer mechanisms and the flow regime transitions are studied in detail.

## Introduction

This is a summary of the research progress on the phenomenological modeling of two-phase flow during 1982 at Argonne National Laboratory. The objective of this NRC sponsored research program is to develop rigorous two-phase flow models and correlations which are the foundation of reliable and accurate LWR safety analyses. The current effort is on the establishment of the two-fluid model, development of scaling criteria, derivation of interfacial transfer terms, and prediction of hydrodynamic transients based on phenomenological modeling. This task will provide overall modeling effort for the basic equations and correlations to be used in large-scale LWR safety codes such as TRAC and RELAP, as well as the scaling criteria for the safety experimental programs. With the present highly advanced capability in numerical analyses, the essential limitations of these codes are imposed by not-well understood two-phase thermo-hydraulics under various accident conditions. Therefore, rigorous two-phase flow models and detailed correlations which are developed under the program will significantly improve the reliability and accuracy of the advanced codes and safety analyses. The modeling efforts cover two-phase equations, interfacial shear, interfacial energy transfer, interfacial area, entrainment, flow regime, and effects of reactor geometry on two-phase thermo-hydraulics and scaling of two-phase phenomena.

Under the program the entrainment and droplet size distribution in annular flow (1,2,3), inverted annular flow thermo-hydraulics, and scaling

criteria for LWR's under natural circulation boiling (4) have been studied in detail. Particular results and accomplishments are listed below:

1. Rate correlations for droplet entrainment and deposition in annular flow (1,2)
2. Interfacial area correlation in annular flow (5)
3. Bubble nucleation site density correlation and bubble transport equation (6)
4. Preliminary assessment of the inverted annular flow hydrodynamics
5. Scaling criteria for natural circulation in two-phase flow (4)

In this paper, only the results related to the inverted annular flow modeling are presented.

## II. Flow Regimes in the Post CHF Region

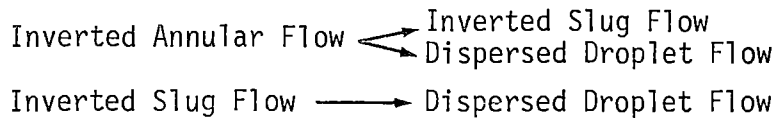
The inverted flow regimes occur after the occurrence of the critical heat flux (CHF). In the post CHF region, the continuous contact between the hot wall and liquid is prevented by various CHF mechanisms. Therefore, the continuous vapor phase is in contact with the wall in the post CHF region. This implies that the structures of flow and interfacial transfer mechanisms are significantly altered by the occurrences of CHF. There are three main flow regimes of importance. These are the inverted annular flow (film boiling), inverted slug flow, and droplet dispersed flow. Any one of them can occur at the dryout point. Furthermore, various flow regime transitions among them in the post CHF region are also possible due to interfacial instabilities, entrainment and phase change.

The above discussion indicates that two types of flow regime criteria are needed for the characterization of flow structures in the post CHF region. The first type is the criteria for the initial flow regime at the point of the dryout. Since the characteristic of the flow inverts at the point of dryout, it is possible to use the inverse form of the conventional flow regime criteria developed previously (7,8). Hence the following scheme is recommended.

| Regime Predicted<br>Assuming no CHF | Regime Just After CHF |
|-------------------------------------|-----------------------|
| Liquid or Bubbly Flow               | → Inverted Annular    |
| Slug or Churn Turbulent             | → Inverted Slug       |
| Annular Flow                        | → Dispersed Droplet   |
| Annular-mist Flow                   | → Dispersed Droplet   |

This indicates that the initial flow regime just after the dryout point depends mainly on the liquid flux, vapor flux, fluid properties, and geometry of the flow channel.

The second type is the flow regime transition criteria within the post CHF region. The possible flow regime transitions are;



It is expected that the liquid core jet stability, entrainment and stability of liquid slugs or droplets are the key mechanisms which determine these flow regime transitions in inverted flow.

In view of the above, the jet disintegration mechanisms have been reviewed in detail (9-18). The existing analytical works and experimental data are on the free liquid jet disintegration in stagnant gas phase. It is obvious that there exist significant differences between the free jet and inverted annular flow. The inverted annular flow is co-axial jets of liquid and vapor, therefore, the pressure and shear force from the outer vapor jet can strongly influence the stability of the liquid jet. Nevertheless, the existing studies on free jet break-up gave significant insight to the inverted annular flow transition.

In the case of a free jet, three main mechanisms of jet break-up have been identified. These are the varicose jet instability, sinuous jet instability, and jet atomization. The varicose instability occurs at low jet velocities and the jet break-up is basically axisymmetric. In this region, the jet length increases with the jet velocity. At higher velocities, the disturbances become asymmetrical and produces sinuous break-up. In this region the jet length decreases with the jet velocity initially, but at higher velocities it can increase again. In the varicose or sinuous region, the resulting droplets are rather large having a dimension similar to the jet diameter. At very high jet velocities, the liquid jet can directly atomize and



become very fine droplets. There are several droplet size correlations (17, 18), however, these correlations are dimensional and their applications are limited.

In view of the significant differences between the free jet break-up and inverted annular flow transitions, a simple simulation experiment using co-axial jets in a glass tube has been carried out. It indicated that there were also three basic mechanisms of liquid jet break-up. In the co-axial jet case, the shear force due to gas flow becomes important at high relative velocities and the entrainment mechanism due to roll waves occurs instead of the atomization. In general, the jet break-up length can be correlated in the following form.

$$\frac{L_J}{D_J \sqrt{We_J}} = f (Re_f, Re_J, \alpha) \quad (1)$$

where  $L_J$ ,  $D_J$ ,  $Re_f$ ,  $We_J$  and  $\alpha$  are the jet break-up length, jet diameter, liquid Reynolds number, jet Weber number, and mean void fraction, respectively. The jet Reynolds number is based on the relative velocity between phases. The void fraction and the jet Reynolds number are additional parameters which characterize the co-axial jet break-up in a tube. It was found that the jet became more unstable as  $Re_J$  increases. On the other hand, the jet became more stable and approached the free jet behavior as  $\alpha$  increased toward unity.

The onset of entrainment due to shearing-off of roll-wave crests can be predicted by the previously developed onset of entrainment criterion (19) for annular flow. For a rough turbulent regime, this is given by

$$\frac{\mu_f V_g}{\sigma} \sqrt{\frac{\rho_g}{\rho_f}} \geq N_\mu^{0.8} \quad (2)$$

where the viscosity number is given by  $N_\mu = \mu_f / (\rho_f \sigma \sqrt{\sigma / \Delta \rho g})^{1/2}$ .

### III. Droplet Size

In the post CHF region, there are several different sources of droplets depending on the mechanisms of droplet generation. The simplest case is the annular flow film dryout. When the CHF occurs in the annular-mist flow, the droplet size can be predicted by the previously developed correlations for

entrained droplets (3). The droplets can be entrained in the upstream annular flow regime, if Eq. (2) is satisfied. Therefore, under this condition at the CHF point, the volume median droplet diameter (3) can be given by

$$D_{vm} = 0.01 \frac{\sigma}{\rho_g j_g^2} Re_g^{2/3} \left( \frac{\rho_g}{\rho_f} \right)^{-1/3} \left( \frac{\mu_g}{\mu_f} \right)^{2/3} \quad (3)$$

where  $j_g$  and  $Re_g$  are the vapor volumetric flux and vapor Reynolds number, respectively. When the CHF occurs below the critical vapor velocity for entrainment or in bubbly, slug or churn turbulent regimes, the above correlation may not be used. The droplet hydrodynamics for these cases appear to be quite complicated due to the droplet size distributions. However, there are some evidences that the rising droplets are mainly in the wake regime (2) having the diameter less than about 1 mm. For these drops the relative velocity can be given by

$$v_r = - \frac{D}{4} \left[ \frac{(g\Delta\rho)^2}{\mu_g \rho_g} \right]^{1/3} \alpha^{1.5} \quad (4)$$

The maximum drop size for the wake regime stable drops is given by

$$D = 4 \sqrt{2} \sqrt{\frac{\sigma}{g\Delta\rho}} N_{\mu g}^{1/3} \quad (5)$$

where the gas viscosity number is given by

$$N_{\mu g} = \mu_g / (\rho_g \sigma \sqrt{\sigma/g\Delta\rho})^{1/2} \quad (6)$$

The inverted annular flow can produce different size droplets. In the varicose or sinuous jet break-up regime, the jet breaks into large liquid slugs having the approximate dimensions of

$$D_s \approx D_j \quad (7)$$

$$L_s \approx 4.5 D_j$$

where  $D_s$  and  $L_s$  are the mean diameter and length of a liquid slug. It appears that these large liquid slugs will then disintegrate due to the standard

droplet break-up criterion based on the Weber number criterion. However, this process has not been confirmed by the experimental observation due to the wetting problem of the glass tube wall in the adiabatic experiment.

In the entrainment regime, it has been observed that the roll-wave crests are entrained by the gas flow. The observed size of the droplets is much smaller ( $\leq 1$  mm) than the jet diameter. However, the droplet size distribution could not be measured due to the same wetting problem of the glass tube.

### Summary

A preliminary study on the hydrodynamics of the inverted annular flow and its transitions to inverted slug and dispersed droplet flows have been carried out. First, a simple procedure to identify the initial inverted flow regimes in the post CHF region is developed. Then the flow regime transitions within the post CHF region and flow characteristics have been studied in terms of the interfacial instabilities.

As a first step, the literature for the break-up of a free liquid jet have been reviewed, then simple simulation experiments of co-axial jets of liquid and gas have been performed. Although the experiments were possible only for downward flow due to wetting problems, valuable information on flow characteristics, regime transitions, interfacial characteristics, slug drop size, and small drop size have been obtained. These formed a foundation for the ongoing preliminary modeling effort.

It has been found that there are basically three different regimes, i.e., the inverted annular, inverted slug, and dispersed droplet flow regimes. The transition from inverted annular to inverted slug can happen in two different modes. The symmetric break-up of a liquid core is called the varicose regime and asymmetric break-up is called the sinuous regime. In both cases the jet breaks into large liquid slugs having a length four to five times the diameter of the jet. It is considered that in the post CHF regime, the large liquid slugs can disintegrate into small drops as the vapor velocity increases due to phase change. At higher gas jet velocity, entrainment due to shearing-off of roll wave crests becomes important. This entrainment process produces small droplets having diameters less than about 1 mm. The onset of this entrainment can be predicted by the previously developed criterion for annular flow.

In view of the several shortcomings of the above simulation experiments such as the wetting problems and flow direction, a new experiment using a heated wall above the rewetting temperature is planned. This will give detailed information on the liquid slug disintegration, entrainment process and small drop size.

#### References

1. M. Ishii and K. Mishima, "Correlation for Liquid Entrainment in Annular Two-phase Flow of Low Viscous Fluid," ANL/RAS/LWR 81-2 (1981).
2. I. Kataoka and M. Ishii, "Mechanism and Correlation of Droplet Entrainment and Deposition in Annular Two-phase Flow," ANL-82-44, NUREG/CR-2885 (1982).
3. I. Kataoka, M. Ishii, and K. Mishima, "Generation and Size Distribution of Droplet in Gas-liquid Annular Two-phase Flow," ANL/RAS/LWR 81-3 (1981).
4. M. Ishii and I. Kataoka, "Scaling Criteria for LWR's under Single Phase and Two-phase Natural Circulation," Joint NRC/ANS Meeting on Basic Thermal Hydraulic Mechanisms in LWR Analysis, Bethesda, Sept. 14-15, 1982.
5. M. Ishii and K. Mishima, "Two-fluid Model and Hydrodynamic Constitutive Relations," to be published in the special issue of Nuclear Engineering and Design (1982).
6. G. Kocamustafaogullari, I. Y. Chen, and M. Ishii, "Correlation for Nucleation Site Density and Its Effect on Interfacial Area," ANL-82-32, NUREG/CR-2778 (1982).
7. A. E. Dukler and Y. Taitel, "Flow Regime Transitions for Vertical Upward Gas Liquid Flow," NUREG-0163 (1977).
8. M. Ishii and K. Mishima, "Study of Two-fluid Model and Interfacial Area," ANL-80-111, NUREG/CR-1873 (1980).
9. C. Weber, "Zum Zerfall eines Flüssigkeitsstrahles," Z. Angew. Math. Mech. 11, p. 136 (1931).
10. E. Tyler and E. G. Richardson, "The Characteristic Curves of Liquid Jets," Proc. Phys. Soc. 37, p. 297 (1925).
11. V. G. Levich, Physicochemical Hydrodynamics, Prentice Hall, Inc., Englewood Cliffs, NJ, p. 626 (1962).
12. R. P. Grant and S. Middleman, "Newtonian Jet Stability," AICHE J. 12, p. 669 (1966).
13. C. C. Miesse, "Correlation of Experimental Data on the Disintegration of Liquid Jets," Ind. and Eng. Chem. 47, p. 1690 (1955).

14. J. H. Lienhard and J. B. Day, "The Breakup of Superheated Liquid Jets," J. Basic Eng. Trans. ASME 88, p. 515 (1970).
15. R. S. Brodkey, The Phenomena of Fluid Motions, Addison-Wesley Publishing Co., Reading, MA, p. 547 (1967).
16. W. Ohnesorge, "Die Bildung von Tropfen an Düsen und die Auflösung flüssiger Strahlen," Z. Angew Math. Mech. 16, p. 355 (1936).
17. S. Nukiyama and Y. Tanasawa, "Experiment on Atomization of Liquid," Trans. JSME, Vol. 5, p. 63 (1939).
18. A. C. Merrington and E. G. Richardson, "The Break-up of Liquid Jets," Proc. Phys. Soc. 59, p. 1 (1947).
19. M. Ishii and M. A. Grofmes, "Inception Criteria for Droplet Entrainment in Two-phase Concurrent Film Flow," AIChE J., Vol. 21, p. 308 (1975).

PHENOMENOLOGICAL MODELING OF TWO-PHASE  
FLOW IN WATER REACTOR AT ANL  
(INVERTED ANNULAR FLOW MODELING)

BY

M. ISHII  
G. DE JARLAIS

REACTOR ANALYSIS AND SAFETY DIVISION

PHENOMENOLOGICAL MODELING AT ANL

- 1) ENTRAINMENT RATE PROCESS IN ANNULAR FLOW.  
DROPLET SIZE & SIZE DISTRIBUTION
- 2) INVERTED ANNULAR FLOW MODELING
- 3) FLECHT-SEASET DATA EVALUATION
- 4) SIMILARITY CRITERIA FOR TWO-PHASE NATURAL CIRCULATION  
SYSTEM

OBJECTIVE: DEVELOP INVERTED ANNULAR FLOW MODEL

- FLOW CHARACTERISTICS & REGIMES
- INTERFACIAL AREA (DROP SIZE)
- INTERFACIAL SHEAR (ROUGHNESS)
- INTERFACIAL HEAT TRANSFER

INVERTED ANNULAR FLOW

(1) POST CHF REGIMES

- INVERTED ANNULAR FLOW
- INVERTED SLUG FLOW
- DISPERSED DROPLET FLOW

• INITIAL FLOW REGIMES (SEE ABOVE)

(2) FLOW REGIME TRANSITION CRITERIA

INVERTED ANNULAR → INVERTED SLUG → DISPERSED

(3) DROPLET SIZE AND INTERFACIAL AREA

LARGE DROPS ← SLUG ← RAYLEIGH JET

SMALL DROPS ← { JET ATOMIZATION  
JET ENTRAINMENT

(4) EXPERIMENTAL PROGRAM

(5) RECOMMENDATION FOR INTERFACIAL TRANSFER CORRELATIONS

NO DIRECT DATA ON TRANSFER

FLOW CHARACTERISTICS → MOST APPROPRIATE CORRELATIONS

FY 1982 EFFORT

INITIAL FLOW REGIMES AT CHF

● REVIEW OF STATE OF THE ARTS

(1) INVERTED ANNULAR FLOW

DATA & MODELS FOR WALL HEAT TRANSFER

LITTLE ON { FLOW CHARACTERISTICS  
INTERFACIAL TRANSFERS

(2) FREE LIQUID JET

JET DISINTEGRATION

JET LENGTH

SOME OF DROP SIZE

(3) INTERFACIAL TRANSFER

{ LIQUID FILM FLOW  
FILM CONDENSATION  
ANNULAR FLOW

● IDENTIFY { MECHANISMS OF LIQUID BREAK-UP  
FLOW & INTERFACIAL CHARACTERISTICS

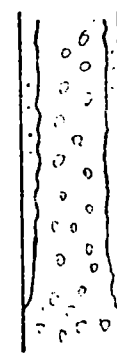
(1) SIMULATING EXPERIMENT OF CO-AXIAL JETS

↳ FLOW REGIMES & REGIME TRANSITIONS  
BREAK-UP LENGTH  
DROPLET SIZE (LARGE & SMALL)

(2) MODELING OF THESE PARAMETERS

● BASED ON ABOVE; CHOICE OF APPROPRIATE TRANSFER CORRELATIONS

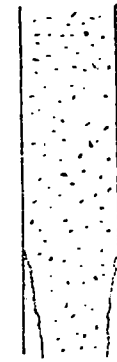
● CRITERIA DEVELOPED BY ISHII & MISHIMA (1980)



INVERTED ANNULAR



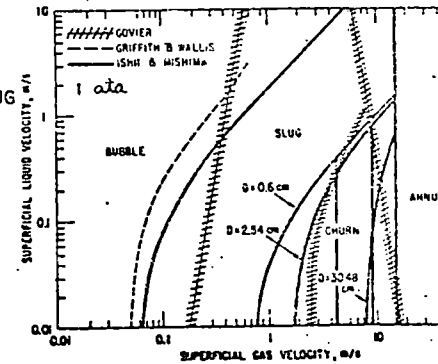
INVERTED SLUG



DISPERSED DROPLET

● BEFORE CHF      Post CHF

{ BUBBLY → INVERTED ANNULAR  
SLUG OR CHURN → INVERTED SLUG  
ANNULAR → DISPERSED DROPLET

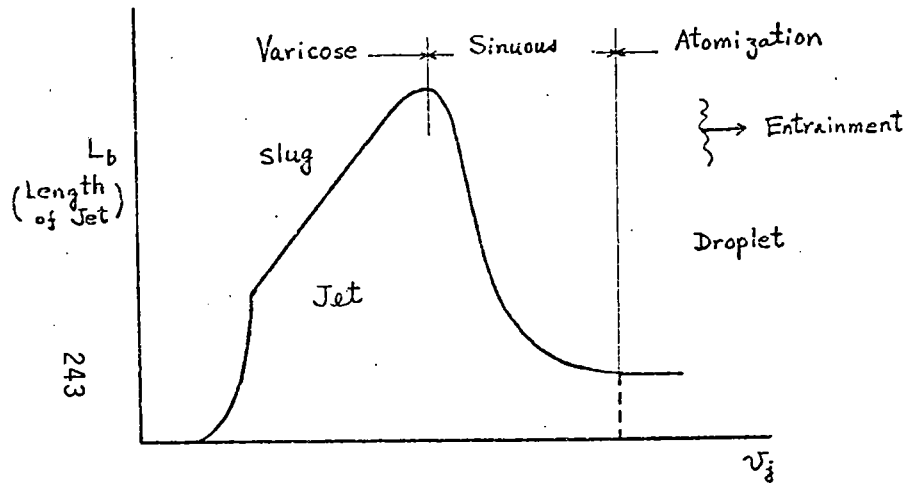


## FLOW REGIME TRANSITION

JET DISINTEGRATION → INVERTED FLOW TRANSITION  
(UNCONFINED)

↑↑  
MODELING  
SIMULATION EXPERIMENT

### (1) RAYLEIGH JET INSTABILITY



- Transition Criteria
- Interfacial Characteristics
  - Interfacial { Area
  - Roughness
  - Droplet Size

## FREE LIQUID JET DISINTEGRATION

(1) VARICOSE REGION  
(SYMMETRIC DISTURBANCE)

TRANSITION CRITERION : ONESORGE  
 { GRANT  
 { TYLER & RICHARDSON

$$RE_J = 340 N_{\mu J}^{-0.27}$$



(2) SINUOUS REGION  
(ASYMMETRIC DISTURBANCE)  
→ SPIRAL

TRANSITION CRITERION : ONESORGE  
MARRINGTON ET AL.

$$RE_J = 280 N_{\mu J}^{-0.82}$$



(3) ATOMIZATION

### IMPORTANT PARAMETERS

$$RE_J = \rho_F U_J D_J / \mu_F$$

$$WE_J = \rho_F U_J^2 D_J / \sigma$$

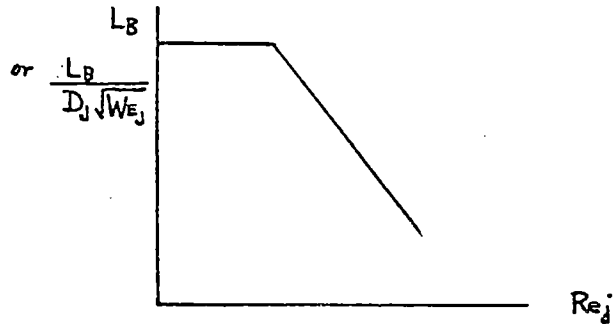
$$N_{\mu J} = \mu_F / \sqrt{\sigma \rho_F D_J}$$

$$N_{\mu J} = \sqrt{WE_J / RE_J}$$





- BREAK-UP LENGTH → LENGTH OF INV. ANNULAR FLOW



$$\left\{ \begin{array}{l} \text{WEBER ET AL. } L_B = 12 \sqrt{We_J} D_J \\ \text{LIENHARD \& DAY } L_B = 2.75 \times 10^{-10} Re_J^{-2} \sqrt{We_J} D_J \end{array} \right.$$

- SLUG LENGTH; MOST DANGEROUS WAVE LENGTH

- HELMHOLTZ INSTABILITY  $\lambda_M = 2\pi \sqrt{\frac{3\sigma}{G\Delta\rho}}$

- RAYLEIGH JET  $\lambda_M = 4.51 D_J$

(CHRISTIANSEN; EFFECT OF 2ND PHASE)  $4.51 \leq \frac{\lambda_M}{D_J} \leq 6.5$

- LARGE DROP SIZE

- TAYLOR WAVE  $D_D \sim \pi \sqrt{\frac{\sigma}{G\Delta\rho}}$

- RAYLEIGH JET  $D_D = 1.89 D_J$

- FOR LARGE JET  $D_J \rightarrow 0.2 \pi \sqrt{\frac{\sigma}{G\Delta\rho}}$

### CRITERIA FOR ONSET OF ENTRAINMENT

- ROLL WAVE ENTRAINMENT;  $Re_F \geq 160$  (VERTICAL UP)

$$\frac{\mu_F J_G}{\sigma} \sqrt{\frac{\rho_G}{\rho_F}} \geq 11.78 N_{\mu F}^{0.8} Re_F^{-1/3} \quad \text{FOR } N_{\mu} \leq \frac{1}{15}$$

$$\geq 1.35 Re_F^{-1/3} \quad N_{\mu} > \frac{1}{15}$$

- ROUGH TURBULENT REGIME;  $Re_F \geq 1635$

$$\frac{\mu_F J_G}{\sigma} \sqrt{\frac{\rho_G}{\rho_F}} \geq N_{\mu F}^{0.8} \quad \text{FOR } N_{\mu} < \frac{1}{15}$$

$$\geq 0.1146 \quad N_{\mu} > \frac{1}{15}$$

- LOW REYNOLDS NUMBER ENTRAINMENT

WEBER NUMBER BASED ON FILM THICKNESS

$$\frac{\mu_F J_G}{\sigma} \sqrt{\frac{\rho_G}{\rho_F}} \geq 1.5 Re_F^{-1/2} \quad Re_F < 160$$

- MINIMUM REYNOLDS NUMBER FOR ENTRAINMENT

$\delta$  < GAS BOUNDARY LAYER

$$(Re_F)_{\text{MIN}} = 155 \left(\frac{\rho_F}{\rho_G}\right)^{3/4} \left(\frac{\mu_G}{\mu_F}\right)^{1.5}$$

SMALL DROPLET SIZE

ORIGIN { JET ATOMIZATION  
JET ENTRAINMENT

ATOMIZED

WEBER  $D_D \sim \frac{12\sigma}{\rho_f u_r^2}$  ; TOO LARGE AT LOW FLOW

NUKIYAMA & TANASAWA (DIMENSIONAL)

$$D_{sm} = 5.85 \frac{\sqrt{2}}{u_r} \sqrt{\frac{\sigma}{\rho_f}}$$

← COMPARATIVE

MERRINGTON & RICHARDSON (DIMENSIONAL)

MODIFIED (ISHII)  $D_{vm} = 573 \left( \frac{\mu_g}{\rho_f u_r} \right) \left( \frac{\mu_f}{\mu_g} \right)^{0.2}$

NOTE  $D \sim \frac{1}{u_r}$  ,  $\nu_f^{1/5}$  (MAY NOT DEPEND ON  $\sigma$ )

VOLUME MEDIAN DIAMETER

$$D_{VM} \doteq 0.01 \frac{\sigma}{\rho_G J_G^2} RE_G^{2/3} \left( \frac{\rho_G}{\rho_F} \right)^{-1/3} \left( \frac{\mu_G}{\mu_F} \right)^{2/3}$$

MAXIMUM DROPLET SIZE

$$D_{MAX} = 3.13 D_{VM}$$

NOTE:

①

$$D_{VM} \sim J_G^{-4/3}$$



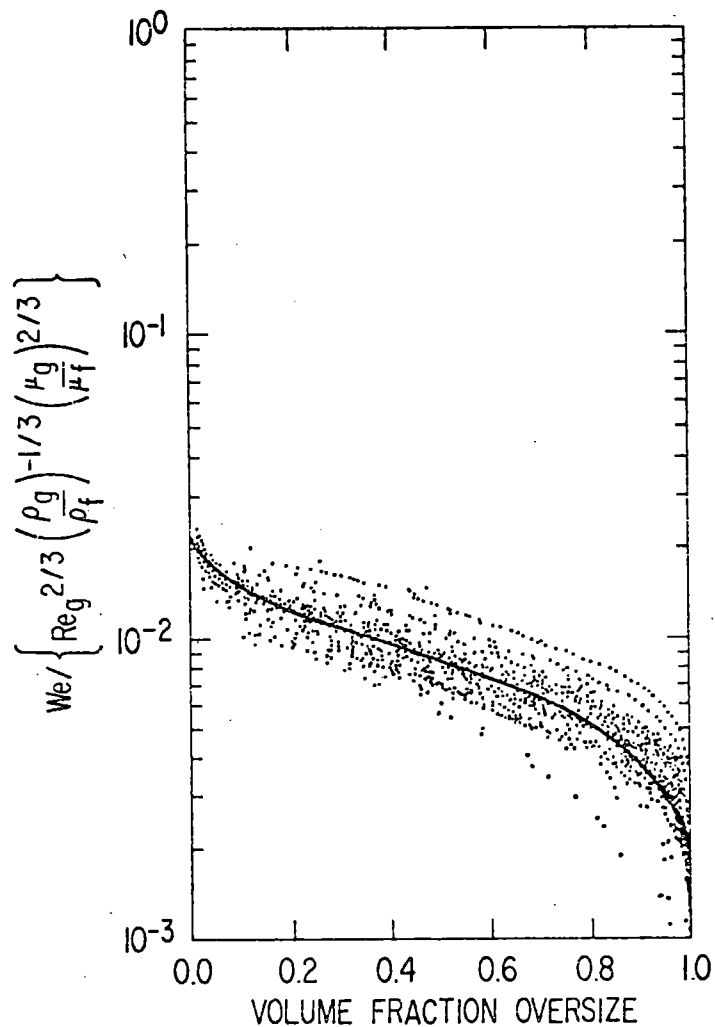
STANDARD  $WE_C$  CRITERIA

$$D_{VM} \sim J_G^{-2}$$

②

PRESENT MODEL → MUCH SMALLER  $D_{VM}$

STANDARD  $WE_C$  → TOO LARGE  $D_{VM}$



Droplet Size Distributions in  $We / \left[ Re_g^{2/3} \left( \frac{\rho_g}{\rho_f} \right)^{-1/3} \left( \frac{\mu_g}{\mu_f} \right)^{2/3} \right]$  vs. Volume Fraction Oversize Plot for Data of Wicks and Dukler, Cousins and Hewitt and Lindsted et al.

### SIMPLE SIMULATION EXPERIMENT

- (1) AIR-WATER SIMULATION EXPERIMENTS
- (2) CO-AXIAL AIR & WATER JET IN GLASS TUBE
- (3) MOTIVATION
  - LACK OF DATA ON
 

|   |                      |
|---|----------------------|
| { | FLOW CHARACTERISTICS |
|   | REGIMES              |
|   | REGIME TRANSITION    |
|   | DROP SIZE            |
  - STUDY THE SIMILARITY WITH FREE JET
- (4) OBJECTIVE
  - FLOW REGIMES & INTERFACIAL CHARACTERISTICS
  - REGIME TRANSITION POINTS
  - INVERTED ANNULAR FLOW DISINTEGRATION LENGTH
  - WAVE LENGTH → LARGE DROP SIZE
  - ATOMIZATION → SMALL DROP SIZE
  - ENTRAINMENT (ROLL WAVE)
- (5) SYSTEM & METHOD
 

|   |           |                               |
|---|-----------|-------------------------------|
| { | ~ 5 μ SEC | HIGH SPEED PHOTOGRAPHY        |
|   | ~ 0.1 MM  | RESOLUTION AT HIGH SPEED FLOW |

  - FLOW CHARACTERISTIC EXPERIMENTS
  - DROP SIZE EXPERIMENTS

EXPERIMENTAL PROGRAM

• JET DISINTEGRATION IN TUBE (PRESENT)

- { JET → WAVE INSTABILITY → SLUG
- { JET → ATOMIZING → DROPLETS
- { JET → ENTRAINMENT → DISINTEGRATION → DROPLETS
- { DROPLET SIZES

• INVERTED FLOW TRANSITION (FUTURE)

FREON + AIR WITH  $T_w > T_o$

• SYSTEM

CO-AXIAL JET OF LIQUID & GAS

UP FLOW OR DOWN FLOW

PHOTO & CINEMATOGRAPH (.8 ~ 15 μSEC)

$D_o = 1.66, 1.36, 1.16 \dots$  CM

$D_i = 1.54, 1.24, 1.08, 0.90, 0.76, 0.60$  CM

$L = 121$  CM

$\alpha_i = .143 - 0.705$

- {  $v_F = 0 \sim 10$  M/SEC
- {  $v_G = 0 \sim 60$  M/SEC

FLOW REGIME/TRANSITION PHOTOGRAPHS

INVERTED ANNULAR FLOW

ADIABATIC H<sub>2</sub>O-N<sub>2</sub> SYSTEM

B2 TEST GEOMETRY:

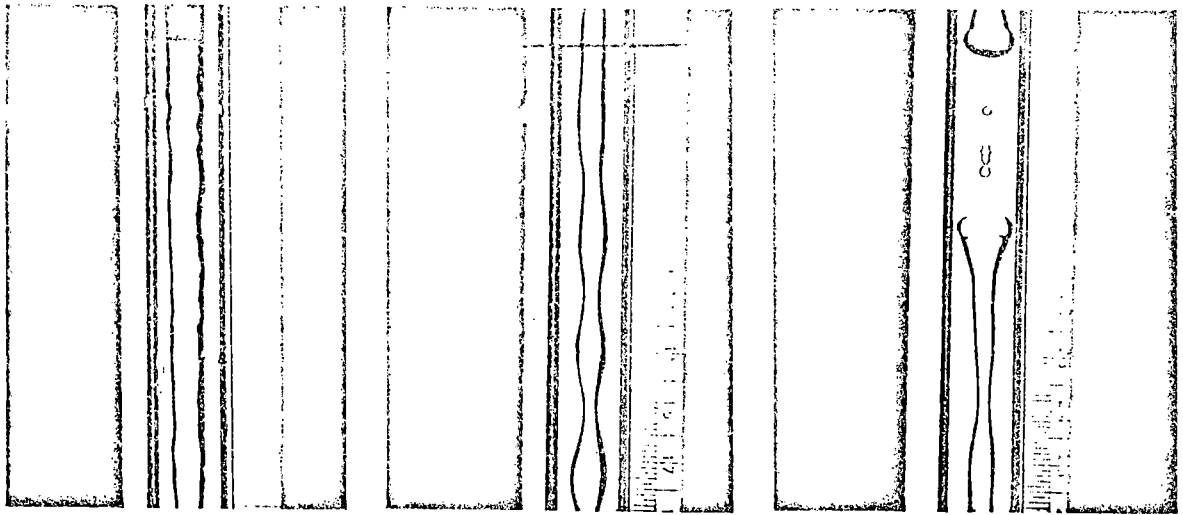
$D_{JET} = 0.873$  CM (AT NOZZLE)

$D_{ANNULUS} = 1.36$  CM

INITIAL VOID FRACTION = 0.685

LOW LIQUID TURBULENCE:  $RE_J \doteq 8000$

HIGH LIQUID TURBULENCE:  $RE_J \doteq 17,000$



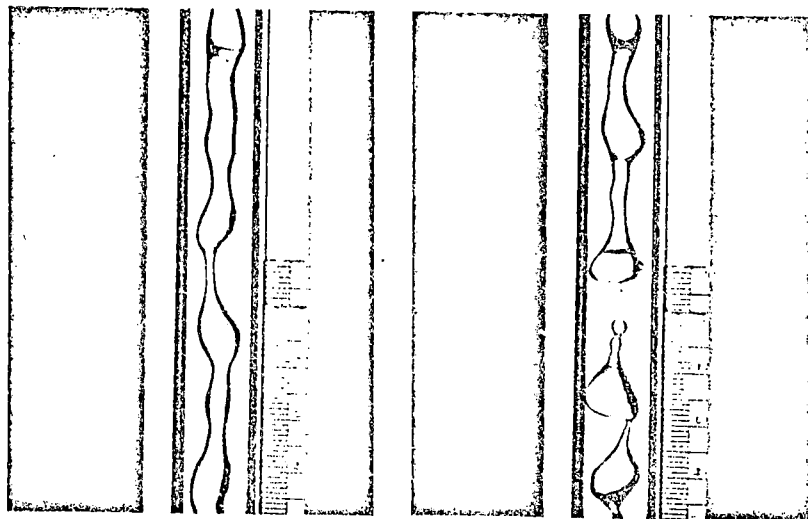
4-1-1

4-1-6

4-1-8

LOW LIQUID TURBULENCE,  
VARICOSE (RAYLEIGH) LIQUID JET

ALL PHOTOS :  $V_{JET} = 1.26 \text{ M/S}$  (AT NOZZLE)  
 $V_{N_2} = .62 \text{ M/S}$  (AT NOZZLE)  
 JET LENGTH  $\approx 50 \text{ CM}$

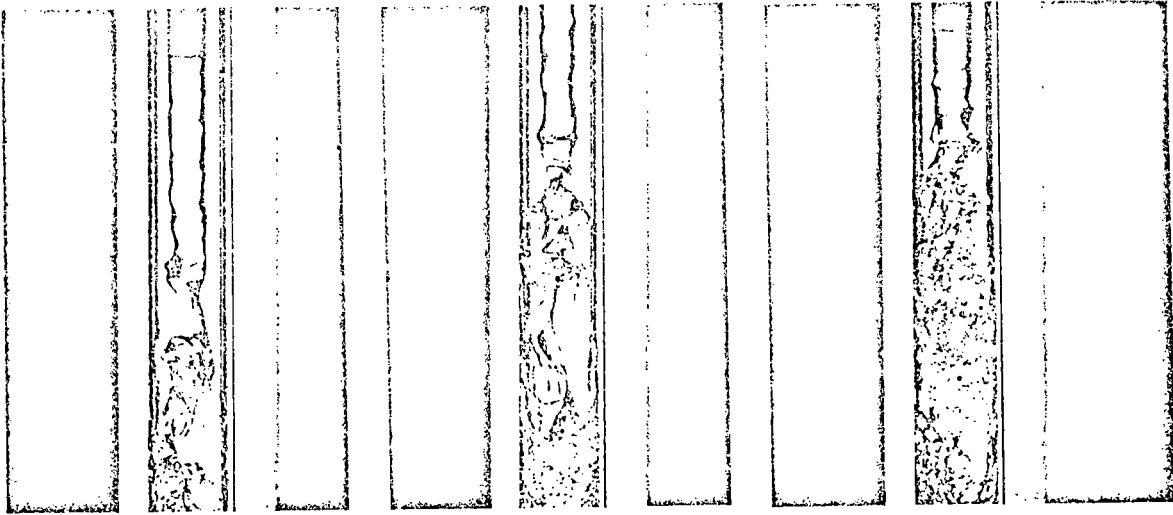


4-1-14

4-1-15

LOW LIQUID TURBULENCE,  
VARICOSE - SINUOUS JET TRANSITION

BOTH PHOTOS :  $V_{JET} = 1.26 \text{ M/S}$  (NOZZLE)  
 $V_{N_2} = 8.0 \text{ M/S}$  (NOZZLE)  
 JET LENGTH  $\approx 28 \text{ CM}$



4-13-2

4-13-7

4-20-14

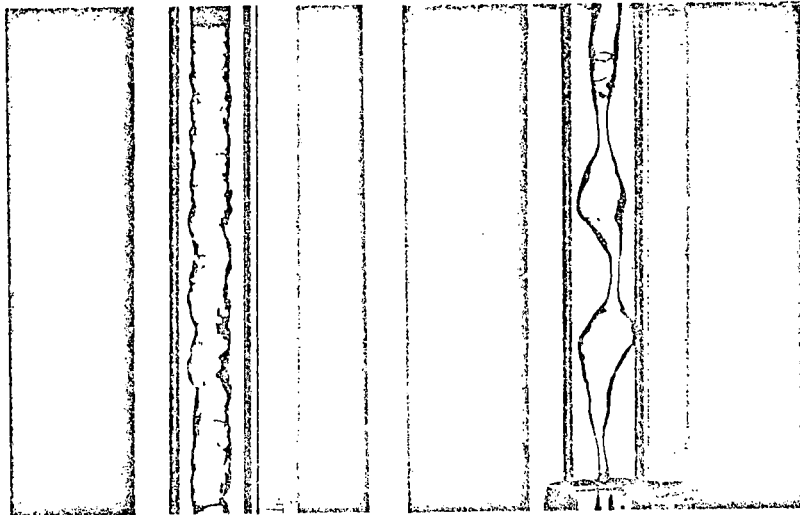
LOW LIQUID TURBULENCE,  
ROLL WAVE BREAKUP

PHOTOS 4-13-2,7 :

$V_{JET} = 1.26 \text{ M/S}$  (NOZZLE)  
 $V_{N_2} = 13.6 \text{ M/S}$  (NOZZLE)  
JET LENGTH  $\hat{=}$  8 CM

PHOTO 4-20-14 :

$V_{JET} = 1.26 \text{ M/S}$  (NOZZLE)  
 $V_{N_2} = 19.8 \text{ M/S}$  (NOZZLE)  
JET LENGTH  $\hat{=}$  4 CM



4-21-5

4-21-8

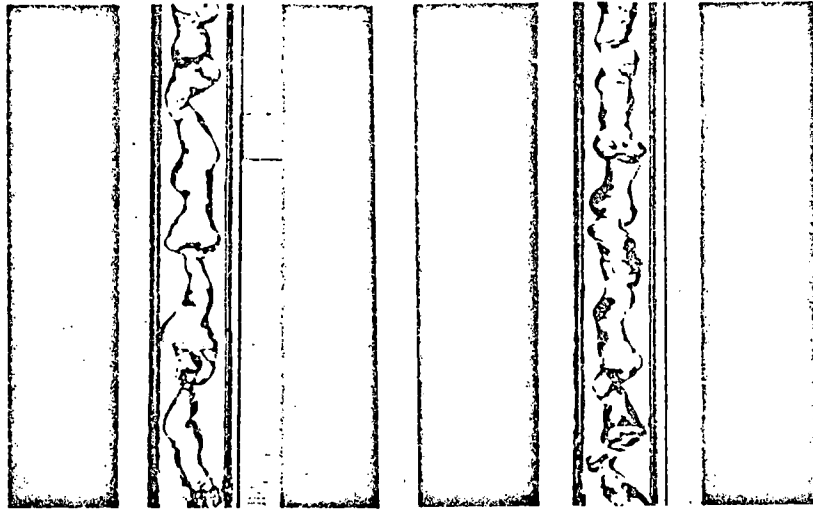
HIGH LIQUID TURBULENCE,  
VARICOSE (RAYLEIGH) LIQUID JET

BOTH PHOTOS :  $V_{JET} = 2.7 \text{ M/S}$  (AT NOZZLE)

$V_{N_2} = .75 \text{ M/S}$  (AT NOZZLE)

249

JET LENGTH  $\hat{=}$  70 CM



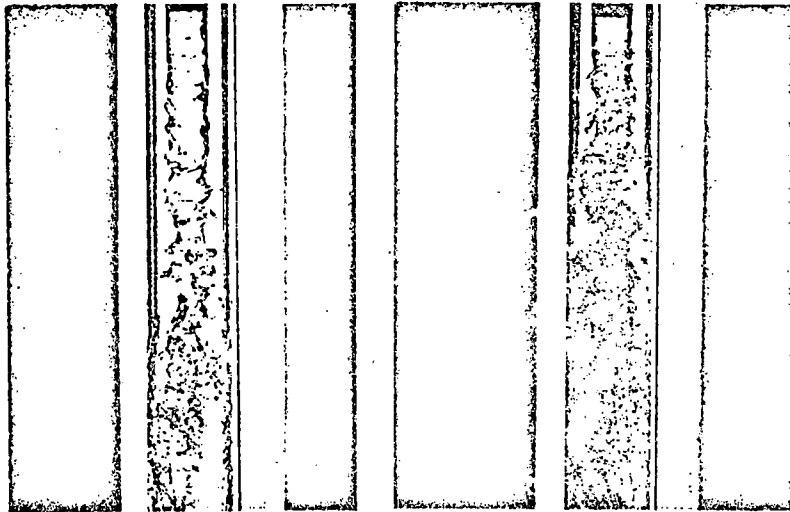
5-3-19

5-3-20

HIGH LIQUID TURBULENCE,  
SINUOUS LIQUID JET

PHOTO 5-3-19 :  $V_{JET} = 2.7$  M/S (NOZZLE)  
 $V_{N_2} = 8.9$  M/S (NOZZLE)  
 JET LENGTH = 35 CM

PHOTO 5-3-20 :  $V_{JET} = 2.7$  M/S (NOZZLE)  
 $V_{N_2} = 10.7$  M/S (NOZZLE)  
 JET LENGTH = 18 CM



5-5-6

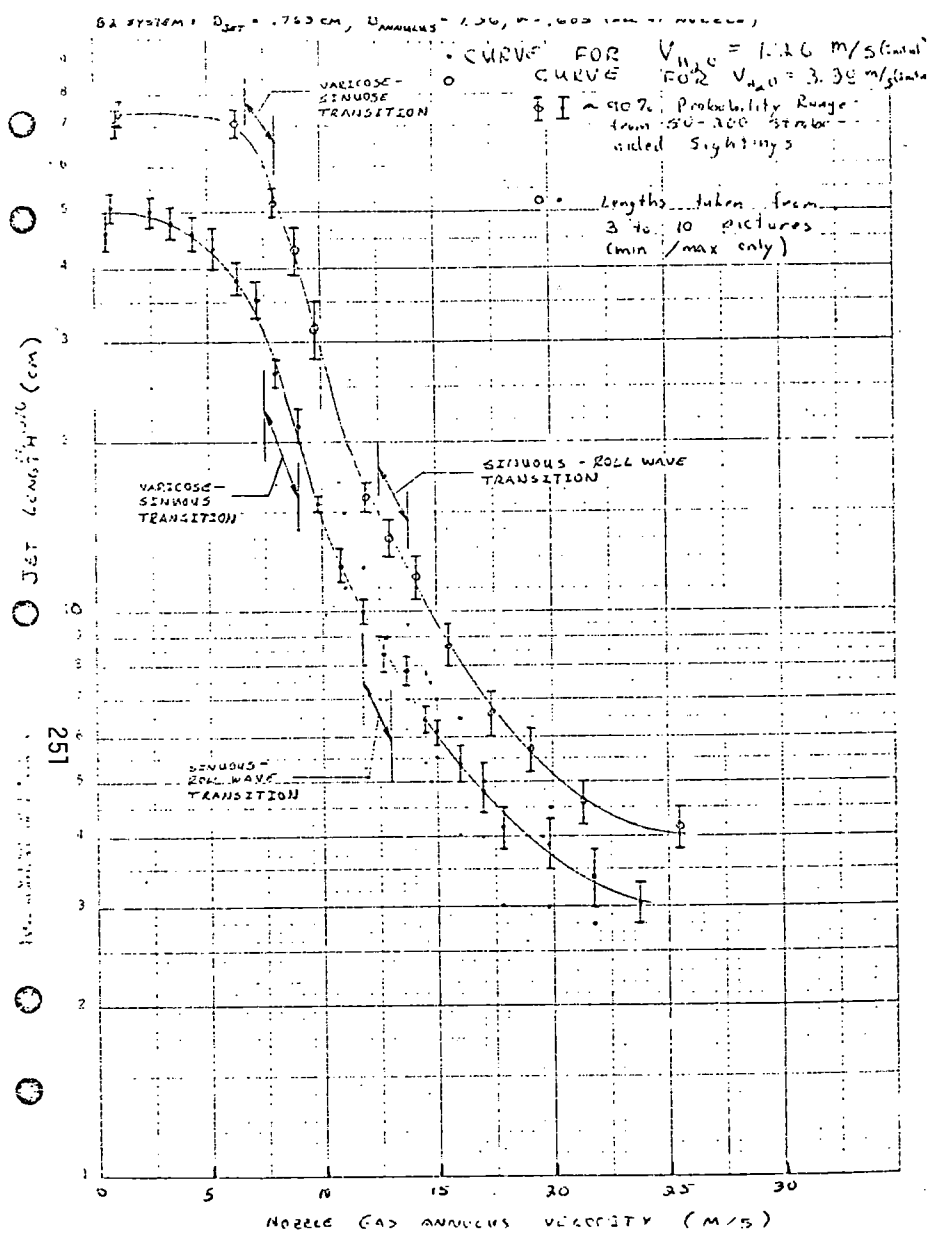
5-5-9

HIGH LIQUID TURBULENCE,  
ROLL WAVE BREAKUP

PHOTO 5-5-6 :  $V_{JET} = 2.7$  M/S (NOZZLE)  
 $V_{N_2} = 17.0$  M/S (NOZZLE)  
 JET LENGTH = 6.5 CM

PHOTO 5-5-9 :  $V_{JET} = 2.7$  M/S (NOZZLE)  
 250  $V_{N_2} = 30.4$  M/S (NOZZLE)  
 JET LENGTH = 3 CM

RESULTS OF EXPERIMENT



(1) JET DISINTEGRATION

VARICOSE } REGIME ~ RAYLEIGH INSTABILITY  
 SINUOUS }

LARGE DROP SIZE ~ 5 D

IDENTIFY PROPER INTERFACIAL TRANSFER CORRELATIONS

- { FILM (DIFFUSION) THEORY
- { SURFACE RENEWAL THEORY
- { LARGE EDDY EFFECT
- { EFFECT OF PHASE CHANGE

(2) ROLL WAVE ENTRAINMENT

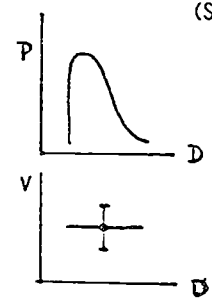
MECHANISM ~ ANNULAR ENTRAINMENT

CRITICAL GAS VELOCITY ~ ONSET CRITERION (ISHII & GROLMES)

DROPLET SIZE - MAXIMUM MEASURED

UNCERTAINTY OF SMALL DROP SIZE { SLUG DISINTEGRATION  
 ENTRAINMENT

FLECHT EXPERIMENT (SEASET) (~200 μSEC) { DROP SIZE  
 DROP VELOCITY



- ONLY IN DISPERSED REGIME
- DROP SIZE DISTRIBUTION → DIFFICULTY OF SMALL DROPS
- VELOCITY DISTRIBUTION → DIFFICULTY OF SMALL DROPS
- + RESOLUTION PROBLEM OF SMALL OR HIGH VELOCITY DROPS



DATA EVALUATION

ADVANTAGE OF HEATED SYSTEM

● AVAILABLE

FLOW CHARACTERISTICS

- FLOW REGIMES
- REGIME TRANSITION
- INTERFACIAL CHARACTERISTICS
- IMMEDIATE LARGE DROP SIZE
- SOME SMALL DROP SIZE

DOWNWARD INVERTED ANNULAR FLOW

● SHORTCOMINGS

● WALL WETTING PROBLEMS

DOWNSTREAM LARGE DROP DISINTEGRATION  
 DOWNSTREAM ROLL WAVE ENTRAINMENT  
 ↓  
 MEASUREMENT OF SMALL DROP SIZE

- UPWARD INVERTED FLOW → UNSTABLE
- NO EFFECT OF PHASE CHANGE (LOCAL)
- NO EFFECT OF SPACERS
- PROPERTY GROUPS UNCHANGED

● RECOMMENDATION OF EXPERIMENT WITH

$T_w > T$  (REWETTING)

CO-AXIAL JETS  
(ADIABATIC)

$T_w > T$  (REWETTING)

(1) SMALL  $\alpha$  (THIN GAS FILM)  
IMPOSSIBLE DUE TO WETTING

POSSIBLE

(2) UP FLOW  
~ IMPOSSIBLE DUE TO { JET EXPANSION  
WETTING

POSSIBLE

(3) LIQUID SLUG BREAKUP  
WALL WETTING BY COLLISION  
SMALL DROP SIZE UNKNOWN

SLUG DISINTEGRATION  
SMALL DROP SIZE

(4) ROLL WAVE ENTRAINMENT  
ONLY INITIAL STAGE  
AFTER ONSET → WETTING

NO WETTING  
DEVELOPMENT OF DIS-  
PERSED FLOW  
SMALL DROP SIZE

~ MAX. SIZE OF SMALL DROPS

(5) EFFECT OF 2 PHASE JET  
IMPOSSIBLE

POSSIBLE

AN LDA IN SITU STUDY OF DROPLET HYDRODYNAMICS  
ACROSS GRID SPACERS IN PWR-LOCA REFLOOD

by

S.L. Lee

S. K. Cho

K. Rob

H. J. Sheen

M. Aghili

College of Engineering and Applied Sciences  
State University of New York at Stony Brook  
Stony Brook, NY 11794

## 1. INTRODUCTION

### A) General

One of the criterias of critical importance for emergency core cooling systems of the nuclear reactors is the prediction of the peak cladding temperature during the transient of the reflood phase of a PWR-LOCA. Ihle et al [1] reported a transient hydraulic experiment on the significant heat transfer mechanisms which are responsible for the development of the cladding temperature transient. These authors presented a typical measured cladding temperature transient near the top end of the heated bundle length compared with corresponding analytical predictions by two computer codes, RELAP4/MOD6 and REFLUX/GRS. The comparison reveals the inadequacy of the assumed heat transfer mechanisms in the analysis which results in significantly higher cladding temperature levels than measured during the initial period of reflooding.

One of the improved heat transfer mechanisms in the case of hot, dry-wall cooling is "bottom flooding". In this technique, the hot, dry-wall is cooled initially by a parallel vapor stream carrying droplets of mostly a few millimeters in size which are entirely generated from the bottom, based on the critical Weber number [2]. Therefore, the cooling is believed to be done primarily by the convection of superheated steam on the assumption of a lack of sufficient population of smaller droplets which usually serve as more efficient cooling agents due to their large surface area to volume ratios. The thermally relatively inactive large droplets ( $>1\text{mm}$ ) can be broken down to more active smaller droplets ( $<100\mu$ ) using grid spacers located at equal

intervals along the entire length of the bundle [3]. Large droplets intercepted by each grid spacer produce a large number of small droplets downstream. The effect of this phenomenon is observed by a sharp dip of the cladding temperature downstream of all grid spacers [4]. Hence, a direct verification of this suggested mechanism of transformation of mist flow across the grid spacer plate is in order.

#### B) Task Objectives

The objectives of this task is to develop correlations for the effect of grid spacers. In detail, they are classified as follows:

1. Develop correlations to predict the rates of droplets re-entrainment in concurrent two-phase flow.
2. Develop correlations for predicting interfacial area density in dispersed flow regimes.
3. Provide data on droplet size distribution, droplet velocity and gas velocity.

## 2. Optical Technique and Instrumentation

#### A) LDA System Arrangement and Methodology

The operational arrangement of the reference-mode laser-Doppler anemometer is shown in the sketch of Figure 1. The incoming laser beam from a 15mw He-Ne laser is split into two beams of unequal intensity, the weaker one for the reference beam and the stronger one for the scattering beam, which are then so polarized that they form at  $45^\circ$  polarization angle with each other. These beams are focussed by a focussing lens to the same point at an angle of 8.14 degrees to form a small measuring volume with a short dimension of about  $240\mu$  as shown in the sketch of Figure 1. Both the

reference beam and the scattered light from the scattering beam on hitting a moving scattering body in the measuring volume are picked up along the direction of the reference beam by a matching receiving lens. The received beam is then passed through a polarization splitter to be split into two beams, one with a polarization orientation the same as that of the scattering beam, and the other with a polarization orientation in the perpendicular direction. The beam with a polarization orientation the same as that of the scattering beam consists of the scattered beam and the component of the reference beam in the same polarization direction and is received through a small aperture by the photo-multiplier tube to produce the Doppler signal through heterodyning.

#### B) Large Particle Measurement Scheme

When a moving spherical particle of a size larger than the size of the reference beam cuts across the reference beam, the outputs of both the photo-multiplier tube and the photo-diode will show a drop from an elevated D.C. voltage to the system electronics noise voltage and after a drop-off period to be followed by a return to the same elevated D.C. voltage. This drop-off period represents the time taken for the center line of the reference beam to transverse across the circular area formed in its plane of intersection with the spherical particle. If this plane of intersection coincides with a vertical plane of symmetry of the spherical body, after the multiplication of a geometrical factor of the cosine of the small angle between the reference beam and the horizontal, this block-off period then represents the time taken for the spherical particle to move a distance of one length of its diameter at the same vertical velocity as outlined in the sketch of Figure 2. With a knowledge of the vertical velocity from the

Doppler signal, one can then obtain the diameter of the spherical particle.

When the plane of intersection of the center line of the reference beam with the spherical particle lies within the smaller dimension of the optical measuring volume from the vertical axis of the particle and the point of detachment, a Doppler signal is registered at the end of the block-off period as shown in Figure 3. The frequency of the Doppler signal gives the vertical velocity of the particle and thus also provides the needed input for converting the measured result of block-off period to the size of the particle. However, the size of the particle so calculated can only be considered approximate due to the combined effects of the finiteness of the size of the optical measuring volume and the size of the effective scattering area of surface of the particle. For large particles of a size larger by an order-of-magnitude or more than the smaller dimension of the optical measuring volume, the error in the particle size so calculated is usually far below two percent. For small particles of a size a few times the magnitude of the smaller dimension of the optical measuring volume, these two effects seem to compensate each other to a great extent in the calculation of the size of the particle.

#### C) Small Particle Measurement Scheme

The optical measuring volume is approximately ellipsoidal in shape with the intensity of illumination falling off from its center in the form of a three-dimensional Gaussian distribution. The particles in the flow for this scheme are assumed to be smaller than the smaller dimension of the optical measuring volume, and in the size range where the aforementioned, previously established monotonical dependence of the scattered

light intensity on the particle size is held valid. It is assumed there is only one particle in the measuring volume at any given time, then the Doppler signal amplitude becomes a function of the location of the particle path through the measuring volume and the scattering particle size as shown in the sketch of Figure 4. For a usually small measuring volume (for example,  $240\mu$  in smaller dimension) and a dilute suspension (say less than  $10^5/\text{cm}^3$ ), this assumption can be shown reasonably sound.

It is also assumed that the predominate direction of the flow is lined up with the measuring direction of the optical measuring system, which is the direction of bisecting line between the axes of the incident and receiving optics at the center of the measuring volume. It is seen that the peak incident light intensity along the particle's path through the measuring volume and the length of path of the particle's center are essentially functions of the location of the path. Since the particle path length is the product of signal path time and particle velocity which is directly proportional the signal Doppler frequency, the three useful characteristic parameters of an idealized Doppler signal, as shown in the sketch of Figure 5, are then the amplitude, Doppler frequency and path time.

A much more serious difficulty in the determination of a particle's path time corresponding to the center of the particle passing through the measuring volume is the broadening of the signal. Due to the finiteness of the size of the particle, the raw Doppler signal is increasingly broadened in time with increase in the particle size. The following scheme has been worked out to convert the measured signal path time for a raw Doppler signal

to the corrected path time corresponding to the center of the particle passing through the measuring volume for the particle size determination.

The central portion of the amplitude of a Doppler signal,  $A$ , varies in a near Gaussian fashion while the amplitude at the two ends of the signal is broadened due to the finiteness of the size of the particle as shown in the sketch of Figure 6. Theoretically, the signal amplitude will asymptotically approach the zero amplitude base level if a truly Gaussian distribution is present. But for a fixed receiving optics, the signal amplitude reaches zero amplitude at both ends in finite time. To describe the central portion of the amplitude of the signal, a false base located at a small platform amplitude increment  $\Delta A_p$  below the base of zero amplitude would have to be designated. To accommodate all of the collected signals, path time and signal amplitude, which are measured at any location of the measuring volume, are converted to the amplitude with maximum path time at the center of the measuring volume by a correction scheme. By this correction scheme, analyzed results can be statistically more stable.

#### D) Instrumentation Development and Computer Interface

A scheme making use of the various signal processors was devised for the validation of the Doppler signal. After such a validation, information on the block-off time, the velocity and the amplitude of Doppler signal for each particle was recorded. The velocity information was easily obtained from the Doppler signal frequency in digital form by using a counter signal processor (T.S.I. Model 1990). The Doppler signal amplitude was detected by first rectifying the signal using a custom-built linear



rectifier, passing the rectified signal through a low-pass filter to obtain the envelope of the signal and finally using a peak detector.

The block-off time of the reference beam for the particle was obtained by using the output of the photo-diode with the proper selection of the threshold level of voltage for the determination of the starting and ending of the blockage. Using a high-speed amplifier and a comparator, a rectangular pulse, the width of which was proportional to the block-off time, was obtained. The width of this rectangular pulse was then measured using a 5 MHz oscillator (Bailey Model TCCO-26LA) and a 20-bit digital counter using integrated circuits (74LS93). Thus all the required parameters were obtained in the digital form.

For signals from each particle which satisfied the aforementioned validation requirements, the four pieces of digital data, viz, a) the number of cycles N selected for the validation of the Doppler signal, b) the time measured for the selected N number of cycles of the Doppler signal, c) the block-off time and d) the Doppler signal amplitude were read into the minicomputer.

For the storage, processing and analysis of data, a PDP-11/34 mini-computer was used. Custom-designed computer interfaces (T.S.I. Models 1998-D-1, 1998-S and 1998-Y) were used to interface the aforementioned electronic circuits to the PDP-11/34 computer interface (DR-11B). The instrumentation block diagram for signal processing and data acquisition is illustrated in Figure 7.

### 3. Flow Arrangements and Experimental Set-up

The general arrangement of the experimental test rig is shown in Figure 8. The flow channel is placed between a 15mw, He-Ne laser and photo-detectors. The flow channel is made of plexiglass with two glass windows. A 2 x 2 bundle of simulated glass rods of approximately 10.75mm outside diameter

is put inside the channel. The total length of the flow channel is 1067mm. The glass rods are arranged with a pitch of 14.30mm. There are a total of three grid spacers, placed at 381mm intervals, and one at the middle is the one designed for mist flow interference studies. The grid spacers are the standard vertical cross-plate design with plate thickness of 0.5mm and plate height of 38mm. Water droplets are supplied to the channel from seven (7) small nozzles. Water is supplied to a specially built distributor and then goes onto the nozzles. This way the pressure drop and flow rate are the same for all the operating nozzles. The set-up of the nozzles is like the cross-plate design and they are placed 75mm below the middle grid spacer cross plates. During the experiment, the nozzles which are on a plane perpendicular to the laser beam are used. The nozzles are spaced at equal distance.

Compressed air is supplied through a honey-comb flow straightener from compressed air line. Drainage ports are provided both at the top and bottom of the channel. Glass windows are needed for the passage of laser beams in the test section of the channel.

#### 4. Detailed Measurement

All the experiments were performed at ambient atmospheric pressure and room temperature. The supplied water had a temperature of 21°C. Inside the channel, a cross-shaped nozzle assembly was located 75mm below the grid spacer. To reduce the noise-to-signal ratio in the LDA measurement, only one line of nozzle assembly, which was perpendicular to the laser beam, was operated. The supplied water flow rate was varied from 205cc/min to 535cc/min. This variation was correspondent to the void fraction from 0.87 to 0.91. The air velocities inside the channel were varied from 11.6m/sec to 17.4/sec.

The measurements were done at two levels above the grid spacer and one level below the grid spacer. As shown in Figure 9, the measurement Location 1 was 5mm below the grid spacer while Location 2 and 3 were 22mm and 100mm above the grid spacer respectively. At every level, the measurements were done 0.9mm away from the center of the grid spacer to eliminate corner effect from a grid spacer joint.

The incoming dispersion contained water droplets of sizes varying from 0.5mm to 2.5mm. But Sauter mean diameter of reentrained small droplets showed that they were independent of other flow parameters. The Sauter mean diameters were calculated from the measured diameters by the following relation:

$$d_{sm} = \frac{\int d^3 N dd}{\int d^2 N dd} \quad (1)$$

where  $d_{sm}$  : Sauter mean diameter.

Finally, all the flow conditions and measured parameters were tabulated at Table 1 and Table 2 with different grid spacer thickness.

## 5. Data Analysis and Correlation

The data analysis is carried out to obtain a clear understanding of the droplet's behavior across the grid spacer. The area density, which represents the ratio between the droplets' area and volume, is an important parameter in heat transfer experiment. In this analysis, a square cross sectional area, which contained four rods and two grid spacers, was considered as a region of interest, as shown in Figure 10. The actual grid spacer thickness was influenced by the incoming droplet size due to the capture of droplets by the side walls of the grid spacer. This effective grid spacer was obtained from a separate experiment which gave a droplet capturing distance as shown in Figure 11.

The detailed area definitions are shown in Figure 10.

Area<sub>base</sub> : Unit base area that one nozzle can cover.

$$\text{Area}_{\text{base}} = 4 \times \ell \quad (2)$$

Area<sub>sc</sub> : Considered total sub-channel area.  
(Areas surrounded by solid line)

$$\text{Area}_{\text{sc}} = (14)^2 - \frac{\pi}{4} (11)^2 = 100.97 \text{mm}^2 \quad (3)$$

Area<sub>Gs</sub> : Effective grid spacer area where supplied large liquid droplets are captured.  
(Area surrounded by dotted line)

$$\text{Area}_{\text{Gs}} = 2 \times 14 \times \ell - \ell^2 \quad (4)$$

Area<sub>Uo</sub> : Unblocked area where supplied large liquid droplets are passing through without hitting the grid spacer.

$$\text{Area}_{\text{Uo}} = \text{Area}_{\text{sc}} - \text{Area}_{\text{Gs}} \quad (5)$$

$\ell$  : Effective thickness of grid spacer which is a function of supplied droplet diameter.

At Location 1, void fraction can be calculated from the following relation:

$$\frac{Q_1}{7} = (1-\alpha)_1 A_{\text{base}} V_{d1} \quad (6)$$

where  $Q_1$  : Water supply rate through 7 nozzles to a grid spacer

$\alpha$  : Void fraction

$A_{\text{base}}$  : Unit base area

$V_{d1}$  : Droplet velocity at Location 1.

If  $Q_1$  and  $V_{d_1}$  are known,  $\alpha$  can be calculated. Then the area density, which is an important parameter in the analysis of droplet evaporation in the hot gas stream, can be calculated from the following equation:

$$\frac{A_1}{V_{t_1}} = \frac{6 (1-\alpha)_1}{d_{sm_1}} \quad (7)$$

If large droplets are moving within the effective grid spacer thickness ( $\ell$ ), they might hit or scratch the grid spacer's side walls. Due to the surface tension and pressure effect, it is assumed that a liquid droplet is stretched and broken at its' neck to generate uniform size small droplets. The supplied input large droplets through Location 1 are assumed to be broken into droplets of two size ranges at Location 2. They are large size droplets (mm range) and small size droplets ( $\mu$  range).

At Location 2, the change of area density has significant meaning, because it explains the breakage of large droplets into small droplets. Now area density calculation at Location 2 will be carried out. The fractional volume ratio is defined as the volume ratio between total droplet volume and small or large droplet volume.

$$\beta_{s,2} = \frac{\int d^3 N dd]_{s,2}}{\int d^3 N dd]_{s+L,2}} \quad (8)$$

$$\beta_{L,2} = \frac{\int d^3 N dd]_{L,2}}{\int d^3 N dd]_{s+L,2}} \quad (9)$$

where  $\beta_{s,2}$  or  $\beta_{L,2}$  : Fractional volume of small or large liquid droplets with respect to the total liquid droplet volume at Location 2.

The supplied water amount through location 1 can be split into two parts which are used up for generating small and large size droplets.

$$(1-\alpha)_{s,1} = (1-\alpha)_1 \beta_{s,2} \quad (10)$$

$$(1-\alpha)_{L,1} = (1-\alpha)_1 \beta_{L,2} \quad (11)$$

where  $(1-\alpha)_{s,1}$  or  $(1-\alpha)_{L,1}$  : Fractional amount of supplied water through Location 1 which corresponds to the volume of small or large droplets at Location 2.

The corresponding fractional area densities at Location 1 are as follows:

$$\left(\frac{A_i}{V_t}\right)_{s,1} = \beta_{s,2} \left(\frac{A_i}{V_t}\right)_1 = \beta_{s,2} \frac{6(1-\alpha)_1}{d_{sm1}} \quad (12)$$

$$\left(\frac{A_i}{V_t}\right)_{L,1} = \beta_{L,2} \left(\frac{A_i}{V_t}\right)_1 = \beta_{L,2} \frac{6(1-\alpha)_1}{d_{sm1}} \quad (13)$$

where:  $\left(\frac{A_i}{V_t}\right)_{s,1}$  or  $\left(\frac{A_i}{V_t}\right)_{L,1}$  : Fractional area density at Location 1 which corresponds to the volume of small or large droplets at Location 2.

From Equations (7), (10), (11), (12) and (13), area density ratios at Location 1 and 2 can be expressed as ratios of inverse of Sauter mean diameters.

$$\frac{\left(\frac{A_i}{V_t}\right)_{s,2}}{\left(\frac{A_i}{V_t}\right)_{s,1}} = \frac{d_{sm,1}}{d_{sms,2}} \quad (14)$$

$$\frac{\left(\frac{A_i}{V_t}\right)_{L,2}}{\left(\frac{A_i}{V_t}\right)_{L,1}} = \frac{d_{sm,1}}{d_{smL,2}} \quad (15)$$

where:  $\frac{\left(\frac{A_i}{V_t}\right)_{s,2}}{\left(\frac{A_i}{V_t}\right)_{s,1}}$  or  $\frac{\left(\frac{A_i}{V_t}\right)_{L,2}}{\left(\frac{A_i}{V_t}\right)_{L,1}}$  : Ratios of area densities for the small or large droplets between Location 1 and Location 2.

As  $d_{sm,1}$ ,  $d_{smL,2}$ ,  $d_{sms,2}$ ,  $\left(\frac{A_i}{V_t}\right)_{s,1}$ ,  $\left(\frac{A_i}{V_t}\right)_{L,1}$  are already known, area densities

for large and small droplets at Location 2 can be calculated. The ratios from Equations (14) and (15) explain how liquid droplets hit the grid spacer and break into small and large droplets. The small droplet's area density ratio at Location 2 was increased about 10 times, while the large droplet's area density ratio at Location 2 was increased only 1.5 times. This explains after liquid droplets breakage, the droplet's surface area was increased

a great deal, and that will enhance the evaporation cooling mechanism. The related specific interfacial area flux for small droplets,  $\left(\frac{A_i}{V_t}\right)_{s,2} \cdot V_{dL,1}$ , or large droplets  $\left(\frac{A_i}{V_t}\right)_{L,2} \cdot V_{dL,1}$  at Location 2 are also calculated.

So far, the region of interest is restricted to the area of effective grid space area. If the whole subchannel area is considered, the area density ratios before and after grid spacer through the subchannel will be as follows:

$$\begin{aligned} \left(\frac{A_i}{V_t}\right)_{AGS} &= \left(\frac{A_i}{V_t}\right)_{BGS} \left(\frac{\text{Area}_{u.o}}{\text{Area}_{s.c}}\right) + \left(\frac{A_i}{V_t}\right)_2 \left(\frac{\text{Area}_{G.S}}{\text{Area}_{s.c}}\right) \\ \left(\frac{A_i}{V_t}\right)_{AGS} / \left(\frac{A_i}{V_t}\right)_{BGS} &= \left(\frac{\text{Area}_{u.o}}{\text{Area}_{s.c}}\right) + \frac{\left(\frac{A_i}{V_t}\right)_2}{\left(\frac{A_i}{V_t}\right)_1} \left(\frac{\text{Area}_{G.S}}{\text{Area}_{s.c}}\right) \end{aligned} \quad (16)$$

Results of calculation are tabulated in Tables 3 and 4 for each of the two different grid spacer thicknesses used respectively.

After the trends of all data have been carefully analyzed, those data were correlated in several ways. All the correlations below are given in non-dimensionalized form and shown in Figures 12-15.

- 1) Sauter mean diameter of the large droplets at Location 2 can be correlated with  $V_a$  and  $h$ .

$$\frac{d_{smL,2}}{d_{smL,1}} = 0.162 (We)^{0.75} \left(\frac{h}{d_{smL,1}}\right)^{0.062}$$

where  $d_{smL,2}$  : Sauter mean diameter of large liquid droplets which were measured at Location 2.



$d_{smL,1}$  : Sauter mean diameter of large liquid droplets  
which were measured at Location 1.

We :  $\frac{\rho_a V_a^2 d_{smL,1}}{\sigma}$  (Weber No.)

$\rho_a$  : Supplied air density.

$V_a$  : Supplied air velocity

$\sigma$  : Surface tension.

h : height of grid spacer plate.

2) Sauter mean diameter of small droplets at Location 2  
is uniform.

$$d_{sms,2} = 1.489 \times 10^{-4} \cdot \frac{\mu_f^2}{\rho_f \sigma}$$

3) Fractional volume of small droplets at Location 2 can  
be correlated with Q and  $V_a$

$$(\beta_{s,2})^{1/5} = 1.752 \left( \frac{V_a}{Q} \right) \left( \frac{1}{We} \right) \left( \frac{d_{smL,1}}{h} \right)^{0.481}$$

where  $\beta_{s,2}$  : Fractional volume of the small liquid  
droplets with respect to the total liquid  
droplets volume at Location 2.

4) The following correlation represents nozzle characteristic:

$$(St)^{1/2} = 1.45 \times 10^{-3} \cdot We^{-1} \cdot Ref^{-1/2} \left( \frac{V_a}{Q} \right)^{1/2} \left( \frac{\rho_a}{\rho_f} \right)$$

St :  $\frac{V_f}{\omega \cdot dN^2}$  (Stokes No.)

$V_f$  : Kinematic viscosity of fluid (water).

$\omega$  : Droplet generation frequency at Location 1.

dN : Nozzle diameter

$Re_f$  :  $\frac{dN Q \rho_f}{\mu_f}$  (fluid Reynold's No.)

$Q$  : Water supply rate through nozzles, per  
unit grid spacer area.

$\mu_f$  : Dynamic viscosity of fluid.

The above correlation gives a relation between droplets generation frequency at Location 1 with  $V_a$  and  $Q$ .

## REFERENCES

1. Ihle, P., Rust, K. and Lee, S. L., "Mist Core Cooling During the Reflood Phase of PWR-LOCA," Proceedings of the International Meeting on Thermal Nuclear Reactor Safety, American Nuclear Society, Chicago, Ill., August 29 - September 2, 1982, in print.
2. Tong, L. S. and Bennet, G. L., "NRC Water-Reactor Safety-Research Program," Nuclear Safety, Vol. 18, No. 1, pp. 1-40, January-February, 1977.
3. Era, A. et al., "Heat Transfer Data in the Liquid Deficient Region for Steam-Water Mixtures at 70 kg/cm<sup>2</sup> Flowing in Tubular and Annular Conduits," Italian Report, CISE-R-184, June 1966.
4. Ihle, P. and Rust, K., "FEBA (Flooding Experiments with Blocked Arrays) - Influence of Blockage Shape," ENR, Hamburg, May 6-11, 1979.

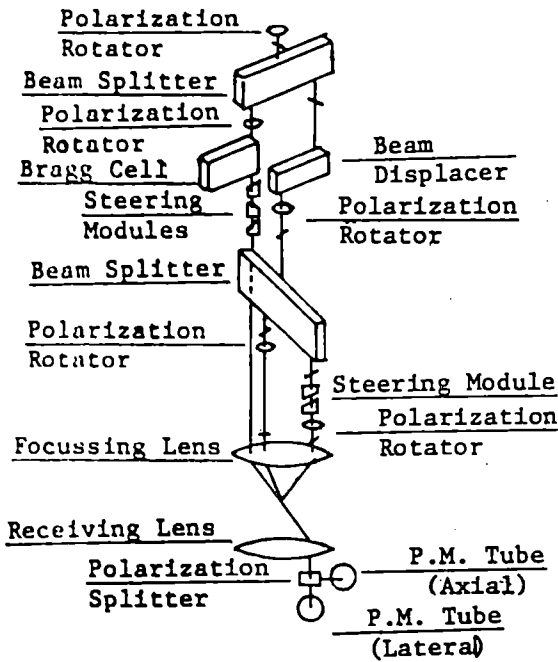


Fig. 1. Optical Arrangement.

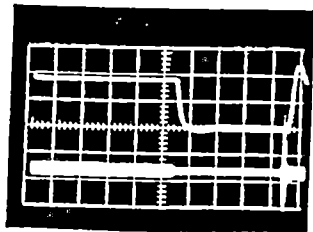


Fig. 3. Photo diode output and doppler signal.

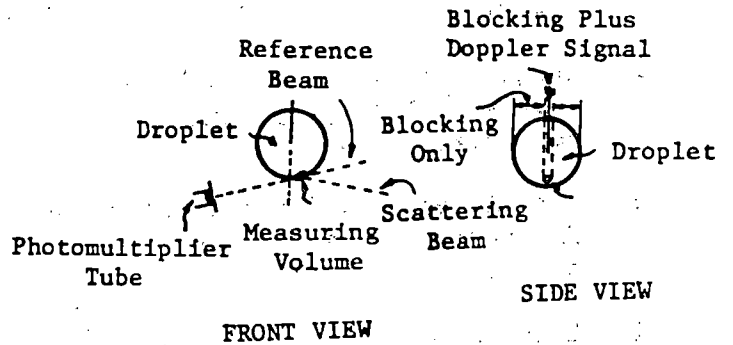


Fig. 2. Laser-Doppler anemometry scheme developed for large-size droplet measurement.

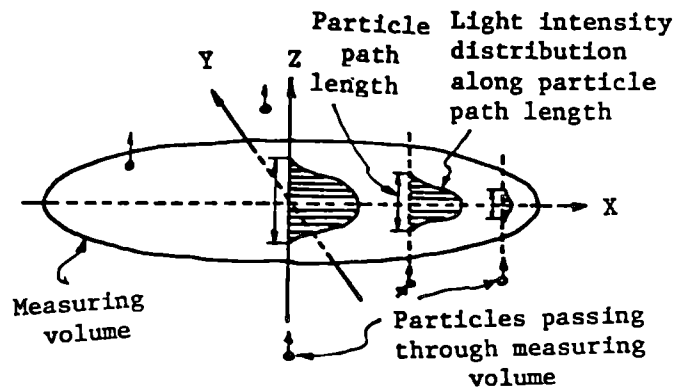


Fig. 4. Sketch of optical measuring volume.

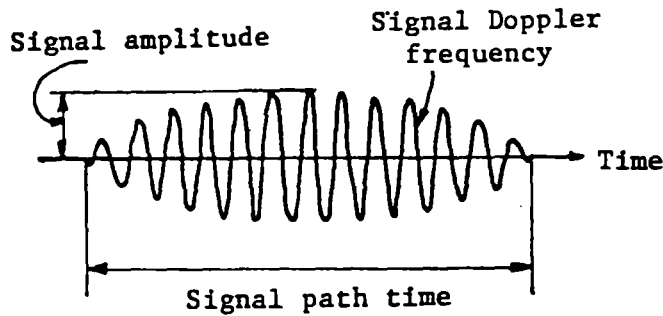


Fig. 5. Sketch of particle Doppler signal.

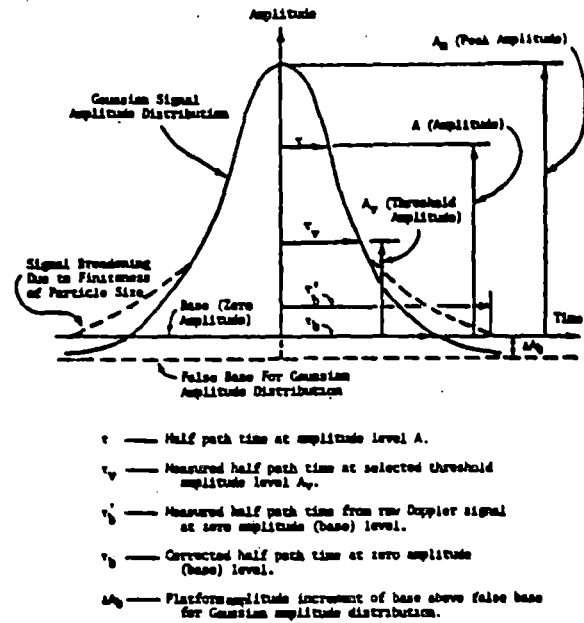
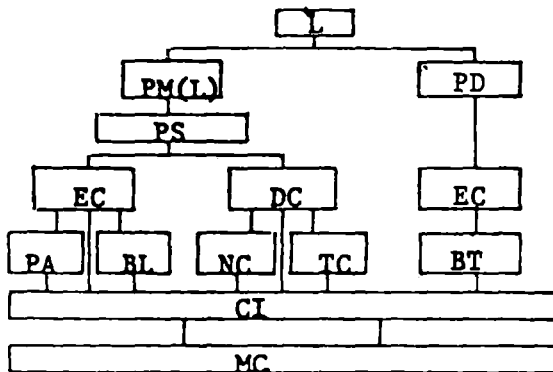


Fig. 6. Signal path time correction scheme.



- L Laser
- PM(L) Photomultiplier (Longitudinal)
- PD Photo Diode
- PS Power Splitter
- EC Electronic Circuits
- DC Digital Counter
- PA Peak Amplitude
- BL Burst Length
- NC Number (N) of Cycles
- TC Time for N Cycles
- CI Computer Interfaces
- MC PDP11/34 Minicomputer
- BT Blocking Time

Fig. 7. Instrumentation block diagram

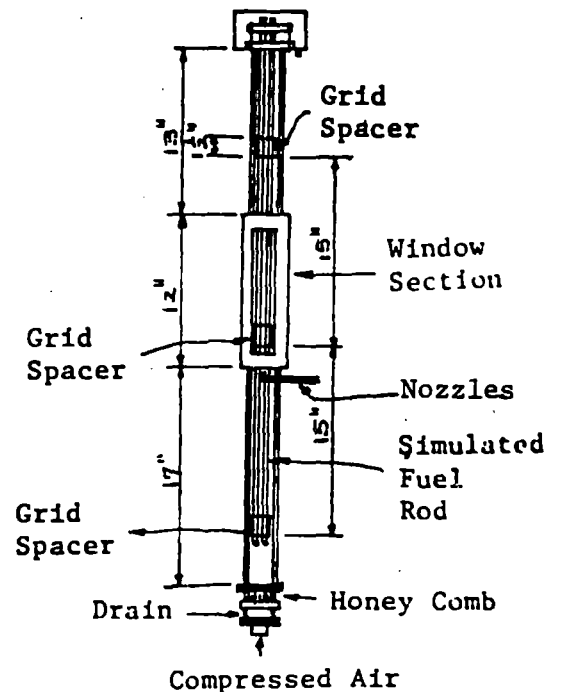
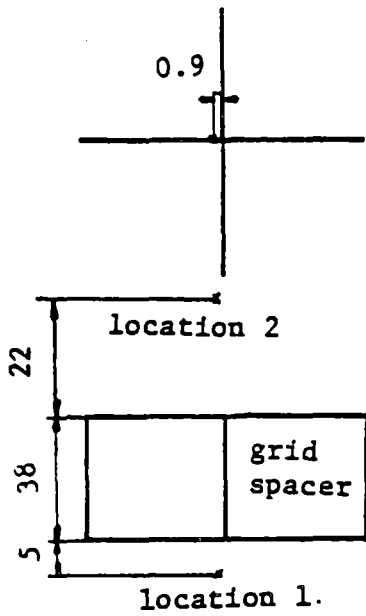


Fig. 8. Channel.



unit: mm

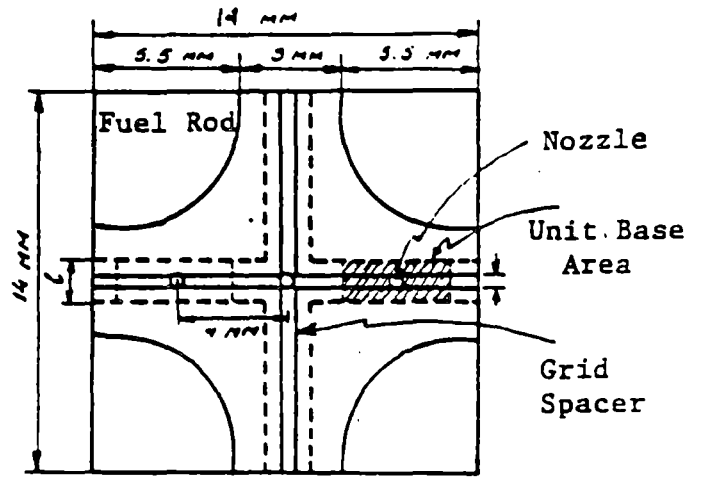


Fig. 10. Geometry of effective grid spacer.

Fig. 9. Measurement locations.

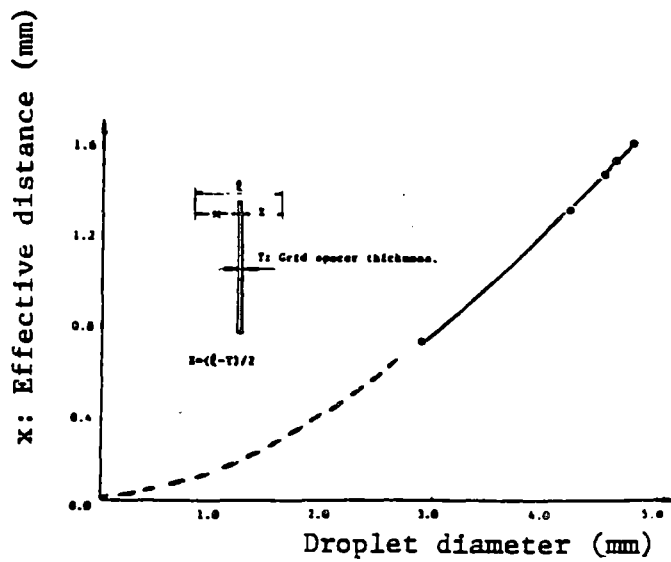


Fig. 11. Measurement of effective grid spacer thickness.

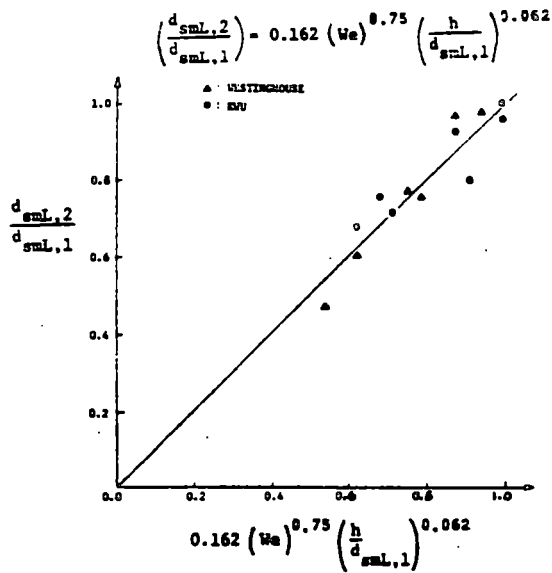


Fig. 12. Sauter mean diameter of large droplets after grid spacer.

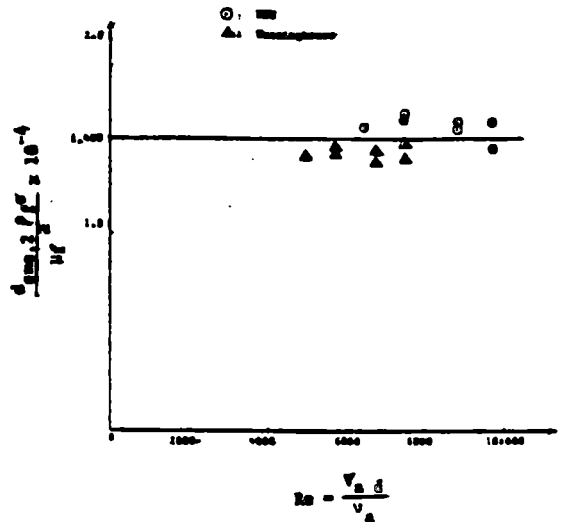


Fig. 13. Sauter mean diameter of small droplets after grid spacer.

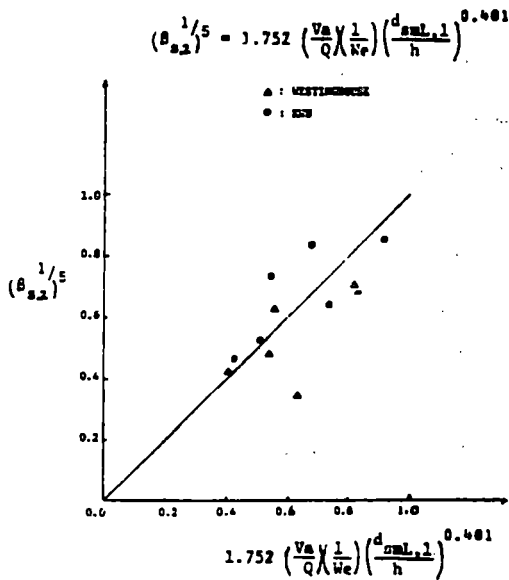


Fig. 14. Fractional volume of small droplets after grid spacer.

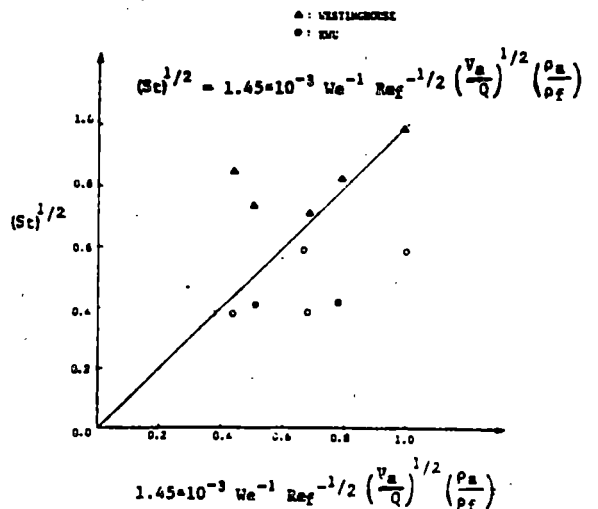


Fig. 15. Nozzle characteristic.

## FINDINGS IN CCTF CORE I TEST

YOSHIO MURAO, TAKASHI SUDOH  
TADASHI IGUCHI, JUN SUGIMOTO  
HAJIME AKIMOTO, TSUTOMU OKUBO  
KEMMEI HIRANO

JAPAN ATOMIC ENERGY RESEARCH INSTITUTE  
AT THE TENTH WATER REACTOR SAFETY RESEARCH INFORMATION MEETING  
OCTOBER 14, 1982

### 1. Introduction

The Cylindrical Core Test Facility (CCTF) is one of the facilities of the Large Scale Reflood Test Program which was initiated in April 1976. The first series of the CCTF test is named CCTF CORE I TEST and was completed in April, 1981.

In the test, the following has been intended to be examined:

(1) The conservativeness of the assumption of the safety analysis with the evaluation model (EM) code. (2) The safety margin on the peak clad temperature. (3) The validity of the models in the EM code and the present BE code for application to the BE code development. For this intension, the twenty-seven runs including the shakedown tests were performed under the various conditions covering the wide spectrum of the refill and reflood phases and analyzed by comparing the results with the results of the reference test, called the base case test and with the results predicted with EM codes, REFLA and TRAC codes.

In the safety analysis with the EM code, using the following results of the system calculations, the temperature response of the hot rod is calculated: (1) the core inlet mass flow rate, (2) the core outlet mass flow rate, (3) the core inlet fluid temperature and (4) the core inlet and outlet pressures.

In the system calculation, usually used is the simplified primary cooling system model coupled with the one-dimensional model of the core with the power rating of the average power rod.

---

The work performed under contracts between Atomic Energy Bureau of Japan and JAERI.



In this calculational procedure, the following is assumed explicitly or implicitly: (1) The one-dimensional treatment of the core thermo-hydrodynamics is valid or acceptable. (2) The correlations of the heat transfer coefficient and the carryover rate fractions obtained from the FLECHT data are valid or conservative. (3) The over-all characteristics of a PWR core can be represented with the averaged power rod and the hot rod analysis gives conservative results. (4) The system model is conservative.

Accordingly necessary is the confirmation of the validity of the above-mentioned assumption and also necessary is the demonstration of the safety margin on the peak clad temperature for confirmation of the validity of the hot rod analysis.

The previous analysis<sup>(1),(2)</sup> showed that the system model assumed in the EM analysis was similar to or more conservative than the phenomena observed in the CCTF test except for the hydrodynamic behaviors in the downcomer.

In this paper, the following items will be discussed:

- (1) One-dimensional treatment of the core hydrodynamics in EM codes.
- (2) Conservativeness of the heat transfer model of EM codes.
- (3) Safety margin of the peak clad temperature.
- (4) Conservativeness of the downcomer hydrodynamic model.

## 2. Experimental

### 2.1 Facility description

The facility is modeled on a 1000 MWe PWR with a cold leg break and has a full-length pressure vessel which includes a core, a downcomer, and lower and upper plenums. The facility has four full-length primary loops with pump simulators and active steam generators, as shown in Fig. 1. The core consists of thirty-two  $8 \times 8$  rod bundles which are electrically heated and are modeled on a  $15 \times 15$  type fuel assembly of a PWR. They are arranged in a cylindrical configuration to minimize the effect of wall surrounding core on the thermo-hydrodynamics. The scaling of flow areas in the system is based on a core flow area scaling ratio of 1/21.4. An Accumulator (Acc) system and a Low Pressure Coolant Injection (LPCI) system are equipped as an Emergency Core Cooling (ECC)

system.

The cross section of the pressure vessel is shown in Fig. 2. The core is subdivided into three power regions. Nine units of core power are independently controlled in order to obtain desired power distribution. Each  $8 \times 8$  rod bundle consists of 12 high powered, 17 medium powered, 28 low powered, and 7 unheated rods. The power ratio of the heated rods is 1.1:1.0:0.95. An axial peaking factor of the heated rod is 1.49. About nine hundred of thermocouples were uniformly distributed in the core to measure the clad surface and fluid temperatures.

The upper plenum internals simulate the former Westinghouse design for the  $17 \times 17$  type fuel assembly. The radial dimensions were scaled down by the ratio of the bundle array sizes between PWRs and the CCTF, that is, 8/15.

The CCTF has the annular downcomer, while, most of reflood facilities including the FLECHT-SET and the PKL facilities have a pipe downcomer instead of an annular downcomer of a PWR. In order to avoid atypical behavior induced by a narrow gap of the simulated downcomer, the scaled core baffle flow area was added to the downcomer flow area. The resultant downcomer gap is 0.065 m. The vessel wall can be preheated to preserve the estimated heat release to a unit fluid volume in the downcomer of a PWR.

In the downcomer, the core, and the lower and the upper plenums, the differential pressures were measured at four directions as shown in Fig. 2. The active steam generators are of the U-tube and shell type. The pump simulators have orifice plates to simulate the flow resistance and vanes to simulate Counter-Current Flow Limitation (CCFL) characteristics of an actual pump.

The containment is simulated by two tanks. The containment tank 1 collects the overflowing water from the downcomer. The liquid level in the tank was precisely measured. The pressure at the containment tank 2 was regulated at a constant in most experiments to simulate a large volume containment of a PWR. The break location is assumed at the outer surface of the biological shielding.

The ECC injection ports are located at four cold legs and the lower plenum. The nozzle of the cold leg port is inclined to the cold leg

pipng by 45 degrees.

In addition to more than 1600 channel data recording, video, 16 mm movie, and 35 mm still cameras are equipped in the system for the flow observation.

## 2.2 Test matrix

A test was designated as the base case test. In order to examine parameter effects of the test conditions, one parameter was usually varied from those of the base case test in each test, as listed in Table 1. Some special effect tests, as given in Table 2, were also conducted to study the phenomena under the conditions extended from those for the parameter effect tests.

The maximum initial clad temperature was usually lower than the value predicted with the EM code, since the guaranteed temperature of the heated rods was 1173 K. The lower initial temperature allowed the higher temperature rise, accordingly it enabled the performance of the more severe experiments.

The Acc and the LPCI flow rates were lowered in order to be conservative. The downcomer wall temperature was higher than the referred value due to the same reason. In order to avoid the unrealistic steam condensation, the Acc water was injected into the lower plenum which had been filled with the saturated water to 0.9 m. The injection location was then switched to the cold legs.

## 3. Results and discussion

### 3.1 One-dimensionality of the core hydrodynamics

In order to show the one-dimensionality of the core hydrodynamics, it is necessary to show that the quench front is, at least, roughly flat in radial direction. Therefore the quench front propagation was examined first. Since it was previously pointed out<sup>(1), (2)</sup> that the bottom quench front progresses roughly one-dimensionally, the bottom quench region was intended to be specified. In the lower two thirds of the core, the bottom quench was observed as shown in Fig. 3. In the upper one ninth, the top quench was observed on every instrumented rods. In the intermediate region, the top quench locally occurred,

as shown in Fig. 4, below the open holes but rarely near the surrounding wall. Since the bottom quench region covers our concerning region to the peak clad temperature, it can be concluded that the quench front advances nearly one-dimensionally in the region.

In the previous report<sup>(1),(2)</sup> axi-symmetric core water accumulation was pointed out. In order to confirm the validity of the one-dimensional treatment of the core hydrodynamics, the uniformity of the azimuthal void fraction distribution was examined under the azimuthally skewed thermal conditions. Figure 5 shows the uniformity of the core water accumulation, since the differential pressures measured at the four directions overlapped with each other. Accordingly the validity of the one-dimensional treatment of the core hydrodynamics, at least, in the bottom quench region has been confirmed.

Figure 6 shows the core water accumulation at the various elevations. This water accumulation suggests the existence and the rapid development of the slug flow above the quench front. Figure 7 shows the comparison of the measured and the predicted void fraction and the core water head. The prediction was made with the void fraction correlation<sup>(3)</sup> for the slug flow under the assumption that the representative rod of the core is the averaged power rod. Except for the early period of the transient, the good agreement of the measured and the predicted is obtained.

Figure 8 shows the measured and the predicted clad surface temperatures of the averaged power rod. The prediction was made with the one-dimensional reflood analysis code, REFLA-1D<sup>(4)</sup>, by using the slug flow void fraction model above quench front and the heat transfer correlation<sup>(5)</sup> for the slug flow. It is found that the slug flow model for the averaged power rod gives a good prediction of the core heat transfer.

Accordingly it can be concluded that the one-dimensional treatment of the core represented by the average power rod is practically valid, and the flow was judged to be the slug flow.

### 3.2 Conservativeness of the heat transfer model of EM codes

Figure 9 shows the comparison of the clad surface temperature measured in the EM test and predicted with the EM code. This figure

indicates that the heat transfer model of the EM code is conservative. It is inferred that the conservativeness was resulted from the lower water density in the flow channel, since the dispersed flow was observed, instead of the slug flow observed in the CCTF tests, in the FLECHT forced flooding tests which is the data base of the EM correlation. Another important point is that the quench front advanced even the carryover rate fraction became nearly unity. This phenomena is reasonable under the existence of the slug flow above the quench front. While the quench front was suppressed to advance when the carryover rate fraction becomes unity in the EM code.

It can be concluded that the heat transfer model built in the EM code is conservative, if the slug flow observed in the CCTF is typical of a PWR.

### 3.3 Safety margin of peak clad temperature

In the most of the CCTF tests, the safety margin of the peak clad temperature (PCT) was not directly evaluated, since the initial clad temperature were lower than that calculated with the EM code.

In order to find the initial temperature effect on the PCT, some parametric tests were performed. Figure 10(a) shows the measured clad surface temperature histories. This indicates that the higher initial clad temperature yields the lower temperature rise defined as the difference between the PCT and the initial clad temperature. Figure 10(b) shows the conservative extrapolation method of the lower initial clad temperature test to the higher.

It was found that the maximum value of the estimated PCTs is much lower than the licensing limitation (1473 K).

### 3.4 Downcomer hydrodynamic model

It was found in the previous analysis<sup>(1),(2)</sup> that the system behaviors observed in the CCTF test were similar to the model assumed in the EM analysis except for the hydrodynamic behaviors in the downcomer, the upper plenum and the broken cold leg nozzle. Since it was found that only downcomer hydrodynamic behaviors do not yield conservative results, the downcomer behavior was analyzed.

Figure 11 shows the downcomer water accumulations with varying

the ECC flow rate. In the base case test, the amount of the injected accumulator (Acc) water was not enough to fill the downcomer and the LPCI flow rate was not enough to condense the steam flowing through the downcomer. This caused the ECC bypass through the downcomer, resulting in the slow water accumulation. In the higher LPCI injection rate test, the water accumulation rate became higher and in the test with the higher Acc and LPCI injection rates, which were predicted with EM code, the water filled the downcomer during the Acc injection period. In the last two cases; however, the downcomer head gradually decreased and this reduced the driving head for flooding. The reduction of the head is caused by the voiding due to heat release from the hot vessel wall. Figure 12 shows the evidence of the effect of the hot wall on the downcomer head.

Accordingly, it can be concluded that the ECC bypass can be neglected under the condition predicted with EM code, however the hot downcomer effect can not be ignored.

#### 4. Conclusion

- (1) Core hydrodynamics can be treated one-dimensionally.
- (2) Much water was accumulated above quench front. The flow above quench front was recognized as slug flow in CCTF.
- (3) Top quench was locally observed. And bottom quench region covers our concerning region on PCT.
- (4) Heat transfer model of EM code is conservative, if the flow observed in CCTF is typical of PWR.
- (5) Quench front advanced even when carryover rate fraction became nearly unity.
- (6) PCT estimated from CCTF data is much lower than licensing limitation.
- (7) ECC bypass in downcomer can be neglected under condition predicted with EM code, however, hot downcomer effect can not be neglected.

## References

- (1) Murao, Y. et al.; CCTF CORE I TEST RESULTS, Presented at the Ninth Water Reactor Safety Information Meeting, Gaithersburg, Maryland, October 28, 1981.
- (2) Murao, Y. et al.; Experimental Study of System Behavior during Reflood Phase of PWR-LOCA Using CCTF, J. Nucl. Sci and Technol., 19 [9], pp 705~719, (1982).
- (3) Murao, Y. and Iguchi, T.; Experimental Modeling of Core Hydrodynamics during Reflood Phase of LOCA, J. Nucl. Sci and Technol., 19 [8], pp 613~627, (1982).
- (4) Murao, Y. and Sugimoto, J.; One-dimensional System Analysis Code for Reflood Phase during LOCA, JAERI-M 9780, (1981).
- (5) Murao, Y. and Sugimoto, J.; Correlation of Heat Transfer Coefficient for Saturated Film Boiling during Reflood Phase Prior to Quenching, J. Nucl. Sci and Technol. 18 [4] 275~284, (1981).

Table 1 Parameter effect tests

| Test parameter  |              |
|---|--------------|
| System pressure (MPa)                                   | 0.15         |
|   | <u>0.20</u>  |
|   | 0.30         |
| ECC injection   |              |
| { Acc rate ( $\times 10^{-3} \text{m}^3/\text{s}$ )     | <u>77.2</u>  |
|   | duration (s) |
| { LPCI rate ( $\times 10^{-3} \text{m}^3/\text{s}$ )    | <u>8.3</u>   |
| High LPCI rate ( $\times 10^{-3} \text{m}^3/\text{s}$ ) | 17.2         |
| Low LPCI rate ( $\times 10^{-3} \text{m}^3/\text{s}$ )  | 4.7          |
| Low Acc rate ( $\times 10^{-3} \text{m}^3/\text{s}$ )   | 67.2         |
| Short Acc duration (s)                                  | 10           |
| Initial clad temperature (K)                            | <u>873</u>   |
|   | 973          |
|   | 1073         |
| Downcomer wall temperature (K)                          | <u>471</u>   |
|   | 392          |
| Loop flow resistance<br>(K-factor)                      | <u>25</u>    |
|   | 35           |

Note: Underlined values are those for the base case test.

Table 2 Special effect tests

| Test                               | Description  |
|------------------------------------|--|
| Coupling tests : FLECHT-SET<br>PKL | Consistency of observed phenomena with other facilities                            |
| Evaluation model test              | Conditions based on EM calculation (high ECC rates, high initial core temperature) |
| Multi-dimensional test             | Thermally skewed core<br>(asymmetric power and initial temperature)                |
| Refill simulation test             | With system depressurization without lower plenum injection                        |
| Loop seal water filling test       | Initially blocked loop seal with saturated water                                   |
| Reproducibility test               | With baffle plates in upper plenum internals                                       |



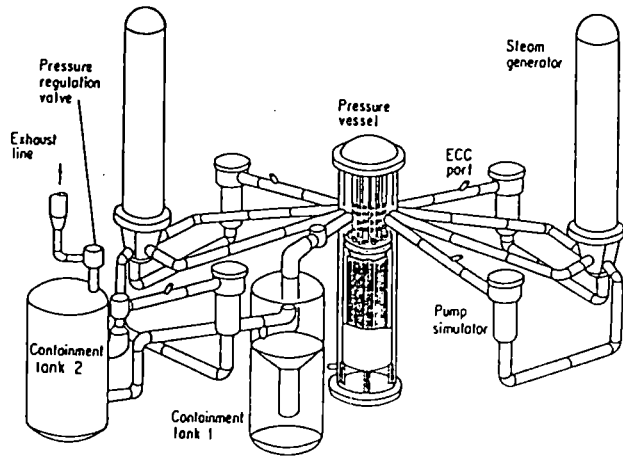


Fig. 1 Cylindrical core test facility

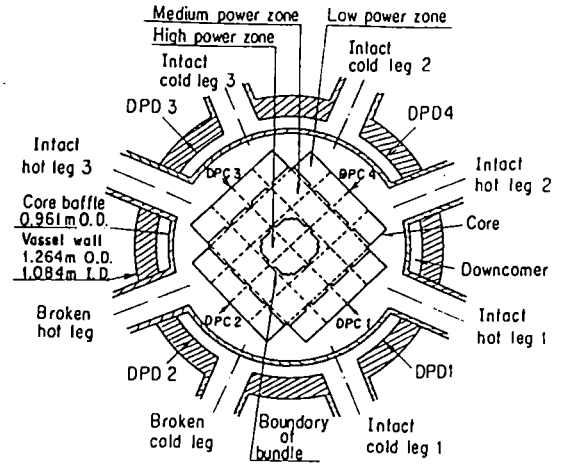


Fig. 2 Cross section of pressure vessel

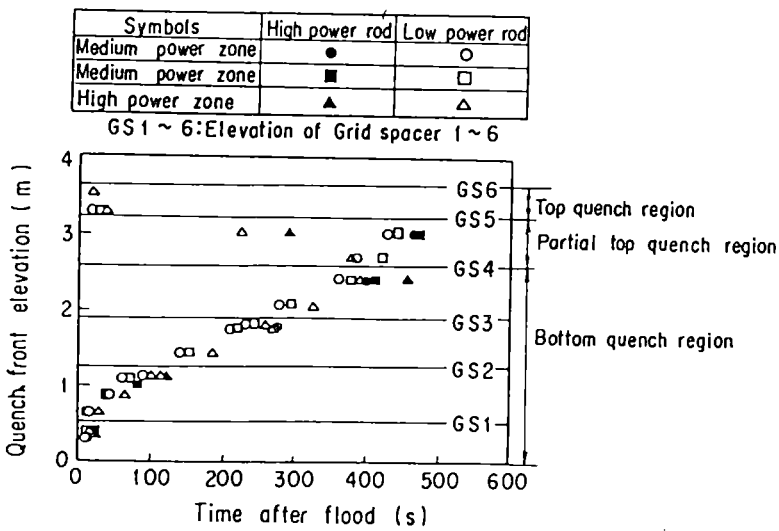


Fig. 3 Quench front propagation in base case test

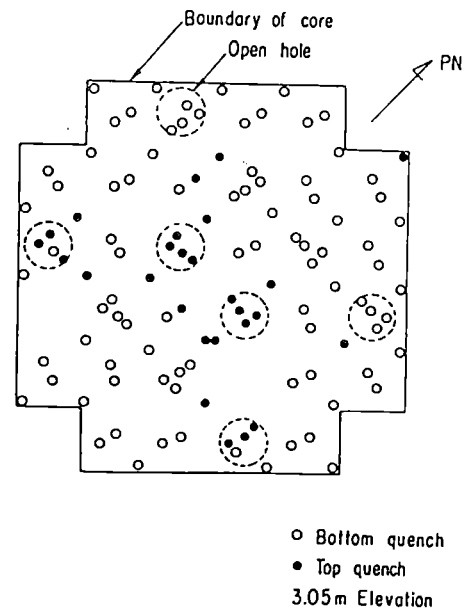



Fig. 4 Relationship of top-quenched rods and open holes in base case test

Note  Hatched band shows the scattering range of four readings of the differential pressures measured at four orientations

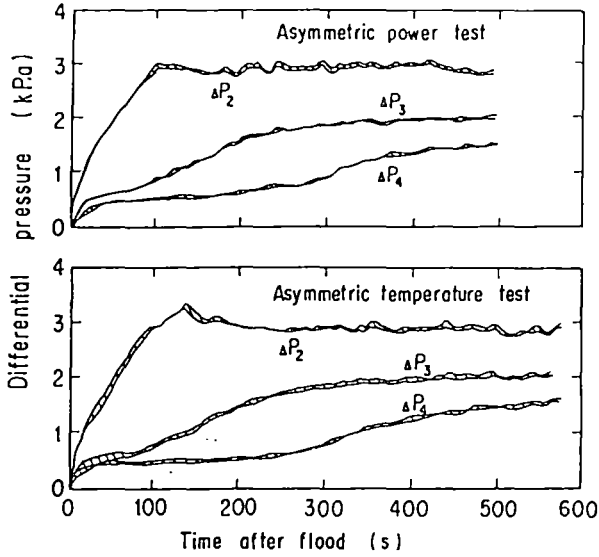


Fig. 5 Uniformity of differential pressures in core in asymmetric power test and asymmetric temperature test

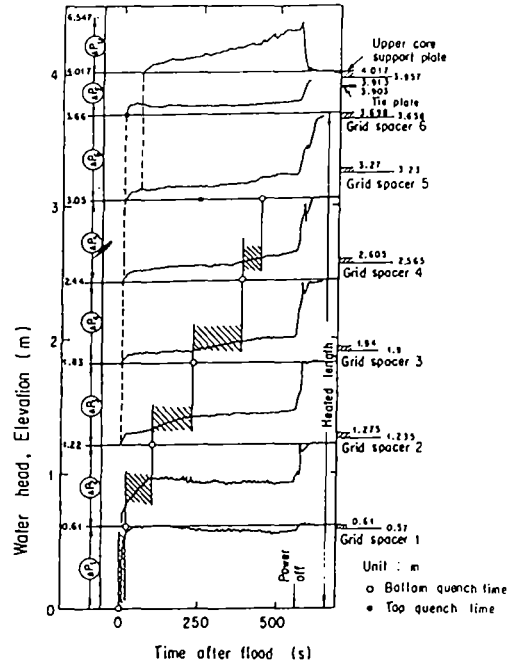


Fig. 6 Comparison of the differential pressures of whole core, end box region and upper plenum

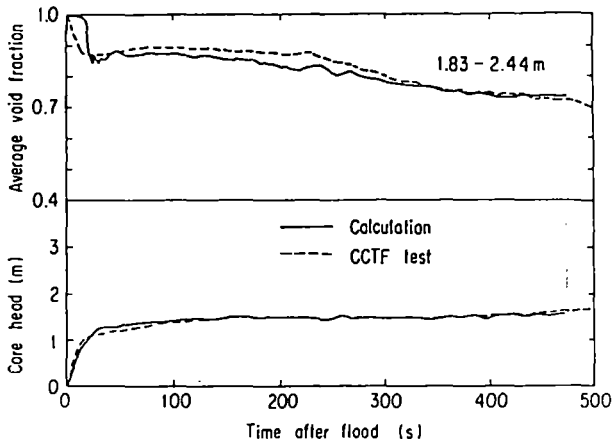


Fig 7 Measured and calculated core head and average void fraction

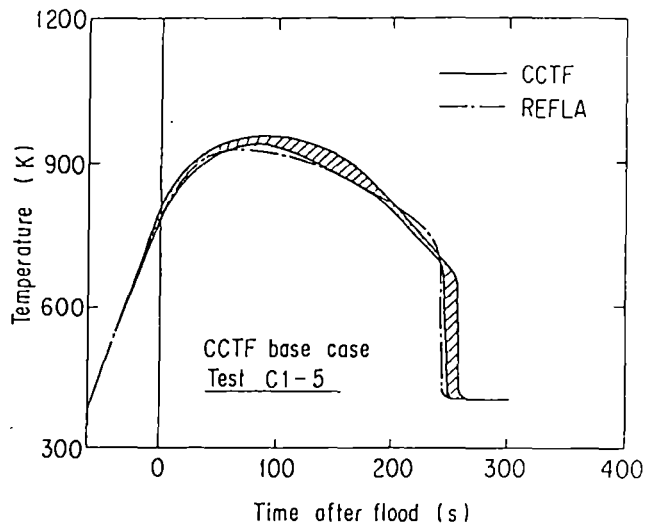


Fig. 8 Measured and calculated clod temperature of the average powered rod

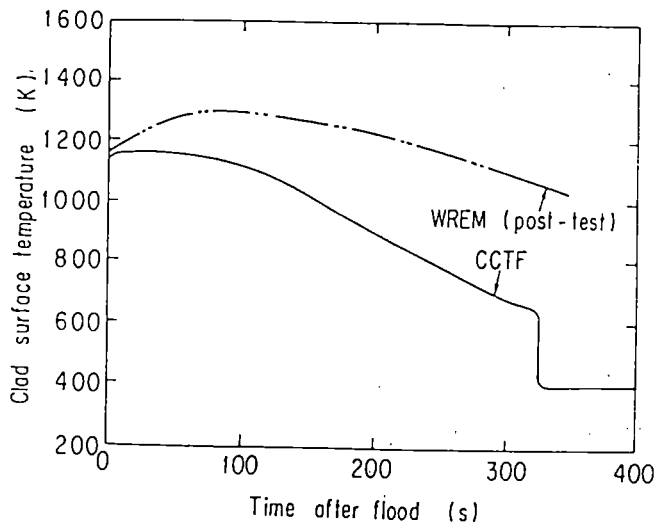


Fig. 9 Clad surface temperature of location of maximum power density

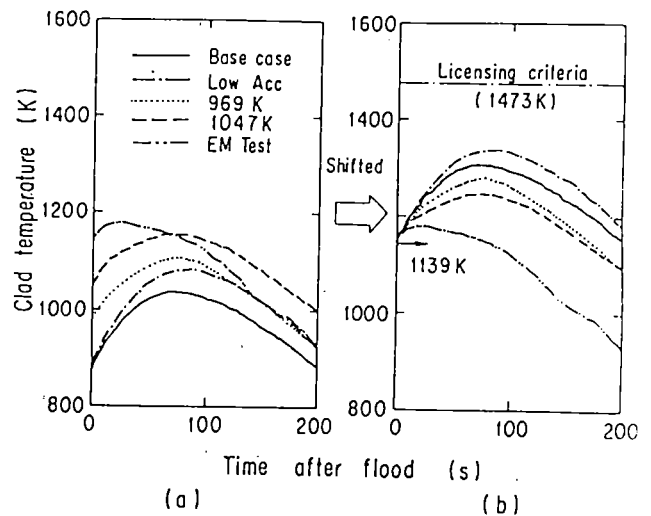


Fig.10 Temperature history and the extrapolation method to a high temperature case

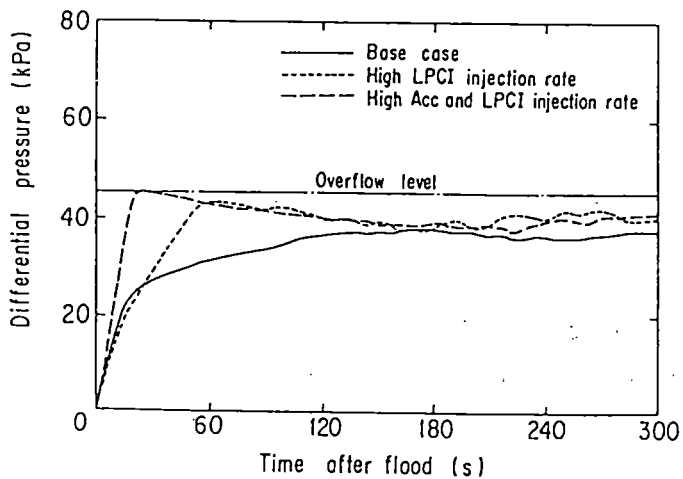


Fig. 11 Differential pressures in downcomer

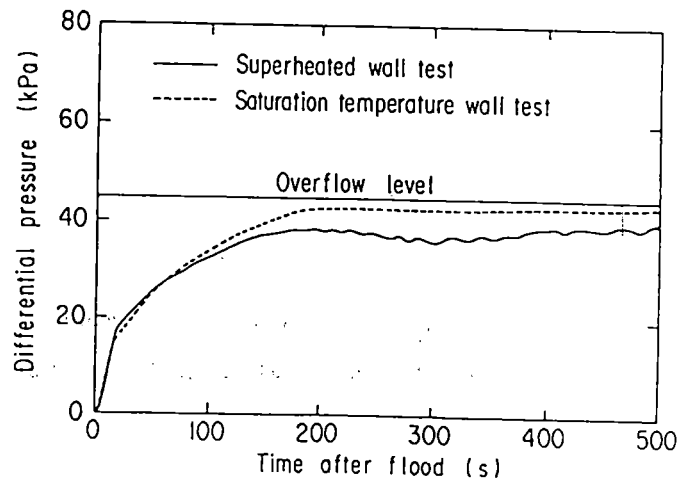


Fig. 12 Differential pressure in downcomer

SCTF Core-I Reflood Test Results

Hiromichi ADACHI, Yukio SUDO, Makoto SOBAJIMA,  
Takamichi IWAMURA, Masahiro OSAKABE,  
Akira OHNUKI, Yutaka ABE and Kemmei HIRANO

Japan Atomic Energy Research Institute

---

The work was performed under contract with the Atomic  
Energy Bureau of Science and Technology Agency of Japan.

## I. Introduction

Slab Core Test Facility (SCTF) Test Program is being performed at Japan Atomic Energy Research Institute (JAERI) as one of the subprograms of Large Scale Reflood Test Program. In Cylindrical Core Test Facility (CCTF) Test Program, another part of the Large Scale Reflood Test Program, system behavior simulation for the last part of blowdown, refill and reflood phases of a LOCA in an actual pressurized water reactor (PWR) is the primary concern. On the other hand, the major objectives in the SCTF Test Program are to clarify the following items:

- (1) Two-dimensional thermo-hydrodynamics in a wide core (chimney effect, sputtering effect, blockage effect, ect.),
- (2) Flow interaction between core and upper plenum (fall back, core entrainment, etc.), and
- (3) Hot leg carryover characteristics (upper plenum entrainment/de-entrainment, counter current flow in hot leg, etc.).

In 1981, thirteen forced-feed flooding tests including two shakedown tests were performed, in which the downcomer was isolated from the lower plenum by inserting a blind plate and emergency core cooling (ECC) water was injected directly into the lower plenum. Results from the system pressure effect tests<sup>(1)</sup> in the forced-feed flooding test series were introduced at the Ninth Water Reactor Safety Research Information Meeting. In the present report, chimney effect, blockage effect and hot leg carryover characteristics shall be discussed based on the data from the other tests in the series.

## 2. Test Facility and Test Conditions

The SCTF is designed and fabricated to simulate a radial slab extracted from a 1,100 MWe PWR core. The facility

dimension is full height, full radius and one bundle width. The volume scaling ratio is about 1/21. The maximum achievable system pressure is 0.6 MPa and the maximum core heating power is 10 MW.

Figure 1 shows the vertical cross-section of the pressure vessel. The simulated core consists of eight electrically heated rod bundles arranged in a row. Each heater rod and non-heated rod are designed principally based on the design of a 15×15 Westinghouse type fuel bundle, i.e., rod diameter and heated length of the heater rod are 10.7 and 3,660 mm, respectively, diameter of the non-heated rod is 13.8 mm and arrangement lattice pitch for these rods is 14.3 mm. The simulated fuel bundle corresponding to the center bundle of the actual core is defined as Bundle 1 and corresponding to the peripheral bundle of the core is defined as Bundle 8. Bundles 3 and 4 are, so called, the blocked bundles and all the heater rods in these two bundles have co-planar blockage sleeves at the mid-plane to simulate ballooned fuel rods. The local blockage fraction is about 60 %. Honeycomb thermal insulator panels are attached to the inner surface of the core barrel to minimize unrealistic thermal effects of the barrel which does not exist in the actual PWR.

Spaces and flow paths such as upper plenum, upper head, core baffle region, lower plenum and downcomer are provided appropriately in the pressure vessel. The downcomer can be isolated from the lower plenum by inserting a blind plate for the forced-feed flooding tests. A hot leg nozzle is provided at one end of the upper plenum. Intact and broken cold leg nozzles are at the upper portion of the downcomer.

Figure 2 shows the flow sheet of the SCTF. The hot leg, steam/water separator, intact cold leg, two broken cold legs, and two containment tanks of the SCTF represent four hot legs, four steam generator inlet plenums, three intact cold legs, two halves of a broken cold leg, and a containment vessel of the actual PWR, respectively. The steam/water

separator has no secondary system, i.e., no heat source. The pump simulator in the intact cold leg has no driving force. Flow resistance of the each cold leg can be adjusted by inserting orifice plates.

The containment tanks-I and II are connected to each other by a pressure equalizing piping and thus the pressures are maintained equal during a test. The containment tank system has a pressure control system so that the pressure can be kept constant or follow a preset pressure transient curve during a test.

The ECCS of SCTF consists of an accumulator injection system (Acc), a low pressure coolant injection system (LPCI) and an upper core support plate (UCSP) water supply tank system. Available injection locations for Acc and LPCI are the intact and broken cold legs, hot leg, downcomer and lower plenum. The UCSP water supply tank system is a special accumulator injection system for SCTF to inject water into the upper plenum from the top and/or the side. It can inject water also into the cold leg via the ECC header.

Major test conditions for the base case test, Test S1-01, are listed in Table 1. Difference in test conditions between each test and the base case test shall be described in the respective discussions.

### 3. Test Results and Discussions

#### 3.1 Chimney Effect

Due to the radial power distribution in the core, steam may flow up through the higher power region at a higher velocity and more water may fall back through the lower power region. The former effect results in higher heat transfer at the hottest zone of the core and the latter effect results in earlier water accumulation in the core and top-down quenching of some fuel rods. Resultantly, quench should occur

earlier and the peak clad temperature should be lower on the whole. These effects of two-dimensional core thermo-hydraulics compose what is called the chimney effect.

To quantitatively clarify the chimney effect, four tests were performed. Initial radial power distributions for the tests which are normalized based on that for the flat power profile test are shown in Fig. 3.

Generally speaking, cooling behavior of a bundle is considered to be a function of the initial rod temperature distribution, the bundle power transient and the transient of hydraulic conditions (in other words, cooling conditions) surrounding the heater rods. By applying different radial power profiles with the same total power, the chimney effect can be clearly observed without affecting the overall conditions such as core outlet steam and water flow rates and water accumulation in the core. Therefore, total powers of tests S1-08 (steep power profile), S1-01 (base case), and S1-11 (Flat power profile) were given as the same for each test. Figure 4 shows the transients of the total and the steam mass velocities at the core exit for each test. Difference between the two curves gives the water mass velocity. The transients are the same among the three tests within the experimental error. Figure 5 shows the transient of the accumulated water mass in the core for each test. Although the steeper radial power profile gives the slightly larger water accumulation, the difference in the accumulated mass among the three tests is very small. The slightly large water mass in the steeper radial power profile test is resulted from the smaller initial stored energy in the core which is described later.

Power effect itself can be clarified by comparing the data from Test S1-01 and those from Test S1-06 (high power) because radial power profiles of the two tests are the same to each other.

To eliminate the effect of initial rod temperature, the same maximum initial rod temperature was applied to the



four tests. Initial rod temperature distributions of Bundle 4 for these tests are shown in Fig. 6. In any bundle other than Bundles 3 and 4, the maximum power bundles, the chimney effect can not be clearly observed because the initial rod temperature in those bundles is different between the tests. On the other hand, the initial stored energy in the core is smaller in the steeper radial power profile test because the stored energy in any bundles other than Bundles 3 and 4 is smaller. Therefore the accumulated water mass in the core is slightly smaller as shown in Fig. 5.

Figure 7 shows the comparison of heat transfer coefficients at the elevation of 1.735 m from the bottom of heated length of Bundle 4 between Tests S1-08 (steep power profile) and S1-11 (flat power profile). In order to clearly observe the effect of hydraulic conditions surrounding the heater rods, the heat transfer coefficients are shown with respect to the distances from the approaching quench fronts. About 20% higher heat transfer coefficient can be seen in Test S1-08, indicating the chimney effect. It can almost cancel the effect of the about 20% higher bundle power in Test S1-08 (See Fig. 3) than Test S1-11; thus quench time at the elevation of 1.735 m of Bundle 4 is almost the same for these two tests as shown in Fig. 8. The same thing can be said also for Bundle 3 because the same bundle power as Bundle 4 was applied. The same characteristics can be seen also at the other two elevations, 0.95 and 2.33 m, in this figure. The data obtained from Tests S1-01 (base case) and S1-06 (high power) are also shown in this figure for reference. Those data shall be discussed in detail later.

Figure 9 shows radial distributions in the quench front level and collapsed water level in the core in Test S1-08 (steep power profile) with time after the beginning of re-flood as a parameter. Effect of radial power profile on quench front level can be seen clearly. However, no noticeable effect on collapsed water level can be seen. This suggests that water distribution in the core is remarkably

flattened by cross-flow across bundles. Because, one-dimensional analysis separately applied to each bundle<sup>(1)</sup> gives an evident radial distribution of collapsed water level.

Existence of the cross-flow across bundles is more directly observed in the horizontal differential pressure data between the two bundles. Figure 10 shows an example. Before 200 sec, the pressure in Bundle 1 is almost the same as that in Bundle 5 and the pressure in Bundle 5 is maintained higher than that in Bundle 8. The almost zero horizontal differential pressure between Bundles 1 and 5 does not always mean no horizontal flow between the two bundles, because two cross-flows with opposite directions from Bundle 1 to Bundle 3 and from Bundle 5 to Bundle 3 can occur. On the other hand, after 200 sec the pressure in Bundle 1 is maintained lower than that in Bundle 5 and the pressure in Bundle 5 is maintained lower than that in Bundle 8.

Behavior in the first half of the transient is variable depending on test and elevation. But characteristics of the second half is qualitatively quite similar in all the tests and all the elevations except for the core inlet at where no higher pressure in Bundle 8 side can be seen. The higher pressure in Bundle 8 side than Bundle 1 side is caused by fall back water flow from the upper plenum.

From Fig. 8, it is concluded that higher total core heating power (Test S1-06) results in delayed quench. However, it is very difficult from the quench time data only to judge whether the delayed quench was directly caused by the higher core heating power itself or indirectly through the different hydraulic conditions of coolant such as smaller water accumulation in the core. This can be made clear by comparing heat transfer coefficients between tests S1-01 (Base case) and S1-06 (high power), because different hydraulic conditions should result in different core cooling ability during transient. As shown in Fig. 11, no significant difference in heat transfer coefficient can be found between the two tests. Therefore, the about 20 % longer quench time

in Test S1-06 shown in Fig. 8 is concluded to be resulted not from the different cooling conditions but mainly from the higher power itself. In other words, chimney effect is not so much affected by the total core heating power if only the radial power profile is the same.

### 3.2 Blockage Effect

Local blockage fraction of SCTF core is only about 60 % but the blocked region occupys two full bundle cross sections. Therefore, effect of a large flow blockage on re-flood core cooling can be observed.

Figure 12 shows a comparison of the quench envelopes between the blocked and unblocked bundles for various tests with different ECC water injection flow rates. The ECC water injection flow rates for each test are given in Table 2 with the nominal core flooding speed which is estimated based on the measured core flow area including the core bypass region and the additional fluid spaces such as the gap between the vessel wall and the core barrel and a lot of instrumentation penetration holes.

It can be concluded from Fig. 12 that the quench envelope is not so much affected by flow blockage except for the just downstream of the blockage sleeves. At the just downstream of the flow blockage, the quench time is slightly shorter than the normal bundle especially when the core inlet flow rate is higher. The slightly longer quench time measured at the downstream of the blockage section (the thermocouple elevations 6 through 9) of Bundle 4 than that for Bundle 5 in Tests S1-05 (low LPCI injection rate), S1-01 (base case), and S1-SH1 (high Acc injection rate) is possible to be caused by the about 5% higher bundle power. However, according to the wide examination of data this cannot be surely concluded because data scattering due to coexistence of bottom-up and top-down quenches is significant in this elevation. Anyway, this difference in quench time between

the Bundles 4 and 5 does not seem to be caused by the blockage effect. Also, the much larger difference in quench time between Bundles 4 and 5 at the thermo-couple elevations 8 and 9 of Test Sl-09 (high Acc and LPCI injection rates) is not caused by the blockage effect.

Figure 13 shows the comparison of the heat transfer coefficients between the blocked and the unblocked bundles for Test Sl-09. When the flow blockage is sufficiently far from the quench front, the effect of the blockage sleeves on the heat transfer coefficient is small. However, when the quench front approaches the blockage section, the heat transfer coefficient at the just downstream of the blockage sleeves is improved substantially and then the quench occurs earlier. The improvement in the heat transfer coefficient and the resultant earlier quench may be caused by the metal-water contact and the heat sink effect of droplets which are encouraged, for example, by drop impact, break-up and mixing effects of the blockage sleeves. The wide examination of heat transfer characteristics shows that this improvement of core cooling can be seen only within about 100 mm downstream from the blockage sleeves and no effect of the blockage sleeves can be observed at the upstream of the blockage section.

Generally speaking, the effect of core flow blockage was insignificant in the past SCTF tests with the local blockage fraction of 60 %, in spite of the two full bundles of blockage region.

### 3.3 Hot Leg Carryover

Figure 14 shows for the base case, Test Sl-01, the transient of the hot leg carryover water flow rate which is defined at the hot leg inlet and estimated with mass balance calculation. The switching time from the Acc injection to the LPCI injection, the beginning time of the reverse flow at the hot leg bottom which is detected with the hot leg spool

piece and observed with the view window, the time of whole core quench and the time when the upper plenum collapsed water level reached the elevation of the hot leg nozzle bottom are referenced on Fig. 12.

The carryover water flow rate increases gradually on the whole although it slightly decreases from about 40 sec after the time when the beginning of the hot leg reverse flow was observed at the view window to the time slightly before the whole core quench. This may be caused by decrease of the steam flow rate from the core. The effect of core outlet steam flow rate can be treated as that of the kinetic energy of steam.

After that, the carryover water flow rate increases as the upper plenum water level rises, and after the arrival of the collapsed water level at the hot leg nozzle bottom it is kept at almost the constant value. This suggests that the upper plenum water began to overflow through the hot leg. From these results, kinetic energy of the steam flow from the core and the collapsed water level in the upper plenum can be considered two of the most important parameters of the hot leg carryover characteristics.

After several trials, the following dimensionless parameter was introduced, as the first approach, to evaluate the effect of these quantities on the hot leg carryover characteristics:

$$F_{UP} = \frac{u_g^2 \rho_g}{g D_{eq} (\rho_l - \rho_g)}$$

where,  $F_{UP}$  represents the ratio of the upper plenum collapsed water level to the elevation of the hot leg nozzle bottom which are measured from the upper surface of the UCSP,  $u_g$  represents the superficial steam velocity at the UCSP holes,  $D_{eq}$  represents the equivalent diameter of the UCSP flow path,  $g$  represents the gravitational acceleration and  $\rho_g$  and  $\rho_l$  represent densities of steam and water, respectively.

The ratio of the hot leg carryover water flow rate to the total core outlet mass flow rate,  $F_B$ , can be correlated with this dimensionless parameter as shown in Fig. 15. Almost all the test data fall near the linearly approximated correlation:

$$0.028(F_B - 0.2) = \frac{F_{UP} u_g^2 \rho_g}{g D_{eq} (\rho_l - \rho_g)}$$

with scattering band of  $\pm 15\%$ . Only exceptions are seen when ECC water injection flow rate is low. This is supposed mainly due to the reason that when the collapsed water level above the UCSP is low the entrained water droplets from the core is directly carried over to the hot leg nozzle, while the entrainment is generated, in the other case, above the UCSP when the steam from the core passes through the water pool. Thus, the sensitivities of both the collapsed water level above the UCSP and the amount of entrained droplets from the core should be different between the case of low ECC water injection rate and the other case.

It must be noted that the correlation can evaluate principally the generation term of entrainment in the region above the UCSP. Of course, de-entrainment on the upper plenum structures is also able to be evaluated indirectly with the core outlet steam flow rate and collapsed water level above the UCSP, however the evaluation is only of the implicit manner. However, this causes no important problems because the data for the various SCTF tests show that more than 80% of carryover water from the core reaches the hot leg inlet, i.e., de-entrainment fraction is less than 20%.

Generally speaking, however, de-entrainment in the upper plenum is still important. In addition, the hot leg flow reversal and the resultant counter-current flow in the hot leg are key phenomena for the prediction of carryover water flow rate to the steam generators (in the case of SCTF, the steam/water separator). These phenomena should be investigated generally in the future.

#### 4. Conclusions

The following conclusions have been obtained from the forced-feed flooding tests with SCTF Core-I.

##### (1) Chimney Effect

- i. Chimney effect was confirmed by comparing the heat transfer coefficients and quench times between the tests with different radial power profiles.
- ii. Cooling of the hottest bundle above the quench front was improved by the chimney effect.
- iii. Cross flow across bundles was confirmed by investigating the collapsed water level distribution in the core and horizontal differential pressure between the two bundles. The cross flow is considered to be caused by the chimney effect.
- iv. The chimney effect was not affected by the total core heating power but by the radial power profile only. Therefore, when the total core heating power was higher but the radial power profile was the same, the heat transfer coefficient was not improved and thus the quench was delayed.

##### (2) Blockage Effect

- i. Blockage effect on reflood core cooling was very small in the case of about 60 % of the local blockage fraction even if the blocked region was as large as the two full bundle cross sections.
- ii. Heat transfer just above the core flow blockage was slightly improved and thus the quench occurred slightly earlier than the unblocked bundles only when the core inlet flow rate was higher.
- iii. The blockage effect was seen only within 100 mm above the core flow blockage.

### (3) Hot Leg Carryover

- i. Carryover water flow rate at the inlet of the hot leg was affected by both the steam flow rate from the core and the collapsed water level above the upper core support plate.
- ii. The carryover flow rate can be evaluated with the dimensionless parameter including the kinetic energy of steam at the upper core support plate holes and the collapsed water level above the upper core support plate. The correlation principally does not directly evaluate the de-entrainment on the upper plenum structures but the generation term of entrainment in the region above the upper core support plate. However, since the de-entrainment fraction was only less than 20 %, the correlation was able to be usefully applied to almost all the SCTF tests.

These conclusions are consistent on the whole with the CCTF test results. Especially, cross-flow across bundles observed in the SCTF tests is expected to remarkably flatten the radial distribution of the core thermal behavior. Resultantly, an one-dimensional average bundle (or rod) analysis for the determination of the core inlet/outlet boundary conditions can be said sufficiently valid. Since the chimney effect acts positively to the core cooling, hottest bundle (or rod) analysis based on the core boundary conditions determined in this way may give the conservative results. These conclusions agree well with those of the CCTF tests. On the other hand, from the view point of the best estimation the chimney effect should be evaluated more quantitatively. Because, the cross-flow across bundles may occur so easily that a fully one-dimensional hottest bundle (or rod) analysis neglecting the cross-flow effect seems to produce too conservative results. Further investigation is, therefore, needed on the chimney effect especially to establish the analytical method to correctly predict the cross-flow effects.



Reference:

- (1) H. Adachi, et al.: SCTF CORE-I TEST RESULTS (SYSTEM PRESSURE EFFECTS ON REFLOODING PHENOMENA), JAERI-M 82-075 (1982), Presented at the Ninth Water Reactor Safety Research Information Meeting, Gaithersburg, Maryland, October 28, 1981.

Table 1 TEST CONDITIONS FOR BASE CASE

|   |   |
|---|---|
| TEST TYPE                               | FORCED FLOODING                                   |
| INITIAL PRESSURE (CORE CENTER)          | 199 kPa   |
| PRESSURE (CONTAINMENT-II)               | 199 kPa   |
| MAX. CORE TEMP. (AT BOCREC)             | 973 K (NOMINAL)                                   |
| POWER HOLDING TIME AFTER ACC INITIATION | 5 SEC (NOMINAL)                                   |
| DECAY CURVE                             | ANS+ACTINIDES+D.N.<br>FROM 30 SEC OF REACTOR TIME |
| MAX. ACC INJECTION RATE                 | 22.4 kg/s   |
| LPCI INJECTION RATE                     | 11.2 kg/s   |
| MAX. CORE INLET SUBCOOLING              | AS LOW AS POSSIBLE                                |

Table 2 ECCS INJECTION RATES FOR SCTF CORE-I FORCED FLOODING TESTS

| TEST   | ACC              |                              | LPCI             |                              | NOTE                      |
|--------|------------------|------------------------------|------------------|------------------------------|---------------------------|
|        | INJ. RATE (kg/s) | NOMINAL FLOOD SPEED * (cm/s) | INJ. RATE (kg/s) | NOMINAL FLOOD SPEED * (cm/s) |                           |
| SI-SHI | 40               | 9.4                          | 11               | 2.6                          | HIGH ACC INJ. RATE        |
| SI-01  | 22               | 5.3                          | 11               | 2.6                          | BASE CASE                 |
| SI-05  | 22               | 5.3                          | 6.5              | 1.5                          | LOW LPCI INJ. RATE        |
| SI-09  | 40               | 9.4                          | 18               | 4.3                          | HIGH ACC & LPCI INJ. RATE |

\* BASED ON MEASURED CORE FLOW AREA INCLUDING CORE BYPASS REGION AND ADDITIONAL FLUID SPACES SUCH AS GAP BETWEEN VESSEL WALL AND CORE BARREL AND INSTRUMENTATION PENETRATION HOLES.

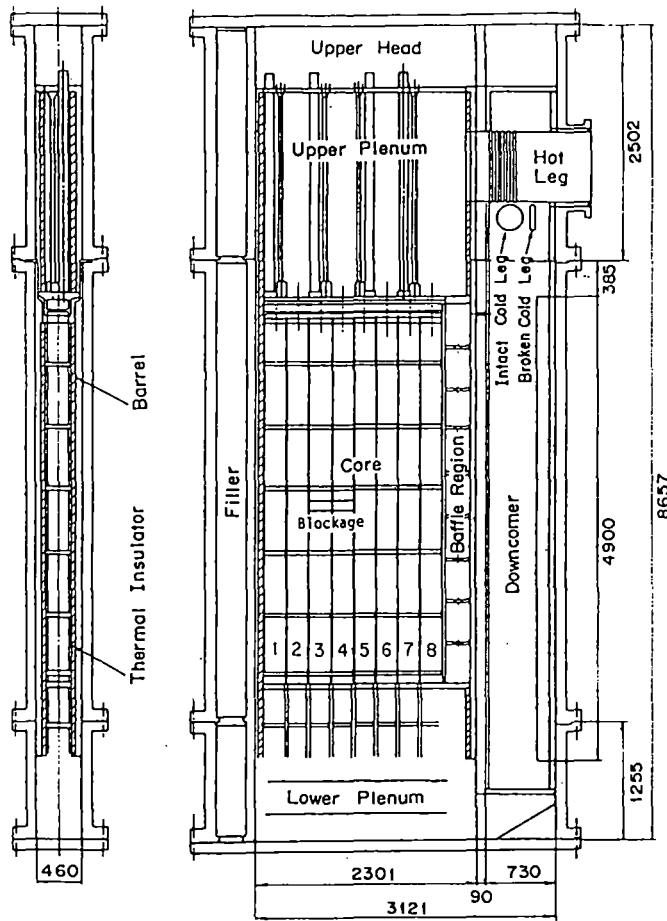


Fig. 1 Vertical Cross Section of SCTF Pressure Vessel

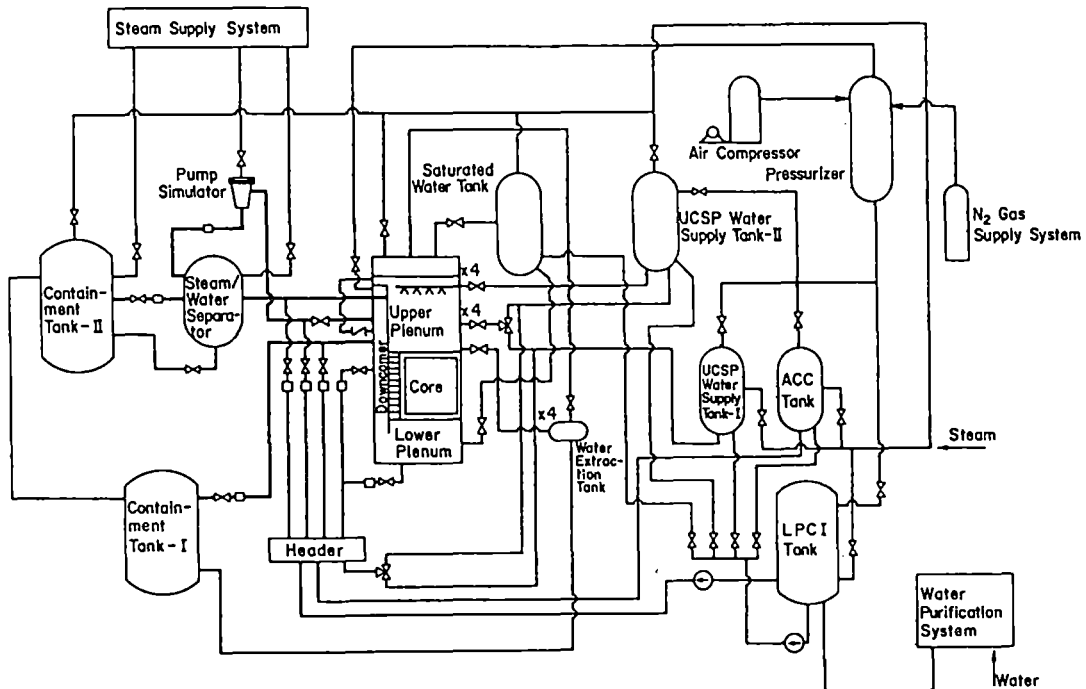


Fig. 2 Flow Sheet of SCTF

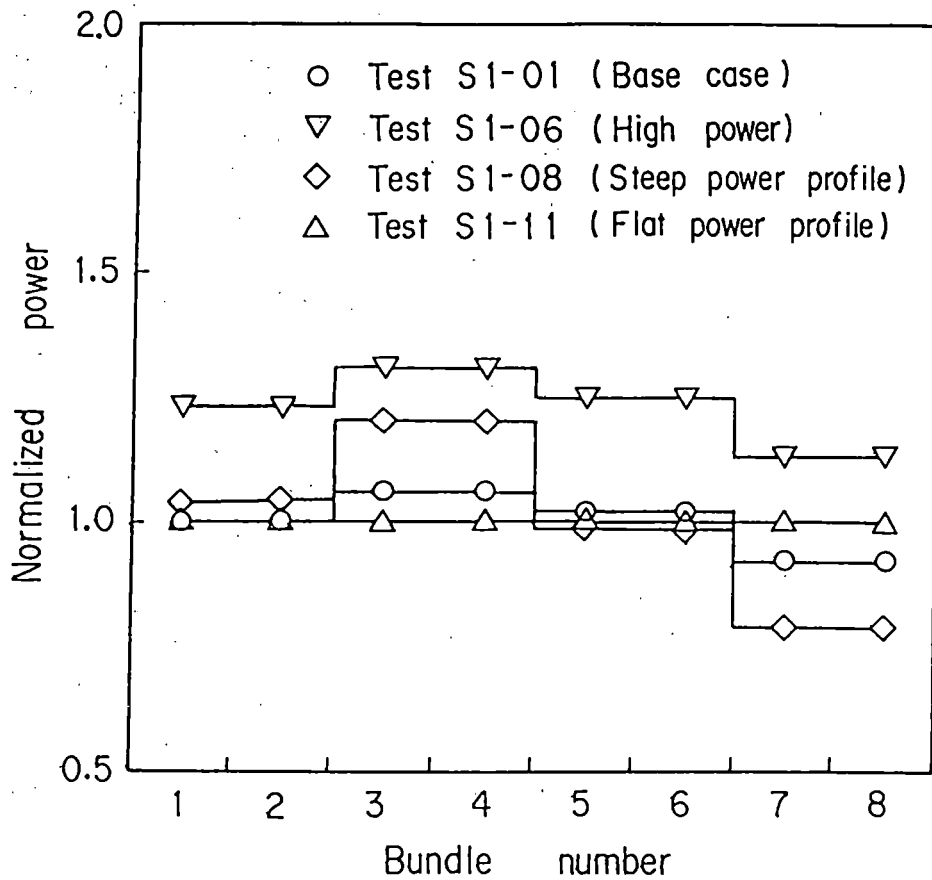


Fig. 3 Radial Power Profiles for Power/Power Distribution Tests

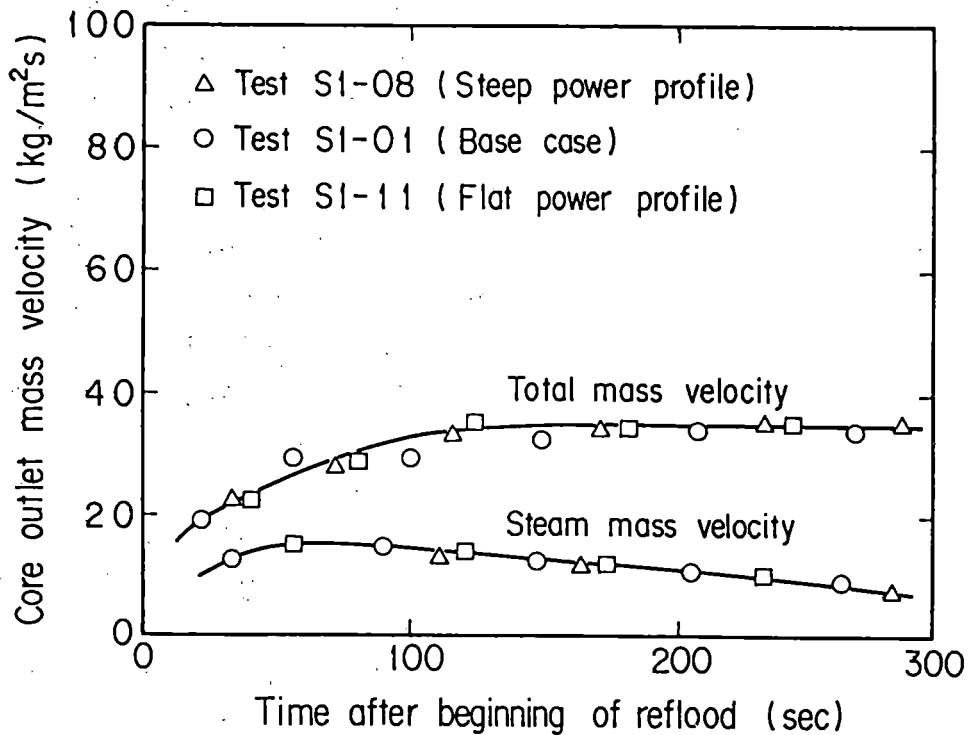


Fig. 4 Core Outlet Mass Velocities in Power Distribution Tests

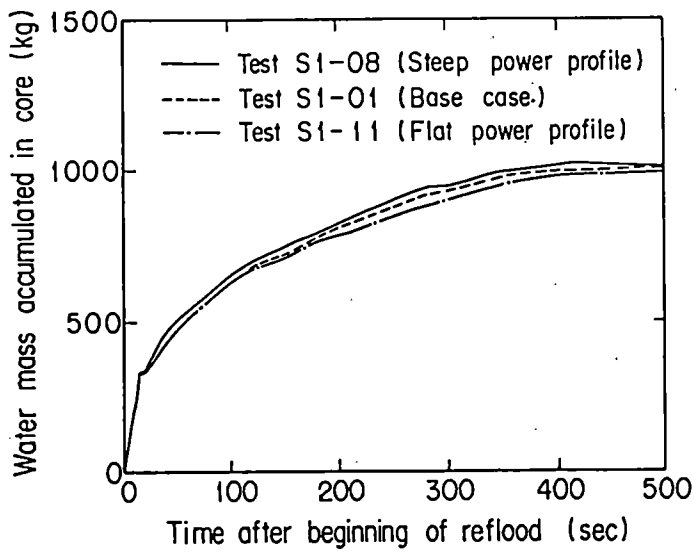


Fig. 5 Water Mass Accumulation in Core in Power Distribution Tests

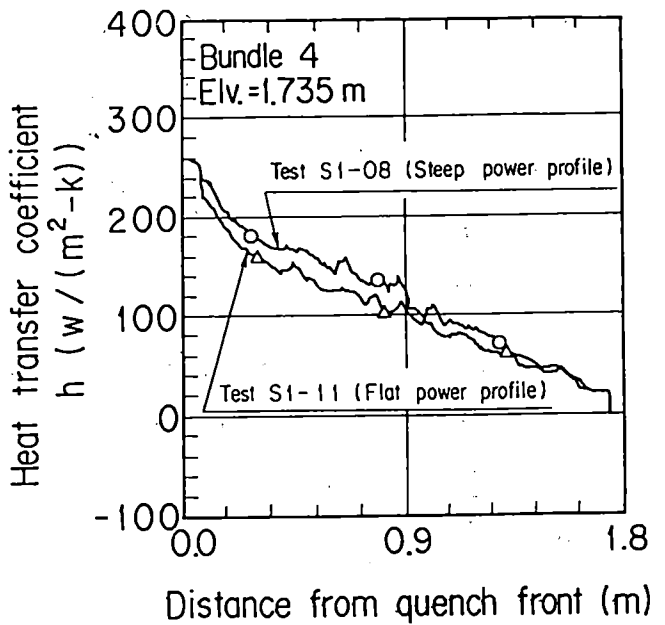


Fig. 7 Heat Transfer Behavior in Power Distribution Tests

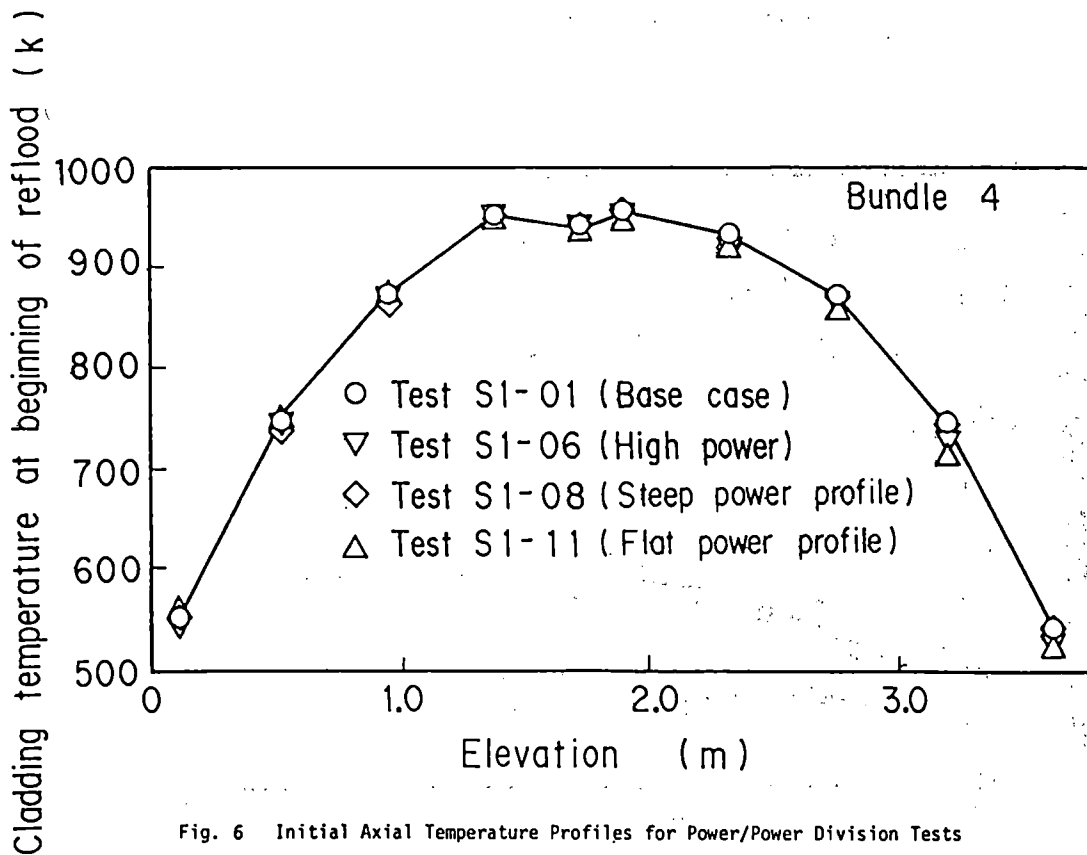


Fig. 6 Initial Axial Temperature Profiles for Power/Power Division Tests

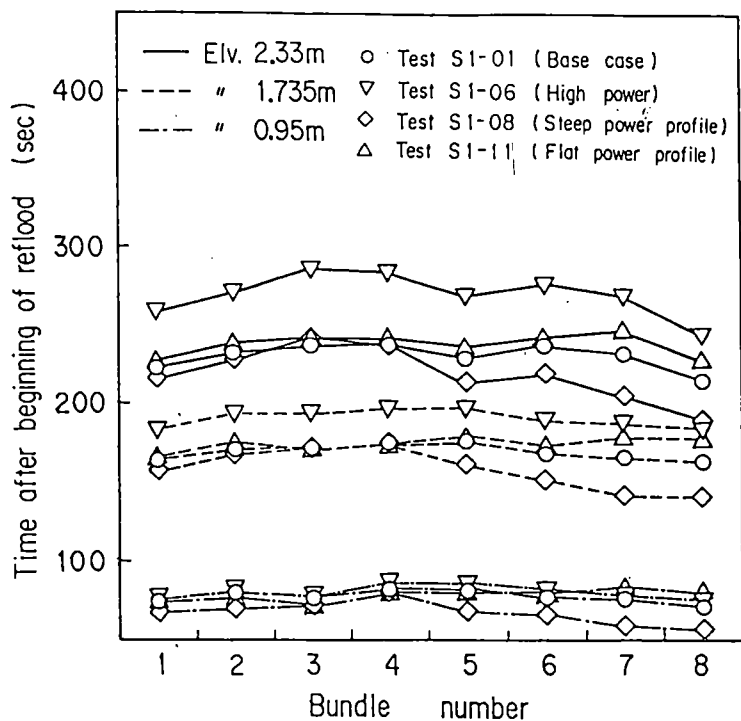
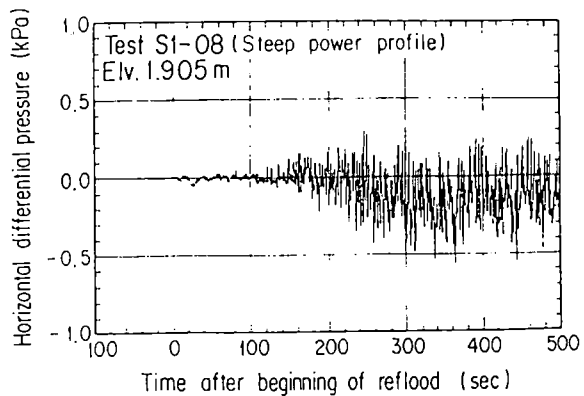
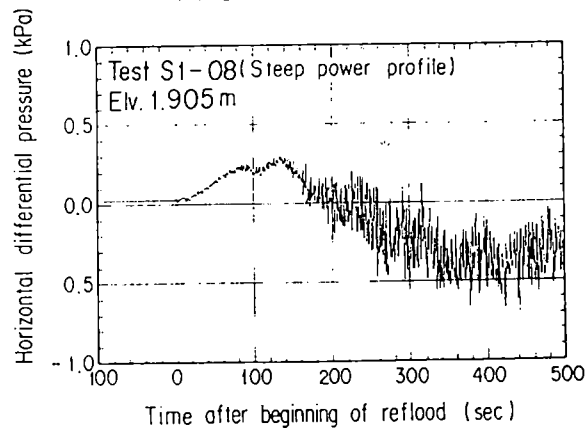


Fig. 8 Quench Time in Power/Power Distribution Tests



(a) Bundle 1 - Bundle 5



(b) Bundle 5 - Bundle 8

Fig. 10 Horizontal Differential Pressure across Bundles for Steep Power Distribution Test

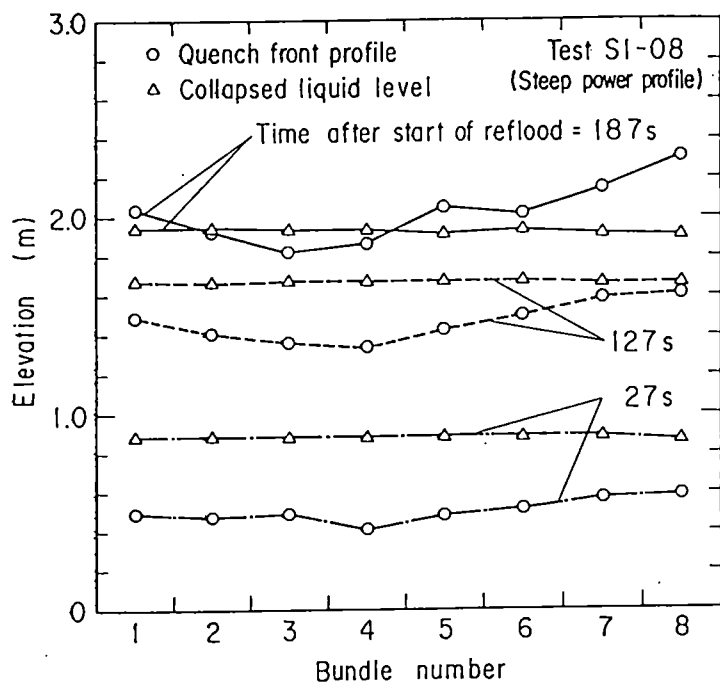


Fig. 9 Quench Front and Collapsed Water Level for Steep Power Distribution Test

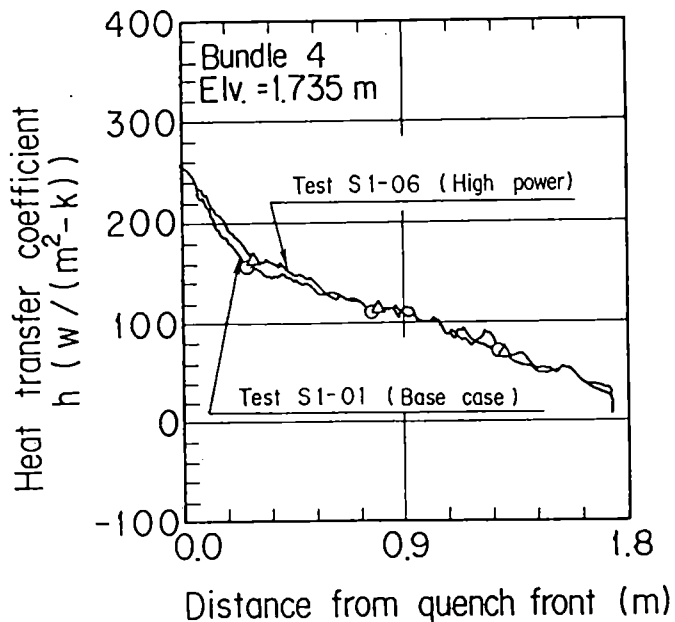


Fig. 11 Heat Transfer Behavior in Power Tests

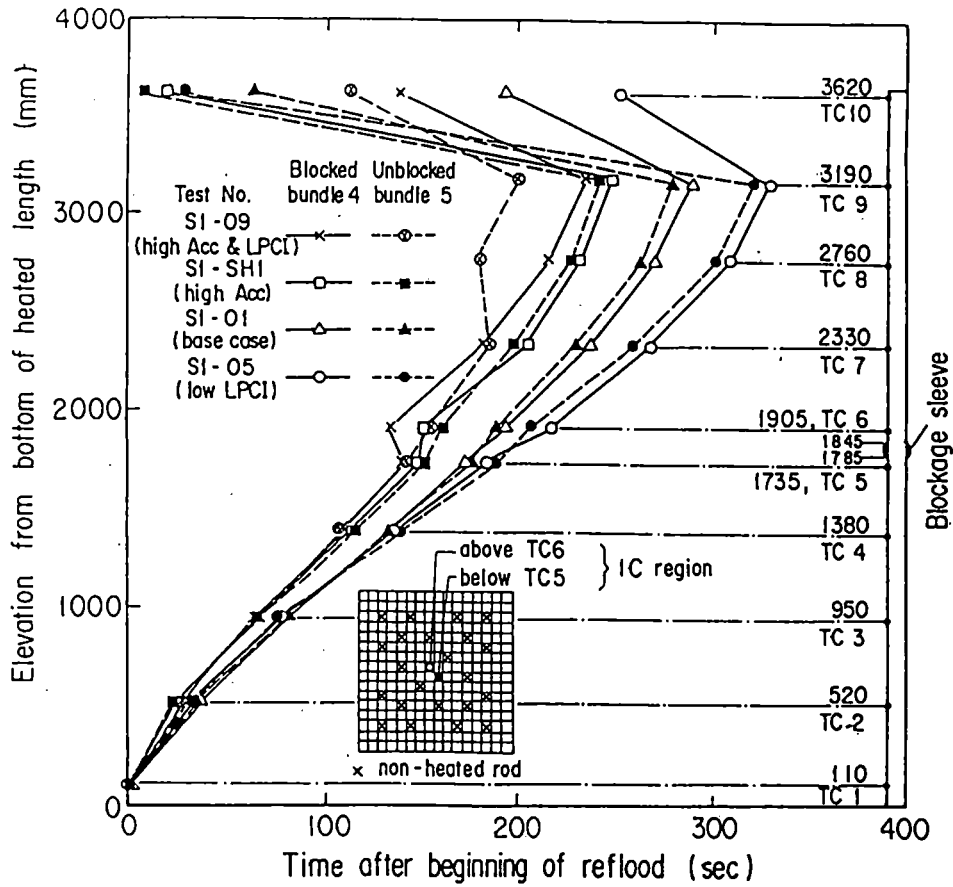
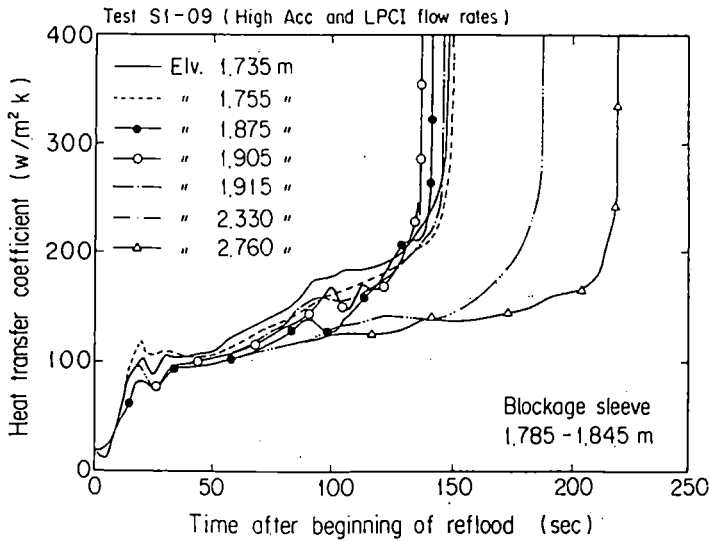
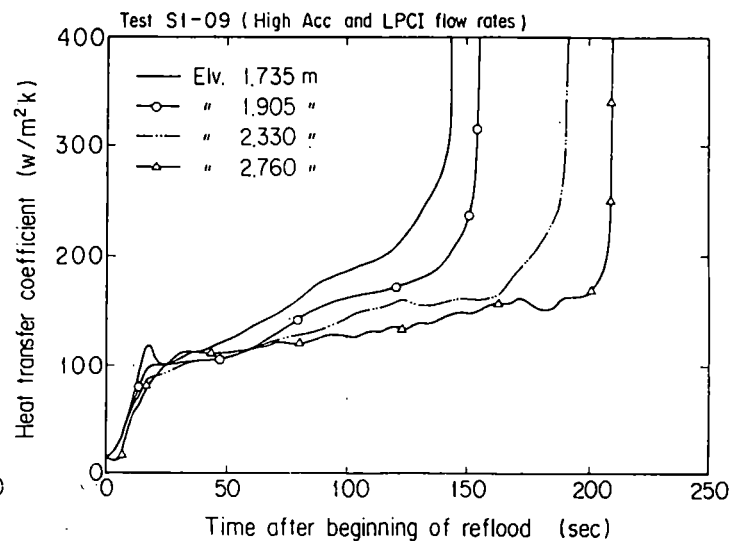


Fig. 12 Comparison of Quench Envelopes between the Blocked and Unblocked Bundles



(a) Bundle 4 (Blocked)



(b) Bundle 2 (Unblocked)

Fig. 13 Heat Transfer Behavior for Blocked and Unblocked Bundles

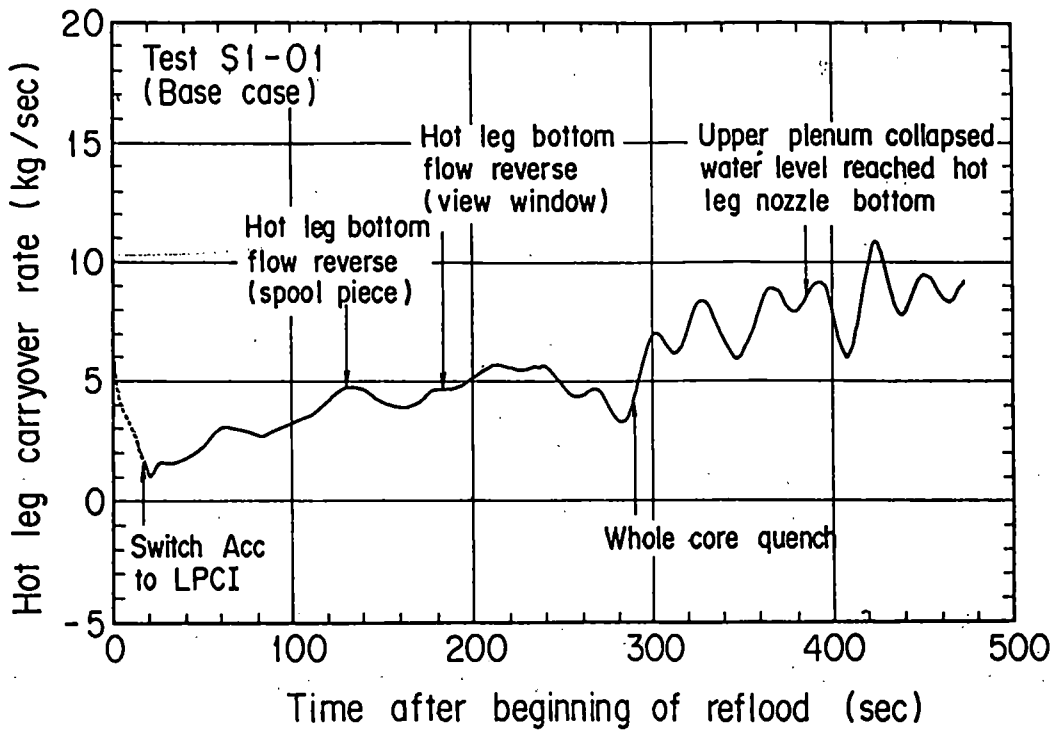


Fig. 14 Hot Leg Carryover Rate for Base Case

- Test S1-01 (Base case)
- △ Test S1-05 (Low LPCI flow rate)
- Test S1-09 (High Acc and LPCI flow rates)

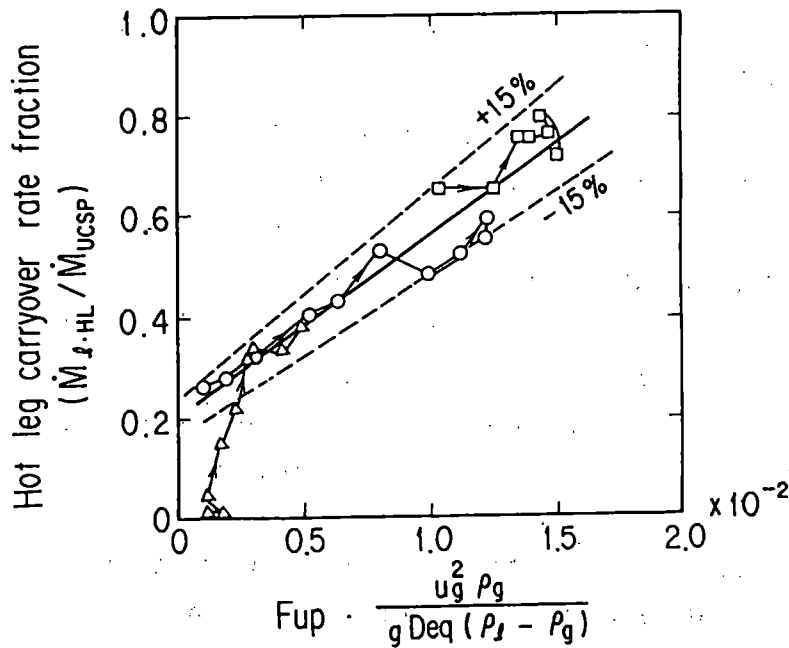


Fig. 15 Hot Leg Carryover Characteristics in ECCS Injection Rate Tests

## TRAC ANALYSIS SUPPORT FOR THE 2D/3D PROGRAM\*

by

Ken A. Williams  
Project Leader  
Energy Division  
Los Alamos National Laboratory  
Los Alamos, New Mexico 87545

The 2D/3D Program is a multinational (Germany, Japan, and the United States) experimental and analytical nuclear reactor safety research program having as its main purpose the investigation of multidimensional thermal-hydraulic behavior during the refill and reflood phases of loss-of-coolant accidents (LOCAs) in pressurized water reactors (PWRs). The German contribution to the program is the planned Upper Plenum Test Facility (UPTF), a full-scale facility with vessel, four loops, and steam-water core simulator. The Japanese are presently operating two large-scale test facilities as part of this program: the Cylindrical Core Test Facility (CCTF) and the Slab Core Test Facility (SCTF). CCTF is a 2000-electrically heated rod, four-loop facility primarily for investigating integral system reflood behavior. SCTF is a 2000-electrically-heated-rod, slab-core (one fuel assembly wide, eight across, and full height), separate-effects reflood facility. Both facilities are scaled on a power-to-volume basis, preserving full-scale elevations, and are much larger than any existing facilities in the United States (including LOFT). All of these facilities are instrumented better than any existing facilities: conventional instrumentation data channels alone are in excess of one thousand in each facility. The United States contribution to the program is the provision of advanced two-phase flow instrumentation and analytical support.

The Los Alamos National Laboratory is the prime contractor to the NRC in the latter activity. The main analytical tool in this program is the

---

\*Work performed under the auspices of the US Nuclear Regulatory Commission.



Transient Reactor Analysis Code (TRAC), a best-estimate, multidimensional, non-equilibrium, thermal-hydraulics computer code developed for the NRC at Los Alamos.<sup>1,2</sup> Through code predictions of experimental results and calculations of PWR transients, TRAC provides the analytic coupling between the facilities and is extending the results to predicting actual PWR behavior.

During the previous fiscal year, the analysis program has matured to the point that it is now playing a central role in the overall 2D/3D program. The TRAC code has been used for a larger number of posttest predictions of both CCTF and SCTF experiments.<sup>3</sup> Through these calculations it has been demonstrated that the code is a reliable tool for predicting the thermal-hydraulic behavior resulting from the parametric variation of test conditions. Specifically, the code has been demonstrated to predict correctly the effects on core reflood resulting from the variation in system operating pressure, ECC subcooling and injection rate, core flooding rate, radial power distribution, local power peaking and the asymmetric initial stored energy of the fuel rods. The twelve experiments to be analyzed in CCTF/SCTF during the next fiscal year will further assess the code's abilities.

Both the experimental findings and the analysis results have a direct and important bearing on licensing issues. Some of the major conclusions that have come from the experiments and that have been predicted by TRAC are the following:

- o Multidimensional hydraulics are responsible for mitigating the thermal consequences of non-uniform power shapes and local power peaking.
- o Core water level stagnation occurs during reflood once the downcomer is filled.
- o Significant bypass of LPCI occurs if the flowrate is increased above the nominal rate.
- o Condensation heating of ECC to near saturation occurs due to superheated vapor exiting the steam generators.
- o Thermal effects of 56% blockages over two adjacent full-scale bundles are not significant during forced-reflood conditions.
- o Significant multidimensional flows in the core during reflood can have an important influence on the thermal response of the fuel cladding even with a symmetrical core power shape.
- o Upper plenum de-entrainment in full-scale hardware can significantly reduce steam binding.

The 2D/3D analysis program is also responsible for providing TRAC calculations of the full-scale PWR's for hypothetical intermediate to large-break LOCAs in the reference US, FRG, and Japan plants. These calculations serve two important functions for this program. First, they determine prototypical initial and boundary conditions about which a range of experimental conditions can be chosen to operate the test facilities. However, the ultimate objective is to allow the overall findings (experimental, analytical, and model development) of the 2D/3D program to be related to actual PWR's. The results from the program to date are very encouraging, and can be summarized as follows. The TRAC calculations of full-scale PWR's exhibit behavior similar to that which has been observed experimentally in the CCTF and SCTF; and this same code has been demonstrated to be a reliable tool for the prediction of these experiments. These PWR calculations demonstrate that a large margin of conservatism exists in present licensing requirements for LBLOCA's. Our best-estimate calculations of these reference PWR's indicate that the peak clad temperature (PCT) occurs during the blowdown phase; the PCT is below 1000 K (1340<sup>o</sup>F).<sup>4</sup>

In conclusion, the analysis effort is functioning as a vital part of the 2D/3D program. Through TRAC analyses the experimental findings can be related from facility to facility; and more importantly, the results of this research program can be directly related to licensing concerns affecting actual PWR's.

## REFERENCES

1. "TRAC-PD2: An Advanced Best-Estimate Computer Program for Pressurized Water Reactor Loss-of-Coolant Accident Analysis," Los Alamos National Laboratory report LA-8709-MS, NUREG/CR-2054 (1981).
2. "TRAC-PF1: An Advanced Best-Estimate Computer Program for Pressurized Water Reactor Analysis," Los Alamos National Laboratory report (to be published).
3. "2D/3D Analysis Program Report - 1981," W. L. Kirchner and K. A. Williams, NUREG/CR-2735, June 1982.
4. "A TRAC-PD2 Analysis of a Large-Break Loss-of-Coolant Accident in a Typical US PWR." J. R. Ireland, NUREG/CR-2775, June 1982.

# PRESENTATION OUTLINE

- OVERVIEW OF ANALYSIS SUPPORT
- KEY LICENSING ISSUES ADDRESSED
- SCTF ANALYSIS RESULTS  
WITH TRAC-PFI
- MULTIDIMENSIONAL THERMAL-HYDRAULIC  
BEHAVIOR IN THE SCTF & CCTF
- SUMMARY OF ANALYSIS FINDINGS  
RELATED TO LICENSING

Los Alamos

**2D/3D ANALYSIS PROGRAM HIGHLIGHTS**  
**SLAB CORE TEST FACILITY (SCTF)**

- **TRAC PREDICTIVE CAPABILITES  
DEMONSTRATED BY BLIND PREDICTIONS  
OF TEN (10) SCTF TESTS TO DATE.**

**ANALYSIS OBJECTIVE**

**SCTF TEST**

|                                   |                           |
|-----------------------------------|---------------------------|
| <b>SYSTEM PRESSURE EFFECTS</b>    | <b>RUNS 506. 507. 508</b> |
| <b>ECC SUBCOOLING EFFECTS</b>     | <b>RUNS 507. 510</b>      |
| <b>RADIAL POWER SHAPE EFFECTS</b> | <b>RUNS 507. 513. 514</b> |
| <b>PEAKED POWER EFFECTS</b>       | <b>RUNS 507. 512</b>      |
| <b>CORE FLOODING RATE EFFECTS</b> | <b>RUNS 507. 511. 515</b> |

# CYLINDRICAL CORE TEST FACILITY (CCTF)

- TRAC PREDICTIVE CAPABILITIES DEMONSTRATED BY CALCULATION OF NINE (9) CCTF TESTS TO DATE.

| ANALYSIS OBJECTIVE   | CCTF TESTS      |
|--|-----------------|
| SYSTEM PRESSURE EFFECTS-----                                 | RUNS 14. 19. 21 |
| LPCI FLOWRATE EFFECTS-----                                   | RUNS 14. 15     |
| EM RADIAL PEAKING EFFECTS-----                               | RUNS 14. 38     |
| CORE FLOODING RATE EFFECTS-----                              | RUNS 14. 25     |
| ASYMMETRIC ROD TEMP EFFECTS---                               | RUNS 14. 39     |
| SYMMETRIC MULTI-D CALCULATION<br>WITH FINE NODALIZATION----- | RUN 14          |
| CORE II BASE CASE PREDICTION----                             | RUN 53          |

Los Alamos

## US/J & FRG REFERENCE PWR CALCULATIONS

- NEW INPUT MODELS FOR REFERENCE  
REACTORS DEVELOPED IN COOPERATION  
WITH VENDORS.
- ALL STEADY STATE RESULTS IN CLOSE  
AGREEMENT WITH THOSE SUPPLIED BY VENDORS.
- LOCA CALCULATIONS PERFORMED  
WITH CURRENT TRAC-PFI.
- REFERENCE REACTORS LBLOCA CALCULATIONS  
WITH BEST-ESTIMATE TRAC CODE DEMONSTRATE  
LARGE MARGIN OF CONSERVATISM  
IN LICENSING REQUIREMENTS.

Lee Almes

## UPPER PLENUM TEST FACILITY (UPTF)

- LOOP OSCILLATION STUDIES IDENTIFIED PROBLEM AREAS FOR UPTF PROTOTYPICAL SIMULATION OF A GPWR.
- EVALUATION OF SEVERAL PROPOSED MODIFICATIONS TO UPTF LOOPS INDICATES THAT NEAR PROTOTYPICAL ECC DELIVERY CAN BE OBTAINED DURING COMBINED INJECTION. NO PROBLEMS ANTICIPATED FOR COLD LEG INJECTION TESTS.
- CORE SIMULATOR STUDIES IN PROGRESS DEMONSTRATE TRAC CAPABILITY TO MODEL FLOODING AT TIE-PLATE/UCSP.

Los Alamos



KEY LICENSING ISSUES ADDRESSED  
BY THE 2D/3D ANALYSIS PROGRAM (1)

♦ SCALING

- . GEOMETRY
- . OPERATING CONDITIONS

♦ MULTIDIMENSIONAL EFFECTS

- . POWER SHAPES
- . SYMMETRICAL CORE TEMPERATURES
- . ASYMMETRICAL CORE TEMPERATURES
- . FULL-RADIUS EFFECTS
- . "HOT-ROD" EFFECT
- . LOCAL POWER PEAKING (EM VALUES)

Los Alamos

KEY LICENSING ISSUES ADDRESSED  
BY THE 2D/3D ANALYSIS PROGRAM (2)

- CORE RECOVERY
  - . CORE WATER LEVEL
  - . STEAM-DROPLET COOLING
  - . PARAMETRIC EFFECT OF PRESSURE
- ECCS EFFECTIVENESS
  - . NOMINAL ECCS FLOWS
  - . HIGH (200 PER CENT) LPCI FLOW RATE.
  - . CONDENSATION HEATING OF ECC

Los Alamos

KEY LICENSING ISSUES ADDRESSED  
BY THE 2D/3D ANALYSIS PROGRAM (3)

- STEAM BINDING
  - . LIQUID CARRYOVER FRACTION
  - . UPPER PLENUM STRUCTURAL DEENTRAINMENT
  - . LOOP EFFECTS - ACTIVE COMPONENTS
- CORE BLOCKAGES
  - . 50 PER CENT BLOCKAGES OVER 2 ASSEMBLIES AT CORE MIDPLANE
  - . FULL-RADIUS EFFECTS

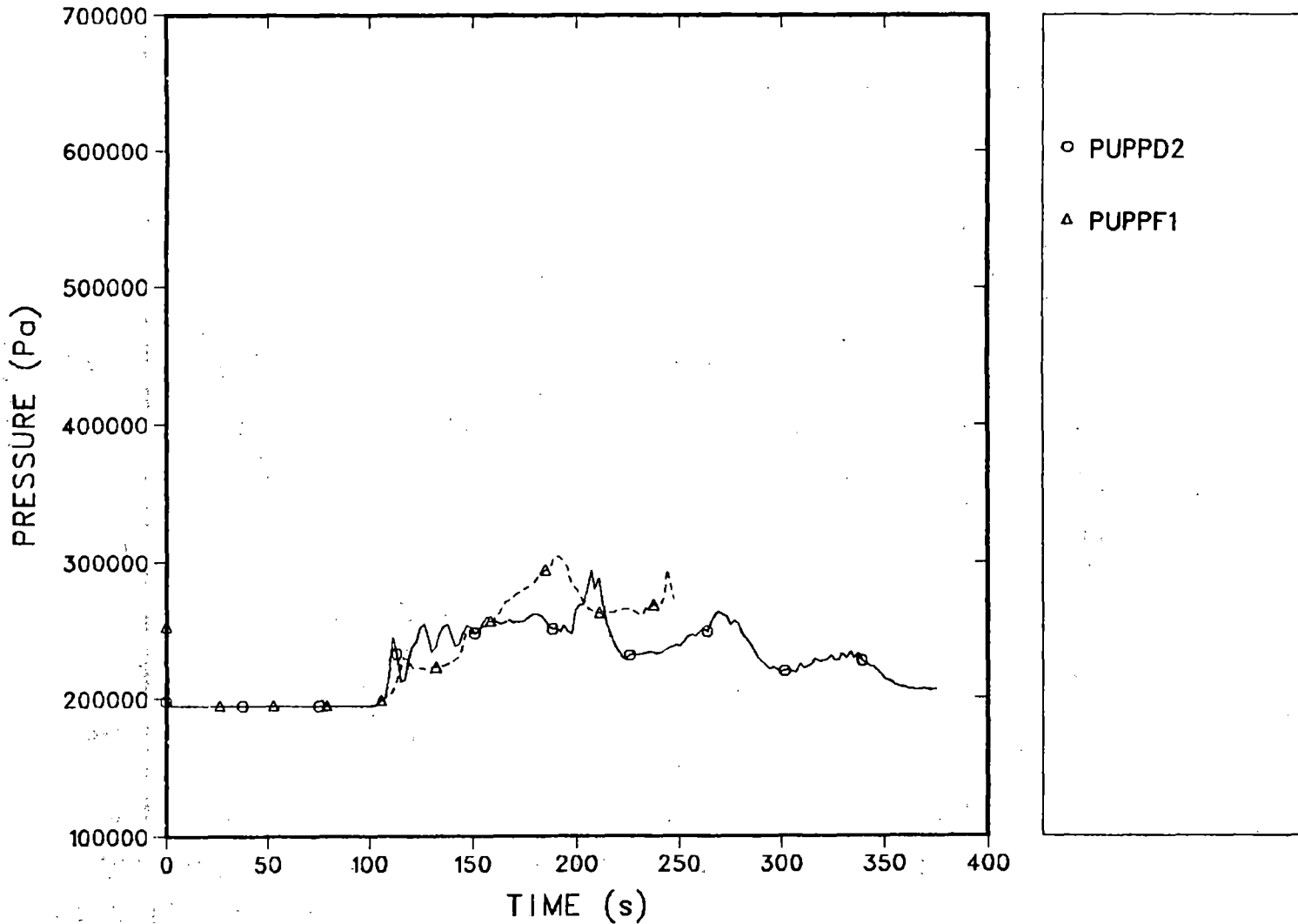
Los Alamos

**RECENT SCTF ANALYSIS RESULTS**

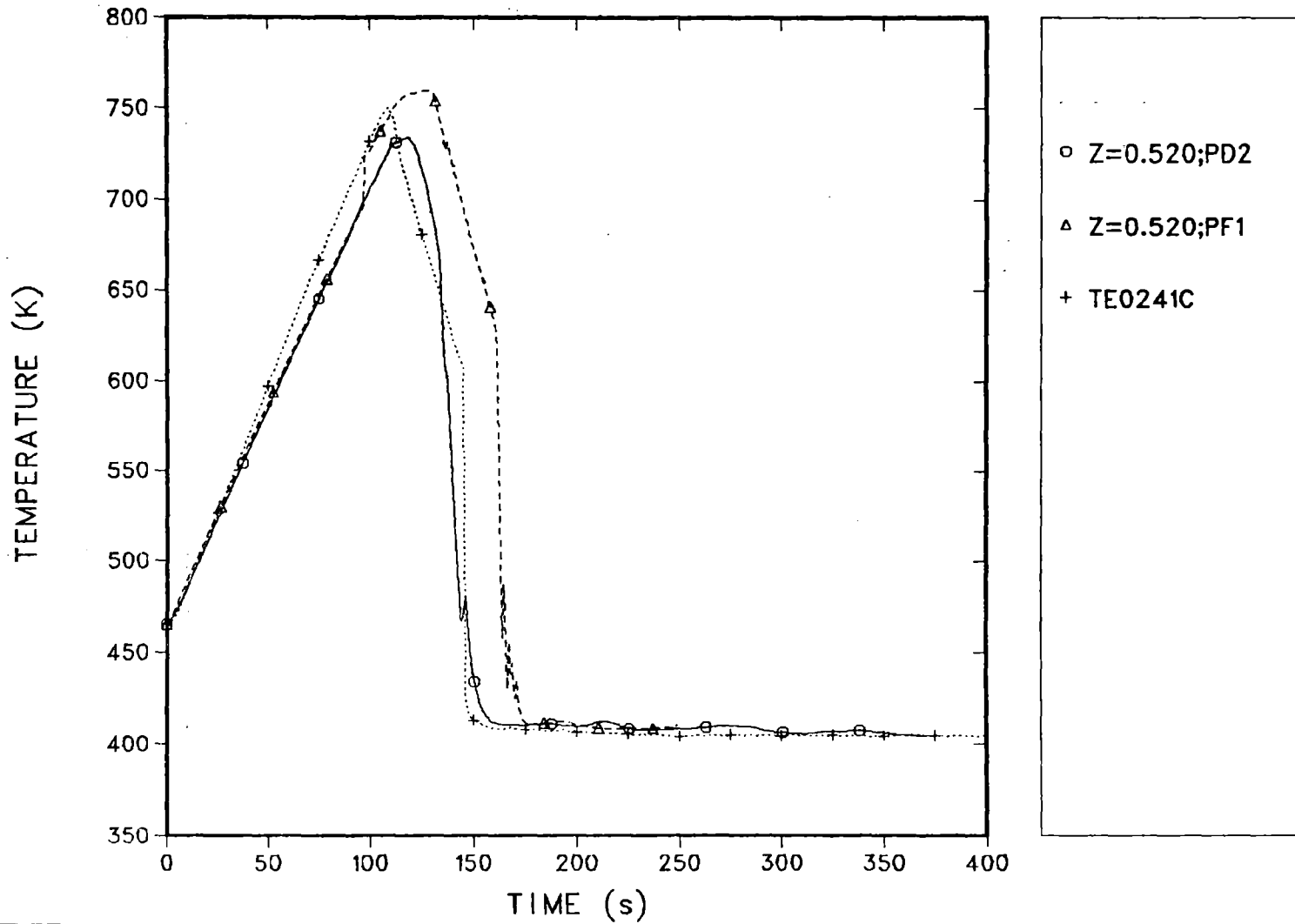
**WITH TRAC-PF1**

**Los Alamos**

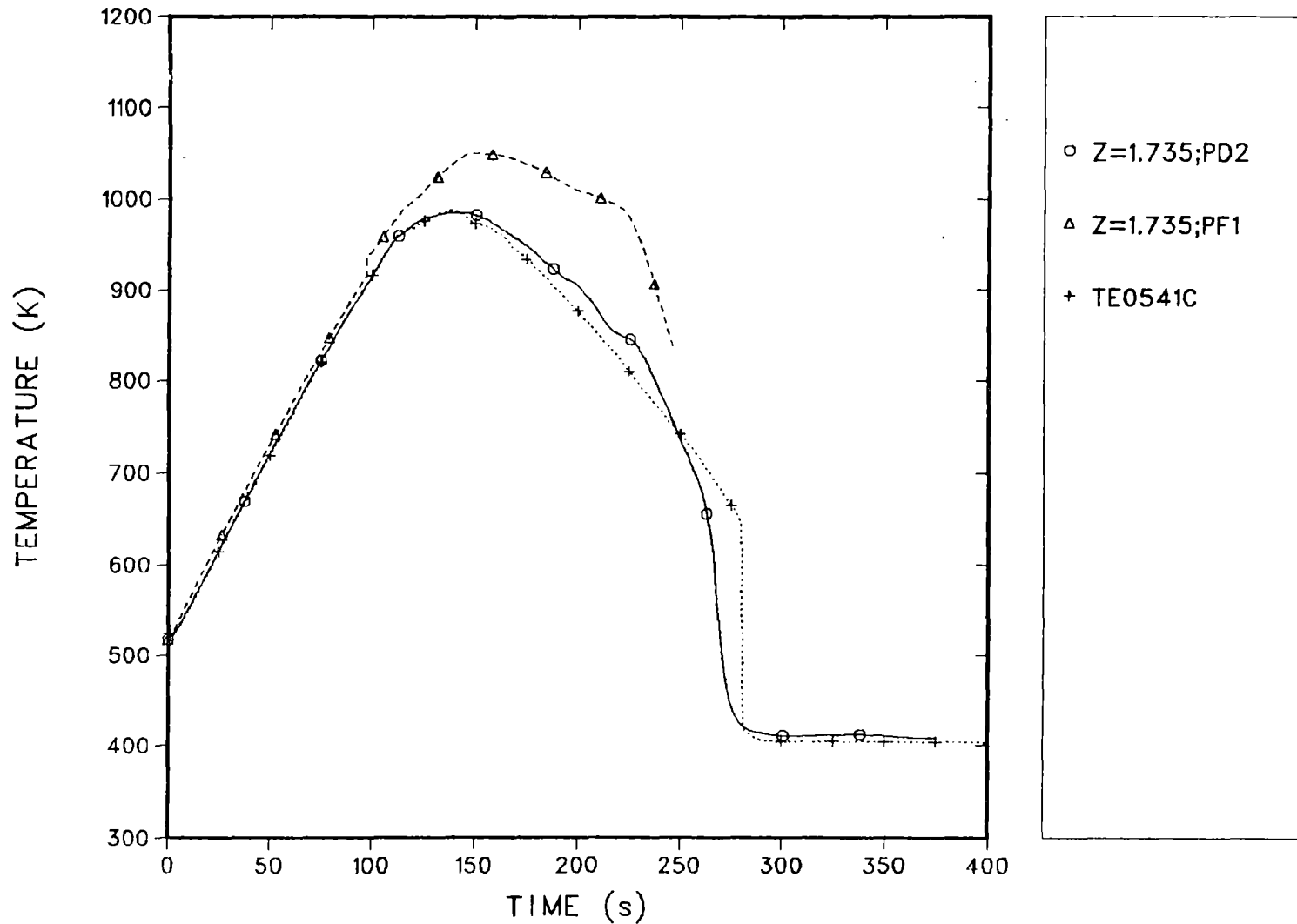
### TRAC PD2/PF1 SCTF BASE CASE CALCULATION COMPARISONS UPPER PLENUM AVERAGE PRESSURE



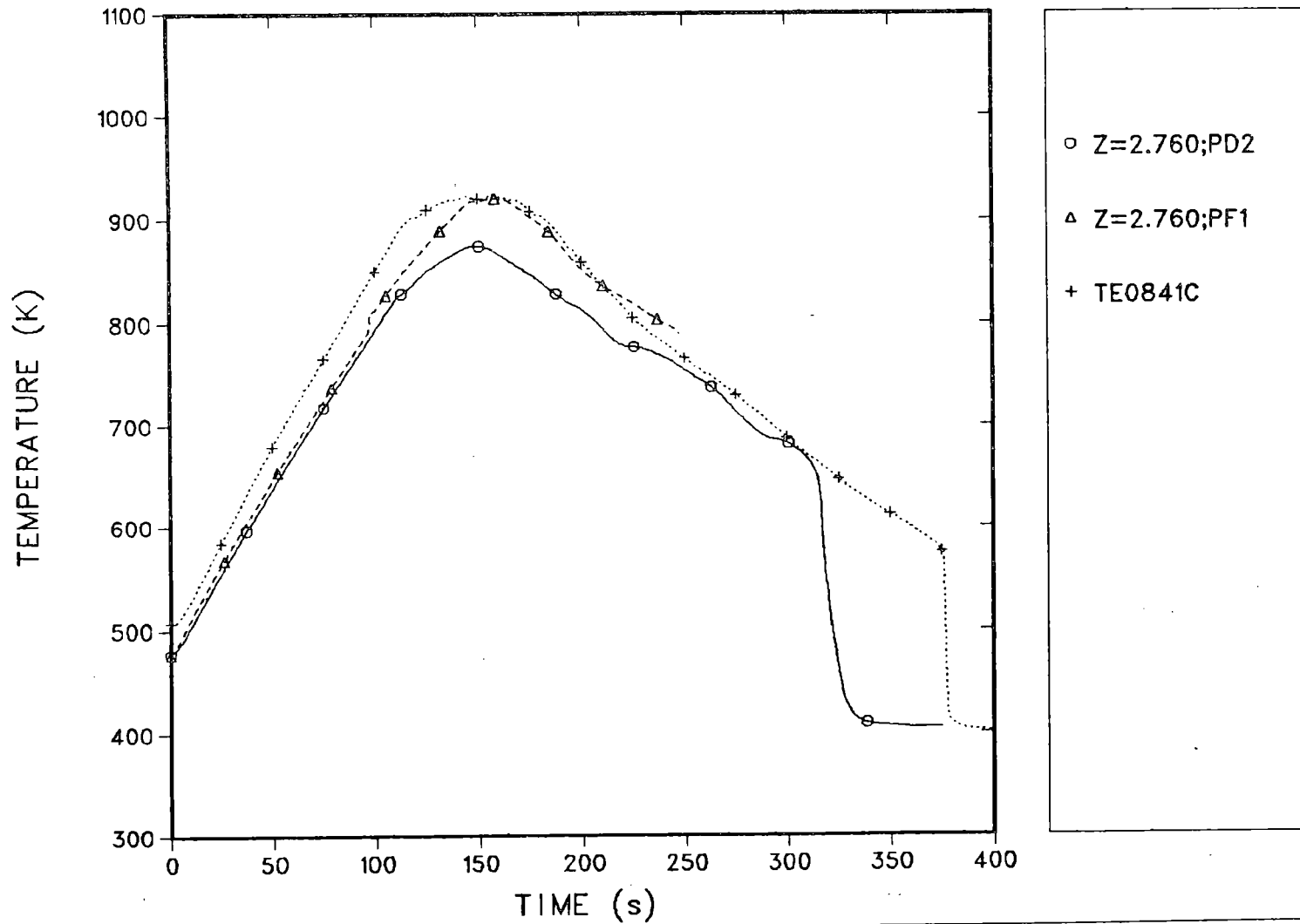
TRAC PD2/PF1 SCTF BASE CASE CALCULATION COMPARISONS  
SURFACE TEMPERATURE FOR ROD 4 AT TC LOCATION 2



TRAC PD2/PF1 SCTF BASE CASE CALCULATION COMPARISONS  
SURFACE TEMPERATURE FOR ROD 4 AT TC LOCATION 5



TRAC PD2/PF1 SCTF BASE CASE CALCULATION COMPARISONS  
SURFACE TEMPERATURE FOR ROD 4 AT TC LOCATION 8





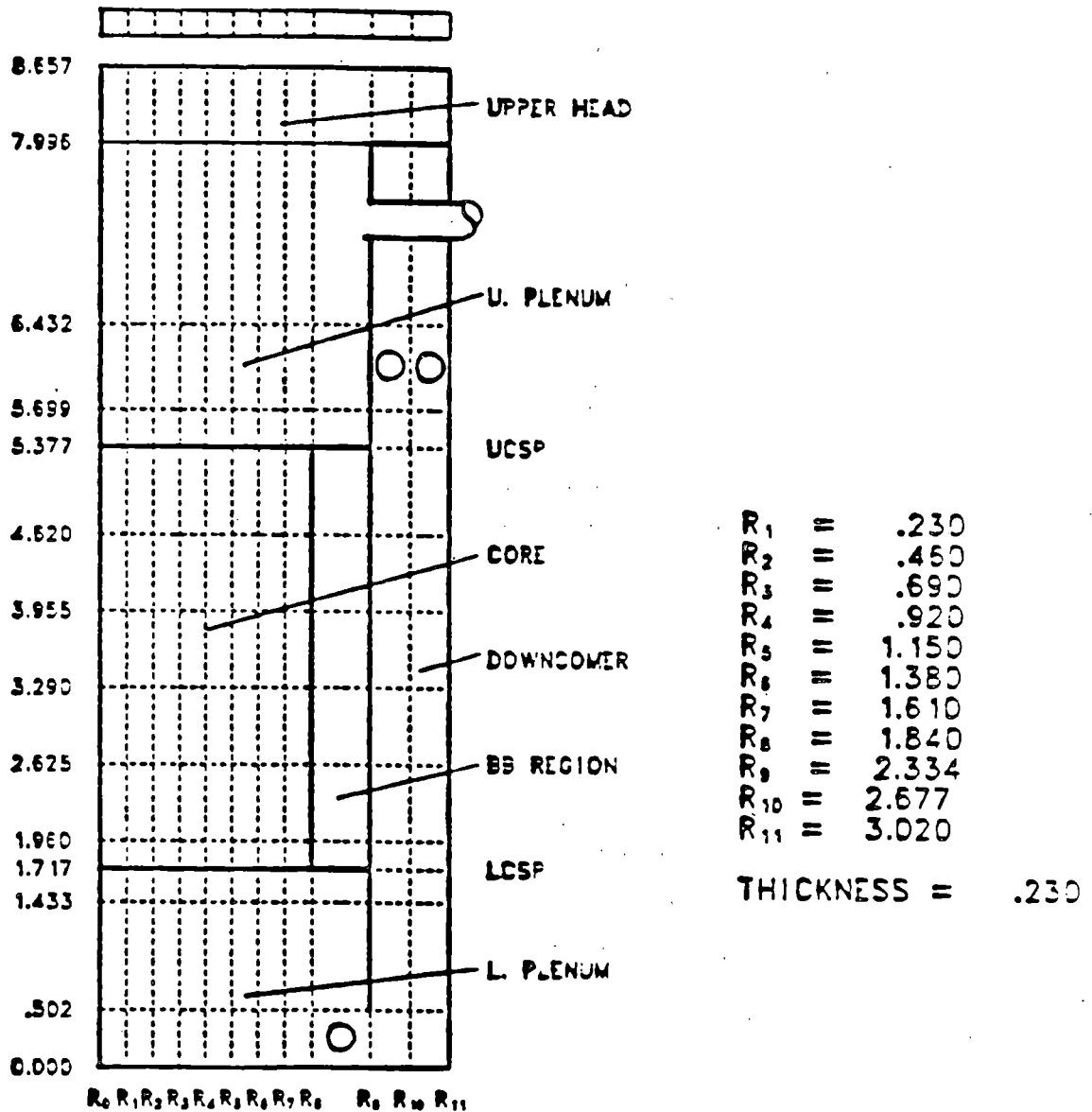
**MULTIDIMENSIONAL THERMAL-HYDRAULIC**

**BEHAVIOR IN THE SCTF AND CCTF**

**Leo Gomes**

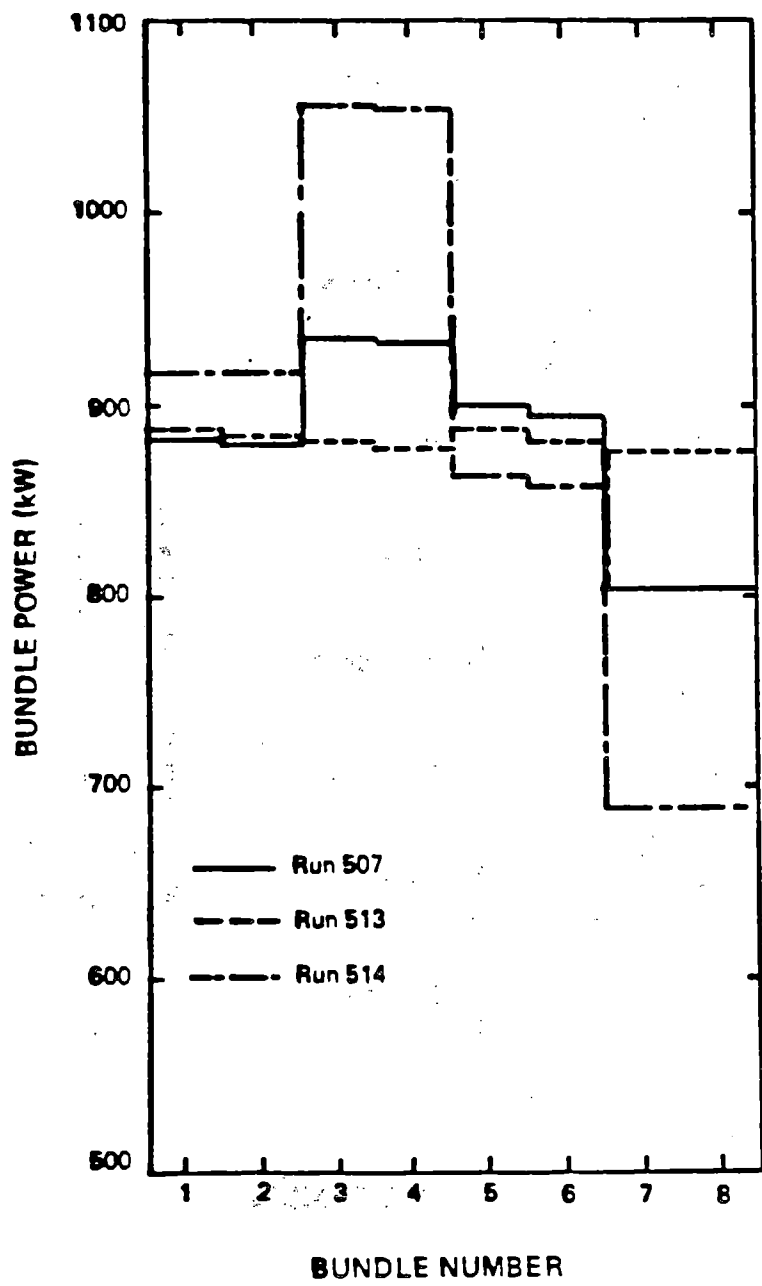
\* RADIAL CORE POWER DISTRIBUTION

- \* Run 507 (Base Case) - Slightly skewed profile
- \* Run 513 - Uniform or flat profile
- \* Run 514 - Highly skewed profile

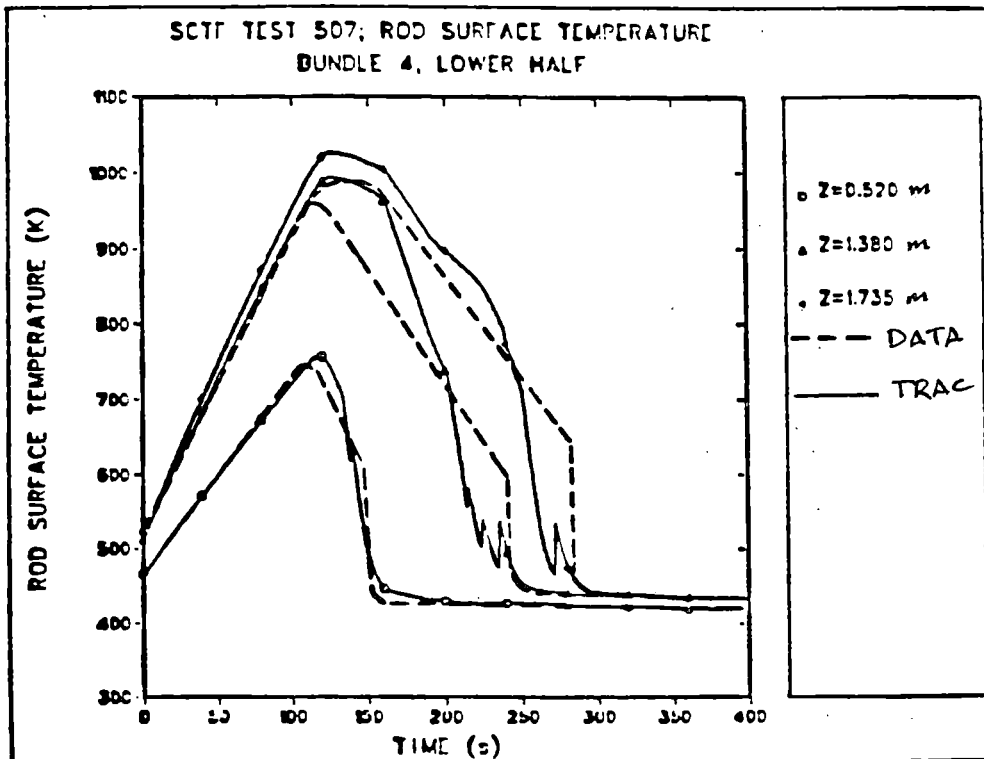
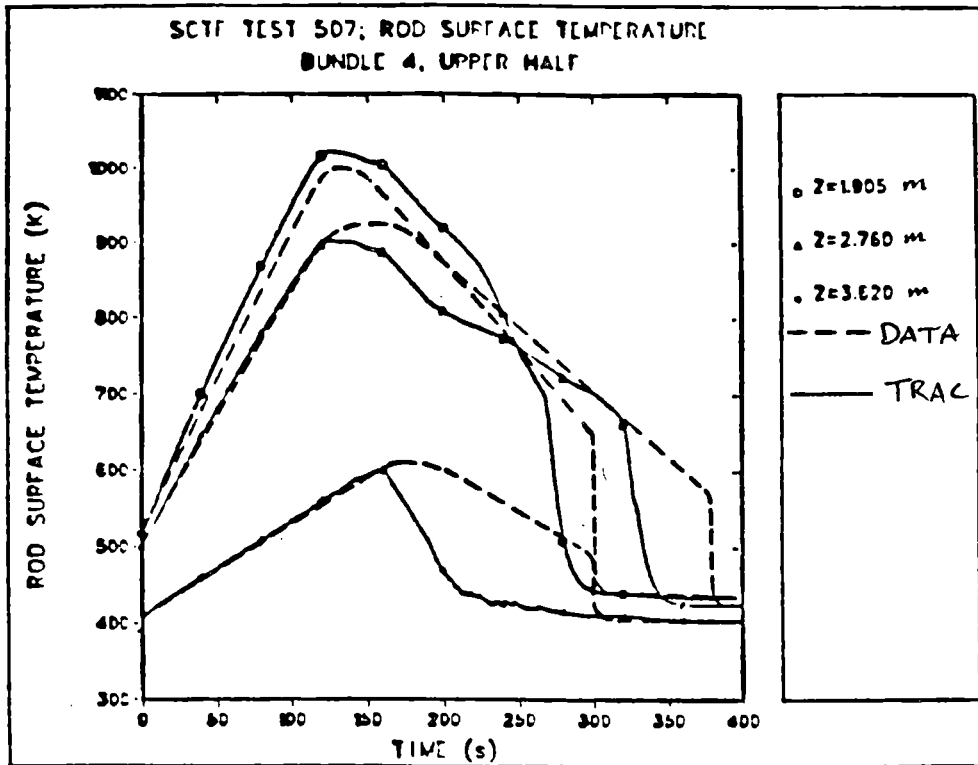


## SCTF VESSEL

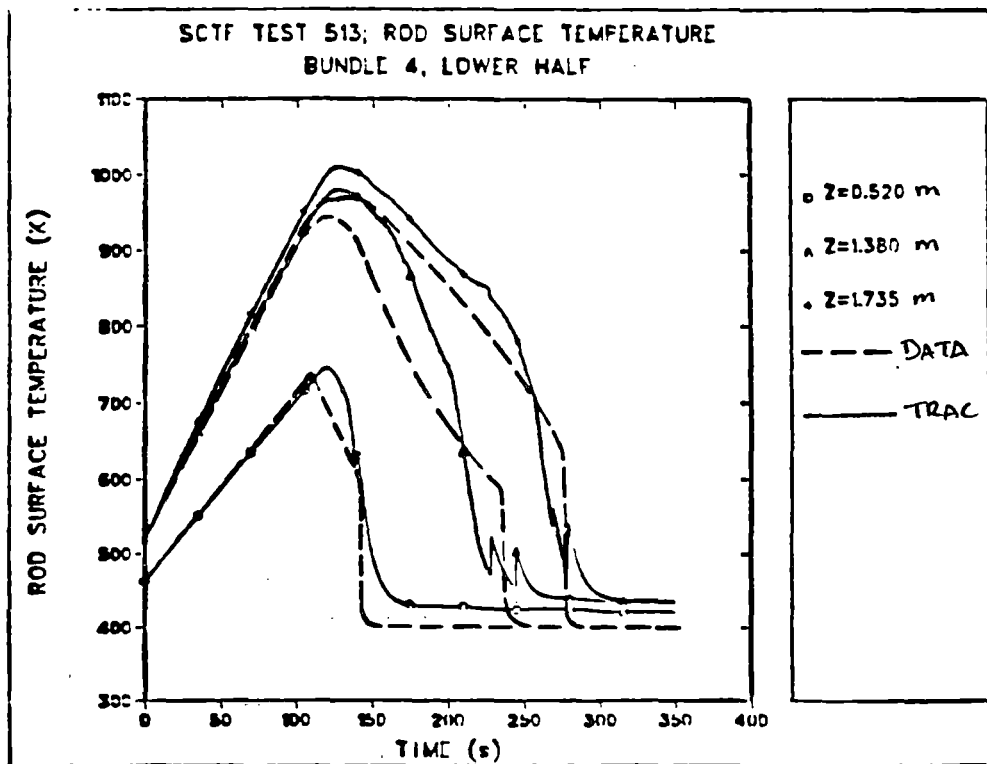
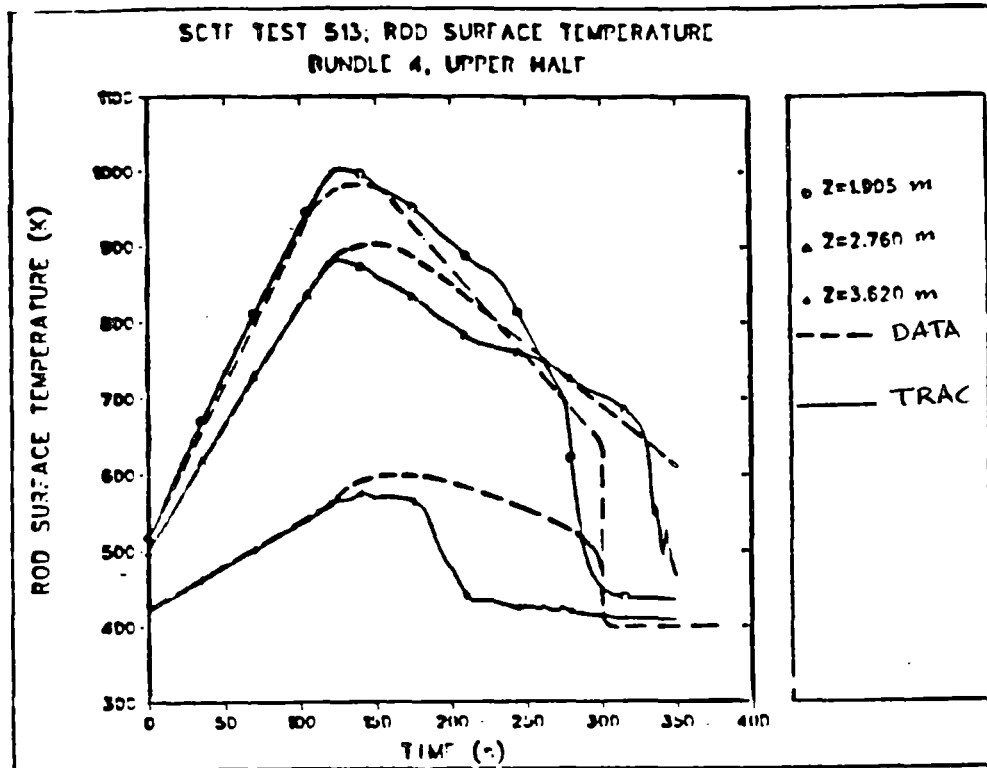
SCTF vessel component noding diagram.



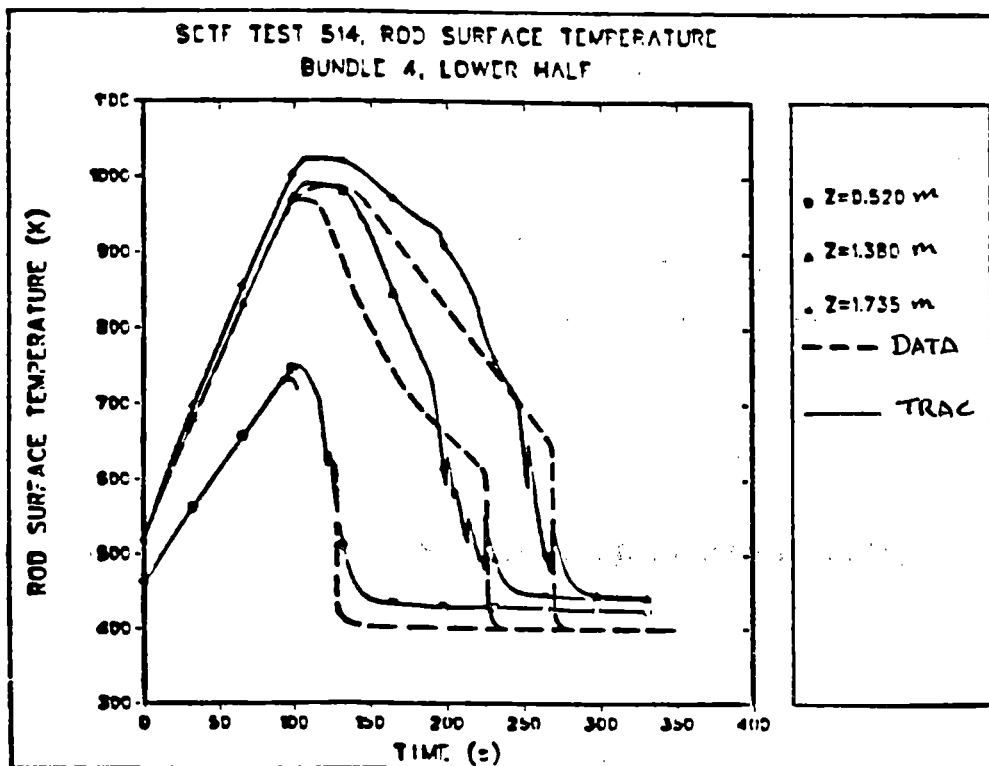
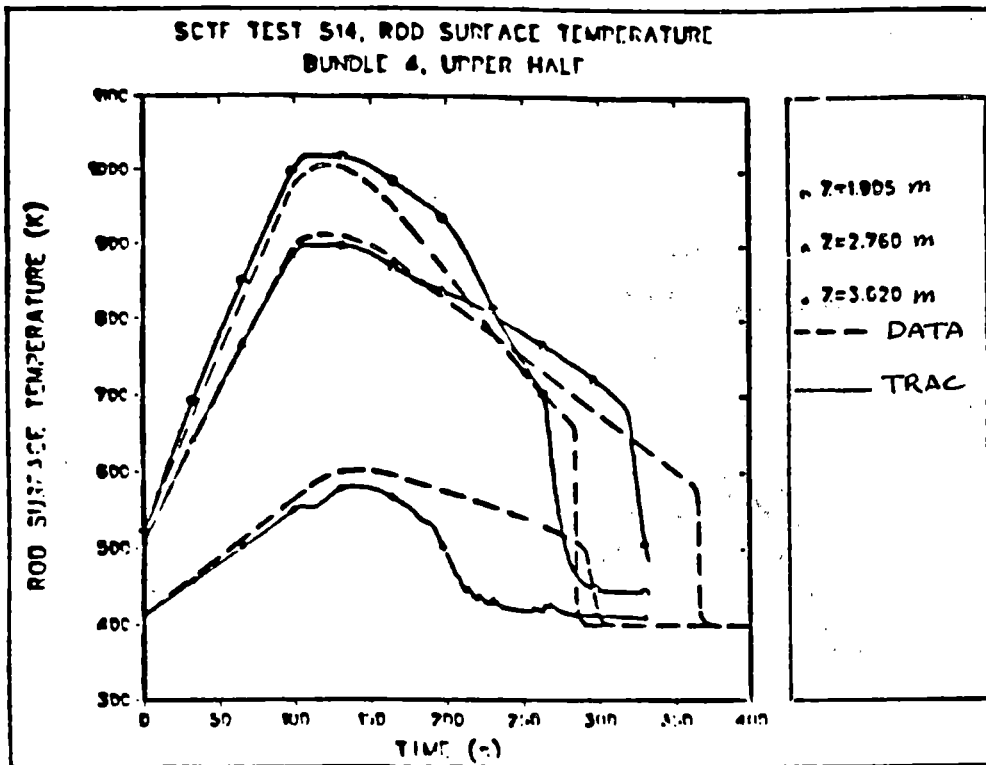
Initial core power distribution for SCTF power effects tests.



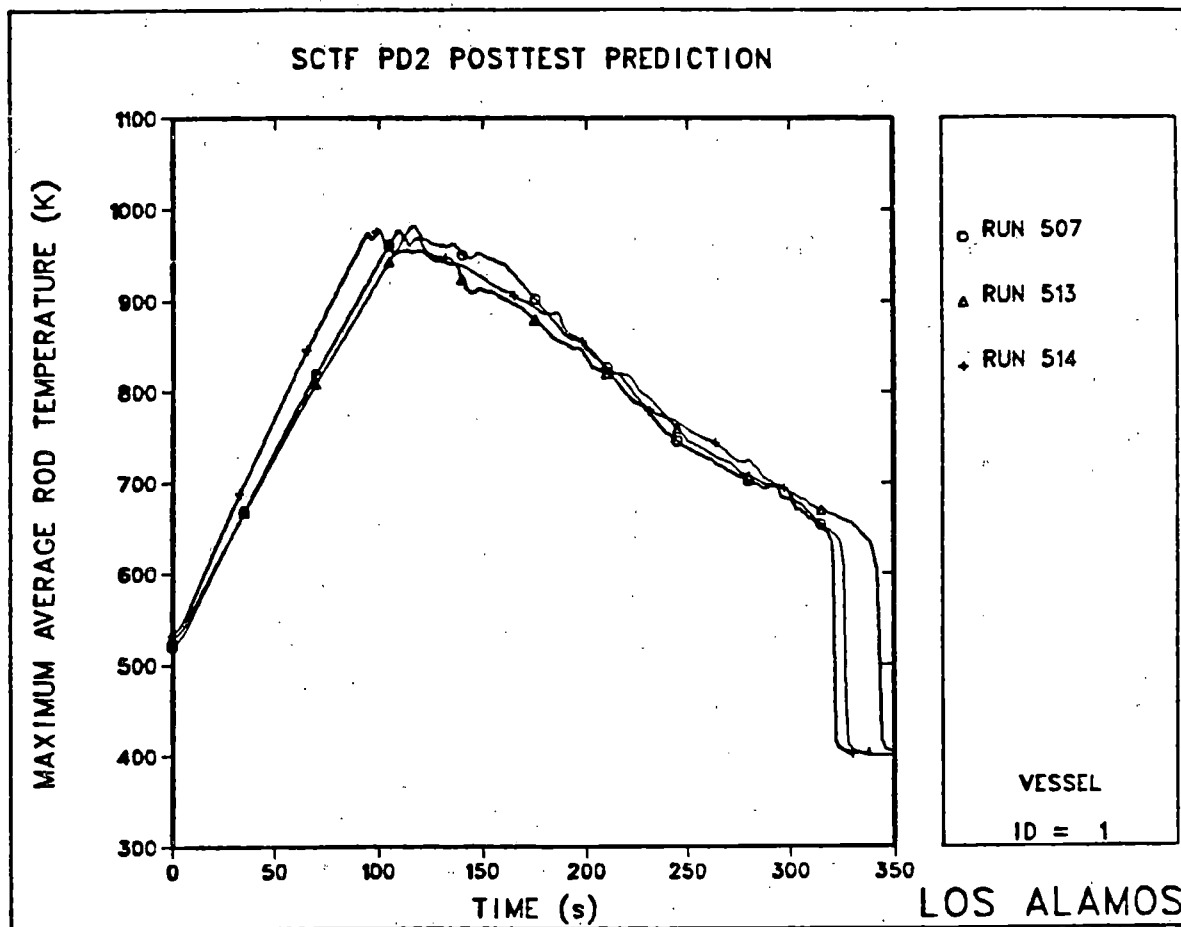
Rod surface temperatures for Bundle 4 of SCTF Run 507.



Rod surface temperatures for Bundle 4 of SCTF Run 513.

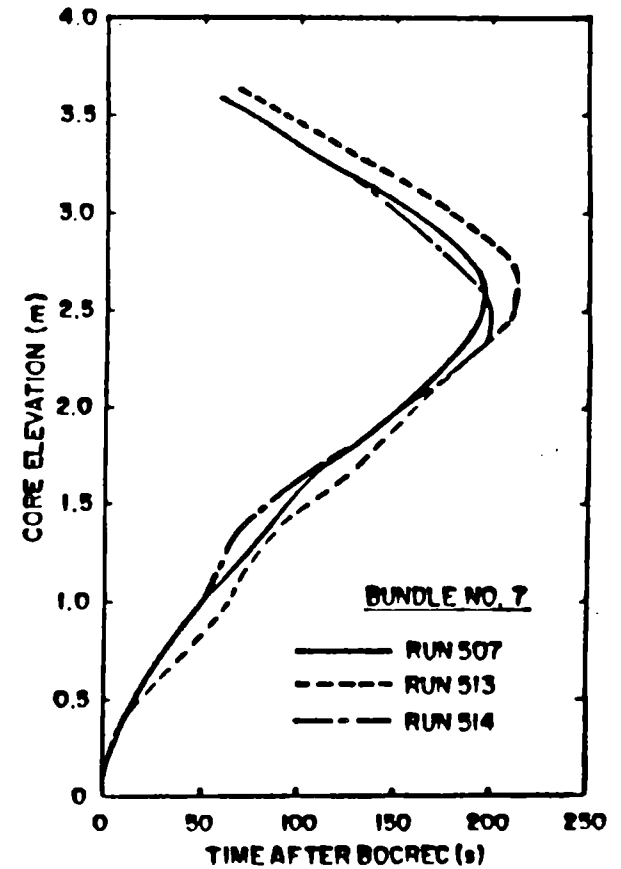
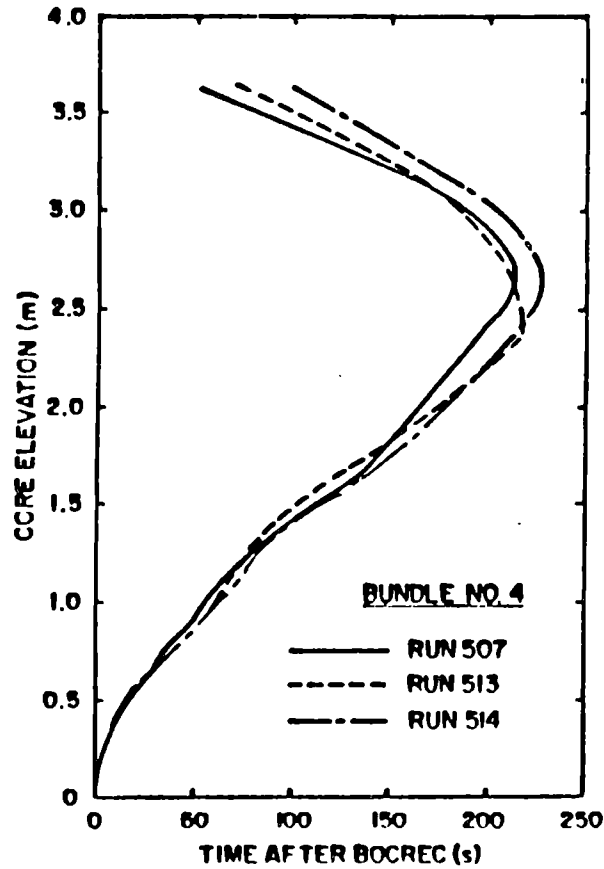
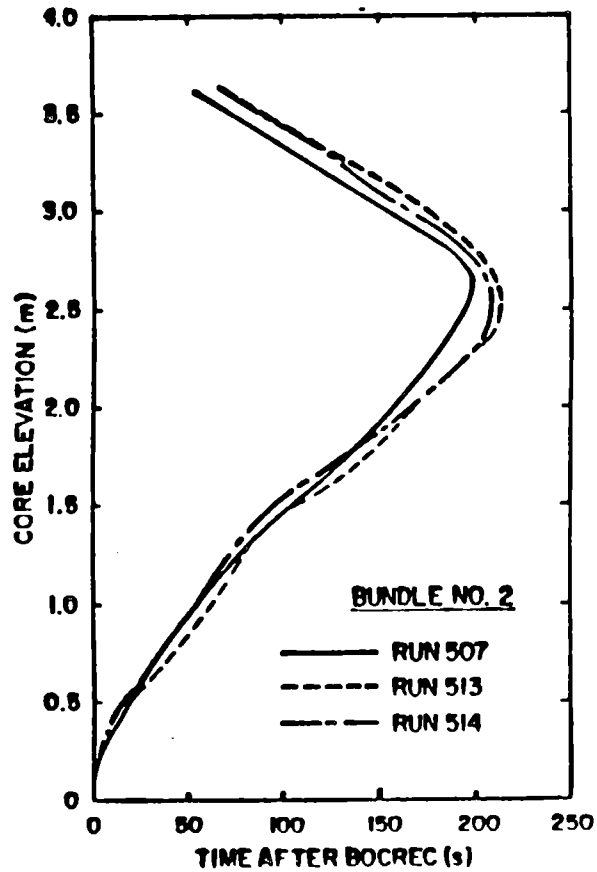


Rod surface temperatures for Bundle 4 of SCTF Run 514.



Maximum rod temperatures for SCTF power-effects tests.

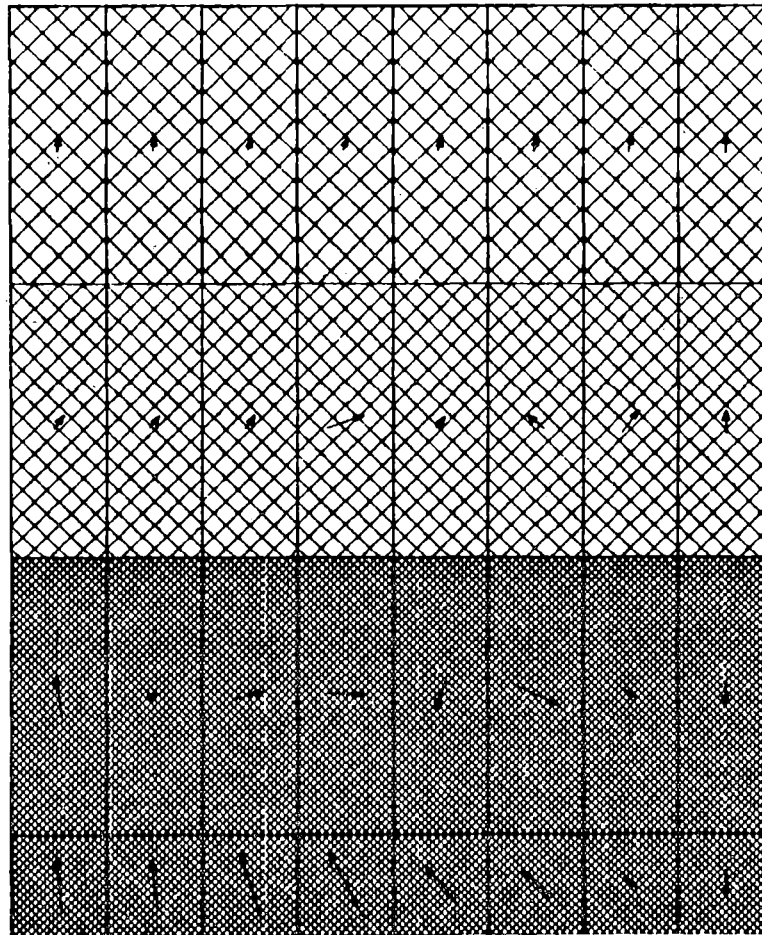
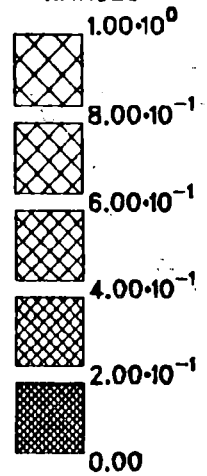




Predicted quench envelopes for SCTF power-effects tests.

SCTF RUN 514 (10/28/81) - LIQUID MASS FLOW

QUANTIZATION  
RANGES



REFERENCE

→  
5.00 kg/s

R = 1 TO 8

Z = 4 TO 7

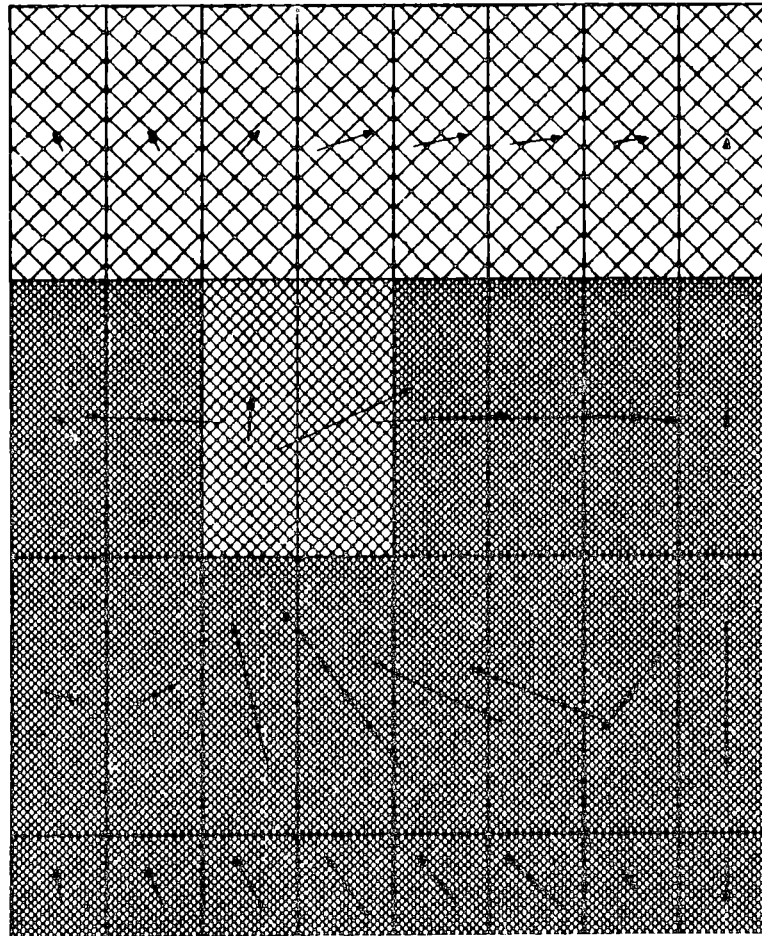
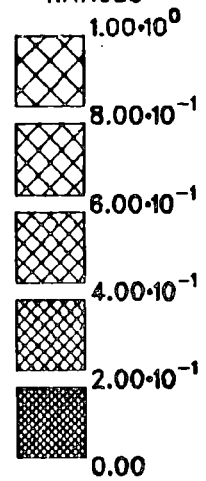
TH = 1

TIME = 150.00s  
20-SECOND MOVING AVERAGE

LOS ALAMOS

SCTF RUN 514 (10/28/81) - LIQUID MASS FLOW

QUANTIZATION  
RANGES



REFERENCE

→  
5.00 kg/s

R = 1 TO 8  
Z = 4 TO 7  
TH = 1

TIME = 200.00s  
20-SECOND MOVING AVERAGE

LOS ALAMOS

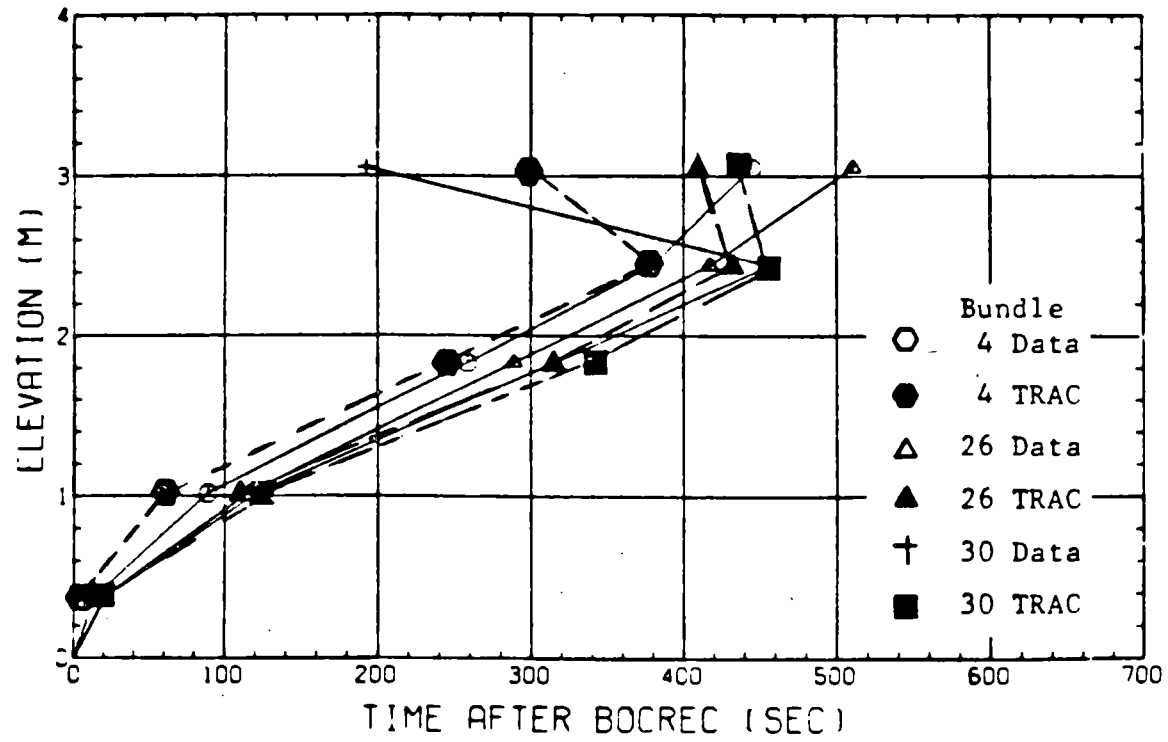
TRAC ANALYSIS OF CCTF RUN38

INITIAL POWER--9.28 MW

LINEAR POWER--1.39 KW/M

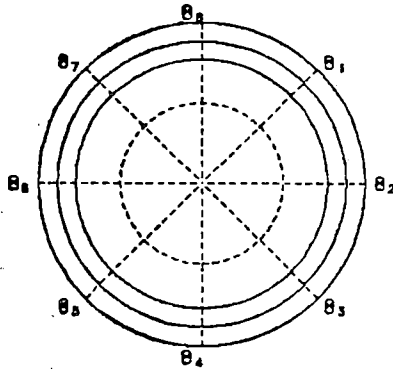
SYSTEM PRESSURE--2.03 BAR

RADIAL POWER SHAPE-1.299:1.092:0.841



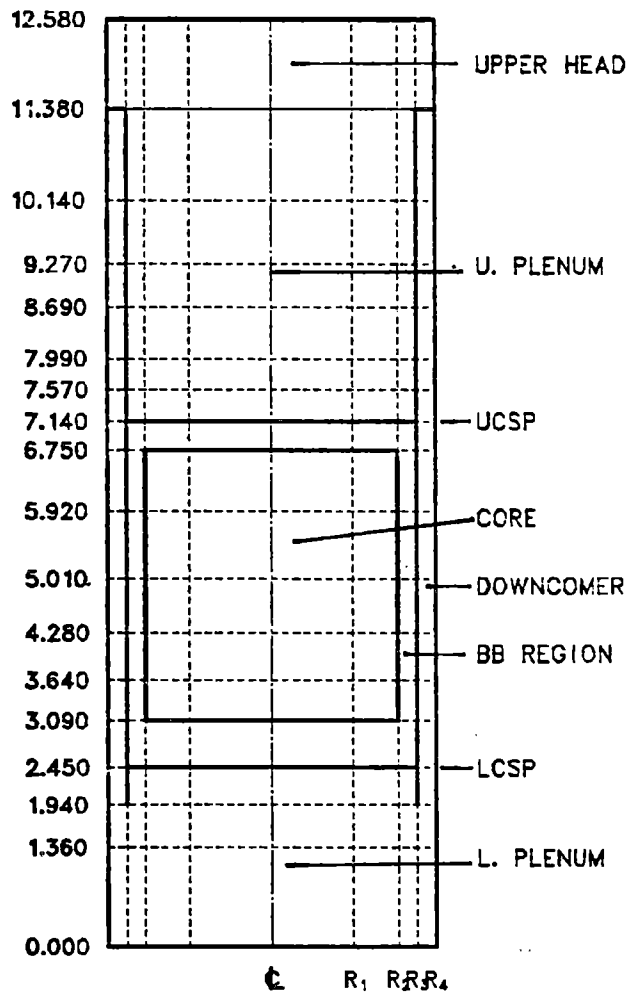
Quench envelopes (CCTF Run 38).

# FULL-SCALE PWR LBLOCA CALCULATIONS

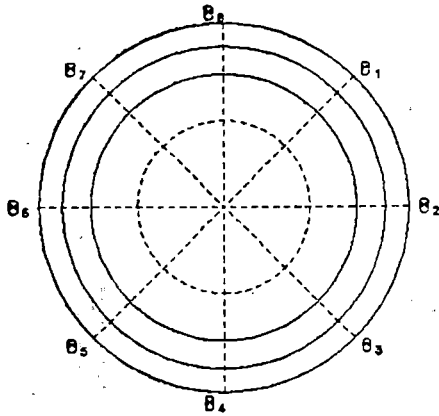


$R_1 = 1.090$   
 $R_2 = 1.690$   
 $R_3 = 1.940$   
 $R_4 = 2.200$

$\theta_1 = 45.0$   
 $\theta_2 = 90.0$   
 $\theta_3 = 135.0$   
 $\theta_4 = 180.0$   
 $\theta_5 = 225.0$   
 $\theta_6 = 270.0$   
 $\theta_7 = 315.0$   
 $\theta_8 = 360.0$

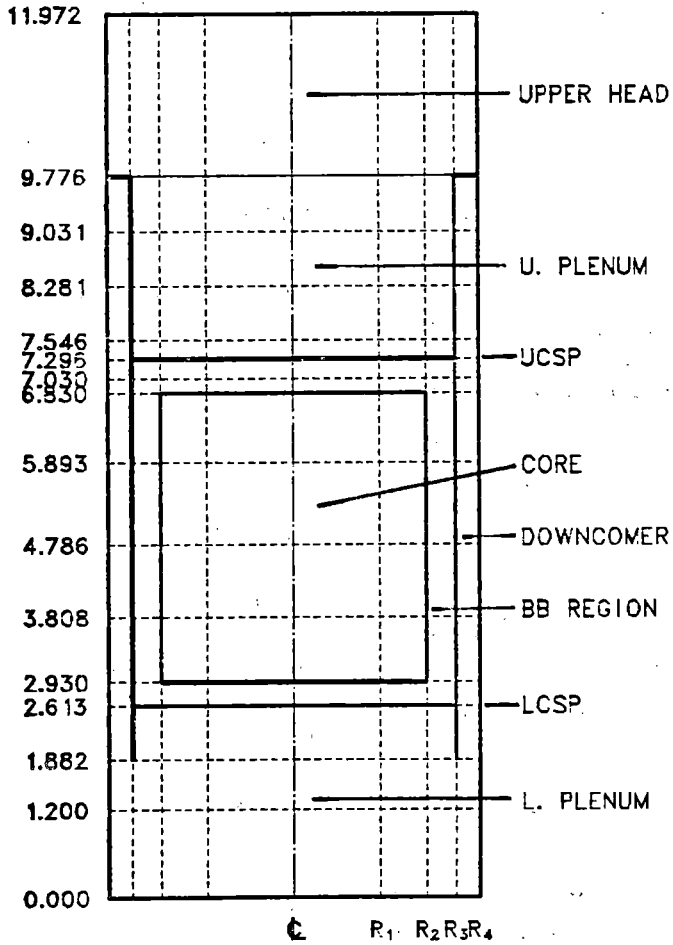


### TRAC MODEL OF US/J PWR



$R_1 = 1.168$   
 $R_2 = 1.803$   
 $R_3 = 2.185$   
 $R_4 = 2.500$

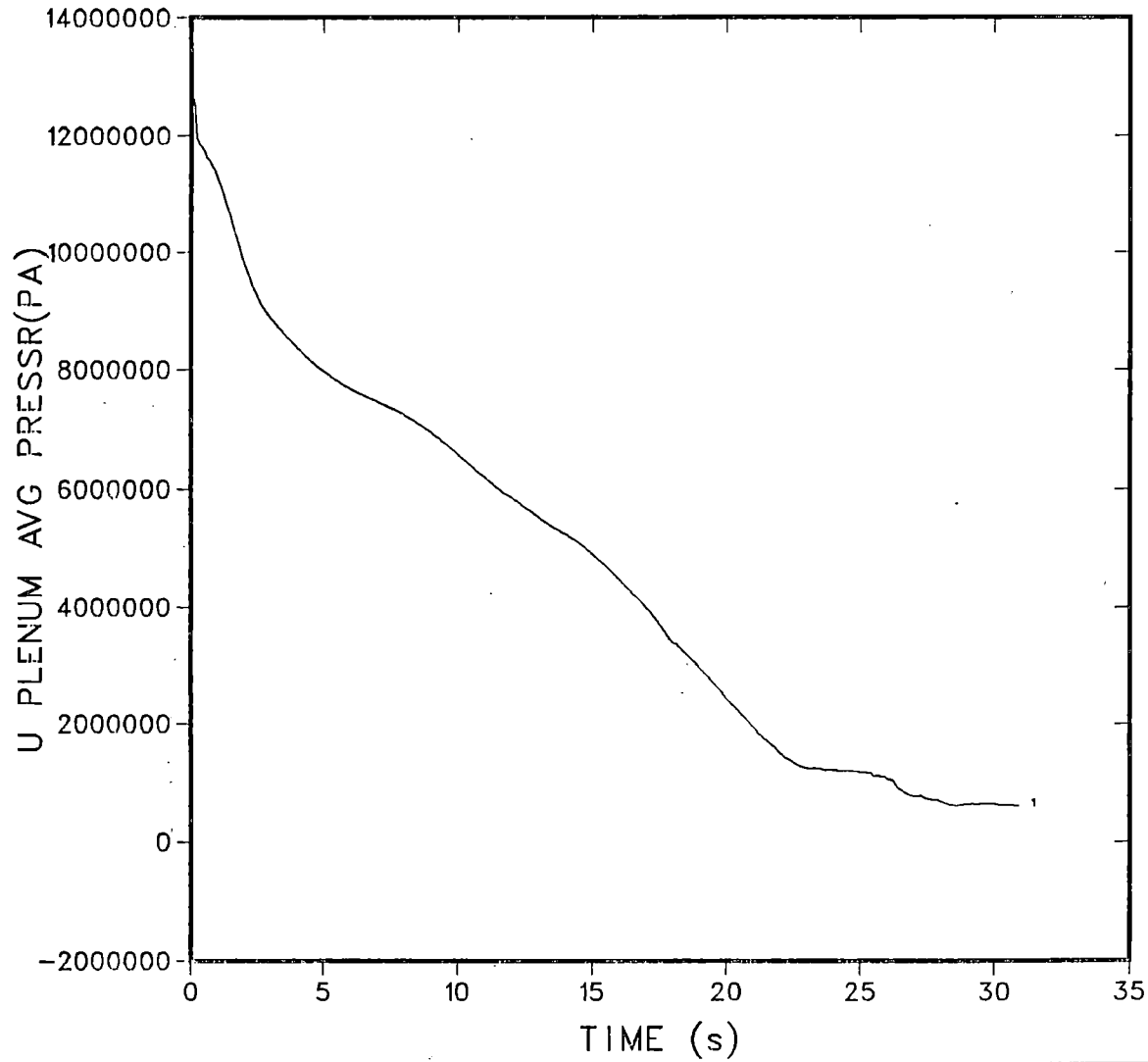
$\theta_1 = 45.0$   
 $\theta_2 = 90.0$   
 $\theta_3 = 135.0$   
 $\theta_4 = 180.0$   
 $\theta_5 = 225.0$   
 $\theta_6 = 270.0$   
 $\theta_7 = 315.0$   
 $\theta_8 = 360.0$



## GPWR VESSEL NODING



GPWR 1982  
TRANSIENT RESTART RUN 1

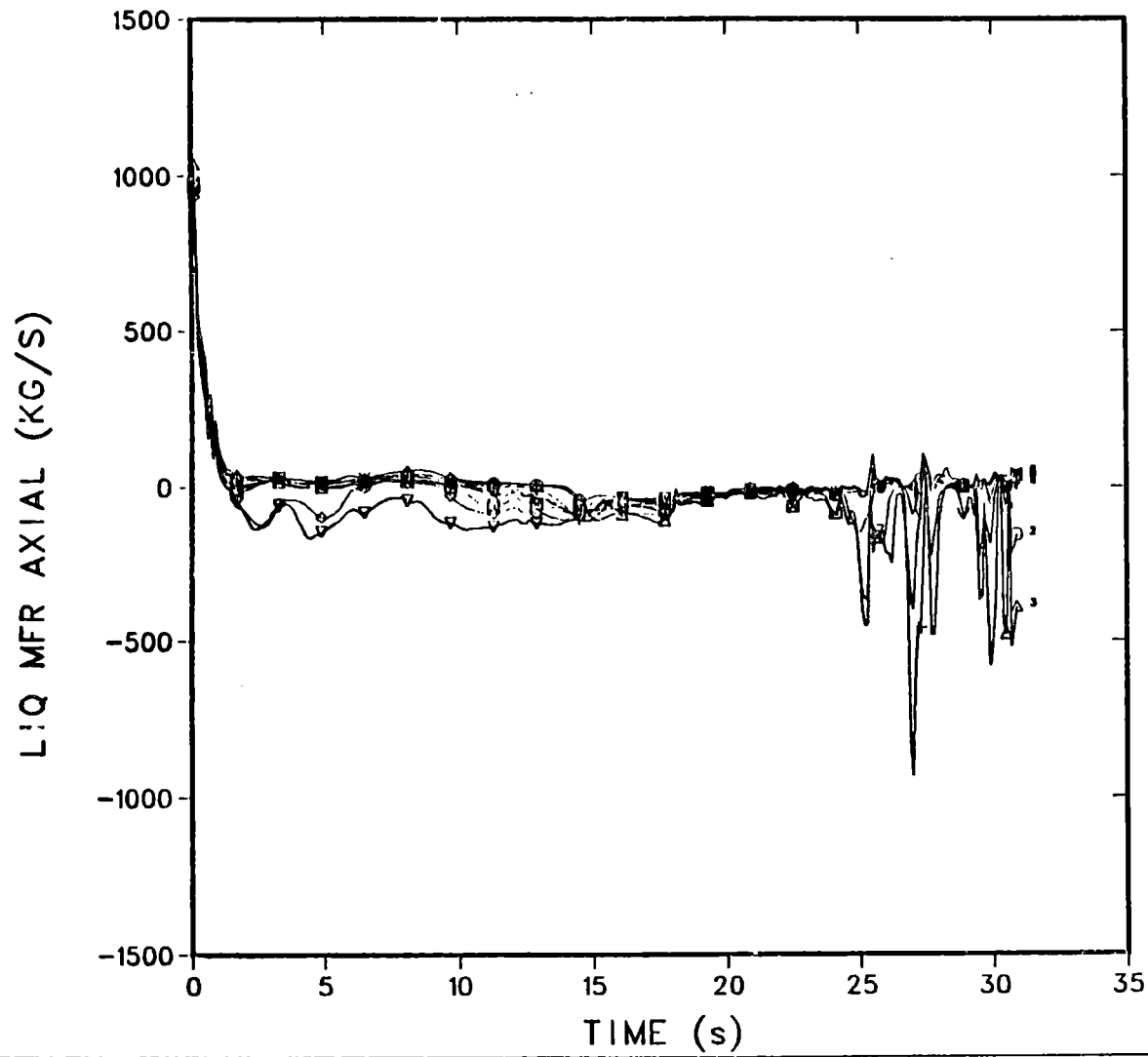


| R | TH | Z |
|---|----|---|
| 1 | 1  | 1 |

VESSEL  
ID = 1

LOS ALAMOS

GPWR 1982  
TRANSIENT RESTART RUN 1

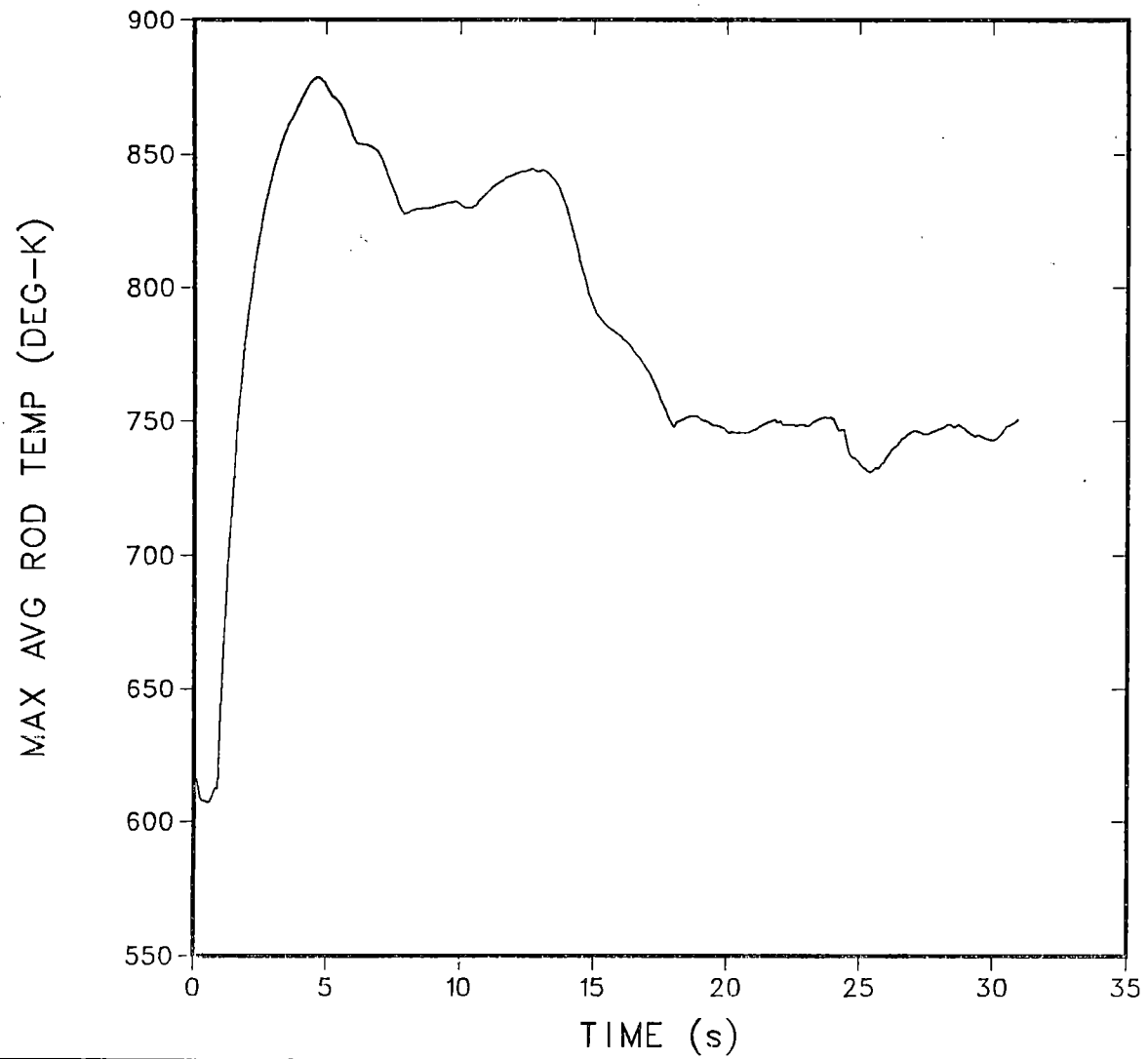


| R | TH | Z   |
|---|----|-----|
| . | 2  | 1 8 |
| o | 2  | 2 8 |
| △ | 2  | 3 8 |
| + | 2  | 4 8 |
| x | 2  | 5 8 |
| ◇ | 2  | 6 8 |
| ▽ | 2  | 7 8 |
| ■ | 2  | 8 8 |

VESSEL  
ID = 1

LOS ALAMOS

GPWR 1982  
TRANSIENT RESTART RUN 1



| R | TH | Z |
|---|----|---|
| 1 | 1  | 1 |

VESSEL  
ID = 1

LOS ALAMOS

# SUMMARY OF ANALYSIS FINDINGS

## RELATED TO LICENSING

Lee Almes

## REACTOR SAFETY ISSUES ADDRESSED BY SCTF ANALYSIS

- MULTIDIMENSIONAL HYDRAULICS MITIGATE SEVERE CONSEQUENCES OF NON-UNIFORM POWER SHAPES AND LOCAL PEAKING.
- IMPROVED UNDERSTANDING OF THERMAL-HYDRAULICS OF CORE REFLOOD IN FULL-RADIUS GEOMETRY.
- THERMAL EFFECT OF 50 PER CENT BLOCKAGES OVER TWO BUNDLES INSIGNIFICANT FOR FORCED REFLOOD CONDITIONS.
- SIGNIFICANT UPPER PLENUM DE-ENTRAINMENT IMPLIES REDUCED STEAM BINDING.

Lee Alamos

## REACTOR SAFETY ISSUES ADDRESSED BY CCTF ANALYSIS

- MULTIDIMENSIONAL HYDRAULICS MITIGATES SEVERE  
CONSEQUENCES OF NON-UNIFORM POWER SHAPES.
- SIGNIFICANT REFLOOD BYPASS OF EXCESS LPCI.
- PRESSURE EFFECTS OF REFLOOD CONFIRMED.
- CORE WATER LEVEL STAGNATES DURING REFLOOD AFTER  
DOWNCOMER FILLS.
- CONDENSATION HEATING OF LPCI REDUCES SUBCOOLING.

Los Alamos

## FULL-SCALE PWR LOCA CALCULATIONS

- **US/JAPAN AND GPWR CALCULATIONS DEMONSTRATE SIGNIFICANT MARGIN OF CONSERVATISM IN LBLOCA LICENSING REQUIREMENTS.**
- **THERMAL-HYDRAULIC PHENOMENA PREDICTED IN LPWR'S CORRELATE WELL WITH 2D/3D EXPERIMENTAL PROGRAM RESULTS.**
- **PEAK CLAD TEMPERATURE OCCUR DURING EARLY BLOWDOWN PHASE WITH BEST-ESTIMATE CALCULATION. PCT LESS THAN 1000 K (1340 F).**

Los Alamos

## TRAC-BD1 CALCULATION FOR TWO-BUNDLE LOOP INTEGRAL RESPONSE

M. Naitoh, T. Matsumoto, M. Murase  
Energy Research Laboratory, Hitachi Co. Ltd.

R. Tsutsumi  
The Tokyo Electric Power Co., Inc.

The two-bundle loop (TBL) facility was constructed to obtain an integral system response during loss-of-coolant conditions in a BWR. The facility consists of two full size electrically heated bundles and two full length jet pumps. TRAC-BD1 is an advanced best estimate computer program for BWR LOCA analysis. This program is used to simulate the Run 106 test data obtained in the TBL. Preliminary results of this activity are given here. Run 106 simulates a guillotine break of the recirculation pipe with an assumption of a low pressure core injection (LPCI) diesel generator single failure. The initial heated power of the two bundles was, respectively, 6MW and 4MW. The TRAC-BD1 vessel nodalization for TBL is shown in Figure 1. Two radial rings, two azimuthal segments and nineteen axial levels were provided in the three-dimensional vessel. Two CHAN components were used to simulate the higher power (6MW) and the lower power (4MW) bundles. Each CHAN contained 18 cells in the axial direction and 4 heater rod groups to describe the thermal radiation. The jet pump was modeled with the five cell JETP component and an extentional PIPE component. The heat transfer between the fluid and the vessel internals and the shroud wall was simulated. The long blowdown line (about 15m), quick opening valve and break nozzle were described by PIPE and BREAK components.

The comparison of calculated and measured steam dome pressure is shown in Figure 2. After 30 sec, the predicted pressure was lower than the data. This was caused by an over calculation of the steam discharge flow from the long blowdown line. In the calculation at about 60 sec, feedwater line flashing occurred. It should be noted the over calculation of steam discharge can only be partially attributed to the code break flow model. A significant portion of the excess flow is believed due to other factors (such as mass distribution errors) which lead to non-prototypical inlet conditions to the break flow model.



The comparisons of calculated and measured rod surface temperature are shown in Figure 3 and Figure 4. In the data, the heat up in the higher power bundle is delayed about 30 sec from that in the lower power bundle. In the calculation, the same result was obtained. It was found that the higher power bundle was cooled by the steam from the lower plenum because of the flow separation effect in the parallel channel. The feed-water line flashing stopped the flow separation. As a result, overall data trends and system behavior were predicted well by TRAC-BD1.

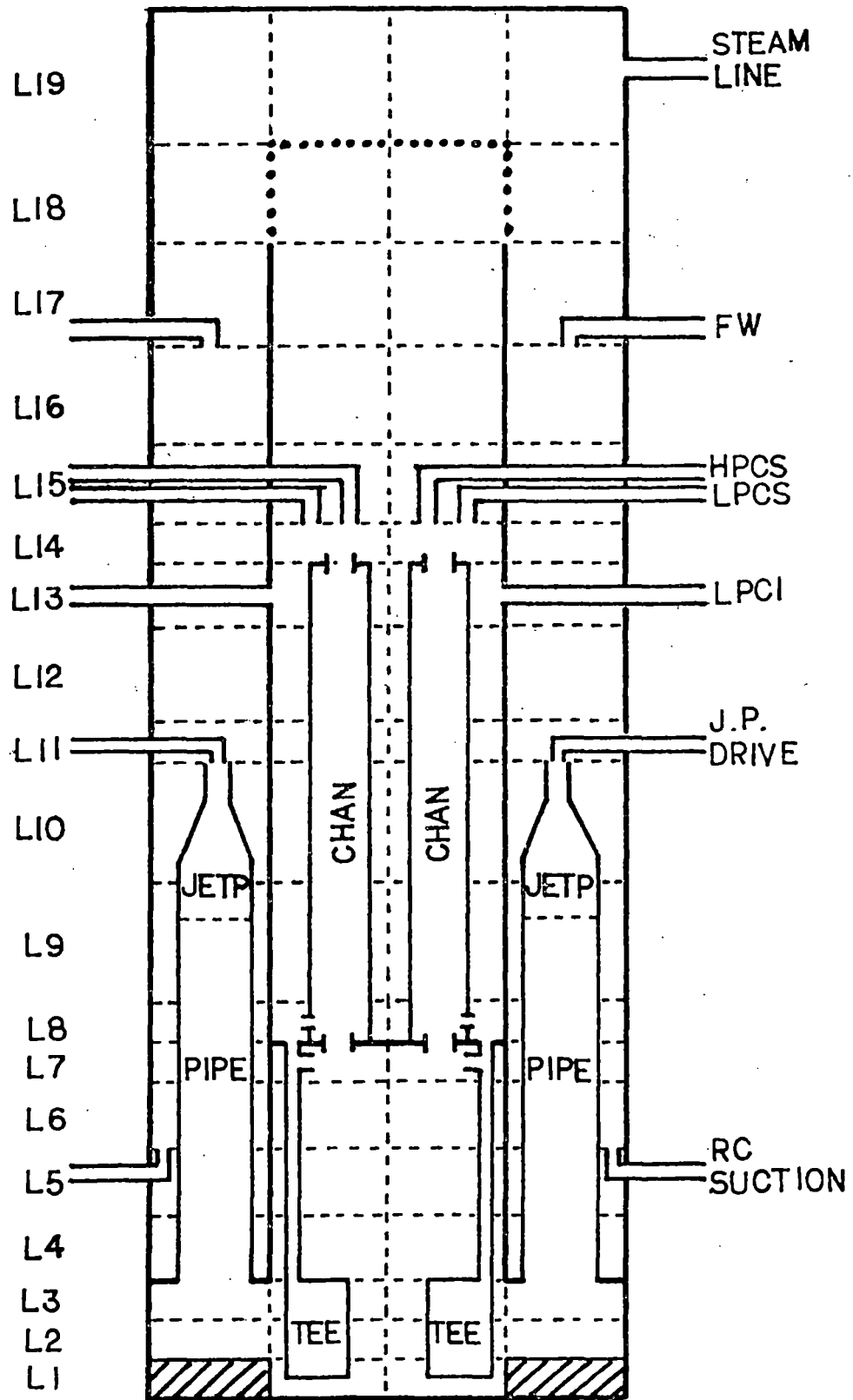


FIG.1 TRAC-BD1 VESSEL MODEL OF TBL1

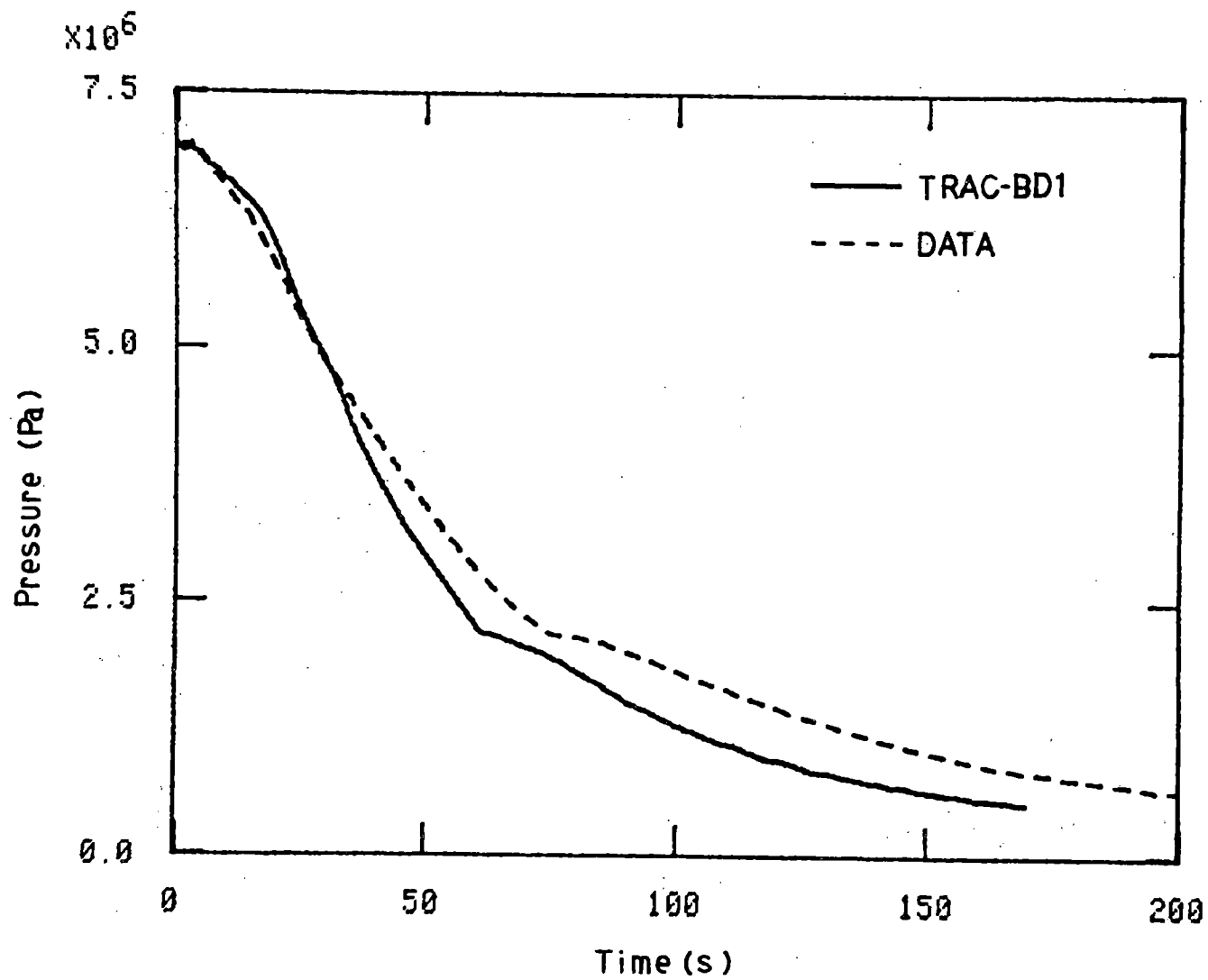


FIG.2 COMPARISON OF STEAM DOME PRESSURE

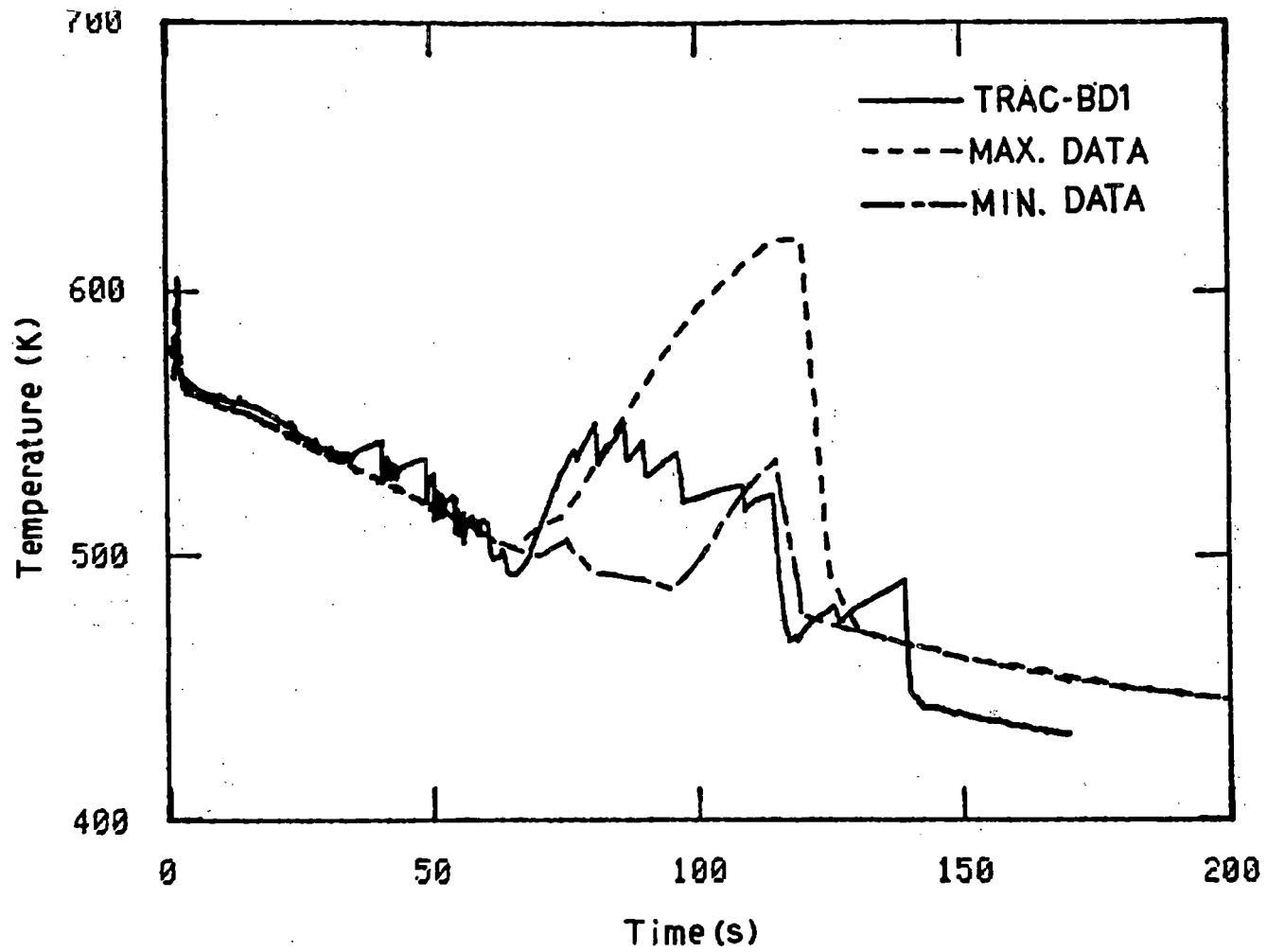


FIG.3 COMPARISON OF ROD SURFACE TEMPERATURE  
IN HIGHER POWER BUNDLE

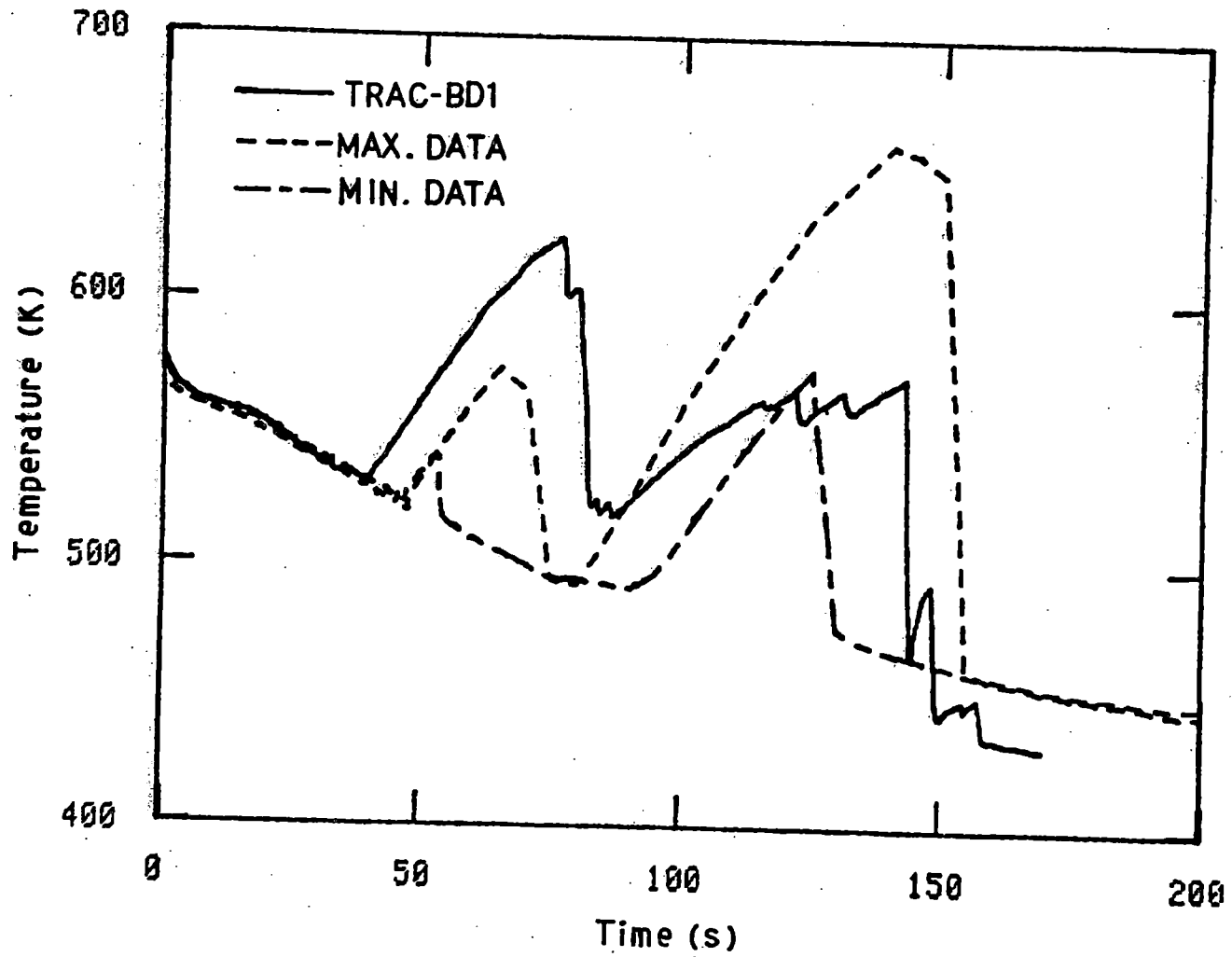


FIG.4 COMPARISON OF ROD SURFACE TEMPERATURE  
IN LOWER POWER BUNDLE

A paper presented at the Tenth Water Reactor Safety Research Information Meeting, October 12-15, 1982, Gaithersburg, Maryland, USA

ROSA-IV Program for the Experimental Study on Small-Break LOCA's and the Related Transients in a PWR

K. Tasaka

Japan Atomic Energy Research Institute  
Tokai-mura, Ibaraki-ken, 319-11, Japan

### Introduction

The emphasis in light water reactor safety research, since the TMI-2 accident, has been on small break loss-of-coolant accidents (SBLOCA's) and transients. The Japan Atomic Energy Research Institute (JAERI) has initiated the Rig of Safety Assessment Number 4 (ROSA-IV) program for study in these areas. The ROSA-IV program consists of the Large Scale Test Facility (LSTF) for system effects tests and the Two-Phase Test Facility (TPTF) for separate effects tests. Experimental results from these facilities will be used to develop and assess a computer code to be used in the analysis of SBLOCA's and transients.

### Scope and Objectives

#### (1) Large Scale Test Facility (LSTF)

LSTF is a large scale (1/48) integral test facility for the study of overall power reactor system behavior during SBLOCA's and anticipated transients. LSTF is designed to explicitly model the major components of the reactor's primary system, secondary system and emergency core cooling system (ECCS). It also models, to the extent required, other plant systems which affect SBLOCA performance (see Fig.1).

The LSTF simulates a 3423 MWt PWR using a 17 x 17 fuel bundle design. The volumetric scale ratio is 1/48 with component elevations maintained at full scale to the maximum extent practicable. Maximum core power is 10 MW which provides the same power input per unit volume as the decay heat core power of the reference PWR below 14% of full power. LSTF has two equal volume active loops, each volumetrically scaled at 2/48, utilizing 207 mm diameter piping. The maximum break size to be investigated will be 10%.

The purpose of LSTF is to provide large scale test data on:

- (a) the effectiveness of the ECCS under SBLOCA and anticipated transient conditions,
- (b) the effectiveness of secondary side cooling via the steam generators (SG's) under SBLOCA and anticipated transient conditions,
- (c) forced and natural circulation cooling in PWR's under various flow regimes and modes of cooling, and the transition from one flow regime or mode of cooling to another,
- (d) the effect of break size and location on system behavior,
- (e) the effect of non-condensable gases on system behavior and
- (f) the effectiveness of alternate system designs and/or operational procedures which are being considered to improve system performance during a SBLOCA and/or plant transient.

The test data, in conjunction with TPTF test data, will be used to develop and verify a SBLOCA computer code model utilizing the RELAP5 computer code.

(2) Two-Phase Test Facility (TPTF)

TPTF is a separate effects test facility for the study of the thermal-hydraulic phenomena in a reactor core, steam generator and coolant system horizontal pipe. The tests to be performed in TPTF will be steady state, two-phase flow experiments. This facility will also be used as a calibration facility for two-phase instrumentation intended for use on LSTF.

TPTF consists of a steam drum for generating high temperature, high pressure steam and water, a steam pump for supplying steam to the test section and a water circulating pump for supplying water to the test section (see Fig.2). The mixture quality will be controlled by changing the flow rates from the steam and water circulating pumps. The maximum water flow rate is 17 kg/s and the maximum steam flow rate is 8.3 kg/s. The maximum pressure and temperature are 12 MPa and 598 K.

The purpose of the TPTF is to provide fundamental thermal-hydraulic data on:

- (a) heat transfer in an uncovered core,
- (b) heat transfer in a SG and
- (c) two-phase flow patterns in a horizontal pipe.

(3) Code Development

In addition to demonstrating the performance of PWR's during SBLOCA's and anticipated transients, the ROSA-IV program will develop and verify a computer code which can accurately model system performance. The computer code is expected to be a two-temperature, two-velocity (2T2V) code and the basis will be the RELAP5 computer code. The results of separate effects testing from TPTF and test results from other sources will be used to modify the basic RELAP5 code as required to provide mathematical correlations and analytical models of the physical phenomena peculiar to long term transients in PWR's. The resulting analytical model will be assessed and verified for accuracy by comparison with test results obtained from LSTF and other integral SBLOCA test facilities (LOFT, Semiscale, PKL, etc.).

Present Status of the ROSA-IV Program

LSTF is now under construction and is scheduled to be completed in November of 1984 with experiments intended to begin at this time.

TPTF was completed in May of 1982. The thermal-hydraulic tests concerning an uncovered core has been started.

Preanalysis with the RELAP5 code is being carried out to help in designing LSTF and determining the test matrix. Comparison of calculated results for a 10% and a 2.5% cold leg break between the reference PWR and LSTF shows relatively good agreement which indicates the LSTF will simulate the overall system performance of the reference PWR.

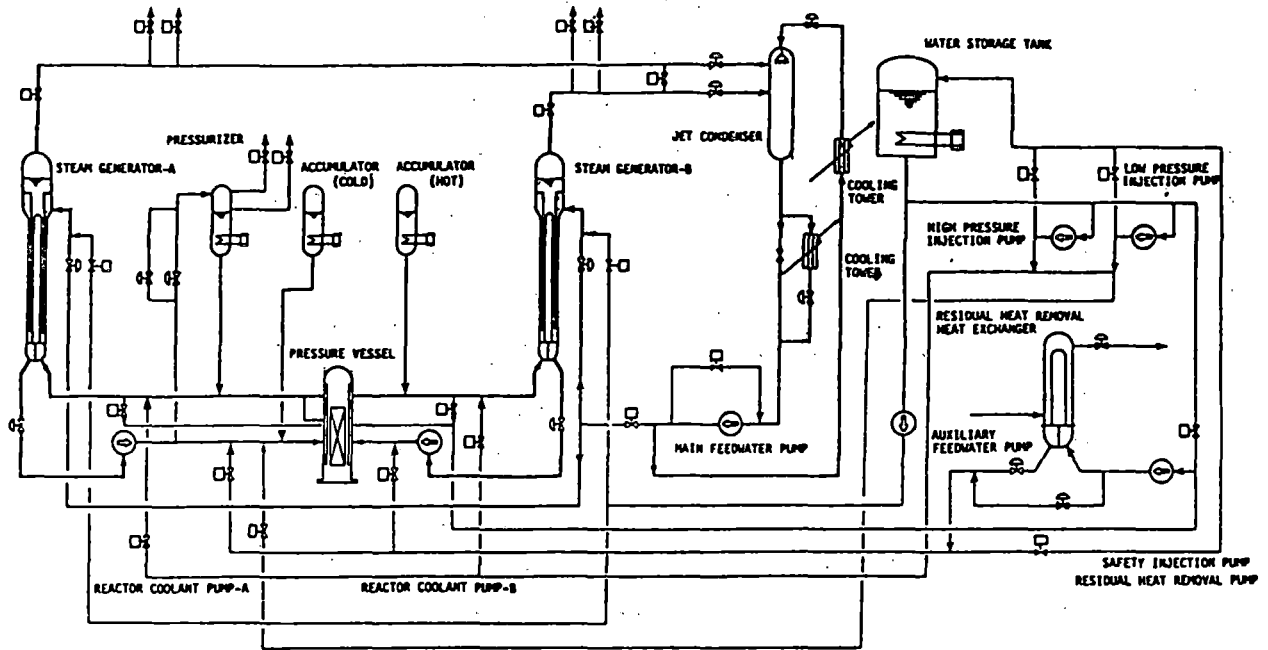


Fig.1 Flow Diagram of Large Scale Test Facility (LSTF).

- D.L : DATA LOGGER
- C : CONDUCTIVITY MEASUREMENT
- D.P : DIFFERENTIAL PRESSURE MEASUREMENT
- F : FLOW MEASUREMENT
- L : LEVEL MEASUREMENT
- P : PRESSURE MEASUREMENT
- T : TEMPERATURE MEASUREMENT

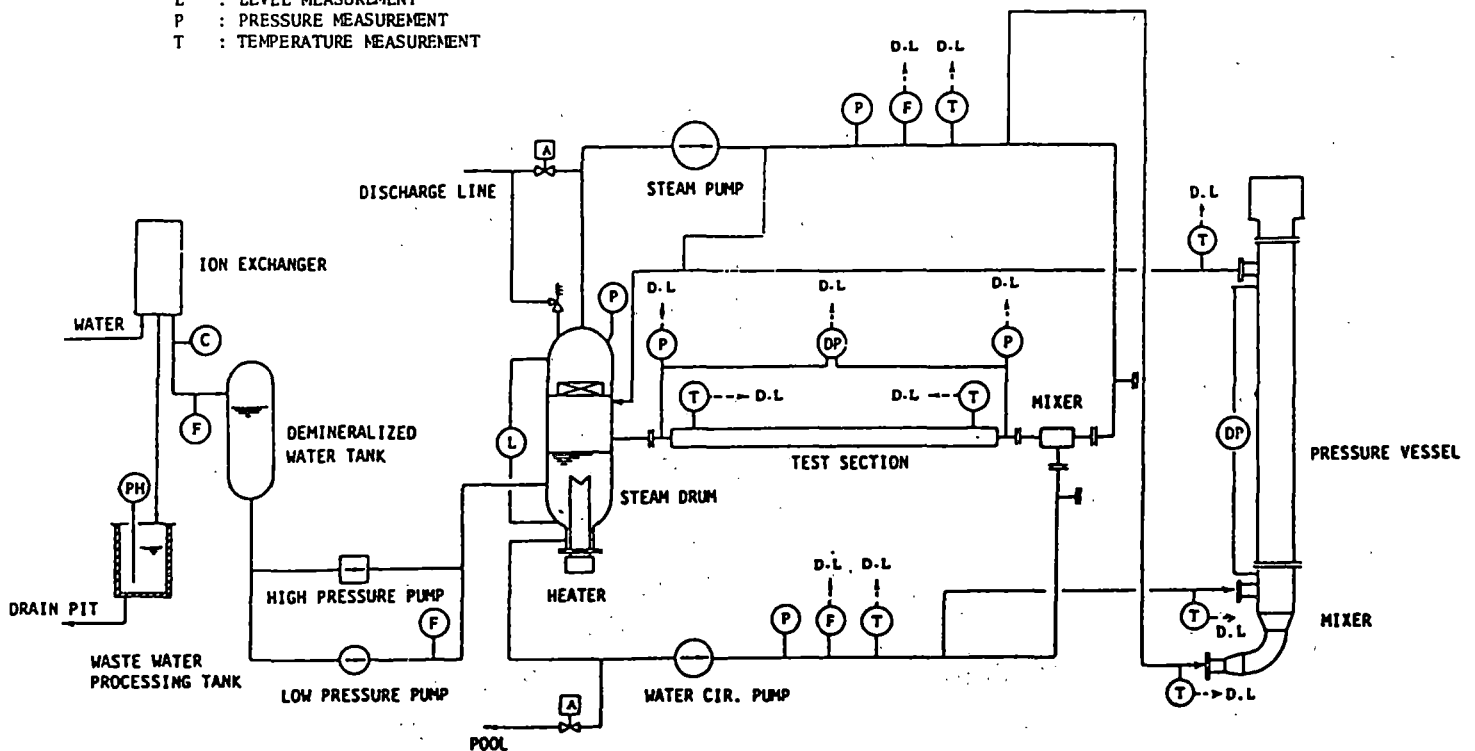


Fig.2 Flow Diagram of Two-Phase Test Facility (TPTF).



## SUMMARY

### TRAC-BD1 Calculation of ESTA Test

N. Abe  
M. Katoh  
H. Nagasaka\*  
H. Aoki\*

Nippon Atomic Industry Group Co., LTD.

\* TOSHIBA Corporation

#### 1. INTRODUCTION

This paper describes analytical results of BWR upper plenum behavior under LOCA using TRAC-BD1 code and comparison with ESTA (Eighteen Degree Sector Test Apparatus) results. TRAC-BD1 is a best estimate system code and features a three dimensional treatment of the BWR pressure vessel and a one dimensional treatment of fuel bundles and pipings. ESTA is the BWR LOCA refill-reflood test facility which mocks up an 18 degrees sector of the BWR with full height from jet pump bottom to standpipe top.

The objective of this study is to verify the predictive capability of the TRAC-BD1 code through the analysis of ESTA saturated CCFL test and subcooled CCFL breakdown tests with special emphasis on multi-dimensional nonequilibrium two phase flow behavior.

#### 2. ANALYTICAL MODEL

For TRAC-BD1 analysis, ESTA was modeled by VESSEL, PIPE, FILL and BREAK components. Pressure vessel was represented by one theta, six radial and seven axial VESSEL component. Fuel bundles were grouped into five radial regions consistent with the measurement locations and modeled by PIPE components. Each fuel bundle PIPE component contained four axial fluid cells and

CCFL condition was checked at the upper tie plate.

TRAC-BD1 uses Kutateladze type correlation for the upper tie plate CCFL. The coefficients of the correlation from ESTA multi-bundle saturated CCFL tests were directly used.

### 3. ANALYTICAL RESULTS AND DISCUSSION

Analyses of ESTA saturated CCFL test and subcooled CCFL breakdown tests were performed by using the TRAC-BD1 code with special emphasis on how TRAC-BD1 can predict multi-dimensional nonequilibrium two phase flow behavior in the upper plenum associated with CCFL and CCFL breakdown at the upper tie plate.

#### 3.1 Saturated CCFL test

The analysis was performed to check the CCFL model of the TRAC-BD1 code for multi-bundle saturated CCFL phenomena. Good agreement between measured and predicted CCFL characteristics indicated that TRAC-BD1 can calculate CCFL phenomena at the upper tie plate.

#### 3.2 Subcooled CCFL Breakdown Tests

ESTA subcooled CCFL breakdown tests were analyzed in order to investigate how TRAC-BD1 can predict the effect of spray temperature on CCFL breakdown. Spray temperature was changed from 303 (K) to 343 (K). Upper plenum was initially filled with two phase mixtures.

Analytical results showed that for higher spray temperature conditions, the continuous CCFL phenomena occurred at the peripheral bundles as well as the central bundles after spray initiation. For lower spray temperature conditions, upper tie plate temperature in the peripheral bundles became subcooled enough to condense upflow steam after spray initiation. As a result, remarkable CCFL breakdown occurred at the peripheral bundles. The other central bundles still remained in CCFL

conditions. These analytical results agreed with ESTA tests qualitatively.

However, calculated fluid temperature profile in the upper plenum was slightly different from the experimental data due to insufficient modeling of the momentum source term to vessel.

#### 4. CONCLUSION

- (1) TRAC-BD1 well predicts multi-bundle saturated CCFL characteristics at the upper tie plate.
- (2) TRAC-BD1 can predict multi-dimensional nonequilibrium two phase thermal hydrodynamic behavior associated with CCFL breakdown at the upper tie plate. TRAC-BD1 also can analyze the effect of spray temperature on CCFL breakdown qualitatively.
- (3) The modeling of the momentum source should be improved to obtain better agreement.
- (4) ESTA tests are useful for the verification and qualification of TRAC-BD1 thermal hydrodynamic models.

THE CATHARE CODE AND ITS  
QUALIFICATION ON ANALYTICAL EXPERIMENTS  
G. HOUDAYER<sup>\*</sup>, J.C. ROUSSEAU<sup>\*\*</sup>, B. BRUN<sup>\*\*\*</sup>

ABSTRACT

OBJECTIVE

CATHARE is an advanced safety code developed by CEA, EDF and FRAMATOME to simulate LOCA on PWR (large and small breaks). It is being done by a joint team (in Grenoble) which is in charge of the experiments analysis, modelling, code writing and assessment.

Associated with code development, an experimental program is performed to study the phenomena occurring during LOCAs. The experimental results are used to qualify and verify the code. The code has to combine and transpose the phenomena occurring in the reactor and then allows safety studies at reactor scale.

CHARACTERISTICS OF CATHARE

CATHARE contains a modelisation of the primary circuit (flow - heat transfers in the walls, in the fuel, in S.G. - oxidation, swelling and rupture of the cladding - power in the core - pumps...).

The thermal and mechanical non-equilibrium must be taken into account (critical flows, cold water injection, stratified flows ...) Therefore the two fluid model was chosen.

---

\* EDF/SEPTEN/EMM - Centre d'Etudes Nucléaires de Grenoble

\*\* CEA/STT/EMM - Centre d'Etudes Nucléaires de Grenoble

\*\*\* CEA/STT/EMA - Centre d'Etudes Nucléaires de Grenoble

The volumes (upper and lower plena, pressurizer, ...) are described with a two-node model (with stratification, entrainment and deentrainment).

CATHARE has a modular structure : the circuit components are simulated by different combinations of elements (1D flow, volume, fuel, wall, grids of transfer laws...) ; any topology can be described.

The 1D flow model is discretized with a staggered mesh scheme. Two options (semi-implicit, fully implicit) can be indifferently used at any time for each 1D component.

A direct method is used to achieve the initial steady state (with the same model).

Then the reactor code can simulate any experiment (transient or steady-state, with or without heat flux, analytical or system tests...).

The grids of transfer laws cover all the needed range of parameters. They contain the synthesis of knowledge from experiments.

#### QUALIFICATION AND VERIFICATION

Our concern is to find out a set of physical laws consistent with the experimental data.

To reach this goal, the data are issued from two different classes of experiments :

- analytical tests from which correlations or models can be found out : this is the qualification of the code
- global tests (ex : system tests) where many phenomena are involved, or where the transient is fast or complex. These tests are needed to verify the code. These verifications give an evaluation of the code accuracy (on complex systems) and may suggest new qualification works.

## QUALIFICATION OF THE CODE

All the correlations, characteristic curves or transfer laws of the models must be found out from the analytical and separate-effect tests :

- transfer laws describing the flow  
(momentum and mass transfers)
- heat transfers at the wall  
(blowdown and reflooding)  
(core and S.G.)
- correlations for specific components
  - pumps
  - upper and lower plena  
(entrainment-deentrainment-stratification)
  - junctions (phase separation)

The work is under progress on the different points and can be illustrated by the determination of momentum and mass transfer laws.

The momentum transfer grid was determined using existing correlations (drift flux, stratification limit, annular flows, and using experimental data from :

- . MOBY DICK air water critical flow test
- . DADINE (void fraction and pressure line measurements in reflooding conditions)
- . REBECA (critical mist flow)
- . ECTHOR (stratification in a U-pipe)

The grid will be improved with further results from SUPER MOBY DICK (flow study, low velocity, high pressure, vertical and horizontal pipe).

The mass transfer law has been elaborated using data from MOBY DICK and SUPER MOBY DICK (critical flow, low and high pressure) and from MARVIKEN CFT.

CANON experiment (blowdown of a pipe  $\phi = 10$  cm,  $L = 4$  m) is a simple global experiment which covers a wide range of parameters. It is used as a first verification of the flow modelisation. Results are good on large breaks but give some discrepancy on small breaks. Sensitivity studies are performed to determine the qualification improvements which have still to be done.

Models elaboration is indeed, an iterative process on all the experimental results, which generates successive "revisions" of the grids. Each new revision must be compared with a check list of experiments (representative of all the experimental results). Comparison of calculated results with these tests gives an estimation of the quality and progress of the qualification.

Revision 1 has already been done. Improvements (revision 2) are being prepared for the first operational version of CATHARE.

#### STATUS AND DEVELOPMENTS

A first version of CATHARE is now completed and is under debugging. It will be operational next year for reactor calculations : two first runs on reactor (large and small breaks) are under way.

Then a systematic verification on system experiments will start. This verification will be done without any tuning of the code : if some improvements are needed they will be studied for a further version of CATHARE.

Meanwhile new modules are being prepared (1D-2 $\phi$  pump, 2D downcomer, detailed S.G., non condensable gaz ...) to be introduced in CATHARE. This new version of CATHARE will be, also, verify on system experiments.

NEPTUN BUNDLE BOIL-OFF AND REFLOODING  
EXPERIMENTAL PROGRAM RESULTS

Presented by S.N. Aksan  
Safety Division, Swiss Federal Institute  
for Reactor Research (EIR)  
5303 Wuerenlingen, Switzerland

The NEPTUN test facility is located at the Swiss Federal Institute for Reactor Research (EIR) in Würenlingen, Switzerland. This project is performed within the framework of an agreement between U.S. Nuclear Regulatory Commission (NRC) and Swiss Federal Office of Energy as participation in International Energy Agency (IEA) safety research projects.

The NEPTUN system as described in reference 1 was initially designed to provide data from low pressure (<5 bar) reflood experiments investigating heat transfer from rod to coolant and the thermal-hydraulic response of the cooling water in a pressurized water reactor (PWR) core. In addition to reflooding experiments, core uncovering (boil-off) experiments to investigate the mixture decrease and resulting fuel rod heatup above the mixture level that may occur in a PWR during a small break loss-of-coolant accident (LOCA) have been performed in the NEPTUN test facility. The reflooding and boil-off experimental data obtained from NEPTUN facility is going to be used in assessing the models developed and may also lead to new model development. The specific objectives of the tests are also related to Loss of Fluid Test (LOFT) data needs. These objectives special interest to LOFT are:



- To obtain electric rod reflood data applicable to LOFT for assessing reflood models.
- To develop and verify heat transfer and fluid carry-over correlations to be used in the above models.
- To obtain data characterizing LOFT core uncover response during a small break loss of coolant experiment.
- To evaluate the accuracy and selective cooling effects of the LOFT cladding-surface thermocouples under reflood and small break core uncover conditions.
- To obtain information on electrical heater rod versus nuclear fuel rod performance during reflood and boil-off conditions.

The NEPTUN system configuration is shown in figure 1. The PWR core is simulated in NEPTUN by a rod bundle containing 33 electrically heated rods and 4 guide tubes. The heater rod bundle cross-section is shown in figure 2. Each heater rod has radial and axial dimensions similar to the LOFT fuel rods, and the heater rod bundle uses typical LOFT fuel assembly spacer grids, axially located identically to LOFT (figure 3). The design of the NEPTUN heater rod allows a continuously variable axial power profile similar to that of LOFT, as shown in figure 4. The main characteristics of the NEPTUN system are:

|                           |                                       |
|---------------------------|---------------------------------------|
| Number of heater rods     | 33                                    |
| Number of guide tubes     | 4                                     |
| Heater rod length         | 1680 mm, corresponding to LOFT        |
| Heater rod outer diameter | 10.72 mm, " " "                       |
| Rod square pitch          | 14.30 mm, " " "                       |
| Spacer                    | grid-type, original LOFT              |
| Power distribution        | chopped cosine, corresponding to LOFT |
| Axial peaking factor      | 1.58 " " "                            |
| Max. linear power rate    | 3.94 KW, simulating decay heat        |
| Max. coolant flow         | 0.65 kg/s                             |

|                            |   |
|----------------------------|---|
| Flooding rate              | 2 to 15 cm/s  |
| Flooding water temperature | 20 to 147 °C  |
| System pressure            | 1 to 5 bar  |
| Initial clad temperature   | up to 900 °C  |
| Thermocouples              | Max. 8 per rod embedded in the clad, additionally there is only one active LOFT thermocouple on each of the five rods with surface thermocouples; the other cladding-surface thermocouples are "dummy" segments (figure 2). |

The instrumentation allows the measurement of cladding, housing, thermal insulation and coolant temperatures, absolute and differential pressures at several axial levels, flow rates, carry over rates and heating power. Further details on NEPTUN test facility is described in reference 1.

The first series of experiments performed in NEPTUN were boil-off tests. This experiment series consisted of eleven experiments consisting of ten boil-off and one adiabatic heat-up tests and summarized in figure 5. Three parameters were varied: rod power, system pressure and initial coolant subcooling. Rod power levels were chosen to represent the nuclear decay power over a range of time as shown in figure 6. System pressure was varied over the 1 to 5 bar range possible in the NEPTUN facility. Experiment repeatability was also tested for both high and low pressure conditions and the system was found to be very repeatable. Experiment numbers 5007 (base case) and 5011 are taken as basis for power levels corresponding to small and intermediate break LOCA decay heat levels, respectively. Therefore, the plots of these experimental results for these two cases will be presented in this paper. Figure 7 presents an overlay of the core power history, core fluid level as measured by the core total  $\Delta p$  measurement and typical responses of the heater rod thermocouples for

the base case. In these experiments, the effects of the surface thermocouples are determined by comparing the cladding temperature (as measured by the LOFT thermocouples) to cladding temperature measurements from thermocouples within the cladding of the NEPTUN heater rod. Overlay plots of the thermocouple responses at a level corresponding to maximum power position on the heaters are shown in figures 8 and 9 for experiment no 5007 and 5011 respectively. As expected, increased core power resulted in more rapid boil-off and cladding heatup. Comparison of base case with low pressure experiments indicate that the lower system pressures result in more rapidly decreasing liquid levels and rod dryouts ranging from 100 - 200 s earlier. As it can be noticed in figures 8 and 9 the LOFT thermocouple is well within the response spread of the internal thermocouples. Dryout times of the internal and external thermocouples were consistent within 10s at any axial elevation. The cladding surface thermocouples measure the true cladding temperatures to within 0 to 20 K for the NEPTUN experiments covering the power levels corresponding to small and intermediate break decay heat levels.

The test matrix for the NEPTUN reflooding experiments is given in figure 10. Total of 29 reflooding tests will be performed. In these tests, the rod power, inlet subcooling, system pressure and flooding rate are the varying parameters. Thirteen tests have already been performed and the rest of the tests will be completed by the end of 1982. In these reflooding tests, NEPTUN bundle with LOFT surface cladding thermocouples is used. The NEPTUN reflooding tests completed till today were performed at 2.3 kw/m peak power, 4.1 bar pressure and 78<sup>0</sup>C subcooling for flooding water. Initial cladding temperature and flooding rate in these tests were varied, as seen in figure 10. Experimental data plots for three different reflooding test are given in figures 11 through 18. The progression of quench front in axial direction is seen from figures 11 to 14. The heater element instrumented with LOFT surface thermocouples gets preferential cooling both from bottom and top and quenches earlier than the other heater rods with embedded ther-

thermocouples. This effect is more pronounced at levels higher than maximum power level (level 4). Figures 15 to 18 shows the temperature histories for low and high flooding rates with different maximum cladding temperatures. The preliminary evaluation of the NEPTUN reflooding data indicates that the LOFT external surface thermocouples have some effect during reflooding. Peak cladding temperatures are reduced about 30-40°C and quench times are 20-70 seconds earlier than rods with embedded thermocouples. Further evaluation of the NEPTUN reflooding data is in progress.

The analysis work both for NEPTUN boil-off and reflooding experimental data have been started. RELAP4/MOD6 and TRAC-BD1 reflooding calculations using NEPTUN data are underway. TRAC-BD1 level tracking and reflooding models will be assessed with NEPTUN data.

#### REFERENCES

1. H. Grütter, F. Stierli, S.N. Aksan, G. Varadi: "NEPTUN Bundle Reflooding Experiments: Test Facility Description" EIR-Report No. 386, March 1980.
2. S. Güntay, L. Nielsen, F. Stierli: "NEPTUN: Information About the Boil-off Experiments" AN-32-81-22 (EIR Internal Report), 20.8.1981.
3. E.L. Tolman, S.N. Aksan: "Summary Results of the NEPTUN Boil-off Experiments to Investigate the Accuracy and Cooling Influence of LOFT Cladding Surface Thermocouples" EGG-LOFT-5554, October 1981.
4. S.N. Aksan: "International Standard Problem (ISP) Proposal: NEPTUN Boil-off and Reflooding Tests" Presented at Ninth Meeting of CSNI Working Group on Emergency Core Cooling and Fuel Behaviour, at IAERI Tokai-Mura, Japan, May 24-28, 1982.

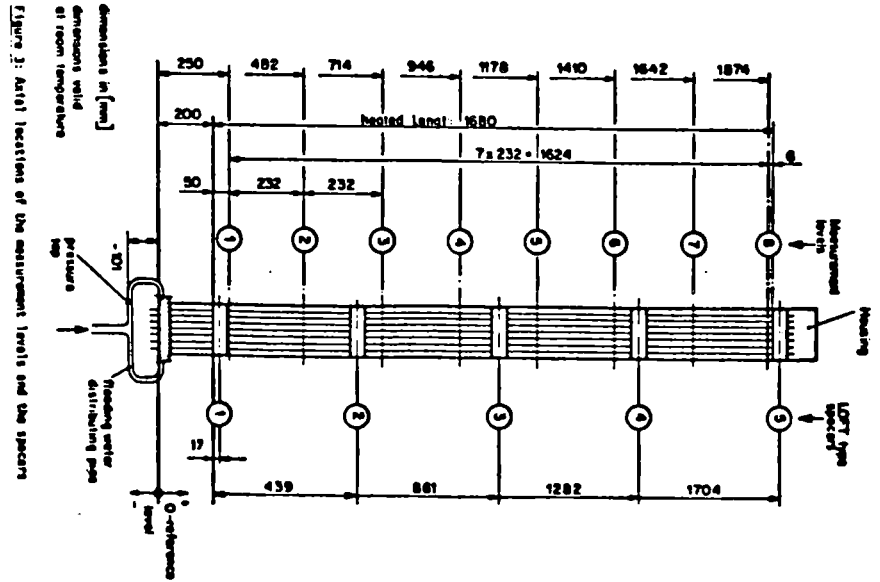
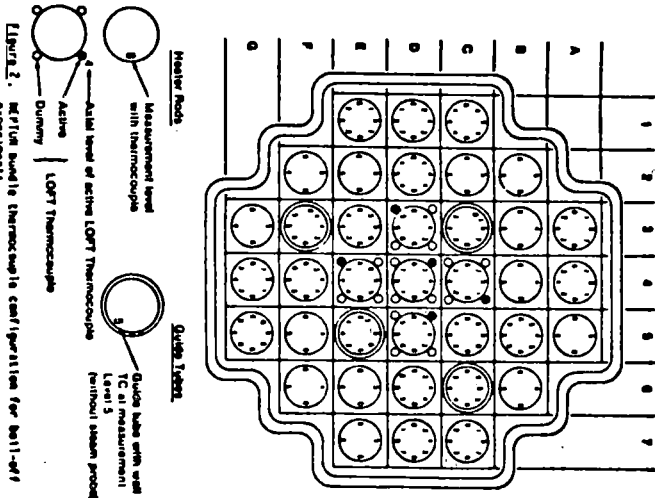
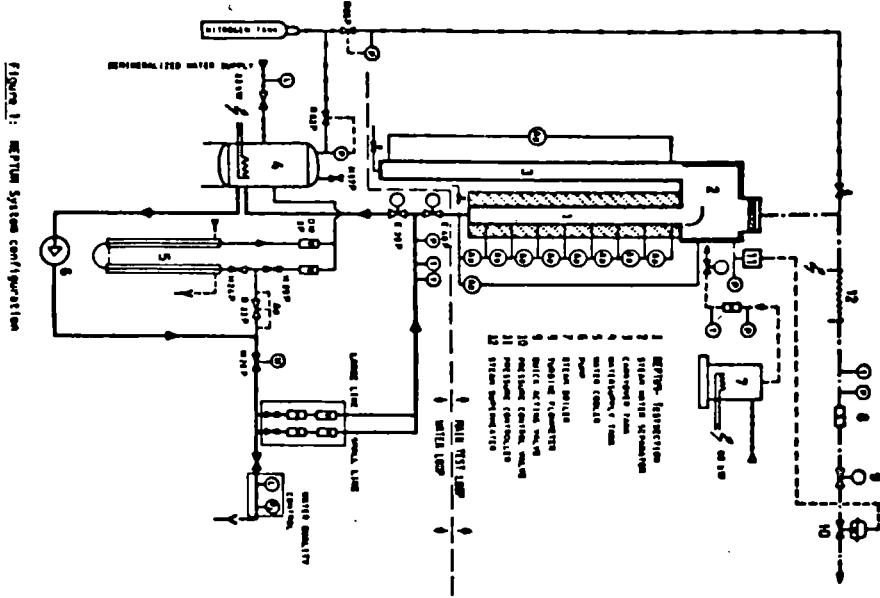


FIGURE 1: REF-TUM System configuration

FIGURE 2: REF-TUM Reactor Grid's Thermocouple configuration for ball-of-steam experiments.

FIGURE 3: Axial locations of the measurement levels and the spacers

Figure 3 SUMMARY OF NEPTUN BOIL-OFF EXPERIMENTS

| Experiment Number | Bed Peak Power (kW/m) | System Pressure (bar) | Initial Coolant Temperature (°C) | Comments  |
|-------------------|-----------------------|-----------------------|----------------------------------|---|
| 5000              | 0.744-0.6             | 1                     | 100                              | Powers were too high for the first test; the data were not evaluated from this experiment       |
| 5001              | 0.744                 | 1                     | 100                              | Repeat experiment at low pressure   |
| 5002              | 0.744                 | 1                     | 100                              | Repeat experiment at low pressure   |
| 5004              | 0.744                 | 5                     | 120                              | Effects of changing rod power and initial coolant subcooling                                    |
| 5005              | 1.276                 | 5                     | 120                              | Effects of changing rod power and initial coolant subcooling                                    |
| 5006              | 1.276                 | 5                     | 140                              | Effects of changing rod power at high system pressure   |
| 5007 <sup>a</sup> | 0.744                 | 5                     | 140                              | Effects of changing rod power at high system pressure   |
| 5008              | 0.319                 | 5                     | 140                              | Effects of changing rod power at high system pressure   |
| 5009              | 1.276                 | 5                     | 140                              | Repeat of high-power, high-pressure experiment 5006 with higher data-scanning rate              |
| 5011              | 2.14                  | 5                     | 110                              | Boil-off test at high power and pressure, corresponding to intermediate break decay heat levels |
| 5012              | 7.2                   | 5                     | stagnant steam                   | Adiabatic heat-up and reflooding. To check the fuel simulation code for heat-up phase           |

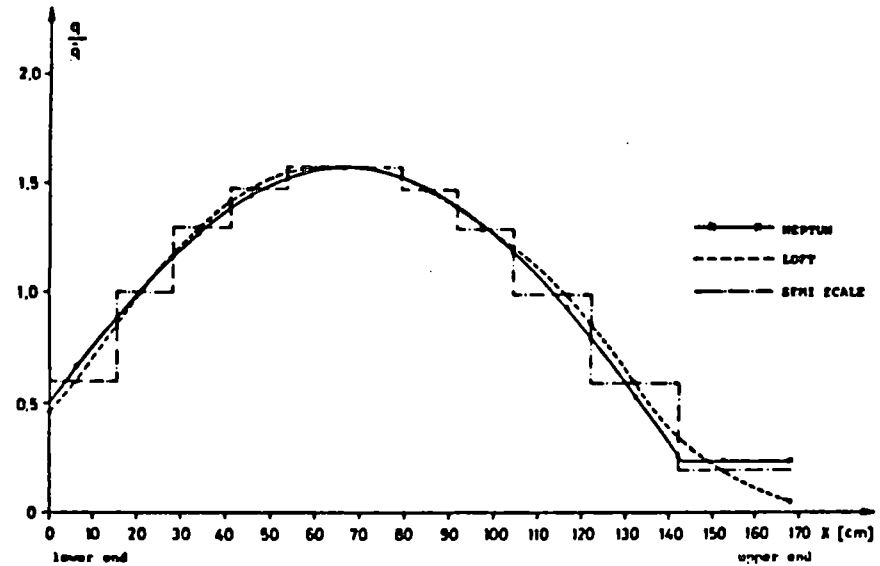


Figure 4: Axial power distribution of the NEPTUN heater rods.

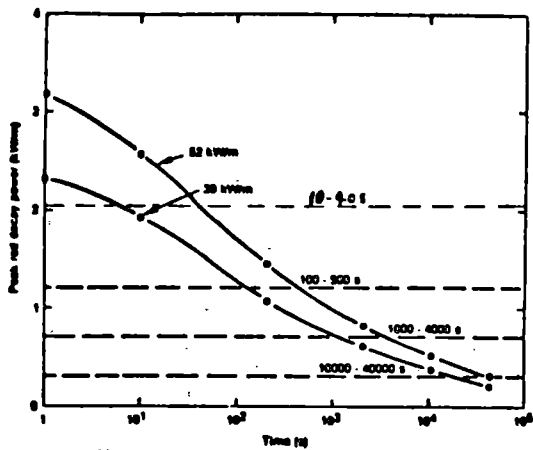


Figure 5. LOFT decay power curves showing power range for NEPTUN ball-off experiments.

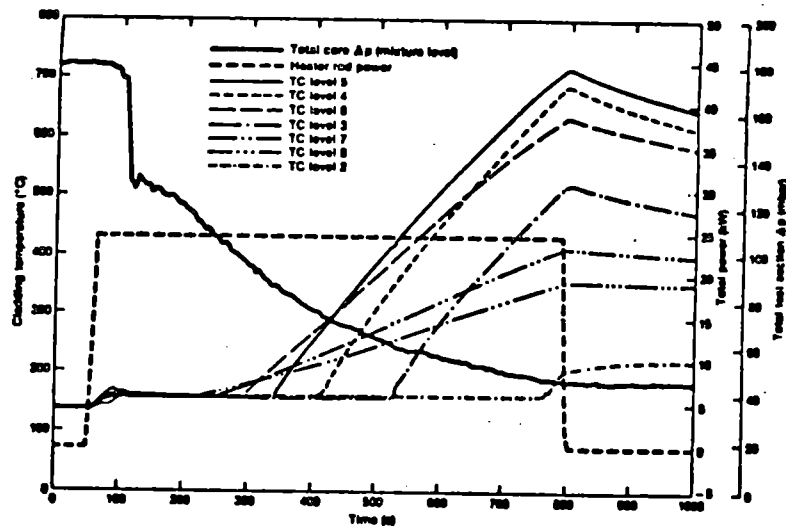


Figure 7. NEPTUN system response--base case (test 507)--high system pressure, intermediate rod power.

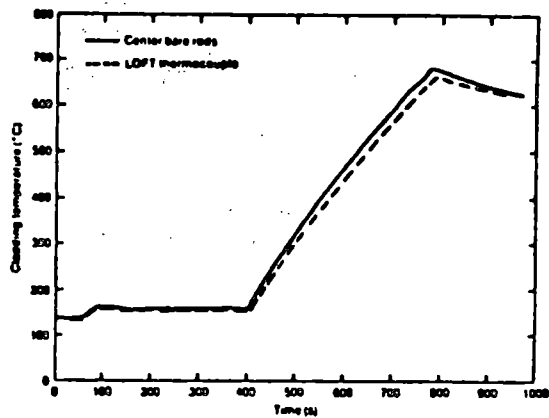


Figure 8. Comparison of center rod internal and LOFT thermocouples (test 507, axial elevation, 946 mm -level 4).

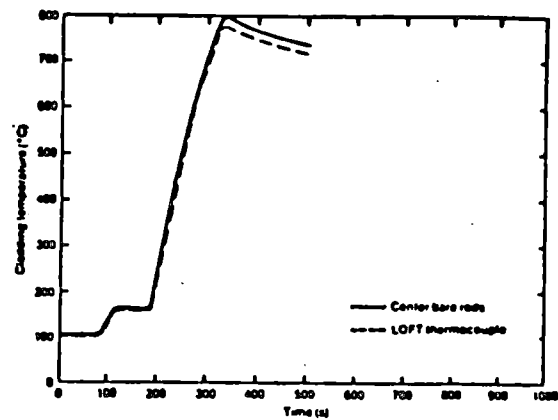


Figure 9. Comparison of center rod internal and LOFT thermocouples (test 5011, axial elevation, 946 mm -level 4).

Figure 10 : Test matrix for NEPTUN reflooding experiments (with LOFT - TC<sub>5</sub>)

|                                    | Reference Tests | Low Subcooling Tests | High Power Tests | Low Pressure Tests |
|------------------------------------|-----------------|----------------------|------------------|--------------------|
| Peaking Power [KW/M]               | 2.3             | 2.3                  | 3.94             | 2.3                |
| Pressure [bar]                     | 4.1             | 4.1                  | 4.1              | 1.0                |
| Subcooling for Flooding [°C] Water | 78              | 11                   | 78               | 78                 |
| Performed tests                    | ■               | ●                    | ▲                | ▼                  |
| Planned tests*                     | □               | ○                    | △                | ▽                  |

\* will be completed by the end of 1982

| Maximum Initial Cladding Temp. [°C] | Flooding Rate [cm/sec] |            |            |    |    |
|-------------------------------------|------------------------|------------|------------|----|----|
|                                     | 1.5                    | 2.5        | 4.5        | 10 | 15 |
| 477                                 | □                      | ■          | ■          | ■  | ■  |
| 597                                 | △                      | □          | ■          | ■  | ■  |
| 757                                 | ○ □<br>▼               | □          | ○ ■<br>△ ▼ | ■  | ■  |
| 867                                 | □                      | ○ □<br>△ ▼ | □          | □  | □  |

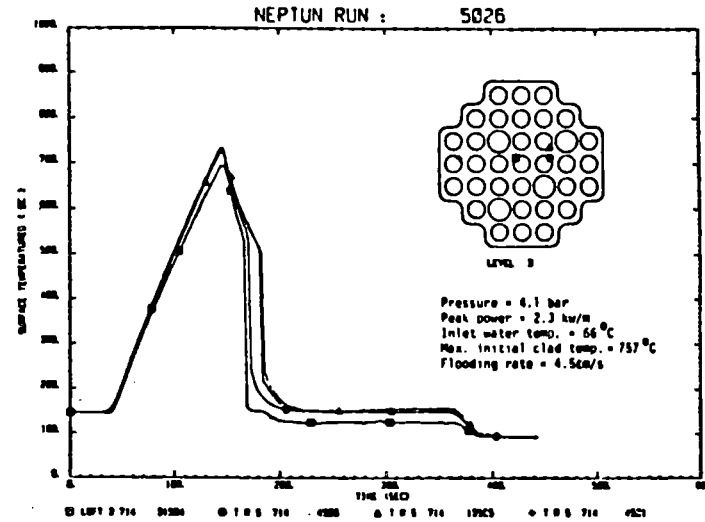


Figure 11: Overlay comparisons of selected NEPTUN thermocouples, axial elevation 3, base case experiment 5026.

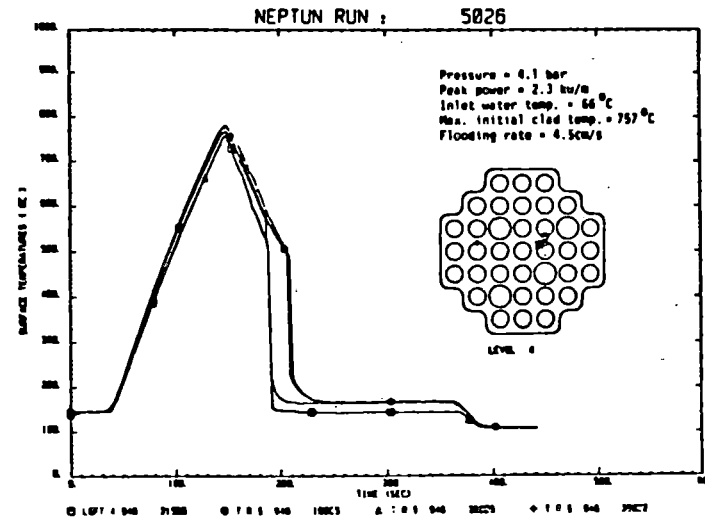


Figure 12: Overlay comparisons of selected NEPTUN thermocouples, axial elevation 4, base case experiment 5026.



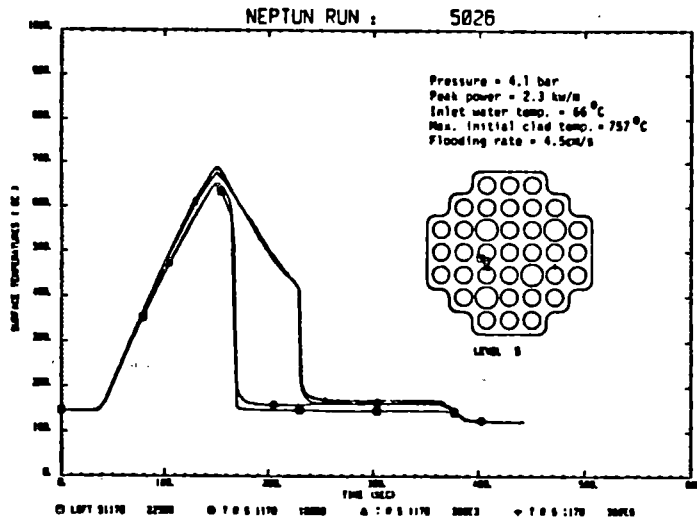


Figure 13: Overlay comparisons of selected NEPTUN thermocouples, axial elevation 5, base case experiment 5026.

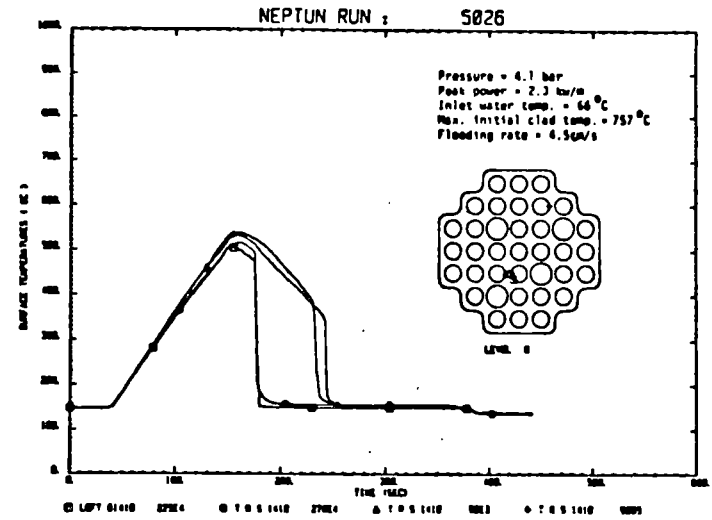


Figure 14: Overlay comparisons of selected NEPTUN thermocouples, axial elevation 6, base case experiment 5026.

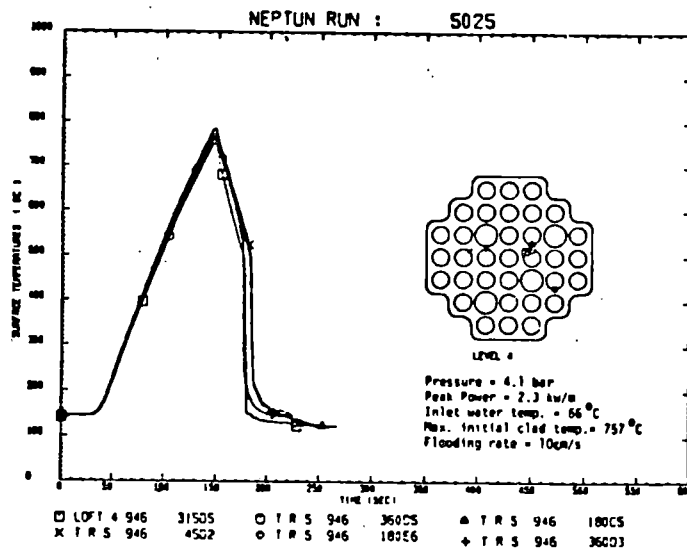


Figure 15: Overlay comparisons of selected NEPTUN thermocouples, axial elevation 4, experiment 5025.

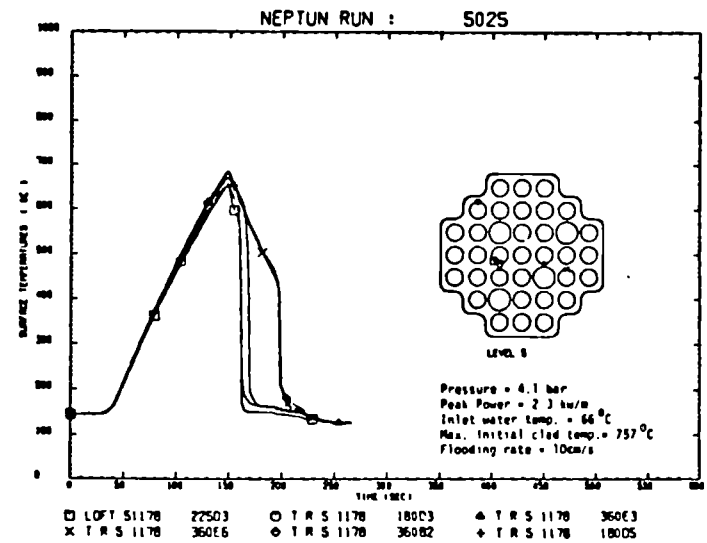


Figure 16: Overlay comparisons of selected NEPTUN thermocouples, axial elevation 5, experiment 5025.

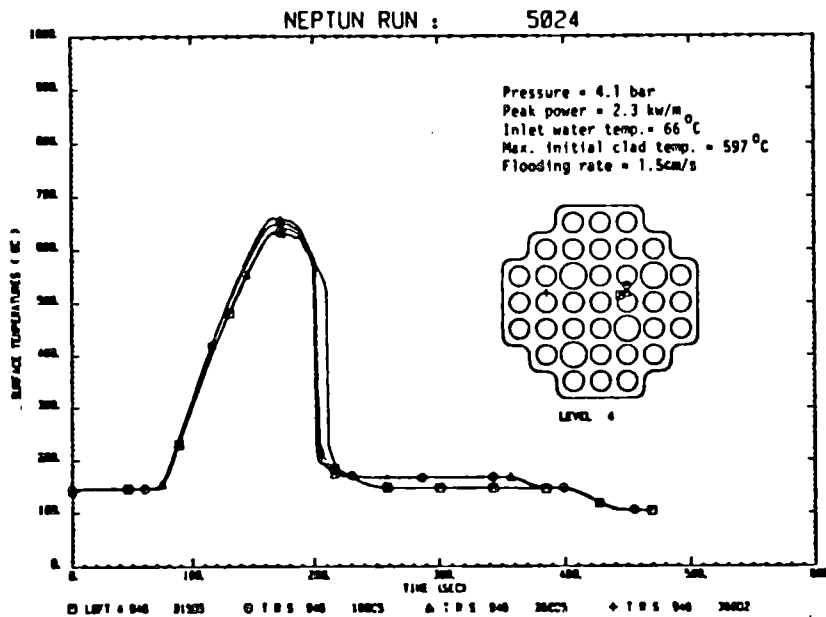


Figure 17: Overlay comparisons of selected NEPTUN thermocouples, axial elevation 4, experiment 5024.

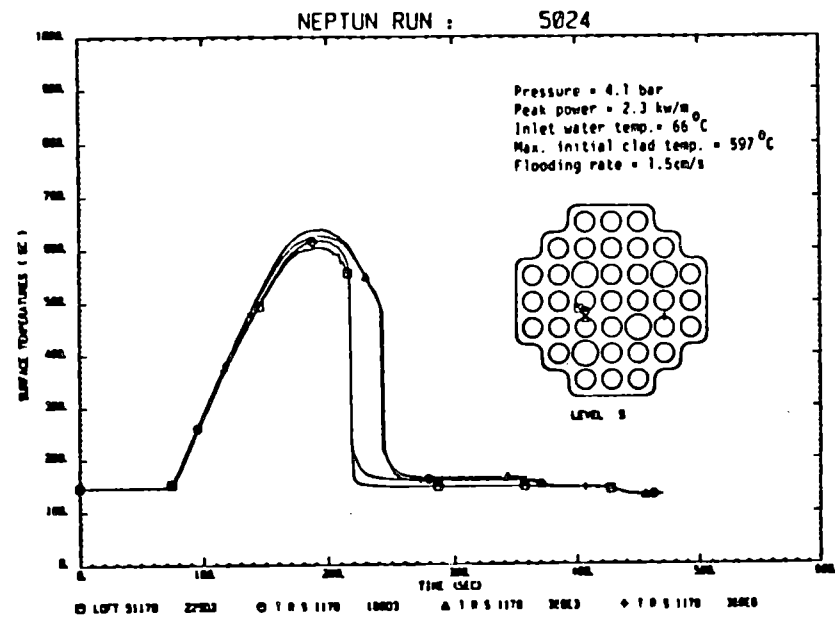


Figure 18: Overlay comparisons of selected NEPTUN thermocouples, axial elevation 5, experiment 5024.

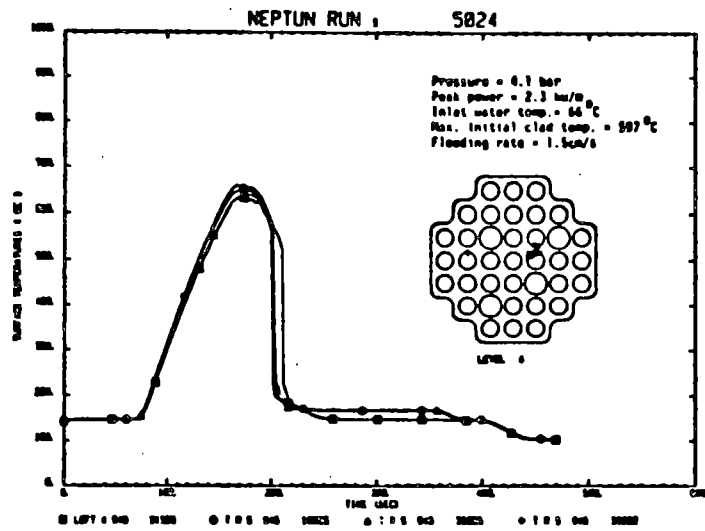


Figure 17: Overlay comparisons of selected NEPTUN thermocouples, axial elevation 4, experiment 5024.

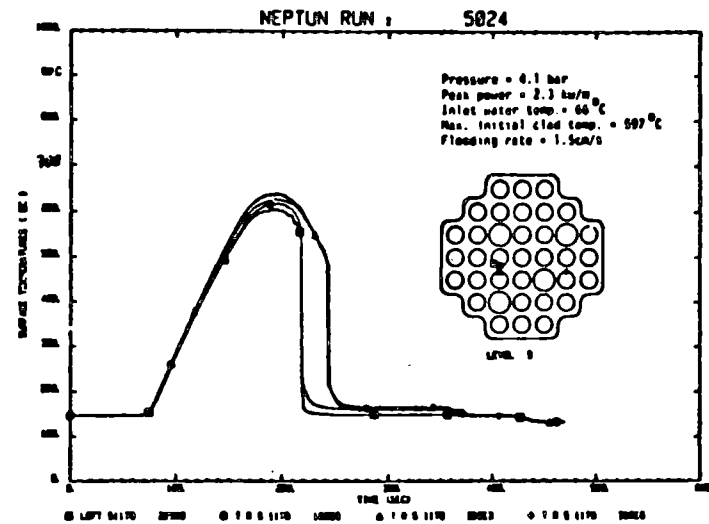


Figure 18: Overlay comparisons of selected NEPTUN thermocouples, axial elevation 5, experiment 5024.

**HDR CORE BARREL DYNAMICS FOR LARGE AND  
SMALL BREAKS INCLUDING NONLINEAR  
STRUCTURAL IMPACT PHENOMENA**

**L. WOLF**

Projekt HDR, Kernforschungszentrum Karlsruhe GmbH  
Postfach 3640, D-7500 Karlsruhe 1,  
Federal Republic of Germany  
Battelle-Institut e.V., Frankfurt,  
Am Römerhof 35, 6000 Frankfurt 90,  
Federal Republic of Germany

This paper summarizes and compares the experimental as well as pre-test calculational results of the four last blowdown tests, V31.2, V32, V33 and V34, with reactor pressure vessel internals (RPV-I) at the HDR-facility. These four tests constitute the Main Test Series of the RPV-I experiments and conclude the experimental efforts during Phase I of the overall HDR-Safety Program /1/ at the same time. The following informations supplement those given last year about the major findings of the Preliminary Test Series /2/.

Figs. 1 and 2 depict the overall HDR-vessel geometry with built-in core barrel and lower end mass ring. The main purpose of the tests is graphically illustrated in Fig. 3, namely demonstrating the effects of fluid/structure coupling under a variety of different initial- and boundary conditions thereby providing a reliable test bed for verifying pertinent computer codes. Fig. 4 presents a flow

sheet of the overall rationale behind the sequence of the various tests. This is supplemented by the set of thermodynamic initial conditions summarized in Fig. 5. From this, the following areas of interest may be deduced as outlined in Fig. 6.

- 1) V31.2: Reproducibility of data after a pause of one year
- 2) V32: German Standard-Problem No. 5: amount of load increase due to increased subcooling in the downcomer compared to V31.2
- 3) V33: Reduction in loads and deformations as result of decreased break size as compared to V32
- 4) V34: Effects of axial and radial core barrel impacts due to nonlinear structural boundary conditions as well as the additional effect of isothermal conditions throughout vessel.

Figs. 7 and 8 depict the allocations of differential pressure and radial displacement sensors mounted at the core barrel for the experiments V31.2 through V34. These figures may be used to identify the coordinates of the positions of these types of sensors for which results and comparisons are shown in the following. Responding to the special needs of test V34, Figs. 9 and 10 present the allocations of the 3 displacement sensors for the purpose of following the axial lifting of the core barrel upper flange.

Because Standard Problem No. 5 is the focal point of this test series, the experimental results of all the other tests will be presented in relation to the findings of V32 in order to more easily comprehend correspondences and deviations. Only for V32 itself and V34 in view of its complexities are additional information supplied.

The increased density and reliability of applied instrumentation in the break nozzle, downcomer, and at the core barrel (see Figs. 7 and 8 for two types of sensors) results in a substantial gain in information about the details of:

- . propagating and reflecting pressure waves (Fig. 12)
- . pressure wave damping effects by abrupt changes in geometry (break nozzle/downcomer), wave spreading, and fluid/structure interactions along and around the downcomer (Fig. 12)
- . local, differential pressures at the core barrel (Fig. 13) as well as across the core barrel diameter in various planes
- . local, relative, radial displacements along and around the core barrel in various planes (Fig. 14 and 15)
- . Symmetry in the core barrel dynamics (Fig. 15)
- . location of maximum displacement in the lower middle section of the core barrel (Fig. 14)
- . Correspondence between small local pressurization and local displacement before the arrival of the depressurization wave (Figs. 13 and 15)
- . local core barrel inside and outside surface strains both in axial and azimuthal directions (Fig. 15) which allow the deduction of stresses as result of both pressure difference (at early times) and thermal driving forcing (at later times) functions
- . axial and radial core barrel impact phenomena (Figs. 22, through 24)

In terms of the aforementioned four problem areas, the following conclusions can be drawn from the experimental evidence presented in Figs. 11 through 24:

- 1) Fig. 11 demonstrates the excellent agreement of V31.2 data with those obtained by V31.0 and V31.1 one year earlier. Thus, a fine record of reproducibility has been established. In retrospective, the new data confirm - as anticipated - the high degree of accuracy and validity of the data even of the earlier experiments /2 - 4/ with reduced instrumentation.
- 2) Figs. 16 and 17 summarize the effects of increased fluid sub-cooling in the downcomer and break nozzle for V32 as compared to V31.2 for some selected quantities. The comparisons show that:
  - . pressure differences, displacements and strains increase by about 10 to 15 %.
  - . core barrel dynamics essentially remain the same.
  - . when there are any noticeable deviations in the temporal behaviors, they occur for times larger 100 ms and are mainly the results of earlier and stronger nonequilibrium effects in the upper plenum and upper core internal regions (pressures drop deep below saturation, believed to be a specific HDR-effect) for V32 than V31.2.
  - . distinct oscillatory pressure fluctuations occur upstream of the break which have not been detected in tests V31.0 through V31.2.

Based on these experimental observations, the following general expectations can be anticipated with respect to the quality of pre-test calculations for the Standard Problem No. 5:

- . Because the experimental data of V32 are sufficiently close to those of V31.0 and V31.1, it must be expected that those institutions which fine-tuned their codes on behalf of V31.1 pre- and post-test calculations should fare very well for the Standard Problem.
  
- . In view of the fact that despite large differences in thermal-fluiddynamic behavior for V32, pressure differences are only mildly affected, it can be anticipated that all codes independent of the sophistication in their fluiddynamic models meet differential pressures well and based upon these driving forcing functions should also result in good agreement with the measured structural data due to tuning the core barrel shell model (see point 1).

With Points 1) and 2) covering the major aspects and primary objectives of fluid/structure interaction phenomena in SP No. 5, the only remaining issues may involve the consistency with which the thermal-fluiddynamic behavior in break nozzle and vessel is presented. Here, larger deviations as compared with the data are to be expected, dependent upon the sophistication of the fluid model used in the codes and the learning effects fed back from the previous tests.

Overall the inspection of the V32-data as compared to V31.2 (V31.1) suggest that SP No. 5 did not pose an insurmountable problem for the participants given the status of predictive quality already reached for the post-test calculational phase of V31.1 /2/.



- 3) The effects of reducing the break cross-sectional area to only 25 % in test V33 are shown in Figs. 18 and 19 in comparison to the base case V32. The data reveal that:
- . the pressures behave totally different as compared to V32 in the break nozzle, reaching the initial pressure level (and even higher) again after the first undershoot.
  - . no nonequilibrium effects occur in the upper plenum and core regions.
  - . local pressure differences, displacements, and strains are effectively reduced. However, only the mass flow shows a linear behavior with break area reduction. All other quantities are only reduced by 12 to 50 % dependent upon the sensor type and its position considered (compare Fig. 25).
  - . the overall temporal behavior of the measured structural quantities is maintained.

For the first time, the V33-data confirm previous analytical results suggesting a nonlinear (i.e. smaller than linear) reduction effect on loads as function of the break area. Most importantly, the measurement techniques have been shown to provide reliable data for small break situations, although a third test with even more reduced break area deems necessary to complete the functional dependence of loads versus break area.

- 4) To assure local radial impact of the core barrel against the RPV inside surface, two snubbers were mounted at the 90° and 270° positions and the core barrel excentrically positioned, touching the 270° positions. Fig. 20 summarizes the relative positions of the core barrel before heat-up, just prior to blowdown and after the

test for two representative axial locations. Needless to say, the reliable control of these clearances is of utmost importance especially for providing the input for post-test calculations. Details of the measurement system and procedures are given in /5,6/.

The measured data of V34 are compared to those of V32 in Figs. 21 through 24. The following main conclusions can be drawn from this evidence:

- . Axial core barrel upper flange impacts (see Fig. 22 bottom and Fig. 23 top) as well as radial core barrel lower end impacts (Fig. 24 top) occurred. Thus, the main objectives of the experiment have been met indicating the validity of procedures and measurement techniques. Post-test visual inspections revealed small plastic marks at the upper flange and at the snubbers supporting the conclusions drawn from the data.
- . The core barrel is lifted axially without tumbling (Fig. 23 top) once the pressure difference (downcomer minus core barrel internal) becomes positive. Fig. 22 depicts this direct correlation.
- . The distinct plateaus in the displacements KS 1030 ( $90^\circ$ ) and KS 1032 ( $270^\circ$ ) clearly indicate radial impact with a prolonged contact time between the surfaces, thereby lowering the frequency of core barrel dynamics by about a factor of 2 when compared to the results of V32 (compare Fig. 15 top); symmetry of the core barrel dynamics is maintained.
- . Displacements in the middle and lower sections of the core barrel are much larger than for the base case (Fig. 25).

- . The maxima in strain histories at the core barrel are unaffected by local impacts; they remain initially same as for V32 and are even greatly reduced during the course of the transients.
- . Signals of the accelerometers mounted at the core barrel as well as at the RPV are not indicative for impact phenomena.
- . No bypass flow effects at the upper flange have been detected from the measurements.
- . The feedback effect of the changed support conditions on the pressure field in the vessel and the differential pressure is small in comparison to the feedback of shell motions; marked deviations are noticeable, starting at the end of the first axial lift-up movement; after that, oscillations of the pressure differences at the core barrel are damped faster than for V32. As a result, the pressure differences for V32 and V34 during the initial blowdown period nearly coincide, suggesting that for the conditions tested the pressure loading for the loose support during this time period may still be well described by the rigidly clamped base case (Fig. 22 top and Fig. 25).

Spikes in the pressure difference histories at about 80 ms and 150 ms may be indicative of the end of the axial core barrel movement (compare top and bottom of Fig. 22).

- . Although the isothermal condition throughout the RPV greatly changes the overall course of the depressurization as compared to V32 (Fig. 21 bottom), it does not significantly affect the pressure loading.

- . In contrast to V32, no two-phase effects have been detected in the upper plenum and core barrel internal regions, rather the pressures linearly decrease with time, suggesting that codes with rather simple approximations for the fluid model should handle this situation well under the given circumstances.

In conclusion, for the first time, the data of V34 provide a meaningful data basis from a large scale experimental investigation for the effects of impacts on fluid- and structural dynamic quantities of interest. The results show that forces, strains, and accelerations induced by impacts on top of the depressurization transients are small. Thus, as Fig. 25 clearly indicates, only displacements differ substantially from the base case V32.

The comparisons between measurements and blind pretest predictions by the codes summarized in Fig. 26 are performed on a test-by-test basis and the results summarized in Figs. 27 through 41. For the sake of clarity, the equivalent network code DAISY is shown together with the mixed-geometry code FLEXWALL, whereas all truly three-dimensional codes for the fluid region inside the RPV are presented together in what follows.

Naturally, of foremost interest are the conclusions which may be derived from the Standard Problem No. 5 (V32) comparisons shown in Figs. 27 through 33. Without forestalling any official comments on these issues, the following first observations may suffice:

- The correct prediction of break nozzle behavior seems to be still a problem for certain codes despite the available evidence provided by previous tests.
- The complete incorporation of "learning effects" from V31.1 and their transfer in model corrections, code improvement and discretization tuning pays back in close agreement of DAISY-

predictions with the data, thereby closing the gap in predictive quality between network and true multidimensional codes.

- Codes based on the mixture of different models and solution schemes are only as good as the weakest member in the model chain and the success of patching the models together. As a result, they show a tendency of overconservatism in the predictions as indicated in Figs. 27 and 28.
- The good agreement of the first displacement maximum is mainly achieved by overpredicting the pressure difference during this time period in the first place.
- Break nozzle phenomena are very well predicted by all multidimensional codes (Fig. 29 top).
- The same is true for the pressure differences and strains (Figs. 29 and 30), which are truly best-estimated by all of the multidimensional codes independent of fluid and structural models. This confirms the already aforementioned speculation that no matter what the differences are in predicting the histories of absolute pressures in downcomer and core barrel internal regions, these deficiencies will not greatly affect the loads.
- As already observed for V31.1, deviations of smaller or larger magnitude still exist in reliably predicting the displacements, noticeably their first maximum. Whether this is only a matter of fineness in the nodalization remains to be seen.
- FLUX-DRIX (FDS) comes closest to the structural data.

- Overall consistency in both fluid- and structural quantities is displayed by K-FIX (LANL) using fully implicit iteration for the field equations (see Figs. 31 through 33), whereas the explicit solution, K-FIX (Battelle) cannot cope with the two-phase situation at later times and results in fluctuations around the data, thereby demonstrating a large robustness of the code.
- Improvements by fully incorporating RPV dynamics into the code FDS seem to be marginal.

Overall, it can be concluded that the predictive quality of codes accounting for fluid/structure interaction effects has generally reached a level which can be considered fully acceptable.

Whereas the V32 data are close to the previous V31.1 results, those of V33 are sufficiently apart to pose yet another stringent test on the predictive capability of participating codes. The comparisons are summarized again in two groups in Figs. 34 through 37 from which the following conclusions can be drawn:

- All codes predict the break nozzle behavior very well.
- In a new situation like this, network and mixed-model codes lose some of their accuracy observed for V32 by substantially overestimating the initial pressure difference histories. Yet, at later times the calculational results follow much closer the data than what was observed for V31.1.
- The multidimensional codes clearly surpass the others in accuracy and consistency as can be seen in Figs. 36 and 37.

- Because no two-phase effects occur in the system during the problem time considered, the fully explicit solution in K-FIX (Battelle) remains appropriate and accurate for a minimum in computation time.

In conclusion to the V33 comparisons one can state that all codes accounting for fluid/structure interaction phenomena have predicted all major trends observed in the experiment. Deviations are towards the conservative side. Multidimensional codes such as FDW and K-FIX (even explicit) have shown again their superiority in pre-test best-estimate predictions in terms of consistency and accuracy. The other codes lost some of their capabilities tuned for higher loading conditions and certainly need readjustments. However, general agreements and overall trends are met much closer than what has been observed for V31.1.

The version FLUX4 which includes fluid-structure interactions with the CB and the RPV together with the algorithm treating impacts described in /7/ provided the only pre-test predictions for the test V34. Additionally, a simple technique accounting for the elastic-plastic behavior of supports has been implemented. In the meantime, a series of post-test calculations has been completed /8/, the best of which is shown together with the pre-test predictions in some of the figures. From the comparisons given in Figs. 38 through 41 the following conclusions can be drawn:

- For reasons already mentioned above in connection with the discussion on the experimental findings, the pre-test analysis already gives generally very good agreement with respect to fluid dynamic quantities. With the exception of overestimating the initial pressure difference by 15 %, the agreement is even better than for V32 because it is not affected by two-phase phenomena which FDW cannot account for.

- The pre-computed displacements do not agree both in amplitudes and oscillatory behaviors because the prespecified initial values for the various gaps differed markedly from the actual ones.
- The good agreement of the fluid dynamic data despite the substantial deficiencies in the structural data confirm again that the feedback of the support parameters and the impacts on the fluid quantities is marginal compared to the feedback induced by the shell motions.
- Adjustment of the input data accounting for the actual gap sizes in post-test calculations as well as support parameters and upper flange stiffness results in extremely good agreement with the data of the axial lift-up movements (not shown) and substantial improvements in radial displacements both in amplitude and frequency (see Fig. 40 and 41 top).
- Strains are already predicted well by the pre-test computations for the same reason as already given above.

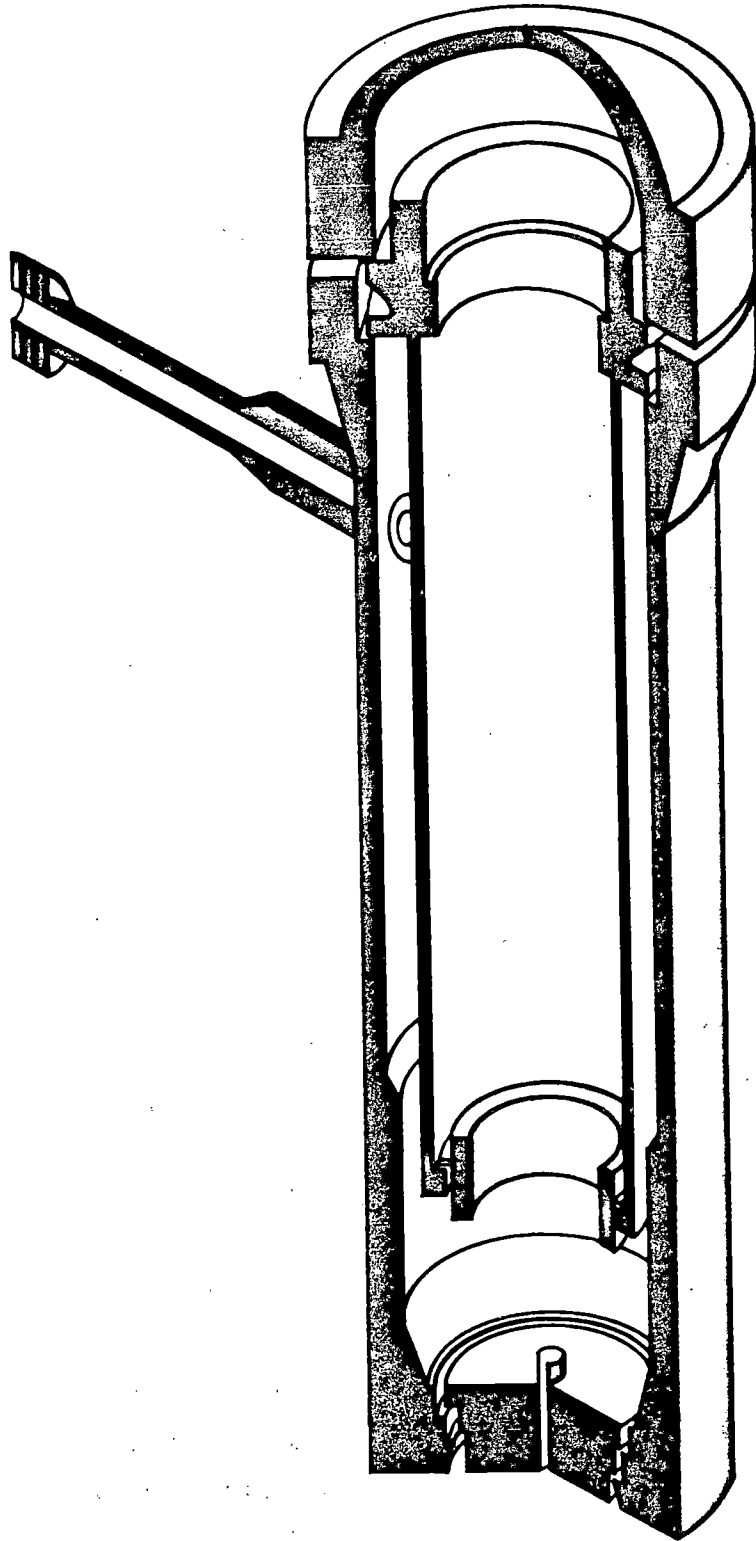
Overall, the code FLUX has demonstrated its ability to predict the complex situation of test V34. Post-test computations matched fairly well the specific structural dynamic effects, although the agreement is not as close as for V32. Remaining differences must be attributed to model uncertainties for the upper CB flange, its stiffness, its support, and possible friction forces affecting its motion.

Overall, it can be concluded that the HDR-RPV-I tests V31.2 through V34 and their accompanying predictions have substantially added to our knowledge of fluid/structure interactions /9/ and the verification process of respective computer codes /3/. Furthermore, they indicate the directions of future research in this area.



## Literature

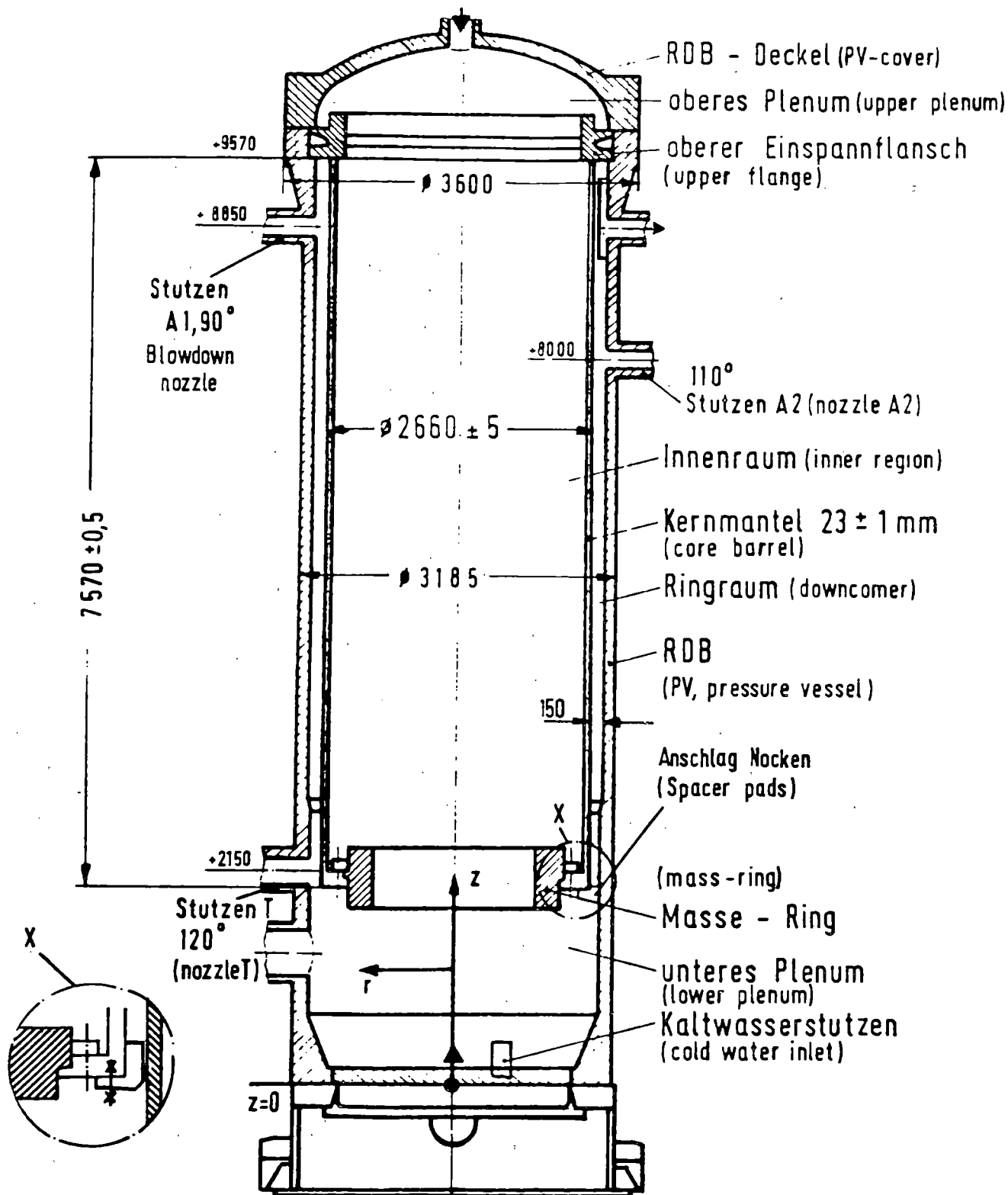
- /1/ HDR Safety Program - General Program -, Status of June 1980, Kernforschungszentrum Karlsruhe
- /2/ Wolf, L.: Experimental and Analytical Results of Coupled Fluid-Structure Interactions During Blowdown of the HDR Vessel, 9th WRSIM, Gaithersburg, MD, USA, Oct. 1981
- /3/ Wolf, L.; Schall, M.; Schumann, U.: Investigation of Reactor Pressure Vessel Internals Following Rupture of Reactor Primary Piping, Tests V31 and V31.1, Quick-Look-Report, (In German), Technical Report No. 17-80, (in press)
- /4/ Schall, M.; Wolf, L.: Evaluation Report on HDR-RPV-I Tests V29.2 Through V31.1 of the Preliminary Test Series, (In German), in preparation
- /5/ Schall, M.; Wolf, L.; Schumann, U.: Investigation of Reactor Pressure Vessel Internals Following Rupture of Reactor Primary Piping, Tests V31.2 Through V34, Quick-Look-Report, (In German), (to appear)
- /6/ Wind, F. et al: Supplemental Report on HDR-RPV-I Tests V31.2 - V34, PHDR-Report 3.303/82, (in press)
- /7/ Schumann, U.: Impacts and Fluid-Structure Interactions in Pressurized Water Reactor Safety Analysis, accepted for publication in Nucl. Engn. Des. (1982)
- /8/ Schumann, U.: Experimental and Computed Results for Fluid-Structure Interactions With Impacts in the HDR Blowdown Experiment, to appear in Nucl. Engng. Des.
- /9/ Wolf, L.: Experimental Results of Coupled Fluid-Structure Interactions During Blowdown of the HDR-Vessel and Comparisons With Pre- and Post-Test Predictions, accepted for publication in Special Issue on FSI-Effects in LWRs, Nucl. Engng. Des., 1982



---

KfK

HDR-REACTOR PRESSURE VESSEL  
WITH CORE BARREL



DETAILS OF HDR-REACTOR PRESSURE VESSEL WITH CORE BARREL



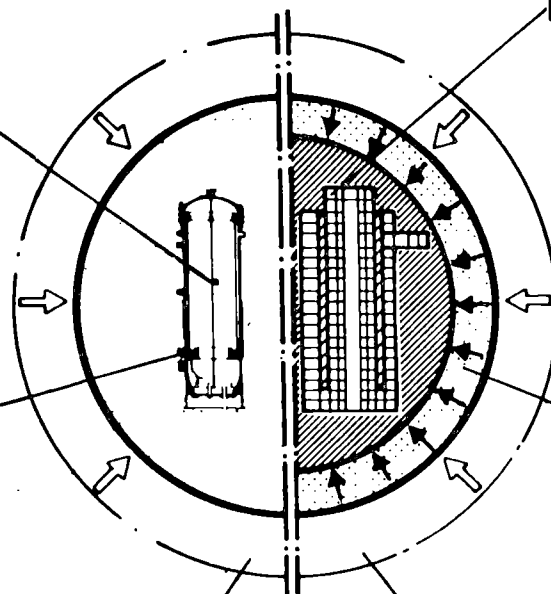
FIG. 2

## A Measurement of Physical Processes

A1 PHENOMENA

A2 DOMINANT EFFECTS

A3 INITIAL-AND BOUNDARY CONDITIONS



## B Computational Simulation of the Physical Processes

B1 MATHEMATICAL MODEL/PROCEDURES

- set of conservation equations
- geometrical modeling
- constitutive equations
- numerical procedures
- degree of coupling

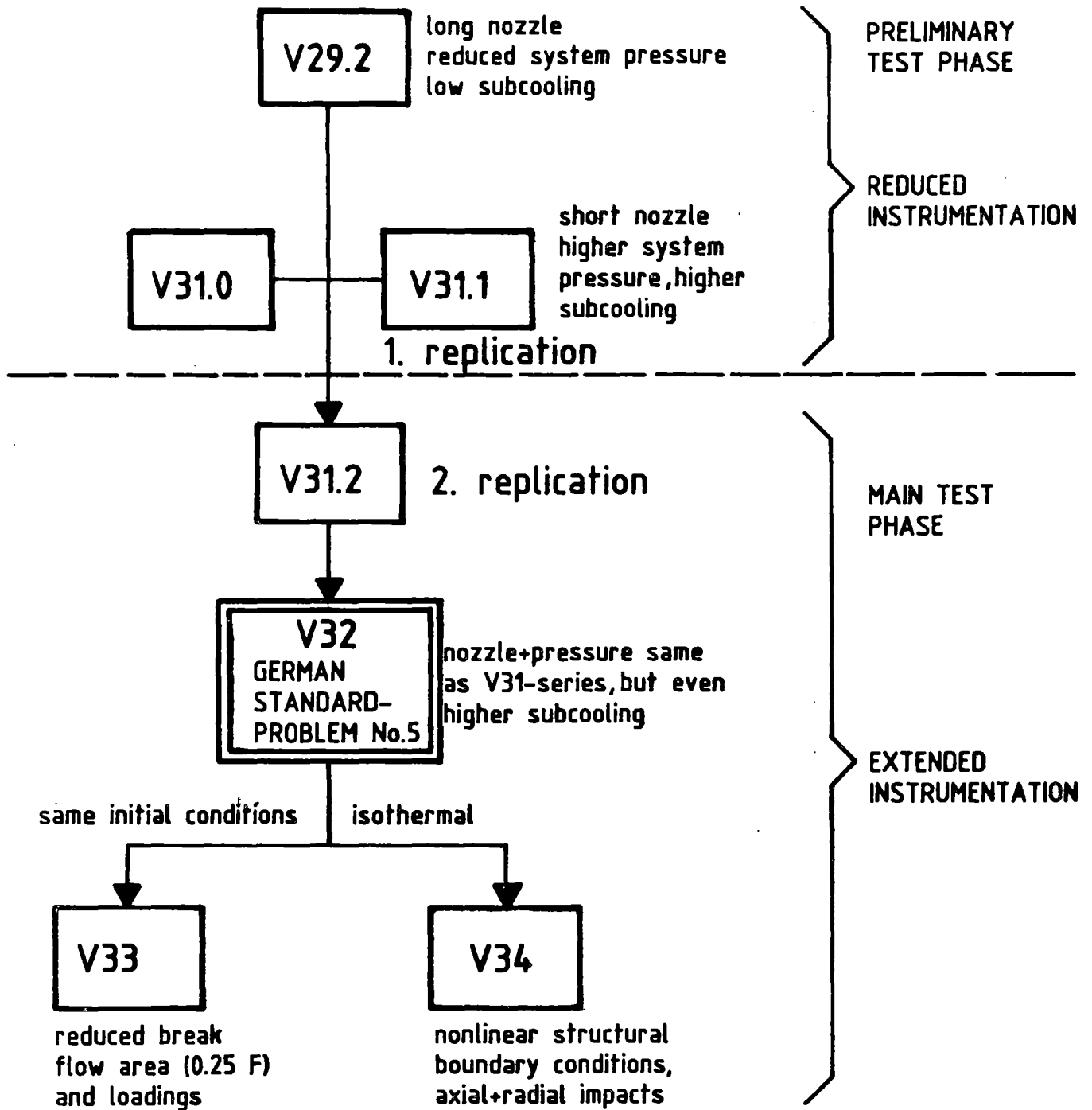
B2 DOMINANT PARAMETERS

- Mass-,Momentum-,Energy-  
Transfer and Interactions  
Fluid / Solid  
Fluid / Fluid
- Damping

B3 MATHEMATICAL SIMULATION OF INITIAL-AND BOUNDARY CONDITIONS

391





SEQUENCE OF HDR-RPV-I TESTS

FIG. 4

| <b>TEST No</b> | <b>Pressure<br/>bar</b> | <b>Upper<br/>Core Temp.<br/>°C</b> | <b>Downcomer<br/>Temperature<br/>°C</b> | <b>Subcooling<br/>Downcomer<br/>Degrees</b> | <b>Length of<br/>break nozzle<br/>m</b> |
|----------------|-------------------------|------------------------------------|---|---|---|
| <b>V 31.2</b>  | <b>110</b>              | <b>308</b>                         | <b>268</b>                              | <b>50</b>                                   | <b>1.369</b>                            |
| <b>V 32</b>    | <b>110</b>              | <b>308</b>                         | <b>240</b>                              | <b>78</b>                                   | <b>1.369</b>                            |
| <b>V 33</b>    | <b>110</b>              | <b>308</b>                         | <b>240</b>                              | <b>78</b>                                   | <b>1.369</b>                            |
| <b>V 34</b>    | <b>110</b>              | <b>240</b>                         | <b>240</b>                              | <b>78</b>                                   | <b>1.369</b>                            |



**TEST MATRIX OF BLOCK I OF MAIN TEST PHASE**

**FIG. 5**

EFFECTS OF:

- . HIGHER DOWNCOMER SUBCOOLING
- . REDUCED BREAK FLOW AREA
- . NONLINEAR STRUCTURAL BOUNDARY CONDITIONS

UPON:

MODELS FOR COUPLED FLUID-STRUCTURE INTERACTIONS

- FLUIDDYNAMICS

- . SINGLE PHASE: PRESSURE WAVE PROPAGATION AND DAMPING,  
1-D AND 2-D BREAK NOZZLE,  
3-D DOWNCOMER AND CORE BARREL INTERNAL
- . TWO PHASE: PRESSURE WAVE PROPAGATION AND DAMPING,  
1-D AND 2-D BREAK NOZZLE,  
3-D CORE BARREL INTERNAL  
  
NON-EQUILIBRIUM EFFECTS AT  
BREAK AND UPPER PLENUM

- STRUCTURAL DYNAMICS

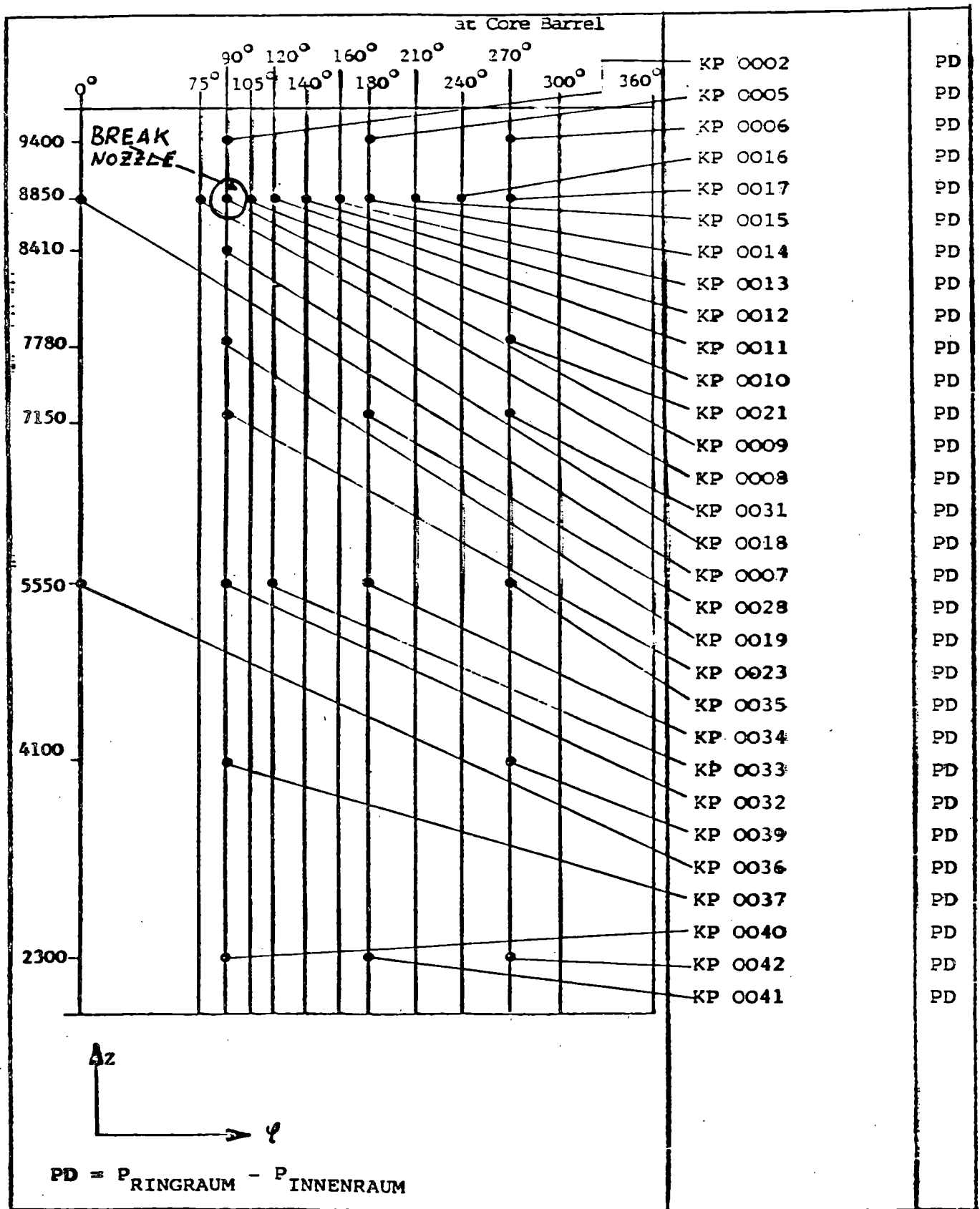
- . CORE BARREL: REL. RADIAL DISPLACEMENTS,  
STRAINS, ACCELERATIONS
- . REACTOR PRESSURE VESSEL: OUTSIDE RPV-SURFACE RADIAL  
DISPLACEMENTS, ACCELERATIONS
- . NONLINEAR UPPER FLANGE  
CLAMPING CONDITIONS: AXIAL AND RADIAL DISPLACEMENTS,  
STRAINS, ACCELERATIONS
- . RADIAL CORE BARREL  
LOWER END IMPACT: REL. RADIAL DISPLACEMENTS,  
STRAINS, ACCELERATIONS,  
PLASTICITY

---

MODELS OF PHENOMENA TO BE TESTED ON THE BASIS  
OF HDR-RPV-I MAIN TEST SERIES DATA

KfK

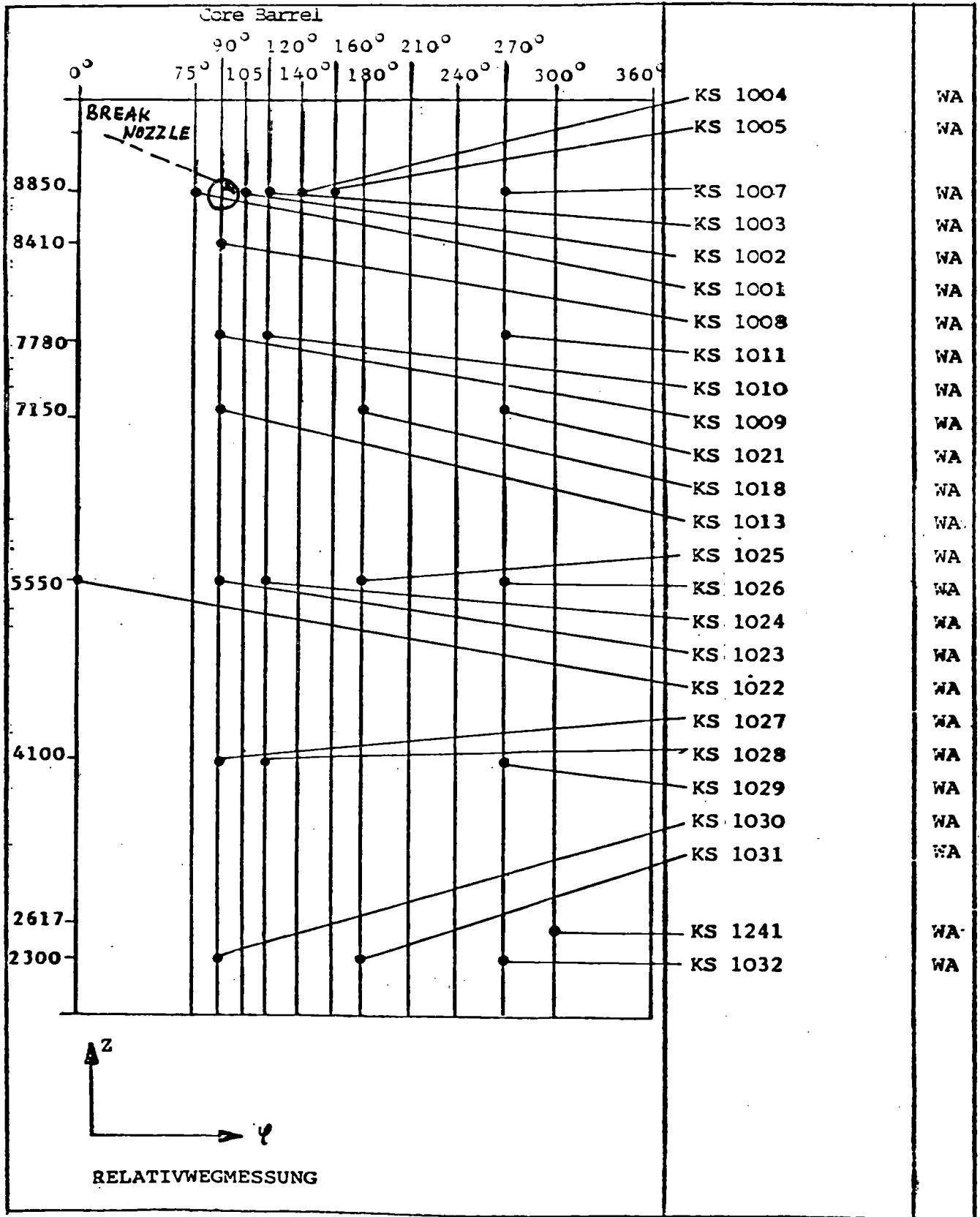
FIG. 6



ALLOCATION OF DIFFERENTIAL PRESSURE SENSORS  
AT CORE BARREL

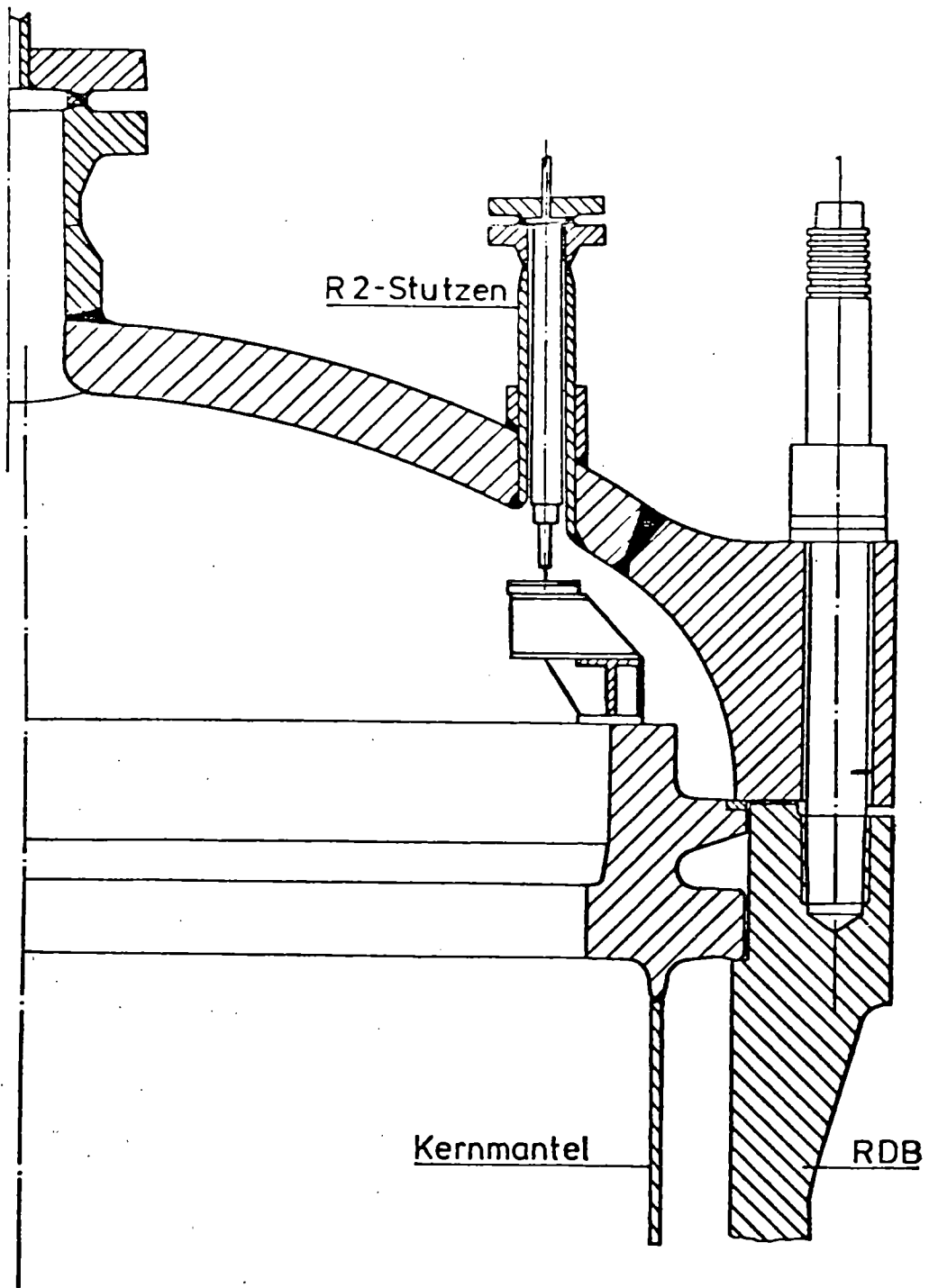
FIG. 7





ALLOCATION OF DISPLACEMENT SENSORS AT CORE BARREL

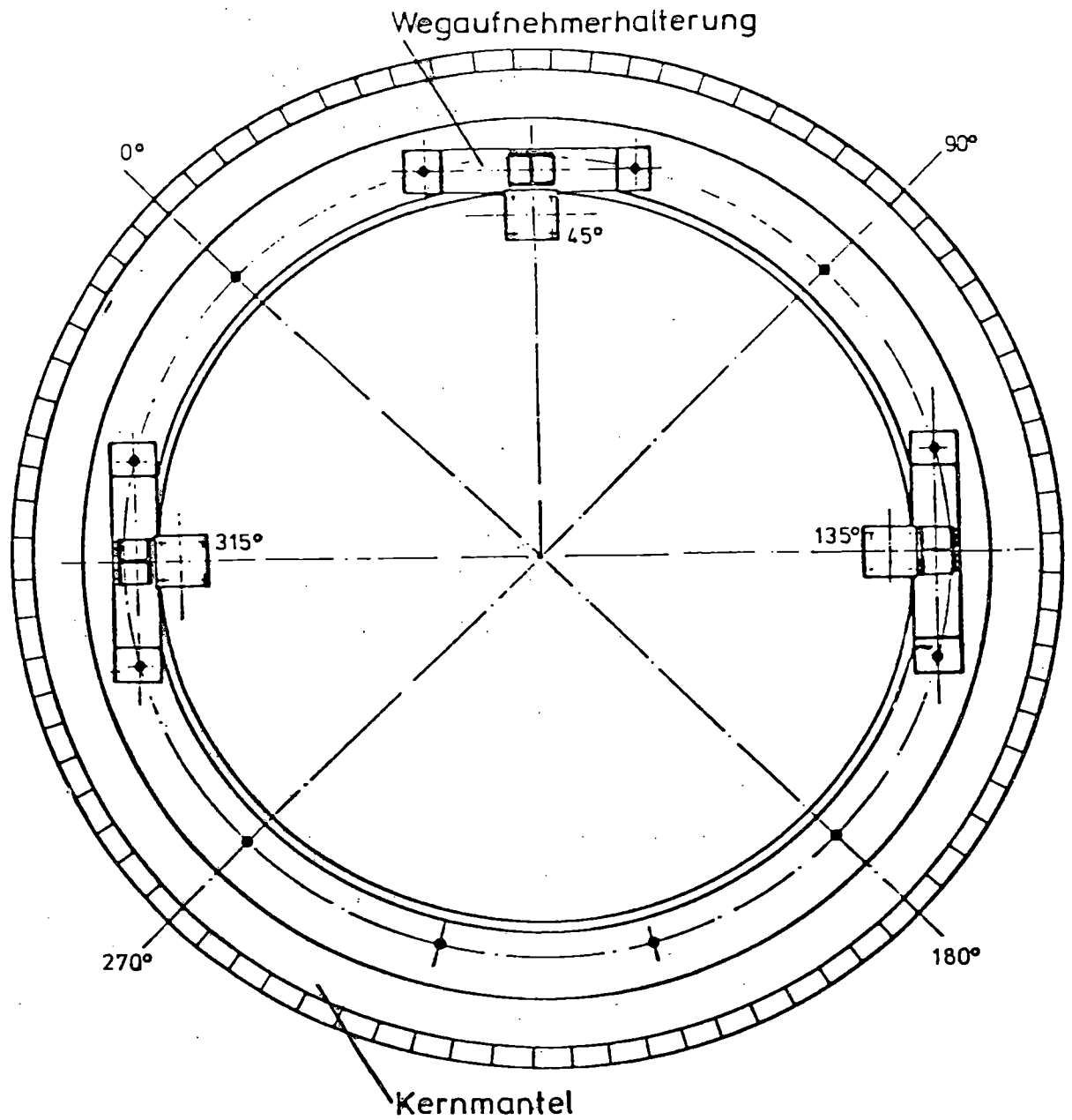
FIG. 8



AXIAL VIEW OF DISPLACEMENT SENSORS AT  
UPPER CORE BARREL FLANGE



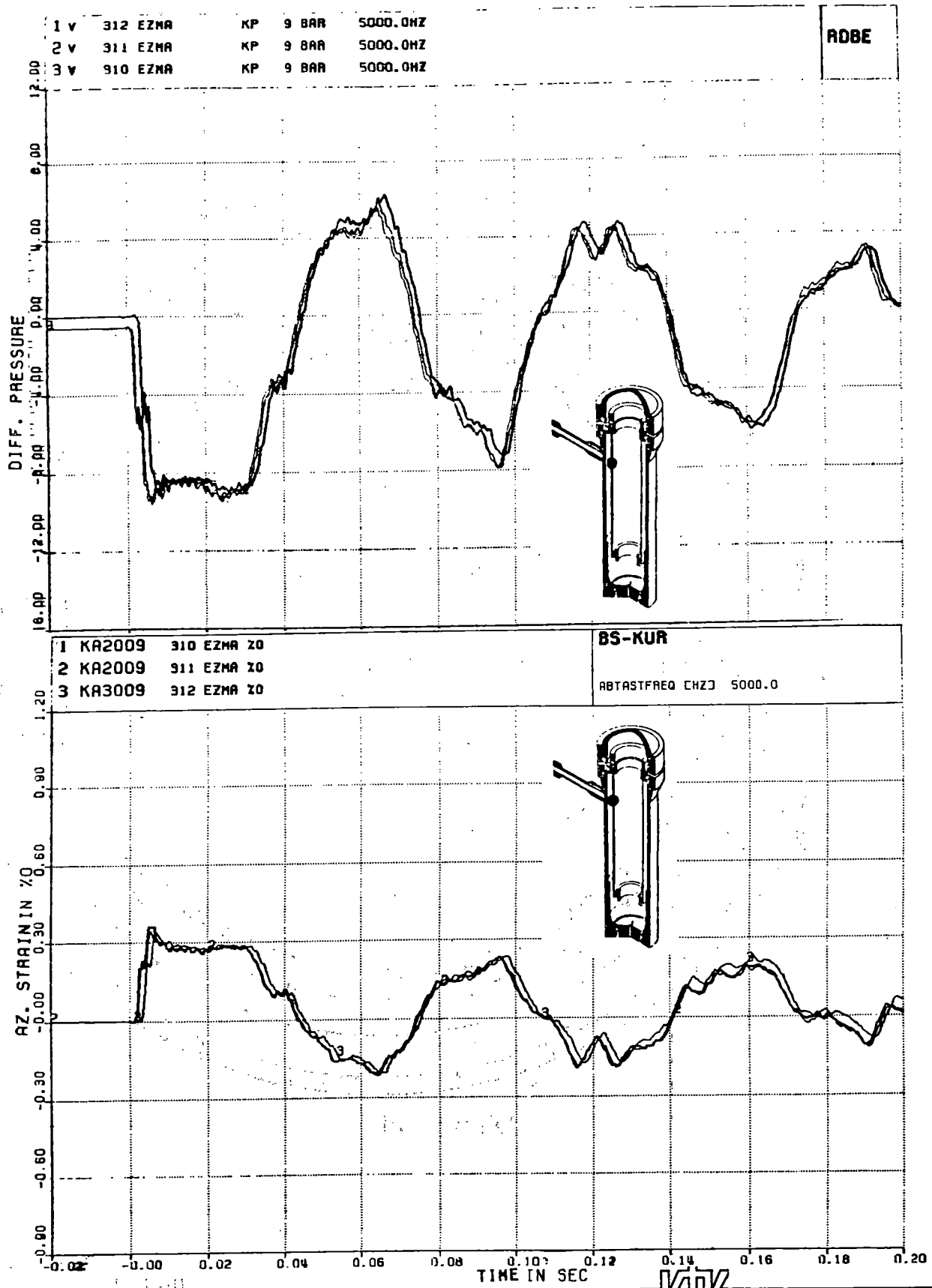
FIG. 9



AZIMUTHAL ARRANGEMENT OF DISPLACEMENT  
SENSORS AT UPPER CORE BARREL FLANGE

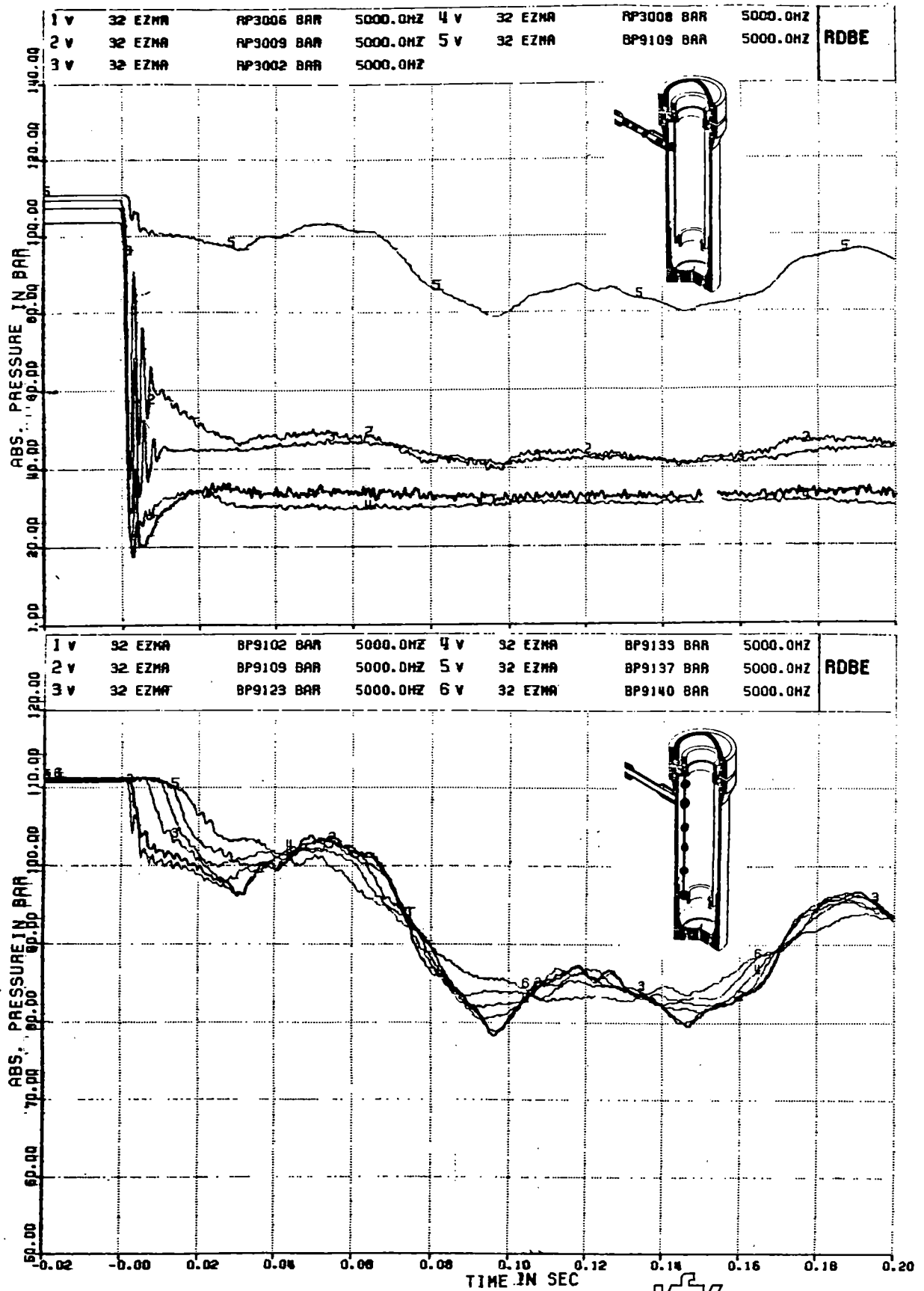


FIG. 10



REPRODUCIBILITY OF DIFF. PRESSURE AND AZIMUTHAL STRAIN FOR 3 RPV-I TESTS V31.0, V31.1, V31.2

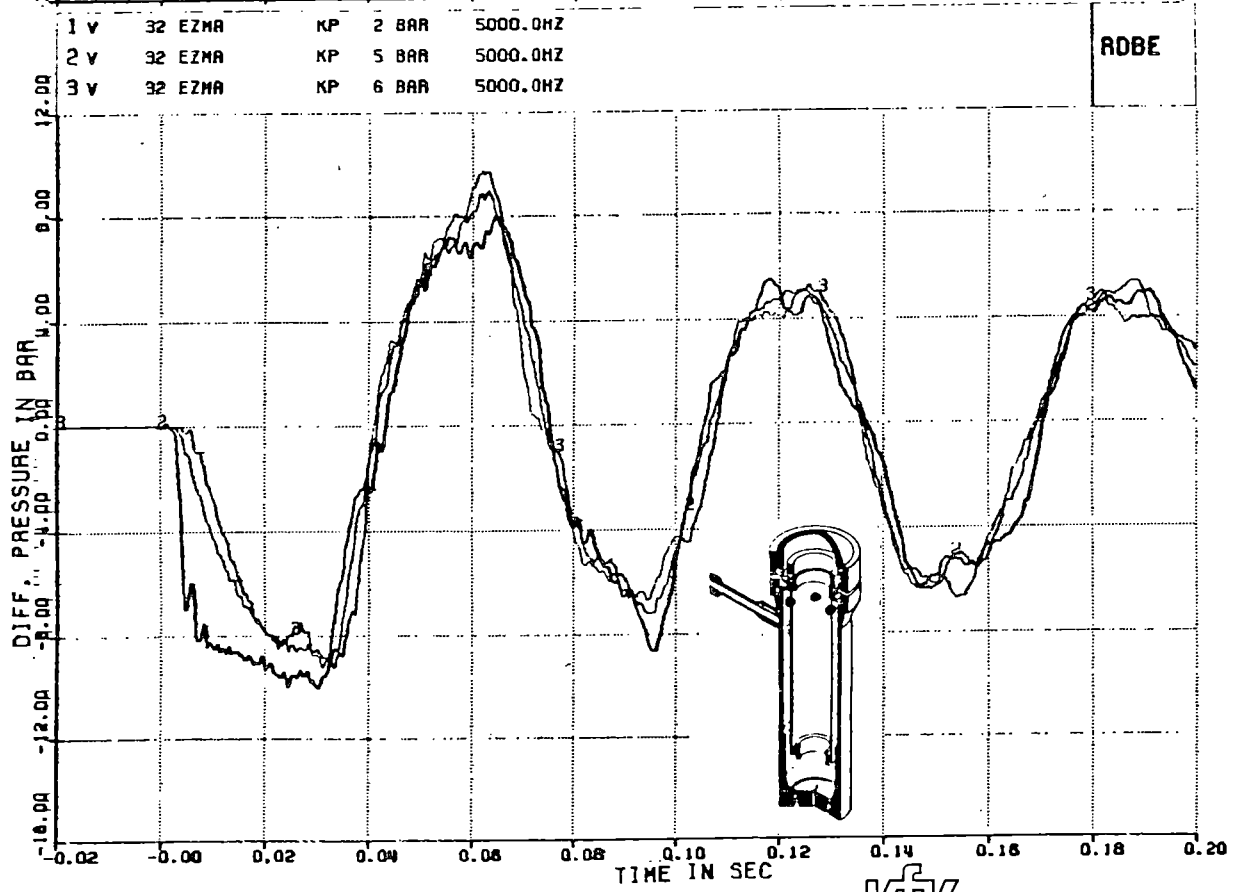
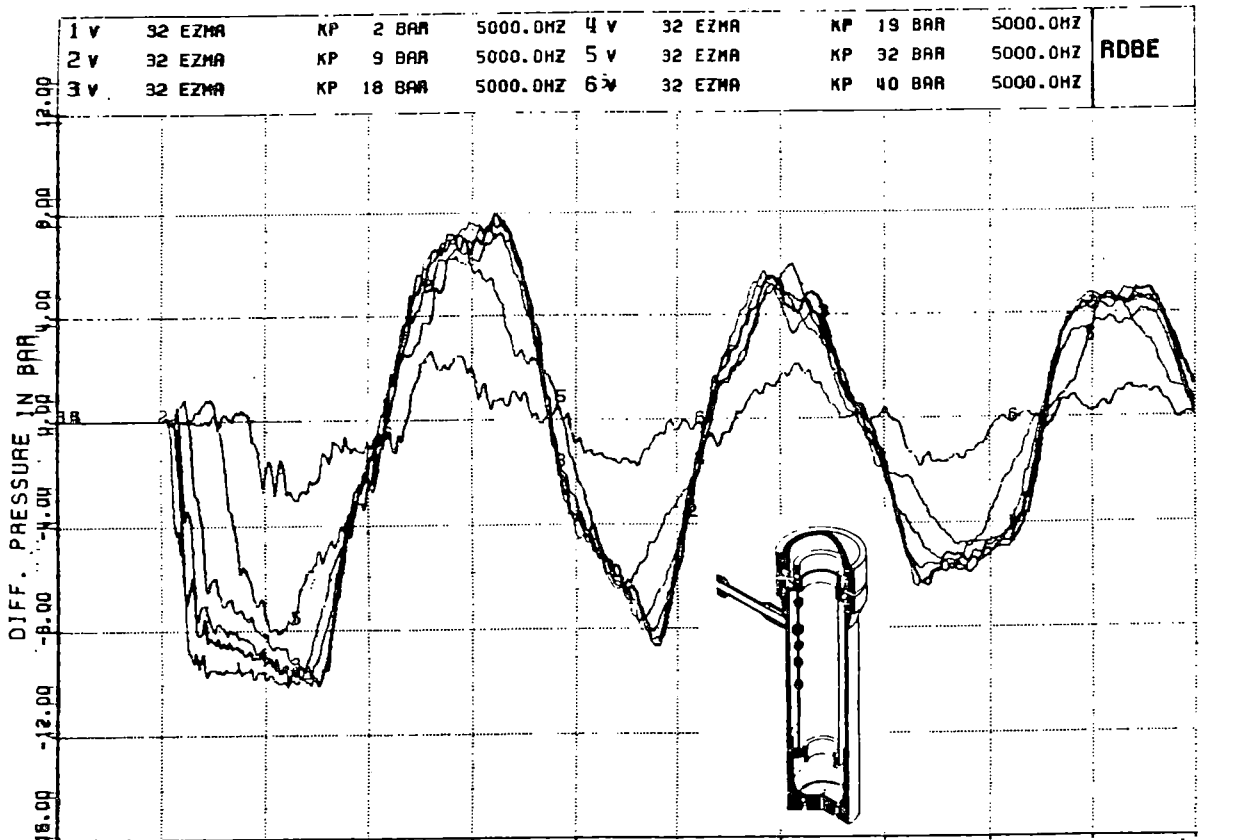
FIG. 11



V32; ABS. PRESSURES AS FUNCTION OF TIME  
ALONG BREAK NOZZLE AND DOWNCOMER



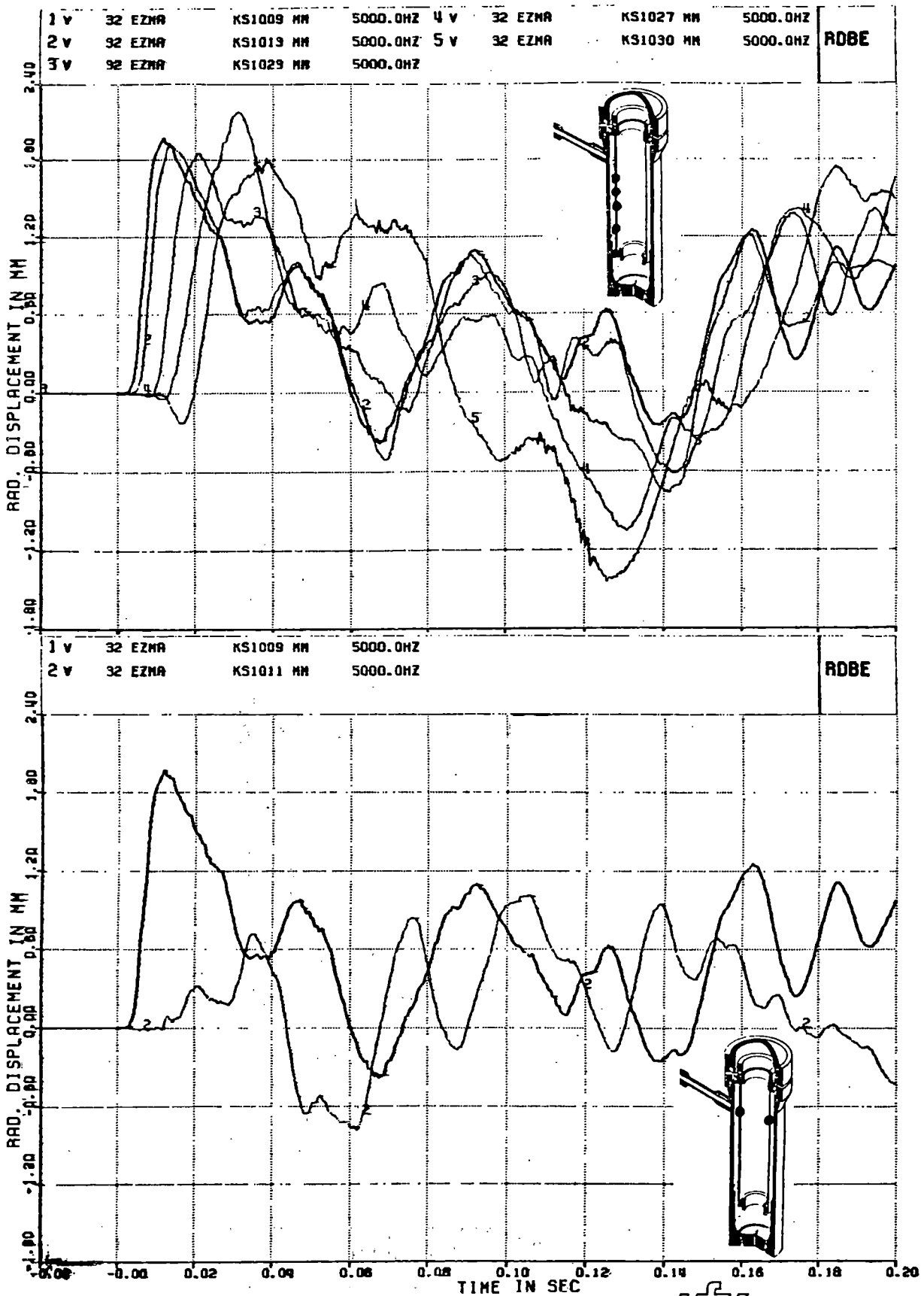
FIG. 12



V32; DIFF. PRESSURES ALONG AND AROUND THE CORE BARREL

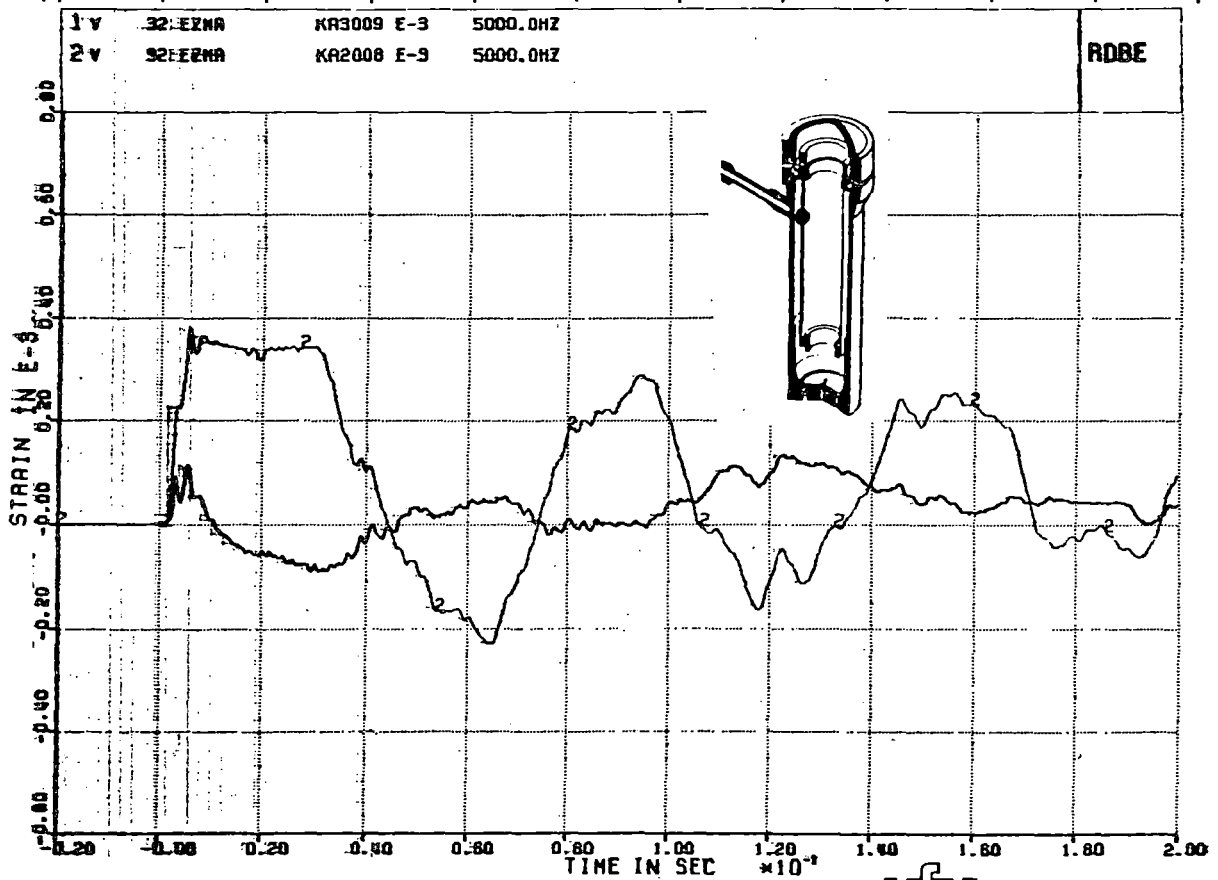
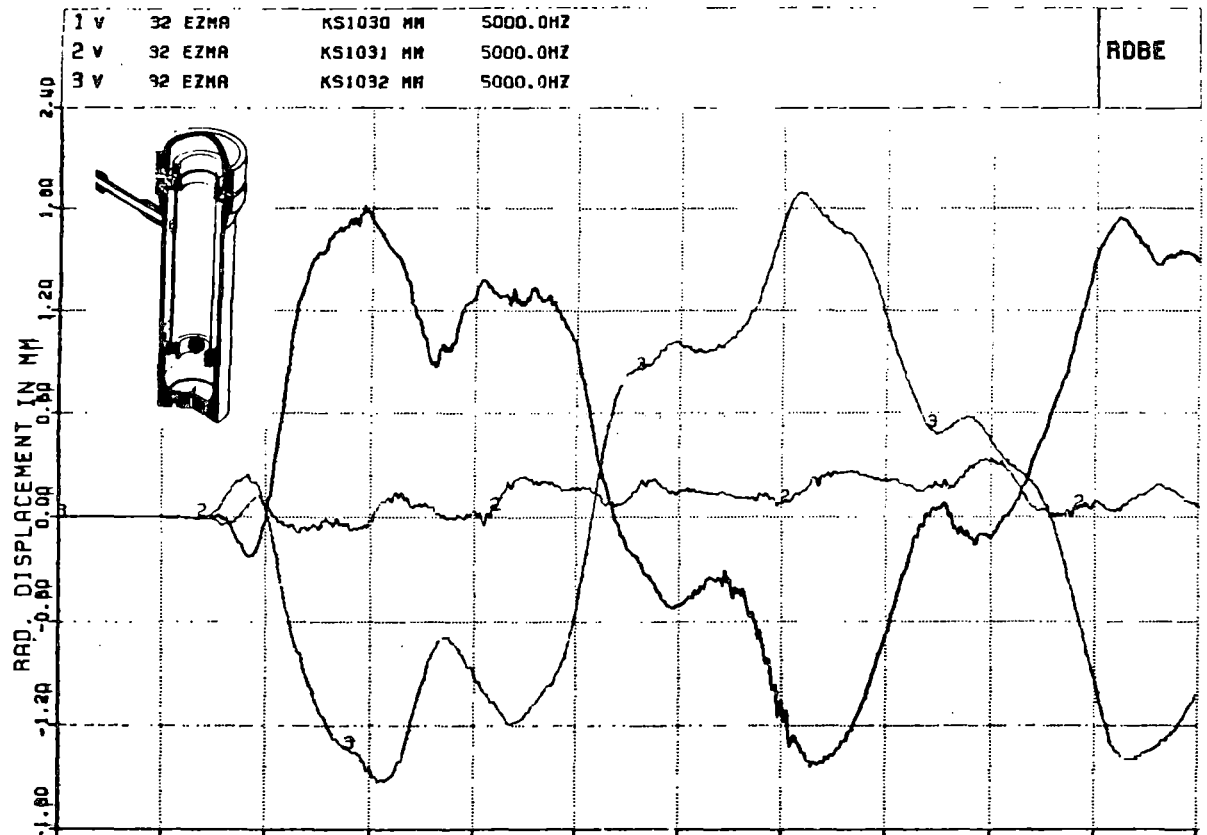


FIG. 13



V32; RAD. RELATIVE DISPLACEMENT ALONG AND AROUND THE CORE BARREL

FIG. 14

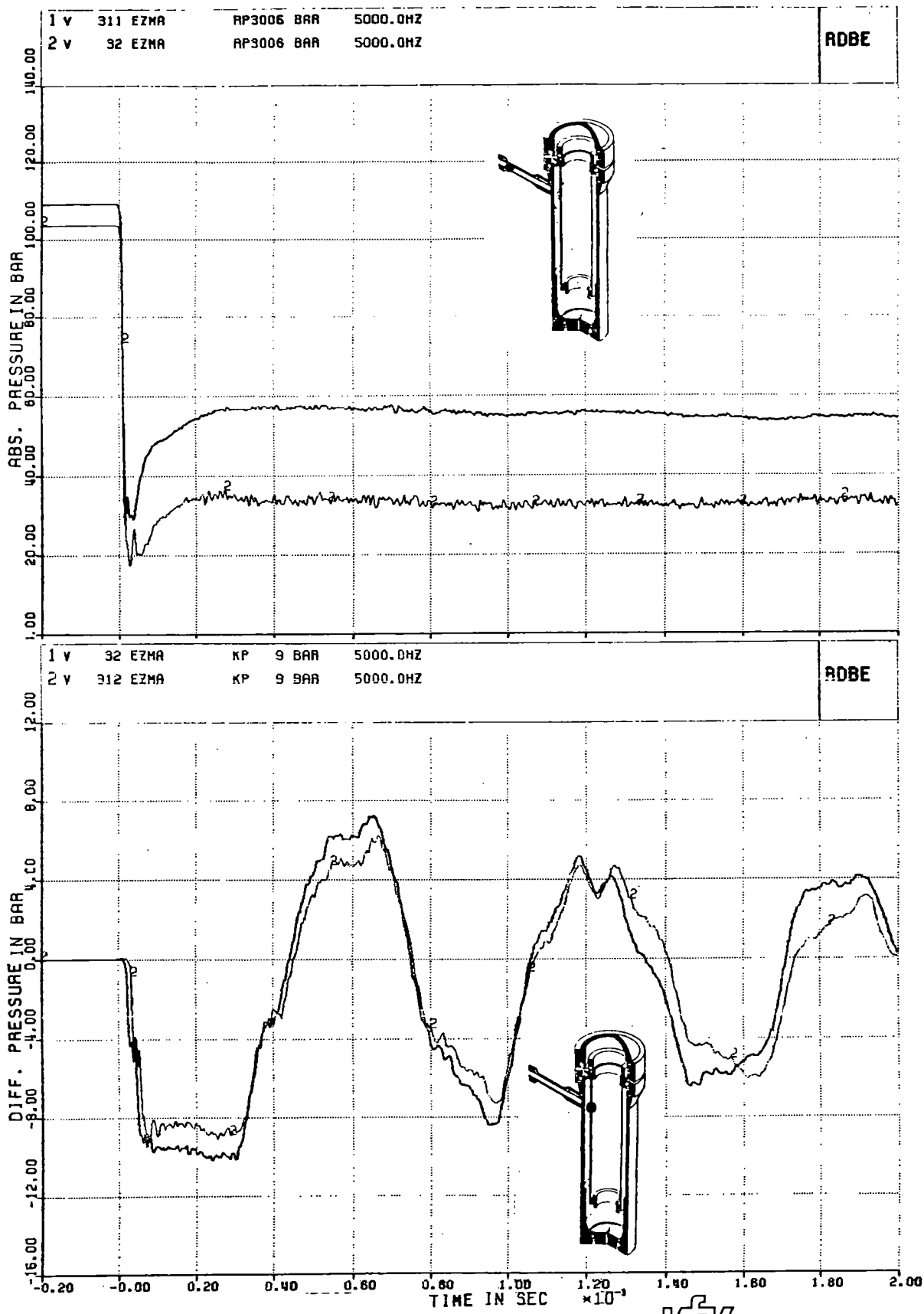


V32; RAD. RELATIVE DISPLACEMENTS AROUND CORE  
 BARREL LOWER END AND AXIAL AND AZIMUTHAL  
 STRAINS AT OUTSIDE CB AT BREAK NOZZLE AXIS

KIK

FIG. 15

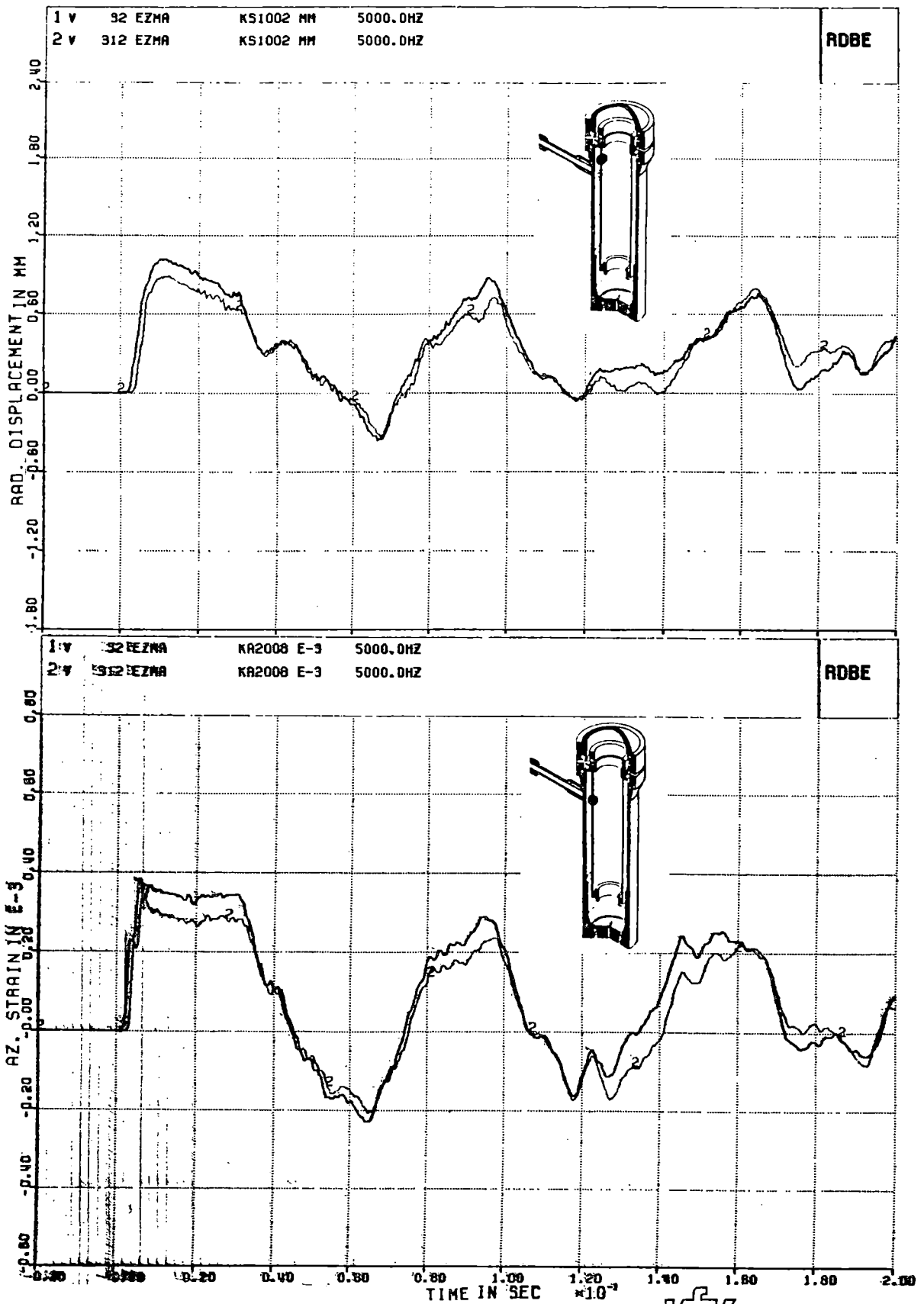




V31.2/V32; COMPARISONS OF ABS. PRESSURES AT BREAK AND DIFF. PRESSURES AT CB AT BREAK NOZZLE AXIS



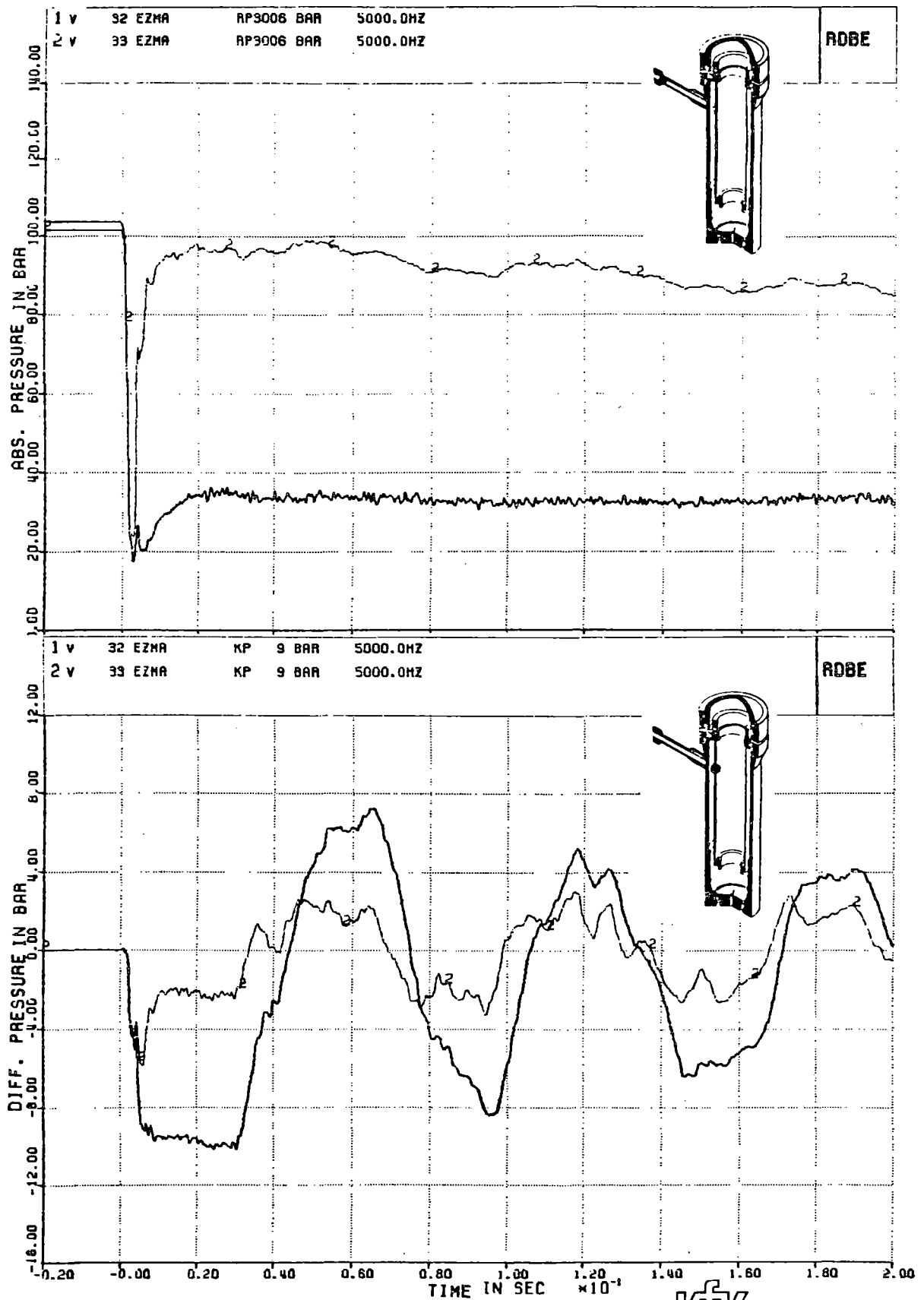
FIG. 16



V31.2/V32; COMPARISONS OF RAD. DISPLACEMENTS AND AZIMUTHAL STRAINS AT OUTSIDE CB

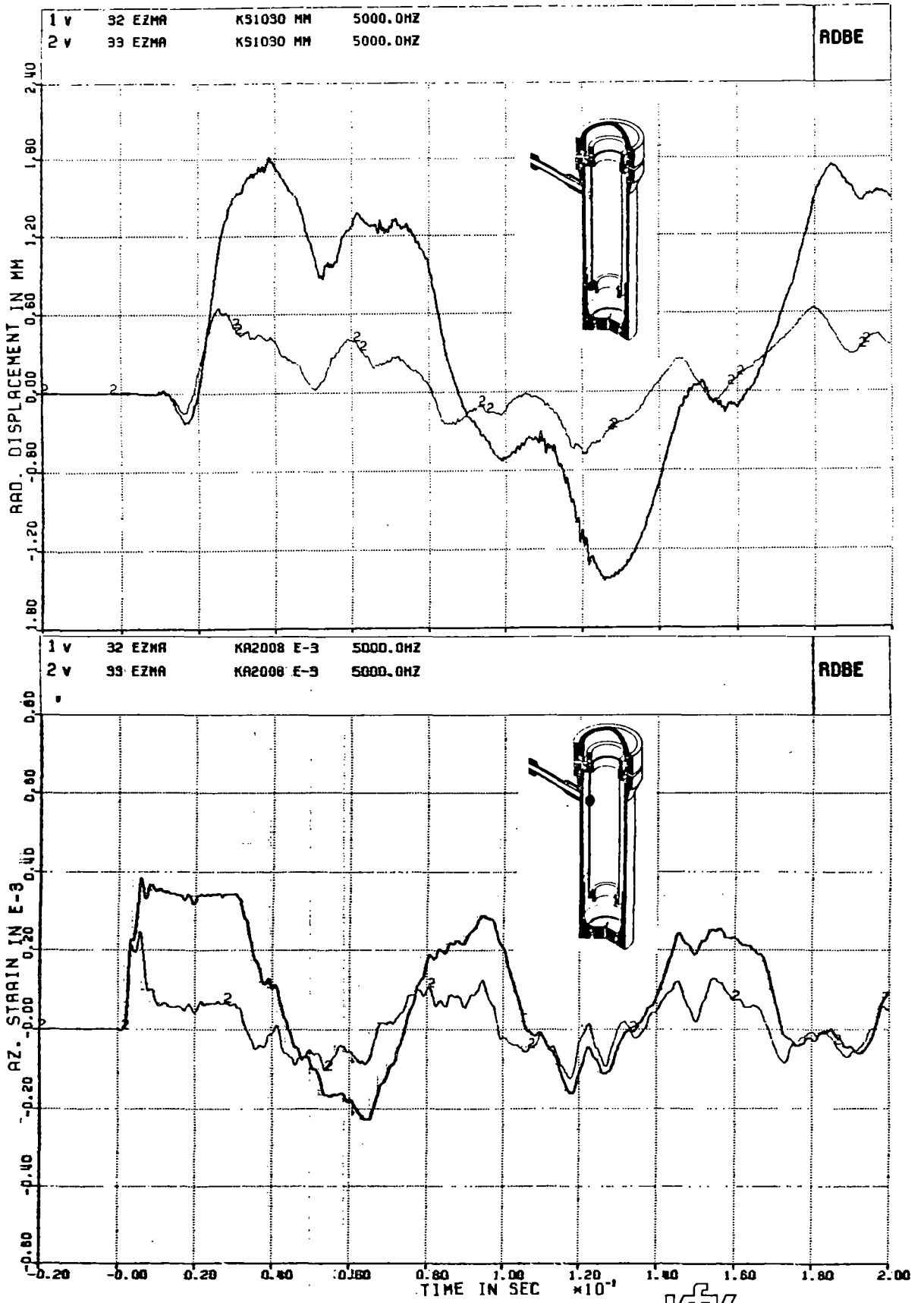


FIG. 17



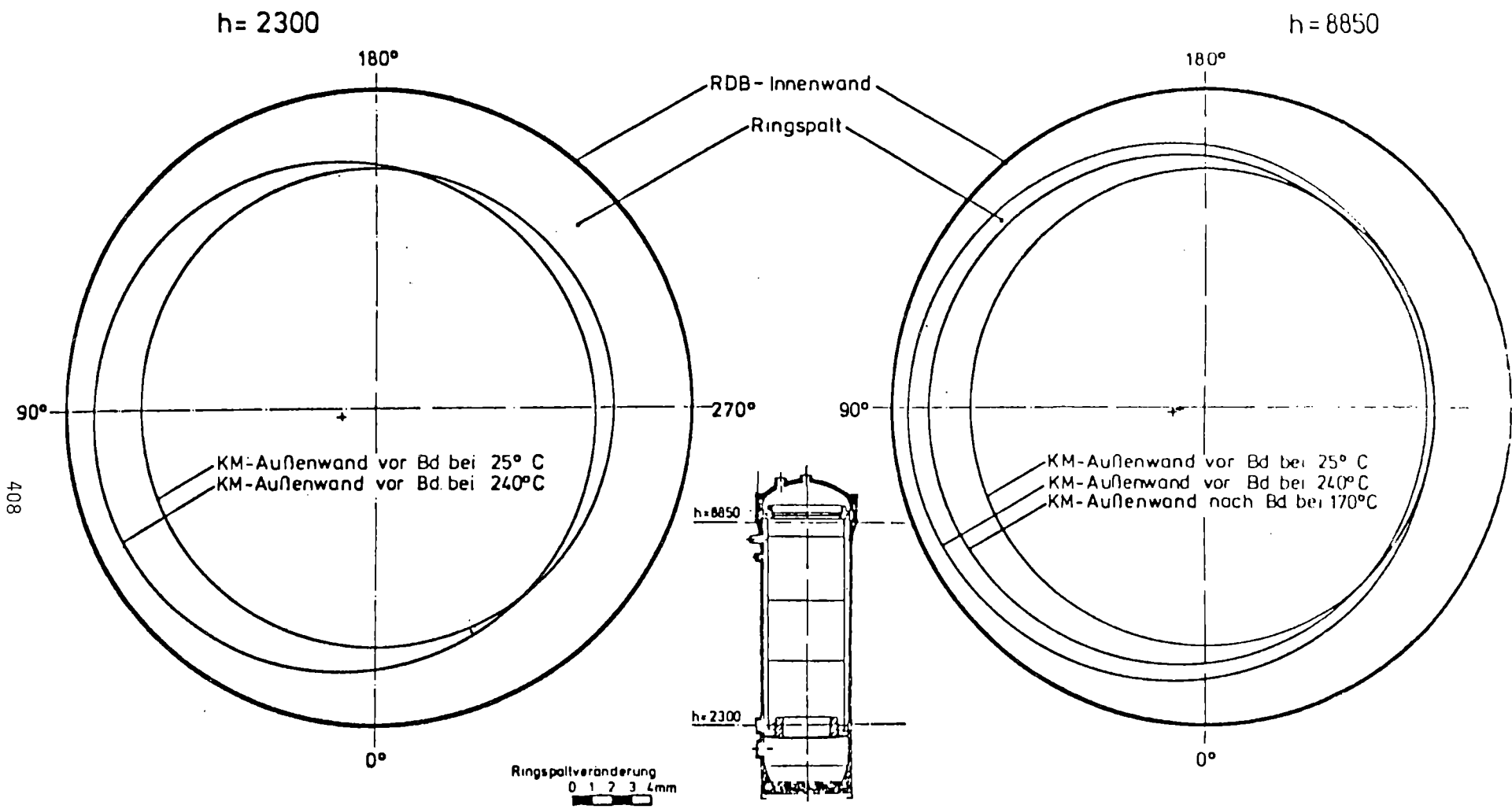
V32/V33; COMPARISONS OF ABS. PRESSURES AT BREAK AND DIFF. PRESSURES AT CB AT BREAK NOZZLE AXIS

FIG. 18



V32/V33; COMPARISONS OF RAD. DISPLACEMENTS AT CB LOWER END AND AZ. STRAINS AT OUTSIDE CB

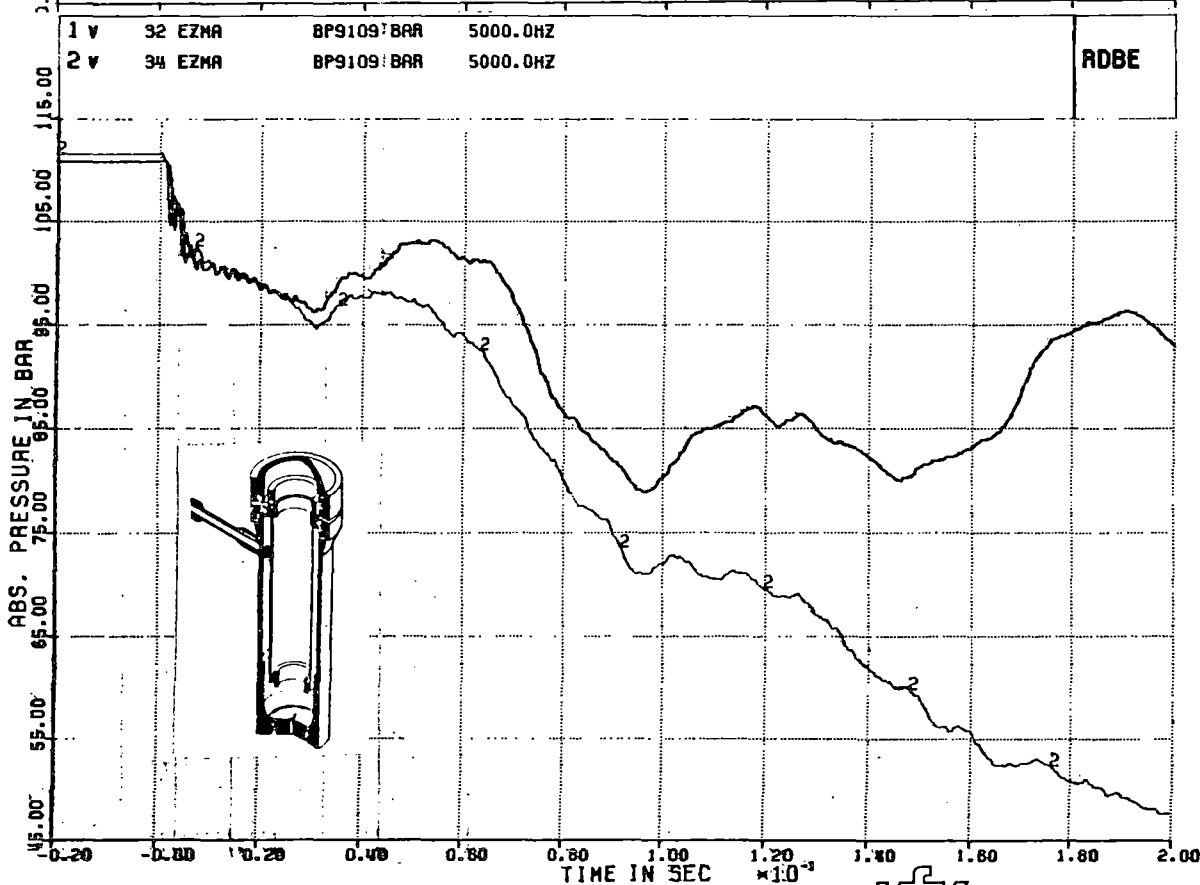
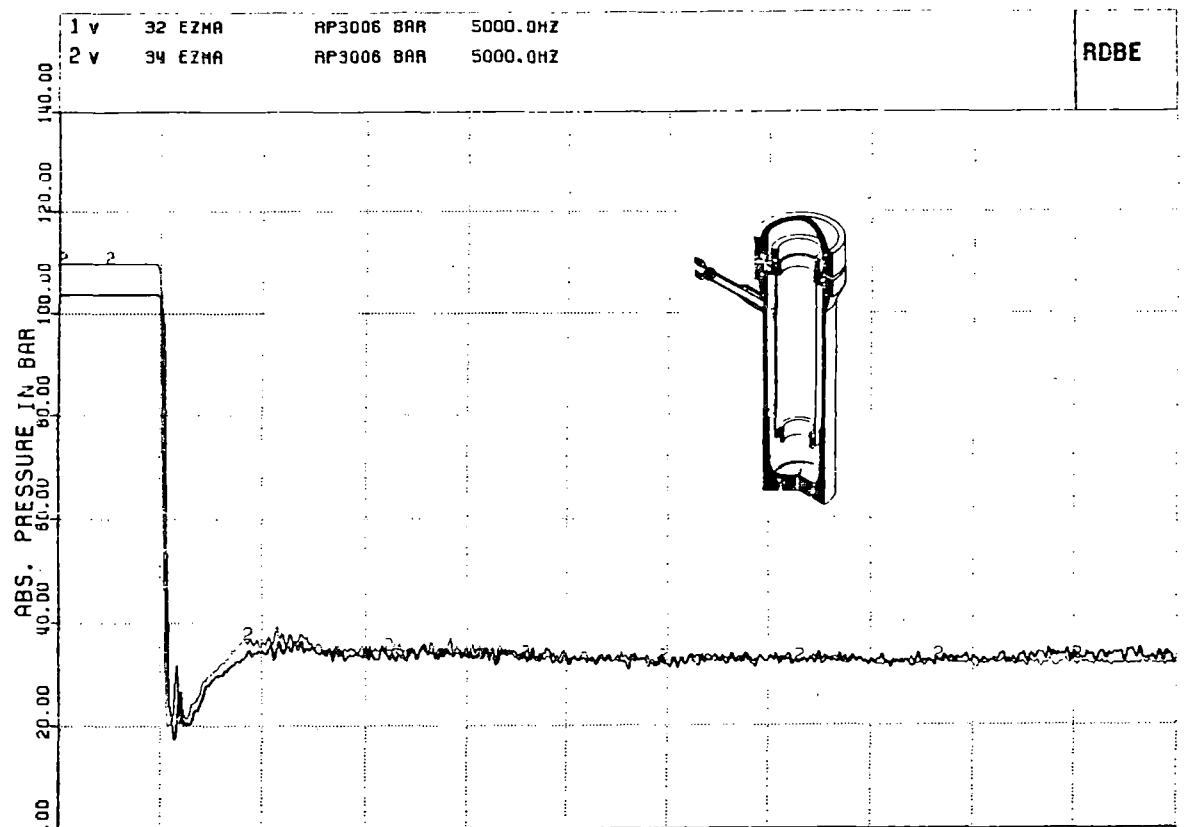
FIG. 19



V34; RELATIVE, RADIAL CHANGES IN CB OUTSIDE SURFACE DISPLACEMENTS DURING HEAT-UP PERIOD AT TWO AXIAL ELEVATIONS



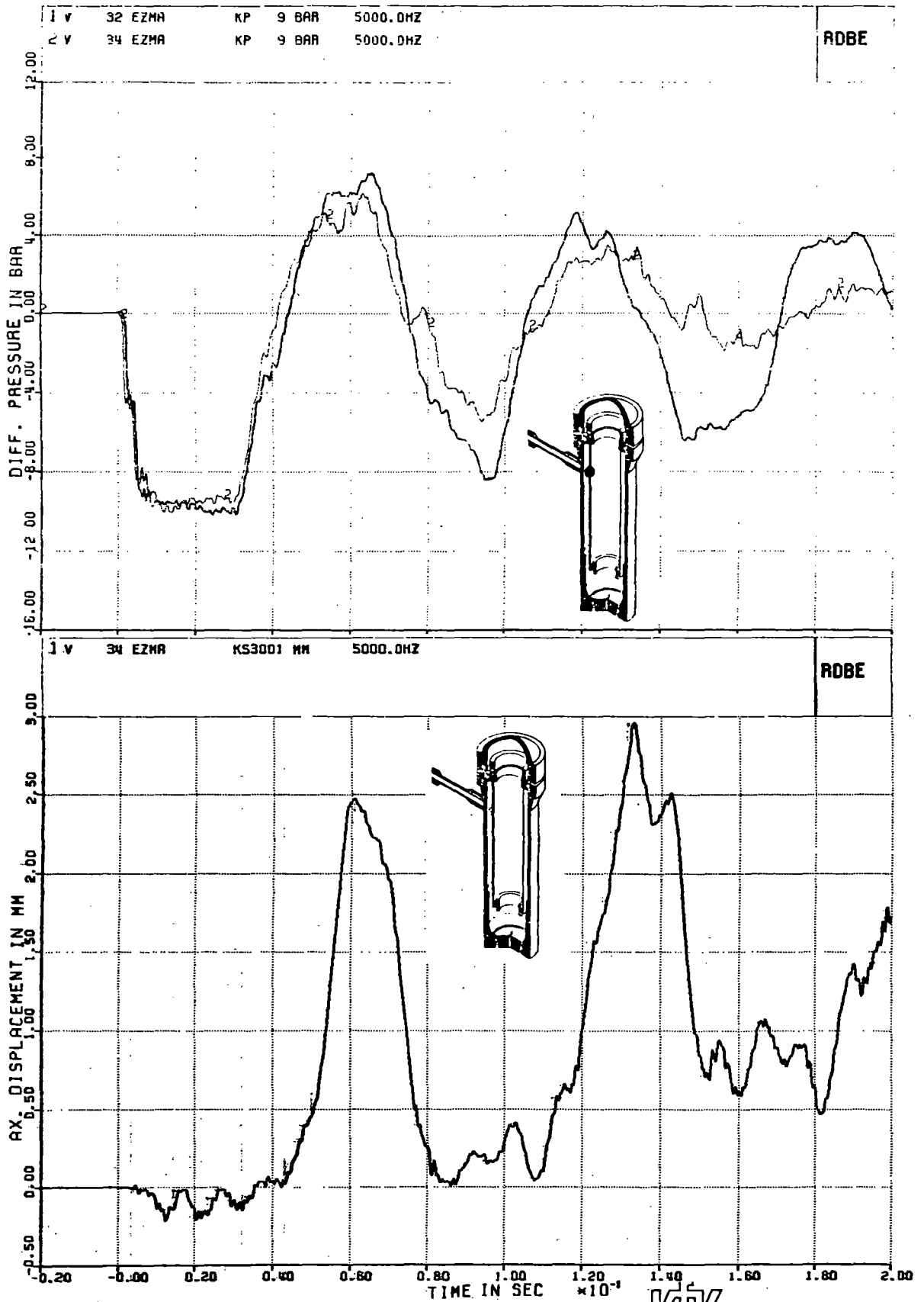
FIG. 20



V32/V34; COMPARISONS OF ABS. PRESSURES AT BREAK AND ABS. PRESSURES IN THE DOWNCOMER AT BREAK NOZZLE AXIS

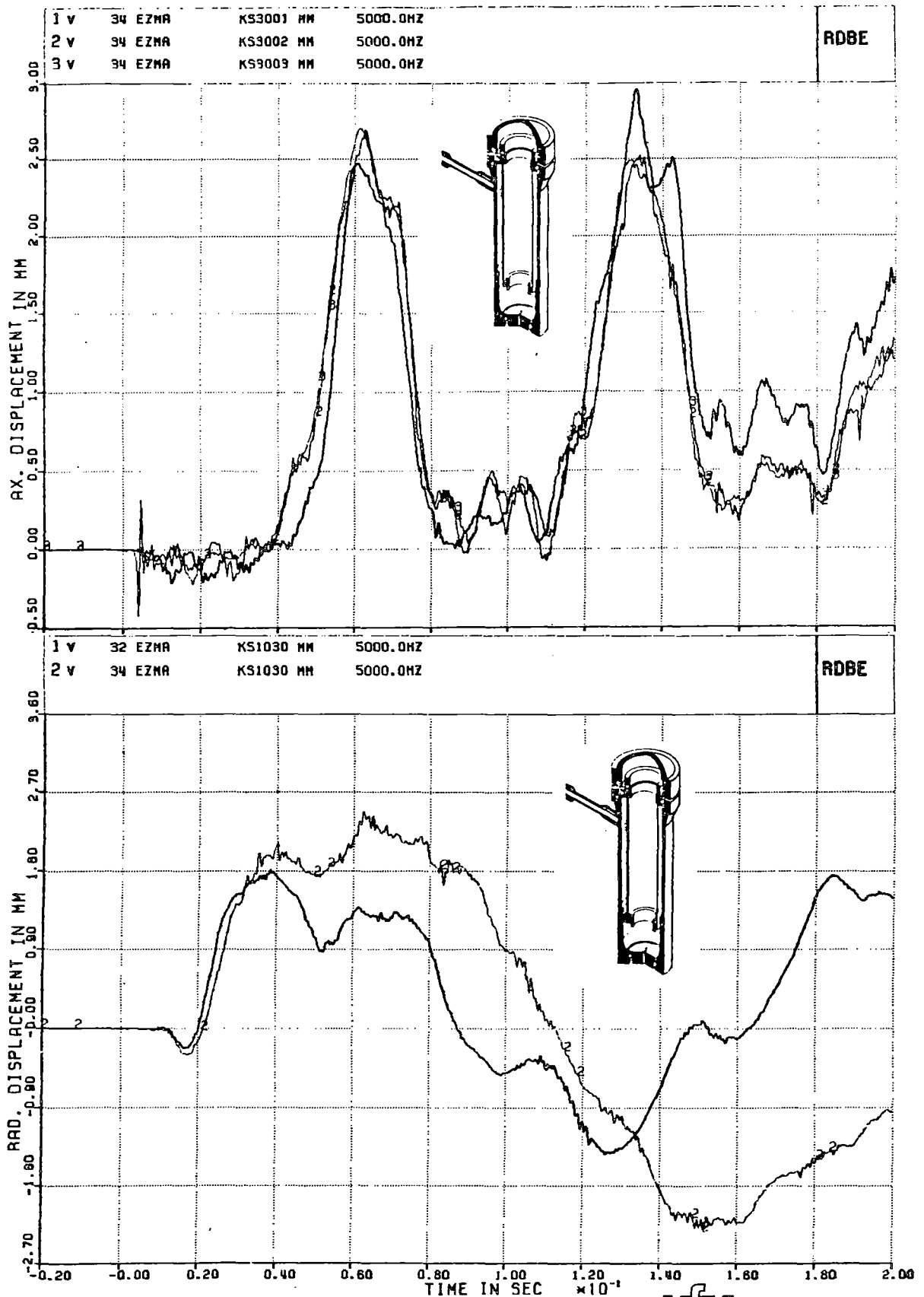


FIG. 21



V32/V34; COMPARISONS OF DIFF. PRESSURES AT CB  
 AT BREAK NOZZLE AXIS AND CB UPPER FLANGE AXIAL  
 DISPLACEMENT

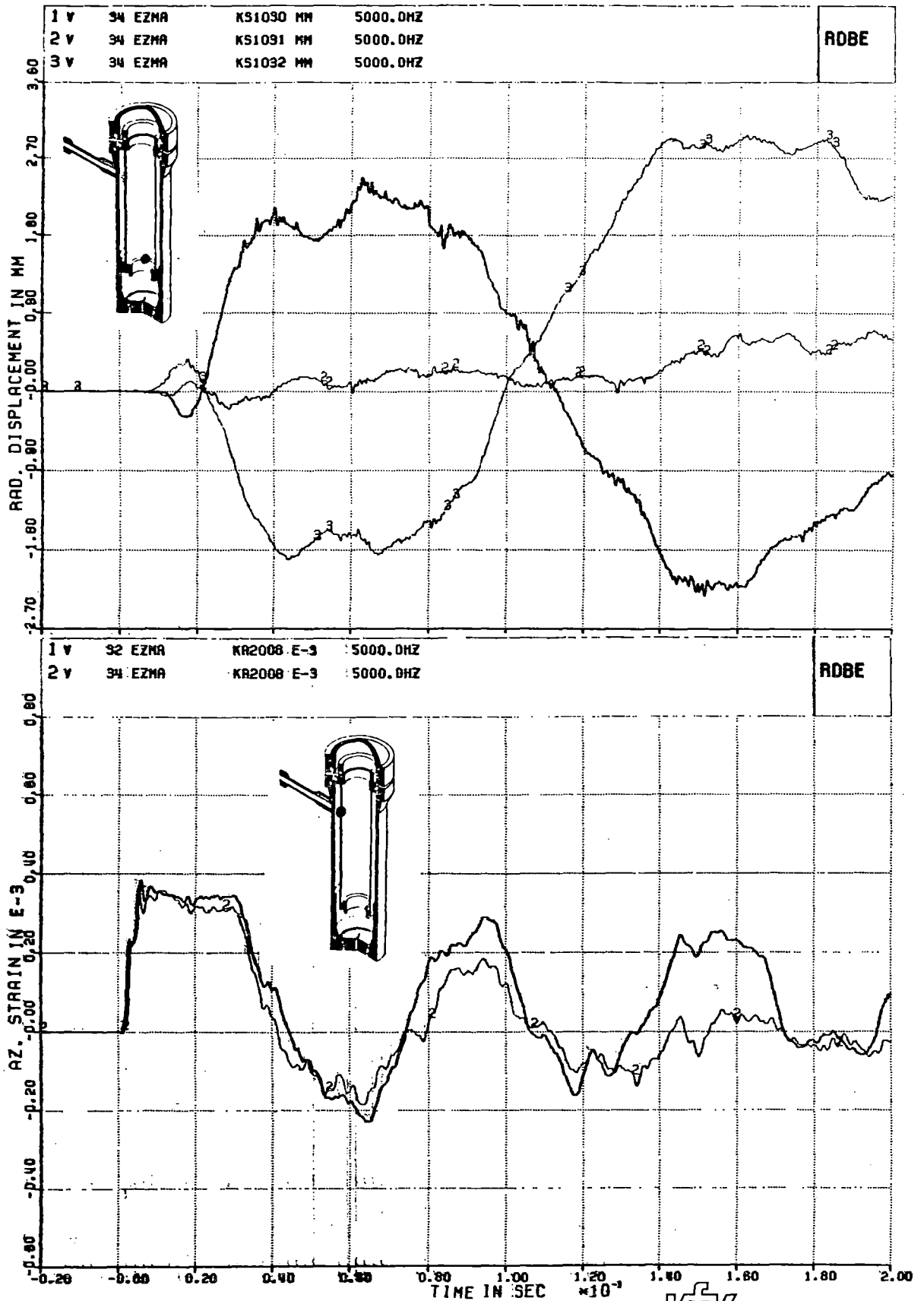
FIG. 22



V32/V34; SUPERPOSITION OF THE 3 AXIAL DISPLACEMENTS OF CB UPPER FLANGE AND REL. RAD. DISPLACEMENTS AT CB LOWER END

FIG. 23





V32/V34; SUPERPOSITION OF REL. RAD. DISPLACEMENTS AT 3 CIRCUMFERENTIAL POSITIONS AT CB LOWER END AND COMPARISONS OF AZIMUTHAL STRAINS

FIG. 24

| QUANTITY     | SENSOR  | V31.2/V32 |      | V33/V32 |      | V34/V32 |      |
|--------------|---------|-----------|------|---------|------|---------|------|
|              |         | min.      | max. | min.    | max. | min.    | max. |
| ABS.PRESS.   | RP 3006 | 1.38      |      | 1.2     |      | 1       |      |
| MASS FLOW    | RM 9090 |           | 0.88 |         | 0.26 |         | 1    |
| DIFF.PRESS.  | KP 0009 | 0.9       | 0.85 | 0.6     | 0.42 | 1       | 1    |
| DIFF.PRESS.  | KP 0032 | 0.87      | 0.84 | 0.5     | 0.33 | 1       | 1    |
| DISPLACEMENT | KS 1002 | 1         | 0.9  | 0.66    | 0.5  | 0       | 0.68 |
| DISPLACEMENT | KS 1023 | 1         | 0.85 | 0.5     | 0.42 | 1.9     | 1.26 |
| DISPLACEMENT | KS 1030 | 0.96      | 0.88 | 0.25    | 0.36 | 1.6     | 1.33 |
| STRAINS      | KA 2008 | 1         | 0.9  | 0.45    | 0.52 | 1       | 1    |
| STRAINS      | KA 3009 | 1         | 1    | 0.5     | 1    | 1.25    | 1    |

RATIO OF AMPLITUDES OF VARIOUS QUANTITIES  
EXPERIMENTALLY OBSERVED DURING HDR-RPV-I  
TESTS V31.2 THROUGH V34



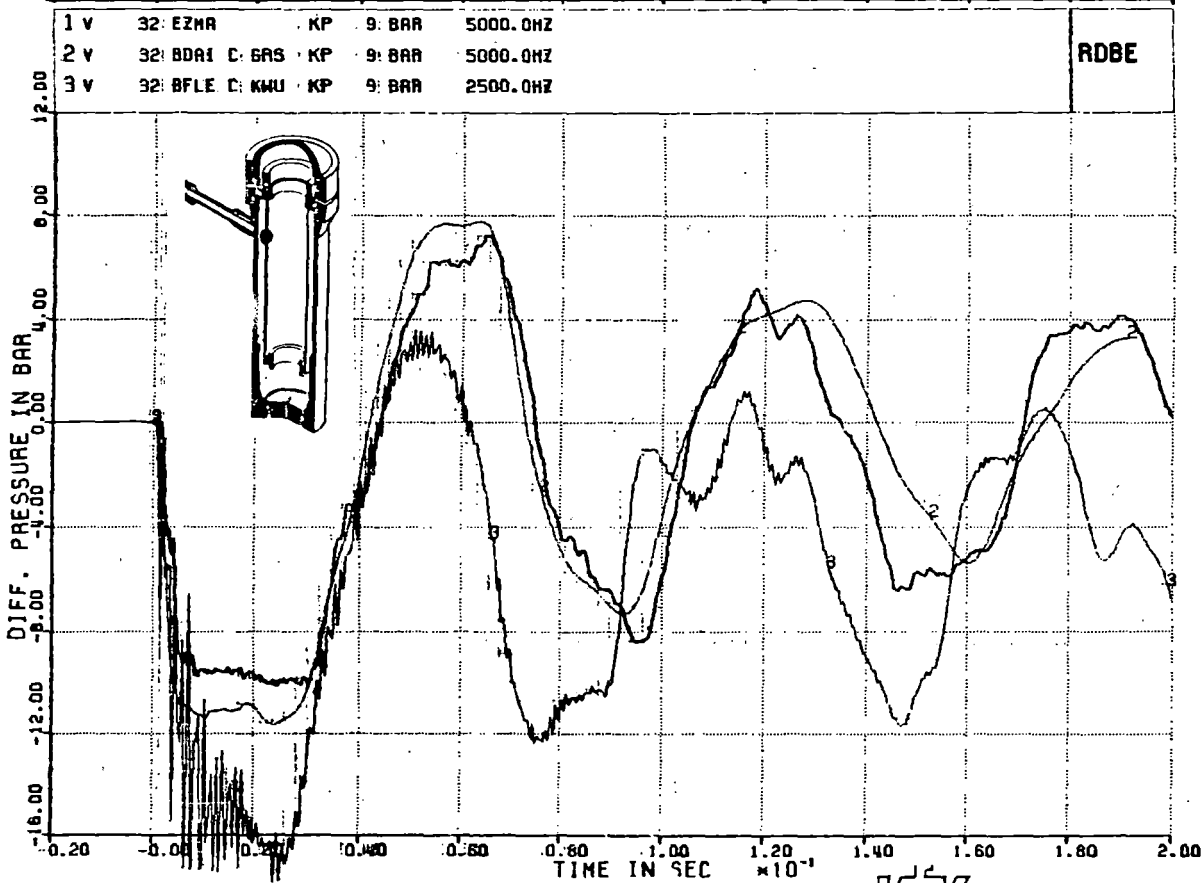
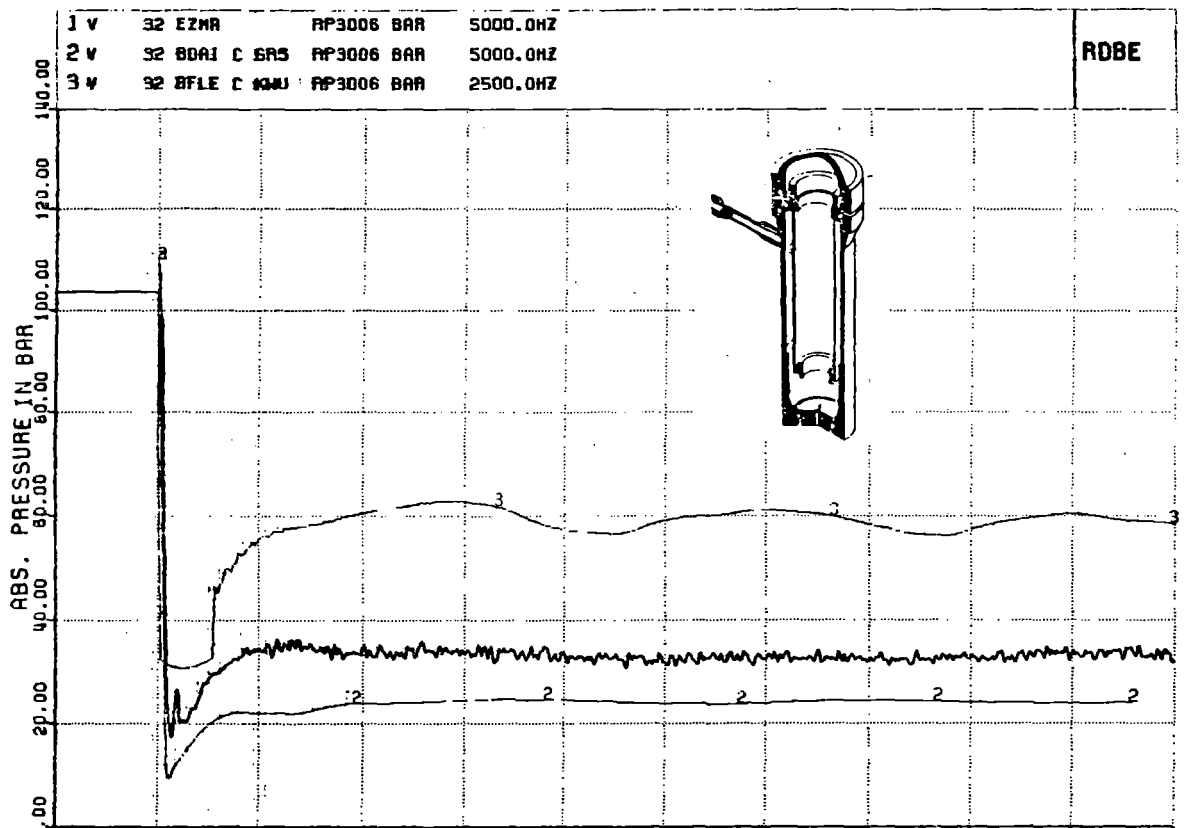
FIG. 25

| Code Abbreviation | Code Name         | Institution Country         | Remarks  |
|-------------------|-------------------|-----------------------------|--|
| DAI               | DAISY             | GRS, Germany                | coupled network  |
| EZMA              | Experimental Data | PHDR, Germany               | coupled  |
| FLE               | FLEXWALL          | KWU, Germany                | coupled; 2 1/2 D downcomer, LECK break nozzle and core representation                                  |
| FDS               | FLUX-DRIX         | IRE-KfK, Germany            | coupled; with pressure boundary calculated at nozzle inlet by DRIX, strong coupling between both codes |
| FDW               | FLUX-DRIX         | IRE-KfK, Germany            | same as above, but weak coupling between both codes  |
| KFXL              | K-FIX(3D,FLX)     | LANL, USA                   | coupled; fully implicit solution   |
| KFXB              | K-FIX(3D,FLX)     | Battelle Frankfurt, Germany | coupled; fully explicit  |
| MFX               | MULTIFLEX         | W, USA                      | coupled network  |
| STE               | STEALTH/WHAMSE    | EPRI, SAI, ITI, USA         | coupled; Lagrange-Euler, rezoning  |



CODES AND THEIR ABBREVIATIONS USED IN THE HDR VERIFICATION PROCESS

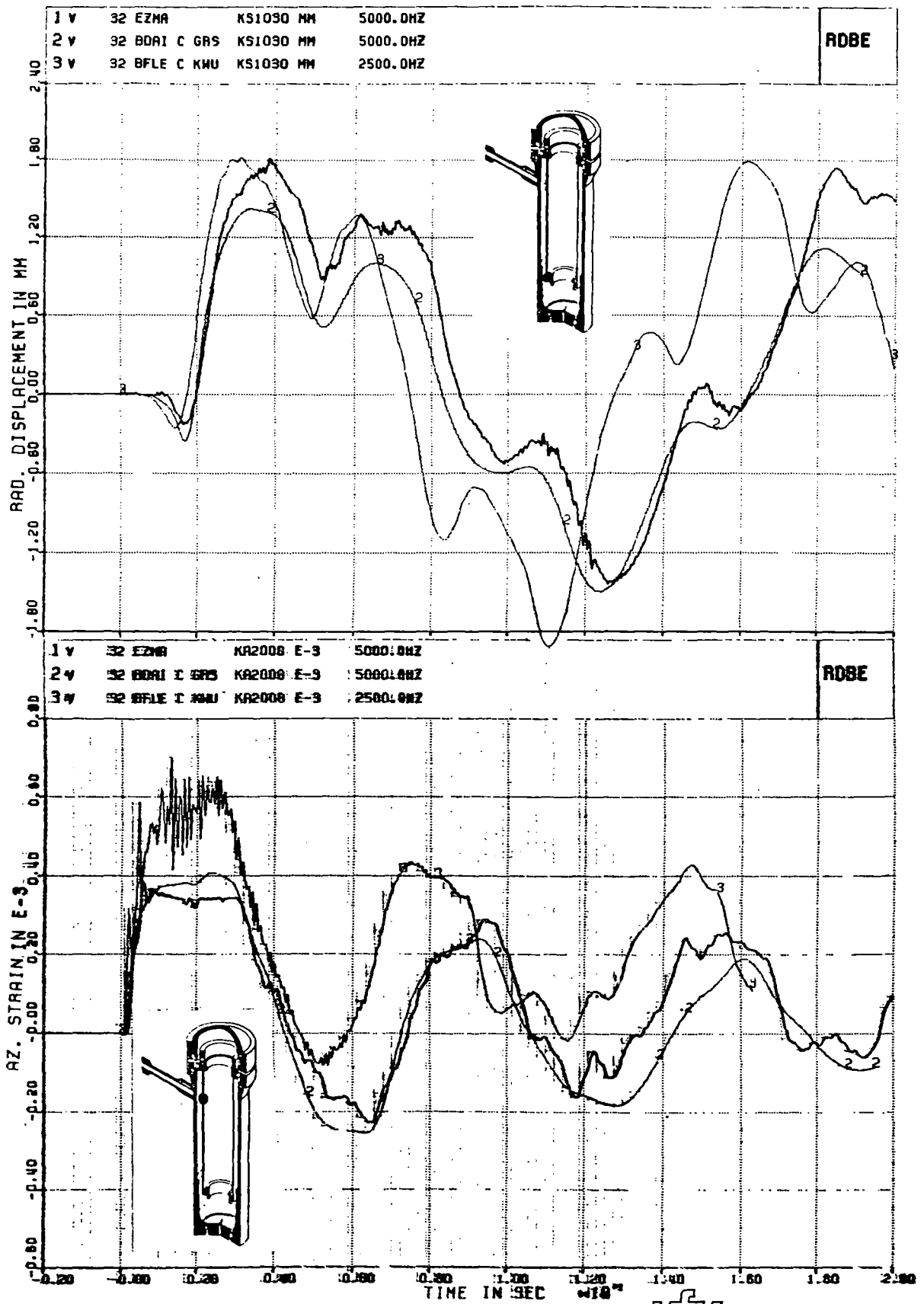
FIG. 26



V32: COMPARISONS OF MEASUREMENTS AND PRETEST CALCULATIONS BY DAISY AND FLEXWALL FOR ABS, AND DIFF. PRESSURES

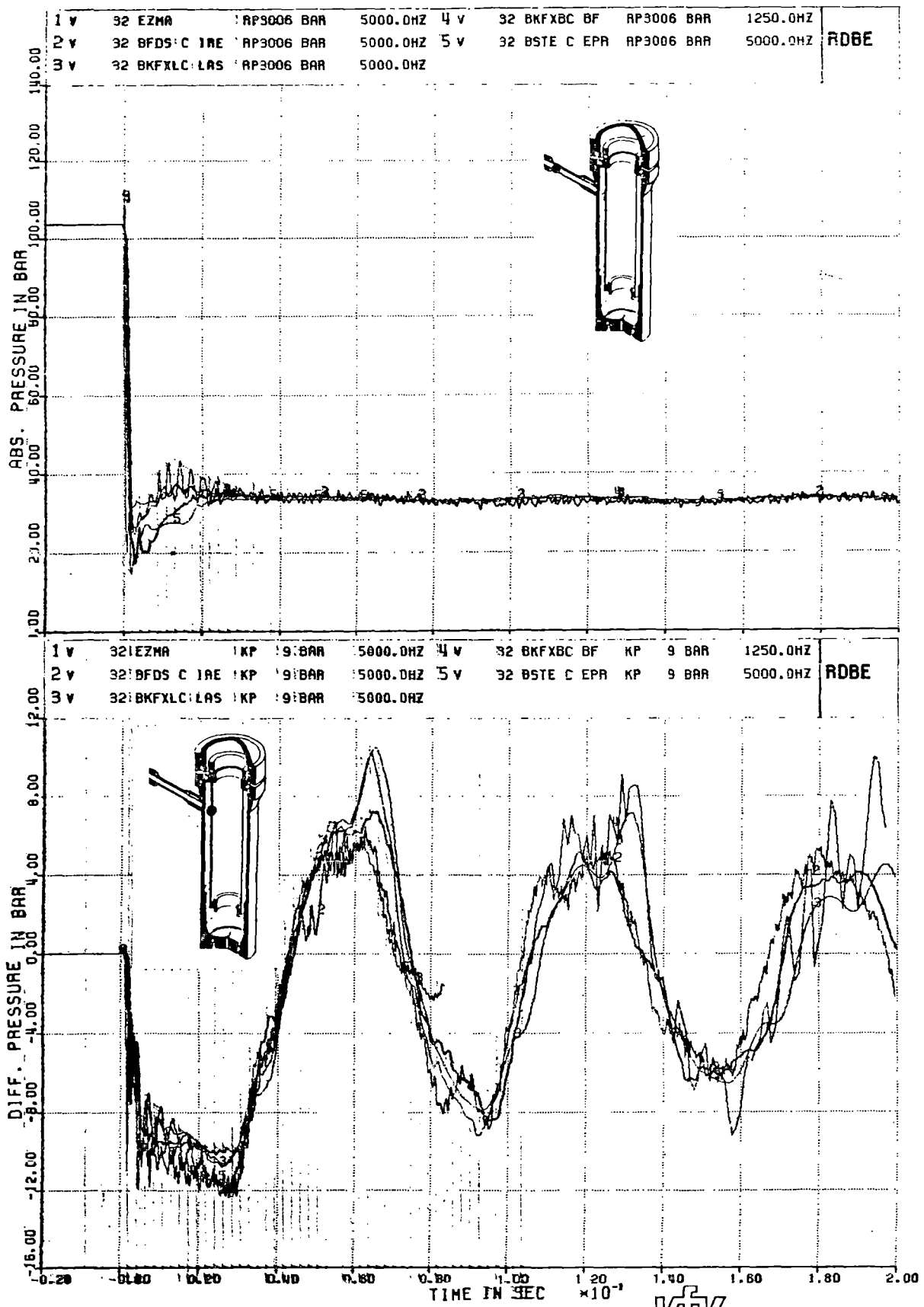


FIG. 27



V32; COMPARISONS OF MEASUREMENTS AND PRETEST CALCULATIONS BY DAISY AND FLEXWALL FOR DISPLACEMENT AND AZ. STRAIN

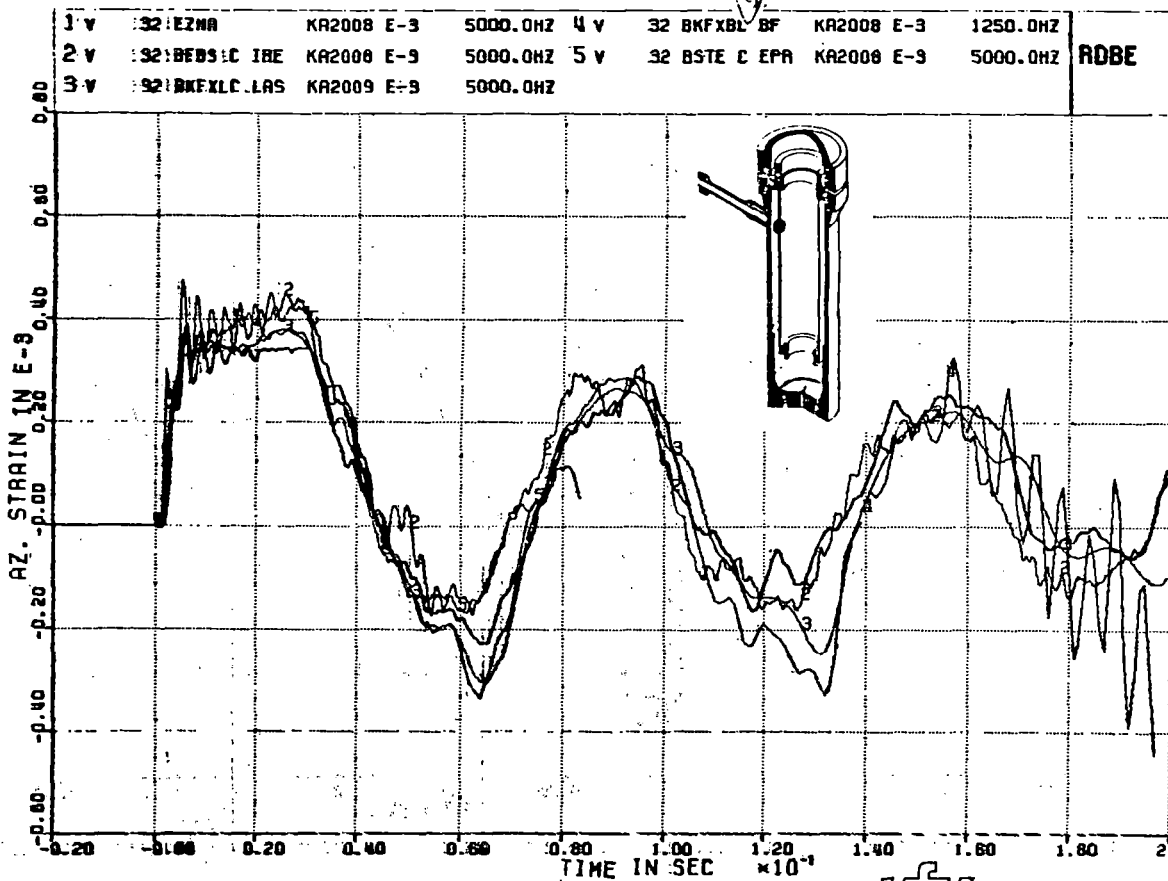
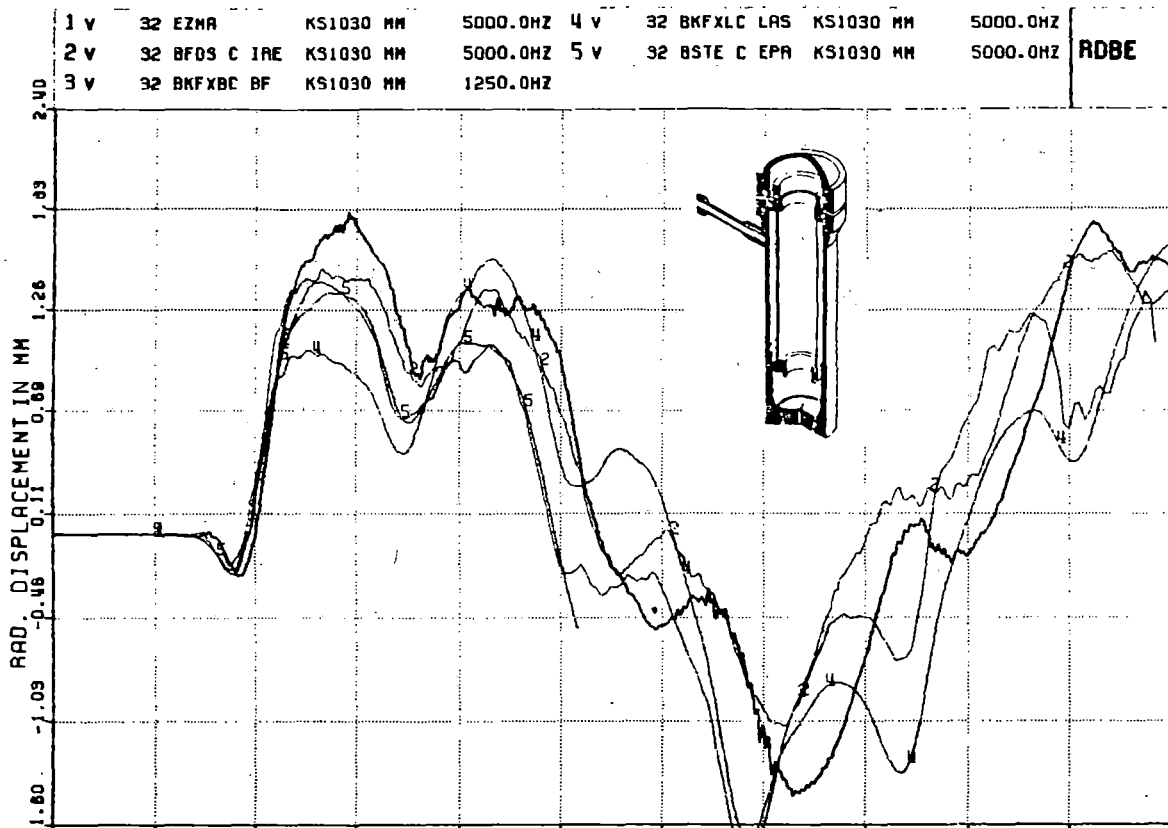
FIG. 28



V32; COMPARISONS OF MEASUREMENTS AND PRETEST CALCULATIONS BY FLUX-DRIX, K-FIX AND STEALTH FOR ABS. AND DIFF. PRESSURES



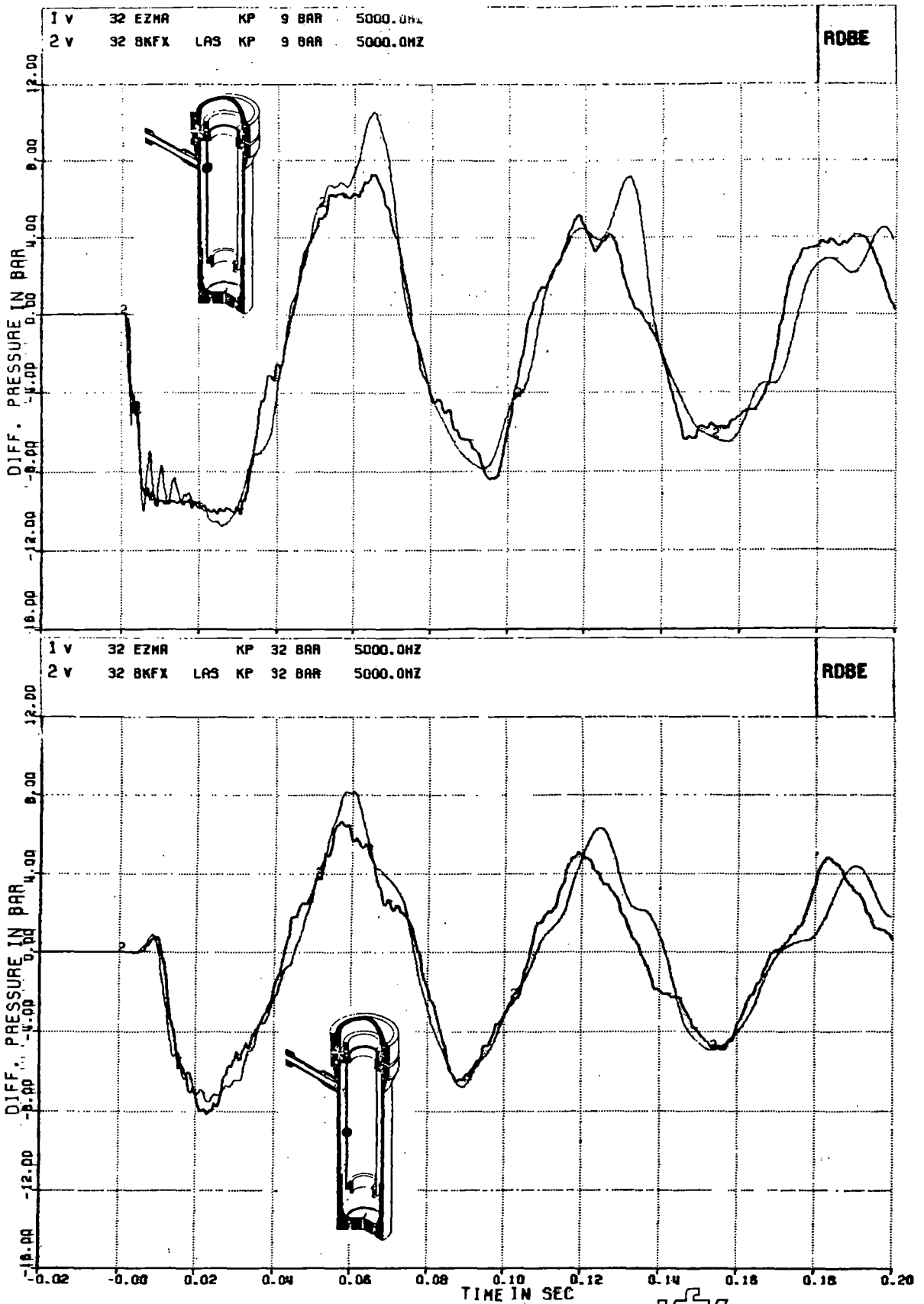
FIG. 29



V32; COMPARISONS OF MEASUREMENTS AND PRETEST CALCULATIONS BY FLUX-DRIX, K-FIX AND STEALTH FOR DISPLACEMENT AND AZ. STRAIN

**KFK**

FIG. 30

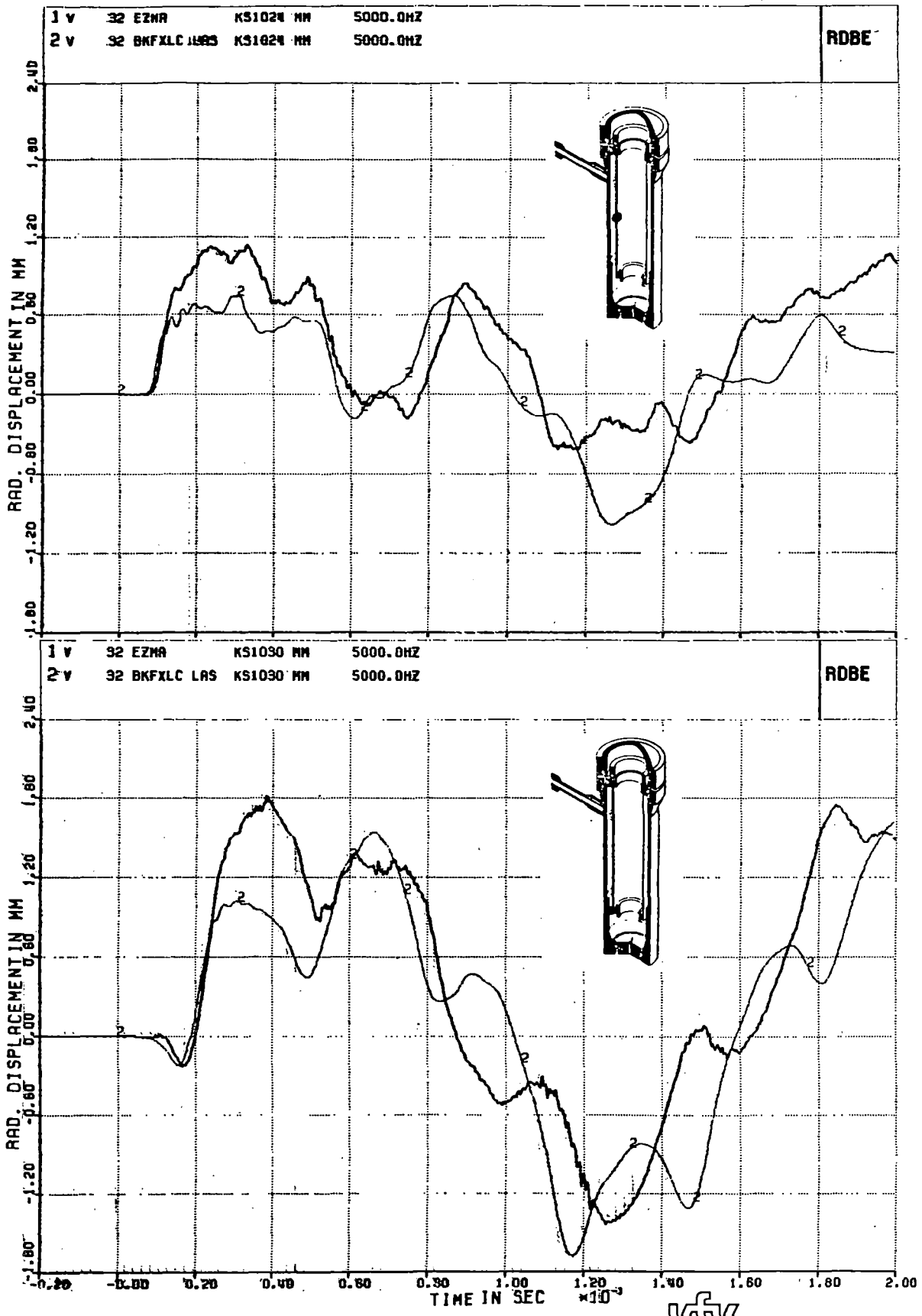


V32; COMPARISONS OF MEASUREMENTS AND LANL-  
PRETEST CALCULATIONS WITH K-FIX FOR DIFF.  
PRESSURES

KFK

FIG. 31

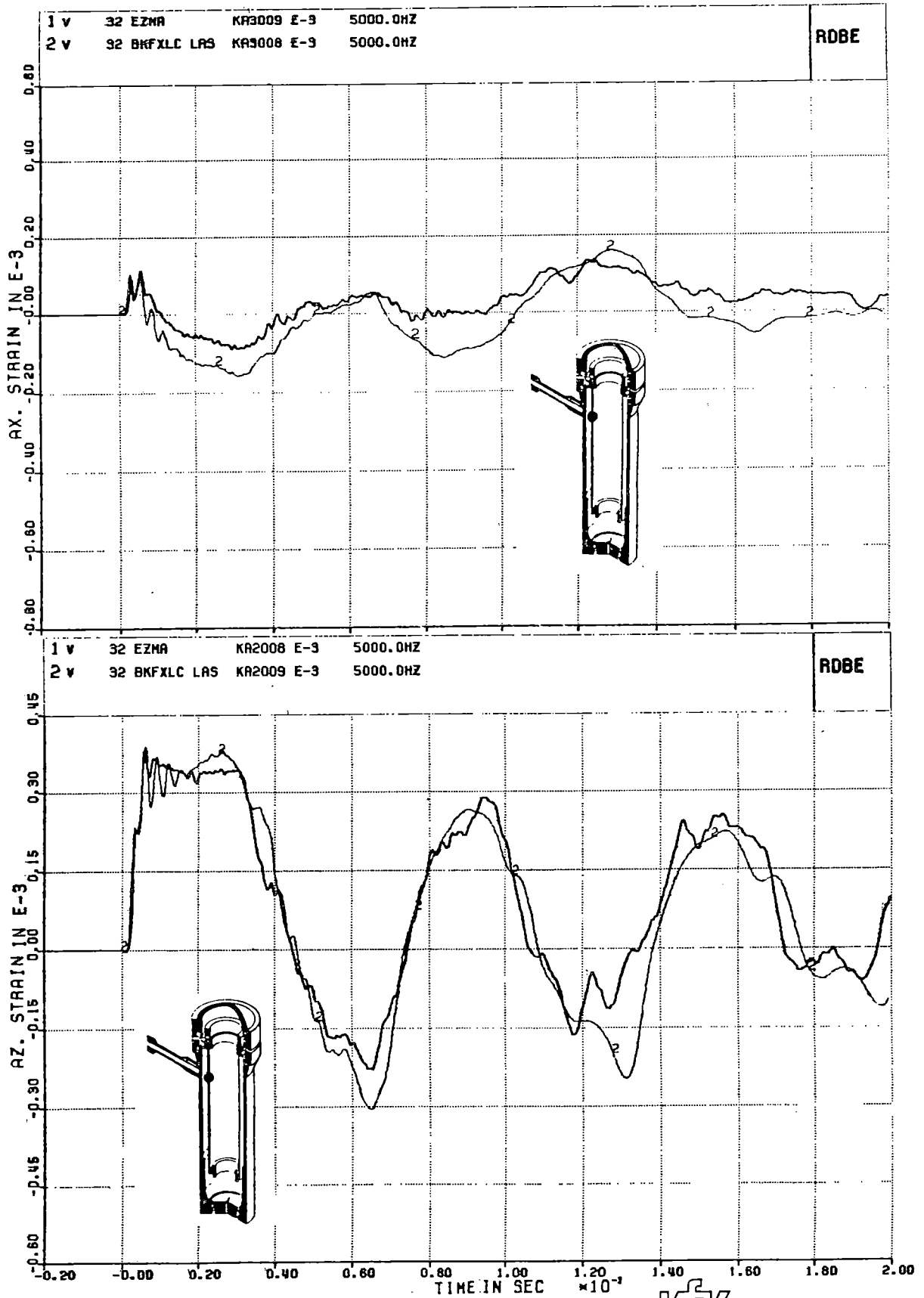




V32; COMPARISONS OF MEASUREMENTS AND LANL-  
PRETEST CALCULATIONS WITH K-FIX FOR RAD.  
DISPLACEMENTS

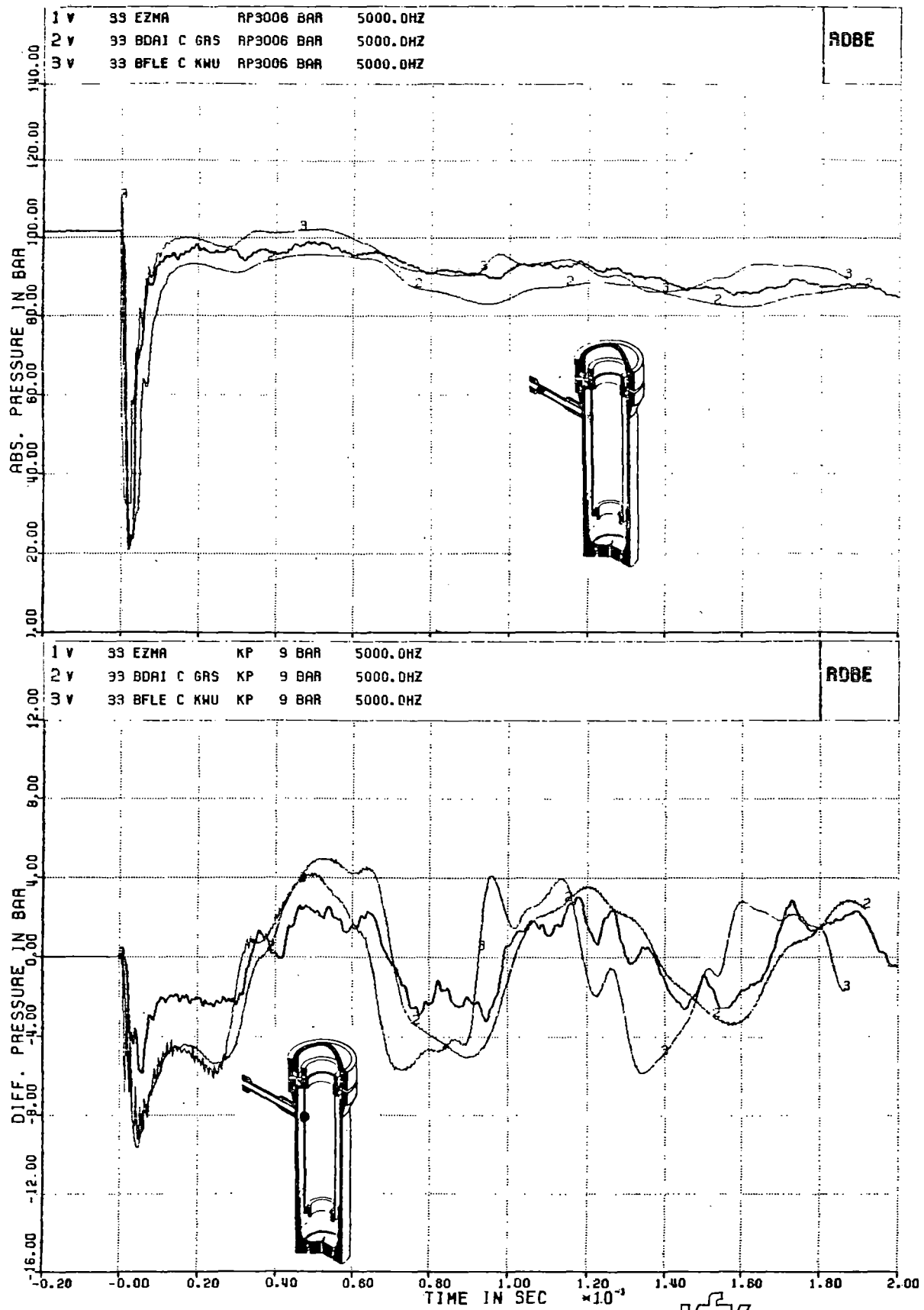


FIG. 32



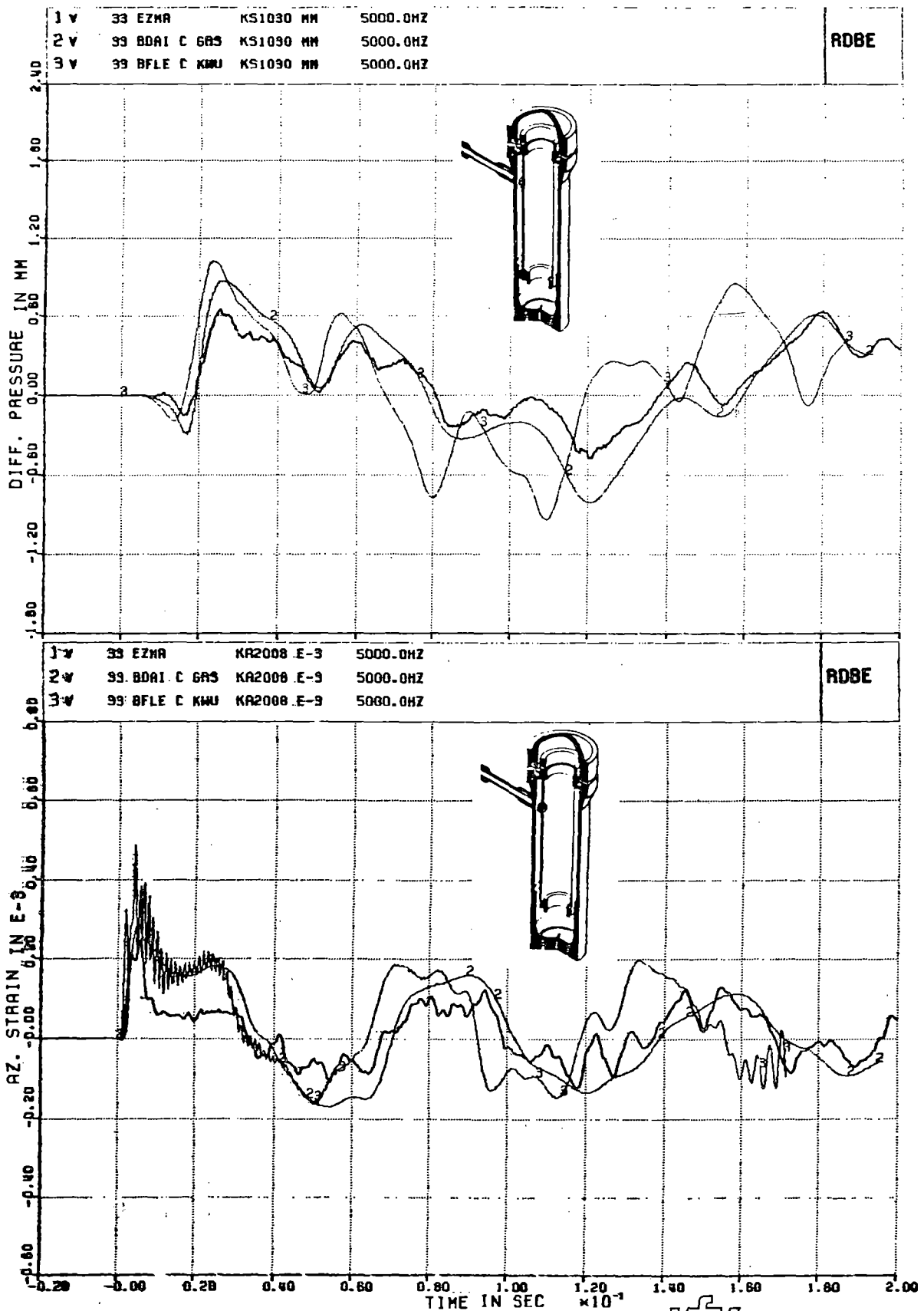
V32; COMPARISONS OF MEASUREMENTS AND LANL-  
PRETEST CALCULATIONS WITH K-FIX FOR AX.  
AND AZ. STRAINS

FIG. 33



V33; COMPARISONS OF MEASUREMENTS AND PRETEST CALCULATIONS BY DAISY AND FLEXWALL FOR ABS, AND DIFF. PRESSURES

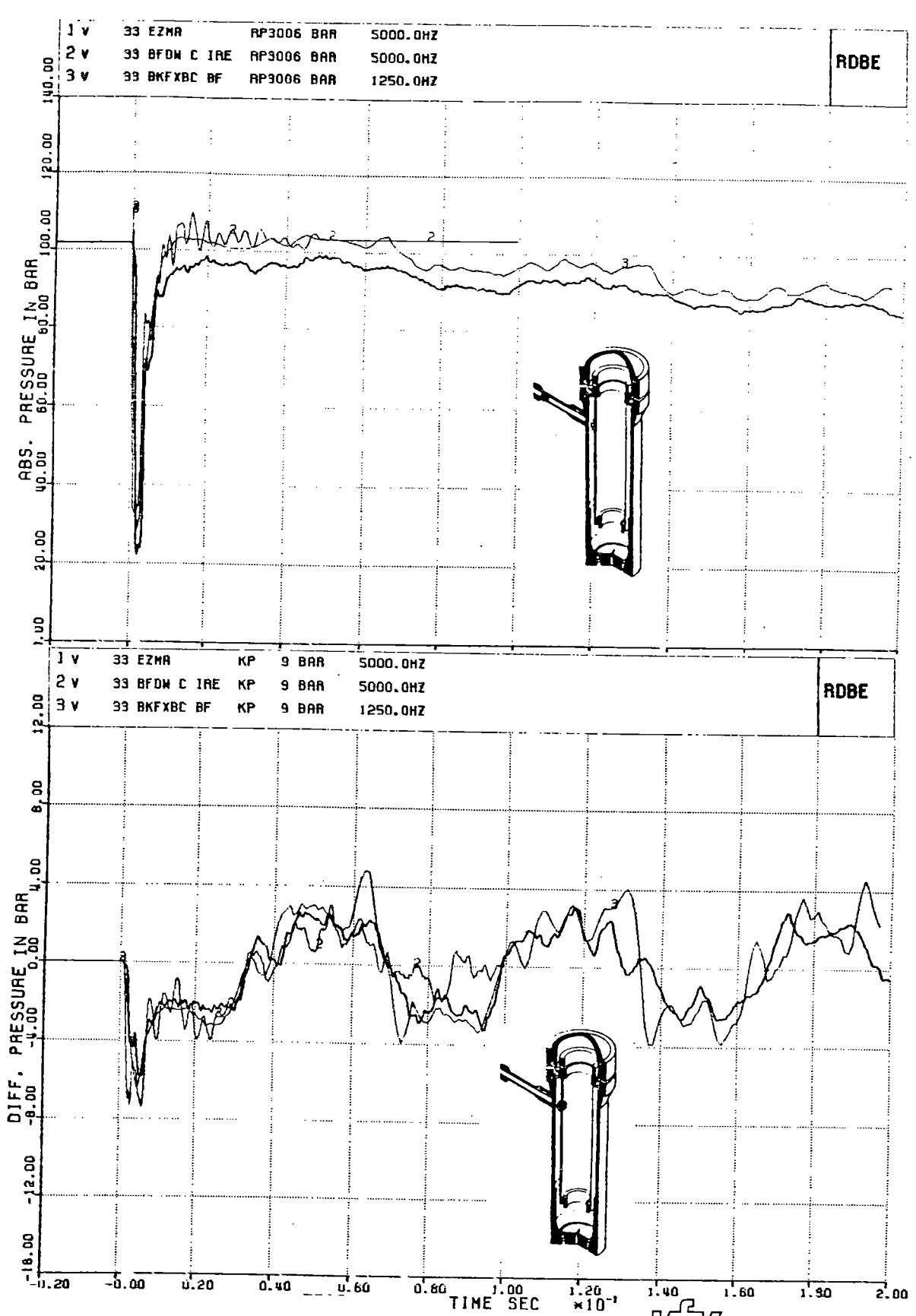
FIG. 34



V33; COMPARISONS OF MEASUREMENTS AND PRETEST CALCULATIONS BY DAISY AND FLEXWALL FOR RAD. DISPLACEMENT AND AZ. STRAIN

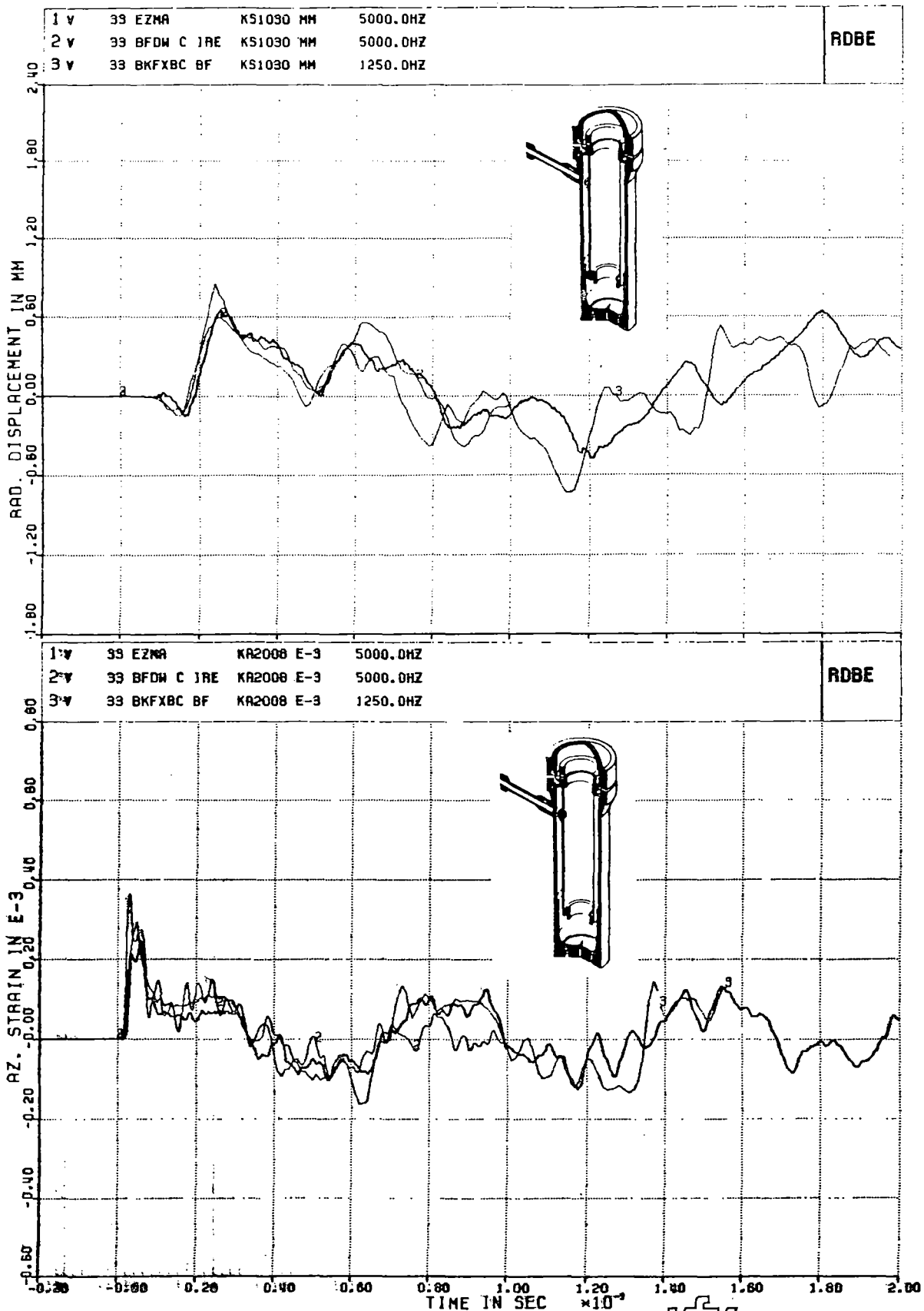


FIG. 35



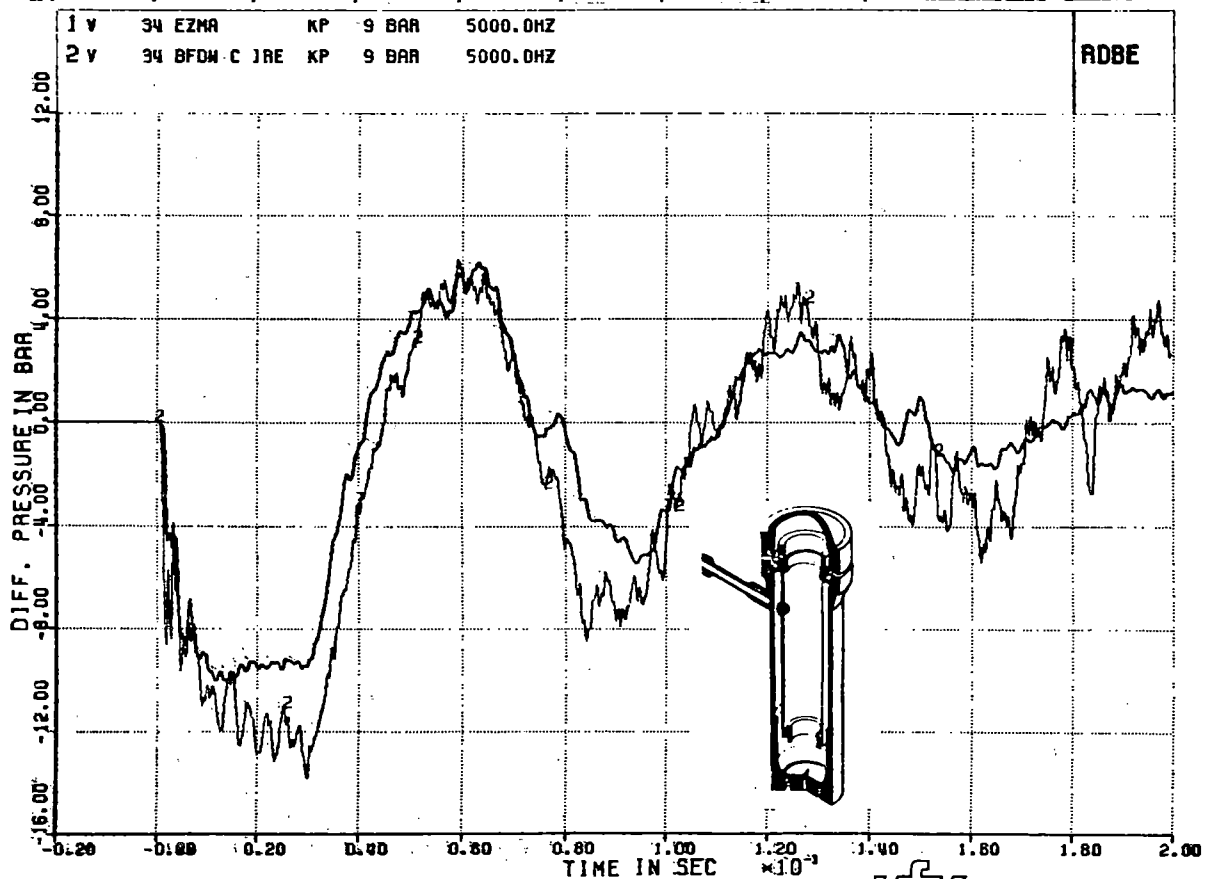
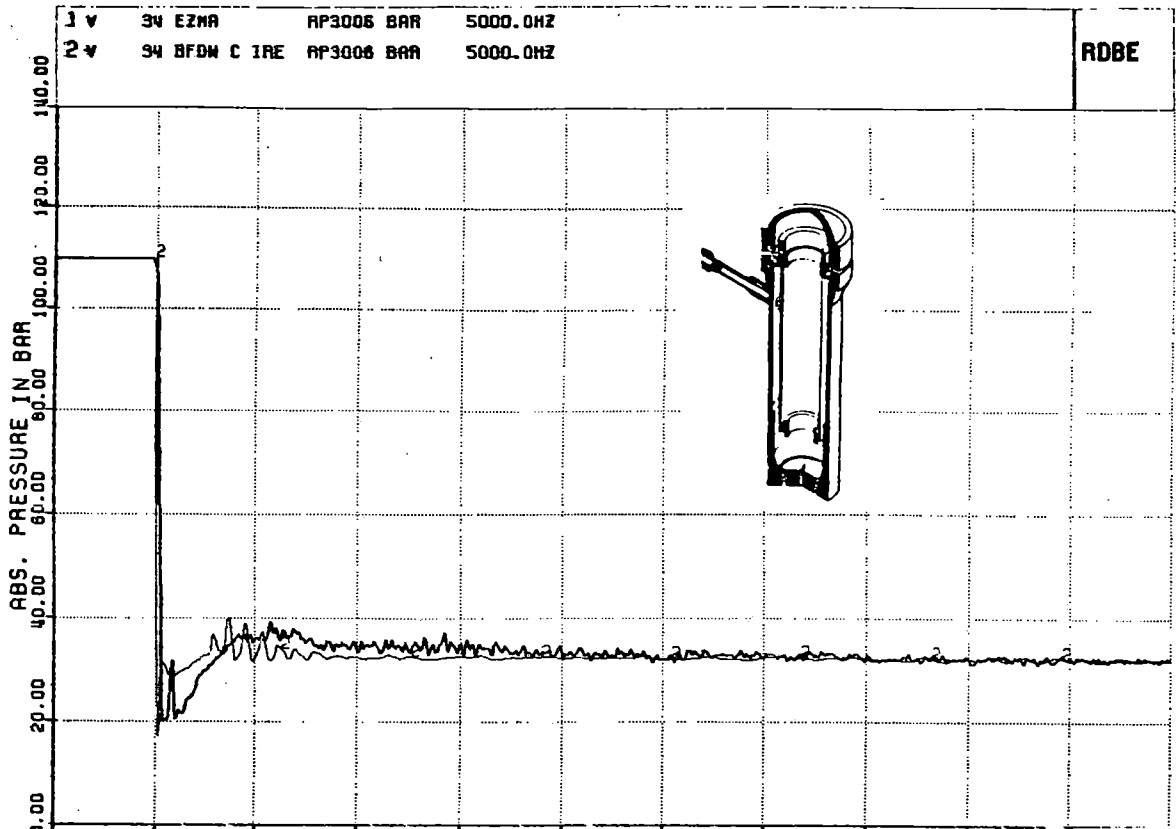
V33; COMPARISONS OF MEASUREMENTS AND PRETEST CALCULATIONS BY FLUX-DRIX AND K-FIX (BATTELLE) FOR ABS. AND DIFF. PRESSURES

FIG. 36



V33; COMPARISONS OF MEASUREMENTS AND PRETEST  
 CALCULATIONS BY FLUX-DRIX AND K-FIX (BATTELLE)  
 FOR RAD. DISPLACEMENT AND AZ. STRAIN

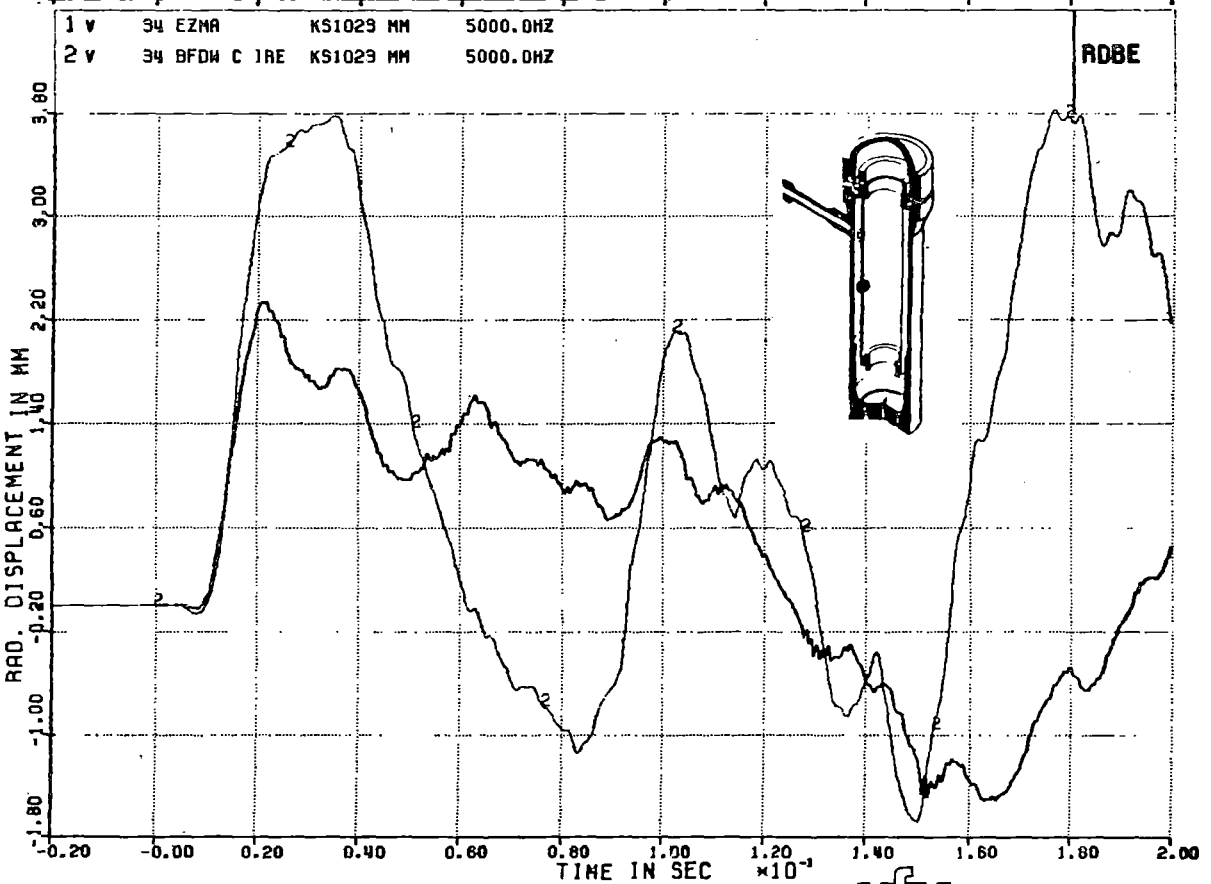
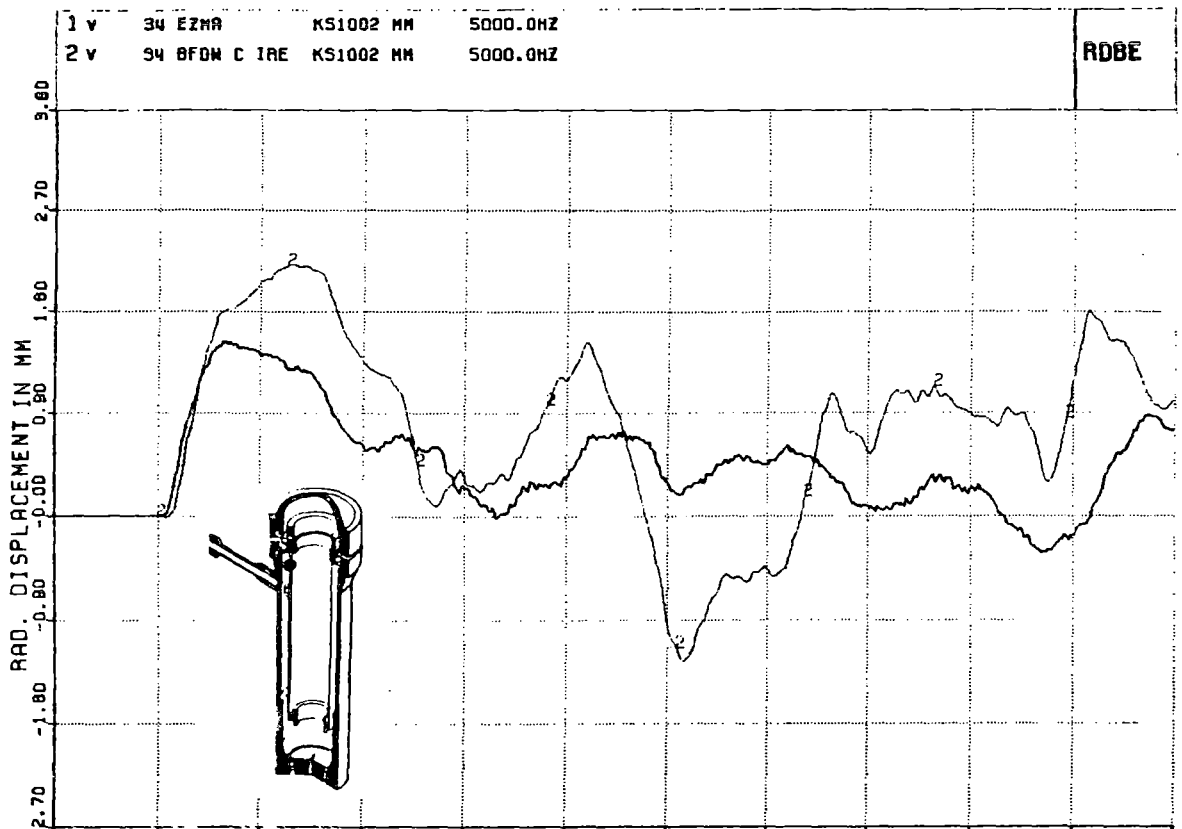
FIG. 37



V34; COMPARISONS OF MEASUREMENTS AND PRETEST CALCULATIONS BY FLUX4-DRIX FOR ABS, AND DIFF. PRESSURES

FIG. 38



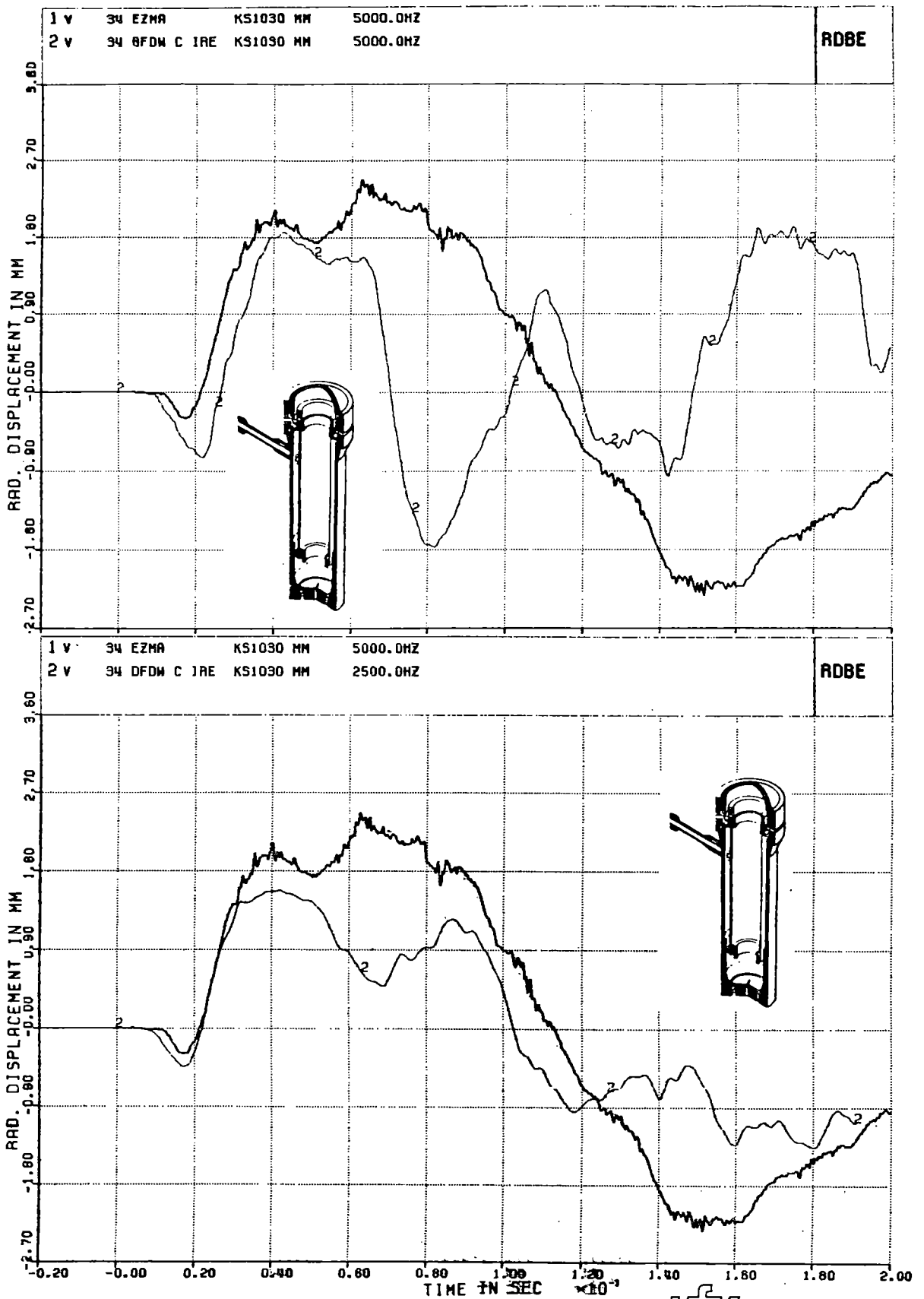


KIK

V34; COMPARISONS OF MEASUREMENTS AND PRETEST CALCULATIONS BY FLUX4-DRIX FOR REL. RAD. DISPLACEMENTS

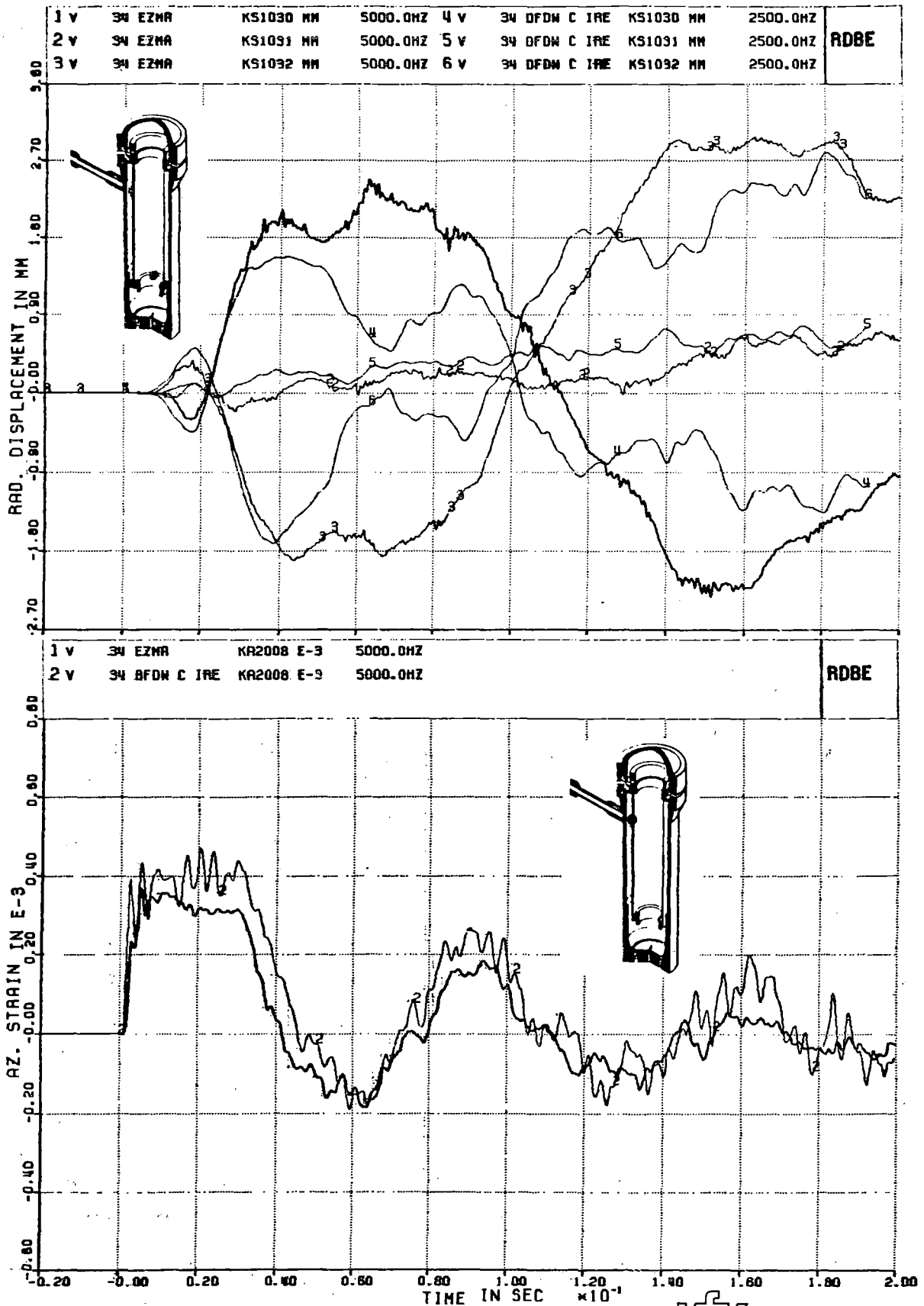
FIG. 39





V34; COMPARISONS OF MEASUREMENTS AND PRE-(TOP) AND POST-(BOTTOM) TEST CALCULATIONS BY FLUX4-DRIX FOR REL. RAD. DISPLACEMENT AT CB LOWER END

FIG. 40



**KfK**

V34; COMPARISONS OF MEASUREMENTS AND POST-TEST CALCULATIONS BY FLUX4-DRIX FOR REL. RAD. DIS-PLACEMENTS AT 3 AZ. POSITIONS (TOP) AND PRETEST CALCULATIONS FOR AZ. STRAIN (BOTTOM)

FIG. 41

|  |  |  |  |  |  |
|--|--|--|--|--|--|
| <b>NRC FORM 335</b><br>(7-77)  |  | <b>U.S. NUCLEAR REGULATORY COMMISSION</b><br><b>BIBLIOGRAPHIC DATA SHEET</b> |  | 1. REPORT NUMBER <i>(Assigned by DDC)</i><br>NUREG/CP-0041, Volume 1 |  |
| 4. TITLE AND SUBTITLE <i>(Add Volume No., if appropriate)</i><br>Proceedings of the Tenth Water Reactor Safety Research Information Meeting  |  |  |  | 2. <i>(Leave blank)</i>  |  |
| 7. AUTHOR(S)<br>Compiled by: Stanley A. Szawlewicz, Consultant   |  |  |  | 3. RECIPIENT'S ACCESSION NO.   |  |
| 9. PERFORMING ORGANIZATION NAME AND MAILING ADDRESS <i>(Include Zip Code)</i><br>U.S. Nuclear Regulatory Commission<br>Office of Nuclear Regulatory Research<br>Washington, DC 20555   |  |  |  | 5. DATE REPORT COMPLETED<br>MONTH   YEAR<br>December   1982          |  |
| 12. SPONSORING ORGANIZATION NAME AND MAILING ADDRESS <i>(Include Zip Code)</i><br>Same as Item 9.  |  |  |  | 6. <i>(Leave blank)</i>  |  |
| 13. TYPE OF REPORT<br>Compilation of Conference Papers   |  |  |  | 7. DATE REPORT ISSUED<br>MONTH   YEAR<br>January   1983              |  |
| 15. SUPPLEMENTARY NOTES  |  |  |  | 8. <i>(Leave blank)</i>  |  |
| 16. ABSTRACT <i>(200 words or less)</i><br><p>This report is a compilation of papers which were presented at the Tenth Water Reactor Safety Research Information Meeting held at the National Bureau of Standards, Gaithersburg, Maryland, October 12-15, 1982. It consists of six volumes. The papers describe recent results and planning of safety research work sponsored by the Office of Nuclear Regulatory Research, NRC. It also includes a number of invited papers on water reactor safety research prepared by the Electric Power Research Institute and various government and industry organizations from Europe and Japan.</p> |  |  |  | 9. PROJECT/TASK/WORK UNIT NO.  |  |
| 17. KEY WORDS AND DOCUMENT ANALYSIS  |  |  |  | 10. CONTRACT NO.   |  |
| 17b. IDENTIFIERS/OPEN-ENDED TERMS  |  |  |  | 11. PERIOD COVERED <i>(Inclusive dates)</i><br>October 12-15, 1982   |  |
| 18. AVAILABILITY STATEMENT<br>Unlimited  |  | 19. SECURITY CLASS <i>(This report)</i><br>Unclassified                      |  | 21. NO. OF PAGES<br>435  |  |
|  |  | 20. SECURITY CLASS <i>(This page)</i><br>Unclassified                        |  | 22. PRICE<br>S   |  |

UNITED STATES  
NUCLEAR REGULATORY COMMISSION  
WASHINGTON, D.C. 20555

OFFICIAL BUSINESS  
PENALTY FOR PRIVATE USE, \$300

FOURTH CLASS MAIL  
POSTAGE & FEES PAID  
USNRC  
WASH. D. C.  
PERMIT No. G-67

| Name | Mail Stop | Due Date |
|------|-----------|----------|
|------|-----------|----------|

Return to: 823 LIBRARY/SNL, MS 0731